Contribution du récepteur 5-HT2B dans la transmission sérotoninergique

Emily Quentin

Université Pierre et Marie Curie

Ecole doctorale Physiologie, physiopathologie et thérapeutique (P2T)

Laboratoire INSERM U839 / Equipe de recherche Luc Maroteaux : Signalisation de la sérotonine dans la plasticité et la pathologie

Contribution du récepteur 5-HT$_{2B}$ dans la transmission sérotoninergique

Par Emily QUENTIN

Thèse de doctorat de Neurosciences

Dirigée par Luc Maroteaux

Présentée et soutenue publiquement le 12 Juillet 2017

Devant un jury composé de :

M. Salah El Mestikawy, Directeur de recherche	Président du Jury
Mme. Françoise Coussen, Directeur de recherche	Rapporteur
Mme. Michèle Darmon, Directeur de recherche	Rapporteur
Mme. Sabine Lévi, Directeur de recherche	Examinateur
M. Philippe Marin, Directeur de recherche	Examinateur

TABLE DES MATIERES

TABLE DES ABREVIATIONS

5-HIAA	5-hydroxyindole acétaldéhyde
5-HT	sérotonine ou 5-hydroxytryptamine
5-HTP	L-tryptophane en 5-hydroxytryptophane
AADC	décarboxylase des acides aminés aromatiques
AC	adénylate cyclase
ALDH2	aldéhyde déshydrogénase2
ATV	aire tegmentale ventrale
BLA	amygdale basolatérale
CaM	calmoduline dépendante du calcium
IPP	channel interacting PDZ protein
COX	cyclooxygénase
CPF	cortex préfrontal
DAG	diacylglycérol
DF	dexfenfluramine
DRN	raphé dorsal
DRM	raphé médian
GABA	acide γ-aminobutyrique
GIRK	G protein-coupled inwardly-rectifying potassium channels
GMPc	guanosine monophosphate cyclique
IP_3	inositol triphosphate
ISRSs	inhibiteurs de la recapture de 5-HT
INADL	inactivation-no afterpotential D-like
LC	locus coeruleus
MAO	monoamine oxydase
Nac	noyau accumbens
NO	oxyde nitrique
cNOS	NO synthase constitutive
iNOS	NOS inductible

nNOS	oxyde nitrique synthase neuronale
P38-MAPK	protéine MAP kinase P38
PATJ	protein associated with tight junction protein
PDGF	facteur de croissance dérivé des plaquettes
PDZ	PSD-95, Discs Large, et Zona Occludens 1 proteins
PIP_2	phosphatidylinositol
PLA2	phospholipase A2
PKA	protéine kinase A
PKC	protéine kinase C
PKG	protéine kinase G
PPI	inhibition du réflexe de sursaut
PSD	densité post-synaptique.
R-5-HT	récepteur sérotoninergique
RCE	Rosa26 : CAG-loxP-STOP-loxP-EGFP
RCPGs	récepteurs couplés aux protéines G
SERT	transporteur de la 5-HT
TIRF	total internal reflexion fluorescent microscopie
TNS	transmission non synaptique
TPH	tryptophane hydroxylase
TS	transmission synaptique
VGLUT	transporteur vésiculaire du glutamate
VMAT	transporteur vésiculaires des monoamines

INDEX DES FIGURES

RESUME

Les neurones sérotoninergiques forment des réseaux complexes avec les autres systèmes de neurotransmission dans le système nerveux central. Le rôle du récepteur 5-HT_{2B} dans ces réseaux est peu connu. L'ablation génétique ou la surexpression virale du récepteur 5-HT_{2B} dans les neurones sérotoninergiques, nous ont permis de mettre en évidence sa participation l'excitabilité de ces neurones. De fait, le récepteur 5-HT_{2B} est nécessaire à l'action des antidépresseurs et de l'ecstasy qui provoquent une accumulation extracellulaire de sérotonine. Aussi, le récepteur 5-HT_{2B} est capable d'agir tel un modulateur positif, à l'opposé des autorécepteurs 5-HT_{1A}, sur l'activité des neurones sérotoninergiques. Ensuite, l'étude de la distribution du récepteur 5-HT_{2B} et de son interaction avec la protéine de pontage CIPP nous a permis de décrire la distribution subcellulaire du récepteur 5-HT_{2B} dans des cultures primaires de neurones d'hippocampe. La co-expression du récepteur 5-HT_{2B} avec CIPP augmente significativement son adressage somatodendritique dans les synapses excitatrices. Au niveau fonctionnel, CIPP augmente la libération dendritique de calcium dépendante de la stimulation du récepteur 5-HT_{2B}. En synergie avec CIPP, cette stimulation augmente le regroupement des récepteurs glutamatergiques NMDA suggérant un rôle dans la plasticité synaptique pouvant expliquer certains résultats précédents.

ABSTRACT

Serotonergic neurons are organized in complex networks interacting with other neurotransmitter systems in the brain. The 5-HT_{2B} receptor contribution in these networks remains unclear. Using 5-HT_{2B} receptor genetic ablation or a viral overexpression in the serotoninergic neurons, we have demonstrated its participation to the excitability of these neurons. In fact, 5-HT_{2B} receptors are necessary for serotonin accumulation induced by ecstasy and antidepressants effects. Moreover, 5-HT_{2B} receptors activation counteracts the 5-HT_{1A} dependant inhibition on serotonergic neurons activity. Here we propose 5-HT_{2B} receptor as positive modulator of serotonergic neurons. Then, studying 5-HT_{2B} receptors and CIPP scaffold protein interaction allow us to identify the subcellular distribution of the receptor and a functional role of CIPP. Indeed, overexpression of both proteins in primary hippocampal cultures of neurons increases 5-HT_{2B} receptors somatodendritic targeting at excitatory synapses. Thus CIPP increases dendritic calcium release dependent on 5-HT_{2B} receptor stimulation. In synergy with CIPP, this stimulation increases NMDA receptors clustering suggesting a role in synaptic plasticity that could explain some of the previous findings.

AVANT PROPOS

Le système sérotoninergique est impliqué dans de nombreuses fonctions physiologiques, par conséquent il a fait l'objet d'un grand nombre d'études touchant différents domaines des neurosciences. Les neurones sérotoninergiques forment des réseaux complexes finement régulés, notamment par l'activation des 14 sous-types de récepteurs sérotoninergiques exprimés par ce réseau neuronal. Elucider le rôle de ces récepteurs est un enjeu majeur de la compréhension des fonctions cognitives pouvant être altérées dans des pathologies psychiatriques telles que la dépression ou l'addiction.

L'ablation génétique ou l'inactivation pharmacologique des récepteurs 2B de la sérotonine (5-HT_{2B}) a été associée à plusieurs phénotypes comportementaux. En effet, la caractérisation phénotypique des animaux transgéniques dépourvus de récepteurs 5-HT_{2B} a mis en évidence une contribution du récepteur dans la prise alimentaire, la dépression, la schizophrénie et l'addiction. Les voies de signalisation du récepteur 5-HT_{2B} ont été bien décrites dans des lignées cellulaires, mais leur distribution et leur fonction neuronale restent encore peu connue. En effet, puisque l'expression du récepteur 5-HT_{2B} est faible dans le cerveau et qu'il n'existe pas d'anticorps spécifique pour ce dernier, il apparait difficile d'extrapoler les données obtenues *in vitro*, aux neurones. Néanmoins, le laboratoire a publié différentes études montrant l'importance du récepteur 5-HT_{2B} dans la transmission sérotoninergique.

Au cours de mon projet doctoral, j'ai participé à plusieurs travaux de recherche visant à éclaircir le rôle des récepteurs 5-HT_{2B} dans les neurones sérotoninergiques et dopaminergiques (Article 1, Annexe2). La comparaison des phénotypes des animaux dépourvus totalement des récepteurs 5-HT_{2B} et ceux n'exprimant pas les récepteurs 5-HT_{2B} uniquement dans les neurones dopaminergiques, a permis d'attribuer certains phénotypes comportementaux aux neurones sérotoninergiques et/ou dopaminergiques (Article 1, Annexe2). Ces travaux nous ont permis également de suggérer que les récepteurs 5-HT_{2B} seraient des modulateurs positifs de l'activité des neurones sérotoninergiques (Article 1). En parallèle, j'ai étudié l'impact de l'interaction des récepteurs 5-HT_{2B} avec la protéine de pontage CIPP sur la signalisation et la distribution des récepteurs dans la lignée cellulaire COS-7 ainsi que dans des cultures primaires de neurones d'hippocampe (Article 2). Sachant que cette protéine de pontage est peu étudiée, nous avons d'abord décrit la distribution subcellulaire de ces protéines. Nous avons par la suite étudié l'impact de l'interaction de CIPP sur 1) les récepteurs 5-HT_{2B}, 2) les récepteurs glutamatergiques de type NMDA et sur 3) la morphologie des épines dendritiques (Article 2).

Enfin, j'ai participé à la description des oligomères des récepteurs 5-HT_2 et à l'étude de leurs impacts sur la signalisation et le couplage des récepteurs 5-HT_2 (Annexe 1).

En résumé, ce manuscrit présente dans une **première partie** la synthèse des études scientifiques décrivant les acteurs du système sérotoninergique et leur régulation. Un chapitre est consacré aux études centrées sur les récepteurs 5-HT_{2B}. Finalement, la contribution des récepteurs 5-HT_1 et 5-HT_2 dans la modulation de la neurotransmission est décrite. Cette section permettra d'introduire la **deuxième partie** qui est la synthèse de nos principaux résultats. Deux études y seront détaillées : l'une portant sur la caractérisation des animaux dépourvus de récepteurs 5-HT_{2B} uniquement dans les neurones sérotoninergiques (*5-$HT_{2B}^{5\text{-}HTKO}$*) (Article 1) et l'autre portant sur l'interaction des récepteurs 5-HT_{2B} avec la protéine de pontage CIPP et l'impact de cette interaction sur la distribution et la fonction du récepteur (article 2). La **troisième partie** du manuscrit sera la synthèse de discussions permettant de mettre en évidence le rôle des récepteurs 5-HT_{2B} dans la transmission sérotoninergique.

.

INTRODUCTION

I. Le système sérotoninergique

A. Généralités

1. Découverte de la sérotonine

Au milieu de XX siècle, une molécule capable d'induire des contractions des muscles lisses des vaisseaux sanguins a été identifiée dans le sérum humain (Rapport et al., 1948) . Il a ensuite été démontré que cette molécule vasoconstrictrice provenait des plaquettes puis, en 1949, Rapport et collaborateurs la caractérise comme sérotonine ou 5-hydroxytryptamine (5-HT) (Page et al., 1948; Rapport et al., 1948; Rapport, 1949) (pour revue Whitaker-Azmitia, 1999).

La 5-HT est synthétisée au niveau périphérique par les cellules entérochromaffines de la muqueuse du tractus gastro-intestinal puis stockée dans les plaquettes. Dans le cerveau, la 5-HT est synthétisée par les neurones du raphé où elle agira en tant que neurotransmetteur, et dans la glande pinéale où elle est utilisée comme précurseur de la mélatonine. Ainsi, le système sérotoninergique est composé d'une entité périphérique comprenant le système nerveux entérique et neuro-endocrine et d'une entité centrale dans le cerveau **(Figure 1)**.

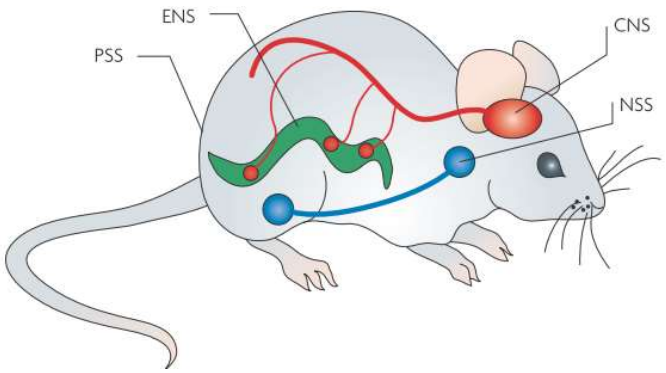

Figure 1 Le système sérotoninergique. *Système sérotoninergique périphérique (en vert ENS: système nerveux entérique et PSS : système sérotoninergique périphérique ; en bleu NSS : système sérotoninergique neuro-endocrine (poumons- cœur- vaisseaux sanguins-pancréas-plaquettes) et central (CNS en rouge) (Murphy and Lesch, 2008).*

2. Métabolisme de la sérotonine

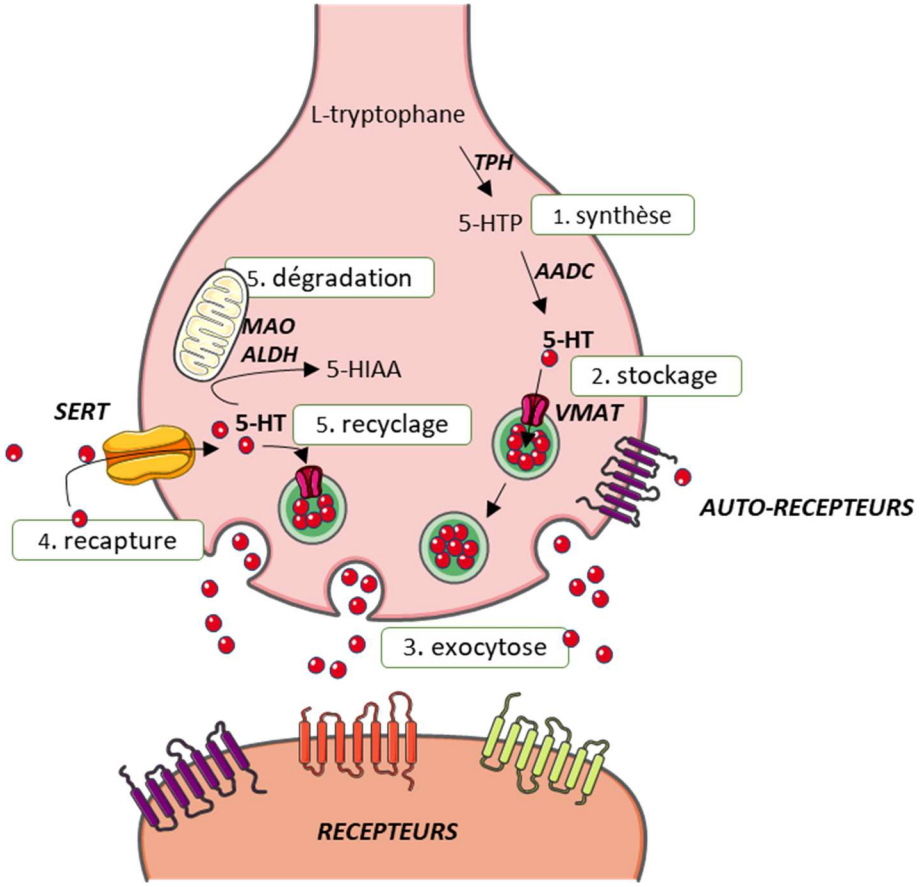

Figure 2 Métabolisme de la sérotonine

La 5-HT est issue de la conversion du L-tryptophane en 5-hydroxytryptophane (5-HTP) par l'enzyme tryptophane hydroxylase (TPH) **(Figure 2)**. Il existe deux isoformes de la TPH, la TPH1 localisée en périphérie dans l'intestin principalement et la TPH2 au niveau du système nerveux central dans le tronc cérébral. Le 5-HTP subit ensuite une décarboxylation par l'action de la décarboxylase des acides aminés aromatiques (AADC) **(Figure 2)**. Cette étape est commune à la synthèse des neuromédiateurs monoaminergiques, *i.e.* la 5-HT, la dopamine et la noradrénaline. La 5-HT est ensuite stockée dans les vésicules synaptiques par le transporteur vésiculaires des monoamines (VMAT) **(Figure 2)** (Kanner and Schuldiner, 1987). Deux isoformes du VMAT ont été identifiés, le VMAT1 localisé dans les cellules entérochromaffines et le VMAT2 localisé dans les neurones et les plaquettes (Erickson et al., 1992; Liu et al., 1992). Les VMATs ont des affinités différentes pour les monoamines (Ki 5-HT = 19+/-5 µM ; Ki Dopamine = 25+/-7 µM ; Ki Noradrénaline =91,5+/-10,5 µM). Ainsi, la régulation du trafic intracellulaire des transporteurs VMAT2 dans les neurones est essentielle pour le stockage et donc la libération des neuromédiateurs (pour revue Fei et al., 2008; Wimalasena, 2011).

La 5-HT est dégradée par la monoamine oxydase (MAO) en 5-hydroxyindole acétaldéhyde (5-HIAA) (**Figure 2**). Il existe deux sous-types de MAO, MAO-A et MAO-B, qui différent par leurs affinités pour les neuromédiateurs monoaminergiques. La MAO-A dégrade préférentiellement la 5-HT et la noradrénaline tandis que la MAO-B dégrade la dopamine (Johnston, 1968; Knoll and Magyar, 1972). La MAO-A est la cible thérapeutique de certains antidépresseurs qui vont bloquer son action et donc empêcher la dégradation de la 5-HT provoquant ainsi une accumulation de 5-HT dans la fente synaptique. Finalement, le 5-HIAA, est dégradé par l'aldéhyde déshydrogénase2 (ALDH2) dans les mitochondries (**Figure 2**).

3. Organisation des neurones sérotoninergiques

La 5-HT est impliquée dans de nombreux processus physiologiques et cognitifs tels que les émotions (Graeff et al., 1996), la régulation des cycles circadiens (Prosser et al., 1990), les cycles veille/ sommeil (Levine and Jacobs, 1992; Portas et al., 2000; Ursin, 2002), la locomotion (Jacobs and Fornal, 1993; White et al., 1996), les comportements sexuels, alimentaires ou sociaux (Weiger, 1997). Cet éventail de fonctions est vraisemblablement dû aux variétés de structures cérébrales dans lesquelles les neurones sérotoninergiques se projettent ainsi qu'aux nombreuses innervations qu'il reçoit.

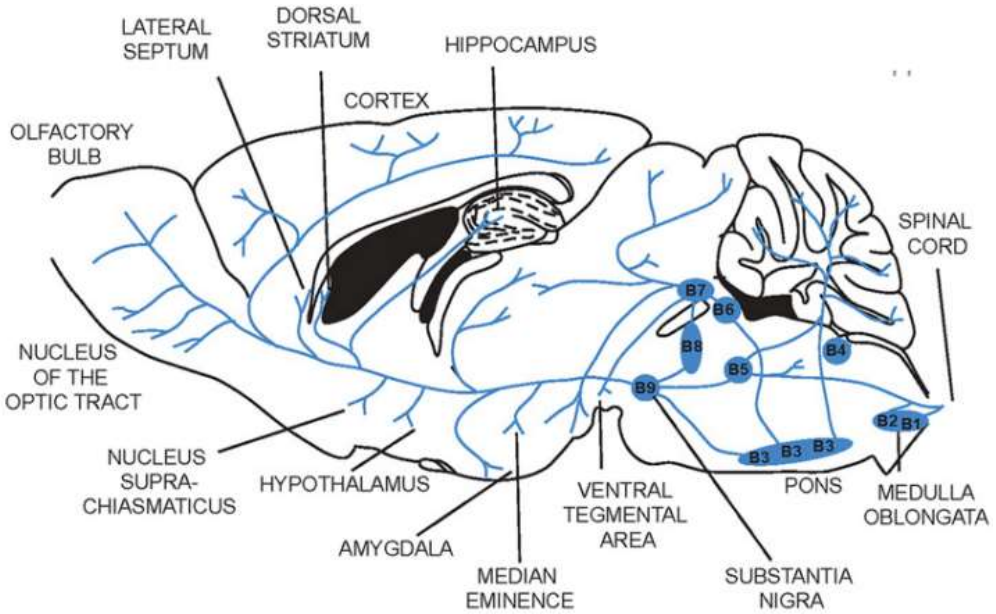

***Figure 3 Distribution des neurones sérotoninergiques**. Les noyaux les plus caudaux (B1-B2-B3) projettent dans la moelle épinière, alors que les noyaux du raphé dorsal (DRN) (B6-B7) et du raphé médian (DRM) (B5-B8) projettent vers des zones cérébrales différentes qui se chevauchent (Voisin et al., 2016).*

Les neurones sérotoninergiques, dont le nombre estimé est d'environ 26 000 (Ishimura et al., 1988), synthétisent et libèrent la 5-HT et sont regroupés en noyaux dans le raphé dorsal (DRN) (noyaux B6-B7), médian (DRM) (noyaux B5-B8) et caudal (noyaux B1-B2-B3) (**Figure 3**). Ces neurones, pauvres en épines dendritiques, ont la particularité d'être riches en axones collatéraux portant un grand nombre de varicosités formant ainsi des synapses dites « en passant » (van der Kooy and Hattori, 1980; Köhler et al., 1982; Descarries et al., 1982; Imai et al., 1986; Gagnon and Parent, 2014).

L'identité des neurones sérotoninergiques est caractérisée par l'expression de marqueurs moléculaires membranaires et intracellulaires. Les marqueurs couramment utilisés sont la TPH2, l'AADC, le transporteur de la 5-HT (SERT), le VMAT2, la MAO-A et la MAO-B et les autorécepteurs sérotoninergiques 5-$HT_{1A/B}$ (pour revue Goridis and Rohrer, 2002). La différenciation des neurones précurseurs en neurones 5-HT exprimant ces marqueurs sérotoninergiques est dépendante de l'expression du facteur de transcription Pet-1 (Liu et al., 2010; Wyler et al., 2016). C'est pourquoi, le promoteur Pet-1 est utilisé dans nos modèles transgéniques de souris knock-out conditionnelles pour les récepteurs 5-HT_{2B} seulement dans les neurones sérotoninergiques (*5-$HT_{2B}^{5\text{-}HTKO}$*).

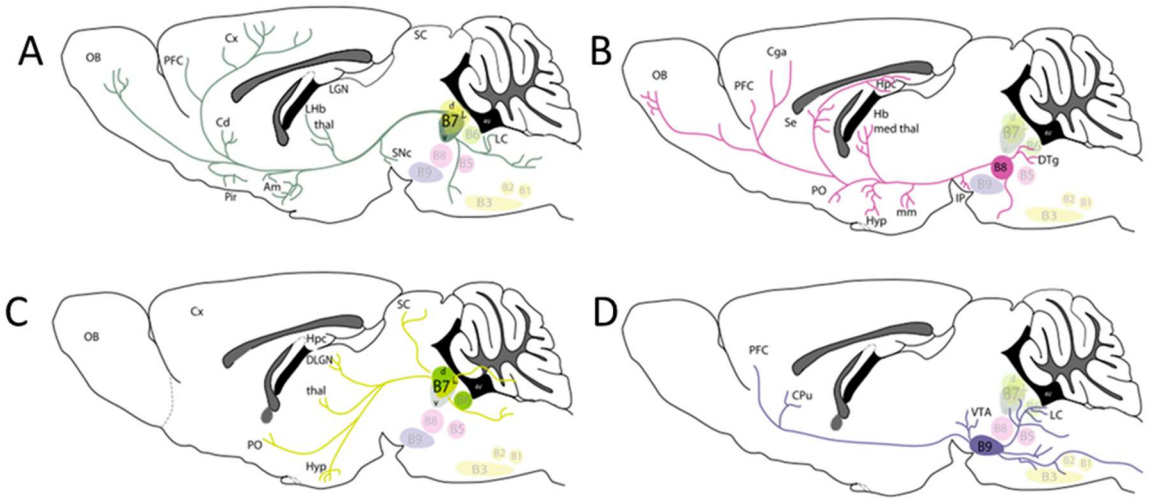

Figure 4 Projections sérotoninergiques en fonction des noyaux du raphé. *Projections issues du noyau B7 (A)(C), B8(C) et B(D) projetant au niveau cortical et central (Muzerelle et al., 2014).*

L'équipe du Pr Gaspar a mis en évidence que les neurones issus du noyau B7 du DRN projettent préférentiellement vers les structures corticales (**Figure 4 A**). Ceux dont les corps cellulaires se situent dans le noyau B8 du MRN ciblent des structures centrales comme l'hippocampe (**Figure 4 B**). Enfin, les neurones issus du raphé supralaminal (B9) projettent au

niveau du cortex préfrontal (CPF), de l'aire tegmentale ventrale (ATV), du locus coeruleus (LC) et aussi sur les neurones 5-HT du raphé (**Figure 4 D**). L'organisation topographique des neurones sérotoninergiques permet d'associer différentes fonctions aux différents noyaux du raphé selon les structures dans lesquelles ils projettent. L'analyse des propriétés électrophysiologiques associée à une étude transcriptomique des neurones 5-HT dans différentes structures cibles a montré que ces différents noyaux sont en réalité des populations bien distinctes avec des caractéristiques physiologiques spécifiques (Beck et al., 2004; Fernandez et al., 2015; Mlinar et al., 2016).

Les populations de neurones sérotoninergiques sont, en général, distinguées par leur localisation dans les noyaux du raphé, leur morphologie et leur profil de décharge électrophysiologique. La mise au point de nouvelles méthodes de dissociation neuronale et de tri par cytométrie en flux associées à des études transcriptomiques a permis de différencier l'origine développementale des populations de neurones sérotoninergiques issus de différents rhombomères exprimant de façon variable des marqueurs génétiques spécifiques (Jensen et al., 2008) tels que la TPH2, le transporteur vésiculaire du glutamate 3 (VGLUT3) et le transporteur de la sérotonine (SERT). Il a été mis en évidence que chaque sous-populations sont associées à des fonctions spécifiques (Okaty et al., 2015; Wyler et al., 2016) .

B. Acteurs de la transmission sérotoninergique

Les différentes modulations du système sérotoninergique sont complexes de par la diversité des réseaux et mécanismes impliqués. Cela inclut notamment la modulation de la signalisation, de l'expression et de la distribution des récepteurs et du transporteur de la 5-HT permettant une régulation fine de la transmission sérotoninergique. Ainsi, un déséquilibre de cette régulation est associé à différentes pathologies psychiatriques.

1. Le transporteur de la sérotonine SERT

La stimulation des neurones sérotoninergiques provoque une libération de 5-HT dans le milieu extracellulaire. Celle-ci est ensuite transportée par le transporteur de la sérotonine SERT vers le milieu intracellulaire. Ainsi, l'action de SERT régule les concentrations extracellulaires de 5-HT et donc la force de la transmission sérotoninergique (Blakely et al., 1991; Torres and Amara, 2007; Steiner et al., 2008). Des perturbations de la modulation de SERT sont associées à de nombreux dérèglements physiologiques et comportementaux.

Les souris invalidées pour le gène codant SERT (*Slc6a4*) montre l'étendue des fonctions affectées par l'absence de SERT et soutient son rôle central dans la transmission sérotoninergique (pour revue Murphy and Lesch, 2008).

i. Distribution

Le SERT est fortement exprimé par les neurones sérotoninergiques du DRN et MRN et plus faiblement par les neurones du raphé caudal (Fujita et al., 1993; Bengel et al., 1997). De fortes densités de SERT ont été observées dans le noyau caudé / putamen, le NAc, l'amygdale, le cortex, la substance noire, le pallidum ventral, le septum et l'hippocampe ; en revanche, de faibles densités ont été observées dans le cervelet (Hensler et al., 1994; Stockmeier et al., 1996; Sur et al., 1996; Bengel et al., 1997; Kish et al., 2005). Au niveau cellulaire, SERT est majoritairement localisé dans les axones à savoir: 1) le long des axones (varicosités), 2) au niveau des terminaisons synaptiques des neurones sérotoninergiques et enfin 3) dans les corps cellulaires des neurones.

ii. Régulations

De par sa fonction unique dans la recapture de la 5-HT, la modulation de SERT est un élément clé dans la transmission sérotoninergique. De nombreux mécanismes modulent les propriétés pharmacologiques, l'expression, le trafic et la distribution de SERT (pour revue Bermingham and Blakely, 2016). SERT est lié à l'enzyme oxyde nitrique synthase neuronale (nNOS) (Chanrion et al., 2007), dont l'activation induit la synthèse d'oxyde nitrique (NO) et de guanosine monophosphate cyclique (GMPc), qui module négativement l'expression du transporteur via la protéine kinase G (PKG) (Launay et al., 2006; Ramamoorthy et al., 2007; Sørensen et al., 2014). Les différents R-5-HT sont couplés à certaines voies de signalisation modulant le SERT mais, pour l'instant, aucune corrélation n'a été mise en en évidence quant à une régulation directe du SERT par les R-5-HT. Enfin, la 5-HT semble exercer un rétrocontrôle sur le SERT en diminuant sa capacité de recapture afin de stabiliser les concentrations de 5-HT extracellulaire *in vitro* (Jørgensen et al., 2014).

De nombreuses protéines kinases ou phosphatases sont impliquées dans la régulation de l'activité du SERT (**Figure 5**). *In vitro*, des phosphorylations dépendantes de la protéine PKA et de la PKC ont lieu au niveau des domaines N et C-terminus du SERT (Blakely et al., 1998). La stimulation de la PKA augmente la phosphorylation du SERT sans affecter sa capacité de transport (Vmax) (Ramamoorthy et al., 1998). Cependant, *in vivo* dans les préparations de

synaptosomes de CPF, la stimulation de la PKA augmente la capacité de transport du SERT (Awtry et al., 2006). La PKC exerce une régulation biphasique du SERT. La première phase est la phosphorylation d'un résidu sérine entrainant la diminution de la capacité de transport du SERT, puis une seconde phosphorylation sur une thréonine provoquant l'internalisation du transporteur (Jayanthi et al., 2005). Le SERT est phosphorylé et son expression est positivement régulée par les agents de la voie de la signalisation de la PKG (Miller and Hoffman, 1994; Ramamoorthy et al., 1998; Zhu et al., 2004a, 2004b; Prasad et al., 2005; Zhang et al., 2007; Wong et al., 2012). Cette régulation est parfois liée à une augmentation de l'expression du SERT à la membrane (Zhu et al., 2004a, 2004b; Prasad et al., 2005; Zhu et al., 2007), parfois liée à une augmentation de sa capacité de transport (Ramamoorthy et al., 2007) (**Figure 5**). Il semble que la PKG phosphoryle la thréonine 276 et maintienne sa conformation ouverte augmentant ainsi l'activité du SERT (Zhang et al., 2014). L'inhibition de la protéine MAP kinase P38 (P38-MAPK) diminue la phosphorylation du SERT et son expression membranaire de surface, alors que son activation augmente la capacité de transport du SERT (Zhu et al., 2004a, 2004b; Prasad et al., 2005; Samuvel et al., 2005; Zhu et al., 2007; Lau et al., 2009; Chang et al., 2012). Cependant, aucun site de phosphorylation par la PKA, la PKC, ni la P38-MAPK n'a été identifié pour le moment mais certains ont été proposés tels que la sérine149, la sérine277 ou la thréonine 603 pour la PKC ; la thréonine 616 pour la P38-MAPK (Sørensen et al., 2014).

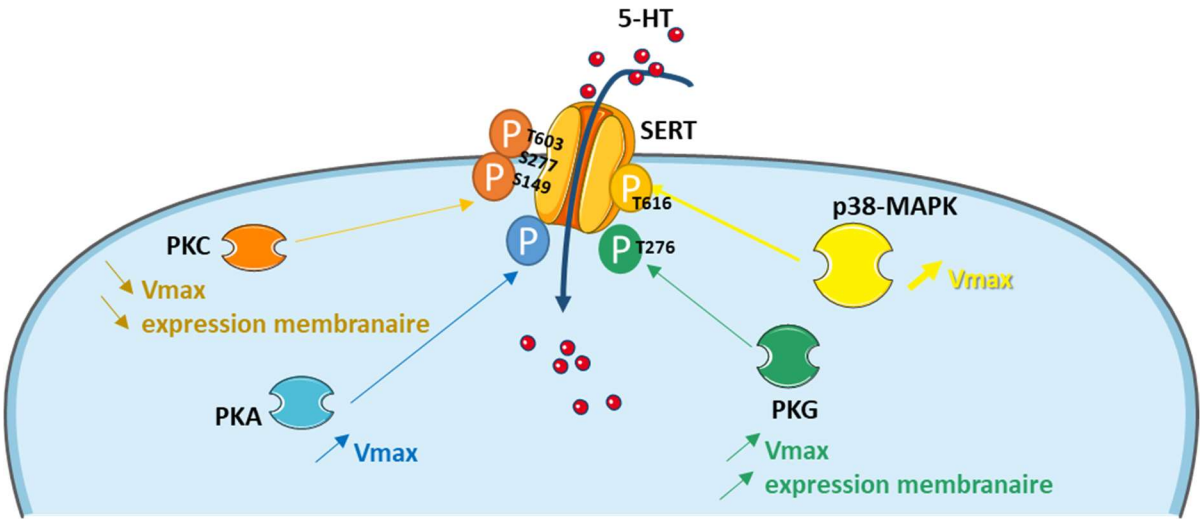

Figure 5 Régulation de SERT par phosphorylation*. Impact de la phosphorylation et sites putatifs de phosphorylations du SERT par les protéines kinases PKC, PKA, PKG et le p38-MAPK sur l'expression membranaire et de l'activité de recapture (Vmax) de SERT.*

2. Les récepteurs sérotoninergiques

La 5-HT est recaptée par le SERT suite à sa libération, d'où son rôle crucial dans l'homéostasie sérotoninergique car elle module la quantité de 5-HT qui va activer les R-5-HT. Ces derniers, par leur couplage à différentes voies de signalisation, vont moduler l'excitabilité des neurones sérotoninergiques, les propriétés pharmacologiques du SERT ou la libération de neuromodulateurs selon s'ils sont exprimés par des neurones sérotoninergiques (autorécepteurs) ou des neurones non sérotoninergiques (hétérorécepteurs). Ce sont donc des acteurs important de la transmission sérotoninergique. Le système sérotoninergique compte le plus grand nombre de sous-type de récepteurs (14 gènes différents). Dans ma thèse, j'ai particulièrement étudié le R-5-HT_{2B}. Ainsi, l'étude des phénotypes induits par la délétion génétique du R-5-HT_{2B} dans les neurones sérotoninergiques nous a permis de développer l'hypothèse selon laquelle le R-5-HT_{2B} pourrait agir tel un modulateur positif de l'activité des neurones sérotoninergiques, à l'inverse du R-5-HT_{1A} (Article 1). De plus, l'article 2 de la partie résultats porte sur l'interaction du R-5-HT_{2B} avec la protéine de pontage CIPP. Ces protéines forment un complexe capable de moduler la distribution des R-5-HT_{2B} et des récepteurs glutamatergiques NMDA (R-NMDA) suggérant un rôle dans la neurotransmission. Enfin, nous avons étudié l'impact fonctionnel de la dimérisation des R-5-HT_2 (Annexe1). C'est pourquoi, dans cette section, je décrirai principalement les récepteurs des familles 5-HT_1 et 5-$HT_{2A/2C}$, les autres familles de récepteurs 5-HT ne seront que brièvement abordées. Enfin, le récepteur 5-HT_{2B} fera l'objet du prochain chapitre.

La majorité des R-5-HT appartiennent à la famille des récepteurs couplés aux protéines G (RCPGs). Les RCPGs répondent à de nombreuses stimulations (odeurs, hormones, neuromodulateurs) et participent aux messages traduisant la perception de la lumière, du goût, du toucher ou de la douleur (pour revue Rosenbaum et al., 2009). Ils partagent tous une structure commune composée de sept domaines transmembranaires, un domaine extracellulaire et un domaine intracellulaire. La liaison de l'agoniste sur son récepteur active les protéines G qui sont composées de trois sous-unités (α, β, γ). Les sous-unités α et $\beta\gamma$ se séparent et agissent individuellement sur leurs effecteurs respectifs (ex. les cyclases, phospholipases ou canaux ioniques). Ce mécanisme de dissociation est souvent accompagné d'un mécanisme de désensibilisation du récepteur par l'action de kinases qui phosphorylent le RCPG le rendant inactif (Pour revue Drake et al., 2006). Ainsi, la stimulation des protéines G active différentes voies de signalisations. Il a également été montré que les protéines G agissent directement sur

le cytosquelette en stimulant la polymérisation / dépolymérisation des microtubules participant ainsi au trafic intracellulaire (Schappi et al., 2014).

Chez l'homme, les R-5-HT sont portés par quatorze gènes différents qui dérivent d'un même ancêtre commun (Barnes and Sharp, 1999). Les R-5-HT appartiennent à deux type de familles: les récepteurs/canaux ioniques 5-HT_3, ayant affinité pour la 5-HT ; et les récepteurs métabotropiques, qui ont une forte affinité pour la 5-HT mais dont l'action est plus lente. Ces derniers sont classés en trois familles selon leur couplage. Les R-5-HT_1 sont couplés à la protéine $G\alpha_i/G\alpha_o$; les R-5-HT_2 sont couplés à la protéine $G\alpha_q$; les R-5-$HT_{4/6/7}$ sont couplés à la protéine G_s et le R-5-HT_5 semble être couplé aux protéines $G\alpha_{i0}$ et $G\alpha_q$ **(Figure 6)** (pour revue Bockaert et al., 2006).

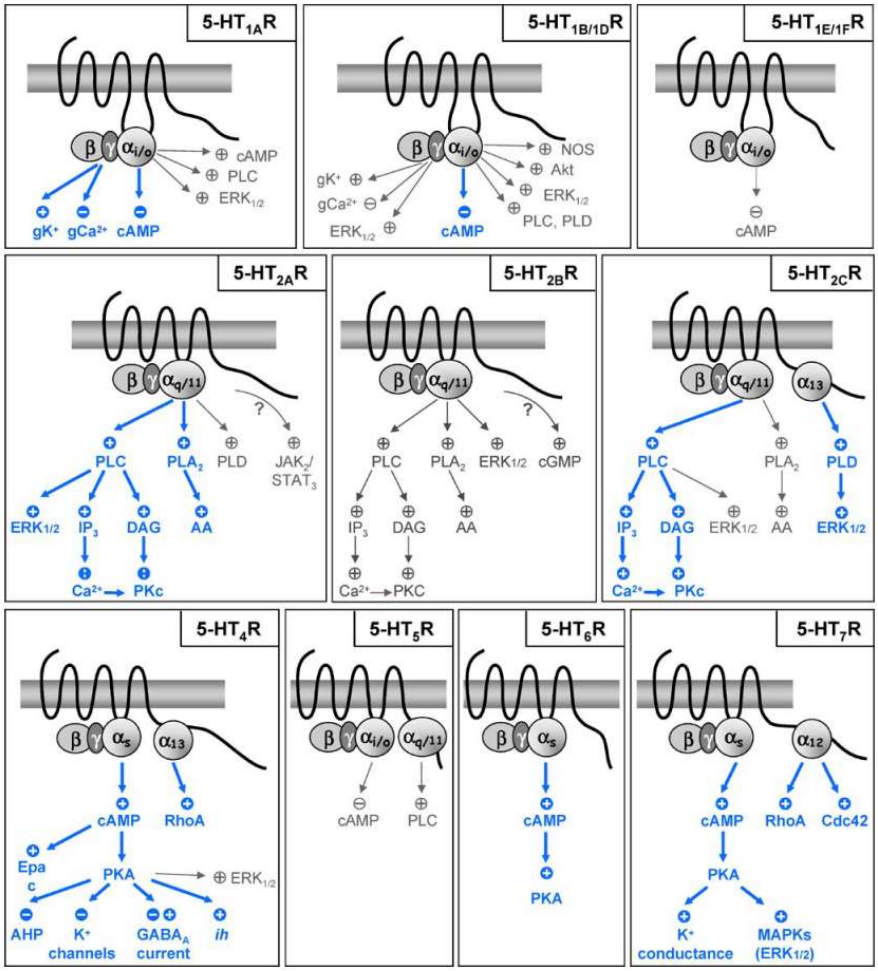

Figure 6 Voies de signalisation associées aux récepteurs sérotoninergiques *Les R-5-HT_1 sont couplés à la protéine $G\alpha_i/G\alpha_o$; les R-5-HT_2 à la protéine $G\alpha_q$; les R-5-$HT_{4/6/7}$ à la protéines G_s et le R-5-HT_5 semble être couplé aux protéines $G\alpha_{i0}$ et $G\alpha_q$ (Bockaert et al., 2006)*

i. Les R-5-HT$_{1A}$ et 5-HT$_{1B}$

Les R-5-HT$_{1A/B}$ sont considérés comme des autorécepteurs négatifs car ils sont exprimés par les neurones sérotoninergiques et diminuent leur activité via leur couplage aux voies $G_{\alpha i}/G_{\alpha o}/G_{\alpha 13}$. Les R-5-HT$_{1B}$ sont retrouvés dans les axones et les R-5-HT$_{1A}$ au niveau somatodendritique dans le DRN et le MRN (Sotelo et al., 1990; Riad et al., 2000).

Les hétérorécepteurs 5-HT$_{1A}$ sont retrouvés principalement au niveau dendritique dans les structures limbiques (septum latéral, gyrus denté, cortex frontal et enthorinal) et faiblement dans le cervelet, le noyau caudé / putamen et la substance noire (Hamon et al., 1990; Pompeiano et al., 1992; Burnet et al., 1995; de Almeida and Mengod, 2008). De façon surprenante, il a été montré que le couplage des R-5-HT$_{1A}$ à ces différentes protéines G varie en fonction des structures dans lesquelles il est exprimé. En effet, dans le CPF le R-5-HT$_{1A}$ est couplé autant à la protéine Gαo que Gα13; dans l'hippocampe, il est majoritairement couplé à la protéine Gαo; et seulement à la protéine Gα13 dans les noyaux antérieurs du raphé (Cour et al., 2006). L'activation des R-5-HT$_{1A}$ inhibe la voie de l'AC (Lanfumey and Hamon, 2000) et active, avec une plus faible efficacité, la PLC (Raymond et al., 2001) ainsi que l'ouverture des canaux potassiques de rectification entrante GIRK favorisant ainsi l'hyperpolarisation des neurones (Colino and Halliwell, 1987; Penington et al., 1992; Bayliss et al., 1997; Montalbano et al., 2015). Leur activation induit aussi la fermeture des canaux calciques de type T (Penington and Kelly, 1990; Penington et al., 1992). L'activation des R-5-HT$_{1A}$ module différemment la voie des MAPK ou ERK selon les tissus. En effet, dans l'hippocampe la stimulation du R-5-HT$_{1A}$ diminue la phosphorylation de ERK, ce qui n'est pas le cas dans le cortex (Chen et al., 2002; Sullivan et al., 2005) **(Figure 7)**. Enfin, la stimulation des R-5-HT$_{1A}$ diminue l'expression et la fonction des récepteurs glutamatergiques NMDA dans les dendrites en diminuant la polymérisation des microtubules (Yuen et al., 2005).

Les R-5-HT$_{1B}$ dont la structure a été cristallisée en 2013 (Wacker et al., 2013; Wang et al., 2013) sont exprimés au niveau des terminaisons synaptiques dans les neurones sérotoninergiques (Riad et al., 2000), dans les neurones dopaminergiques, glutamatergiques et GABAergiques où ils exercent leur action inhibitrice sur l'activité neuronale (Pazos and Palacios, 1985; Voigt et al., 1991; Riad et al., 2000). Ces récepteurs sont couplés aux protéines Gαi/Gαo induisant l'inhibition de l'adénylate cyclase (AC), l'ouverture des canaux GIRK, la fermeture des canaux calcique de type T/L et ainsi l'activité des neurones (Ghavami et al., 1997; Le Grand et al., 1998; Lin et al., 2002) **(Figure 7)**.

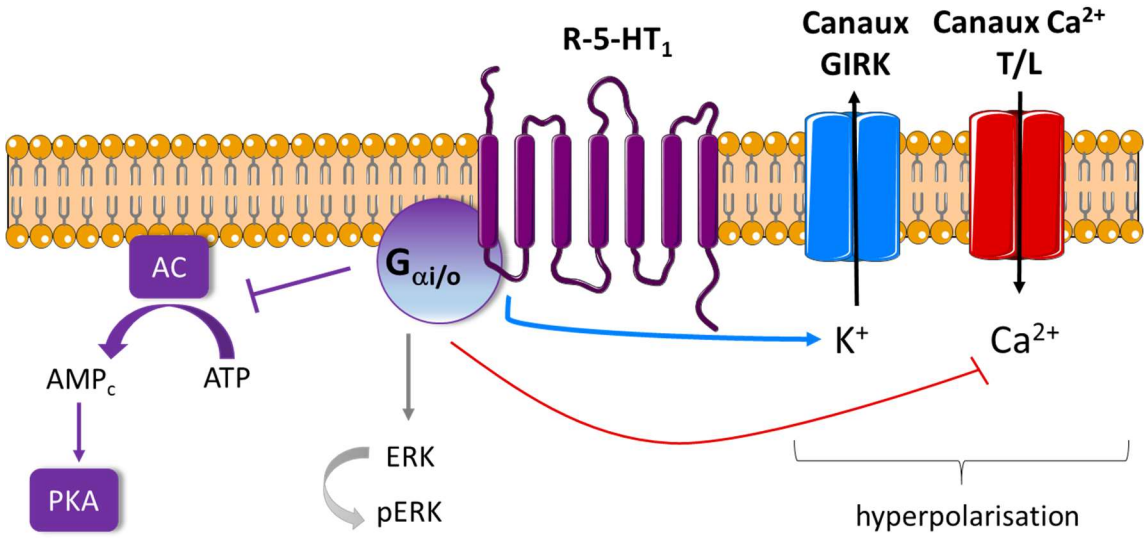

Figure 7 Voies de signalisation des récepteurs 5-HT$_1$. *Les R-5-HT$_1$ sont couplés négativement à la voie AC / PKA / AMP$_c$ par l'intermédiaire des protéines G$_{αi/o}$. Leur activation diminue la libération de neuromodulateurs par les neurones en augmentant les courants sortants potassiques$^+$ et en diminuant les courants entrants calciques$^+$. La stimulation du R-5-HT$_{1A}$ régule également la phosphorylation de ERK.*

ii. Les R-5-HT$_{2A/2C}$

Les gènes codant pour les différents types de R-5-HT$_2$ sont relativement similaires bien que le *HTR2C* (R-5-HT$_{2C}$) possède un intron supplémentaire et subit une édition de son mRNA. Les épissages alternatifs des transcrits codant pour les R-5-HT$_2$ ne semblent pas produire d'isoformes fonctionnels de ces récepteurs (pour revue Wirth et al., 2016). Les R-5-HT$_2$ partagent 46 à 50% d'homologie de séquence et sont couplés à la protéine G$_{αq/11}$. Leur stimulation active la voie de la PLC, induisant l'hydrolyse du phosphatidylinositol (PIP$_2$) en inositol triphosphate (IP$_3$) et diacylglycérol (DAG) (Conn and Sanders-Bush, 1984). L'IP$_3$ sert de second messager pour induire la libération des stocks intracellulaires de calcium tandis que le DAG va activer la PKC. Les R-5-HT$_2$ activent également la voie de la phospholipase A2 (PLA2) provoquant la libération d'acide arachidonique par son couplage à la protéine G$_{α1/13}$. La voie des MAP kinase ERK1/2 peut aussi être activée par la stimulation des R-5-HT$_2$ (Kurrasch-Orbaugh et al., 2003). Enfin la stimulation des R-5-HT$_{2A}$ active l'ouverture des canaux calciques voltage dépendant Cav1.2 et la stimulation des R-5-HT$_{2C}$ provoque la fermeture des canaux GIRK ou Kv (Day et al., 2002; Speake et al., 2004; Blomeley and Bracci, 2009) **(Figure 8)**.

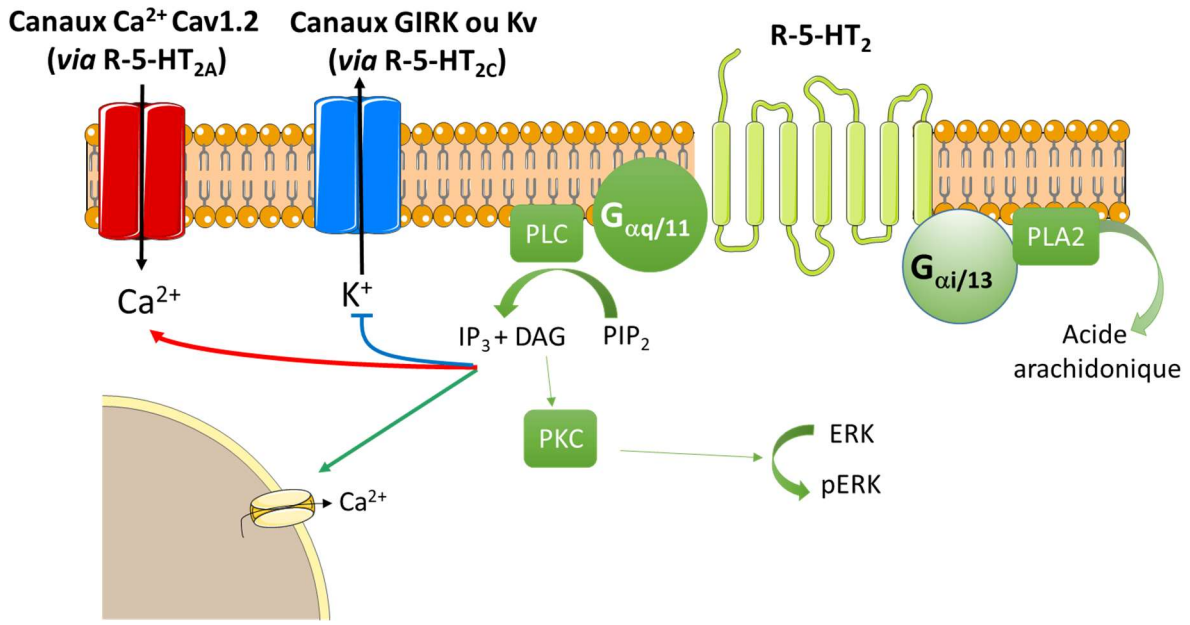

Figure 8 Voies de signalisation des récepteurs 5-HT₂. *La stimulation des R-5-HT₂ induit plusieurs voies de signalisation (PLC / DAG / PKC / Ca^{2+}) via la protéine $G_{\alpha q}$. Les R-5-HT₂ induisent aussi la phosphorylation de la kinase ERK.*

Les R-5-HT$_{2A}$ et 5-HT$_{2C}$ partagent de nombreuses propriétés et sont tous deux liés avec la protéine PSD-95 qui module leur maintien au niveau des épines dendritiques (Xia et al., 2003a, 2003b). L'association de PSD-95 avec le R-5-HT$_{2A}$ favorise son maintien à la membrane tandis que l'association avec le R-5-HT$_{2C}$ promeut son internalisation. Le maintien des R-5-HT$_{2C}$ se fait par le biais de la protéine de pontage MPP3 (Gavarini et al., 2006; Jones et al., 2009).

Les R-5-HT$_{2A}$ sont fortement exprimés au niveau cortical (néocortex, cortex enthorinal et piriforme), tubercule olfactif, le gyrus denté, et la corne ventrale de la moelle épinière (Pazos et al., 1985; Pompeiano et al., 1994; López-Giménez et al., 1997). Les R-5-HT$_{2A}$ sont exprimés au niveau somatodendritique dans de nombreuses structures limbiques et corticales dans les neurones GABAergiques et glutamatergiques (De Almeida and Mengod, 2007; Weber and Andrade, 2010).

Les R-5-HT$_{2A}$ sont associés aux protéines de type calmodulines dépendantes du calcium (CaM) via leur extrémité C-terminale dont le site de liaison est superposé au site de phosphorylation de la PKC permettant ainsi une régulation fine. En effet, la phosphorylation de l'extrémité C-terminale des R-5-HT$_{2A}$ favorise son internalisation; tandis que la liaison de la calmoduline

empêche cette phosphorylation et permet ainsi son maintien à la membrane (Turner and Raymond, 2005). Les R-5-HT_{2A} sont retrouvés dans des radeaux lipidiques complexes contenant entre autres des cavéoline1 ce qui faciliterait l'interaction du récepteur avec la protéine Gαq (Bhatnagar et al., 2004).

Le R-5-HT_{2C} est fortement exprimé dans le plexus choroïde , où il joue un rôle dans la régulation de la production de fluide cérébro-médullaire (Sanders-Bush and Breeding, 1988). Des niveaux plus faibles de R-5-HT_{2C} sont observés dans les zones corticales (noyau olfactif, cortex piriforme, cortex cingulaire), le système limbique (Nac, hippocampe et amygdale), les ganglions de la base (noyau caudé et substance noire) et plusieurs noyaux du tronc cérébral ainsi que dans la moelle épinière (López-Giménez et al., 1997; Pompeiano et al., 1994).

L'ARN messager des R-5-HT_{2C} est sujet à des éditions « *editing* » engendrant la substitution de certains nucléotides (C en U ou A en I) changeant ainsi certains acides aminés. Cet effet peut affecter la structure de la protéine et sa fonction (Gurevich et al., 2002; Kawahara et al., 2008). Concernant l'ARN messager des R-5-HT_{2C}, ce sont des substitutions de type A/I qui ont été observées. Cette édition induit la formation de 24 isoformes différents chez la souris (Fitzgerald et al., 1999; Kawahara et al., 2008), influençant les propriétés du récepteur, notamment sa cinétique d'internalisation et son activité intrinsèque (Porter et al., 2001). Ce processus est tissu-dépendant, c'est pour cela que l'on ne retrouve que 7 isoformes dans le cerveau chez le rat et 23 chez l'homme. Pour certains isoformes du R-5-HT_{2C}, les récepteurs sont directement liés à la β-arrestine, induisant son internalisation (Marion et al., 2004). Au vu des phénotypes des souris invalidées pour le gène codant 5-HT_{2C}, il semble que ce récepteur soit impliqué dans la prise alimentaire, la régulation de l'humeur et de l'anxiété et dans la récompense.

iii. Les autres R-5-HT

Le R-5-HT_3 est le seul sous type des R-5-HT étant un canal ionique, il est perméable au sodium, potassium et au calcium et est composé de quatre domaines transmembranaires et une extrémité N-terminale extracellulaire. Ce récepteur est localisé dans les terminaisons axonales, les corps cellulaires et les épines dendritique où il participe aux réponses excitatrice rapides ainsi que dans les interneurones (Emerit et al., 2016; Yakel and Jackson, 1988). Il a été montré que le R-5-HT_3 est exprimé dans le système limbique, l'hippocampe, l'amygdale et au niveau cortical (pour revue Lummis, 2012). La stimulation des R-5-HT_3 permet l'activation de la nNOS, provoquant des courants chlore sortants, dépendants du GMP cyclique. La stimulation

des R-5-HT_3 induit la libération de glutamate dans la médulla oblongata (cerveau médian) (Ashworth-Preece et al., 1995). De même, les R-5-HT_3 sont exprimés par les interneurones de l'amygdale basolatérale (BLA) où ils facilitent la libération de GABA par ces neurones (Koyama et al., 2002), suggérant un rôle pro-nociceptif (Suzuki et al., 2004).

Les R-5-HT_4 sont majoritairement exprimés dans le système limbique (amygdale, Nac et hypothalamus) et dans l'hippocampe (pour revue Bockaert and Dumuis, 1998; Bockaert et al., 2004). Leur couplage aux protéines G stimule l'activité de l'AC et donc la production d'AMPc. Ce couplage stimule l'ouverture de canaux calciques et la fermeture de canaux potassiques, contribuant ainsi à l'excitabilité des neurones (Lucas and Debonnel, 2002).

Peu de choses sont connues à propos des **R-5-HT_5**, ils semblent être exprimés dans les neurones et les astrocytes (Nelson, 2004). Les R-5-HT_5 modulent les concentrations calciques via les récepteurs ryanodine et leur activation induit l'ouverture des canaux potassiques de rectification entrante GIRK. Les R-5-HT_5 sont exprimés dans les neurones du cortex, l'hippocampe, du cervelet et l'habénula (Matthes et al., 1993). Enfin, ces récepteurs joueraient un rôle dans les processus circadiens de veille/éveil (pour revue Thomas, 2006).

Les R-5-HT_6 sont exprimés dans différentes structures limbiques et corticales dans le soma ou les terminaisons axonales (Ruat et al., 1993; Gérard et al., 1996). Ils sont associés à de nombreuses voies de signalisation telle que la voie de l'AC, la voie Fyn qui régule les canaux potassique, la voie ERK1/2, la voie Jun et la voie mTOR impliquées dans le développement neuronal (Marcos et al., 2010) . Ce récepteur module la libération de plusieurs neuromédiateurs et participent à de nombreux processus physiologiques qui, en cas de dérégulation, peuvent être associés à certaines pathologies dégénératives et/ou psychiatriques comme Alzheimer par exemple. Les agonistes/antagonistes des R-5-HT_6 les ont récemment proposés comme cibles thérapeutiques et les résultats semblent être très prometteurs dans des études précliniques (pour revue Karila et al., 2015).

Les R-5-HT_7 sont localisés au niveau somatique et extrasynaptique, majoritairement dans des interneurones GABAergiques, dans des structures telles que l'hypothalamus, le thalamus, le cortex et l'hippocampe. Ces récepteurs jouent un rôle dans la plasticité synaptique en modifiant la morphologie des épines dendritiques via leur couplage à la protéine Gαs, activant les voies ERK et Ras-MEK (Norum et al., 2003, 2005; Kvachnina et al., 2005).

iv. Oligomérisation

Les RCPGs forment des oligomères par l'association de deux ou plusieurs récepteurs, que l'on appelle protomères et l'association de deux protomères forme un dimère ; lorsque les récepteurs sont de différents types on parle alors d'hétérodimères et d'homodimères quand ils sont identiques. Ces dimérisations affectent la signalisation du ou des récepteurs impliqués (pour revue Borroto-Escuela et al., 2017). La moitié des R-5-HT forment des homodimères et/ou des hétérodimères avec d'autres R-5-HT ou d'autres systèmes de neurotransmission. Ces mécanismes semblent donc importants dans la régulation de la transmission sérotoninergique par la modulation des propriétés des R-5-HT (pour revue Herrick-Davis, 2013). La dimérisation des R-5-HT_2 a fait l'objet d'un article publié en Mars 2017 dans *The Journal of Biological Chemistry* présenté en Annexe 1.

Homodimères

La formation d'homodimères des R-5-HT a d'abord été mise en évidence pour les R-5-HT_{1B} et 5-HT_{1D} *in vitro* (Halazy et al., 1996; Xie et al., 1999). Par la suite plusieurs études ont montré que les R-5-$HT_{1A/1B/2A/2B/2C/4/7}$ forment des homodimères fonctionnels (Xie et al., 1999; Salim et al., 2002; Herrick-Davis et al., 2004; Berthouze et al., 2005; Kobe et al., 2008; Mancia et al., 2008; Brea et al., 2009; Woehler et al., 2009; Teitler et al., 2010; Paila et al., 2011; Pellissier et al., 2011; Moutkine et al., 2017). Ce processus a été démontré comme étant physiologique et faisant partie du processus de maturation dans le réticulum endoplasmique **(Figure 9)**.

Hétérodimères

Les **R-5-HT_{1A}** forment des hétérodimères avec les récepteurs μ-opioïdes (Cussac et al., 2012), les récepteurs de l'adénosine A2A (Łukasiewicz et al., 2007), les récepteurs $GABA_B$ (Salim et al., 2002). Les R-5-HT_{1A} forment aussi des oligomères avec les isorécepteurs de la Galanine 1 et 2, induisant des régulations allostériques de chacun des protomères et affectant par conséquent les voies de signalisation associées (Fuxe et al., 2012a) **(Figure 9)**.

Les **R-5-HT_{1B}** et les **R-5-HT_{1D}** sont aussi capable de se dimériser *in vitro* (Xie et al., 1999) et cette association augmenterait l'affinité des récepteurs 5-HT_{1D} pour la 5-HT (Halazy et al., 1996) **(Figure 9)**.

Les **R-5-HT$_{1A}$** et les **R-5-HT$_7$** sont capables de former des hétérodimères *in vivo* et *in vitro*. Les hétérodimères des R-5-HT$_{1A}$ et R5-HT$_7$ régulent l'activité des canaux GIRK dans des lignées cellulaires et dans les neurones de l'hippocampe (Renner et al., 2012). L'hétérodimerisation diminue le couplage des R-5-HT$_{1A}$ avec la protéine Gαi et diminue l'activité des GIRK, indiquant un rôle inhibiteur du protomère 5-HT$_7$ (Renner et al., 2012) **(Figure 9)**.

Les **R-5-HT$_{2A}$** et les récepteurs métabotropiques glutamatergiques mGlur2 forment des hétérodimères (González-Maeso et al., 2008; Moreno et al., 2011). Cette dimérisation est absente chez les animaux dépourvus de mGlur2 et on constate une suppression des effets psychoactifs du DOI qui sont dépendants du R-5-HT$_{2A}$ (Moreno et al., 2012). La dimérisation des R-5-HT$_{2A}$ avec le récepteur mGlur2 entraine une augmentation du nombre de sites de liaison des R-5-HT$_{2A}$ et une diminution des sites de mGlur2, bien que leur expression totale ne soit pas affectée. Ce qui signifie que les dimères sont exprimés en surface mais que les R-5-HT$_{2A}$ sont plus disponibles ou « stimulables » que ceux des mGlur2 ce qui favorise la signalisation des R-5-HT$_{2A}$ au détriment des mGlur2 (Baki et al., 2016). Les R-5-HT$_{2A}$ forment aussi des dimères avec les récepteurs dopaminergiques D2 (Albizu et al., 2011; Łukasiewicz et al., 2011). Cette dimérisation est cruciale car elle augmente l'affinité des R-5-HT$_{2A}$ pour le DOI et diminue le couplage du R-5-HT$_{2A}$ pour la voie de la PLC probablement par des modulations allostériques (Albizu et al., 2011) **(Figure 9)**.

Certains isoformes des **R-5-HT$_{2C}$** sont capables de se dimériser avec les récepteurs de la ghréline GHS-R1a. Ces deux RCPGs participent individuellement à la régulation de la prise alimentaire. Cette dimérisation diminue l'expression membranaire du GHS-R1a et donc les voies de signalisation qui lui sont associées, proposant ainsi une nouvelle forme de régulation des récepteurs de la ghréline dans ce processus (Schellekens et al., 2013) **(Figure 9)**.

Les sous-types de **R-5-HT$_2$** forment des homodimères (5-HT$_{2A/2A}$, 5-HT$_{2B/2C,}$ mais pas 5-HT$_{2B/2B}$) et des hétérodimères (5-HT$_{2A/2B}$, 5-HT$_{2A/2c}$, 5-HT$_{2B/2C}$) fonctionnels. La présence du protomère 5-HT$_{2C}$ masque le site de liaison des R-5-HT$_{2A}$ ou des R-5-HT$_{2B}$. Au niveau fonctionnel cette dimérisation va promouvoir la signalisation du R-5-HT$_{2C}$ au détriment de celle des R-5-HT$_{2A}$ ou des R-5-HT$_{2B}$ *in vitro* et *in vivo*. Ceci ouvre de nouvelles perspectives dans la compréhension du fonctionnement des R-5-HT$_2$ notamment dans les structures exprimant un ou plusieurs sous-types de R-5-HT$_2$ (Moutkine et al., 2017) (Annexe 1) **(Figure 9)**.

Les R-5-HT$_4$ forment des hétérodimères avec les récepteurs β2-adrénergiques, cependant l'impact fonctionnel reste encore à être étudié (Berthouze et al., 2005).

	Homodimères	*Hétérodimères*
R-5-HT$_{1A}$	✓	R-5-HT$_7$ (↘ couplage G$_{a1}$ du R-5-HT$_{1A}$ et ↘activité GIRK) R-5-HT$_{1D}$ (↗ affinité du R-5-HT$_{1D}$ pour la 5-HT) R-A2A, R-GABA$_B$, R-Galanine 1/2
R-5-HT$_{1B}$	✓	
R-5-HT$_{2A}$	✓	mGlur2 (↗nombre de site de liaison R-5-HT$_{2A}$ et affinité du DOI) (↘ nombre de site de liaison mGlur2) R-5-HT$_{2C}$ (perte de la signalisation dépendante des R-5-HT$_{2A}$) (le protomère 5-HT$_{2C}$ masque les sites de liaison des R-5-HT$_{2AB}$)
R-5-HT$_{2B}$	X	R-5-HT$_{2C}$ (perte de la signalisation dépendante des R-5-HT$_{2B}$) (le protomère 5-HT$_{2C}$ masque les sites de liaison des R-5-HT$_{2B}$)
R-5-HT$_{2C}$	✓	GHS-R1a (↘expression et signalisation de GHS-R1a)
R-5-HT$_4$	✓	R-β-2 adrénergique
R-5-HT$_7$	✓	R-5-HT$_{1A}$ (↘ couplage G$_{a1}$ du R-5-HT$_{1A}$ et↘ activité GIRK)

Figure 9 Impact de l'oligomérisation des R-5-HT

Pour conclure, les mécanismes d'hétérodimerisation produisent différents types de modulations. En effet, cela provoque des changements de l'affinité à certains ligands, des modifications du trafic intracellulaire et/ou de l'expression membranaire aboutissant à des modulations des voies de signalisation des différents récepteurs. D'autres mécanismes interviennent et modulent ces paramètres. En effet, les protéines de pontages jouent un rôle crucial dans la distribution et la fonction des R-5-HT dans la transmission sérotoninergique.

C. Protéines associées aux récepteurs sérotoninergiques

1. Protéines PDZ

Les protéines de pontage modulent les clusters de récepteurs aux neuromédiateurs, les voies de signalisation, le trafic des récepteurs/canaux membranaires ou encore agissent directement sur le cytosquelette, ce qui impacte la morphologie des épines dendritiques. Beaucoup des protéines de pontage interagissent grâce à leurs domaines PDZ. Ce terme provient des trois premières protéines découvertes possédant ces domaines : **P**SD-95, « ***D****iscs Large* », et « ***Z****ona Occludens 1 proteins* ». Ces domaines peuvent être multiples, ce qui leur permet des interactions variées et constituent le ciment des complexes protéiques et leur localisation en micro domaines dans la synapse. Au niveau sémantique, les protéines de pontages portent des domaines PDZ tandis que les protéines se liant à celles-ci portent des sites liaison aux domaines PDZ.

Il existe environ 400 types de protéines liant les domaines PDZ, et en général les sites de liaisons aux domaines PDZ se situent au niveau de l'extrémité C-terminale de la protéine cible. Dans les neurones, les protéines retrouvées dans la densité post-synaptique (PSD) sont riches en domaines PDZ, ce qui permet la formation de microdomaines fonctionnels finement régulés impliqués dans la transmission synaptique ainsi que dans sa régulation (Good et al., 2011). Les protéines à domaines PDZ jouent des rôles très variés notamment dans la régulation des voies de signalisation et du trafic intracellulaire (pour revue : Dunn and Ferguson, 2015).

Les domaines PDZ ont des structures similaires, bien que leur homologie de séquence ne soit que de 30%. Ces domaines sont composés de six brins β antiparallèles et deux hélices α, la liaison peptidique se situant au niveau du brin β et l'hélice α (Cabral et al., 1996). Les extrémités N- et C-terminale des domaines PDZ sont situées à proximité l'une de l'autre en face de la liaison peptidique permettant la régulation des interactions protéiques (Cabral et al., 1996) (**Figure 10**).

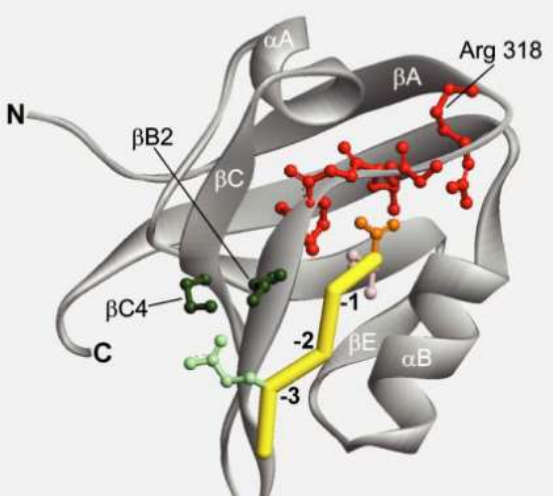

Figure 10 Structure du domaine PDZ3 de la protéine PSD-95 (en gris) lié à un site de liaison au domaine PDZ d'une extrémité C-terminale (en jaune). *Extrémité N- et C- terminal de PSD-95 sur la gauche. En gris, les 6 brins β (βA–βB2–βC–βC4-βE ; βD non visible sous cet angle) et les deux hélices α (αA en haut et αB en bas). En rouge le motif conservé de l'extrémité C-terminale (Arg-318 et Gly-Leu-Gly-Phe), en orange la partie libre (R/K–XXX-) (Sheng and Sala, 2001)*

Les domaines PDZ reconnaissent des motifs spécifiques au niveau de l'extrémité C-terminale de la protéine cible ; ces motifs sont fortement conservés entre les différentes protéines et sont composés de motifs Glycine-Leucine-Glycine-Phénylalanine (GLGF). La composition des domaines PDZ est constante, R/K-XXX-GLFG (**Figure 10**). 1) Le deuxième et quatrième résidu du motif GLFG sont toujours hydrophobes, 2) la deuxième glycine est toujours conservée et 3) la première glycine peut parfois être remplacée par une sérine, une thréonine ou une proline. L'intérêt des deux résidus hydrophobes dans ce motif est la création d'une « poche » au sein du domaine PDZ. Ainsi, c'est la nature du premier résidu et des résidus hydrophobes qui permet de sélectionner l'interaction protéique et donc de donner sa spécificité au domaine PDZ (Doyle et al., 1996).

Dans la majorité des cas le deuxième résidu est un résidu phosphorylable (tyrosine, thréonine ou sérine) permettant ainsi la régulation de l'interaction protéique. La phosphorylation de ce résidu peut affecter l'affinité des protéines entre elles et donc leur capacité de maintenir cette interaction. La phosphorylation des différents domaines PDZ est réalisée par des kinases spécifiques, étant elles même activées ou inhibées par les voies de signalisation dépendantes de l'activité synaptique (pour revue Sheng and Sala, 2001).

Par exemple, l'interaction entre le canal potassique Kir2.3 et la PKA est abolie lorsque la sérine en position 2 du motif de Kir2.3 est phosphorylée (Cohen et al., 1996).

Ces protéines à domaines PDZ peuvent être modulées de façon allostérique selon la distribution spatiale des acides aminés (Reynolds et al., 2011). L'extrémité C-terminale des protéines peut se « replier », modifiant ainsi la conformation spatiale et induisant son auto-inactivation. Enfin elles peuvent avoir des propriétés différentes par épissage alternatif, les isoformes d'une même protéine pouvant contenir plus ou moins de domaines PDZ (Sierralta and Mendoza, 2004).

2. Protéines PDZ associées aux R-5-HT

Les R-5-$HT_{2/4/7}$ interagissent avec des protéines PDZ via le motif de liaison aux domaines PDZ situés sur leur extrémité C-terminale (pour revue Marin et al., 2012). La protéine MUPP1 fut la première protéine PDZ identifiée pour son interaction avec les R-5-HT_{2C} dont l'association est modulée par la phosphorylation du deuxième résidu conservé du motif de liaison PDZ (Ullmer et al., 1998) **(Figure 11)**. L'association de MUPP1 avec les récepteurs 5-$HT_{2A/2B/2C}$ a été confirmée (Bécamel et al., 2001).

Les R-5-$HT_{2A/C}$ sont associés à la protéine PSD-95, qui potentialise leurs voies de signalisation en diminuant leur internalisation (Bécamel et al., 2002; Xia et al., 2003a, 2003b). Cependant, les sous-types de R-5-HT_2 semblent s'associer à des partenaires bien spécifiques (Bécamel et al., 2004; Gavarini et al., 2004): le R-5-HT_{2A} est plutôt associés aux protéines PDZ post-synaptiques tandis que les R-5-HT_{2C} peuvent aussi s'associer à des protéines présynaptiques telles que Veli3/CASK/Mint1 (Bécamel et al., 2004; Gavarini et al., 2006). Finalement, les R-5-HT_4 sont associés aux protéines MPP3, veli-3, NHERF-1, CIPP, nNOS, SNX-27 (Joubert et al., 2004) **(Figure 11)**.

Les R-5-HT_{2B} sont associées aux protéines PDZ nNOS, α-syntrophine, « channel interacting PDZ protein » (CIPP), la protéine associée aux synapses de 102 kDa (SAP-102), le transporteur ioniques NHERF **(Figure 11)**. Seules les interactions entre le R-5-HT_{2B}/NOS (Manivet et al., 2000; Launay et al., 2006), 5-HT_{2B}/SAP-102 (non publiées) et 5-HT_{2B}/CIPP (non publiées) ont été étudiées. Au cours de ma thèse, j'ai commencé à étudier l'interaction 5-HT_{2B}/SAP-102 qui sera détaillée dans le chapitre suivant puis j'ai approfondi par l'étude de l'interaction 5-HT_{2B}/CIPP qui se trouve dans la partie résultat de ce manuscrit (Article 2).

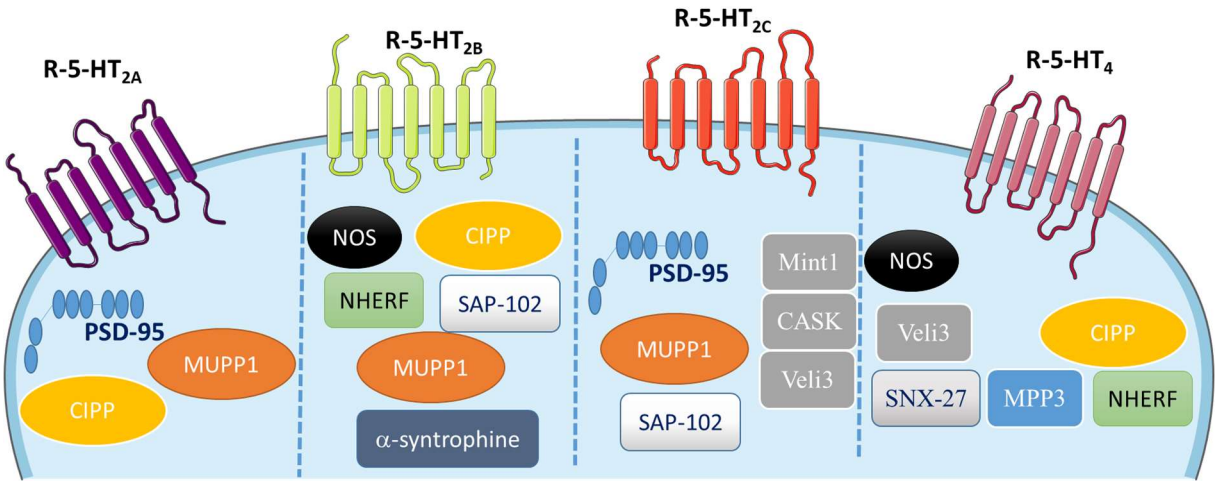

Figure 11 Protéines PDZ associées aux R-5-HT$_{2A/2B/2C/4}$

3. Autres protéines (GRK-b-arrestine, canaux ioniques, Yif, CAM)

Les R-5-HT$_{1A}$ et R-5-HT$_{1B}$ étant dépourvu de domaines de liaison aux protéines PDZ, d'autres molécules associées à leur expression membranaire ont été identifiées.

Les R-5-HT$_{1A}$ sont également associés à la protéine Yif1B, cette interaction est essentielle à l'adressage du R-5HT$_{1A}$ vers les dendrites distales des neurones (Carrel et al., 2008). Yif1B recrute d'autres protéines du trafic intracellulaire dans les vésicules cargos transportant les R-5-HT$_{1A}$ (Awabdh et al., 2012; Darmon et al., 2015). De plus, dans les neurones d'hippocampe en culture, Yif1B joue un rôle plus général dans le trafic intracellulaire, plus précisément entre le réticulum endoplasmique et l'appareil de Golgi (Alterio et al., 2015).

Les R-5-HT$_{1B/4}$ se lient à la protéine p11, une protéine de pontage associée à de nombreux canaux ioniques (TRPV, TASK1, Nav1.8). La protéine p11 augmente l'expression membranaire des R-5-HT$_{1B}$ mais également des R-5HT$_4$ en culture cellulaire potentialisant ainsi leurs voies de signalisation. De plus, les animaux invalidés pour le gène codant pour p11 présentent des comportements de type dépressif, probablement suite à une altération de la distribution des R-5-HT$_{1B/4}$ (Svenningsson et al., 2006; Svenningsson and Greengard, 2007; Warner-Schmidt et al., 2009).

Une interaction avec la CaM a été établie pour les R-5-HT$_{1A/2A/2C}$ (Della Rocca et al., 1999; Bécamel et al., 2002; Turner et al., 2004a; Labasque et al., 2008). Les sites de liaison à la CaM des R-5-HT sont superposés aux sites de phosphorylations de la PKC, suggérant une modulation des récepteurs par ces deux protéines. La liaison de la CaM et la phosphorylation des récepteurs par la PKC auraient des effets opposés sur les R-5-HT$_{2A}$ en diminuant ou potentialisant respectivement son association aux protéines G (Turner and Raymond, 2005).

4. CIPP

CIPP (« *channel interacting PDZ protein* ») a été identifié pour la première fois en 1998 par Kurshner *et al.* (Kurschner et al., 1998). Cette équipe a effectué un échantillonnage aléatoire à l'aide d'un peptide artificiel portant la séquence du site de liaison aux domaines PDZ « V-S-D-L » présent sur l'extrémité C-terminale d'un certain nombre de protéines. Cette technique a permis d'isoler, à partir d'une bibliothèque d'ADN complémentaire de cerveaux souris, les protéines capables de s'associer à ce motif (Kurschner and Morgan, 1995). Ainsi CIPP, une protéine de 612 acides aminés contenant quatre domaines PDZ, a été identifiée. Les quatre domaines PDZ de CIPP présentent une homologie de séquence avec les domaines PDZ de la protéine PSD-95: le domaine PDZ1 de CIPP présente 38% d'homologie avec le PDZ1 de PSD-95 et il y a 47, 49, et 36% d'homologie entre CIPP-PDZ2, CIPP-PDZ3 et CIPP-PDZ4 avec PSD-95-PDZ2, respectivement (Joo and Pei, 2008).

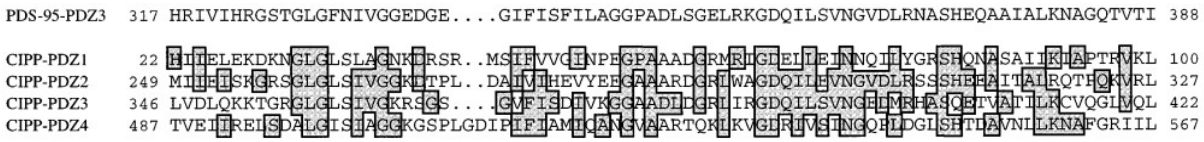

Figure 12 Homologies de séquence entre les PDZ de CIPP et le PDZ3 de PSD-95 *(Kurschner et al., 1998)*

Deux transcrits différents ont été identifiés par « *Northern Blot* » : un premier long de 8000 nucléotides présent dans les reins et un second court de 3760 paires de bases présent dans le cerveau (Kurschner et al., 1998). La forme longue de CIPP en périphérie est aussi appelée PATJ pour *« PALS1-associated tight junction* protein », composée de dix domaines PDZ (1835 acides aminés) et exprimée aussi dans le rein. Cette protéine est localisée au niveau des jonctions serrées et des jonctions adhérentes et joue un rôle important dans la polarité des cellules rénales (en collaboration avec MUPP1, un partenaire des R-5-HT$_{2A/2C}$) (Pieczynski and Margolis, 2011). Le gène codant PATJ et CIPP possède différents noms : INADL

(« *inactivation-no afterpotential D-like* »), PATJ « *protein associated with tight junction protein* » et CIPP, et génère différents isoformes de la même protéine contenant un nombre différent de domaines PDZ (Alpi et al., 2009).

Kurschner et collaborateurs ont montré par hybridation *in situ* que CIPP est exprimée fortement dans de nombreuses structures cérébrales telles que le cervelet (**cb**), les colliculus inférieurs (**ic**), les noyaux vestibulaires (**vn**), les noyaux facials (**VII**) et le thalamus (**thal**), la zone de transition dorsale (**DTr**), le tronc cérébral ainsi que les bulbes olfactifs (**ob**). En revanche, aucun des transcrits de CIPP n'a été retrouvé dans le cortex (**Ctx**) et l'hippocampe (**hc**) (Kurschner et al., 1998) **(Figure 13)**. Récemment, il a été montré que les ARN messagers du R-5-HT_{2B} et de CIPP sont exprimés dans les mêmes neurones sérotoninergiques. Cependant, il est important de préciser que les taux d'expressions sont très faibles et que l'expression protéique reste à quantifier (Okaty et al., 2015).

Ainsi, l'objectif de l'article 2 a été d'étudier la distribution du R-5-HT_{2B} transfecté ou non avec CIPP dans des lignées cellulaires et des cultures primaires de neurones d'hippocampe qui n'expriment pas CIPP de façon endogène (Kurschner et al., 1998) **(Figure 13)**.

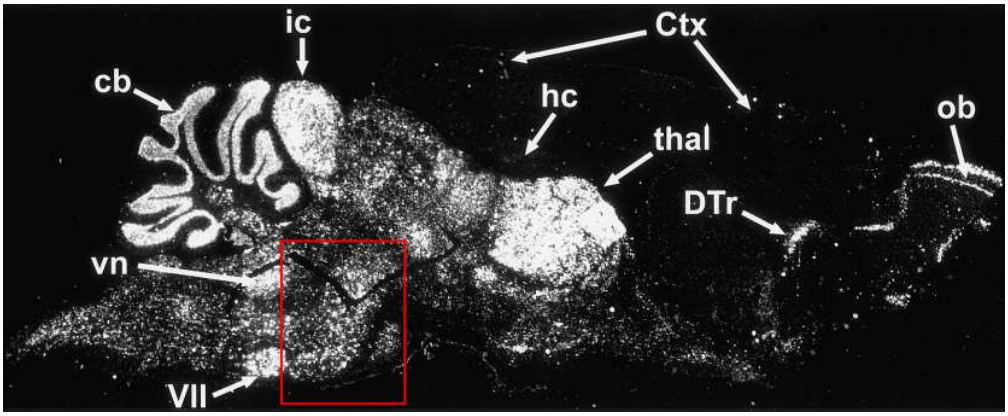

Figure 13 Distribution de l'ARN messager de CIPP dans le cerveau *(Kurschner et al., 1998)*

Un interaction entre CIPP et les sous-unités NR2A/B/C/D des récepteurs NMDA ainsi qu'avec les canaux potassiques de rectification entrante Kir4.1 et 4.2 et les protéines neurexine et neuroligine a été démontrée par double-hybride chez la levure et précipitation par la GST (Kurschner et al., 1998) **(Figure 14)**. La co-expression de CIPP avec les canaux Kir4.1 ou 4.2, dans la lignée cellulaire Cos-7, induit une augmentation des courants potassiques. Cependant, le canal Kir 4.2 n'est pas exprimé dans le cerveau, cette interaction a probablement lieu dans

les reins avec la protéine PATJ. Contrairement à Kir 4.1 qui est exprimé dans le cerveau et le rein, et est fortement exprimé dans les mêmes structures cérébrales que CIPP.

CIPP interagit aussi avec la protéine IRSp53 (« *insulin receptor tyrosine kinase substrate protein p53* »), un effecteur des petites protéines G Rac1 et cdc42 (Alpi et al., 2009) . Il a été montré que IRSp53 interagit avec PSD-95 et que cette liaison augmente la densité des épines dendritiques des cultures de neurones d'hippocampe (Choi et al., 2005). Lorsque CIPP et IRSp53 sont co-exprimés, dans des cellules Cos-7, on observe l'apparition de protrusions apicales (ou *puncta*) qui ne sont pas des vésicules mais de complexes protéiques dans lesquels on retrouve ces deux protéines (Alpi et al., 2009). Cet effet a été reproduit dans d'autres lignées cellulaires telles que les cellules HEK-293T, HeLa et dans la lignée cellulaire HN9.10e (dérivées de neuroblastomes de rats). Les auteurs ont aussi montré que CIPP interagit avec la protéine Cypine, dont le rôle est de participer à l'assemblage des microtubules (Akum et al., 2004; Alpi et al., 2009). Cypine s'associe à CIPP via son domaine PDZ1, cependant lorsque la protéine IRSp53 est exprimée la protéine Cypine interagit avec le domaine PDZ2 de CIPP (Barilari and Dente, 2010). Dans des cellules exprimant CIPP/Cypine/IRSp53, CIPP co-immunoprécipite Cypine et IRSp53 indiquant qu'elles forment un complexe tripartite **(Figure 14)**. Dans la lignée neuronale utilisée (HN9.10^{e}) la privation de sérum induit la formation de neurites. Lorsque le complexe CIPP/IRSp53/Cypine est exprimé et que les cellules sont privées de sérum, le complexe protéique est localisé dans ces neurites (Barilari and Dente, 2010).

En résumé, ces observations sont intéressantes car la neuroligine est une protéine d'adhésion associée à PSD-95 (Hata et al., 1996; Irie et al., 1997) **(Figure 14)**; mais aussi à la protéine neurexine avec qui elle forme un complexe transynaptique permettant la différentiation et le maintien des éléments pré et post-synaptiques (Dean et al., 2003; Chih et al., 2005). Les protéines IRSp53 et Cypine participent à la signalisation et la morphologie des neurones (Akum et al., 2004; Choi et al., 2005). De plus, les canaux Kir de rectification entrante participent à la repolarisation des neurones suite à une stimulation. Enfin, les R-NMDA sont des éléments clés dans la neurotransmission et la plasticité. Le fait que CIPP soit associé à ce panel de protéines sérotoninergiques suggère un rôle possible dans la transmission sérotoninergique. Cette hypothèse est confortée par le fait que CIPP interagisse également avec le R-5-HT$_{2A}$ (Bécamel et al., 2004), le R-5-HT$_4$ (Joubert et al., 2004) et SERT (Chanrion et al., 2007). Sachant que les récepteurs NMDA interagissent avec CIPP et IRSp53, il est envisageable 1) que les récepteurs NMDA fassent partie de ce complexe multi-protéiques et 2) que

l'expression des récepteurs NMDA puisse être modulée par ces différents effecteurs. Cependant, d'autres expériences sont nécessaires pour confirmer ces hypothèses.

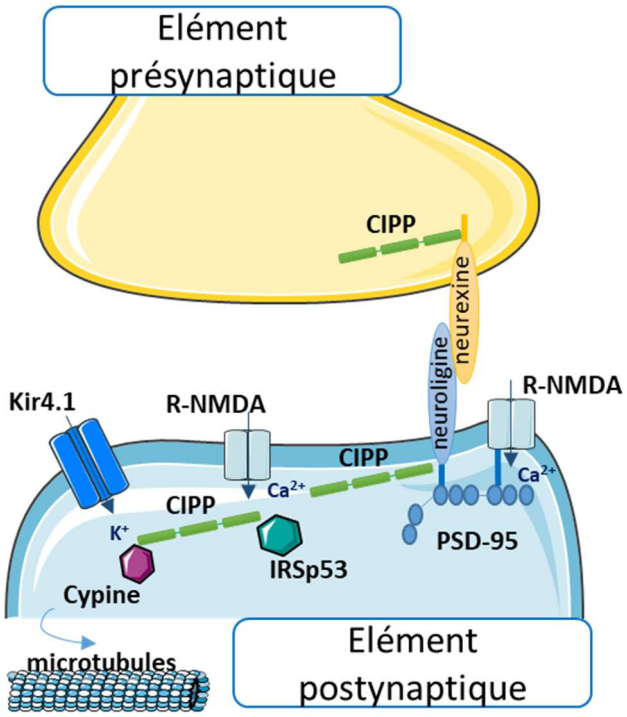

Figure 14 Représentation schématique des protéines associées à la protéine CIPP.

Pour finir, ces données m'ont permis de proposer un axe d'étude quant à l'interaction des R-5HT$_{2B}$ et de la protéine de pontage CIPP. Nous savons que la protéine CIPP interagit avec de nombreuses protéines synaptiques comme les R-NMDA, qu'elle est capable de potentialiser l'effet de certains effecteurs synaptiques comme Kir 4.1 ou de former des complexes tripartites avec des protéines impliquées dans la morphologie des dendrites comme le complexe IRSp53/Cypine ou le complexe neuroligine/neurexine **(Figure 14)**. L'étude de l'interaction des R-5-HT$_{2B}$ avec CIPP a permis, pour la première fois, d'étudier ce récepteur dans un modèle physiologique de neurones. Notamment sa distribution et son activité en présence ou non de CIPP, ce qui n'avait jamais été décrit. Sachant que la fonction de CIPP n'est pas très documentée, cette étude a permis aussi d'approfondir le rôle de cette protéine et d'ouvrir des perspectives dans le trafic intracellulaire ou la morphologie des neurones. Enfin, sachant que CIPP interagit avec les R-NMDA ; que l'activation des R-5-HT$_{2A/C}$ (Yuen et al., 2008) augmente l'expression des R-NMDA à la surface à l'inverse des R-5-HT$_{1A}$ (Yuen et al., 2005) dans des cultures de neurones corticaux ; alors il m'a paru judicieux d'étudier le rôle du R-5-HT$_{2B}$ et CIPP sur l'expression des R-NMDA (Article 2).

II. Le récepteur 5-HT$_{2B}$

A. Généralités

Le R-5-HT$_{2B}$ a été cloné à partir de banques d'ADN complémentaire de souris (Choi et al., 1996; Loric et al., 1992) puis de rats (Wainscott et al., 1993) et enfin chez l'humain (Kursar et al., 1994; Schmuck et al., 1994; Wainscott et al., 1996). Le R-5-HT$_{2B}$ humain présente 79 et 82% d'homologies de séquence avec les R-5-HT$_{2B}$ de rat et de souris, respectivement, mais conserve les mêmes propriétés pharmacologiques pour les agonistes et les antagonistes du récepteur (Choi et al., 1994; Maroteaux et al., 2017). Chez l'humain le gène codant le R-5-HT$_{2B}$, d'une taille de 16,8 kb, est localisé sur le chromosome 2 dans le locus 2q36.3-37.1 (Le Coniat et al., 1996). Pour toutes les espèces, ce gène est composé de 4 exons (dont 1 non codant) et de 3 introns et génère une protéine de 479 acides aminés (Colas et al., 1997; Horton et al., 1996).

L'ARN messager du R-5-HT$_{2B}$ a été détecté en périphérie dans le cœur, les reins, et les poumons mais aussi dans le cerveau adulte de rat (Choi and Maroteaux, 1996; Choi et al., 1994) notamment dans l'hippocampe, le noyau paraventriculaire du thalamus, les noyaux du raphé dorsal, le locus cœruleus, l'habénula, le cortex et le cervelet (Bonaventure et al., 2002) **(Figure 15)**. La purification des neurones sérotoninergiques de souris adultes et l'analyse transcriptomique de leur contenu cellulaire a confirmé une expression faible du R-5-HT$_{2B}$ dans certains noyaux du raphé (Okaty et al., 2015).

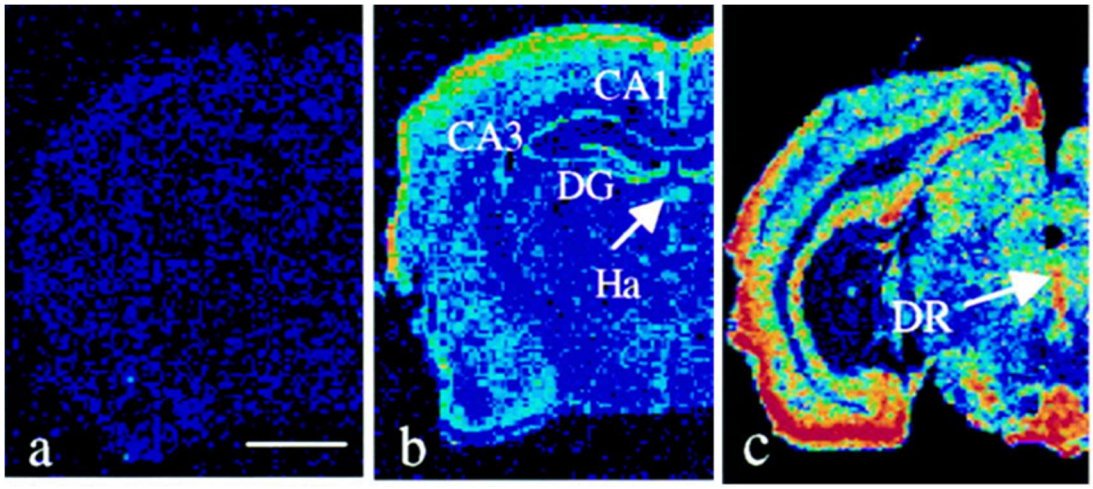

Figure 15 Détection de l'ARN messager du récepteur 5-HT$_{2B}$. *Barre d'échelle 0,3 cm. (Bonaventure et al., 2002)*

La structure 3D du R-5-HT_{2B} a été déduite de sa cristallisation (Wacker et al., 2013, 2017; Wang et al., 2013). Comme tous les RCPGs, le R-5-HT_{2B} est composé de sept domaines transmembranaires hydrophobes, trois boucles extracellulaires, une extrémité N-terminale extracellulaire et une extrémité C-terminale intracellulaire. Ce récepteur possède un site putatif de N-glycosylation dans son extrémité N-terminale (sauf chez le rat), un pont disulfure, un site de palmitoylation, des sites consensus de phosphorylations et une séquence de liaison aux domaines PDZ dans son extrémité C-terminale (Manivet et al., 2000, 2002) **(Figure 16)**.

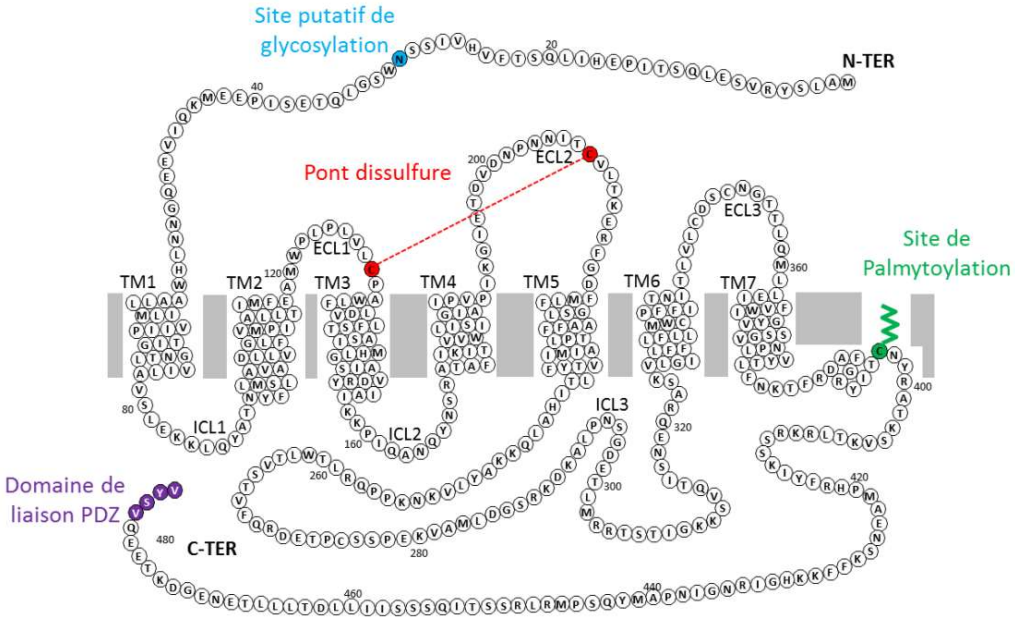

Figure 16 Topologie du récepteur 5-HT$_{2B}$ humain

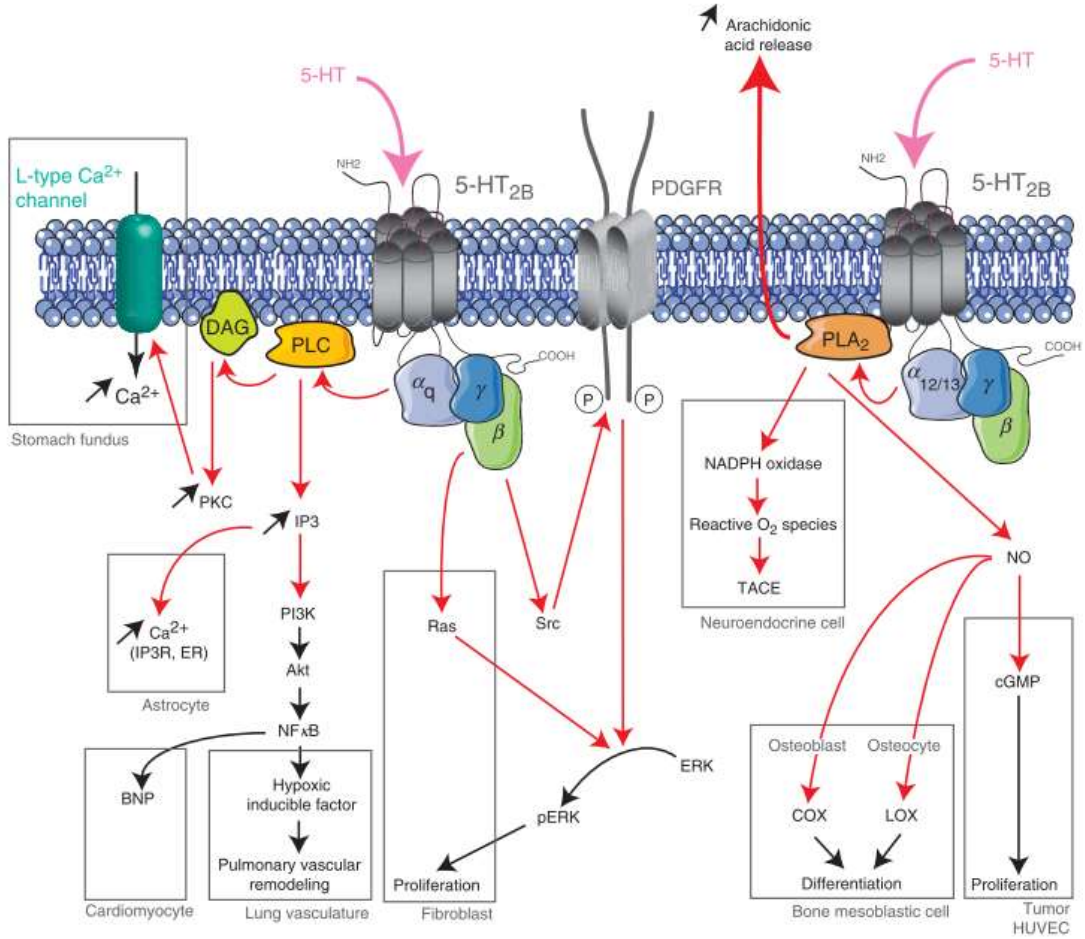

Figure 17 Voies de signalisation induites par l'activation des récepteurs 5-HT$_{2B}$ *(Masson et al., 2012)*

La stimulation du R-5-HT_{2B} par la 5-HT dans les cellules CHO induit l'internalisation de 80% des récepteurs après cinq minutes de stimulation, suggérant une dynamique rapide du récepteur (Porter et al., 2001).

- Les R-5-HT_{2B} sont couplés aux protéines Gαq qui activent la PLC et induisent la production d'IP_3 et de DAG **(Figure 17)**, à la fois dans des cellules transfectées transitoirement et dans les lignées stables (HEK293, AV-12 A600K-2-3-MTX, LMTK, 1C11, CHO) (Kellermann et al., 1996). Cette stimulation induit l'entrée de calcium dans la cellule par les canaux calciques de type L (Baxter et al., 1994; Cox and Cohen, 1996; Sandén et al., 2000).

- La stimulation de PLC permet également l'activation de PI3-kinase et par conséquent la stimulation de la voie NFκB (Launay et al., 2002; Nebigil et al., 2003a) **(Figure 17)**. Ces voies sont importantes dans les processus de développement car l'ablation génétique du R-5-HT_{2B} est associée à un fort taux de létalité durant l'embryogenèse (Nebigil et al., 2000).

- L'activation des protéines G permet l'activation de la protéine Ras et donc l'activation de la voie ERK, elle-même impliquée dans la prolifération des fibroblastes en synergie avec les récepteurs PDGF (facteur de croissance dérivé des plaquettes) **(Figure 17)** (Launay et al., 1996).

- De plus, le R-5-HT_{2B} est associé, via son site de liaison aux domaines PDZ, à la NOS, engendrant la production de GMP cyclique par la NO synthase constitutive (cNOS) et la NOS inductible (iNOS) (Manivet et al., 2000) **(Figure 17)**.

- Finalement, le récepteur peut également se coupler à la voie de la phospholipase A2 (PLA2), permettant la libération d'acide arachidonique. Ceci induit la production de prostaglandines par activation de la cyclooxygénase (COX) (Tournois et al., 1998). L'activation de la PLA2 active aussi la NADPH oxydase et induit la production de radicaux libres oxygénés (Schneider et al., 2006) **(Figure 17)**.

B. Caractérisation fonctionnelle des mutants du récepteur 5-HT_{2B}

1. Contribution de l'extrémité C-terminale

i. Gain de fonction du mutant R393X

L'extrémité C-terminale du R-5-HT_{2B} est fondamentale dans l'expression et la cinétique d'internalisation du R-5-HT_{2B}. En effet, la délétion de cette extrémité chez les mutant R393X supprime l'internalisation du récepteur, tout en favorisant son couplage à la protéine $G_{\alpha 13}$ et la prolifération cellulaire. Etant donné que la délétion de l'extrémité C-terminale ne supprime pas le site de palmitoylation (cystéine en position 385), ces résultats suggèrent que celui-ci est important dans l'ancrage du récepteur à la membrane. La mutation R393X a été trouvée chez l'homme et associée à l'hypertension pulmonaire induite par la prise de dexfenfluramine (Deraet et al., 2005).

ii. Perte de fonction du mutant R388W

Des expériences préliminaires effectuées au cours de mon stage de master 2 et au début de ma thèse, ont porté sur l'étude d'une autre mutation de l'extrémité C-terminale du R-5-HT_{2B}, la mutation R388W. Celle-ci a été retrouvée chez une sous-population de personnes prédisposées à l'impulsivité (Bevilacqua et al., 2010). Chez ce variant, contrairement à la mutation R393X, l'extrémité C-terminale est intacte. En revanche, l'arginine en position 388 située juste après le site de palmitoylation (cystéine en position 385) est substituée par un tryptophane. Les conséquences de cette substitution sont dramatiques car l'expression membranaire du R-5-HT_{2B} est perdue. Cette perte d'expression est probablement due à une mauvaise conformation des R-5-HT_{2B}, entrainant leur dégradation et/ou à un défaut de translocation à la membrane **(Figure 18)**. Ces expériences n'ont cependant pas été approfondies car l'absence d'expression du récepteur, liée à la mutation R388W, peut être assimilée aux animaux invalidés pour le gène codant le R-5-HT_{2B} (*Htr2b*$^{-/-}$), dont les phénotypes seront détaillés plus loin dans ce chapitre**.**

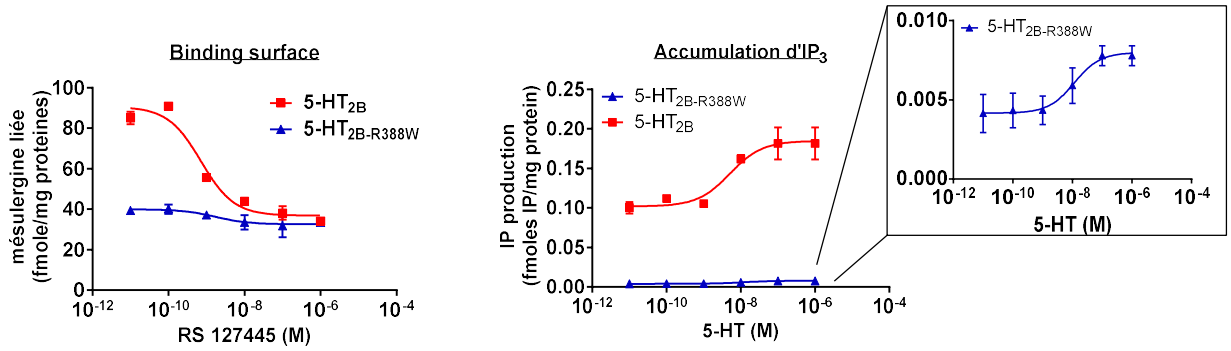

Figure 18 Propriétés pharmacologiques du mutant 5-HT$_{2B-R388W}$ comparées à celles du R-5-HT$_{2B}$ non muté (5-HT$_{2B}$). *Mesure de l'expression membranaire (« binding surface ») et de la production d'inositol phosphate induite par la 5-HT.*

2. Contribution de l'extrémité N-terminale

i. Phénotype du polymorphisme R6G ; E42G

L'extrémité N-terminale joue aussi un rôle dans les voies de transduction du R-5-HT$_{2B}$. Le polymorphisme R6G;E42G, retrouvé dans une sous-population de personnes ayant développé une addiction, induit une substitution au début de l'extrémité N-terminale (Lin et al., 2004). Cette double mutation provoque des variations de couplage par rapport au récepteur non muté (Belmer et al., 2014). En effet, ce polymorphisme induit une augmentation de l'activité de la voie de la PKC sans changer l'expression du R-5-HT$_{2B}$ à la surface de la membrane. Ce récepteur muté est internalisé plus tardivement que le récepteur non muté et l'affinité de la 5-HT et de l'agoniste BW723C86 est augmentée d'un facteur cinq. Enfin, ce polymorphisme est associé à une augmentation de prolifération cellulaire (Belmer et al., 2014).

C. Interactions du récepteur 5-HT$_{2B}$

1. Les récepteurs 5-HT$_{1B}$ et 5-HT$_{2B}$

La co-expression du R-5-HT$_{2B}$ avec le R-5-HT$_{1B}$ module la cinétique d'internalisation du R-5-HT$_{2B}$ dans la lignée cellulaire LMTK$^-$(Janoshazi et al., 2007). En effet, les auteurs ont montré que les R-5-HT$_{1B}$ et R-5-HT$_{2B}$ ont des cinétiques d'internalisation spécifiques lorsqu'ils ne sont pas co-exprimés. Cependant, leur co-expression et leur stimulation par des agonistes accélèrent de cinq fois la cinétique d'internalisation du R-5-HT$_{2B}$. Cet effet n'est pas supprimé par l'application d'un antagoniste du R-5-HT$_{2B}$, suggérant que c'est la stimulation du R-5-HT$_{1B}$

qui est impliquée dans l'internalisation du R-5-HT$_{2B}$ et non sa propre stimulation. En revanche, les récepteurs ne semblent pas colocalisés, supportant l'hypothèse selon laquelle la signalisation du R-5-HT$_{1B}$ modulerait les mécanismes d'internalisation du R-5-HT$_{2B}$. L'internalisation du R-5-HT$_{1B}$ est dépendante des cavéolines, contrairement au R-5-HT$_{2B}$. Cependant, lorsque les deux récepteurs sont co-exprimés, l'internalisation du R-5-HT$_{2B}$ devient partiellement dépendante des cavéolines, tandis que l'internalisation du R-5-HT$_{1B}$ devient complétement indépendante des cavéolines (Janoshazi et al., 2007). Ces résultats indiquent que la signalisation des R-5-HT est plus complexe lorsqu'ils sont co-exprimés probablement par l'interaction de leurs voies de signalisation.

2. Modulation de SERT par le couplage 5-HT$_{2B}$ / NOS

Après stimulation par la 5-HT, les R-5-HT$_{2B}$ activent à la voie de la NOS. L'activation de la NO induit une cascade de transduction qui peut aboutir à des phosphorylations de SERT. Ces phosphorylations changent les propriétés du transporteur, en particulier sa capacité de lier les antidépresseurs inhibiteurs de la recapture de 5-HT (ISRSs) et sa capacité de recapture de la 5-HT qui devient alors maximale. En présence de 5-HT, l'expression de SERT à la membrane diminue. L'activation des R-5-HT$_{2B}$ participe à ce mécanisme d'inhibition. En effet, lorsque la 5-HT active le R-5-HT$_{2B}$, la PKC induit des phosphorylations de SERT diminuant son expression à la membrane et ses capacités de recapture de la 5-HT. Les R-5-HT$_{2B}$ pourraient donc agir sur l'homéostasie des neurones sérotoninergiques en modulant les capacités de recapture de SERT ou en les modulant négativement en présence de 5-HT (Manivet et al., 2000; Launay et al., 2006).

D. Fonctions physiologiques et pathologiques du R-5-HT$_{2B}$

1. Au niveau périphérique

La 5-HT participe à la régulation des centres respiratoires situés au niveau médullaire dans le complexe pre-Bötzinger. L'injection locale d'agoniste des R-5-HT$_{2B}$ (BW723C86) induit une excitation tonique de l'activité des neurones. Cet effet est également observé lors de l'application d'un agoniste des R-5-HT$_{2A/2B/2C}$, le α-méthyl 5-HT. L'effet de l'α-méthyl 5-HT sur la respiration est bloqué par l'application d'antagonistes du R-5-HT$_{2A}$. Une injection locale de BW723C86 induit une augmentation de la fréquence respiratoire. Cet effet est bloqué par l'application d'antagoniste des R-5-HT$_{2B}$ mais pas par des antagonistes des R-5-HT$_{2A}$.

L'ensemble de ces résultats indique que l'excitation tonique des neurones de l'hypoglosse fait intervenir les R-5-$HT_{2A/2B}$ (Günther et al., 2006; Niebert et al., 2011) **(Figure 20)**.

Les R-5-HT_{2B} participent aussi au développement des os. En effet, l'expression des R-5-HT_{2B} augmente au cours de la différenciation des ostéoblastes. Une étude a montré que les femelles *Htr2b*$^{-/-}$ présentent une densité osseuse plus faible que les souris sauvages et que cette diminution s'intensifie avec l'âge (Collet et al., 2008). La diminution de la densité osseuse est associée à une réduction des phosphatases alcalines dans les cellules précurseurs de la moelle osseuse. De plus, la prolifération cellulaire des ostéoblastes est diminuée chez ces animaux, induisant un retard dans la différenciation des cellules. La suppression pharmacologique ou génétique du R-5-HT_{2B} induit une diminution de l'incorporation de calcium dans les ostéoblastes. Cette étude a donc montré que le R-5-HT_{2B} facilite le recrutement et la prolifération des ostéoblastes et que son absence peut induire des troubles de type osteopénie voire de l'ostéoporose avec l'âge (Collet et al., 2008) **(Figure 20)**.

Un des nombreux processus physiologiques dans lesquels la 5-HT est impliquée est la perception de la douleur notamment via la participation des R-5-HT_{2B}. La perception de la douleur, ainsi que sa modulation, sont intégrées au niveau des ganglions rachidiens dorsaux exprimant, entre autres, les R-5-HT_{2B}. La stimulation des R-5-HT_2, ou l'injection de 5-HT dans cette structure, est associée à une hyperalgésie (sensation anormalement douloureuse et exagérée) pouvant être reversée par l'application d'antagonistes 5-$HT_{2B/2C}$. Le rôle des R-5-HT_{2B} dans l'hyperalgésie serait dû à l'activation de la PKC et de la phosphorylation des récepteurs NMDA, qui provoquerait une hyperexcitabilité des neurones de la moelle épinière (Aira et al., 2013, 2014). Enfin, dans le cas de l'allodynie, pathologie où un stimulus sensoriel non douloureux provoque une sensation de douleur, le R-5-HT_{2B} est une cible potentielle de par son implication dans la perception sensorielle, son inhibition spécifique permettrait de diminuer cette sensation inadaptée et invalidante (Lin et al., 2011; Urtikova et al., 2012) **(Figure 20)**.

Le R-5-HT_{2B} joue un rôle clé dans le système cardiovasculaire pendant le développement et à l'âge adulte. En effet, l'inactivation du R-5-HT_{2B} au stade embryonnaire est létale *in utero* causée par des altérations de la fonction cardiaque. Ces défauts de maturations sont dus à l'absence de différenciation des précurseurs cardiaques en cellules trabéculaires. Cependant, lorsque les animaux survivent, ils présentent une hypoplasie cardiaque due à un défaut de prolifération et de développement cardiaque (Nebigil et al., 2000).

A contrario, la surexpression des R-5-HT$_{2B}$ dans les cellules cardiaques, induit une prolifération cellulaire excessive engendrant, en autres une hypertrophie des valves cardiaques. Cette hyperplasie est associée à une augmentation de la taille et du nombre de cardiomyocytes ainsi qu'une forte accumulation de mitochondries dans ces cellules. Ce modèle de surexpression peut donc être utilisé comme modèle d'hypertrophie cardiaque (Nebigil and Maroteaux, 2001; Nebigil et al., 2003b, 2003b; Hajjo et al., 2010; Monassier et al., 2010) **(Figure 20)**.

2. Au niveau central

Le R-5-HT$_{2B}$ joue un rôle prépondérant durant le développement du système nerveux périphérique et central notamment de par son expression sur les microglies, les macrophages résidents du cerveau. Ces derniers participent aux phénomènes de raffinement et de maturation synaptique au cours du développement. Suite à une injection locale de 5-HT sur tranche de cerveau, les microglies migrent et émettent des prolongements dirigés vers le site d'injection. De façon surprenante, cet effet n'a pas été observé chez les souris *Htr2b*$^{-/-}$. De plus, les souris *Htr2b*$^{-/-}$ présentent des altérations de la distribution des projections ipsilatérales des neurones projetant de la rétine au thalamus. Cette observation suggère que la délétion du R-5-HT$_{2B}$ est associée à des déficits dans l'élimination des neurones au cours du développement (Kolodziejczak et al., 2015) **(Figure 20)**.

3. Contribution du récepteur 5-HT$_{2B}$ dans les pathologies psychiatriques

i. Prise alimentaire

La dexfenfluramine (DF), un dérivé d'amphétamine, a été largement utilisée pour lutter contre l'obésité. Ce trouble de la prise alimentaire a été corrélé avec une perturbation de la transmission sérotoninergique. La dexfenfluramine a pour effet d'agir sur le SERT et induire une sortie massive des stocks intracellulaires et ainsi une accumulation extracellulaire de 5-HT. Cette molécule a été retirée du marché à cause des effets secondaires désastreux tels que l'hypertension pulmonaire et des valvulopathies. Notre laboratoire a étudié le rôle du R-5-HT$_{2B}$ dans la prise alimentaire et sur les effets de la DF chez des souris sauvages et des souris *Htr2b*$^{-/-}$. Les effets anorexigènes de la DF sont abolis chez les souris *Htr2b*$^{-/-}$. Cet effet a été reproduit après un traitement aigu avec l'antagoniste du R-5-HT$_{2B}$, le RS127445. Des expériences de microdialyse ont montré que la DF induit un pic de libération de 5-HT au niveau du thalamus une heure après l'injection. Ce pic étant fortement diminué chez les souris *Htr2b*$^{-/-}$, cela indique que le récepteur joue un rôle dans la transmission sérotoninergique au

niveau hypothalamique. Des expériences sur des synaptosomes issus de souris sauvages et *Htr2b*$^{-/-}$ ont montré que les synaptosomes issus des souris *Htr2b*$^{-/-}$ ne relarguent pas la 5-HT en réponse à la DF, contrairement aux synaptosomes issus des souris témoins. Ces résultats indiquent donc que le R-5-HT$_{2B}$ exprimés dans les neurones du raphé participent fortement à la libération de 5-HT via SERT induite par la DF (Banas et al., 2011) **(Figure 20)**.

ii. Impulsivité

Le séquençage du génome d'une population finlandaise de faible variabilité génétique a identifié un polymorphisme du gène *HTR2B* Q20* qui fait apparaitre un codon stop au début du gène. Ce polymorphisme est fréquemment associé à une population présentant une forte incidence de comportements impulsifs. L'impulsivité est un comportement caractérisé par une action sans anticipation, une diminution du contrôle inhibiteur ou une absence de considération des conséquences. Des défauts de la fonction cognitive, de l'attention ou des processus de la récompense sont associés à l'impulsivité, qui est retrouvée dans les cas de suicide, d'addiction, de violence, ainsi que dans l'hyperactivité, les déficits d'attention et divers troubles de la personnalité. Des études ont relié l'impulsivité et la violence à des variations génétiques, notamment dans le gène *MAOA* et des récepteurs dopaminergiques D1 (Brunner et al., 1993; Sabol et al., 1998; Misener et al., 2004; Winstanley et al., 2006, 2006).

Le polymorphisme *HTR2B* Q20* est associé à une perte d'expression du R-5-HT$_{2B}$, c'est pourquoi les auteurs l'ont comparé avec celui des souris *Htr2b*$^{-/-}$ (Bevilacqua et al., 2010). Les souris *Htr2b*$^{-/-}$ présentent une augmentation de leurs activités locomotrices lors des transitions jour/nuit reflétant une augmentation de la locomotion en réponse à un nouvel environnement ainsi qu'une augmentation de l'activité exploratoire face à un nouvel objet. Une augmentation de la locomotion après administration d'agonistes des récepteurs dopaminergiques D1 aussi été observée chez ces souris *Htr2b*$^{-/-}$. Enfin, ces animaux présentent une intolérance aux délais avant l'obtention d'une récompense, ainsi qu'une augmentation des taux plasmatiques de testostérone. Ces données ont mis en évidence une corrélation des phénotypes des souris *Htr2b*$^{-/-}$ avec les données retrouvées chez les humains impulsifs portant le polymorphisme *HTR2B* Q20* (Bevilacqua et al., 2010).

La population portant le polymorphisme *HTR2B Q20** a été étudiée en 2015 dans le but d'évaluer l'existence d'une corrélation entre l'agressivité et la prise d'alcool. Cette étude basée sur un panel de tests psychologiques portant sur l'agressivité/l'impulsivité a mis en évidence

que les porteurs de ce polymorphisme présentent un profil passif et une susceptibilité à développer des comportements agressifs particulièrement sous l'influence de l'alcool (Tikkanen et al. 2015) **(Figure 20)**.

iii. Schizophrénie

L'ablation génétique des R-5-HT_{2B} est associée à un comportement impulsif (Bevilacqua et al., 2010) qui est associée à une perturbation du système dopaminergique, comme c'est le cas dans la schizophrénie. C'est pourquoi, les comportements des souris *Htr2b*$^{-/-}$ ont été étudiés plus en détails afin de déterminer avec précision si ces animaux présentent des comportements de type psychotique.

Le test comportemental d'inhibition du réflexe de sursaut (PPI) fait référence à un stimulus acoustique fort qui fera sursauter l'animal (stimulus de sursaut) associé à un pré-pulse de faible intensité qui, s'il survient auparavant, atténuera la réponse suscitée par le stimulus fort. Chez l'humain, les troubles psychotiques, en particulier la schizophrénie, diminuent ce réflexe de sursaut et c'est également le cas chez les souris *Htr2b*$^{-/-}$ **(Figure 19)**.

De plus, la suppression génétique ou pharmacologique des R-5-HT_{2B} est associée à des défauts d'interactions sociales, de mémorisation spatiale et une hyperlocomotion face à la nouveauté par rapport aux animaux sauvages sans que les capacités motrices basales ne soient affectées (Doly et al., 2008). Chez ces animaux l'injection d'antagonistes des R-NMDA ou d'amphétamine provoque une réponse locomotrice supérieure aux animaux sauvages, ce qui renforce l'idée d'une action synergique des différents neuromédiateurs. Dans le cadre d'apprentissages associatifs, les souris *Htr2b*$^{-/-}$ ont un fort pourcentage d'échecs dans les tests de mémorisation à long et court terme. Enfin, ces animaux présentent des variations dans les stades de sommeil par rapport aux souris sauvages **(Figure 19)**.

Certains de ces phénotypes sont supprimés après quatre semaines de traitement à l'halopéridol, un antipsychotique antagoniste des récepteurs dopaminergiques D2. Cet ensemble de données comportementales a permis d'approfondir les phénotypes des souris *Htr2b*$^{-/-}$ qui présentent des comportements psychotiques **(Figure 20)**. Ceci montre que ce récepteur joue un rôle important dans de nombreux comportements impliquant le système sérotoninergique, glutamatergique et dopaminergique (Pitychoutis et al., 2015).

Functional domain	Factor tested	$Htr_{2B}^{-/-}$
Behavior		
Locomotor activity	Response to novelty	↑
	Response to dizocilpine	↑
	Response to amphetamine	↑
Sensorimotor gating	Prepulse inhibition	↓
Attention	Latent Inhibition	×
Cognitive function	Novel object recognition memory (short term)	↓
	Novel object recognition memory (long term)	↓
	Contextual fear memory	↓
	Cued fear memory	↓
	Social memory	↓
Social interaction	Sociability	↓
	Juvenile conspecific	↓
Sleep architecture	Wakefulness	↑
	NREM sleep	↓
	REM sleep	—
	REM latency	↓

Figure 19 Phénotypes comportementaux des souris Htr2b$^{-/-}$ *(Pitychoutis et al., 2015)*

iv. Vulnérabilité aux drogues d'abus

Lin et collaborateurs ont découvert un polymorphisme du gène *HTR2B* faisant apparaitre des mutation R6G/E42G affectant l'extrémité N-terminale du R-5-HT$_{2B}$ (Lin et al., 2004; Belmer et al., 2014). Cette mutation induit des variations des propriétés pharmacologiques des R-5-HT$_{2B}$ (*e.g.* ralentissement de la cinétique d'internalisation, augmentation de l'activité de la voie de la PKC, augmentation de l'affinité pour la 5-HT). Cette mutation a été identifiée chez une population montrant des prédispositions à développer une dépendance pour les drogues d'abus, suggérant que le R-5-HT$_{2B}$ participe à la transmission synaptique notamment dans le circuit de la récompense (Lin et al., 2004).

- Cocaïne

Le R-5-HT$_{2B}$ participe aux effets psychoactifs de la cocaïne. L'injection de cocaïne induit de la libération de dopamine dans le NAc et le striatum dorsal et une augmentation de la locomotion. Un traitement avec l'antagoniste du R-5-HT$_{2B}$ induit une diminution de la libération de dopamine dans le NAc *« shell »* en condition basale par rapport aux témoins. Cependant, cette libération de dopamine n'est pas affectée suite à l'injection de cocaïne. À l'inverse, l'injection d'antagonistes du R-5-HT$_{2B}$ ne change pas la libération de dopamine dans

le NAc « *core* », ni dans le striatum dorsal. Cependant, les antagonistes des R-5-HT_{2B} diminuent l'hyperlocomotion induite par l'agoniste des récepteurs dopaminergiques D2 (quinpirole) (Devroye et al., 2015). Cette étude suggère également que le R-5-HT_{2B} est un nouvel élément à prendre en compte dans l'étude de l'effet des drogues d'abus. Dans ce contexte, nous avons étudié le rôle du R-5-HT_{2B} dans les effets psychoactifs de la cocaïne. Cette étude, incluant des analyses comportementales et moléculaires chez les souris est présentée dans la partie l'Annexe 2 de ce manuscrit.

- Ecstasy ou MDMA (3,4-methylenedioxymethamphetamine)

Le rôle des R-5-HT_{2B} a aussi été étudié dans les effets psychoactifs de l'ecstasy ou MDMA (3,4-methylenedioxymethamphetamine). Le MDMA, dérivé de l'amphétamine, se fixe principalement au SERT et au transporteur de la dopamine (DAT) à plus forte dose. Le MDMA est un substrat du SERT et induit une sortie massive des stocks intracellulaires et ainsi une accumulation extracellulaire de 5-HT et dopamine. De façon surprenante, les souris *Htr2b*$^{-/-}$ne présentent pas les phénotypes comportementaux induits par l'injection de MDMA observés chez les souris témoins. En effet, l'injection de MDMA produit une augmentation de la locomotion et une augmentation de la libération de 5-HT dans le Nac et l'ATV chez les souris témoins mais pas chez les souris *Htr2b*$^{-/-}$. Ces effets sont reproduits par l'injection aigüe d'antagonistes du R-5-HT_{2B} (Doly et al., 2008, 2009). Chez les souris sauvages et *Htr2b*$^{-/-}$, le DAT et le SERT sont exprimés de la même façon et conservent leurs capacités de recapture la dopamine ou la 5-HT. Ainsi, ces résultats suggèrent un effet dynamique et rapide des R-5-HT_{2B} sur ces mécanismes de libération de 5-HT (Doly et al., 2008, 2009). Les effets renforçants du MDMA ont été évalués chez ces animaux dans un test de préférence de place conditionnée. Le principe de ce test est que l'animal passe plus de temps dans le compartiment où il a reçu la drogue, par association du lieu avec le stimulus récompensant. Dans le cas de souris sauvages, le MDMA induit un renforcement. Ce renforcement n'a pas été observé chez les souris *Htr2b*$^{-/-}$sauf lors de l'administration de la dose la plus élevée de MDMA (30mg/kg) (Doly et al., 2008, 2009). Au niveau moléculaire, l'effet du MDMA induit une augmentation de la phosphorylation des protéines ERK1/2 dans le NAc « *shell* » reflétant les effets renforçants de la drogue chez des souris sauvages. Cependant, la phosphorylation des protéines ERK1/2 est identique chez les souris *Htr2b*$^{-/-}$ayant reçu une injection saline ou de MDMA (10mg/kg). Une augmentation de la phosphorylation des protéines ERK1/2 chez les souris *Htr2b*$^{-/-}$ est observée seulement lors de l'administration de 30mg/kg de MDMA.

Ces études montrent que les R-5-HT_{2B} jouent un rôle important dans les effets psychoactifs du MDMA en modulant la transmission sérotoninergique et dopaminergique, et jouent aussi un rôle dans les effets renforçants de cette drogue (Doly et al., 2008, 2009).

v. Dépression- Inhibiteurs sélectifs de la recapture de la sérotonine (ISRSs)

Les antidépresseurs de la classe des inhibiteurs sélectifs de la recapture de la sérotonine (ISRSs) ciblent SERT et bloquent son activité de recapture. Ce blocage induit une augmentation des taux de 5-HT extracellulaires modulant ainsi l'expression des R-5-HT au niveau présynaptique et postsynaptique. Le rôle des R-5-HT_{2B} a été étudié chez la souris durant un traitement aigu et chronique aux ISRSs (fluoxetine et paroxetine). Dans le test de nage forcée, la prise d'ISRS a pour effet de diminuer le temps d'immobilité des animaux. Cependant, cet effet n'est pas observé chez les souris *Htr2b*$^{-/-}$. Ce résultat est reproduit suite à l'administration d'antagoniste du R-5-HT_{2B}. A l'inverse, l'injection d'agonistes du R-5-HT_{2B} chez des souris sauvages reproduit l'effet des ISRSs sur le temps d'immobilité dans le test de nage forcée. Ces résultats indiquent que la stimulation spécifique du R-5-HT_{2B} produit un effet similaire aux antidépresseurs (Diaz et al., 2012).

Il a été montré qu'un traitement chronique aux ISRSs induit des effets neurogéniques et stimulent la prolifération cellulaire dans l'hippocampe chez des souris sauvages (Santarelli et al., 2003). Cet effet n'est pas observé chez les souris *Htr2b*$^{-/-}$. Le traitement chronique de souris sauvage avec l'agoniste du R-5-HT_{2B} reproduit les effets neurogéniques observés chez les souris sauvages traitées aux ISRSs. Ces résultats indiquent que l'absence du R-5-HT_{2B} est suffisante pour altérer les effets neurogéniques induits par les ISRSs et sa stimulation est suffisante pour reproduire ces effets (Diaz et al., 2012). Des expériences de microdialyse ont été effectuées sur les animaux *Htr2b*$^{-/-}$afin d'observer l'effet des ISRSs sur l'accumulation de 5-HT après une injection aigue. De façon surprenante, les ISRSs induisent une accumulation de 5-HT extracellulaire significativement plus faible chez les souris *Htr2b*$^{-/-}$ou chez les souris sauvages traitées avec un antagoniste du R-5-HT_{2B}. Cette expérience indique donc que le blocage aigu des récepteurs supprime les effets d'une injection aigüe des ISRSs (Diaz et al., 2012). Les concentrations basales de 5-HT étant similaires pour les deux génotypes cet effet n'est pas le résultat d'une hyposérotoninergie (Diaz et al., 2012). SERT est exprimé de la même façon et possède les même propriétés de recapture chez les souris *Htr2b*$^{-/-}$et chez les souris sauvages, suggérant que SERT n'est pas impliqué dans les phénotypes observés (Diaz et al., 2012).

Les R-5-HT_{1A} participent aussi aux effets chroniques des antidépresseurs ISRSs. En effet, l'accumulation permanente de 5-HT extracellulaire induit une désensibilisation des R-5-HT_{1A}, réduisant leur action inhibitrice sur les neurones sérotoninergiques, et permettant ainsi de restaurer une transmission sérotoninergique normale. Cependant ni l'expression, ni la fonction pré- et post-synaptiques des R-5-HT_{1A} ne sont modifiées chez les animaux sauvages et *Htr2b*$^{-/-}$ suggérant que le R-5-HT_{1A} ne participe pas aux phénotypes observés chez ces *Htr2b*$^{-/-}$ (Diaz et al., 2012).

La caractérisation phénotypique des souris *Htr2b*$^{-/-}$suite à l'administration des ISRSs, indique qu'elles présentent des comportements mimant un traitement avec des antidépresseurs. En effet, les souris *Htr2b*$^{-/-}$ ont 1) une diminution de latence à se nourrir en cas de privation de nourriture, 2) une augmentation de l'expression basale de BDNF qui est un facteur de croissance exprimé au cours de la prolifération cellulaire dans l'hippocampe, et enfin 3) une augmentation de la consommation de sucrose qui diminue lors des symptômes de type dépressifs (anhédonie) (Diaz et al., 2016). Cependant les souris *Htr2b*$^{-/-}$peuvent également développer des phénotypes dits « dépressifs » suite à l'application d'un stress chronique de quatre semaines sans que les ISRSs ne soient efficaces. En conclusion, les souris *Htr2b*$^{-/-}$ présentent un profil de résistance aux antidépresseurs et pourraient être un bon modèle d'étude pour tester de nouveaux types d'antidépresseurs destinés aux individus résistants aux ISRSs (Diaz et al., 2016) **(Figure 20)**.

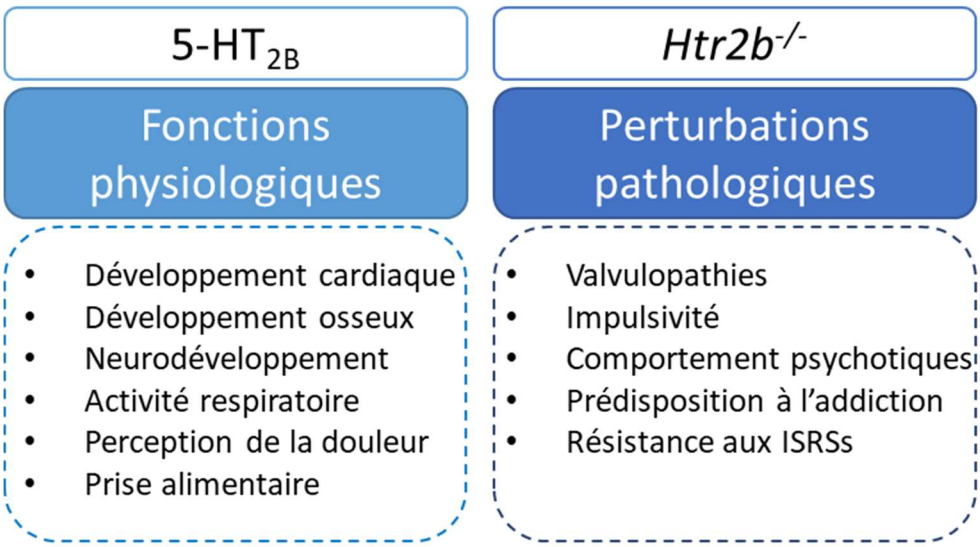

Figure 20 Fonctions physiologiques et pathologiques du R-5-HT_{2B}

III. Transmission sérotoninergique

A. Mode de neurotransmission

Dans le système nerveux central il existe deux modes principaux de communications. Le mode le plus classique proposé est la transmission électrochimique au niveau d'une synapse composée de deux entités structurales bien définis, 1) l'élément présynaptique (ou bouton axonal) contenant les vésicules de neuromédiateurs dans la zone active et 2) l'élément postsynaptique (ou épine dendritique) portant les différents récepteurs des neuromédiateurs ainsi que les canaux et effecteurs de la signalisation. Il existe aussi un mode de transmission « non-synaptique », qui n'a pas lieu entre deux éléments pré- et post-synaptiques comme décrit précédemment, et dans lequel la libération des neuromédiateurs a lieu dans un espace pseudo-ouvert. Ainsi la transmission synaptique (TS) est définie par la « *wiring transmission* » et la transmission non synaptique (TNS) par le « *volume transmission* » (Agnati et al., 1995; Zoli and Agnati, 1996).

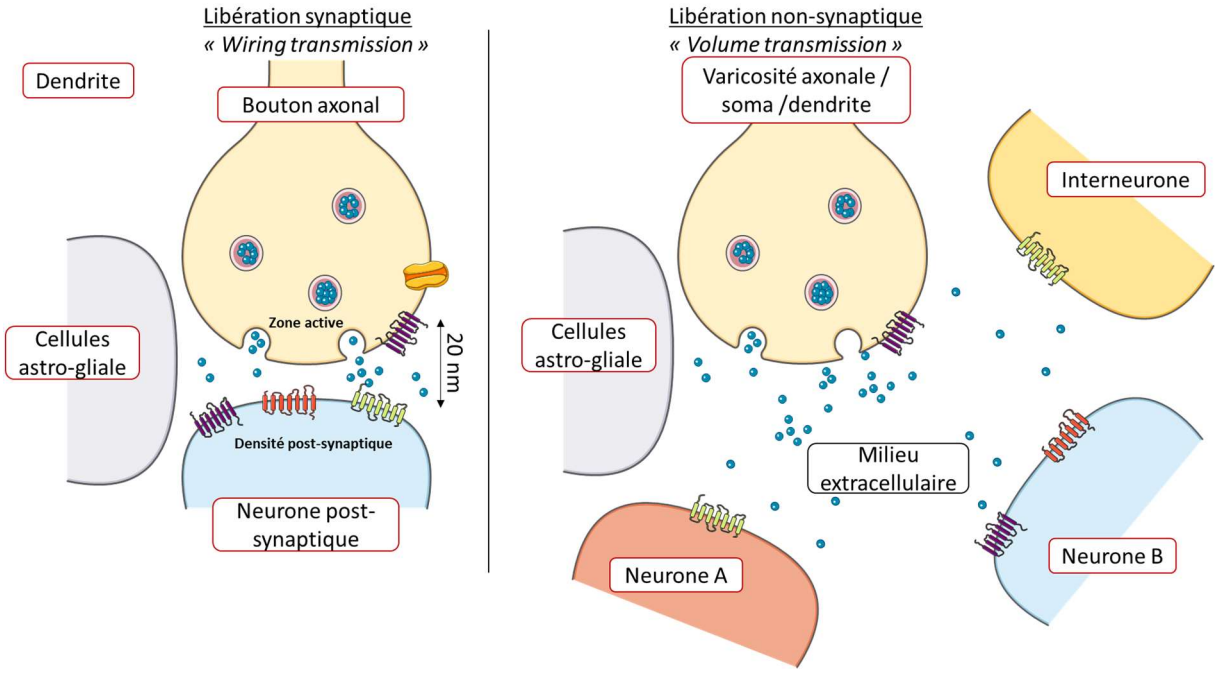

Figure 21 Représentation schématique de la libération synaptique et de libération non-synaptique de neuromédiateur*. A gauche, la TS implique des éléments pré- et post-synaptiques structurellement définis par un bouton axonal qui libère des neuromédiateurs, au niveau de la zone active dans un espace clos qu'est la synapse, qui activent les récepteurs présents sur la densité post-synaptique d'une épine dendritique. A droite, la TNS est induite par une libération extrasynaptique de neuromédiateur par une varicosité axonale ou une dendrite ou le soma d'un neurone dans le milieu extrasynaptique et ainsi active des récepteurs portés par différents types cellulaire (neurone A, neurone B, interneurone)*

La TS est définie comme un mode de communication entre une seule source et une seule cible dans l'espace clos/étanche/restreint qu'est la fente synaptique (environ 20 nm). La TS transmet un signal rapide, fiable, dont le mécanisme est couteux en énergie et impliquant une forte concentration de neuromédiateurs. La TNS est un mode de communication issu d'une seule source pouvant affecter plusieurs cibles (Agnati et al., 1995). Ce signal diffus est décrit comme lent, peu fiable, peu couteux en énergie, dans un espace plus grand que la fente synaptique (> 20 nm) et impliquant une faible concentration de neuromédiateurs. L'imagerie par microscopie électronique a montré que les sites de libération extrasynaptique sont riches en vésicules denses aux électrons (Bruns and Jahn, 1995; Kuffler et al., 1987) et en vésicules claires (Bruns and Jahn, 1995). Les mécanismes de libération extrasynaptique ont lieu par

exocytose des vésicules, par transport inverse des transporteurs membranaires, par la formation de pores ou par diffusion à travers la membrane plasmique (Trueta et al., 2012). De plus, l'existence de ce type de libération est supportée par la distribution extrasynaptique de canaux et des récepteurs aux neuromédiateurs notamment des systèmes monoaminergiques ou glutamatergiques (Aoki et al., 1987, 1994; Nusser et al., 1994; Sesack et al., 1994). Enfin, les deux types de neurotransmission existent pour les systèmes monoaminergiques, la proportion de TS par rapport à la TNS dépend de l'hétérogénéité de la morphologie et l'arborisation des axones et dendrites. Par exemple, les neurones dopaminergiques possèdent de nombreuses varicosités axonales formant des synapses et les neurones noradrénergiques et sérotoninergiques ont beaucoup d'axones collatéraux portant des varicosités non-synaptiques (Séguéla et al., 1988, 1989, 1990; Descarries et al., 1990; Oleskevich et al., 1991).

Le fait que ces deux modes de neurotransmission aient des cinétiques, des couts énergétiques et des cibles différentes suggère des rôles spécifiques. Ainsi, la TS favoriserait des messages rapides et intenses impliqués dans des comportements rapides ou des réponses aigües tandis que la TNS pourrait être impliquée dans des processus à long terme comme la régulation des états émotionnels ou encore pourrait agir comme des molécules de « guidage » notamment au cours de la neurogenèse et du raffinement synaptique. De plus, le processus de TNS pourrait activer les cellules astrogliales proches qui sont impliquées dans la régulation de microcircuits de neurones. Certains suggèrent que la fonction principale de la TNS serait de réguler la TS (Fuxe et al., 2012b). Il est également probable que ces deux mécanismes soient indépendants En effet, au vu de leurs cinétiques de transmission, la TNS participerait à l'état physiologique de base des neurones, ou à la régulation locale des neurones tandis que la TS aurait plutôt vocation à transmettre une information rapidement et efficacement.

B. Libération de la sérotonine

Les neurones sérotoninergiques issus de raphé projetant au niveau de la corne ventrale de la moelle épinière (Kiehn et al., 1992; Alvarez et al., 1998) et de la substance noire (Moukhles et al., 1997) créent principalement des synapses classiques. Les axones des neurones sérotoninergiques projetant sur la corne dorsale de la moelle épinière (Ridet et al., 1993) et sur le NAc (Van Bockstaele and Pickel, 1993) ne portent pas de structures synaptiques. Il existe donc bien des sous-populations de neurones sérotoninergiques n'utilisant pas les mêmes modes de neurotransmission. Ceci est supporté par le fait qu'au niveau hippocampique, les neurones sérotoninergiques issus du MRN forment des synapses classiques avec les

interneurones (Freund and Buzsáki, 1996; Varga et al., 2009) tandis que les neurones issus du DRN contiennent beaucoup de varicosités et forment peu de synapses (Kosofsky and Molliver, 1987). Les neurones du DRN contiennent des structures synaptiques et non synaptiques et sont donc capables d'utiliser les deux types de transmissions. De plus, il semble que les neurones utilisant soit la TS ou la TNS appartiennent à différentes populations de neurones sérotoninergiques (Chazal and Ralston, 1987).

1. Libération synaptique de sérotonine

La 5-HT est stockée dans des vésicules synaptiques claires et denses (Kuffler et al., 1987; Van Bockstaele et al., 1994). La libération de la 5-HT contenue dans ces vésicules (Henderson, 1983; Bruns and Jahn, 1995) est induite par la dépolarisation de l'élément présynaptique, dépendante du calcium qui permet la fusion des vésicules synaptiques avec la membrane plasmique dans la zone active (Katz and Miledi, 1970; Llinás et al., 1981; Dietzel et al., 1986). L'exocytose des vésicules dans la zone active fait intervenir des complexes moléculaires spécifiques qui participent à la modulation du cytosquelette et donc au transport, à l'amorçage et à la fusion avec la membrane plasmique (Szule et al., 2012). Le cycle de remplissage, amorçage et exocytose dure environ 30 secondes après stimulation (Ryan et al., 1993; Wölfel and Schneggenburger, 2003). La présence de vésicules claires est aussi une source de libération de 5-HT et leur exocytose est dépendant de la formation des potentiels d'actions (Bruns and Jahn, 1995). Ces deux types de vésicules contiennent sensiblement la même quantité de neuromédiateurs (Bruns and Jahn, 1995). La transmission sérotoninergique est dépendante des capacités de recapture du transporteur SERT axonal et des courants calciques entrants (Bruns et al., 1993). La libération de 5-HT provoque une diminution de l'amplitude des potentiels d'action par l'activation des autorécepteurs inhibiteurs 5-$HT_{1A/1B}$ (Cercós et al., 2009) et une hyperpolarisation des neurones (Baumann and Waldmeier, 1984; Blier et al., 1989; Becquet et al., 1990).

2. Libération extrasynaptique de sérotonine

Différentes techniques sont utilisées pour indiquer la présence de sites de libération extrasynaptique. La présence et la diffusion de 5-HT peuvent être évaluées en microscopie 3-Photons (Kaushalya et al., 2008a, 2008b) ou par ampérométrie à l'aide d'une fibre de carbone qui est placée dans le milieu extracellulaire. La libération de 5-HT produira ainsi un signal oxydatif mesurable (Bruns et al., 2000). La présence de vésicules plus ou moins grosses et

denses aux électrons est observée en microscopie électronique. Récemment, le suivi des vésicules d'exocytose pendant une stimulation a été observé en microscopie TIRF (« *total internal reflexion fluorescent microscopie* ») (Sarkar et al., 2012). Enfin, la distribution des récepteurs et transporteurs est observée en microscopie plein champ suite à des marquages par des anticorps spécifiques. Différentes observations permettent de suggérer une libération extrasynaptique de 5-HT (pour revue Trueta and De-Miguel, 2012):

1) La distribution homogène des R-5-HT et de SERT dans différents compartiments cellulaires (axone, soma, dendrite) suggère un rôle de ces récepteurs hors des synapses (Ridet et al., 1994; Bunin and Wightman, 1999). En effet, le R-5-HT_{1A} est retrouvé dans le soma et les dendrites des neurones sérotoninergiques du DRN (Kia et al., 1996; Riad et al., 2000) ; et le SERT dans des sites extrasynaptiques sur les axones projetant dans le cortex et le raphé (Zhou et al., 1998).

2) La présence de vésicules contenant la 5-HT localisées dans le soma, les dendrites et les varicosités axonales non accolées à un élément post-synaptique (Liposits et al., 1985; Chazal and Ralston, 1987; Descarries and Mechawar, 2000).

3) Enfin, la quantité de neurotransmetteurs retrouvée au niveau somatique ou dendritique par rapport aux terminaisons axonales (Bruns et al., 2000). Pour le système sérotoninergique, une quantité similaire de 5-HT est retrouvée dans les boutons synaptiques, le soma ou les dendrites (Kaushalya et al., 2008b). De plus, les concentrations extracellulaires de 5-HT augmentent en réponse à une stimulation extrasynaptique (Bunin and Wightman, 1999; Sakurai and Katz, 2003).

i. Somatodendritique

Il a été montré chez le rat et dans les neurones Retzius de sangsue, que le soma des neurones sérotoninergiques contient des amas vésiculaires périnucléaires et sous-membranaires suggérant une capacité de libération extrasynaptique de 5-HT (Coggeshall, 1972; Rude et al., 1969; Trueta et al., 2012).

Dans les neurones Retzius de sangsue, la libération somatique de 5-HT, qui a été mise en évidence par ampérométrie (Bruns et al., 2000), active l'ouverture de canaux ioniques via la PKC (Sanchez-Armass et al., 1991). Trueta *et al*. ont montré que cette libération dure quelques minutes suite à une stimulation électrique (Trueta et al., 2003). Plus précisément, l'exocytose

des vésicules commence une dizaine de secondes après la stimulation et se termine quelques minutes après, permettant une diffusion de 5-HT jusqu'à plusieurs micromètres (Perrier and Cotel, 2008). Après exocytose, ces vésicules sont regroupées puis dirigées au niveau périnucléaire (Trueta et al., 2012). Une stimulation électrique moyenne (induction d'un potentiel d'action) provoque l'ouverture de canaux calciques de type L (Beck et al., 2001; Lohr et al., 2001; Trueta et al., 2003) ; tandis qu'une stimulation de plus forte intensité (train de potentiels d'action) produit une entrée massive de calcium qui active la CaM et la libération des stocks intracellulaires de calcium (Trueta et al., 2004) via des R-5-HT_2 (Leon-Pinzon et al., 2014). Il est important de noter que les canaux calcique de type L n'interviennent pas dans la libération synaptique et sont donc spécifiques de la libération extrasynaptique (pour revue Catterall, 2011). En résumé, l'exocytose de 5-HT a lieu suite à une stimulation électrique qui induit l'ouverture des canaux calciques de type L, puis est renforcée par l'activation des R-5-HT_2 qui, par leur couplage à la voie de la PLC, va amplifier la libération de 5-HT (Leon-Pinzon et al., 2014).

Dans les neurones du DRN de rat, la libération des vésicules contenant la 5-HT peut être provoquée par une dépolarisation des neurones (Kaushalya et al., 2008b); par la stimulation des canaux calciques voltage-dépendant (De Kock et al., 2006); ou par l'activation des récepteurs glutamatergiques AMPA (De Kock et al., 2006; Colgan et al., 2009). Dans ces neurones, la libération de 5-HT est possible grâce à la présence de VMAT2 qui transporte la 5-HT dans les vésicules **(Figure 22)**. Le remplissage des vésicules a lieu au repos pour former des stocks et également pendant la stimulation (Colgan et al., 2009). La libération de 5-HT suit une cinétique lente (*i.e.* demi vie d'environ 200ms) et peut diffuser jusqu'à 20µm (Bunin and Wightman, 1999) typique d'une transmission de type TNS.

ii. Dendritique

Les dendrites des neurones sérotoninergiques du DRN contiennent des grosses vésicules denses aux électrons ainsi que des vésicules claires plus petites, regroupées au niveau extrasynaptiques ou au niveau de synapses dendro-dendritiques (Liposits et al., 1985; Kapadia et al., 1985; Chazal and Ralston, 1987; Colgan et al., 2012). Une étude récente a permis d'établir que la libération de 5-HT par les dendrites distales ne partage pas tous les mécanismes de libération des dendrites proximales dans les neurones de DRN de rat. Les auteurs ont décrit ces mécanismes dans des renflements en forme de fuseau (diamètre maximal de 1,4 µm) qu'ils définissent comme des « puncta », portant des vésicules claires ou denses aux électrons.

Ces structures expriment le transporteur VMAT2 colocalisé avec la 5-HT et le marqueur dendritique MAP2. Ces « puncta » sont huit fois plus concentrés en 5-HT que les terminaisons axonales. Dans ces structures, l'activation des R-NMDA, de même que l'injection locale de glutamate, induit une libération de 5-HT dendritique (Colgan et al., 2012). L'activation des R-NMDA, sans la propagation de potentiel d'action, est suffisante pour reproduire cet effet, indiquant que la libération somatodendritique de 5-HT extrasynaptique est potentialisée par les afférences glutamatergiques. Cette libération est dépendante de l'ouverture des canaux calciques de type L mais complètement indépendante de la formation de potentiel d'action contrairement aux dendrites proximales (Colgan et al., 2012) **(Figure 22)**.

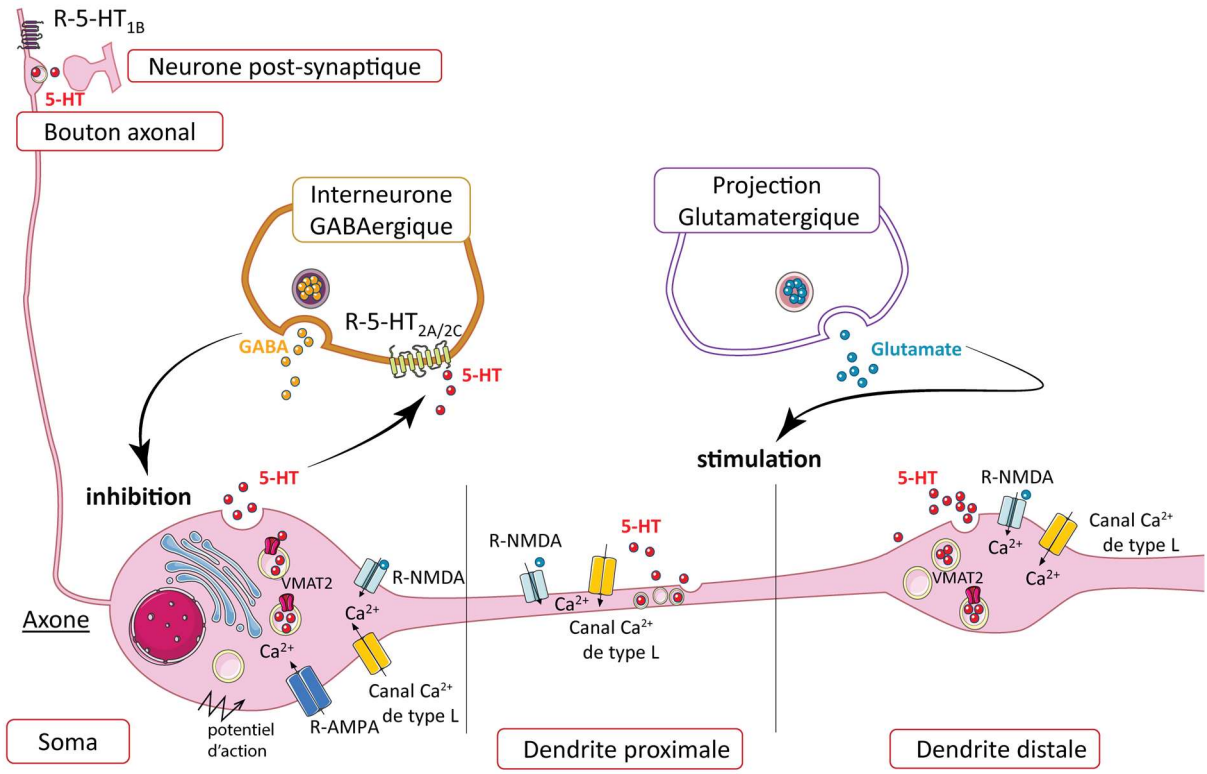

Figure 22 Mécanismes de libération somatodendritique de 5-HT par les neurones sérotoninergiques de DRN de le rat. *La libération extrasynaptique de 5-HT est induite par le glutamate libéré par les projections glutamatergiques. La libération de 5-HT par le soma et la dendrite proximale est dépendante des potentiels d'action, des R-NMDA et des R-AMPA ainsi que des canaux calciques de type L induisant des influx calciques. La libération de 5-HT par la dendrite distale est dépendante des R-NMDA et des canaux calciques de type L. La 5-HT libérée active les R-5-HT$_{2A/2C}$ présents sur les interneurones GABAergiques*

Pour conclure, la libération extrasynaptique de neuromédiateurs sans barrière physique permet la diffusion du signal selon un gradient dépendant des paramètres physicochimiques du milieu extracellulaire (température, pH, pression, présence de cellules gliales ou neurones) (Carmignoto, 2000; Vizi et al., 2004) et donc la capacité d'activer les récepteurs ou transporteurs ayant une forte affinité pour le neuromédiateur. En résumé, la libération de 5-HT, induite par la stimulation des R-AMPA/NMDA dans le soma et préférentiellement des R-NMDA dans les dendrites, augmente le rétrocontrôle inhibiteur des interneurones GABAergiques portant les R-5-HT_2 (Liu et al., 2000; De Kock et al., 2006; Colgan et al., 2009, 2012). Ainsi l'activation des récepteurs glutamatergiques et la propagation des potentiels d'action en même temps pourraient augmenter la libération de 5-HT et la force de la transmission sérotoninergique. Les afférences glutamatergiques et les neurones sérotoninergiques pourraient être actifs de façon synchrone afin de renforcer ce signal. Ces mécanismes peuvent *in fine* affecter le taux de décharge des neurones, leurs excitabilités, et les réponses des cellules astrogliales environnantes **(Figure 22)**.

C. Modulation de la transmission sérotoninergique

1. Hétéro-régulation

i. Par les neurones glutamatergiques et GABAergiques

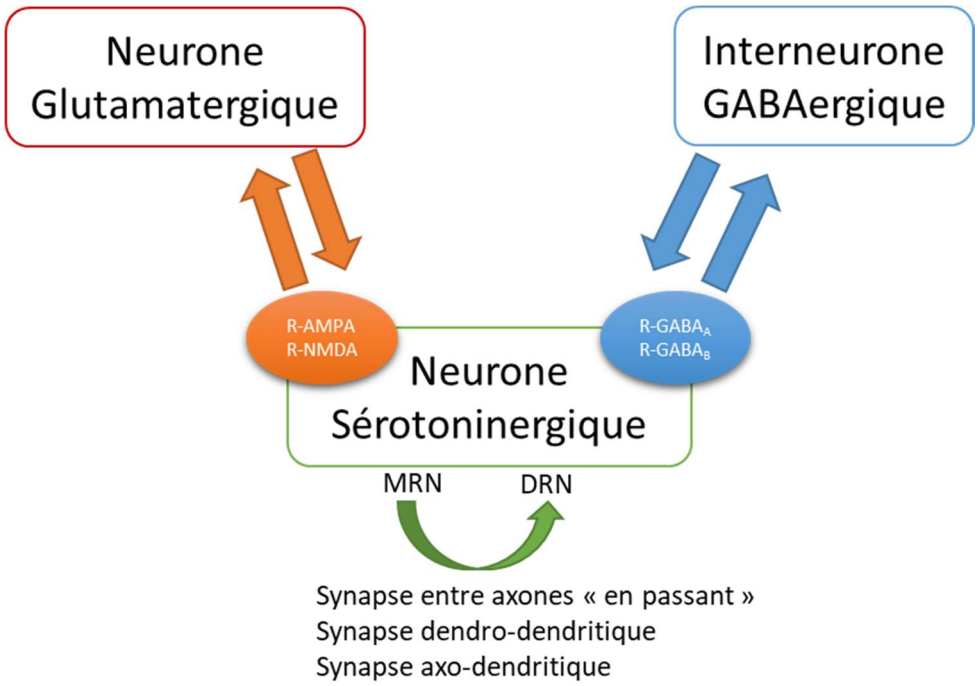

Figure 23 Représentation schématique de la régulation des neurones du raphé. *Afférences glutamatergiques et GABAergiques sur les neurones sérotoninergiques (orange et bleu). Autorégulation des neurones sérotoninergiques (en vert)*

Les neurones ciblés par les neurones sérotoninergiques, tels que les neurones de l'hippocampe ou les neurones du CPF ou de l'habénula latérale, ciblent en retour les interneurones GABAergiques localisés dans le raphé qui vont par la suite moduler les neurones sérotoninergiques (Varga et al., 2003; Torres-Escalante et al., 2004; Varga et al., 2009). Ainsi, les neurones sérotoninergiques sont modulés par les interneurones GABA (acide γ-aminobutyrique) ou les projections glutamatergiques. Les neurones sérotoninergiques peuvent également y être régulé par rétrocontrôle (i.e. par les neurones sérotoninergiques) via 3 types de synapses (1) les synapses dendrodentritiques (entre deux dendrites); (2) les synapses dites « en passant » sur les axones collatéraux ou (3) par contacts axodendritiques entre les neurones sérotoninergiques du DRN et ceux du MRN **(Figure 23)**.

Un autre mécanisme de régulation a été observé dans le raphé où l'on observe la formation de triades synaptiques composées d'un neurone sérotoninergique accolé à un élément GABAergique ou un élément glutamatergique et un troisième élément synaptique (Soiza-Reilly et al., 2013).

La libération de GABA par les interneurones provoque une diminution de l'activité tandis que le glutamate va potentialiser l'activité des neurones sérotoninergiques (Pan and Williams, 1989; Levine and Jacobs, 1992; Becquet et al., 1993a, 1993b), pour revue Maejima et al., 2013). Ces modulations sont possibles par l'expression des récepteurs ionotropiques de type $GABA_A$ (Tao and Auerbach, 2000) et des récepteurs glutamatergiques AMPA et NMDA (Gartside et al., 2007) par les neurones sérotoninergiques **(Figure 23)**. Ces neurones expriment aussi les récepteurs métabotropiques $GABA_B$ qui induisent l'ouverture des canaux GIRK diminuant le taux de décharge (Innis and Aghajanian, 1987; Williams et al., 1988; Bayliss et al., 1997). De plus, les récepteurs $GABA_B$ sont situés dans des structures extrasynaptiques suggérant une participation à la transmission non synaptique de 5-HT (Varga et al., 2002). Concernant les récepteurs métabotropiques glutamatergiques, peu de choses sont connues mais il semble que le blocage des mGlur2/3 induisent une augmentation de l'activité des neurones sérotoninergiques et la libération de 5-HT dans le CPF (Kawashima et al., 2005).

Le système glutamatergique, par l'activation des R-NMDA, est capable de stimuler la libération de 5-HT dans le raphé et il a été observé que le DRN est plus sensible à cet effet que le MRN ; tandis que le système GABAergique va avoir l'effet opposé dans le DRN et le MRN (Tao and Auerbach, 2000; Tao et al., 1996). L'application d'antagonistes des récepteurs $GABA_A$ induit une augmentation de la libération de 5-HT dans le DRN mais pas le MRN. De plus, l'application d'antagonistes des récepteurs glutamatergiques diminue la libération de 5-HT plus fortement dans le MRN que dans le DRN. Ces observations indiquent que le système glutamatergique aurait un effet excitateur plus fort sur les neurones du MRN que ceux du DRN; tandis que le système GABAergique aurait un effet inhibiteur plus fort sur les neurones du DRN que du MRN (Tao and Auerbach, 2003) **(Figure 24)**.

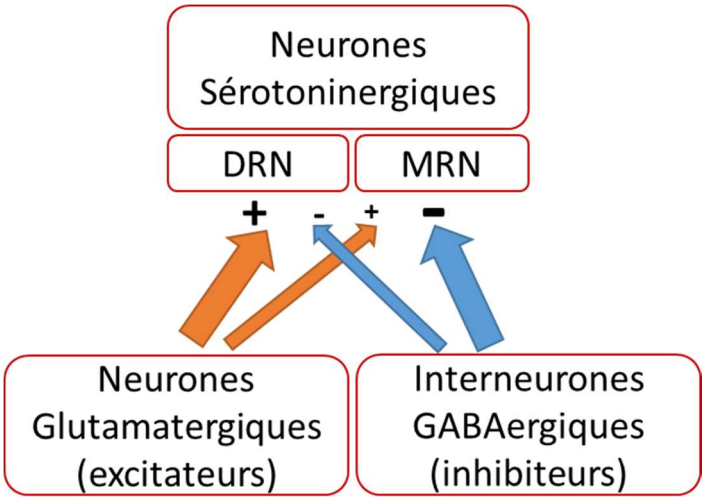

Figure 24 Régulation des neurones sérotoninergiques du DRN et du MRN par les neurones glutamatergiques et GABAergiques

ii. Co-libération de glutamate

Certains neurones sérotoninergiques sont capables de libérer de la 5-HT ainsi que du glutamate (Johnson, 1994). Cette catégorie de neurones est identifiable par l'expression de marqueurs glutamatergiques tels que les transporteurs vésiculaires VGLUTs, transportant le glutamate dans les vésicules synaptiques (Herzog et al., 2001, 2004; Hioki et al., 2010; Gagnon and Parent, 2014). Une étude a quantifié la proportion de neurones sérotoninergiques exprimant les VGLUTs dans les synapses en utilisant la synapsine comme marqueur présynaptique, PSD-95 comme marqueur post-synaptique et TPH comme marqueur sérotoninergique. Ils ont abouti à la conclusion que 28% des neurones sérotoninergiques expriment VGLUT1, 23% le transporteur VGLUT2 et 32% le transporteur VGLUT3 dans les synapses excitatrices (Soiza-Reilly and Commons, 2011). Ces observations indiquent qu'environ un tiers des neurones sérotoninergiques expriment un transporteur glutamatergique vésiculaire, ce qui est en faveur de l'hypothèse selon laquelle les neurones sérotoninergiques pourraient libérer de la 5-HT et du glutamate. VGLUT3 a été proposé comme participant à la co-libération de glutamate et de sérotonine car il est principalement exprimé dans des neurones non glutamatergiques (Gras et al., 2002).

Il a été montré que 50% des varicosités présentent une colocalisation de VGLUT3, VMAT2 et de 5-HT dans le cortex prélimbique (Amilhon et al., 2010). De façon surprenante cette étude a aussi montré que VGLUT3 est rarement colocalisé avec SERT, ce qui a été

reproduit sur culture de neurones sérotoninergiques (Amilhon et al., 2010; Voisin et al., 2016). En résumé, il existe différentes populations de neurones 5-HT/Glutamatergiques selon les marqueurs qu'ils expriment au niveau des projections axonales: (1) 5-HT, VMAT2, SERT, (2) 5-HT, VMAT2, SERT, VGLUT3, (3) 5-HT, VMAT2, VGLUT3 **(Figure 25)**.

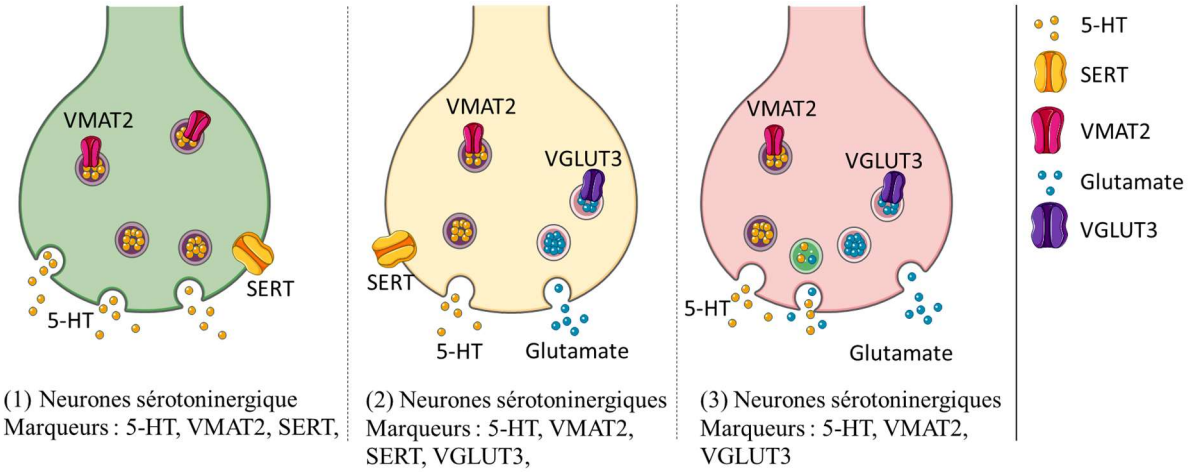

Figure 25 Hétérogénéité des terminaisons sérotoninergiques co-exprimant le transporteur VGLUT3. *Trois populations sont représentées, de gauche à droite : (1) neurones libérant de la 5-HT, (2) neurones libérant de la 5-HT et du glutamate, (3) neurones libérant de la 5-HT et du glutamate mais n'exprimant pas SERT.*

Au niveau fonctionnel, l'absence de VGLUT3 induit une diminution du nombre et du taux de survie des neurones sérotoninergiques, alors que la distribution et le nombre de varicosités exprimant SERT ne sont pas modifiés (Voisin et al., 2016). Ces observations suggèrent donc que le glutamate, via VGLUT3, a bien un rôle fonctionnel dans les neurones sérotoninergiques. Au niveau comportemental, la stimulation optogénétique des neurones sérotoninergiques du DRN exprimant VGLUT3 augmente la fréquence de décharges des neurones de l'ATV et du Nac ce qui est associé à une potentialisation de l'effet récompensant du sucrose (Liu et al. 2014). Cet effet est diminué par l'application d'un antagoniste glutamatergique ou des R-5-HT$_{2A/2C}$ et chez les animaux invalidés pour les gènes TPH2 ou VGLUT3. Ces observations confirment l'action synergique du glutamate et de la 5-HT dans la transmission synaptique notamment dans la récompense (Liu et al. 2014). De plus, il est important de noter que les neurones sérotoninergiques sont capables de libérer de la 5-HT hors des synapses dans lesquels ils pourraient aussi libérer du glutamate.

iii. Régulation par les R-5-HT$_{1A}$ et 5-HT$_2$

Il est important de préciser qu'en général la majorité des auteurs utilisent l'agoniste DOI pour étudier les R-5-HT$_2$ dans la transmission synaptique et qu'ils attribuent les effets observés aux R-5-HT$_{2A/2C}$ bien que le DOI soit un agoniste ayant des affinités similaires pour tous les R-5-HT$_2$ (pKi$_{5\text{-HT2A}}$ = 8.04 ± 0.05 ; pKi$_{5\text{-HT2B}}$ = 7.78 ± 0.09 ; pKi$_{5\text{-HT2C}}$ = 7.73 ± 0.04) (Maroteaux et al., 2017).

Les interneurones GABAergiques expriment des R-5-HT$_2$ dont l'activation stimule la libération de GABA qui inhibe les neurones sérotoninergiques (Xu et al., 1998; Liu et al., 2000; Leysen, 2004). Ces interneurones expriment aussi les R-5-HT$_{1A}$ (Kishimoto et al., 2001; Koyama et al., 2002; Katsurabayashi et al., 2003) et les 5-HT$_3$ (Koyama et al., 2002; Katsurabayashi et al., 2003; Turner et al., 2004b) dont l'activation inhibe ou stimule respectivement la libération de GABA dans de nombreuses structures telles que le gyrus denté, le cortex enthorinal, piriforme, frontal et l'habénula latéral (pour revue Ciranna, 2006).

Les R-5-HT$_{1A}$ sont largement exprimés dans les neurones glutamatergiques du CPF et suppriment leur activité spontanée. De plus, l'activation des R-5-HT$_{1A}$ réduit l'expression des récepteurs NMDA dans les dendrites (Yuen et al., 2005). Cependant, cet effet est compensé par la stimulation des R-5-HT$_2$ dans ces mêmes neurones (Yuen et al., 2008). De plus, la stimulation des R-5-HT$_{2A}$ dans les neurones pyramidaux augmente la formation de courants post-synaptiques excitateurs (Aghajanian and Marek, 1997) ainsi que dans les neurones dorsolatéraux du noyau septal par l'activation de la PKC (Hasuo et al., 2002). De même, l'activation des R-5-HT$_2$ induit des phosphorylations des canaux potassiques Kv1.1 et Kv1.2 et inhibe leurs ouvertures, potentialisant la libération de glutamate dans le CPF (D'Adamo et al., 2013).

Les mécanismes de régulation par les R-5HT$_{1A}$ et 5-HT$_2$ sont complexes car l'activation des R-5-HT$_{1A}$ diminue la libération de glutamate et de GABA et celle des R-5-HT$_2$ l'augmente. Comme les systèmes sérotoninergiques, glutamatergiques et GABAergiques sont fortement interconnectés il est compliqué d'associer des fonctions spécifiques de ces récepteurs dans la modulation de tous ces systèmes.

2. Autorégulation par les R-5-HT$_1$ et les R-5-HT$_2$

Au niveau somatodendritique et axonal, l'inhibition de l'activité des neurones sérotoninergiques est due à la présence des autorécepteurs inhibiteurs 5-HT$_{1A/1B}$ (Sprouse and Aghajanian, 1987; Blier et al., 1989; Sharp et al., 1989; Riad et al., 2000) qui activent l'ouverture des canaux potassiques de rectification entrante « GIRK » (« *G protein gated inwardly rectifying potassium* ») (Colino and Halliwell, 1987; Mlinar et al., 2015; Montalbano et al., 2015) et ferment les canaux calciques de type N et P/Q (Colino and Halliwell, 1987; Penington and Kelly, 1990; Penington et al., 1992; Bayliss et al., 1997) **(Figure 26)**. Ce mécanisme induit une hyperpolarisation des neurones et limite leur capacité de développer un potentiel d'action. De plus, les R-5-HT$_{1B}$ limitent la libération de 5-HT par les varicosités axonales (Sprouse and Aghajanian, 1987; Boeijinga and Boddeke, 1993; Morikawa et al., 2000) en augmentant la capacité de recapture du SERT (Hagan et al., 2012) **(Figure 26)**.

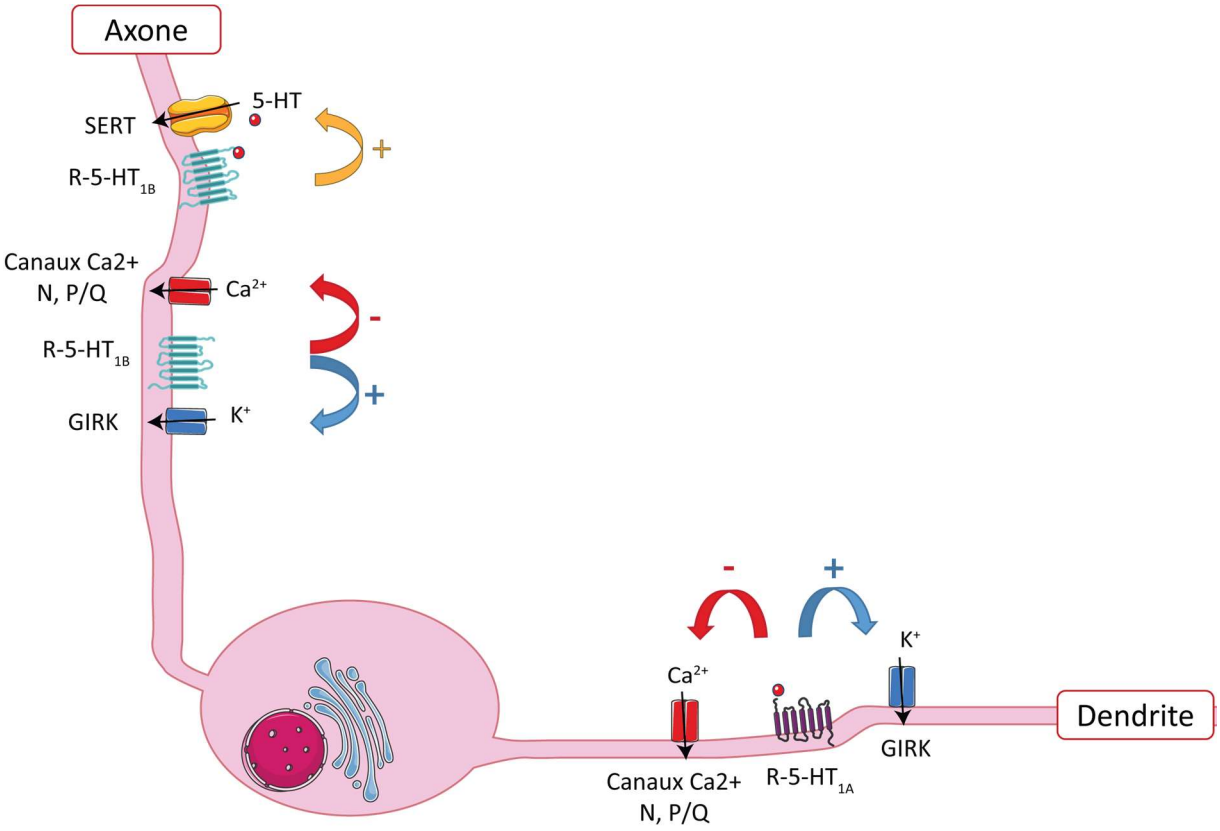

Figure 26 Représentation schématique de la régulation des neurones sérotoninergiques par les autorécepteurs 5-HT$_{1A}$ dendritique et 5-HT$_{1B}$ axonal. *Les R-5-HT$_{1A}$ inhibent l'ouverture des canaux calciques N, P/Q et activent l'ouverture des canaux GIRK, Les R-5-HT$_{1B}$ inhibent l'ouverture des canaux calciques N, P/Q et active l'ouverture des canaux GIRK et de SERT.*

La réduction de l'expression des R-5-HT_{1A} par l'injection d'ARN interférant dans le DRN produit de forts effets antidépresseurs, probablement dus à la suppression du rétrocontrôle négatif du récepteur sur l'activité des neurones sérotoninergiques (Bortolozzi et al., 2012). De plus, sa suppression génétique chez les souris 5-HT_{1A} KO provoque un comportement anxieux à l'état basal. Les souris 5-HT_{1A} KO présentent une plus forte augmentation de libération de la 5-HT comparées aux souris sauvages en réponse au stress (Richardson-Jones et al., 2010). Ces phénotypes auraient une origine développementale car l'inactivation ou le blocage pharmacologique de ce récepteur à l'âge adulte ne reproduit pas ces phénotypes contrairement à une suppression pendant la deuxième et la troisième semaine après la naissance.

De plus, le traitement chronique par les ISRS provoque une diminution de l'expression des R-5-HT_{1A} dans les neurones sérotoninergiques. Cette diminution d'expression des R-5-HT_{1A} explique probablement le retard clinique de l'effet antidépresseur des ISRS en régulant l'excitabilité des neurones sérotoninergiques (Santarelli et al., 2003; Adell et al., 2005; Richardson-Jones et al., 2010; Rainer et al., 2012). Chez les souris SERT KO, les R-5-HT_{1A} sont désensibilisés dans les noyaux du raphé tandis qu'ils sont intacts dans les neurones post-synaptiques (Fabre et al., 2000). Cette désensibilisation des R-5-HT_{1A} serait vraisemblablement due à l'accumulation chronique de 5-HT dans le raphé, en absence de SERT. Cependant, cette accumulation de 5-HT n'est pas suffisante au niveau des projections sérotoninergiques pour reproduire cet effet (Soiza-Reilly et al., 2015).

Enfin, les R-5-HT_{1A} semblent participer au fait que les neurones sérotoninergiques aient des profils électrophysiologiques différents. En effet, l'effet inhibiteur des R-5-HT_{1A} est supérieur dans les neurones du DRN que du MRN suggérant un plus fort rétrocontrôle dans le DRN (Beck et al., 2004).

Concernant les R-5-HT_2, aucun mécanisme n'a clairement été décrit dans les neurones sérotoninergiques de rat ou de souris. Cependant, une étude effectuée sur le hamster a reproduit l'effet inhibiteur des R-5-HT_{1A} dont l'activation par la 5-HT induit l'ouverture des canaux GIRK dans les neurones sérotoninergiques du DRN. La 5-HT produit une dépolarisation des neurones. Cette dépolarisation est bloquée par différents antagonistes spécifiques des R-5-HT_2 (mésulergine , kétansérine) mais pas des antagonistes des R-5-HT_3 ou 5-HT_4 (Craven et al., 2001).

Sur des coupes de DRN de rat, la 5-HT induit des courants sortants (hyperpolarisants) et des courants entrants (dépolarisants) dans les neurones sérotoninergiques et non sérotoninergiques. La totalité des courants sortants sont reproduits par l'application d'un agoniste des R-5-HT_{1A} (5-CT) et 47% des courants entrants par un agoniste des R-5-HT_2 (DOI) dans les neurones sérotoninergiques (Marinelli et al., 2004). Dans les neurones non sérotoninergiques, 100% des neurones répondent au 5-CT et 75% au DOI. Enfin 31% des neurones sérotoninergiques et 75% des neurones non sérotoninergiques répondent au 5-CT et au DOI (Marinelli et al., 2004). Ces observations indiquent donc que les neurones sérotoninergiques et non sérotoninergiques sont hétérogènes par l'expression des différents R-5-HT. Ces données suggèrent aussi que les R-5-HT_2 exprimés par les neurones sérotoninergiques participeraient à la transmission synaptique.

	Neurones sérotoninergiques	Neurones non sérotoninergiques
Courants sortants (agoniste R-5-HT_{1A})	96%	100%
Courants entrants (agoniste R-5-HT_2)	47%	75%
Courants entrants et sortants (agonistes R-5-$HT_{1A/2}$)	31%	75%

***Figure 27 Hétérogénéité des neurones du raphé**. Proportion de neurones sérotoninergiques et non sérotoninergiques du DRN produisant des courants sortants (hyperpolarisants) dépendants des R-5-HT_{1A} ou des courants entrants dépendants des R-5-HT_2 d'après (Marinelli et al., 2004)*

OBJECTIFS DE L'ETUDE

Mon projet de thèse s'est déroulé dans la continuité des études effectuées jusqu'alors dans le laboratoire portant sur la fonction du R-5-HT_{2B} dans le cerveau. Au cours des dernières années, le laboratoire a démontré un rôle insoupçonné du R-5-HT_{2B} dans le système nerveux. En effet, suite à la génération des animaux 5-$HT_{2B}^{-/-}$, différentes études ont permis d'ouvrir de nombreuses perspectives quant au rôle de ce récepteur dans plusieurs processus. Ces animaux présentent des comportements impulsifs, ce qui a été corrélé avec un polymorphisme perte de fonction dans le gène *HTR2B* associé à une forte impulsivité et des comportements suicidaires chez l'homme. Ces récepteurs contribuent aussi aux effets comportementaux et physiologiques de dérivés de l'amphétamine (MDMA-ecstasy) et des antidépresseurs ISRS qui sont supprimés chez les animaux 5-$HT_{2B}^{-/-}$.

A mon arrivée au laboratoire, deux principaux axes ont été proposés : l'un visant à approfondir le rôle du R-5-HT_{2B} dans les neurones sérotoninergiques et/ou dopaminergiques afin de préciser l'origine des phénotypes des animaux 5-$HT_{2B}^{-/-}$ et l'autre visant à approfondir la caractérisation fonctionnelle des R-5-HT_{2B} notamment son interaction avec les protéines de type PDZ. Ces protéines de pontage ont été identifiées par l'équipe de Philipe Marin par une approche protéomique associant chromatographie d'affinité à l'aide d'un peptide synthétique contenant le site de liaison aux domaines PDZ du R-5-HT_{2B} et spectrométrie de masse.

Au cours de la première partie de ma thèse, j'ai généré et amplifié les lignées de triples transgéniques dépourvues de R-5-HT_{2B} (5-$HT_{2B}^{flox/flox}$) dans les neurones sérotoninergiques (Pet1-cre) exprimant la GFP (RCE) comme rapporteur uniquement dans les neurones recombinés. Les réponses comportementales en réponse au MDMA et aux ISRSs ont ainsi été effectuées et ont permis de terminer le projet présenté dans l'Article 1 de ce manuscrit. Dans cette étude, nous montrons la contribution du R-5-HT_{2B} dans les effets psychoactifs du MDMA ainsi que dans les effets comportementaux et neurogéniques des ISRSs. Ces molécules, induisant une accumulation extracellulaire de 5-HT, ont principalement servi d'outils pour étudier le rôle du R-5-HT_{2B} dans la transmission sérotoninergique. Ceci nous a permis de proposer un rôle de modulateur positifs du R-5-HT_{2B} sur l'activité des neurones sérotoninergiques, à l'inverse du R-5-HT_{1A}.

Dans la seconde partie de ma thèse, j'ai étudié le rôle de l'interaction du R-5-HT_{2B} avec la protéine CIPP. J'ai tout d'abord confirmé leur interaction puis j'ai montré qu'elle induit un gain de fonction de la voie de la PLC du R-5-HT_{2B} sans affecter l'expression du récepteur ni la capacité de couplage aux protéines G. J'ai alors suggéré que CIPP pourrait regrouper le

récepteur dans des régions riches en effecteurs expliquant le gain de fonction induit par CIPP. En collaboration avec Sabine Lévi, j'ai alors étudié la distribution du R-5-HT_{2B} et de CIPP dans des cultures primaires d'hippocampe. C'est alors que, pour la première fois, nous avons observé que le R-5-HT_{2B} est restreint au niveau somatodendritique tandis que CIPP est retrouvé dans tous les compartiments des neurones. J'ai ensuite étudié l'impact de cette interaction sur l'adressage synaptique, l'internalisation et la signalisation calcique du R-5-HT_{2B}. Enfin, sachant que CIPP interagit aussi avec les R-NMDA, j'ai proposé que CIPP puisse regrouper le R-5-HT_{2B} et le R-NMDA. Pour cela, j'ai étudié l'impact de la stimulation du R-5-HT_{2B} sur la distribution des R-NMDA en présence ou non de CIPP.

RESULTATS

Article 1

Positive regulation of raphe serotonin neurons by serotonin 2B receptors

Arnauld Belmer, Emily Quentin, Silvina L. Diaz, Bruno P. Guiard, Sebastian P. Fernandez, Stéphane Doly, Sophie M. Banas1, Pothitos M. Pitychoutis, Imane Moutkine, Aude Muzerelle, Anna Tchenio, Anne Roumier, Manuel Mameli, and Luc Maroteaux

1. Le récepteur 5-HT$_{2B}$: un modulateur positif de l'activité des neurones sérotoninergiques

(Soumis)

Les R-5-HT$_2$ ont été associés à des pathologies telles que l'addiction à la cocaïne (pour revue Cunningham, K. A. et al., 2013), au MDMA (Fletcher et al., 2002) ou dans la dépression (pour revue Carr and Lucki, 2011). En particulier, les travaux du laboratoire ont montré que le R-5-HT$_{2B}$ participe aux effets du MDMA et des ISRSs. En effet, la délétion génétique ou l'inhibition pharmacologique provoque une perte des effets comportementaux induits par le MDMA (Doly et al., 2008, 2009) et des ISRSs (Diaz et al., 2012, 2016). Puisque ces molécules induisent une accumulation de 5-HT extracellulaire, par leur action sur SERT, ces résultats suggèrent que le R-5-HT$_{2B}$ participe activement à la transmission sérotoninergique. Cette hypothèse est renforcée par le fait que la stimulation des R-5-HT$_{2B}$, par un agoniste, reproduit les effets induits par les ISRSs ainsi qu'une réduction des comportement anxieux dans différents paradigmes comportementaux (Kennett et al., 1996; Diaz et al., 2012). Par ailleurs, Doly et collaborateurs ont montré que l'infusion d'agoniste des R-5-HT$_{2B}$ induit une libération de 5-HT dans le raphé (Doly et al., 2008). L'ensemble de ces données nous indique que le R-5-HT$_{2B}$ est important dans la transmission sérotoninergique mais les mécanismes d'action selon son expression par les neurones sérotoninergiques ou non sérotoninergiques (interneurones GABA, neurones glutamatergiques ou dopaminergiques) restent encore à déterminer.

A. Caractérisation des animaux *5-HT$_{2B}^{5\text{-}HTKO}$*

Dans cette étude, nous avons voulu préciser le rôle du R-5-HT$_{2B}$ dans la physiologie des neurones sérotoninergiques. Pour cela, nous avons mis au point une lignée de souris n'exprimant pas le R-5-HT$_{2B}$ spécifiquement dans les neurones du raphé (*5-HT$_{2B}^{5\text{-}HTKO}$*). Cette lignée a été obtenue par le croisement d'animaux exprimant la cre-recombinase sous le contrôle du promoteur Pet1, responsable de l'identité des neurones sérotoninergiques, avec des animaux dont le premier exon codant du gène *Htr2b* est flanqué de sites lox. Ainsi, le R-5-HT$_{2B}$ est supprimé seulement dans les neurones sérotoninergiques. Enfin, pour vérifier que les neurones sont correctement recombinés, cette lignée a été croisée avec la lignée RCE (Rosa26 : CAG-loxP-STOP-loxP-EGFP) qui exprime la protéine fluorescente GFP uniquement dans les cellules exprimant la cre-recombinase (Mao et al., 2001) **(Figure 28)**.

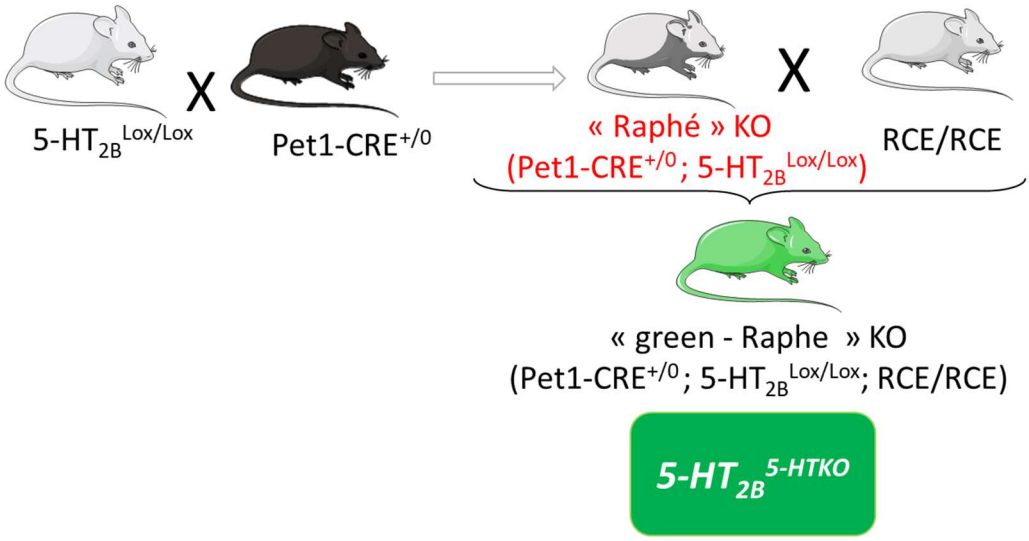

Figure 28 Génération de la lignée 5-HT$_{2B}^{5\text{-}HTKO}$. *En haut à gauche, le croisement permettant l'obtention des animaux dépourvus de R-5-HT$_{2B}$ seulement dans les neurones sérotoninergiques. En haut à droite, croisement avec la lignée RCE exprimant la GFP sous le contrôle de la cre-recombinase permettant l'obtention d'animaux dépourvus de R-5-HT$_{2B}$ et exprimant la GFP dans les neurones sérotoninergiques 5-HT$_{2B}^{5\text{-}HTKO}$.*

La caractérisation comportementale des animaux *Htr2b*$^{-/-}$ nous a permis de montrer que certains phénotypes des souris *Htr2b*$^{-/-}$ sont conservés.

En effet, chez ce modèle animal, les ISRSs n'induisent pas d'effet antidépresseur aigu, évalué par le test de nage forcée ; ni d'effet chronique neurogénique, évalué par l'analyse de la prolifération dans l'hippocampe. De plus, les effets psychoactifs induit par le MDMA (augmentation de la locomotion et sensibilisation locomotrice) ne sont pas observés par rapport aux souris témoins. En revanche, les effets hallucinogènes du DOI, un agoniste des R-5-HT$_{2A/2B/2C}$, évalués par le nombre de mouvements de tête spécifiquement induit par les hallucinogène (*« head-twitch »*) sont augmentés.

Ces résultats ont permis de vérifier que le R-5-HT$_{2B}$ participe aux effets des composés ciblant spécifiquement les acteurs du système sérotoninergique. En effet, les hallucinogènes, dont le DOI, activent les R-5-HT$_{2A}$ et le MDMA et les ISRSs ciblent SERT. Le transporteur SERT étant le principal régulateur des concentrations de 5-HT, il était crucial de savoir si l'absence de R-5-HT$_{2B}$ affecte l'expression ou les propriétés pharmacologiques de ce dernier. Des expériences de liaison et de recapture, sur synaptosomes, ont montré que SERT n'est pas affecté chez les animaux *5-HT$_{2B}^{5\text{-}HTKO}$*.

B. Le R-5-HT$_{2B}$ participe à l'activité des neurones sérotoninergiques

Des mesures électrophysiologiques *in vitro*, sur tranches issues d'animaux sauvages exprimant la GFP dans les neurones sérotoninergiques, ont montré que l'application d'un agoniste du R-5-HT$_{2B}$ (BW723C86) provoque une augmentation de la fréquence de décharge des neurones sérotoninergiques. Ces données montrent, pour la première fois, un effet positif des R-5-HT$_{2B}$ sur l'activité électrique des neurones sérotoninergiques.

Des mesures électrophysiologiques *in-vivo*, dans le DRN d'animaux anesthésiés, ont montré que les neurones des animaux *5-HT$_{2B}^{5\text{-}HTKO}$* n'ont pas la même activité que ceux des animaux témoins. En effet, la délétion du R-5-HT$_{2B}$ induit une diminution de la proportion de neurones déchargeant à une forte fréquence (4-5 Hz) et une augmentation du nombre de neurones déchargeant à une faible fréquence (0-1 Hz). Ces observations indiquent que le R-5-HT$_{2B}$ peut participer à l'excitabilité des neurones sérotoninergiques.

L'excitabilité des neurones 5-HT a été mesurée *ex-vivo* sur des tranches issues d'animaux infecté par un virus Flex-DIO. Cette construction Flex-DIO contient la séquence codant la protéine d'intérêt (R-5-HT$_{2B}$ ou *Tomato*) qui est flanquée de sites loxP orientés dans le sens inverse l'un de l'autre. La cre-recombinase clive et inverse les sites LoxP permettant ainsi l'expression de la protéine. Nous avons effectué cette infection sur des animaux exprimant la cre-recombinase et la GFP dans les neurones sérotoninergiques et dont le gène *Htr2b* est intact. Ainsi, nous avons développé un modèle de surexpression du R-5-HT$_{2B}$ dans les neurones sérotoninergiques. Cette surexpression virale du R-5-HT$_{2B}$ dans le noyau B7 du raphé provoque une augmentation significative de l'excitabilité des neurones sérotoninergiques par rapport aux souris infectées avec un virus contrôle induisant l'expression de la protéine fluorescente *Tomato*. Ces résultats confirment donc le fait que le R-5-HT$_{2B}$ participe à la modulation positive de l'activité des neurones 5-HT.

L'absence d'anticorps spécifique du R-5-HT$_{2B}$ rendant l'analyse de la distribution du récepteur impossible, nous avons fait en sorte que la construction virale du R-5-HT$_{2B}$ contienne un marqueur HA. Dans cet article, ces injections nous ont permis de surexprimer le R-5-HT$_{2B}$ dans les neurones 5-HT et de mesurer l'excitabilité des neurones. Par ailleurs, ce modèle nous sert aussi dans une étude en cours portant sur la distribution du R-5-HT$_{2B}$ dans les neurones 5-HT (axones, dendrites, synapses excitatrices et/ou inhibitrices). Ce modèle va nous permettre de déterminer la distribution du R-5-HT$_{2B}$ par rapport aux différents marqueurs sérotoninergiques (SERT, VMAT, TPH2).

C. Dualité fonctionnelle des R-5-HT$_{1A}$ et des R-5-HT$_{2B}$

Le R-5-HT$_{1A}$ est le principal autorécepteur inhibant l'activité des neurones sérotoninergiques. C'est pourquoi, nous avons testé le rôle excitateur du R-5-HT$_{2B}$ sur celui du R-5-HT$_{1A}$ chez des animaux sauvages.

Dans un premier temps, nous avons enregistré *in vivo* la fréquence de décharge des neurones sérotoninergiques en appliquant des concentrations croissantes de 8-OH-DPAT, inhibant ainsi l'activité des neurones sérotoninergiques de façon dose dépendante. Ensuite, nous avons réitéré cette expérience chez des souris préalablement traitées avec l'agoniste du R-5-HT$_{2B}$ et nous avons observé que la capacité d'inhibition du R-5-HT$_{1A}$ était significativement plus faible pour une même dose de 8-OH-DPAT. C'est-à-dire qu'en présence d'agoniste du R-5-HT$_{2B}$, il faut des concentrations plus fortes de 8-OH-DPAT pour obtenir la même inhibition de l'activité des neurones sérotoninergiques. Ceci montre que la modulation positive des neurones 5-HT par le R-5-HT$_{2B}$ est suffisante pour contrebalancer l'auto-inhibition induite par le R-5-HT$_{1A}$.

Au niveau comportemental, l'inhibition de la transmission sérotoninergique par le 8-OH-DPAT provoque une diminution de la température corporelle. Afin de savoir si l'effet positif du R-5-HT$_{2B}$ peut agir sur cet effet, nous avons mesuré la température corporelle en réponse au 8-OH-DPAT chez des animaux pré-traités avec une solution saline ou avec l'agoniste du R-5-HT$_{2B}$. Chez les animaux ayant reçu une injection d'agoniste du R-5-HT$_{2B}$, le retour à une température corporelle normale est plus rapide que chez les animaux ayant reçu une solution saline.

Ces données confirment la capacité des R-5-HT$_{2B}$ à moduler l'activité des neurones sérotoninergiques de façon opposée au R-5-HT$_{1A}$.

D. Conclusion

Cette étude a permis de montrer que les R-5-HT$_{2B}$ exprimés par les neurones sérotoninergiques modulent positivement l'activité des neurones 5-HT. Cette modulation positive dépendante des R-5-HT$_{2B}$ est suffisamment importante pour pouvoir contrer les effets inhibiteurs des autorécepteurs 5-HT$_{1A}$ au niveau comportemental. Enfin, le R-5-HT$_{2B}$ est nécessaire à l'action des molécules induisant une accumulation extracellulaire de 5-HT (MDMA, ISRSs).

E. Contribution personnelle

Dans cette étude, j'ai pris en charge les lignées de souris *5-HT$_{2B}^{5\text{-}HTKO}$* et effectué les croisements permettant d'obtenir les deux lignées de transgéniques conditionnelles dans les neurones sérotoninergiques exprimant la GFP (Pet1cre/0 ; fl/fl ; RCE/RCE et Pet1cre/0; RCE/RCE). J'ai participé aux tests de locomotion et de sensibilisation induit par le MDMA dans ces lignées. Sur les animaux *5-HT$_{2B}^{5\text{-}HTKO}$*, j'ai effectué les marquages contre la 5-HT afin de montrer la colocalisation avec la GFP et vérifié que les neurones recombinés sont bien sérotoninergiques. J'ai effectué le clonage du R-5-HT$_{2B}$ pour la création du virus, que j'ai ensuite injecté en stéréotaxie dans le noyau (B7) du raphé. Enfin, j'ai effectué les marquages afin de déterminer l'expression et la diffusion du virus dans les neurones du raphé.

Title. Positive regulation of raphe serotonin neurons by serotonin 2B receptors.

Short title. **5-HT$_{2B}$ receptors in serotonergic neurons**

Author List. Arnauld Belmer[1,3*], Emily Quentin[1*], Silvina L. Diaz[1,4], Bruno P. Guiard[2], Sebastian P. Fernandez[1,5], Stéphane Doly[1,6], Sophie M. Banas[1], Pothitos M. Pitychoutis[1,7], Imane Moutkine[1], Aude Muzerelle[1], Anna Tchenio[1,8], Anne Roumier[1], Manuel Mameli[1,8], and Luc Maroteaux[1]

[1] INSERM UMR-S 839, F75005, Paris, France; Sorbonne Universités, UPMC Univ Paris 6, F75005, Paris; Institut du Fer à Moulin, F75005, Paris.

[2] Research Center on Animal Cognition, Center for Integrative Biology, Toulouse, France; Université Paul Sabatier, Toulouse, France; UMR5169 CNRS, Toulouse, France

Present adresses:

[3] Translational Research Institute, Queensland University of Technology, Brisbane Qld 4059, Australia

[4] IBCN - Paraguay 2155, 3º piso, C1121ABG Buenos Aires, Argentina

[5] IPMC – CNRS UMR7275 660 Route des Lucioles Sophia-Antipolis 06560 Valbonne France

[6] Université Clermont Auvergne, INSERM, NEURO-DOL, F-63000 Clermont-Ferrand, France.

[7] Department of Biology & Center for Tissue Regeneration and Engineering at Dayton (TREND), University of Dayton, 300 College Park, Dayton, 45469-2320, Ohio, USA

[8] Dept. Fundamental Neurosciences (DNF) The University of Lausanne, Rue du Bugnon 9 1005 Lausanne Switzerland

*Equal contributors

Corresponding author: Luc Maroteaux, Institut du Fer à Moulin UMR-S839 INSERM/UPMC 17 rue du Fer à Moulin 75005 Paris Email: luc.maroteaux@upmc.fr; Tel: (33) 01 45 87 61 23 Fax: (33) 01 45 87 61 32

Number of words in abstract: 248 ; Number of words in text: 4180. Number of tables: 0; Number of figures: 5; Number of supplementary material 1.

Keywords: Serotonin, electrophysiology, viral overexpression, conditional knockout, MDMA, SSRI.

Abstract.
Background: The activity of neurons synthetizing serotonin in raphe nuclei can be modulated not only by 5-HT_{1A} but also by 5-HT_2 receptors with responses ranging from inhibition to excitation. However, direct roles of 5-HT_2 receptors have not been yet clearly established. In this work, we tested the hypothesis that the 5-HT_{2B} receptor directly regulates raphe serotonin neuron activity.

Methods: We used a combination of pharmacologic and genetic approaches with *in-vivo* and *ex-vivo* electrophysiology, viral-mediated overexpression,and behavior in mice to study the raphe serotonin neuron functions.

Results: Stimulation with a 5-HT_{2B} receptor agonist, BW723C86, increased raphe serotonin neuron firing frequency as shown by electrophysiological cell-attached recordings. Independently, viral overexpression of 5-HT_{2B} receptors in dorsal raphe neurons increased their excitability in current-clamp electrophysiological recordings. In addition, BW723C86 counteracted the 8-OHDPAT-dependent *in-vivo* 5-HT_{1A} autoreceptor-dependent reduction in firing rate and hypothermic response. By developing a conditional genetic ablation strategy to eliminate *Htr2b* gene expression specifically and exclusively from Pet1-positive serotonin neurons ($Htr2b^{5\text{-}HTKO}$ mice), we observed that MDMA behavioral and sensitizing effects were eliminated in $Htr2b^{5\text{-}HTKO}$ mice. As well, acute behavioral and chronic neurogenic effects of fluoxetine were abolished in $Htr2b^{5\text{-}HTKO}$ mice. Dorsal raphe serotonin neuron of $Htr2b^{5\text{-}HTKO}$ mice displayed a shift toward low firing frequency of compared to control $Htr2b^{lox/lox}$ mice as assessed by *in-vivo* extracellular recordings. The increase in head twitch response to DOI further confirmed the lower serotonergic tone in these conditional mutant mice.

Conclusions: Together, these observations established the 5-HT_{2B} receptor as a direct positive modulator of serotonin neurons.

Introduction

Serotonin (5-Hydroxytryptamine, 5-HT) innervates the forebrain, including the cerebral cortex. These 5-HT neurons originates predominantly from the rostral cell group of neurons in the dorsal raphe nucleus (DRN)[1, 2]. DRN neurons express many serotonergic markers including tryptophan hydroxylase (TPH2-*Tph2*), 5-HT transporter (SERT-*Slc6a4*), 5-HT_{1A} (Htr_{1A}) and 5-HT_{1B} (Htr_{1B}) receptors. The negative 5-HT_{1A} autoreceptor expression is restricted to the somatodendritic compartment of 5-HT neurons, whereas 5-HT_{1B} autoreceptors are targeted to axonal terminals[3]. The existence of synaptic vesicles in 5-HT neuron dendrites led to the suggestion that autoinhibition is mediated via dendritic release of 5-HT[4]. In fact, the 5-HT_{1A} autoreceptor activation by released 5-HT in the DRN elicits an outward current carried through G protein-coupled inwardly-rectifying potassium channels of the Kir3 (GIRK-*Kcnj*) family leading to membrane hyperpolarization and the inhibition of 5-HT neuron firing[5]. However, the activity of 5-HT DRN neurons can be modulated not only by 5-HT_{1A} but also by 5-$HT_{2A/B/C}$ receptors triggering inward currents[6-10]. DRN neurons can thus respond to 5-HT with responses ranging from inhibition to excitation depending on a balance of functional 5-HT_{1A} and 5-$HT_{2A/B/C}$ receptors[11]. However, direct roles of 5-HT_2 receptors have not been yet clearly established for 5-HT neurons.

In humans, a lack of 5-HT_{2B} receptor is associated with 5-HT-dependent phenotypes, including impulsivity and suicidality[12]. Pharmacological experiments in rats indicated that the 5-HT_{2B} receptor preferential agonist BW723C86[13] exhibited anxiolytic-like properties[14-16]. In mice, stimulation of 5-HT_{2B} receptor by BW723C86 induced a serotonin specific reuptake inhibitor (SSRI)-like action in the in the forced swimming test (FST), which is abolished in mice knocked-out (KO) for 5-HT_{2B} receptor gene ($Htr2b^{-/-}$)[17]. In addition to impulsive behavior[12], $Htr2b^{-/-}$ mice display a global deficit in sensorimotor gating as well as novelty-induced hyperlocomotion. These phenotypes have been related to positive symptoms observed in schizophrenia[18], a disorder commonly associated to a deregulation of the 5-HT systems.

Further evidence indicated that 5-HT_{2B} receptors could modulate directly or indirectly 5-HT neurons. Indeed, genetic (KO) or pharmacologic manipulation (antagonist) of 5-HT_{2B} receptors also interferes with the effects of molecules that directly target 5-HT systems including SERT-targeting antidepressant SSRIs, amphetamine-derivatives 5-HT releasers MDMA and dexfenfluramine[19-21]. For examples, long-term behavioral and neurogenic SSRI effects were also abolished after either genetic ablation or chronic exposure to pharmacologic antagonists of 5-HT_{2B} receptors[22], and could be mimicked by chronic exposure to BW723C86. As well the enhanced locomotor response to the psychostimulant MDMA was abolished[20].

Altogether, these studies suggest that 5-HT_{2B} receptors could be implicated in 5-HT-dependant behavior by acting onto the 5-HT neurons. Nevertheless, the precise localization and way of action of 5-HT_{2B} receptors to triggers such behavioral effects are still poorly investigated. Main difficulties include the lack of specific antibody as well as the low level of expression of 5-HT_{2B} receptors in mouse[23] or human brains[24, 25]. Nevertheless the expression of the 5-HT_{2B} receptor mRNA was confirmed in several brain nuclei including the DRN[26] in rats. Besides, study using single cells PCR[22] permitted to established the presence of neurons expressing 5-HT_{2B} together with 5-HT_{1A} receptors and TPH2, pointing out a 5-HT_{2B} receptor expression not only in raphe but more precisely in some 5-HT neurons. Finally, local infusion of BW723C86 in the DRN produced a robust accumulation of extracellular 5-HT that is blocked by RS127445, a selective 5-HT_{2B} receptor antagonist [20] supporting a functional role of this receptor within the raphe. Despite the evidence of 5-HT_{2B} receptor expression in 5-HT neurons, its precise role in 5-HT neurons function remain elusive since pharmacologic manipulation or general knockout does not permit to distinguish effects due to direct activation in 5-HT neuron from action at other part of the brain (or circuit rearrangement for general KO).

In the present work, we tested the hypothesis that the 5-HT_{2B} receptor is a direct regulator of 5-HT neurons activity. *Ex-vivo* electrophysiological recordings of identified raphe 5-HT neurons revealed that stimulation of the 5-HT_{2B} receptor can increase firing frequency of raphe neurons. Furthermore, a 5-HT_{2B} receptor overexpression in raphe 5-HT neurons triggers a higher excitability of 5-HT neurons. *In-vivo* experiments revealed that stimulation of the 5-HT_{2B} receptor acts in an opposite way to the negative autoreceptor 5-HT_{1A}. Using a conditional ablation of the 5-HT_{2B} receptor gene specifically in raphe 5-HT neurons, we show that many phenotypes (MDMA and DOI psychoactive effects, SSRI antidepressant effects) observed in complete *Htr2b*$^{-/-}$ mice can be reproduced and support a reduced serotonergic tone. Together, these findings established for the first time that the 5-HT_{2B} receptor acts as a direct positive modulator of 5-HT neurons.

Materials and Methods (see extended methods in supplementary materials)

Animals- *Htr2b*$^{-/-}$ mice on a 129S2 background were compared to 129S2 *Htr2b*$^{+/+}$ mice (8-10 wks. old); *Htr2b*$^{fl/fl}$ mice generated on a mixed 129S2.B6 background were backcrossed >10 times onto the 129S2 strain. All experiments involving mice were approved by the local ethical committee (N° 1170.02).

Ex-vivo **electrophysiology-Cell attached** -Electrophysiological recordings and molecular characterization of 5-HT neurons was conducted in acute brain slices from male Pet1-EGFP mice aged 3–4 weeks old according to published procedures[27].

Viral constructs and stereotaxic injection -The 5-HT$_{2B}$-HA was cloned into a pAAV-EF1A-DIO-WPRE-pA vector (Addgene), packaged into AAV2.9 serotype and titers of 10^{12}–10^{13} viral particles/ ml were obtained (UNC Vector Core, Chapel Hill USA). AAV2.9 DIO-Tomato was used as a control. AAVs were injected in the B7 raphe nuclei of *Pet1cre*$^{0/+}$*; RCE/RCE* following procedure described[28].

Ex-vivo **electrophysiology-Current clamp** -Mice of either sex aged ~9 weeks were deeply anesthetized with ketamine and xylazine (150 mg/kg and 10 mg/kg, respectively; i.p.; Sigma-Aldrich, France) and immediately sacrified. Coronal brain slices containing the raphe nucleus were prepared as previously described[29].

8-OHDPAT-induced hypothermia -Body temperature was then measured every 10 min after the injection during 40 additional minutes[30].

In-vivo **electrophysiology of DRN 5-HT neurons** -The extracellular recordings of the 5-HT neurons in the DRN were performed according to[31]. The DRN 5-HT neurons were identified according to the criteria of Aghajanian and Vandermaelen[32].

Generation of *Htr2b* floxed mice -*Htr2b*$^{fl/fl}$ mice were inactivated for *Htr2b* in 5-HT neurons by crossing with e*Pet1-Cre* mice[33] generating *Pet1-Cre*$^{+/0}$*; Htr2b*$^{lox/lox}$ conditional knockout mice (*Htr2b*$^{5\text{-}HTKO}$) and *Pet1-Cre*$^{0/0}$*; Htr2b*$^{lox/lox}$ littermate controls (*Htr2b*$^{lox/lox}$). This strain was generated on a mixed 129S2.B6 background used as F3 offspring of the 129S2 strain. Efficiency of recombination was tested using of *Pet1-Cre*$^{+/0}$;*Gt(ROSA)26Sor*$^{tm1.1(CAG-EGFP)Fsh}$ (*Htr2b*$^{5\text{-}HTKO}$*;RCE*) mice, who express GFP in 5-HT neurons only after Cre recombination.

Locomotor response to novelty and MDMA-induced hyperlocomotion and sensitization - Locomotor activity was measured as previously described[20], in a circular corridor with four infrared beams placed at every 90° (Imetronic, Passac, France). MDMA-induced locomotor sensitization was performed in a two-injection protocol as previously described[19].

Prepulse Inhibition (PPI) of acoustic startle- Sensorimotor gating was assessed as previously described[18].

Forced Swimming Test -Mice FST was conducted essentially as described by[17].

Fluoxetine treatments, Proliferation assay -Flx dose selection and FST were performed as described[17]. Neurogenesis study was performed as described[22].

Synaptosome study -Crude synaptosomes were prepared as previously described[34]. Synaptosomes 5-HT uptake and citalopram competition experiments were performed as described [20].

DOI-induced head-twitch -DOI-induced head twitch experiment was performed in clear plastic cages lined with bedding. Head-twitches (lateral movements of the head from side to side) induced by DOI (10 mg/kg, ip) were scored for 30 minutes immediately after administration, by two experimenters and individual scores were averaged.

Statistical analysis- To determine differences between the experimental groups, responses were analyzed by Two-tailed unpaired Student´s t test or Mann-Whitney test when distribution is not normal or a Two-way analysis of variance (ANOVA) with Bonferroni's test was used for *post hoc* multiple comparisons. In all cases, $P < 0.05$ was considered statistically significant.

Results

E*x-vivo* electrophysiological responses to 5-HT$_{2B}$ receptor stimulation and overexpression

To examine a direct role of 5-HT$_{2B}$ receptors on 5-HT neuron activity, we first performed cell-attached electrophysiological recordings of identified DRN 5-HT neurons expressing GFP (*Pet1cre$^{0/+}$; RCE/RCE* mice). *In-vivo*, DRN neurons fire in a regular pattern at 0.5–5 Hz. However, 5-HT neurons in *ex-vivo* brain slices are electrically quiescent, but an excitatory noradrenergic tone facilitates firing[35]. In order to reproduce noradrenergic input, subsaturating concentrations of phenylephrine (Phe, 100-300 nM)[36] were added to the bath. Low concentration (100 nM) of Phe was unable to initiate regular firing nor was application of the preferential 5-HT$_{2B}$ receptor agonist BW723C86 (1µM). However, 300 nM Phe was able maintained a regular firing and subsequent application BW723C86 (1µM) induced a significant increase in firing frequency (1.73 ± 0.23-fold, *n* = 8) compared to Phe alone (unpaired t-test, $t_{14} = 2.99$, $P = 0.0098$, n = 8; **Fig. 1A**). These data were the first to indicate that 5-HT$_{2B}$ receptor stimulation could increase raphe 5-HT neuron electrical activity *ex-vivo*.

To further establish that 5-HT$_{2B}$ receptors can directly affect 5-HT neuron activity, adeno-associated viruses (AAV2.9) were used to obtain a conditional overexpression of 5-HT$_{2B}$-HA-tagged receptor exclusively in 5-HT raphe neurons. AAV-DIO-5-HT$_{2B}$-HA or control AAV-DIO-Tomato virus was unilaterally injected into B7 raphe nucleus of *Pet1cre$^{0/+}$;RCE/RCE* mice (**Fig. S1A**). We confirmed the proper injection site by colocalization of either Tomato expression or HA immunofluorescence with GFP positive 5-HT neurons (**Fig. S1B**). Coronal raphe-containing brain slices were used for recordings of GFP positive 5-HT neuron excitability performed in current clamp mode using a solution containing synaptic blockers for AMPA, GABA and NMDA receptors. Recordings at various current steps showed that the number of action potentials obtained in function of the current injected was significantly increased in 5-HT neurons overexpressing 5-HT$_{2B}$ receptors. Two-way ANOVA RM, showed a main effect of overexpression, ($F_{1, 39} = 4.94$ *P = 0.032*) (**Fig. 1B**). Input resistance value from recorded neurons was also significantly increased in 5-HT$_{2B}$-HA overexpressing neurons (unpaired t-test $t_{39} = 2.054$, $P = 0.047$) (**Fig. 1C**). This implies increased density of open ion channels upon 5-HT$_{2B}$ receptor overexpression. *Ex-vivo* recordings of raphe neurons revealed that overexpression of 5-HT$_{2B}$ receptor in 5-HT neurons increases their excitability.

In-vivo responses to 5-HT$_{1A}$ and 5-HT$_{2B}$ receptor agonists

The activity of 5-HT neurons is negatively modulated by somatodendritic 5-HT$_{1A}$ autoreceptors. To confirm these initial *ex-vivo* results, we assessed the putative effects of stimulating 5-HT$_{2B}$ receptors on 5-HT$_{1A}$ autoreceptor functional activity and hypothesized that it works in an opposite way to 5-HT$_{1A}$ negative regulatory activity. The 5-HT$_{1A}$ autoreceptors are activated by 5-HT released from 5-HT collaterals. This stimulation elicits an outward current leading to inhibition of 5-HT neuron firing. We thus tested the effect of BW723C86 (5 mg/kg sc) on 8-OHDPAT-induced inhibition of neuronal firing frequency *in-vivo*. Interestingly, 8-OHDPAT was significantly less potent in suppressing 5-HT neuronal firing activity after BW723C86 injection and ED50 was shifted about 3.3-fold from 45 to 148 µg/kg (**Fig. 2A**) although BW723C86 alone did not modify firing (not illustrated). ANOVA RM analysis showed a main effect of BW723C86 treatment ($F_{6, 54} = 31.14$; *P < 0.0001*) and Bonferroni's *post-hoc*

analysis a reduced effect of 8-OHDPAT (at 50 and 100 mg/kg sc) on 5-HT neuronal firing activity (**Fig. 2A**).

Although the mechanism of 5-HT_{1A} receptor agonist-induced hypothermia is poorly defined[37], the 8-OHDPAT-induced hypothermia in mice is known to be mediated by 5-HT_{1A} autoreceptor[38]. We then used the 8-OHDPAT-induced hypothermia as readout of the functional status of 5-HT_{1A} autoreceptor and tested the effect of stimulating 5-HT_{2B} receptors. In agreement with the above-mentioned effect on firing, a pretreatment with BW723C86 (5 mg/kg sc) was able to reduce significantly the ability of 8-OHDPAT (0.3 mg/kg sc), to induce hypothermia in WT mice (**Fig. 2B**). ANOVA RM analysis showed a significant interaction between the time and treatment ($F_{9, 54} = 10.34$; $P < 0.0001$). Bonferroni's *post-hoc* analysis showed a significant reduction by BW723C86 (at t70 and 80 min post-injection) of the 8-OHDPAT-induced hypothermia (**Fig. 2B**). These data indicate that 5-HT_{1A} autoreceptor inhibitory activities can be attenuated by concomitant activation of 5-HT_{2B} receptors.

Absence of response to MDMA in *Htr2b$^{5\text{-}HTKO}$* mice

To further establish the functions of 5-HT_{2B} receptors in 5-HT neurons, we developed mice with conditional ablation of the 5-HT_{2B} receptor gene specifically in raphe 5-HT neurons by inserting recombination sites (loxP) flanking the *Htr2b* second exon (*Htr2b$^{fl/fl}$*). Crossing with mice expressing the Cre recombinase under the *Pet1* gene promoter, whose expression in the brain is restricted to 5-HT neurons and their postmitotic precursors[33], we generated *Pet1-Cre$^{+/0}$; Htr2b$^{lox/lox}$* mice (*Htr2b$^{5\text{-}HTKO}$*) (**Fig. S2A**). Restricted recombination in raphe 5-HT neurons was revealed by analysis of raphe DNA and RCE reporter (**Fig. S2B-C**). The *Htr2b$^{5\text{-}HTKO}$* mice injected with MDMA (20 mg/kg) did not display locomotor responses in contrast to control *Htr2b$^{lox/lox}$* littermate mice (**Fig. 3A-C**). Two-way ANOVA RM analysis showed a main effect of genotype ($F_{1, 14} = 5.106$; $P = 0.0403$), and Bonferroni's *post-hoc* analysis a significant difference between genotypes from t=25 to t=45 min post-injection (**Fig. 3A**). Furthermore, the analysis of the total locomotor activity over the first 60 min after MDMA injection revealed a significantly lower locomotion in *Htr2b$^{5\text{-}HTKO}$* compared to control *Htr2b$^{lox/lox}$* mice, with a main effect of genotype ($F_{1, 60} = 4.612$; $P = 0.0358$) (**Fig. 3B**).

We further assessed the contribution of raphe 5-HT_{2B} receptors to MDMA-induced locomotor sensitization using a two-injection protocol in *Htr2b$^{5\text{-}HTKO}$* mice (**Fig. 3C**)[39]. In *Htr2b$^{5\text{-}HTKO}$* mice, no change in locomotor response could be observed after a second injection of MDMA (20 mg/kg) (1st inj=254 ± 132 *vs.* 2nd inj=353 ± 174, n=8) (**Fig. 3C**). However, a second injection significantly increased the hyperlocomotor response elicited by the first in *Htr2b$^{lox/lox}$* control mice (1st inj= 639 ± 222 *vs.* 2nd inj= 1291 ± 295 1/4 of turns, P <0.0001, n=8). ANOVA RM analysis showed a main effect of genotype ($F_{1, 14} = 5.106$; $P = 0.0403$). These results indicate a lack of behavioral and sensitizing effects of MDMA in *Htr2b$^{5\text{-}HTKO}$* mice and confirmed that these *Htr2b$^{-/-}$* mice phenotypes were due to the elimination of this receptor in 5-HT neurons.

Absence of response to the SSRI Fluoxetine in *Htr2b$^{5\text{-}HTKO}$* mice

A classical test for the acute response to SSRIs is the forced swimming test (FST). We tested the effect of acute Flx injection (3 mg/kg, ip, the optimal dose in 129S2 strain[17]) in FST. Administration of Flx in *Htr2b$^{5\text{-}HTKO}$* mice did not affect immobility time. However, a significant reduction of immobility time was observed in control *Htr2b$^{lox/lox}$* littermates (**Fig. 4A**). Two-way ANOVA analysis showed a significant time x genotype interaction ($F_{1, 24} = 10.67$; $p<0.003$) and Bonferroni's *post-hoc* analysis showed the only significant difference between vehicle and Flx-treated *Htr2b$^{lox/lox}$* controls (**Fig. 4A**).

Long-term effects of SSRI are known to trigger hippocampus subgranular zone (SGZ) neuronal proliferation. We performed a daily ip injection for 4 weeks of Flx (3 mg/kg) and looked for BrdU

incorporation in SGZ neurons of the hippocampus. Chronic injection of Flx in *Htr2b*$^{5\text{-}HTKO}$ mice did not produce any change in BrdU incorporation, while a significant increase was detected in controls *Htr2b*$^{lox/lox}$ littermates (**Fig. 4B**). Two-way ANOVA analysis showed a trend for time x genotype interaction ($F_{1, 26} = 3.88$; *P = 0.059*) and Bonferroni's *post-hoc* analysis showed only a significant difference between vehicle and Flx-treated *Htr2b*$^{lox/lox}$ controls (**Fig. 4B**). These results indicate a lack of both acute behavioral and chronic neurogenic effects of SSRIs in *Htr2b*$^{5\text{-}HTKO}$ mice.

We recently reported that *Htr2b*$^{-/-}$ mice display novelty-induced hyperlocomotion and a global deficit in sensorimotor gating. However, locomotor activity in a new environment was not different between *Htr2b*$^{5\text{-}HTKO}$ and *Htr2b*$^{lox/lox}$ littermate control mice over a 60-minute period (**Fig. S3A**). Similarly, prepulse inhibition (PPI) of startle reflex and startle amplitude were not different between *Htr2b*$^{5\text{-}HTKO}$ and *Htr2b*$^{lox/lox}$ littermate control mice (**Fig. S3B**). Although present in *Htr2b*$^{-/-}$ mice, these deficits are not reproduced in mice lacking the 5-HT_{2B} receptor selectively in 5-HT neurons and thus rely on 5-HT_{2B} receptor expressed in other cell type.

Since SERT targeting drug (MDMA and Flx) action is affected by the lack of 5-HT_{2B} receptors in 5-HT neurons, we next determined whether this lack could alter SERT expression or function in whole brain synaptosome preparations from *Htr2b*$^{5\text{-}HTKO}$ mice. Heterologous competition binding experiments showed no difference in the density of citalopram binding sites (Bmax; 305±18 vs. 389±26 fmol/mg of protein) or in paroxetine affinity (Ki; 0.4±0.1 vs. 0.17+0.06 nM) between *Htr2b*$^{5\text{-}HTKO}$ mice and their *Htr2b*$^{lox/lox}$ littermate control mice (**Fig. 4C**). Additionally, 5-HT uptake experiments showed no difference in 5-HT transport maximum velocity (Vmax; 5.57±0.32 vs. 6.49±0.38 fmol/sample/min) or apparent affinity for 5-HT (Km 40.7±2.6 vs. 27.7±2.5 nM) between *Htr2b*$^{5\text{-}HTKO}$ mice and their *Htr2b*$^{lox/lox}$ littermate controls (**Fig. 4C**). Together, these results demonstrated that selective ablation of 5-HT_{2B} receptors in raphe 5-HT neurons eliminates SSRI action but does not affect SERT expression and activity.

Htr2b$^{5\text{-}HTKO}$ mice display a hyposerotonergic phenotype

To determine whether the 5-HT_{2B} receptor had an overall effect on serotonergic tone, we measured the firing rates of 5-HT DRN neurons in *in-vivo* anesthetized animals. Neurons were included in the analysis based on the characteristics of their action potentials, and averaged traces of these action potentials[36]. *Htr2b*$^{5\text{-}HTKO}$ mice display a higher percentage of 5-HT neurons discharging with a low firing mode (16.1% vs. 9.3% <1 Hz) and a lower percentage of 5-HT neurons with a high firing mode (5.9% vs. 13.9% >4 Hz) relative to *Htr2b*$^{lox/lox}$ mice. Overall DRN 5-HT neurons in *Htr2b*$^{5\text{-}HTKO}$ mice are more likely to fire at lower rates (1.88 ± 0.11 Hz; n=118) than *Htr2b*$^{lox/lox}$ control mice. We observed a trend toward reduced mean firing rates in *Htr2b*$^{5\text{-}HTKO}$ compared to *Htr2b*$^{lox/lox}$ (Mann-Whitney test, P = 0.13) (**Fig. 5A**).

The head-twitch response (HTR) is a rhythmic paroxysmal rotational head movement that occurs in mice and rats treated by a variety of serotonergic hallucinogens, including LSD and DOI[40]. This behavior is specifically linked to 5-HT_{2A} receptor activation, since selective 5-HT_{2A} receptor antagonists block the HTR induced by DOI and other hallucinogens, and is absent in *Htr2a*$^{-/-}$ mice[40]. A drastic increase in the number of DOI-induced HTR was observed in the *Tph2-R439H* knock-in mouse[37] (a mouse model with 60-80% reduction in TPH2 activity and thus with low serotonergic tone). Here, we studied the ability of DOI (5 mg/kg ip) to cause HTR in *Htr2b*$^{-/-}$ and *Htr2b*$^{5\text{-}HTKO}$ mice (**Fig. 5B**). DOI induced a greater HTR in *Htr2b*$^{-/-}$ than in control mice (+94%; $t_{10} = 2.43$, n = 6, P = 0.036, unpaired t-test) (**Fig. 5B**). Similarly an increase in HTR was observed in *Htr2b*$^{5\text{-}HTKO}$ mice, as compared to *Htr2b*$^{lox/lox}$ littermate control (+61%, $t_{13} = 2.23$, n = 7-8, P = 0.044, unpaired t-test). These results reveal that ablation of 5-HT_{2B} receptors in raphe 5-HT neurons is sufficient to modify their firing rate and increase the behavioral response to DOI, supporting a lowering of serotonergic tone.

Discussion

In the present work, we show that stimulation of 5-HT_{2B} receptors increased the firing rate of 5-HT neurons in slices and the local overexpression of 5-HT_{2B} receptors in raphe 5-HT neuron increases their excitability. In addition, the *in-vivo* 5-HT_{2B} receptor stimulation counteracts the 5-HT_{1A} receptor-dependent reduction in firing rate of raphe 5-HT neurons and hypothermic response. To the opposite, mice lacking 5-HT_{2B} receptors exclusively in 5-HT neurons, *Htr2b*$^{5\text{-}HTKO}$ mice, display several 5-HT-dependent deficits including (i) an absence of behavioral and sensitizing effects of MDMA, (ii) a lack of acute behavioral and chronic neurogenic action of the SSRI Flx, and (iii) an increased number of low firing neuron and of DOI-induced HTR, that support a reduced serotonergic tone.

There is a growing consensus that DRN 5-HT neurons are non-homogeneous. Heterogeneity of DRN neurons has been suggested by anatomical, biochemical and electrophysiological properties[11, 27, 41-44]. Sub-populations of 5-HT neurons, either within the DRN or between various raphe nuclei, are interconnected, or form complex circuits[45-47]. The activity of some 5-HT DRN neurons has been shown to be modulated by both 5-HT_{1A} and 5-$HT_{2A/B/C}$ receptors[7, 9]. Identified 5-HT DRN neurons are known to respond to 5-HT_{1A} receptor agonists[6, 8] by a 5-HT-induced outward current[6-10]. A significant proportion of TPH2-positive neurons (about 50%) also respond to 5-HT_2 receptor activation by an inward current[11]. Tonic spiking of 5-HT neurons establishes 5-HT levels in synapses. We show here by electrophysiological cell-attached recordings of identified raphe 5-HT neurons that stimulation of 5-HT_{2B} receptors by BW723C86 increases their firing frequency. Independent electrophysiological current-clamp recordings of identified DRN 5-HT neurons revealed a higher excitability of 5-HT neurons overexpressing 5-HT_{2B} receptors. These results confirm that 5-HT_{2B} receptors are able to positively control the excitability of 5-HT neurons. Furthermore, *in-vivo* extracellular recordings that *Htr2b*$^{5\text{-}HTKO}$ mice display a shift toward low firing rate of 5-HT neurons. The lack of 5-HT_{2B} receptors in 5-HT neurons in *Htr2b*$^{5\text{-}HTKO}$ mice confirms the need for 5-HT_{2B} receptors in regulating serotonergic tone, and stimulation of 5-HT_{2B} receptors increases 5-HT neurons firing in an opposite manner to 5-HT_{1A} autoreceptors.

The unique control of dendritic 5-HT release has important implications for DRN physiology and the SSRI action. Packaging by the vesicular monoamine transporter (VMAT2) is essential for 5-HT transmission and glutamate receptor activation in dorsal raphe brain slice evoked somatic release by vesicle exocytosis[48]. SSRIs and MDMA are SERT-targeting drugs. The lack of effects of these drugs in the absence of 5-HT_{2B} receptors in 5-HT neurons raises the possibility that these receptors directly interact with 5-HT transporter. However, the apparent lack of modification in SERT uptake and expression lowers this possibility. 5-HT released within the DRN induces feedback inhibition of 5-HT neuron activity by stimulating somatodendritic 5-HT_{1A} negative autoreceptors and appears to result from the local release rather than the extended diffusion of 5-HT throughout the extracellular space[49]. The hypothermic response to 8-OHDPAT, known to be mediated by 5-HT_{1A} auto- but not hetero-receptors in mice[38], is attenuated by the 5-HT_{2B} receptor agonist BW723C86 or in hyposerotonergic mice with reduction in TPH2 activity, the *Tph2-R439H* knock-in mice[37, 50]. In addition, these *Tph2-R439H* knock-in mice displayed exaggerated HTR after injection of DOI[37], as either full *Htr2b*$^{-/-}$ or raphe selective *Htr2b*$^{5\text{-}HTKO}$ mice. The degree of 5-HT system autoinhibition has been deduced from functional assays using activation of 5-HT_{1A} receptors with direct agonists, for example blunted hypothermia. Richardson-Jones et al.,[38] generated a mouse strain differing in 5-HT_{1A} autoreceptor expression by approximately 30-40% below the WT level (1A-Low). The 1A-Low mice showed reduced 8-OHDPAT-induced hypothermia and their neurons exhibited a shift toward higher firing rates. In the absence of 5-HT_{2B} receptors in 5-HT neurons, we found a shift toward lower frequency firing neurons. Together with reduced 8-OHDPAT-induced hypothermia and higher HTR, these findings support that the lack of 5-HT_{2B} receptor in 5-HT neurons generates hyposerotonergic mice. Thus serotonergic tone results from the opposite control exerted by 5-HT_{1A} and 5-HT_{2B} receptors, and explains the lack of response to SERT blockers (Flx) and releasers (MDMA) in *Htr2b*$^{5\text{-}HTKO}$ mice.

Chronic SSRI responses are usually ascribed to desensitization of somatodendritic 5-

HT_{1A} receptors. Recent works using a chemogenetic approach (e.g., Designer Receptors Exclusively Activated by Designer Drugs-DREADDs) showed that short- and long-term CNO mactivation of DRN 5-HT neurons expressing the Gq-coupled M3Gq DREADD induced an increase in 5-HT levels and firing rate and antidepressant-like behavioral responses[51, 52]. We showed previously that activating 5-HT_{2B} Gq-coupled receptors with BW723C86 mimics both acute and chronic behavioral and neurogenic effects of SSRI antidepressants, including novelty suppressed feeding test (NSF) and FST[17, 22]. We found here that knocking-out the 5-HT_{2B} receptors specifically from 5-HT neurons in *Htr2b*$^{5\text{-}HTKO}$ eliminates acute behavioral and chronic neurogenic effects of Flx. It appears thus that 5-HT_{2B} receptors contribute to SSRI therapeutic effects by their direct stimulation on adult 5-HT neurons.

The reason why the positive action of 5-HT_{2B} receptors acting in an opposite manner to 5-HT_{1A} autoreceptors has not yet been identified could have several explanations. For example, the 5-$HT_{2A/2C}$ receptor mRNAs have been shown to be expressed by γ-Aminobutyric acid (GABA) inhibitory interneurons located in the DRN. Systemic administration of DOI increases c-fos immunoreactivity in GABAergic interneurons of the DRN[53] supporting that DOI reduces the firing of 5-HT neurons by increasing GABA release in the DRN. The local application of DOI (a 5-$HT_{2A/2B/2C}$ receptor agonist) in this area induces a dose-dependent increase in the frequency of inhibitory postsynaptic currents (IPSCs)[9]. This local inhibitory mechanisms cooperating with 5-HT_{1A} negative autoreceptors, obviously masked the presence of the positive 5-HT_{2B} receptor-dependent regulatory mechanisms in DRN neurons.

An unsolved question is why both positive and negative autoreceptors are needed to regulate 5-HT neuron activity. In the nucleus locus coeruleus (LC), the major noradrenergic nucleus of the brain, resting membrane potential and a pattern of spontaneous firing neurons are affected by both α1- and α2-adrenergic receptors activation[54] in newborns. The application of the α2-adrenergic receptor agonists activates GIRK channels, resulting in membrane hyperpolarization and inhibition of the spontaneous firing of the action potentials[55]. By contrast, stimulating α1-adrenergic receptors, known to couple to a Gq protein, induced membrane depolarization and accelerated spontaneous firing rates in neonatal rat LC neurons[56] and alterations of these may trigger pathological conditions[54]. Mixtures of positive and negative feedback has been modeled and shown to be necessary to create single pulses or oscillatory signal outputs[57], which are important for neuronal functions. Our findings established that 5-HT_{2B} receptors expressed by 5-HT neurons act in an opposite manner to 5-HT_{1A} autoreceptors. The 5-HT_{2B} receptor can thus be considered as a positive modulator of serotonergic tone that increases 5-HT neuron excitability. The observed hyposerotonergy in KO mice could explain violent impulsivity and suicidality associated to a loss-of-function poymorphism in *HTR2B* gene observed in human[12]. This positive modulation has to be taken into account in the studies of the regulatory mechanisms of 5-HT neurons including those of antidepressants.

Author Contribution.
Arnauld Belmer, performed initial behavioral characterization of conditional mice, and MDMA's experiment

Emily Quentin performed mice breeding, viral overexpression and behavioral experiments

Silvina L. Diaz performed SSRI's experiment on mice

Bruno P. Guiard, performed the studies on 5-HT receptor electrophysiology *in-vivo*

Sebastian P. Fernandez performed the studies on 5-HT receptor electrophysiology on slices,

Stéphane Doly performed pharmacological assessment

Sophie M. Banas performed mice breeding and behavioral experiments

Pothitos M. Pitychoutis performed PPI experiments

Imane Moutkine designed and produced viral vectors

Aude Muzerelle performed stereotaxic viral injection

Anna Tchenio performed 5-HT receptor electrophysiology on slices

Anne Roumier participated in the studies on 5-HT receptor electrophysiology on slices, experimental design, and funding

Manuel Mameli supervised 5-HT receptor electrophysiology on slices, experimental design and provided funding

Luc Maroteaux supervised the analysis, experimental design, wrote the paper and provided funding

Acknowledgment.
We thank the Mouse Clinical Institute (Strasbourg) for *Htr2b* floxed mice production, Evan Deneris for providing *Pet1-Cre*$^{+/0}$ mice, Mythili Savariradjane and the Imaging facility of the IFM, and Natacha Roblot and the IFM animal facility.

Funding Sources
This work has been supported by funds from the *Centre National de la Recherche Scientifique*, the *Institut National de la Santé et de la Recherche Médicale*, the *Université Pierre et Marie Curie*, and by grants from the *Fondation pour la Recherche Médicale* "Equipe FRM DEQ2014039529", the French Ministry of Research (Agence Nationale pour la Recherche ANR-12-BSV1-0015-01 and the Investissements d'Avenir programme ANR-11-IDEX-0004-02). LM's team is part of the École des Neurosciences de Paris Ile-de-France network and of the Bio-Psy Labex and as such this work was supported by French state funds managed by the ANR within the Investissements d'Avenir programme under reference ANR-11-IDEX-0004-02. A Roumier has been supported by grants from the *Université Pierre et Marie Curie (Emergence-UPMC program) and* the Bio-Psy Labex. S. Doly has been supported by a fellowships of the Lefoulon-DeLalande foundation, SL Diaz from the Region Ile de France DIM STEM and from the ANPCyT (PICT 2013-3225), CONICET (PIP-11220130100157CO), and University of Moron (PID 2015), and E. Quentin by a PhD fellowship from the Region Ile de France DIM Cerveau et Pensée.

Conflict of Interest
The authors declare no conflict of interest.

References

1. Okaty BW, Freret ME, Rood BD, Brust RD, Hennessy ML, Debairos D *et al.* Multi-Scale Molecular Deconstruction of the Serotonin Neuron System. *Neuron* 2015; **88**(4)**:** 774-791.

2. Commons KG. Ascending serotonin neuron diversity under two umbrellas. *Brain Structure and Function* 2016; **221**(7)**:** 3347-3360.

3. Riad M, Garcia S, Watkins KC, Jodoin N, Doucet E, Langlois X *et al.* Somatodendritic localization of 5-HT1A and preterminal axonal localization of 5-HT1B serotonin receptors in adult rat brain. *The Journal of Comparative Neurology* 2000; **417**(2)**:** 181-194.

4. Andrade R, Huereca D, Lyons JG, Andrade EM, Mcgregor KM. 5-HT1A Receptor-Mediated Autoinhibition and the Control of Serotonergic Cell Firing. *ACS Chem Neurosci* 2015; **6**(7)**:** 1110-1115.

5. Aghajanian GK, Lakoski JM. Hyperpolarization of serotonergic neurons by serotonin and LSD: studies in brain slices showing increased K+ conductance. *Brain Research* 1984; **305**(1)**:** 181-185.

6. Beck SG, Pan Y-Z, Akanwa AC, Kirby LG. Median and dorsal raphe neurons are not electrophysiologically identical. *J Neurophysiology* 2004; **91**(2)**:** 994-1005.

7. Craven RM, Grahame-Smith DG, Newberry NR. 5-HT1A and 5-HT2 receptors differentially regulate the excitability of 5-HT-containing neurones of the guinea pig dorsal raphe nucleus in vitro. *Brain Research* 2001; **899**(1-2)**:** 159-168.

8. Kirby LG, Pernar L, Valentino RJ, Beck SG. Distinguishing characteristics of serotonin and non-serotonin-containing cells in the dorsal raphe nucleus: electrophysiological and immunohistochemical studies. *Neuroscience* 2003; **116**(3)**:** 669-683.

9. Liu R, Jolas T, Aghajanian G. Serotonin 5-HT(2) receptors activate local GABA inhibitory inputs to serotonergic neurons of the dorsal raphe nucleus. *Brain Research* 2000; **873**(1)**:** 34-45.

10. Xu ZQ, Zhang X, Pieribone VA, Grillner S, Hökfelt T. Galanin-5-hydroxytryptamine interactions: electrophysiological, immunohistochemical and in situ hybridization studies on rat dorsal raphe neurons with a note on galanin R1 and R2 receptors. *Neuroscience* 1998; **87**(1)**:** 79-94.

11. Marinelli S, Schnell SA, Hack SP, Christie MJ, Wessendorf MW, Vaughan CW. Serotonergic and nonserotonergic dorsal raphe neurons are pharmacologically and electrophysiologically heterogeneous. *J Neurophysiol* 2004; **92**(6)**:** 3532-3537.

12. Bevilacqua L, Doly S, Kaprio J, Yuan Q, Tikkanen R, Paunio T *et al.* A population-specific HTR2B stop codon predisposes to severe impulsivity. *Nature* 2010; **468**(8)**:** 1061-1066.

13. Banas SM, Doly S, Boutourlinsky K, Diaz SL, Belmer A, Callebert J *et al.* Deconstructing antiobesity compound action: requirement of serotonin 5-HT2B receptors for dexfenfluramine anorectic effects. *Neuropsychopharmacology* 2011; **36**(2)**:** 423-433.

14. Kennett GA, Bright F, Trail B, Baxter GS, Blackburn TP. Effects of the 5-HT2B receptor agonist, BW 723C86, on three rat models of anxiety. *Br J Pharmacol* 1996; **117**(7)**:** 1443-1448.

15. Kennett GA, Ainsworth K, Trail B, Blackburn TP. BW 723C86, a 5-HT2B receptor agonist, causes hyperphagia and reduced grooming in rats. *Neuropharmacology* 1997; **36**(2)**:** 233-239.

16. Kennett GA, Trail B, Bright F. Anxiolytic-like actions of BW 723C86 in the rat Vogel conflict test are 5-HT2B receptor mediated. *Neuropharmacology* 1998; **37**(12)**:** 1603-1610.

17. Diaz SL, Maroteaux L. Implication of 5-HT2B receptors in the serotonin syndrome. *Neuropharmacology* 2011; **61:** 495-502.

18. Pitychoutis P, Belmer A, Moutkine I, Adrien J, Maroteaux L. Mice lacking the serotonin Htr2B receptor gene present an antipsychotic-sensitive schizophrenic-like phenotype. *Neuropsychopharmacology* 2015; **40**(12)**:** 2764-2773.

19. Doly S, Bertran-Gonzalez J, Callebert J, Bruneau A, Banas SM, Belmer A *et al.* Role of serotonin via 5-HT2B receptors in the reinforcing effects of MDMA in mice *PLoS ONE* 2009; **4**(11)**:** e7952.

20. Doly S, Valjent E, Setola V, Callebert J, Herve D, Launay JM *et al.* Serotonin 5-HT2B receptors are required for 3,4-methylenedioxymethamphetamine-induced hyperlocomotion and 5-HT release in vivo and in vitro. *J Neurosci* 2008; **28**(11)**:** 2933-2940.

21. Banas S, Doly S, Boutourlinsky K, Diaz S, Belmer A, Callebert J *et al.* Deconstructing antiobesity compound action: requirement of serotonin 5-HT2B receptors for dexfenfluramine anorectic effects. *Neuropsychopharmacology* 2011; **36:** 423–433.

22. Diaz SL, Doly S, Narboux-Nême N, Fernandez S, Mazot P, Banas S *et al.* 5-HT2B receptors are required for serotonin-selective antidepressant actions. *Mol Psychiatry* 2012; **17:** 154-163.

23. Loric S, Launay J-M, Colas J-F, Maroteaux L. New mouse 5-HT2-like receptor: Expression in brain, heart, and intestine. *FEBS L* 1992; **312:** 203-207.

24. Kursar JD, Nelson DL, Wainscott D, Baez M. Molecular cloning, functional expression, and mRNA tissue distribution of the human 5-hydroxytryptamine2B receptor. *Mol Pharmacol* 1994; **46:** 227-234.

25. Choi D-S, Birraux G, Launay J-M, Maroteaux L. The human serotonin 5-HT2B receptor: pharmacological link between 5-HT2 and 5-HT1D receptors. *FEBS L* 1994; **352:** 393-399.

26. Bonaventure P, Guo H, Tian B, Liu X, Bittner A, Roland B *et al.* Nuclei and subnuclei gene expression profiling in mammalian brain. *Brain Res* 2002; **943**(1)**:** 38-47.

27. Fernandez SP, Cauli B, Cabezas C, Muzerelle A, Poncer J-C, Gaspar P. Multiscale single-cell analysis reveals unique phenotypes of raphe 5-HT neurons projecting to the forebrain. *Brain Structure and Function* 2016; **221**(8)**:** 4007-4025.

28. Muzerelle A, Scotto-Lomassese S, Bernard JF, Soiza-Reilly M, Gaspar P. Conditional anterograde tracing reveals distinct targeting of individual serotonin cell groups (B5-B9) to the forebrain and brainstem. *Brain Structure and Function* 2016; **221**(1)**:** 535-561.

29. Maroteaux M, Mameli M. Cocaine evokes projection-specific synaptic plasticity of lateral habenula neurons. *J Neurosci* 2012; **32**(36)**:** 12641-12646.

30. Bill DJ, Knight M, Forster EA, Fletcher A. Direct evidence for an important species difference in the mechanism of 8-OH-DPAT-induced hypothermia. *Br J Pharmacol* 1991; **103**(4)**:** 1857-1864.

31. Rainer Q, Nguyen HT, Quesseveur G, Gardier AM, David DJ, Guiard BP. Functional status of somatodendritic serotonin 1A autoreceptor after long-term treatment with fluoxetine in a mouse model of anxiety/depression based on repeated corticosterone administration. *Molecular Pharmacology* 2012; **81**(2)**:** 106-112.

32. Aghajanian GK, Vandermaelen CP. Intracellular recording in vivo from serotonergic neurons in the rat dorsal raphe nucleus: methodological considerations. *J Histochem Cytochem* 1982; **30**(8)**:** 813-814.

33. Scott MM, Wylie CJ, Lerch JK, Murphy R, Lobur K, Herlitze S *et al.* A genetic approach to access serotonin neurons for in vivo and in vitro studies. *Proc Natl Acad Sci U S A* 2005; **102**(45)**:** 16472-16477.

34. Gray EG, Whittaker VP. The isolation of nerve endings from brain: an electron-microscopic study of cell fragments derived by homogenization and centrifugation. *J Anat* 1962; **96:** 79-88.

35. Haddjeri N, Lavoie N, Blier P. Electrophysiological evidence for the tonic activation of 5-HT(1A) autoreceptors in the rat dorsal raphe nucleus. *Neuropsychopharmacology* 2004; **29**(10)**:** 1800-1806.

36. Vandermaelen CP, Aghajanian GK. Electrophysiological and pharmacological characterization of serotonergic dorsal raphe neurons recorded extracellularly and intracellularly in rat brain slices. *Brain Res* 1983; **289**(1-2)**:** 109-119.

37. Jacobsen JPR, Siesser WB, Sachs BD, Peterson S, Cools MJ, Setola V *et al.* Deficient serotonin neurotransmission and depression-like serotonin biomarker alterations in tryptophan hydroxylase 2 (Tph2) loss-of-function mice. *Mol Psychiatry* 2012; **17**(7)**:** 694-704.

38. Richardson-Jones JW, Craige CP, Guiard BP, Stephen A, Metzger KL, Kung HF *et al.* 5-HT1A autoreceptor levels determine vulnerability to stress and response to antidepressants. *Neuron* 2010; **65**(1)**:** 40-52.

39. Valjent E, Bertran-Gonzalez J, Aubier B, Greengard P, Hervé D, Girault J-A. Mechanisms of locomotor sensitization to drugs of abuse in a two-injection protocol. *Neuropsychopharmacology* 2010; **35**(2)**:** 401-415.

40. Halberstadt AL. Recent advances in the neuropsychopharmacology of serotonergic hallucinogens. *Behavioural brain research* 2015; **277:** 99-120.

41. Calizo LH, Akanwa A, Ma X, Pan Y-Z, Lemos JC, Craige C *et al.* Raphe serotonin neurons are not homogenous: Electrophysiological, morphological and neurochemical evidence. *Neuropharmacology* 2011; **61**(3)**:** 524-543.

42. Vasudeva RK, Lin RCS, Simpson KL, Waterhouse BD. Functional organization of the dorsal raphe efferent system with special consideration of nitrergic cell groups. *J Chem Neuroanat* 2011; **41**(4)**:** 281-293.

43. Andrade R, Haj-Dahmane S. Serotonin neuron diversity in the dorsal raphe. *ACS Chem Neurosci* 2013; **4**(1)**:** 22-25.

44. Kiyasova V, Fernandez SP, Laine J, Stankovski L, Muzerelle A, Doly S *et al.* A genetically defined morphologically and functionally unique subset of 5-HT neurons in the mouse raphe nuclei. *J Neurosci* 2011; **31**(8)**:** 2756-2768.

45. Bang SJ, Jensen P, Dymecki SM, Commons KG. Projections and interconnections of genetically defined serotonin neurons in mice. *European J Neurosci* 2012; **35**(1)**:** 85-96.

46. Gaspar P, Lillesaar C. Probing the diversity of serotonin neurons. *Philos Trans R Soc Lond, B, Biol Sci* 2012; **367**(1601)**:** 2382-2394.

47. Altieri SC, Garcia-Garcia AL, Leonardo ED, Andrews AM. Rethinking 5-HT1A receptors: emerging modes of inhibitory feedback of relevance to emotion-related behavior. *ACS Chem Neurosci* 2013; **4**(1)**:** 72-83.

48. Colgan LA, Putzier I, Levitan ES. Activity-dependent vesicular monoamine transporter-mediated depletion of the nucleus supports somatic release by serotonin neurons. *J Neurosci* 2009; **29**(50)**:** 15878-15887.

49. Courtney NA, Ford CP. Mechanisms of 5-HT1A receptor-mediated transmission in dorsal raphe serotonin neurons. *J Physiol* 2016; **594**(4)**:** 953-965.

50. Mosienko V, Matthes S, Hirth N, Beis D, Flinders M, Bader M *et al.* Adaptive changes in serotonin metabolism preserve normal behavior in mice with reduced TPH2 activity. *Neuropharmacology* 2014; **85:** 73-80.

51. Urban DJ, Zhu H, Marcinkiewcz CA, Michaelides M, Oshibuchi H, Rhea D *et al.* Elucidation of The Behavioral Program and Neuronal Network Encoded by Dorsal Raphe Serotonergic Neurons. *Neuropsychopharmacology* 2016; **41**(5)**:** 1404-1415.

52. Teissier A, Chemiakine A, Inbar B, Bagchi S, Ray RS, Palmiter RD *et al.* Activity of Raphé Serotonergic Neurons Controls Emotional Behaviors. *Cell reports* 2015; **13**(9)**:** 1965-1976.

53. Boothman LJ, Sharp T. A role for midbrain raphe gamma aminobutyric acid neurons in 5-hydroxytryptamine feedback control. *Neuroreport* 2005; **16**(9)**:** 891-896.

54. Igata S, Hayashi T, Itoh M, Akasu T, Takano M, Ishimatsu M. Persistent α1-adrenergic receptor function in the nucleus locus coeruleus causes hyperexcitability in AD/HD model rats. *Journal of Neurophysiology* 2014; **111**(4)**:** 777-786.

55. Aghajanian GK, VanderMaelen CP. alpha 2-adrenoceptor-mediated hyperpolarization of locus coeruleus neurons: intracellular studies in vivo. *Science (New York, NY)* 1982; **215**(4538)**:** 1394-1396.

56. Williams JT, Marshall KC. Membrane properties and adrenergic responses in locus coeruleus neurons of young rats. *J Neurosci* 1987; **7**(11)**:** 3687-3694.

57. Brandman O, Meyer T. Feedback loops shape cellular signals in space and time. *Science (New York, NY)* 2008; **322**(5900)**:** 390-395.

Figure 1

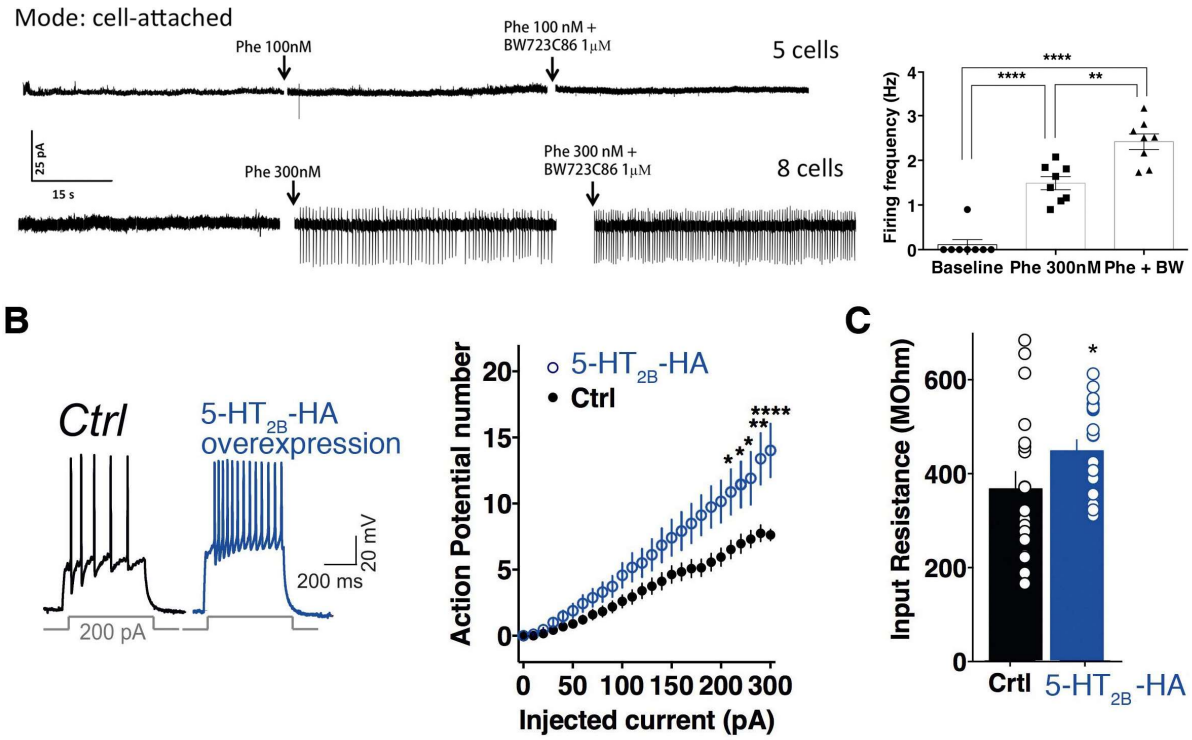

Figure 1 - *Ex-vivo* electrophysiological recordings - A) Recordings of identified ePet1-GFP 5-HT neuron of *ex-vivo* WT slices. In single identified ePet1-GFP 5-HT neuron, cell-attached recordings made in the presence of 100 nM phenylephrine did not show response (top line). In these slices treated with subsaturating concentration of phenylephrine (300 nM), cell firing was observed and BW723C86 (1 µM) increased significantly the firing rate of these identified raphe neurons. Representative traces (left) and quantification (right) reveal a significant BW723C86-induced increase in firing. Vertical scale bar represents 25 pA. (RM one way ANOVA $F_{(7, 14)} = 2.745$; **P<0.01; data are means ± SEM, n = 8 per group). **B**) Current clamp recordings of *ex-vivo* slices overexpressing 5-HT$_{2B}$-HA receptor in 5-HT neuron. (Left) Sample traces of action potential for a +200 pA current step in the different experimental groups. (Middle) Quantification of the number of action potentials obtained in function of the current injected shows significant increase in action potential number in mice overexpressing 5-HT$_{2B}$-HA receptor in 5-HT neurons compared to controls: n = 20-21 cells; n = 3-4 mice per group; two-way ANOVA RM, Bonferroni posttest, *P<0.05, **P<0.01, ****P<0.0001). Data are means ± SEM. **C**) Input resistance values. Bar graph and scatter plot for input resistance values shows that input resistance was also increased in mice overexpressing HA-5-HT$_{2B}$ receptor in 5-HT neuron (input resistance; *Pet1-Cre$^{+/0}$:RCE* mice vs. *Pet1-Cre$^{+/0}$;AAV-DIO-HA-Htr2b;RCE* mice unpaired t-test, *P = 0.047). Data are means ± SEM.

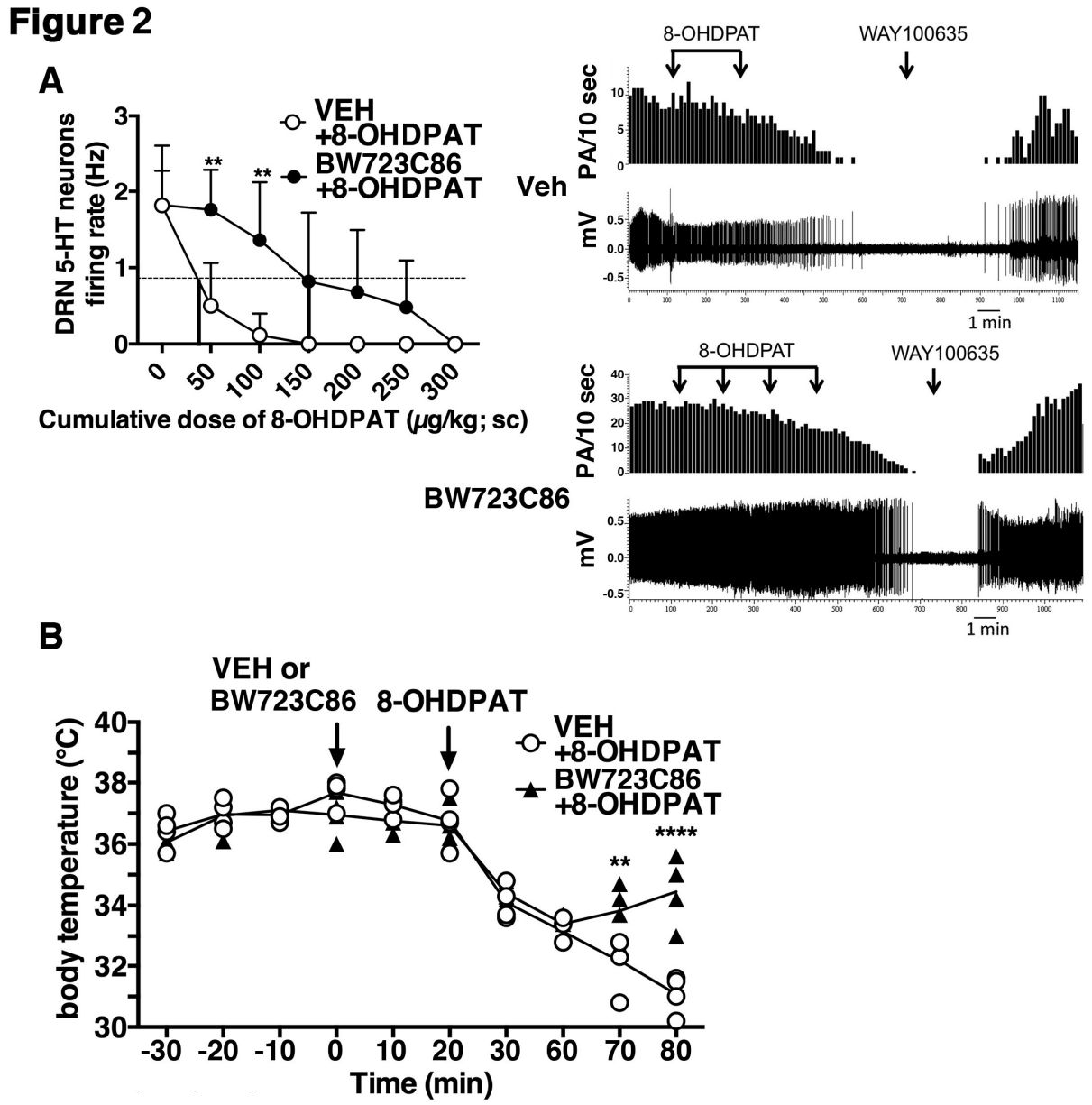

Figure 2 - *In-vivo* responses of WT mice to 5-HT$_{2B}$ and 5-HT$_{1A}$ receptor agonists - A) *In-vivo* extracellular electrophysiological recordings of raphe neurons. (Left) BW723C86 (5 mg/kg sc) counteracted the 5-HT$_{1A}$ agonist 8-OHDPAT (0.05 mg/kg; sc) inhibitory effects to 5-HT neuron firing; n=5-6 mice per group (Two-way ANOVA RM followed by Bonferroni's multiple comparisons test **P<0.01). Data are means ± SD. (Right) Examples of typical recordings of DRN 5-HT neurons obtained in each experimental group. Each arrow represents an injection of 8-OHDPAT (0.05 mg/kg; sc). The injection of the 5-HT$_{1A}$ receptor antagonist WAY100635 (0.3 mg/kg sc) completely reversed the inhibitory effect of 8-OHDPAT. **B)** *In-vivo* hypothermic effects. The 5-HT$_{2B}$ receptor agonist BW723C86 (5 mg/kg sc) injected 20 min before test is able to counteract the 5-HT$_{1A}$ agonist 8-OHDPAT (0.3 mg/kg sc) hypothermic effects on WT mice, n = 4 per group (Two-way ANOVA RM followed by Bonferroni's multiple comparisons test, **P<0.01, ****P<0.0001).

Figure 3

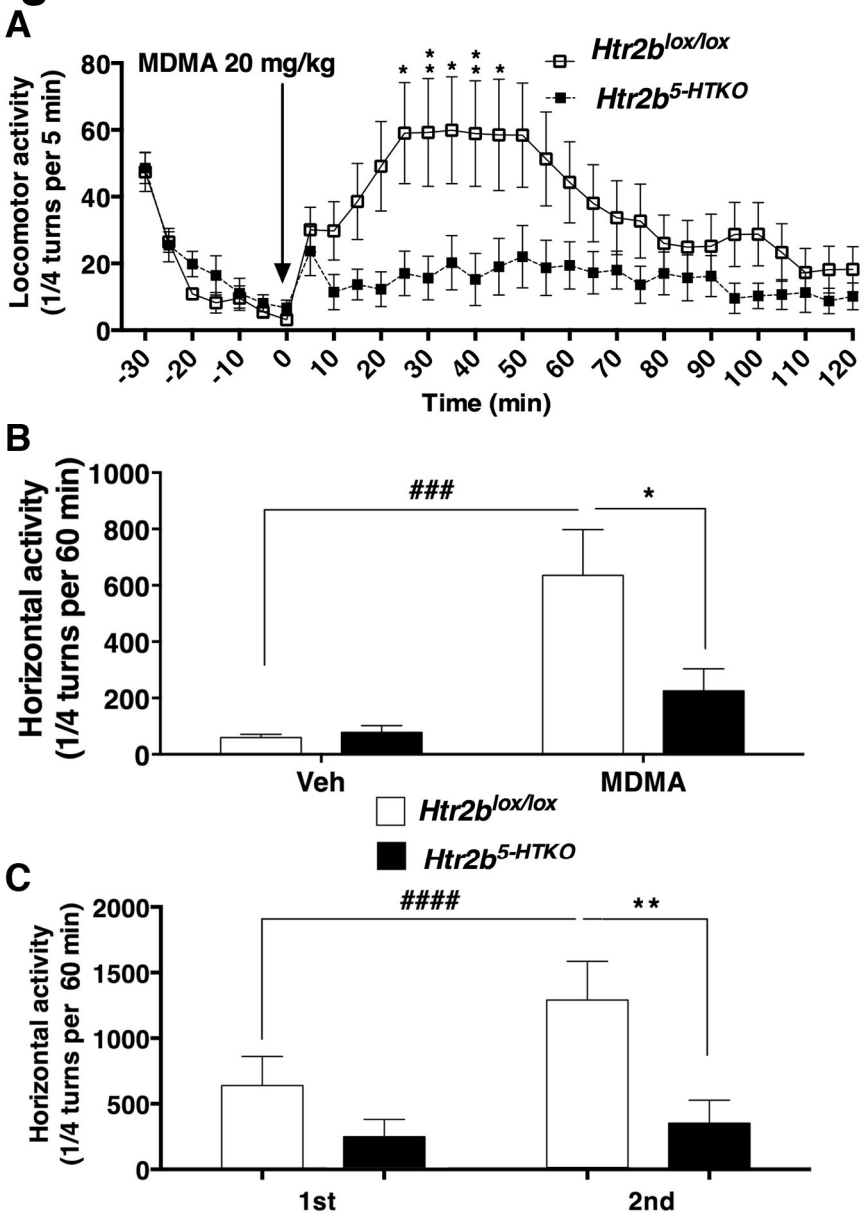

Figure 3- Lack of behavioral responses to 5-HT releaser MDMA in *Htr2b*$^{5\text{-}HTKO}$ mice - A) MDMA-induced locomotion. Mice were injected with MDMA (20 mg/kg ip) after 30 minutes habituation (arrow). A lack of MDMA-induced locomotion was observed in *Htr2b*$^{5\text{-}HTKO}$ mice, while control *Htr2b*$^{lox/lox}$ mice showed a clear increase in locomotion. Data between 0 to 60 min were analyzed using two-way ANOVA RM (means ± SEM, n = 16 per group). A Bonferroni posttest was also applied on each graph, *P<0.05; **P<0.01. **B**) Cumulative MDMA-induced locomotion. Cumulative locomotion during the first hour following MDMA injection showed a significant difference between the two genotypes. Data between 0 to 60 min were analyzed using two-way ANOVA (means ± SEM, n = 16 per group). A Bonferroni posttest was also applied on each graph, *P<0.05 *Htr2b*$^{5\text{-}HTKO}$ vs. *Htr2b*$^{lox/lox}$; ###P<0.001 MDMA vs. Veh. **C**) Locomotor sensitization by two MDMA injection protocol. MDMA (20 mg/kg ip) increased locomotor activity after the first injection (1st) in control *Htr2b*$^{lox/lox}$ mice but not in *Htr2b*$^{5\text{-}HTKO}$ mice. The stimulant effect of a challenge dose of MDMA (20 mg/kg ip) 7 days later (2nd) was significantly enhanced compared to the first injection in control *Htr2b*$^{lox/lox}$ mice, while it had no effect in *Htr2b*$^{5\text{-}HTKO}$ mice. Data were analyzed using two-way ANOVA RM (means ± SEM, n = 8 per group). A Bonferroni posttest was also applied on each graph, **P<0.01 *Htr2b*$^{5\text{-}HTKO}$ vs. *Htr2b*$^{lox/lox}$; ####P<0.0001 1st vs. 2nd.

Figure 4

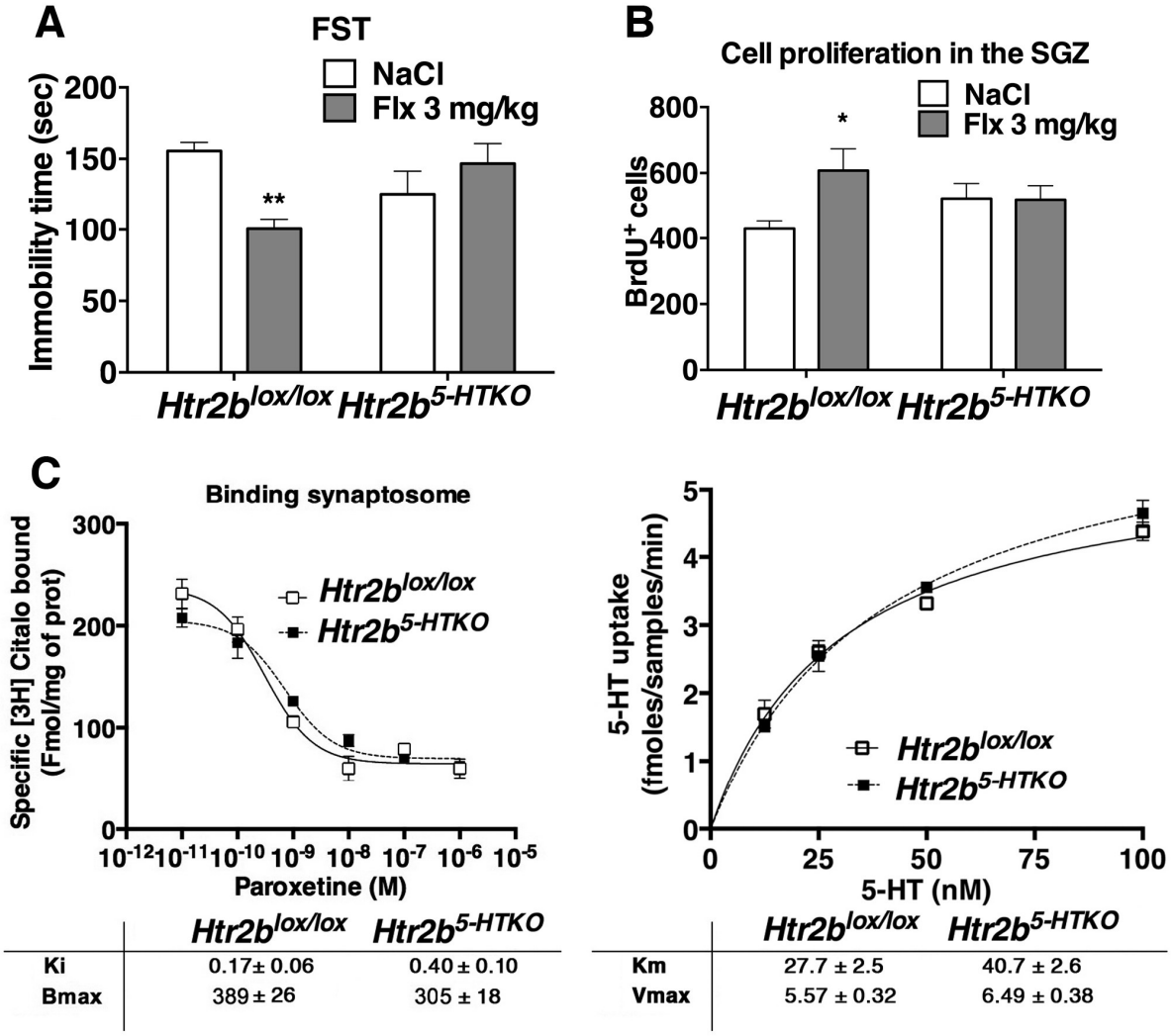

	Htr2b lox/lox	Htr2b 5-HTKO
Ki	0.17± 0.06	0.40 ± 0.10
Bmax	389 ± 26	305 ± 18

	Htr2b lox/lox	Htr2b 5-HTKO
Km	27.7 ± 2.5	40.7 ± 2.6
Vmax	5.57 ± 0.32	6.49 ± 0.38

Figure 4- SSRI Fluoxetine action is abolished in *Htr2b*$^{5\text{-}HTKO}$ mice - A) Forced swimming test (FST). The time spent immobile in the FST was determined in control *Htr2b*$^{lox/lox}$, and in *Htr2b*$^{5\text{-}HTKO}$ mice 30 min after Flx (3 mg/kg ip) injection. The lack of acute Flx effect in FST on *Htr2b*$^{5\text{-}HTKO}$ mice confirmed that Flx needs raphe neurons expressing 5-HT$_{2B}$ receptors. Two-way ANOVA, Bonferroni posttests; **P<0.01; data is expressed as mean ± SEM (n = 7-8 per group). **B**) Neurogenesis in subgranular zone (SGZ) of the hippocampus. The SSRIs Flx (3 mg/kg/day ip), daily injected for 4 weeks, induced a significant increase in neuron proliferation in the SGZ of the hippocampus of control *Htr2b*$^{lox/lox}$ mice, but no effect was observed in *Htr2b*$^{5\text{-}HTKO}$ mice. Two-way ANOVA, Bonferroni posttests; *P<0.05; data are expressed as mean ± SEM (n = 7-8 per group). **C**) SERT expression and function. (Left) SERT expression in conditional *Htr2b*$^{5\text{-}HTKO}$ and *Htr2b*$^{lox/lox}$ control mice was evaluated using heterologous radioligand competition binding assays with [^{3}H]citalopram on synaptosomes membranes prepared from whole brain. No differences in the affinity (Ki) or expression (Bmax) between *Htr2b*$^{5\text{-}HTKO}$ and *Htr2b*$^{lox/lox}$ genotypes were observed. (Right) SERT uptake activity. Saturation isotherms of [^{3}H]5-HT uptake in conditional *Htr2b*$^{5\text{-}HTKO}$ and *Htr2b*$^{lox/lox}$ control mice synaptosomal preparation from whole brain were similar for both strains of mice. Nonlinear regression analysis did not reveal differences in the Km or *V*max. Shown are representative curves of at least 2 independent experiments performed in duplicates. Data are expressed as mean ± SEM.

Figure 5

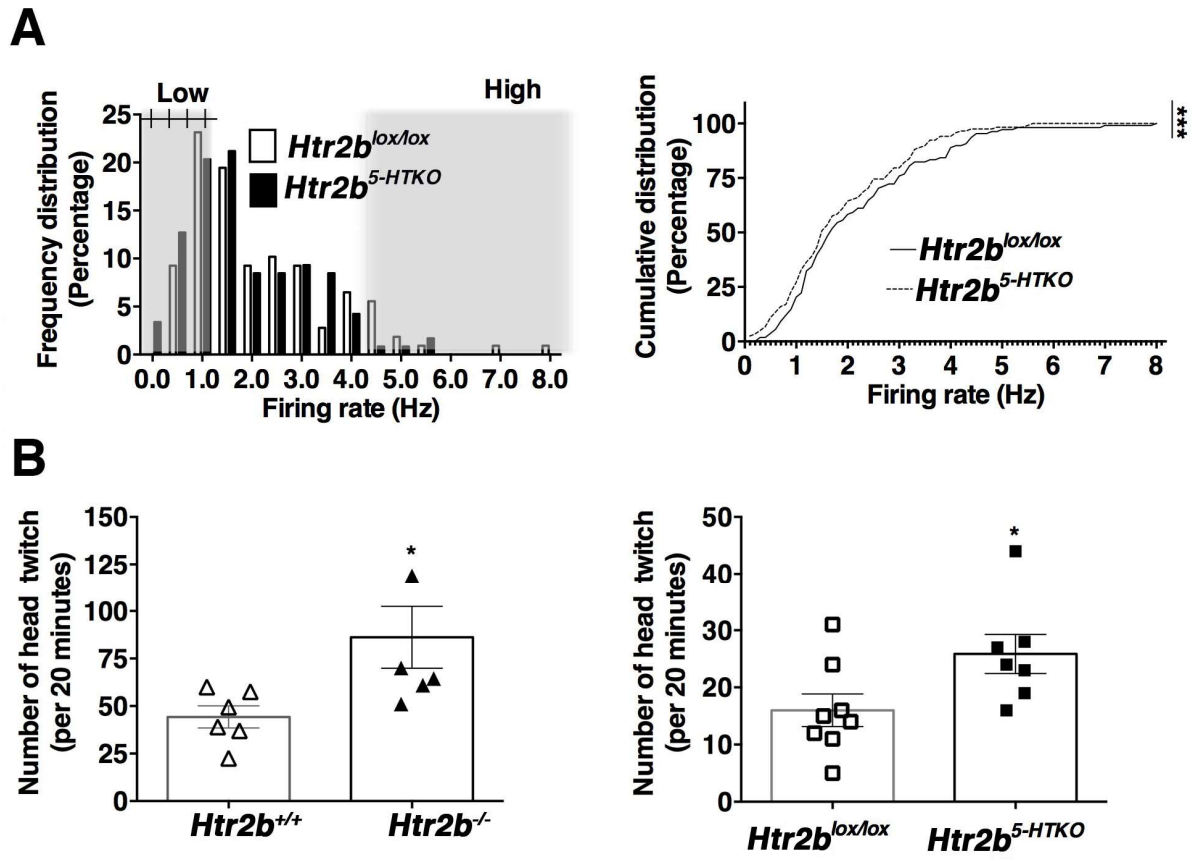

Figure 5 - Hyposerotonergic phenotype of *Htr2b$^{5\text{-}HTKO}$* mice - A) *In-vivo* extracellular recordings of DRN 5-HT neurons. (Left) The firing frequency of DRN 5-HT neurons in both genotypes revealed a shift from high to low firing rates. (Right) Spontaneous firing rates for individual raphe neurons in an *in-vivo* anesthetized preparation of animals revealed a significant reduced cumulative distribution of firing rate in *Htr2b$^{5\text{-}HTKO}$* mice compared to control *Htr2b$^{lox/lox}$* mice (n = 108 and 118 neurons, respectively; Kolmogorov-Smirnov test; P=0.0008). **B**) Head twitch response (HTR) to DOI. Control and mutant mice were ip injected with DOI (5 mg/kg ip) 15 min before test and the HTR was scored for 20 min. DOI-induced HTR was significantly increased in *Htr2b$^{-/-}$* mice (t_{10}=2.43, *P=0.036; unpaired t-test) and in conditional *Htr2b$^{5\text{-}HTKO}$* (t_{13}=2.32, *P=0.044; unpaired t-test) compared to respective control mice. Data are means ± SEM, n = 6-8 per group.

Positive regulation of raphe serotonin neurons by serotonin 2B receptors.

Arnauld Belmer*, Emily Quentin*, Silvina L. Diaz, Bruno P. Guiard, Sebastian P. Fernandez, Stéphane Doly, Sophie M. Banas, Pothitos M. Pitychoutis, Imane Moutkine, Aude Muzerelle, Anna Tchenio, Anne Roumier, Manuel Mameli, and Luc Maroteaux

INSERM UMR-S 839, F75005, Paris, France; Sorbonne Universités, UPMC Univ Paris 6, F75005, Paris; Institut du Fer à Moulin, F75005, Paris.

Supplemental Informations

Inventory of Supplemental Information

The supplementary information submitted consists in 3 Supplementary Figures corresponding to constructs and control experiments of Virus injection, behavioral investigations of basal locomotion and prepulse inhibition o startle reflex, and constructs and control experiments of conditional mutant together with materials and methods that were only briefly described in the main article.

Materials and methods

Animals

Wild type 129S2 mice (8-10 week old) used as a control group were derived from heterozygote crosses and were bred at our animal facility. The temperature was maintained at 21±1°C, under 12/12h light/dark. Food for laboratory mice (SAFE A03, France; 3200 kcal/kg, moisture 12%, proteins 21%, lipids 5%, carbohydrates 52%, fibers 4%, and mineral ash 6%) and water were available *ad libitum*. Male mice were housed in groups of 3-5 of the same genetic background after weaning. Mice were moved to experimental room in their home cage at least 5 days prior to testing to allow for habituation to the environment and stayed there until the end of the experiments. The total number of animals per group was defined according to the standard deviation and the difference score observed for each small group in a pilot experiment and according to previous results from our laboratory. Mice were randomly assigned to different experimental groups of about 4 to 6 animals and independent experiments were performed at least 2-3 times. Behavioral studies were carried out in the afternoon (14:00–20:00). The observer was blind to experimental conditions being measured. Electrophysiological recording, behavioral tests, and animal care were conducted in accordance with the standard ethical guidelines (National Institutes of Health's 'Guide for the care and use of Laboratory animals,' and European Directive 2010/63/ UE). All experiments involving mice were approved by the local ethical committee (N° 1170.02).

Cell-attached *ex-vivo* electrophysiological recordings

Electrophysiological recordings and molecular characterization of 5-HT neurons was conducted in acute brain slices from male Pet1-EGFP mice aged 3–4 weeks old according to published procedures[1]. Deeply anesthetized mice were decapitated and the brain was rapidly dissected out. Coronal slices (250 µm) containing the DR and MR were prepared with a vibratome (Microm HM650 V, Thermo Scientific) and placed in aCSF containing (in mM): 11 glucose, 2.5 KCl, 26.2 NaHOC3, 1 NaH2PO4, 124 NaCl, 2 CaCl2, 2 MgCl2 bubbled with a mixture of 95 % O2/5 % CO2 After a 1-h recovery period, individual slices were placed in an electrophysiology chamber continuously perfused with aCSF maintained at 31 °C. Neurons were visualized by combined epifluorescent and infrared/differential interference contrast

visualization using an Olympus BX51WI upright microscope holding 59 and 409 objectives. Expression of green fluorescent protein was detected with an Endow GFP/EGFP Bandpass filter (Chroma Technology Corp, USA, #41017). Borosilicate glass pipettes (3–5 MΩ) were made in a HEKA PIP5 puller and filled with 140mM NaCl solution. Single EGFP-positive neurons were approached with a pipette and a giga-ohm seal was established. Signals were collected and stored using a Multiclamp 700B (Molecular Devices, Sunnyvale, CA, USA), Digidata 1440A converter and pCLAMP 10.2 software (Molecular Devices, CA, USA). To reproduce noradrenergic drive that facilitates serotonergic neuron firing during wakefulness, aCSF was supplemented with subsaturating concentrations of the α1 adrenergic receptor agonist phenylephrine (PE; 100-300 nM)[2].

Viral constructs and stereotaxic injections into B7 raphe nuclei

A triple HA tag (3xPYDVPDYA) was inserted in-frame in 5' of the 5-HT_{2B} cDNA using complementary oligo annealing. Then, 5-HT_{2B}-HA was cloned into a pAAV-EF1A-DIO-WPRE-pA conditional vector (Addgene) to get pAAV-EF1A-DIO-5-HT_{2B}-HA-WPRE-pA (**Fig. S2**). The construct was packaged into AAV2.9 serotype and titers of 10^{12}–10^{13} viral particles/ ml were obtained (UNC Vector Core, Chapel Hill USA). DIO-Tomato AAV2.9 particles were used as a control. AAVs were injected in the B7 raphe nuclei of *Pet1cre$^{0/+}$; RCE/RCE* following procedure described in Muzerelle *et al* [3]. Briefly, four weeks-old Pet1cre$^{0/+}$; RCE/RCE mice were anesthetized with ketamine (150 mg/kg) / xylazine (10 mg/kg) (Sigma-Aldrich Co., MO, USA) before surgery. To maintain the skull position zt 10° in order to target B7nuclei, the palate bar was adjusted after measuring the dorsoventral bregma and lambda positions (0.5 from lambda; 1 mediolateral and-3.2 dorsoventral). Single injections (20 nl) were performed using a pulled glass capillary (30 to 50 lm tip diameter; PCR micropipette, Drummond Scientific company) fixed to an adapter specially designed to be mounted on the oil hydraulic micromanipulator MO-10 (Narishige, Japan). The capillary was left in the target site for 5 min after injection to prevent backflow. After 3 weeks of recovery and viral transgene expression, deeply anesthetized (Pentobarbital 0.5 mg/g) mice were fixed by intracardiac perfusion of 4 % paraformaldehyde in 0.1 M phosphate-buffered saline (PBS; pH 7.4). Brains were post-fixed overnight in the same solution. Fifty-micrometer-thick sections were cut with a VT1000S (Leica) then stored in PBS1X-azide 0.001% solution.

Immunofluorescence

Immunofluorescent staining was performed using free-floating procedures. Sections were washed 3 times in PBS1X, permeabilized in PBS1X-Triton 0.25% and incubated in blocking solution PBS1X-Triton 0.25%-BSA 1%-goat serum 5% for 1 hour. Sections were then incubated overnight with anti HA antibody (C29FA, Cell Signaling, 1:500). Sections were washed in PBS1X-Triton 0.25% and incubated with secondary antibody (goat anti-rabbit CY3 Jackson laboratory, 1:500). Images were acquired using a 40 X objective on a Leica DM6000 upright epifluorescence microscope with a 12-bit cooled CCD camera (Micromax; Roper Scientific) run by MetaMorph software (Roper Scientific). Exposure time was determined on bright control cells to avoid pixel saturation (**Fig. S2**).

Ex-vivo electrophysiology

Mice aged ~9 weeks were anesthetized with ketamine and xylazine (150 mg/kg and 10 mg/kg, respectively; i.p.; Sigma-Aldrich, France). Coronal brain slices containing the raphe nucleus were prepared as previously described[4]. Briefly, coronal raphe-containing brain slices (250 μm) were prepared in bubbled ice-cold 95% O2/5% CO2-equilibrated solution containing (in mM): 110 choline chloride; 25 glucose; 25 NaHCO3; 7 MgCl2; 11.6 ascorbic acid; 3.1 sodium pyruvate; 2,5 KCl; 1.25 NaH2PO4; 0.5 CaCl2. Slices were stored at room temperature in 95% O2/5% CO2–equilibrated artificial cerebrospinal fluid (ACSF) containing (in mM): 124 NaCl; 26.2 NaHCO3; 11 glucose; 2.5 KCl; 2.5 CaCl2; 1.3 MgCl2; 1 NaH2PO4. Recordings (flow rate of 2.5 ml/min) were obtained under an Olympus-BX51 microscope (Olympus, France) at the temperature of 30 °C. Currents were amplified, filtered at 5 kHz and digitized at 20 kHz. Access resistance was monitored by a step of −40 pA (0.1 Hz).

Experiments were discarded if the access resistance increased more than 20%. Recordings of neuronal excitability were performed in current clamp mode using an internal solution containing (in mM): 140 potassium gluconate, 4 NaCl, 2 MgCl2, 1.1 EGTA, 5 HEPES, 2 Na2ATP, 5 sodium creatine phosphate, and 0.6 Na3GTP (pH 7.3 with KOH). The liquid junction potential was ~12 mV. Synaptic blockers for AMPA- (NBQX, 20 μM), GABA (picrotoxin, 100 μM) and NMDA receptors (AP5 50 μM) were added to the aCSF. Cells were maintained at -65mV throughout the experiment.

Data Analysis

All drugs were obtained Hello Bio (Bristol, UK) and dissolved in water. Online/offline analysis was performed using IGOR-6 (Wavemetrics, US) and Prism (Graphpad, US). Sample size required for the experiment was empirically tested by running pilots experiments in the laboratory. Data distribution was assumed to be normal, and single data points are always plotted. Compiled data are expressed as mean ± s.e.m. Significance was set at $p < 0.05$ using Student's t-test and two-way ANOVA.

***In-vivo* electrophysiology of DR 5-HT neurons.**

Mice were anaesthetized with chloral hydrate (400 m/kg; i.p.) and mounted in a stereotaxic frame. Additional anesthesia (50–100 mg/kg; i.p.) was given as necessary to maintain a full anesthetic state, characterized by the absence of response to a tail pinch. Body temperature was maintained at 37 °C throughout the experiments using a thermistor-controlled heating pad (Astro-Med, Elancourt, France). The extracellular recordings of the 5-HT neurons in the dorsal raphe (DR) were performed using single-barreled glass micropipettes (Stoelting, Dublin, Ireland) pulled on a pipette puller (Narishige, Tokyo, Japan) preloaded with a 2 M NaCl solution. Their impedance typically ranged between 2.5 and 5 MΩ. The single-barreled glass micropipettes were positioned 0.2–0.5 mm posterior to the interaural line on the midline and lowered using a hydraulic micropositioner (Kopf Instruments) into the DR, usually attained at a depth between 2.5 and 3.5 mm from the brain surface. To increase the signal-to-noise ratio, we used a current amplifier (BAK Electronics, Mount Airy, MD, USA) connected to the active filter Humbug (Quest scientific, DIPSI, Châtillon, France). The presumed DR 5-HT neurons were then identified according to the criteria of Aghajanian and Vandermaelen[5], that is, a slow (0.5–2.5 Hz) and regular firing rate and long-duration (2–5 ms) bi- or triphasic extracellular waveform. Neuronal activity was recorded in real time using Spike2 software (Cambridge Electronic Design, Cambridge, UK), which was also used to analyze neurons offline. For all dose–response curves, only one neuron was recorded and tested from each animal. In the latter experiments cumulative dose of 8-OHDPAT (0,05 – 0,3 mg/kg; s.c.) were injected every 3 minutes in mice pre-treated with BW723C86 or its vehicle.

8-OHDPAT-induced hypothermia

Body temperature was assessed intrarectally, using a lubricated probe (BIO-BRET-3) inserted approximately 2 cm and monitored with a thermometer (Bioseb, France). Four baseline body temperature measurements were taken as a control measure. Ten minutes after the fourth baseline measurement, animals received vehicle or BW723C86 and 20 minutes later they received 8-OHDPAT (0,3 mg/kg s.c.). Body temperature was then measured every 10 min after the injection during 40 additional minutes[6].

Generation of *Htr2b* floxed mice. Genomic contigs of *Htr2b* encompassing exon 1 and 2 and flanking sequence were obtained by screening of a 129S2 mouse genomic library. For the gene targeting construct, a 10 kb BamHI-XhoI fragment containing the two first exons was selected, while a 4 kb SacI-SacI fragment containing exon 2, which includes the ATG start codon and 5' UTR was used to induce the targeted deletion (**Fig. S2**). A LoxP site was inserted in the 5'-UTR and a neomycine-resistance (NEO) cassette flanked by two LoxP sites in the ClaI site of the second intron. Then, the SacI-SacI fragment comprising the floxed construct was excised and electroporated into 129S2 embryonic stem (ES) cells which were subjected to G418 selection. Targeted homologous recombination was confirmed by PCR and Southern blot analysis. A positive ES clone was injected into C57Bl/6NCrl blastocysts and

implanted into pseudopregnant mice. A chimeric male displaying germ-line transmission was then used to propagate the floxed *Htr2b* (*Htr2b*$^{fl/fl}$) allele on a C57Bl/6NCrl background for the two first generations.

Htr2b$^{lox/+}$ mice were backcrossed on 129S2 background (originally obtained from Charles River Laboratories, L'Arbresle, France) for 8 generations. Female *Htr2b*$^{lox/lox}$ mice were then generated by heterozygous mating. All genotyping was performed by PCR amplification of tail-tip DNA. The WT and floxed alleles were independently detected using 2 sets of primers: F1-R2 5'-CTAACATTTTTCATCCACATCTA / ACTTTAATTGGGACTCGCTGAT-3' (WT) and F1-R1 5'-CTAACATTTTTCATCCACATCTA / TCCCTCGAAGCTTATCGGCGCG-3' (floxed). These primers amplified a 1016bp (WT) or 1056bp band respectively. Male heterozygous *ePet1-Cre*$^{+/0}$ breeders on C57Bl6 background were kindly provided by P. Gaspar (Institut du Fer a Moulin, Paris, France) (BAC–ePet-Cre) mice[7], and Cre-bearing male mice were backcrossed on 129S2 background for 8 generations. The *ePet1-Cre* allele was detected by PCR with the following primers: 5'-CTTCTGTCCGTTTGCCGGTCGTGG/ TTTTGCACGTTCACCGGCATCAACG-3' that amplified a band of 264 bp. Heterozygous e*Pet1-Cre* males on 129sv background were intercrossed with *Htr2b*$^{lox/lox}$ females until generation of *Pet1-Cre*$^{+/0}$*; Htr2b*$^{lox/lox}$ conditional knockout mice (*Htr2b*$^{5\text{-}HTKO}$) and *Pet1-Cre*$^{0/0}$*; Htr2b*$^{lox/lox}$ littermate controls (*Htr2b*$^{lox/lox}$). These mice were then bred to *Gt(ROSA)26Sor*$^{tm1.1(CAG-EGFP)Fsh}$ mice (Jackson Lab) that express EGFP after recombination to generate the triple transgenic line *Pet1-Cre*$^{+/0}$*; Htr2b*$^{lox/lox}$*;Gt(ROSA)26Sor*$^{tm1.1(CAG-EGFP)Fsh}$ (*Htr2b*$^{5\text{-}HTKO}$*;RCE*) to verify proper recombination and to identify 5-HT neurons.

Behavioral experiments

Locomotor response to novelty and MDMA-induced hyperlocomotion and sensitization

Locomotor activity was measured as previously described[8], in a circular corridor with four infrared beams placed at every 90° (Imetronic, Passac, France). Eight to nine weeks-old conditional KO and littermate control mice were injected with a saline solution and individually placed in the activity box for 30 min during 3 days consecutively for habituation before experiments (**Fig. S3A**). On the experiment day, mice were placed in the activity box for 30 min for basal locomotor activity recording and then injected with MDMA (20 mg/kg, ip). Locomotor activity was recorded for two hours.

MDMA-induced locomotor sensitization was performed in a two-injection protocol as previously described[9]. Briefly, 8-9 week-old conditional KO and littermate control mice received a first injection of MDMA (20 mg/kg) and the locomotor activity was recorded for two hours. Mice were then challenged seven days later with a second injection of MDMA (20 mg/kg) and locomotor activity was recorded for two hours.

Prepulse Inhibition (PPI) of acoustic startle

Sensorimotor gating was assessed as previously described[10]. PPI was indexed by the percentage inhibition of the startle response at each level of prepulse intensity by using the following formula: % PPI = [(mean reactivity on pulse-alone trials- mean reactivity on prepulse-pulse trials)/mean reactivity on pulse-alone trials] x 100%. % Average PPI values were calculated from all PPI values across all the four prepulse intensities.

Forced Swimming Test

Mice FST was conducted essentially as described by[11]. Briefly, swim sessions were conducted by placing male mice individually in a plastic cylinder (26 cm tall × 17 cm in diameter) filled with water (24–26°C) to a depth of 15 cm. The depth was deep enough so that mice could not support themselves by placing their paws or tail on the base of the cylinder. Standard 6-min test duration was employed,

and immobility time was only measured during the last 4 minutes of the test period. Mice were judged to be immobile when no additional activity was observed other than that required to keep their head above water. After removing mice from water, they were dried and placed in their home cage. Each animal was challenged once. Injections were administered 30 minutes before the test session.

Chronic treatments, Proliferation assay

Fluoxetine (3 mg/kg/day) or vehicle (0.9% NaCl) was injected once daily for 4 weeks. WT male mice chronically treated with daily i.p. injections of Flx or Veh. The last day of this 4-week experimental protocol, mice received 2 injections of 150 mg/kg BrdU (2-h interval between injections). Then, 24 hours after BrdU administration, mice were perfused and brains were recovered for cell proliferation studies. Newborn cells were detected by peroxidase immunostaining of BrdU, an exogenous marker of cell division. Free-floating sections were first incubated overnight in 0.1% H_2O_2. After rinsing, sections were exposed to 2 N HCl for 1 h for deoxyribonucleic acid hydrolysis, immediately rinsed in 1X PBS and blocked in 0.2% gelatin and 0.5% triton in 1X PBS solution for 1 h. Sections were then incubated overnight with the primary antibody (rat anti-BrdU 1:400; AbDserotec OBT0030; clone BU1/75-ICR1) at 4°C, and, after washing, exposed to the secondary biotinylated antibody (goat anti rat, 1:400; Vector) for 2 h at room temperature and to 1:400 Streptavidin-biotinylated horseradish peroxidase complex (Amersham). Sections were incubated in Tris 0.1M-DAB 3%-triton 0.1% solution for 30 min, and finally, 5‰ of H_2O_2 was added for 45 min to reveal peroxidase activity. After rinsing in Tris 0.05 M, sections were mounted and cover-slipped in Mowiol mounting medium. Cell counting and identification of newly formed cells was performed by optical microscopy as described[12].

DOI-induced head-twitch

DOI-induced head twitch experiment was performed in clear plastic cages lined with bedding. Head-twitches (lateral movements of the head from side to side) induced by DOI (10 mg/kg, IP) were scored for 30 minutes by two experimenters and individual scores were averaged (**Fig. S3B**).

Statistical analysis- To determine differences between the experimental groups, responses were analyzed by either an unpaired Student´s t test or a two-way analysis of variance (ANOVA) with genotypes, time, or treatments as main factors, depending on the experimental design. Previously, normal distributions and homoscedasticity were verified by Shapiro-Wilk's test and Levene's test, respectively. Bonferroni's test was used for *post-hoc* comparisons. In all cases, $p < 0.05$ was considered statistically significant.

Pharmacological experiments

Synaptosome preparation

Crude synaptosomes were prepared as previously described[13]. Briefly, conditional KO mice and littermates controls were rapidly sacrificed by cervical dislocation. The brains were harvested on ice and homogenized in ice-cold sucrose 0.32M solution. Homogenates were centrifuged at 1000g for 10 min at 4°C. Supernatants were centrifuged at 15000 g for 30 min at 4°C. Crude synaptosome pellets were resuspended in Krebs-Ringer-Hepes solution (125 mM NaCl; 3 mM KCl; 1.2 mM $CaCl_2$; 1.2 mM MgSO4; 1 mM NaH_2PO_4; 22 mM $NaHCO_3$; 10 mM Glucose; 100 µM ascorbic acid; 100 µM pargyline; pH 7,4). Protein content was determined by Bradford assay (Bio-Rad, Marnes-la-Coquette, France).

Serotonin uptake

Synaptosomes (200 ± 50 µg) were incubated with 6 concentrations (0, 6.25, 12.5, 25, 50 and 100 nM) of [^{3}H] 5-HT for 30 min at room temperature. In parallel, non-specific uptake was determined by addition of paroxetine 1µM. Synaptosomes were harvested (Brandell harvester) on GF/B filtermats,

washed 3 times with ice-cold Krebs-Ringer-Hepes solution containing 1µM paroxetine to prevent 5-HT release. Filtermats were incubated in scintillation cocktail (Ultima Gold, Perkin Elmer, Courtaboeuf, France) and counted in a scintillation counter. Non-specific uptake was subtracted from total uptake to calculate the specific uptake.

Competition binding

Synaptosomes (200 ± 50 µg) were incubated with 5 nM of [^{3}H] Citalopram and 6 concentrations (10^{-11}, 10^{-10}, 10^{-9}, 10^{-8}, 10^{-7}, 10^{-6} M) of paroxetine for 1 hour at room temperature. Synaptosomes were harvested (Brandell harvester) on GF/B filters, washed 3 times with ice-cold Krebs-Ringer-Hepes solution. Filtermats were incubated in scintillation cocktail (Ultima Gold, Perkin Elmer, Courtaboeuf, France) and counted in a scintillation counter.

[^{3}H]Radioligands and drugs

Fluoxetine hydrochloride (Biotrend, Switzerland), Paroxetine hydrochloride hemydrate, (±) 8-hydroxy-2-(di-n-propylamino) tetralin hydrobromide (8-OH-DPAT), 1-[5-(2-thienylmethoxy)-1H-3-indoyl] propan- 2-amine hydrochloride (BW723C86) (Tocris), and (±)-2,5-Dimethoxy-4-iodoamphetamine hydrochloride (DOI), (±)-1-(3,4-Methylenedioxyphenyl)-2-butanamine hydrochloride (MDMA) (Sigma-Aldrich, Saint-Quentin Fallavier, France) were dissolved in 0.9% (w/v) NaCl solution (saline). [^{3}H]5-HT Trifluoroacetate (85.6 Ci/mmol) and [^{3}H]citalopram (86 Ci/mmol) were purchased from Perkin Elmer (Courtaboeuf, France). 5-Bromo-2'deoxyuridine (BrdU) (Sigma, B9285) was dissolved in 0.9% NaCl at 50°C, and the pH was set at 7.4 with NaOH 10M.

References

1. Fernandez SP, Cauli B, Cabezas C, Muzerelle A, Poncer J-C, Gaspar P. Multiscale single-cell analysis reveals unique phenotypes of raphe 5-HT neurons projecting to the forebrain. *Brain Structure and Function* 2016; **221**(8)**:** 4007-4025.

2. Vandermaelen CP, Aghajanian GK. Electrophysiological and pharmacological characterization of serotonergic dorsal raphe neurons recorded extracellularly and intracellularly in rat brain slices. *Brain Res* 1983; **289**(1-2)**:** 109-119.

3. Muzerelle A, Scotto-Lomassese S, Bernard JF, Soiza-Reilly M, Gaspar P. Conditional anterograde tracing reveals distinct targeting of individual serotonin cell groups (B5-B9) to the forebrain and brainstem. *Brain Structure and Function* 2016; **221**(1)**:** 535-561.

4. Maroteaux M, Mameli M. Cocaine evokes projection-specific synaptic plasticity of lateral habenula neurons. *J Neurosci* 2012; **32**(36)**:** 12641-12646.

5. Aghajanian GK, Vandermaelen CP. Intracellular recording in vivo from serotonergic neurons in the rat dorsal raphe nucleus: methodological considerations. *J Histochem Cytochem* 1982; **30**(8)**:** 813-814.

6. Bill DJ, Knight M, Forster EA, Fletcher A. Direct evidence for an important species difference in the mechanism of 8-OH-DPAT-induced hypothermia. *Br J Pharmacol* 1991; **103**(4)**:** 1857-1864.

7. Scott MM, Wylie CJ, Lerch JK, Murphy R, Lobur K, Herlitze S *et al.* A genetic approach to access serotonin neurons for in vivo and in vitro studies. *Proc Natl Acad Sci U S A* 2005; **102**(45)**:** 16472-16477.

8. Doly S, Valjent E, Setola V, Callebert J, Herve D, Launay JM *et al.* Serotonin 5-HT2B receptors are required for 3,4-methylenedioxymethamphetamine-induced hyperlocomotion and 5-HT release in vivo and in vitro. *J Neurosci* 2008; **28**(11)**:** 2933-2940.

9. Doly S, Bertran-Gonzalez J, Callebert J, Bruneau A, Banas SM, Belmer A *et al.* Role of serotonin via 5-HT2B receptors in the reinforcing effects of MDMA in mice *PLoS ONE* 2009; **4**(11)**:** e7952.

10. Pitychoutis P, Belmer A, Moutkine I, Adrien J, Maroteaux L. Mice lacking the serotonin Htr2B receptor gene present an antipsychotic-sensitive schizophrenic-like phenotype. *Neuropsychopharmacology* 2015; **40**(12)**:** 2764-2773.

11. Diaz SL, Maroteaux L. Implication of 5-HT2B receptors in the serotonin syndrome. *Neuropharmacology* 2011; **61:** 495-502.

12. Diaz SL, Doly S, Narboux-Nême N, Fernandez S, Mazot P, Banas S *et al.* 5-HT2B receptors are required for serotonin-selective antidepressant actions. *Mol Psychiatry* 2012; **17:** 154-163.

13. Gray EG, Whittaker VP. The isolation of nerve endings from brain: an electron-microscopic study of cell fragments derived by homogenization and centrifugation. *J Anat* 1962; **96:** 79-88.

14. Banas S, Doly S, Boutourlinsky K, Diaz S, Belmer A, Callebert J *et al.* Deconstructing antiobesity compound action: requirement of serotonin 5-HT2B receptors for dexfenfluramine anorectic effects. *Neuropsychopharmacology* 2011; **36:** 423–433.

Figure S1

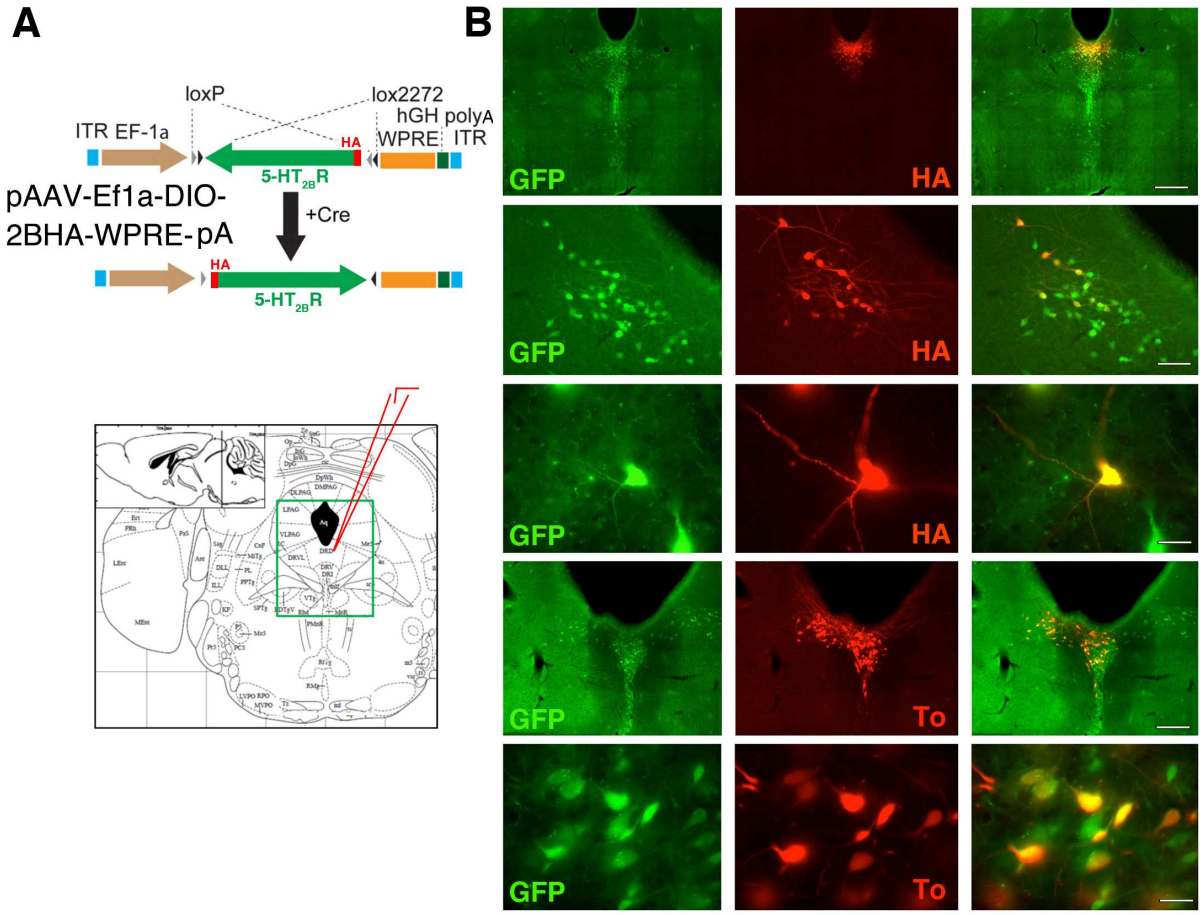

Figure S1 - Stereotaxic injection of *AAV-DIO-tomato* or *AAV-DIO-5-HT$_{2B}$HA* virus in B7 raphe nuclei. A) Viral construct, injection site and transgenes expression. The Double-floxed Inverse Orientation (DIO) AAV construct allows Cre-mediated expression of the transgene. **B)** Correct expression was assessed by visualization of Tomato (To) or 5-HT$_{2B}$HA immunofluorescence (HA) in GFP positive Pet1-Cre neurons (GFP) by fluorescence microscopy. Scale bars 10 µm; 30 µm, 100 µm.

Figure S2

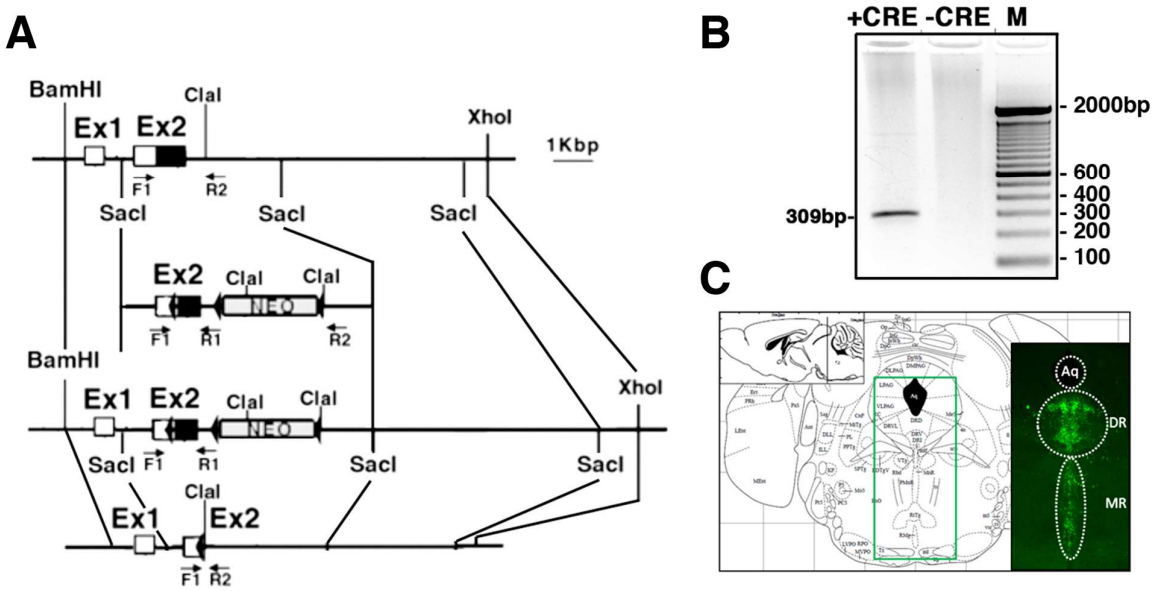

Figure S2 - Conditional deletion of *Htr2b* and genotyping. A) Top: *Htr2b* locus indicating the positions of exons, (Exon 1, Ex1; Exon 2, Ex2) and restriction sites used for the targeting construct. Middle: targeting vector designed to floxed exon 2 by homologous recombination in genomic DNA generating the targeted locus (below). Exons 1– 2 are depicted by white (untranslated) and black boxes (coding) and Neomycin resistance by grey box (NEO). Bottom: sequenced-verified structure of the *Htr2b* null allele (KO) after excision by Cre recombinase of the sequence flanked by LoxP sites (triangles). Horizontal arrows illustrate the position of primers used for genotyping (F1, R1, R2). **B)** Genomic DNA of raphe from *Pet1-Cre*$^{+/0}$*;Htr2b*$^{fl/fl}$ mice was extracted and analyzed by PCR, revealing the effective proper recombination (F1, R2 amplimers, 309 bp). **C)** Efficient Cre recombination in serotonin neurons. Immunofluorescence reveals the GFP expression in serotonin neurons, as seen by confocal microscopy in coronal section of raphe of *Pet1-Cre*$^{+/0}$;*RCE* mice. Aq: Aqueduct (Sylvius); DR: Dorsal raphe; MR: Median raphe.

Figure S3

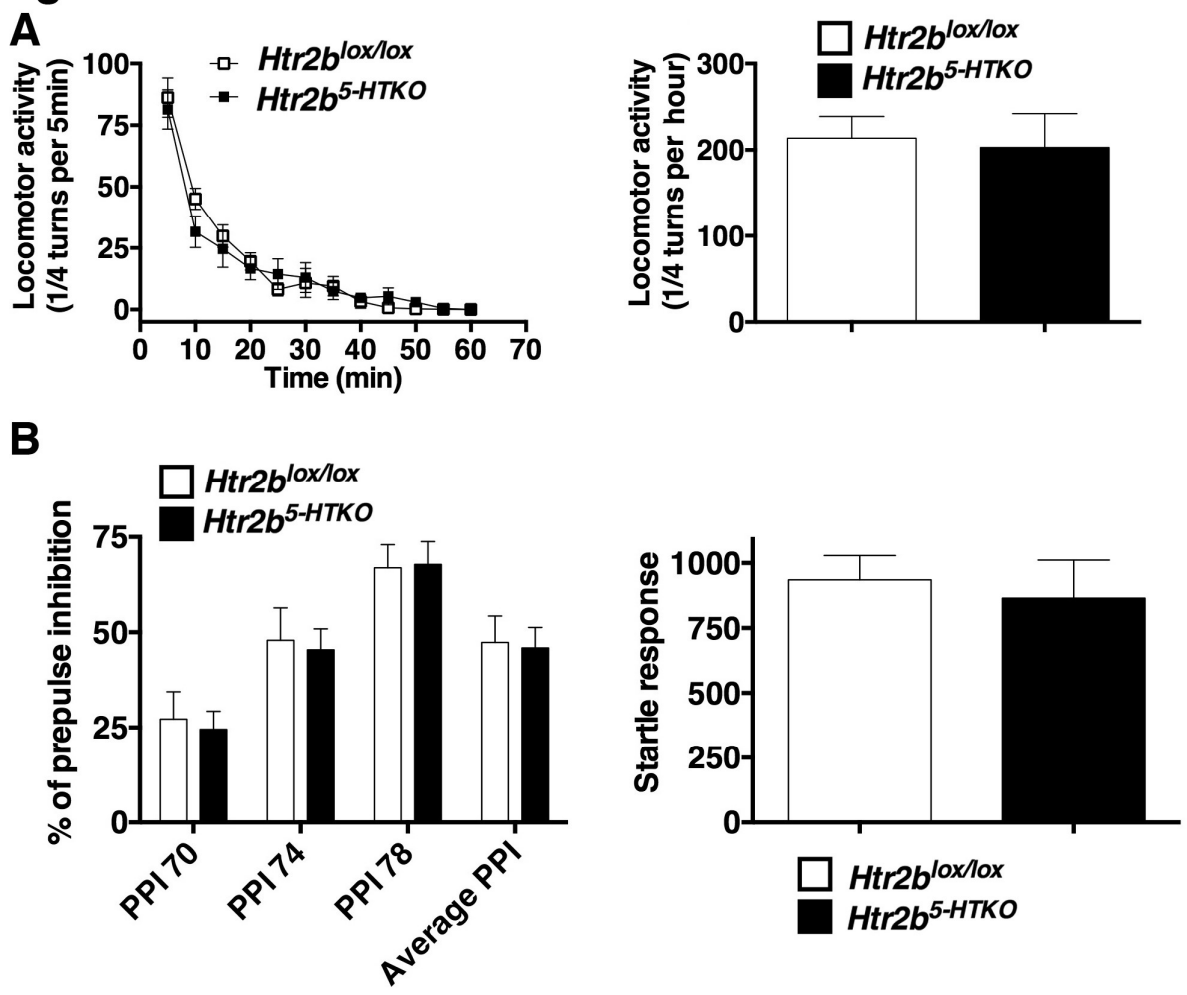

Figure S3 - Behaviors that are not affected in *Htr2b*$^{5\text{-}HTKO}$ mice lacking 5-HT$_{2B}$ receptor selectively in 5-HT neurons- A) Spontaneous locomotion in a novel environment. The total locomotor activity of the control *Htr2b*$^{lox/lox}$ mice, and of the *Htr2b*$^{5\text{-}HTKO}$ mice was not significantly difference in the first session in actimeter (n = 8 per group; data are expressed as mean ± SEM). **B**) Prepulse inhibition of startle reflex. Prepulse inhibition (PPI) was not different from *Htr2b*$^{lox/lox}$ control animals in conditional *Htr2b*$^{5\text{-}HTKO}$ mice across prepulse intensities over 70 db and in average of all intensities (n = 8 per group; data are expressed as mean ± SEM) with no change in startle response (right). Defects of PPI observed in full *Htr2b*$^{-/-}$ mice[10] are not reproduced in conditional raphe *Htr2b* ablation, as novelty-induced hyperlocomotion[8, 9, 14].

Article 2

CIPP scaffold protein interacts with the C-terminus of 5-HT$_{2B}$ receptors to promote NMDA receptor clustering

Emily Quentin, Imane Moutkine, Benjamin Chanrion, Marion Russeau, Philippe Marin, Sabine Levi, and Luc Maroteaux

---

2. Interaction du récepteur 5-HT$_{2B}$ avec la protéine de CIPP

(En préparation)

Dans les neurones, les RCPGs sont distribués grâce à leurs interactions avec différentes protéines d'adressage, de pontage ou d'échafaudage régulant ainsi leur trafic intracellulaire, leur cinétique d'internalisation ou encore leurs voies de signalisation. Les protéines de pontage contiennent différents domaines de liaison permettant la formation de complexes protéiques fonctionnels. Notamment via leurs domaines PDZ auxquels se fixent les RCPGs par leur extrémité C-terminale (pour revue Dunn and Ferguson, 2015). Des approches protéomiques ont permis d'identifier les protéines de pontage associées aux R-5-HT et montrer, par exemple, l'association des R-5-HT$_{2C}$ avec PSD-95 ou des R-5-HT$_{2A/2B/2C}$ avec MUPP1 (pour revue Marin et al., 2012) **(Figure 29)**. Au vu des phénotypes des animaux *5-HT$_{2B}^{5-HTKO}$*, il est apparu nécessaire d'étudier la distribution des R-5-HT$_{2B}$ et d'examiner les interactions protéiques de ce récepteur et l'impact fonctionnel potentiel de cette interaction.

Protéines communes aux R-5-HT$_{2A/C}$ | Protéines communes aux R-5-HT$_{2A/B}$ | Protéines communes aux R-5-HT$_{2B/C}$ | Protéines communes aux R-5-HT$_{2A/B/2C}$

Receptor	Associated protein	Site of interaction	Function of interaction
5-HT$_{2A}$	PDZ protein*	Ct	Targeting
	PSD-95	Ct	Targeting, expression, signalling,
	MUPP1	Ct	response to hallucinogens and antipsychotics
	SAP97	Ct	Trafficking, Targeting
	MAGI2	Ct	Targeting, trafficking
	MPP3	Ct	Signalling
	CIPP	Ct	Targeting
	Caveolin-1	Ct	Signalling
	ARF1-6	Ct	Desensitization, cross-talk with growth factors,
	MAP1A	i3	functional selectivity
	JAK2/STAT3	Ct, i3	Signalling
	RSK2		
	Calmodulin		
5-HT$_{2B}$	PDZ proteins*	Ct	NO signalling
	MUPP1	Ct	
5-HT$_{2C}$	PDZ proteins *	Ct	Desensitization
	MUPP1	Ct	Aggregation, phosphorylation
	PSD-95	Ct	Desensitization, Trafficking, Expression, Signalling
	SAP97	Ct	Desensitization, Trafficking
	SAP102	Ct	G-independent signalling
	MAGI-2	Ct	Dephosphorylation, responses to drugs
	MPP3	Ct	of abuse (cannabis)
	Veli3/CASK/Mint1	Ct	
	Calmodulin	Ct	

Figure 29 Fonction et sites d'interaction des protéines associées aux R-5-HT$_2$. *D'après (Marin et al., 2012)*

A. Identification des protéines PDZ associées au R-5-HT$_{2B}$ dans le cerveau

Les 14 derniers acides aminés du R-5-HT$_{2B}$ ont été utilisés comme sonde pour identifier les protéines interagissant avec le récepteur dans le cerveau de souris (Bécamel et al., 2004). Ces protéines ont été identifiées par l'équipe de Philipe Marin par une approche protéomique associant chromatographie d'affinité à l'aide d'un peptide synthétique du R-5-HT$_{2B}$ et spectrométrie de masse. Afin d'identifier le site d'interaction de ces protéines avec le R-5-HT$_{2B}$, le site de liaison au domaine PDZ a été tronqué (R-5-HT$_{2B}$ΔPDZ). Cinq protéines ont été identifiées : α1-syntrophine, NHERF, nNOS, SAP-102 et CIPP. Parmi ces protéines, nous avons choisi de nous concentrer sur la protéine CIPP du fait de son interaction avec les R-NMDA et le complexe transynaptique neuroligine-neurexine suggérant un rôle dans la transmission synaptique. Nous avons confirmé, en transfectant CIPP et le R-5-HT$_{2B}$ dans la lignée cellulaire COS-7, que ces protéines co-immunoprécipitent et que cette interaction est supprimée en tronquant le domaine de liaison aux sites PDZ du récepteur

B. Impact fonctionnel de l'interaction du R-5-HT$_{2B}$ avec CIPP sur la voie de la PLC

La co-expression du R-5-HT$_{2B}$ avec CIPP, dans les cellules COS-7 transféctées, n'affecte pas l'expression totale et membranaire du récepteur. Pour montrer cela, nous avons appliqué des concentrations croissantes d'un antagoniste du R-5-HT$_{2B}$ (10^{-6} à 10^{-12} M, RS127445) dans un milieu contenant une concentration fixe d'un antagoniste tritié du récepteur (mésulergine, 1 nM). Ceci induit une compétition entre les deux antagonistes pour lier le R-5-HT$_{2B}$. La quantité d'antagoniste tritié détectée reflète le nombre de site « liables » de récepteurs (Bmax). Sachant que la mésulergine et le RS127445 ne possèdent qu'un seul et même site de liaison sur le récepteur, le Bmax calculé reflète l'expression du R-5-HT$_{2B}$. Cette expérience a été effectuée sur des préparations de membrane de cellules transfectées lysées, nous permettant d'évaluer l'expression totale du récepteur. Cette expérience a été reproduite sur des cellules en culture non lysées, ainsi comme le site de liaison des ligands se situe sur la partie extracellulaire du récepteur, ceci nous permet d'évaluer l'expression de surface du R-5-HT$_{2B}$. Nos résultats ont montré que, ni l'expression totale, ni l'expression de surface ne sont affectées en présence de CIPP.

Pour évaluer l'impact fonctionnel de cette co-expression nous avons stimulé les cellules transfectées avec des concentrations croissantes (10^{-6} à 10^{-12} M) d'agoniste total (5-HT) ou partiel (DOI). Ces expériences étant effectuées en présence d'un bloqueur de la dégradation de l'IP_3 (LiCl), la mesure de l'accumulation d'IP_3 reflète l'activité de la voie de la PLC induite par l'activation du R-5-HT_{2B}. L'utilisation d'un agoniste partiel et total nous permet d'appliquer un modèle mathématique développé par Black et Leff en 1983 et d'évaluer la capacité de couplage du R-5-HT_{2B} à la voie de la PLC (Black and Leff, 1983).

En condition basale et en réponse à l'activation du R-5-HT_{2B} (10^{-6} à 10^{-11} M), l'accumulation d'IP_3 mesurée est significativement plus forte en présence de CIPP, indiquant que CIPP potentialise la voie de la PLC associée au R-5-HT_{2B} sans affecter son expression membranaire ni sa capacité de couplage aux protéines Gαq.

C. Distribution subcellulaire du R-5-HT_{2B} et de CIPP

Dans le but d'approfondir cette interaction dans un modèle plus physiologique, en collaboration avec Sabine Lévi, nous avons transfecté ces deux protéines dans des cultures primaires d'hippocampe. Le choix d'utiliser des cultures primaires de neurones d'hippocampe s'est imposé du fait de la difficulté de cultiver et transfecter des neurones sérotoninergiques.

L'ARN messager codant le R-5-HT_{2B} a été localisé dans l'hippocampe, le noyau paraventriculaire du thalamus, les noyaux du raphé dorsal, le locus cœruleus, l'habénula, le cortex et le cervelet (Bonaventure et al., 2002) **(Figure 15)**. L'ARN messager codant CIPP a été identifié dans le cervelet, les colliculus inférieurs, les noyaux vestibulaires, les noyaux facials, le thalamus, le tronc cérébral ainsi que les bulbes olfactifs (Kurschner et al., 1998) **(Figure 13)**. Sachant que l'ARN messager du R-5-HT_{2B} est retrouvé dans l'hippocampe, il est probable que les mécanismes d'adressage du récepteur soient présents et que sa distribution soit physiologique bien que nous utilisions un modèle de surexpression. De plus, étant donné que CIPP n'est pas exprimé dans l'hippocampe, nous suggérons que les effets observés sont dus à la transfection de CIPP et non pas à la présence de CIPP endogène. Enfin, le milieu de culture que nous avons utilisé pour la culture des neurones d'hippocampe ne contient pas de sérum afin d'éviter que le R-5-HT_{2B} ne soit stimulé par la présence de 5-HT dans le sérum.

Les propriétés des clusters de R-5-HT_{2B}, de R-NMDA et de CIPP ont été évaluées à l'aide du logiciel Metamorph (nombre, aire, intensité). Sachant que la résolution optique d'un microscope confocal en profondeur est d'environ 400 nm (pour un marquage et une configuration optique parfaits) et qu'une dendrite fait environ 1 µm d'épaisseur, nous

considérons que les objets ne peuvent pas être séparé du fait de la résolution du microscope. C'est pourquoi, nous effectuons une projection des images obtenues sur une même dendrite avant d'effectuer les analyses. Les marquages protéiques sont mesurés par l'application d'un seuil déterminé manuellement, à l'aveugle, afin de ne pas inclure de marquages non spécifiques. Les analyses de colocalisation ont été effectuées avec le logiciel Metamorph. Les clusters protéiques sont définis de la même façon que précédemment sur les images brutes et non modifiées de chacun des marquages. Ensuite, le logiciel superpose les images et détermine les clusters superposés et définis les propriétés de chacun des marquages (nombre, aire, intensité) et des propriétés spécifiques des marquages colocalisés ou non colocalisés. Du fait de la résolution en x du microscope confocal (200 nm), nous considérons qu'une augmentation de l'aire est significative seulement lorsque la taille des clusters est supérieure à la résolution optique ou lorsque la variation est supérieure à 50%. Dans le cas contraire, l'analyse de l'aire des clusters n'est pas prise en compte dans les interprétations des résultats.

Les R-5-HT_{2B} sont observés au niveau somatodendritique et CIPP dans tous les compartiments cellulaires (soma, dendrite, axone). De façon surprenante, CIPP augmente de façon significative l'aire et l'intensité des clusters de R-5-HT_{2B} mais pas sa localisation dans les compartiments cellulaires **(Figure 30)**. Ceci pourrait expliquer le gain de fonction de la signalisation du récepteur. En effet, en regroupant les R-5-HT_{2B}, CIPP favoriserait le maintien du récepteur ou le localiserait dans des régions riches en protéines G. Nous avons, par la suite, co-transfecté des marqueurs de synapses excitatrices (Homer-GFP) ou inhibitrices (gephyrine-GFP) avec le R-5-HT_{2B} en présence ou non de CIPP. Ceci nous a permis de montrer que CIPP favorise l'expression du R-5-HT_{2B} dans les synapses excitatrices au détriment des synapses inhibitrices, ceci étant abolis lorsque le site de liaison aux domaines PDZ est tronqué (R-5-HT_{2B}ΔPDZ).

D. Impact fonctionnel de l'interaction du R-5-HT_{2B} avec CIPP sur la voie de la signalisation calcique

Au niveau fonctionnel, la stimulation du R-5-HT_{2B} avec un agoniste spécifique (BW723C86-1 µM) diminue rapidement (10 min) la densité, l'aire et l'intensité des clusters de R-5-HT_{2B} à la surface. Cet effet est conservé en présence de CIPP indiquant que CIPP n'empêche pas l'internalisation des R-5-HT_{2B}. Sachant que le R-5-HT_{2B} est couplé à la voie de la PLC et que celle-ci induit la libération de calcium dans les neurones, nous avons mesuré la libération de calcium suite à une stimulation des R-5-HT_{2B} (BW723C86-1 µM). Le signal calcique a été observé en utilisant la sonde calcique fluo4-AM perméable et qui pénètre donc

dans les cellules. Le signal calcique a été mesuré en microscopie confocale *« spinning disc »* dans une chambre chauffée et dans un milieu physiologique (MEM-R). Les images ont été acquises toutes les 500 ms avec un temps d'exposition faible, permettant le maintien de l'intégrité des neurones au cours de l'acquisition. Pour analyser le signal calcique, le signal a été acquis pendant 30 secondes afin de mesurer le signal calcique de base avant stimulation. Ainsi, le signal calcique observé pendant la stimulation a été normalisé par le signal basal et le bruit de fonds de la caméra a été soustrait pour extraire seulement les signaux induits par la stimulation. La présence de CIPP n'affecte pas la cinétique de libération de calcium mais augmente significativement l'ampleur du pic de libération de calcium (+45% des neurones exprimant seulement le R-5-HT_{2B}), indiquant que la présence de CIPP induit une augmentation de la libération de calcium dépendante de la stimulation du récepteur **(Figure 30)**. Ces résultats associés à ceux obtenus sur l'activation de la voie de la PLC sur la lignée cellulaire COS-7, suggèrent que CIPP potentialise la signalisation du R-5-HT_{2B} par son action sur la distribution cellulaire du récepteur.

E. Impact de la stimulation du R-5-HT_{2B} sur la morphologie des épines dendritiques

La morphologie des épines dendritiques a été étudiée à partir de neurones transfectés avec le R-5-HT_{2B}, CIPP ainsi qu'une protéine GFP cytosolique. La morphologie des épines a été identifiée à l'aide du logiciel Neuron Studio (Dumitriu et al., 2011). Ainsi les épines dendritiques de type filopodes sont identifiées par leur absence de « tête », celles de types *« stubby »* sont identifiées par leur absence de « cou » et enfin celles de types *« mushroom »* sont identifiées par la présence d'un « cou » et d'une « tête ». Un paramètre supplémentaire est la mesure du ratio entre le diamètre de la « tête » et la longueur du « cou » de l'épine. Lorsque ce ratio est égal à 1 :1 (tête : cou), cela correspond à une morphologie de type *« mushroom »*. Lorsque le ratio est supérieur ou égal à 1 :2,5 (tête : cou) alors le cou est trop long pour que l'épine soit considérée comme *« mushroom »*., elle est donc catégorisée comme filopode (Dumitriu et al., 2011).

Sachant que CIPP cible le R-5-HT_{2B} dans les synapses excitatrices, il pourrait aussi affecter la morphologie des épines dendritiques. La co-expression de CIPP et du R-5-HT_{2B} diminue le nombre et la densité des épines dendritiques en condition basales. De plus, la stimulation du R-5-HT_{2B} induit des variations de la morphologie des épines dendritiques. Ces variations semblent plus grandes lorsque CIPP n'est pas exprimé, notamment pour les épines de type *« stubby »,* suggérant que CIPP pourrait participer au maintien de la morphologie des épines dendritiques **(Figure 30)**.

F. Impact du R-5-HT$_{2B}$ et de CIPP sur la distribution des R-NMDA

Kurschner *et al.,* (1998) ont mis en évidence que CIPP interagit aussi avec les récepteurs NMDA, c'est pourquoi nous avons étudié la distribution des R-NMDA endogènes en condition basale et suite à la stimulation de neurones exprimant CIPP et/ou le R-5-HT$_{2B}$. De façon surprenante, l'expression de CIPP suffit à augmenter le nombre de clusters de R-NMDA et à diminuer leur intensité, indépendamment de la présence des R-5-HT$_{2B}$. Cette observation indique que CIPP est capable d'avoir un impact sur la distribution des R-NMDA.

La stimulation du R-5-HT$_{2B}$, diminue progressivement l'intensité de R-NMDA sans affecter le nombre de cluster, suggérant que la stimulation du R-5-HT$_{2B}$ provoquerait une dégradation des R-NMDA en absence de CIPP **(Figure 30)**. A l'inverse, en présence de CIPP, la stimulation du R-5-HT$_{2B}$ augmente rapidement l'intensité des R-NMDA, suggérant qu'il y a un recrutement de R-NMDA en réponse à cette stimulation **(Figure 30)**.

G. Conclusion

Dans cette étude, nous avons mis en évidence que l'interaction protéique du R-5-HT$_{2B}$ et de la protéine de pontage CIPP favorise la signalisation du R-5-HT$_{2B}$ dans la lignée cellulaire COS-7 et les cultures de neurones primaires d'hippocampe. Nous avons montré que CIPP et R-5-HT$_{2B}$ modulent la distribution des R-NMDA ainsi que la morphologie des épines dendritiques. La stimulation du R-5-HT$_{2B}$ affecte la morphologie des épines dendritiques et induit l'internalisation du récepteur même en présence de CIPP. Enfin, la stimulation du R-5-HT$_{2B}$ favorise l'agrégation des R-NMDA, en présence de CIPP, suggérant que l'interaction CIPP/R-5-HT$_{2B}$ pourrait participer à la transmission synaptique excitatrice.

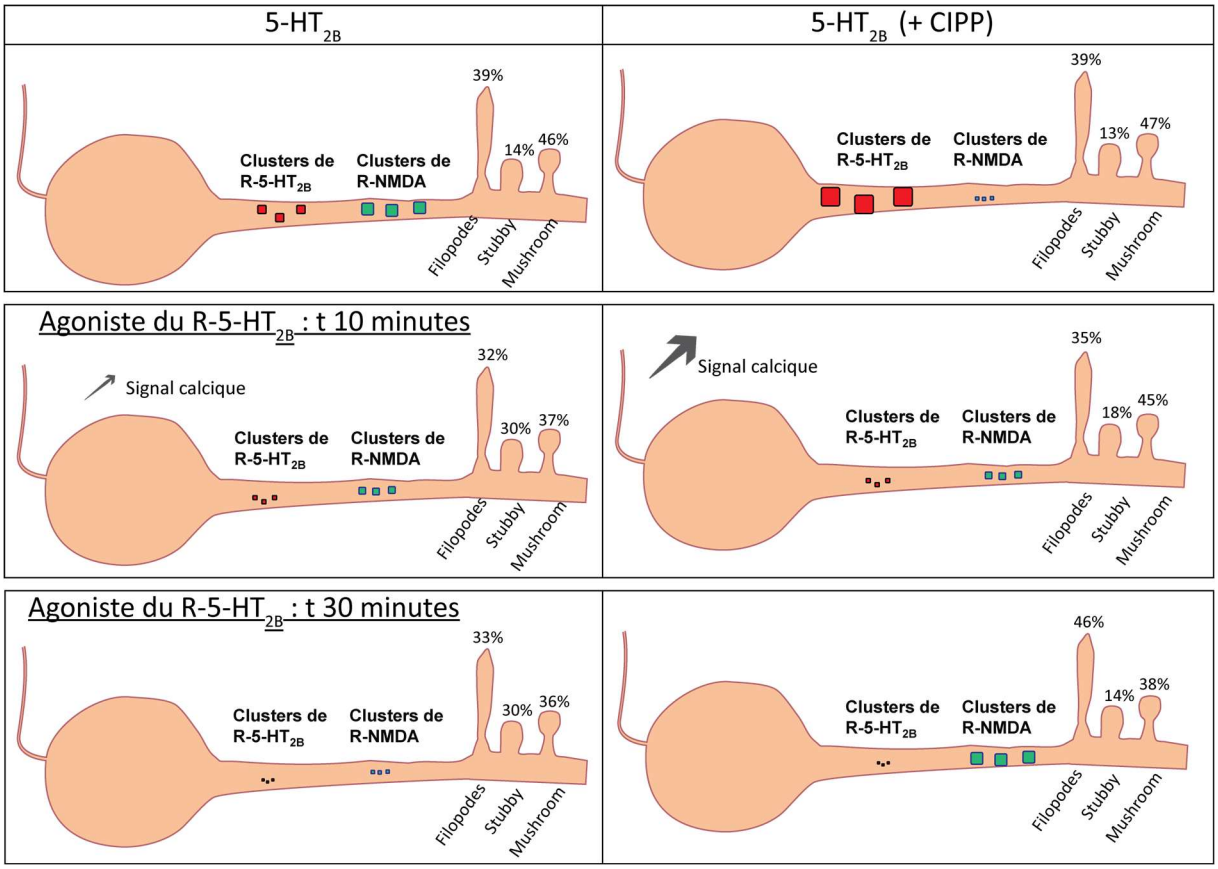

Figure 30 Représentation schématique des effets induits par la stimulation du R-5-HT$_{2B}$ dans des neurones exprimant ou non la protéine CIPP*. La distribution du R-5-HT$_{2B}$ est plus diffuse qu'en présence de CIPP tandis que les R-NMDA forment de plus gros clusters. La stimulation du R-5-HT$_{2B}$ provoque un pic de calcium, supérieur en présence de CIPP. La stimulation du R-5-HT$_{2B}$ induit son internalisation indépendamment de CIPP. La stimulation du R-5-HT$_{2B}$ induit une dispersion des R-NMDA (en absence de CIPP) ou le regroupement des R-NMDA (en présence de CIPP). La stimulation des R-5-HT$_{2B}$ induit des variations morphologiques de plus grandes ampleurs des épines dendritiques, en absence de CIPP.*

H. Contribution personnelle

Dans cette étude, j'ai effectué toutes les expériences excepté l'analyse protéomique et la préparation de cultures primaires de neurones d'hippocampe.

Title. CIPP scaffold protein interacts with the C-terminus of 5-HT2B receptors to promote NMDA receptor clustering

Short title. **5-HT_{2B} receptors interactions with CIPP**

Author List. Emily Quentin (1), Imane Moutkine (1), Benjamin Chanrion (2), Marion Russeau (1), Philippe Marin (2), Sabine Levi (1)*, and Luc Maroteaux (1)*

(1) INSERM UMR-S 839, F75005, Paris, France; Sorbonne Universités, UPMC Univ Paris 6, F75005, Paris; Institut du Fer à Moulin, F75005, Paris.
(2) Département de Neurosciences, Centre National de la Recherche Scientifique, UMR-5203, Institut de Génomique Fonctionnelle, F-34094 Montpellier, France; Département de Neurosciences, Institut National de la Santé et de la Recherche Médicale, U1191, F-34094 Montpellier, France; and Université de Montpellier, F-34094 Montpellier, France

Corresponding authors: Luc Maroteaux and Sabine Lévi, Institut du Fer à Moulin UMR-S839 INSERM/UPMC 17 rue du Fer à Moulin 75005 Paris Email: luc.maroteaux@upmc.fr; Tel: (33) 01 45 87 61 23 Fax: (33) 01 45 87 61 32

Keywords: Serotonin 5-HT_{2B} receptors, Scaffold protein, NMDA receptors, dendritic spines.

Abstract

Serotonin is involved in many psychiatric diseases including depression, addiction, impulsivity or psychosis. Humans lacking the serotonin receptor subtype 2B (5-HT_{2B}), a Gq-protein-coupled receptor, present more frequent impulsive, aggressive and suicidal behaviors. The mechanisms underlying the 5-HT_{2B}-receptor function remain unknown; in particular the distribution of the 5-HT_{2B} receptor and its putative associated protein at central synapses are not described. The present study focused on putative 5-HT_{2B} receptor association with scaffold proteins by its PDZ binding motif located at the C-terminus. Using peptide affinity chromatography combined with mass spectrometry, we found that the 5-HT_{2B} receptor PDZ binding motif recruits channel interacting PDZ protein (CIPP), a multivalent PDZ domain protein known to interact with the serotonin transporter and glutamate N-methyl-D-aspartate (NMDA) receptors. In transfected Cos-7 cells, we found that interaction between 5-HT_{2B} receptors and CIPP significantly enhanced receptor-operated inositol phosphate production without affecting the receptor membrane and intracellular expression levels or coupling efficacy. Studies in transfected hippocampal neurons revealed that CIPP-5-HT_{2B} receptor interaction allows targeting the receptor at excitatory glutamatergic synapses. This was associated with the reorganization of NMDA receptor clusters and change in the maturation of dendritic spines. Upon agonist stimulation, CIPP potentiated the 5-HT_{2B} receptor signaling in neurons, thus delaying the agonist-induced loss of mature dendritic spines. This work support that CIPP participates in the formation of a signaling platform at glutamatergic synapses, and allows the recruitment of the 5-HT_{2B}-receptor signaling and the fine tuning of NMDA receptors function in structural plasticity.

Introduction

Serotonin (5-HT) is a neurotransmitter involved in pathological conditions such as addiction, impulsivity, psychosis and depression, and in many physiological functions (sleep, mood, food intake ...). The variety of serotonin action is reflected by numerous 5-HT receptors. The serotonin receptor subtypes 2 comprises 5-HT_{2A}, 5-HT_{2B} and 5-HT_{2C} that are Gαq-coupled receptors and display distinct pharmacological properties. In humans, a lack of 5-HT_{2B} receptor is associated with 5-HT-dependent phenotypes, including impulsivity and suicidality (Bevilacqua et al., 2010). In addition to impulsive behavior (Bevilacqua et al., 2010), *Htr2b*$^{-/-}$ mice display a global deficit in sensorimotor gating as well as novelty-induced hyperlocomotion; these phenotypes have been related to positive symptoms observed in schizophrenia (Pitychoutis et al., 2015), a disorder commonly associated to a deregulation of the 5-HT systems. Recent studies suggested that 5-HT_{2B} receptors could be implicated in 5-HT-dependent behavior by acting on 5-HT neurons (Diaz et al., 2012). In frog motoneurons, electrophysiological and pharmacological studies have shown a potentiation of N-methyl-D-aspartate (NMDA)-induced depolarization by activation of 5-HT_{2B} receptors (Holohean and Hackman, 2004). More recently, Bigford et al. (2012) showed that 5-HT_{2B} receptor can immunoprecipitate GluN1 (NR1), supporting that 5-HT_{2B} receptors may form distinct multiprotein complexes with functionally assembled NMDA receptors and may affect NMDA receptor-induced motoneuron responses (Bigford et al., 2012). Nevertheless, the precise way used by 5-HT_{2B} receptors to trigger neuronal effects is still poorly understood.

In neurons, G protein–coupled receptors (GPCRs) and ion channels are targeted to the membrane of synaptic terminals in and around the postsynaptic density (PSD). Each receptor is targeted to specialized membrane domains via the interaction of scaffolding proteins with the receptors. These scaffold proteins contain multiple protein-protein interaction domains that allow them to interact with a multitude of structural and signaling proteins and hold them in close proximity with one another. Of these scaffolding proteins, postsynaptic density protein of 95 kilodaltons (PSD-95), disc large, zona occludens-1 (PDZ) domain–containing proteins provide direct contact with both GPCRs and ion channels at the postsynaptic density. PDZ proteins are not only important for targeting GPCRs, but they have a role in regulating signaling protein complexes (Dunn and Ferguson, 2015). Using the yeast two-hybrid system, a cDNA clone encoding a novel protein interacting with the C-terminal domain of the 5-HT_{2C} receptor was identified (Ullmer et al., 1998). The protein, named MUPP1 (multi-PDZ-domain protein-*Mpdz*), contains thirteen PDZ domains and no obvious catalytic domain. MUPP1 increases the expression of 5-HT_{2A} receptors in cell periphery (Jones et al., 2009).

From human epithelial cells, a cDNA for a paralogue of *Mpdz*/MUPP1 was obtained and encodes a human INAD-Like protein (INADL-inactivation-no afterpotential D-like)-PATJ (PALS1-protein associated with Lin-seven-associated tight junction protein), a protein containing several PDZ domains (Lemmers et al., 2002). The channel-interacting PDZ domain protein (CIPP) correspond to the last four PDZ domain of INADL/PATJ and is expressed in brain neurons of various areas including the cerebellum, inferior colliculus, vestibular nucleus, facial nucleus, thalamus, and brainstem (Philipp and Flockerzi, 1997). A robust interaction between the 5-HT_{2A} receptor and CIPP was initially found, whereas CIPP did not significantly associate with the 5-HT_{2C} receptor (Becamel et al., 2004). By analogy to MUPP1, it is likely that CIPP PDZ2 (INADL PDZ8) interacts with 5-HT_2 receptors (Assémat et al., 2013).

Here, we report a strong interaction between the 5-HT_{2B} receptor and CIPP, which induces an increase in 5-HT_{2B}-receptor coupling efficacy in non-neuronal and neuronal cells. We present evidences that CIPP targets 5-HT_{2B} receptors at excitatory glutamatergic synapses, increasing intracellular calcium levels. This has for consequence to increase NMDA receptor clustering and dendritic spine maturation. Our data support a role of the CIPP-5-HT_{2B} receptor scaffold in the regulation of the glutamatergic synapse function.

Results

Recruitment of CIPP by the 5-HT$_{2B}$-receptor PDZ binding domain. To get novel insight into the role of 5-HT$_{2B}$ receptors expressed in neurons, we sought to identify its PDZ partners in brain using an affinity purification coupled to mass spectrometry (AP-MS) proteomic strategy, which has already proved efficiency for characterizing specific PDZ binding partners of 5-HT$_{2A}$ and 5-HT$_{2C}$ receptors (Becamel et al., 2004). Two-dimensional (2-D) gel analysis of affinity-retained proteins in experiments using the 5-HT$_{2B}$ C-terminal peptide and the corresponding peptide lacking the receptor PDZ binding motif (3 C-terminal residues) as baits, showed the specific recruitment by the full-length peptide of a protein of around 70 kDa that appears as a train of spots on the 2-D gels (**Fig. 1A**). This protein was identified as CIPP (or INAD-like protein isoform 3) by peptide mass fingerprint (Mascot Score, 153, $p = 8.7 \times 10^{-11}$). Co-immunoprecipitation followed by Western blotting confirmed association of CIPP with full length 5-HT$_{2B}$ receptor expressed in COS-7 cells and that 5-HT$_{2B}$ receptor/CIPP interaction is abolished by the deletion of the receptor PDZ binding motif (**Fig. 1B**).

Recruitment of CIPP by the PDZ binding domain of the 5-HT$_{2B}$ receptor increases signaling without changing Gq-coupling efficacy. To better understand the role of CIPP interactions, we started investigating the functional impact of 5-HT$_{2B}$ receptor and CIPP co-expression. Using radiolabeled ^{3}H-Mesulergine binding, a 5-HT$_{2B}$ receptor antagonist (pKi = 8.46 ± 0.05) (Maroteaux et al., 2017), we quantified the total expression (lyzed cell membrane) and the surface expression (living cells) of 5-HT$_{2B}$ receptor in the presence or not of CIPP. First, we observed that CIPP co-expression did not affect total- (Welch corrected t-test p = 0.7) or plasma-membrane 5-HT$_{2B}$-receptor expression (Welch corrected t-test p = 0.1) (**Fig. 2A**). In order to analyze signaling properties of 5-HT$_{2B}$ receptors, we stimulated cells with increasing concentrations of a full 5-HT$_{2B}$ receptor agonist (5-HT) or a partial agonist (DOI) and quantified the amount of inositol phosphate accumulated. Co-expression of 5-HT$_{2B}$ receptors with CIPP increased basal (p = 0.0075 for 5-HT, p = 0.0055 for DOI) and stimulated inositol phosphate signaling pathway (p = 0.0157 for 5-HT, p = 0.0015 for DOI) (**Fig. 2B**). Data were further analyzed using Black and Leff operational model in order to determine any change in the power of agonists to activate the Gq pathway, which is represented by the $\log(\tau/K_A)$ with (K_A) affinity for the receptor and (τ) coupling efficacy in activating a particular signaling pathway (Graphpad Prism 6 Software) (Black and Leff, 1983; Kenakin et al., 2012). No significant difference was found in Gq-coupling properties. For 5-HT, 5-HT$_{2B}$ receptor $\log(\tau/K_A)$ =7.99 ± 0.24 compared to 5-HT$_{2B}$ receptor/CIPP $\log(\tau/K_A)$ = 8.02 ± 0.21, (Welch corrected t-test p = 0.93). For DOI, 5-HT$_{2B}$ receptor $\log(\tau/K_A)$ = 7.19 ± 0.16 compared to 5-HT$_{2B}$ receptor/CIPP $\log(\tau/K_A)$ = 7.09 ± 0.66, (p = 0.53, n=3-5). These results indicated that CIPP did not affect the affinity of the 5-HT$_{2B}$ receptor for the Gq protein nor changed the coupling efficacy to the Gq protein in COS-7 cells (**Fig. 2B**). Therefore, CIPP increases 5-HT$_{2B}$-receptor signaling without changing the receptor property or membrane turnover.

CIPP increases the membrane clustering of 5-HT$_{2B}$ receptors. If CIPP is involved in the gain of signaling activity of 5-HT$_{2B}$ receptors, it could affect its subcellular distribution. In order to investigate the subcellular distribution of 5-HT$_{2B}$ receptors in a more physiological context, we use primary cultures of hippocampal neurons. In the absence of antibody against 5-HT$_{2B}$ receptor or CIPP, we transfected constructs with HA- and FLAG- N-terminus tagged 5-HT$_{2B}$ receptor and CIPP, respectively. We assessed quantitatively the distribution of 5-HT$_{2B}$ receptors in the presence (or not) of CIPP. Colocalization analyzes of 5-HT$_{2B}$ receptor and CIPP clusters showed that both proteins were strongly colocalized (Total: 73.2%, Surface: 68.4% of colocalization). By comparing the total labeling of 5-HT$_{2B}$ receptor (permeabilized cells) to surface labeling (performed at 4°C), we observed that CIPP increased surface and total 5-HT$_{2B}$-receptor cluster area (145.8 ± 16.8% for total 5-HT$_{2B}$ receptors, n=18, Mann-Withney t-test p = 0.04; and 156.6 ± 15.5% for surface receptor, n=18, p = 0.007) but not the cluster

number (**Fig. 3**). CIPP increased significantly the 5-HT_{2B}-receptor density per cluster (integrated intensity 244.8 ± 22.4% for total 5-HT_{2B} receptor, n=18, Mann-Withney t-test p = 0.0007 and 214.0 ± 28.5% for surface receptor, n=28, p = 0.004) compared to the receptor alone. Thus, CIPP increases the size of platforms recruiting the 5-HT_{2B} receptor associated signaling pathway.

CIPP targets the 5-HT_{2B}-receptor at glutamatergic synapses via PDZ binding. We identified CIPP expression in the somatic, dendritic and axonal compartments, while 5-HT_{2B} receptor expression was restricted to somato-dendritic compartments (**Fig. 4A**). This result was confirmed by a labeling using neurofilamin as axonal marker (data not illustrated). Hippocampal cultures of neurons were then transfected by 5-HT_{2B}-HA-tagged-receptor and a Gephyrin-finger-GFP protein as postsynaptic marker of inhibitory synapses or a Homer-GFP protein, as postsynaptic marker of excitatory synapses in presence or not of CIPP-Flag protein. Coexpressing a Homer-GFP protein, we found that CIPP increased the colocalization of 5-HT_{2B}-HA-tagged-receptor with Homer-GFP (+25%, n=11) and thus the expression of 5-HT_{2B} receptors close to excitatory dendritic spines (Mann-Withney t-test p = 0.0097) (**Fig. 4B**). Conversely, coexpressing a Gephyrin-finger-GFP, we found that CIPP reduced the colocalization of 5-HT_{2B}-HA-tagged-receptor with Gephyrin-finger-GFP (-50%, n=10), and thus the expression of 5-HT_{2B} receptors close to dendritic inhibitory synapses (Mann-Withney t-test p = 0.026) (**Fig. 4B**). Truncation of PDZ binding domain of 5-HT_{2B}-receptor C-terminus (5-$HT_{2B}\Delta$PDZ) suppressed the effect of CIPP and reduced receptor expression at excitatory synapses compared to non-truncated 5-HT_{2B} receptor (Mann-Withney t-test, p = 0.034, 5-HT_{2B} vs. 5-$HT_{2B}\Delta$PDZ receptor; p = 0.002, 5-HT_{2B} vs. 5-$HT_{2B}\Delta$PDZ receptor in the presence of CIPP, n=9-11). This result validates the need for the 5-HT_{2B}-receptor PDZ domain to allow CIPP to enrich the receptor at excitatory dendritic synapses.

CIPP controls the maturation of dendritic spines. If co-expression of CIPP and 5-HT_{2B} receptors target the receptor to excitatory glutamatergic synapses, it could also affect dendritic spine morphology. It is generally accepted that synaptogenesis begin with the formation of immature thin dendritic spines, the so-called filopodia and that spine maturation promotes the selection of large mushroom-type spines (Hering and Sheng, 2001). We classified into three groups, the thin, stubby, and mushroom spines (**Fig. 5A**). We investigated the contribution of CIPP in dendritic spine maturation by measuring spine head diameter in neurons expressing the 5-HT_{2B} receptors in the absence or presence of CIPP. Cumulative distribution showed that neurons co-expressing CIPP and the 5-HT_{2B} receptor have dendritic spine with increased head diameter compared to neurons expressing 5-HT_{2B} receptors alone (n=527 spines for 5-HT_{2B} alone and n=333 spines in presence of CIPP, Kolmogorov t-test p < 0.0001) (**Fig. 5B**). The co-expression of CIPP and 5-HT_{2B} receptors doesn't affect spines morphology but globally reduced the spine density (1.82 ± 0.13 spines/µm for cell expressing only 5-HT_{2B} receptors, compared to 1.12 ± 0.17 spines/µm in presence of CIPP, Mann-Whitney t-test p = 0.01) (**Fig. 5C**).

CIPP has been shown to interact with NMDA receptors (Kurschner et al., 1998), one of the main neurotransmitter receptor and signaling effector that shapes glutamatergic synapses. We thus studied the influence of CIPP on NMDA receptor clustering in neurons. Expressing CIPP alone or in the presence of the 5-HT_{2B} receptor increased NMDA receptor (NR1 subunit) cluster number as compared to neurons expressing the 5-HT_{2B} receptor alone (CIPP, 140.1±15.1% n=22, CIPP+5-HT_{2B} receptor=149±13.82 %, n=49) (**Fig. 5D**). In contrast, CIPP decreased the density of NMDA receptor molecules per cluster in the absence or presence of the 5-HT_{2B} receptor (t20-5-HT_{2B} receptor = 54.66 ± 13.97% n=25; t20-CIPP+5-HT_{2B} receptor = 89.87 ± 1.97%, n=38). Therefore, CIPP redistributes NMDA receptors at the surface of neurons. It induces the formation of larger clusters with more disperse molecules within the cluster.

CIPP does not prevent the agonist-induced membrane removal of 5-HT$_{2B}$ receptors. We stimulated neurons expressing 5-HT$_{2B}$ receptors in the presence (or not) of CIPP with the 5-HT$_{2B}$-receptor agonist, BW723C86 (1µM) and quantified the number of 5-HT$_{2B}$-receptor clusters, their area and density per clusters at different time points (t0-10-20min). Agonist stimulation induces a significant decrease in surface 5-HT$_{2B}$-receptor cluster number in the presence or not of CIPP (**Fig. 6**). The area of 5-HT$_{2B}$-receptor clusters decreased after BW723C86 stimulation in the absence of CIPP (t20 = 49.34% of t0 p = 0.0006, n=13-17) as in the presence of CIPP (t20 = 52.24% p<0.0001, n=18) (**Fig. 6**). Agonist stimulation decreased in 10 min the density of surface 5-HT$_{2B}$ receptor per clusters in the absence (integrated intensity t10 = 30.16% of t0, n=18) or in the presence of CIPP (t10 = 37.83% of t0 p = 0.0003, n=28) (**Fig. 6**). The overall loss of receptors was higher in the presence of CIPP since the density of receptors per cluster is almost twice that of neurons expressing the receptor alone (at t0, the integrated intensity is 214% that of 5-HT$_{2B}$ receptor expressed alone). Altogether, these results indicate that the activation of the 5-HT$_{2B}$-receptor induces its internalization that cannot be prevented by the presence of CIPP.

CIPP increases calcium coupling of 5-HT$_{2B}$ receptors in hippocampal neurons. The 5-HT$_{2B}$-receptor stimulation activates the PLC pathway, which induces inositol phosphate production, and diacylglycerol production that stimulates release of calcium intracellular pool. We stimulated hippocampal neurons expressing 5-HT$_{2B}$ receptors in the presence (or not) of CIPP with BW723C86 (1µM) and followed calcium signal using fluo-4 AM probe. In primary dendrites, the 5-HT$_{2B}$-receptor stimulation induces calcium peak 3.06 to 4.68 second after bath application of the agonist. Co-expression of the two proteins did not affect the time course of intracellular calcium increase but increased significantly the peak height (109.8 ± 2.9% of basal activity for 5-HT$_{2B}$ receptor alone and 154.5±5.9% for 5-HT$_{2B}$ receptor with CIPP, p = 0.016; Mann-Whitney t-test; n=3–5 independent experiments, with >50 ROI measurements). Co-expression of CIPP also affected the area under the curve in each condition, which was significantly increased (3-fold) in the presence of CIPP (2682 ± 81% of basal activity for 5-HT$_{2B}$ receptor alone vs. 8299 ± 229% for 5-HT$_{2B}$ receptor with CIPP) (**Fig. 7**). These results confirmed that CIPP, by shaping 5-HT$_{2B}$-receptor clusters, potentiates receptor-signaling activity in neurons.

CIPP promotes NMDA receptor clustering upon 5-HT$_{2B}$-receptor stimulation. Since we previously observed that CIPP redistributes NMDA receptors at the surface of neurons, with larger clusters and more disperse NMDA receptors within the cluster, we checked the effect of 5-HT$_{2B}$-receptor stimulation on NMDA receptor clusters. In neurons transfected with 5-HT$_{2B}$ receptors alone, agonist stimulation did not affect number but slowly decreased the density of NMDA receptor per clusters (integrated intensity t30 = 54.66 ± 7.86% of 5-HT$_{2B}$ receptors t0, n=53, p = 0.03 t0 vs. t30 Mann-Withney t test; n = 41 from 3 independent cultures) (**Fig. 8**). On the contrary in the presence of CIPP, agonist stimulation, which also did not affect the number of NMDA receptor clusters, quickly increased the density of NMDA receptor per clusters (t0 = 56.35 ± 4.65%, n=49, t5 = 102.4 ± 13.7% of 5-HT$_{2B}$ receptor alone, n=36, p = 0.0024) (**Fig. 8**). To sum up agonist stimulation of 5-HT$_{2B}$ receptor alone induces a slow decrease of NMDA receptor density per cluster. In the presence of CIPP, 5-HT$_{2B}$-receptor stimulation produces an increase in NMDA receptor density per cluster. Therefore, 5-HT$_{2B}$-receptor activation in the presence of CIPP reverses the dispersing effect of CIPP alone on the clustering of NMDA receptors.

CIPP delays the loss of mature dendritic spines upon 5-HT$_{2B}$-receptor stimulation. After having noticed that CIPP changes the NMDA receptor distribution, we tested the effects of 5-HT$_{2B}$-receptor stimulation. We found that receptor activation led to a partial loss of mature mushroom-type spines (**Fig. 9A**). Stimulation of 5-HT$_{2B}$ receptors induced a faster decrease in mature spines density in the absence of

CIPP (t0 = 46.46 ± 1.49%, t10 = 37.18 ± 2.12%, Mann-Withney t test p<0.0001; n = 40-50 from 4-5 cultures) than in the presence of CIPP (t0 = 47.71 ± 1.51%, t20 = 37.79 ± 1.45%, p<0.0001) (**Fig. 9A**). The decrease in the number of mature dendritic spines was accompanied by a decrease in the density of thin spines (t0 = 39.07 ± 1.47%, t10 = 32.09 ± 1.08%, p = 0.0001) in neurons expressing the 5-HT_{2B}-receptor alone (**Fig. 9C**). In contrast, cells expressing CIPP together with the 5-HT_{2B} receptor displayed increased number of thin spines (t0 = 39.03 ± 1.43%, t20 = 46.35 ± 1.59%, p<0.0001) (**Fig. 9C**). An increase in the density of stubby spines was seen upon 5-HT_{2B}-receptor stimulation (t0 = 14.47 ± 1.49%, t10 = 30.73 ± 1.05%, p<0.0001) (**Fig. 9B**), and co-expression of CIPP was without effect in stubby spine number (t0 = 13.05 ± 1.593%, t20 = 14.85 ± 1.876%, p=0.3192) (**Fig. 9B**) upon BW723C86 bath application. Therefore the 5-HT_{2B} receptor activation alters the maintenance of mature dendritic spines; the mature spines returning to an immature state. CIPP cannot prevent the loss of mature spines although influencing the transition to a more immature state.

Discussion

Here, we report that direct interactions of 5-HT_{2B} receptors with CIPP increase inositol phosphate signaling in COS-7 cells and calcium signaling in hippocampal neurons. We show that CIPP shapes 5-HT_{2B} and NMDA receptors dendritic clusters. Agonist stimulation of 5-HT_{2B} receptors induces morphological changes of dendritic spines morphology and 5-HT_{2B}-receptor internalization, independently of CIPP expression. Finally, NMDA clustering is promoted by 5-HT_{2B}-receptor stimulation in the presence of CIPP, supporting a role of these interactions in controlling neuronal excitatory events.

We identified by a proteomic approach, a protein interacting with 5-HT_{2B} receptor PDZ binding site (VSYV) in mouse brain, the channel interacting PDZ protein (CIPP). Few studies focused on CIPP, which is a scaffold protein composed of four PDZ domains. CIPP has been reported to associate to the PDZ binding site of Kir4.1 and Kir4.2 potassium channel family members, as well as NMDA receptor NR2 subunits (Kurschner et al., 1998), IRSp53, Cypin, (Alpi et al., 2009; Barilari and Dente, 2010) and acid-sensing ionic channel 3 (Anzai et al., 2002). CIPP was proposed to be a bridge between cypin and IRSp53 to form complex of proteins and to induce the recruitment and rearrangements of cytoskeleton proteins (Alpi et al., 2009; Barilari and Dente, 2010). Here we show that the co-expression of the CIPP scaffolding protein with 5-HT_{2B} receptor increases the basal and stimulated accumulation of second messenger induced by 5-HT_{2B} receptor full agonist (5-HT) or partial agonist (DOI) without affecting receptor total or surface expression. In addition “operational model” fitting of second messenger accumulation dose response curves indicates similar ability of the receptor to bind the agonist and the G protein reflected by the same activity ratio (Kenakin and Christopoulos, 2013). CIPP expression induces a stronger increase of calcium peak induced by receptor stimulation compared to neuron expressing only 5-HT_{2B} receptor, confirming that CIPP also promotes 5-HT_{2B}-receptor signaling in neurons.

PDZ proteins are important in synaptic transmission since they contribute to signaling, trafficking, and cytoskeletal rearrangements in both presynaptic and postsynaptic elements (Dunn and Ferguson, 2015; Feng and Zhang, 2009). CIPP has been suggested to be involved in cytoskeleton reorganization in HEK-293T (Alpi et al., 2009). In neuronal HN9.10e and PC12 transfected cell line, CIPP colocalized with IRSp53 and Cypin at the tip of induced neurites supporting a possible role in the formation of neuronal protrusions (Barilari and Dente, 2010). In cultured hippocampal neuron, transfection of 5-HT_{2B}-HA tag receptor allowed for the first time to describe 5-HT_{2B}-receptor subcellular distribution. We observed that 5-HT_{2B}-receptor expression is restricted to the somato-dendritic domain and excluded from axons. 5-HT_{2B} receptors form cluster in dendritic spines and the expression of CIPP increased significantly the 5-HT_{2B}-receptor density per cluster. Moreover CIPP is able to shape 5-HT_{2B}-receptor cluster. Indeed co-expression induces an increased cluster area, and amount of 5-HT_{2B}-

receptors per cluster. CIPP clusterizes 5-HT_{2B} receptors and also significantly increases the colocalization of 5-HT_{2B} receptors with Homer protein a marker of excitatory synapses. The colocalization of gephyrin protein, a marker of inhibitory synapses, with 5-HT_{2B} receptors decreases in the presence of CIPP. These interactions are suppressed by deletion of PDZ binding site of the receptor, supporting the ability of CIPP to target 5-HT_{2B} receptors specifically to excitatory synapses via the C-terminus of the receptor. Therefore CIPP targets the 5-HT_{2B} receptors to glutamatergic synapses, allowing a fine and rapid regulation of intracellular calcium signaling cascade at this site.

It is now accepted that thin filopodia spines are immature, whereas mushroom and stubby spines are mature (Hering and Sheng, 2001) and that immature spines are more mobile. PDZ scaffold proteins allow the formation of microdomains at the post-synaptic density specialized in shaping specific pathway responses (Good et al., 2011). The 5-HT_{2A} receptors have been shown to colocalize with PSD-95 and with MUPP1 in a subset of dendritic spines of rat cortical pyramidal neurons, in addition to dendritic shafts. PSD-95 was reported to be important for 5-HT_{2A} receptors targeting in dendrites of cultured cortical pyramidal neurons (Xia et al., 2003b). PSD-95 interaction has subsequently been shown to drive the targeting of 5-HT_{2A}- and 5-HT_{2C}-receptors to apical dendrites and to control their turnover *in-vivo* (Abbas et al., 2009). In cultured cortical neurons, the 5-HT_{2A}-receptor activation by DOI induced a transient increase in dendritic spine size, as well as phosphorylation of p21-activated kinase, a downstream target of the neuronal Rac guanine nucleotide exchange factor (RacGEF) kalirin-7 (Jones et al., 2009). Here, in basal activity conditions, we observed that the presence of CIPP decreased spine density. However, spine head diameter was increased in the presence of CIPP, supporting the notion that CIPP can affect the maturation of dendritic spines. We further show that stimulating 5-HT_{2B} receptors destabilized the mature spines and CIPP could delay this effect, allowing to maintain the mature spines.

The association with PSD-95 was shown to enhance 5-HT_{2A} receptor-mediated signal transduction, via the inhibition of agonist-induced 5-HT_{2A} receptor internalization in HEK-293 cells (Xia et al., 2003a). PSD-95 was shown to increase desensitization of the 5-HT_{2C} receptor-mediated Ca^{2+} responses, while MPP3 prevented its desensitization. The effects of these PDZ proteins on the desensitization of the Ca^{2+} response were correlated with a differential regulation of cell surface expression of the receptor (Gavarini et al., 2006). Our results indicate that 5-HT_{2B}-receptor stimulation induces an internalization of the receptor reflected by the decrease of the number and area of the clusters. The presence of CIPP does not prevent the decrease of receptor per cluster. Stimulation of 5-HT_{2B} receptors could thus induce its fast internalization removing the receptor from clusters.

NMDA receptor is an important regulator of calcium signaling in neurons. Indeed *in-vitro* and *in-vivo* experiment showed that activation of NMDA receptors could cause rapid elongation of filopodia, formation of novel spines, or shrinkage of existing ones. High-frequency focal synaptic stimulation of neurons in hippocampal slices evoked growth of small filopodia-like protrusions that was prevented by blockade of NMDA receptors (Maletic-Savatic et al., 1999). Kurschner et al., (Kurschner et al., 1998) suggested a potential role of CIPP in NMDA receptor functions due to its association to NR2 subunits. Accordingly, we show here in hippocampal neurons that CIPP increases the number of NMDA receptor clusters independently of 5-HT_{2B} receptors. Furthermore, agonist stimulation of 5-HT_{2B} receptors induces fast increase of NMDA cluster intensity in the presence of CIPP without affecting cluster number. Therefore, CIPP acts synergistically to promote clustering of NMDA and 5-HT_{2B} receptors that improves 5-HT_{2B} receptor signaling. In serotonergic neurons of dorsal raphe nuclei, endogenous NMDA receptor activation induced presynaptic release of serotonin (de Kock et al., 2006). Therefore, association between CIPP, NMDA and 5-HT_{2B} receptors may participate to synaptic function including in raphe serotonin neurons.

Materials and methods

Plasmid Constructs- Human 5-HT_{2B} receptor or mouse CIPP-3Xflag cDNAs were subcloned into pSG5 mammalian expression vector (Green et al., 1988) or pCAGGS (Niwa et al., 1991). PCAGGS-5-HT_{2B}-3XHA construct was obtained from pCAGGS-5-HT_{2B} by insertion of a Triple HA tag (YPYDVPDYA) to the N-terminal extremity of 5-HT_{2B} receptors. PCAGGS-5-HT2B-ΔPDZ-3XHA was obtained by targeted substitution in order to create stop codon before the PDZ binding site (EEQ/*V**SYV**).

COS-7 Cell Culture- COS-7 cells were cultured as monolayers in Dulbecco 's modified Eagle 's medium (DMEM) (Glutamax-GIBCO/Invitrogen, Carlsbad, CA) supplemented with 10% fetal calf serum (Biowest SAS, Nuaillé, France) and 1% penicillin/streptomycin (Sigma-Aldrich, St. Louis, MO), in 9-cm dishes (Falcon/Corning Life Sciences, Tewksbury, MA). Cells were incubated at 37°C in a 5% CO_2 atmosphere. Cells were 70% confluent when transfected in 6 well plates for Inositol phosphate accumulation, in 24 well plates for surface binding and in 9 cm dishes for total binding and co-immunoprecipitation/western-blot using Genjuice (Merck Chemicals Limited, Nottingham, England), according to the manufacturer's protocol, in an complete DMEM.

Peptide affinity chromatography and mass spectrometry

A synthetic peptide comprising the 14 C-terminal amino acids of the mouse 5-HT_{2B} receptor and the corresponding peptide lacking the receptor PDZ binding motif (95% purity, Eurogentec) were coupled *via* their N-terminal extremities to activated CH-sepharose 4B (GE-Healthcare). Ten µg of each immobilized peptide were incubated with CHAPS-solubilized proteins from mice brain (10 mg per condition) overnight at 4°C and affinity-retained proteins were resolved on 2-D gels and detected by silver staining, as previously described (Becamel et al., 2004). Proteins of interest were excised, digested in gel using trypsin (Gold, Promega), and peptides were analyzed using an Ultraflex MALDI-TOF-TOF mass spectrometer (Bruker Daltonik). Analyses were performed in reflectron mode with an accelerating voltage of 25 kV and a delayed extraction of 50 ns. Spectra were analyzed using the FlexAnalysis software (version 2.4, Bruker Daltonik) and auto-proteolysis products of trypsin (mol wt: 842.51, 1045.56, 2211.10, 2383.90) were used as internal calibrates (Becamel et al., 2004). Identification of proteins was performed by peptide mass fingerprint using the free Mascot Web server (http://www.matrixscience.com/search_form_select.html) and the SwissProt or NCBIprot databases (containing 16,838 and 172,881 *Mus musculus* sequences, respectively). The following parameters were used for database interrogation: mass tolerance of 100 ppm; fixed chemical modification, carbamidomethylation of cysteins; variable chemical modification, oxidation of methionines; matching peptides with one missed cleavage accepted only when they included two consecutive basic residues or when arginine or lysine residues were followed by one or several acidic residues inside the peptide amino acid sequence.

Co-immunoprecipitation and Western-blotting

COS-7 cells transfected with 10µg of DNA with a ratio of 1:1 (5-HT_{2B}-HA / empty vector; 5-HT_{2B}ΔPDZ-HA / empty vector; CIPP-flag / empty vector 5-HT_{2B}-HA / CIPP-Flag; 5-HT_{2B}ΔPDZ-HA / CIPP-Flag) and cultured two days before scrapping. Cells were centrifuged and suspended in CHAPS lysis buffer and sonicated during 30 s. Cells were next solubilized during 5 hours at 4°C under gentle agitation. Lysates were centrifuged (1,000 g) in order to pellet non solubilized membranes. Protein concentration of supernatant was evaluated using Pierce™ Coomassie Protein Assay Kit. Lysates were co-imunoprecipitated with anti-flag or anti HA beads (SIGMA, ANTI-FLAG M2 Affinity Gel) overnight at 4°C with gentle agitation. Total lysates and immunoprecipitates were separated by

SDS/PAGE-10 % (wt/vol) gels and transferred electrophoretically to nitrocellulose membranes. Inputs represent 5% of the total protein amount used for immunoprecipitations. Blots were probed with anti-HA, or anti-Flag antibodies (1:1,000). Anti-mouse and anti-rabbit antibodies (1:10,000) were used as secondary antibodies. Immunoreactive bands were detected using the Odyssey software. Three independent experiments were performed.

Inositol phosphate accumulation

COS-7 cells were transfected with 3µg of DNA (1:1 ratio for co-transfection) in 6 wells plate using Genjuice transfectant reagent in complete medium. Twenty-four hours later cells were trypsinized (Trypsin 1X 0.05% EDTA; Invitrogen) and plated in 96 wells plate (30,000 cells/well). The next day, complete medium is replaced by serum free medium. The day of the experiment, media was replaced by stimulation buffer with LiCl in order to inositol phosphate degradation (NaCL 146 mM, KCl 4.2mM, $MgCl_2$ 0.5mM, $CaCl_2$ 1mM, Hepes 10 mM, Glucose 5.5 mM, LiCl 50 mM, pH 7.4). Cells were stimulated during two hours at 37°C with different concentration of full and partial agonists, serotonin and DOI respectively (10^{-11} to 10^{-5} M in stimulation buffer) (Sigma). Stimulation solution was replaced by lysis buffer (IP one HTRF Kit, Cisbio, France) during one hour. Lysates were distributed to 384 well plates and IP1 was labeled using HTRF reagents. The assay is based on a competitive format involving a specific antibody labeled with Terbium Cryptate (donor) and IP1 coupled to d2 (acceptor). After one-hour incubation with HTRF reagent the plate was read using according to manufacturer instructions. At least five independent experiments were performed in duplicate.

Binding Assays

Surface binding. COS-7 cells were transfected with 10µg of DNA in 9 cm dishes using Genjuice transfectant reagent in complete medium. Twenty-four hours later cells were trypsinized and plated in 24 wells plate. The day before experiment media was replaced by serum free media. Last day the media is replaced by Krebs-Ringer-Hepes buffer (130 mM NaCl, 1.3 mM KCl, 2.2 mM, $CaCl_2$, 1.2 mM NaH_2PO_4 , 1.2 mM $MgSO_4$, 10 mM Hepes, 10 mM glucose, pH 7.4). Cells were incubated with constant concentration of [^{3}H]-Mesulergine (1 nM) and with increasing concentration of RS127445 a 5-HT_{2B} specific antagonist (Sigma). RS127445 was diluted in Krebs-Ringer-Hepes buffer at 10^{-11} to 10^{-6} M final concentration. Cells were then incubated for 90 minutes at room temperature and then washed twice on ice with cold PBS. Then cell were washed cells were lysed using SDS 1% during 1 hour. Finally lysate was transferred in 4 ml of scintillation tubes and scintillation cocktail were added to the samples. The radioactivity was counted using a scintillation counter (Beckman Coulter).

Total Binding. COS-7 cells were transfected cells in 9-cm dishes using Genjuice transfectant reagent in complete medium. The day after media is replaced by serum free media. Next day, cells were scraped on ice, then centrifuged for 5 minutes at 3,000 rpm at 4°C. Cell pellets were dissociated and lysed in 1 ml of binding buffer (50 mM Tris HCl, 10 mM $MgCl_2$, 0.1 mM EDTA, pH 7.4) and centrifuged for 30 minutes at 10,000 g. Membrane preparations were then suspended in 5 ml of PBS. Aliquots of membrane suspension (200 µl/well about 50 µg/well) were distributed in 96 deep well plates. The lysates were incubated at room temperature during 90 minutes with 25 µl of [^{3}H]-Mesulergine diluted in binding buffer at a final concentration of 1 nM and 25 µl/well of increasing concentrations of RS127445 5-HT_{2B} specific antagonist (from 10^{-11} to 10^{-6} M final concentration in binding buffer). Membranes were harvested by rapid filtration onto Whatman GF/B glass fiber filters (Brandel, Gaitherburg, MD) pre-soaked with cold saline solution and washed 3 times with cold saline solution to reduce nonspecific binding. Filters were placed in 6-ml scintillation vials and allowed to dry overnight. The next day, 4 ml of scintillation cocktail were added to the samples, which were counted as before. At least three independent experiments were performed in duplicate.

Hippocampal neuronal culture and transfection.

Hippocampal neurons were prepared as described previously (Chamma et al., 2013; Gauvain et al., 2011) from embryonic day 19 Sprague-Dawley rat pups. Tissue was then trypsinized (0.25% v/v) and mechanically dissociated in 1x HBSS containing 10 mM HEPES (Invitrogen). After dissociation, cells were plated on glass coverslips (Assistent) precoated with 80 g/ml poly-D,L-ornithine (Sigma-Aldrich) in plating medium composed of MEM (Sigma) supplemented with horse serum (10% v/v; Invitrogen), L-glutamine (2 mM), and Na pyruvate (1 mM) (Invitrogen) at a density of 3.4×10^4 cells.cm^{-2} and maintained in a CO2 incubator set at 37°C. After attachment for 2–3 h, cells were incubated in maintenance medium that consists of Neurobasal medium supplemented with B27 (1x), L-glutamine (2 mM), and antibiotics (Invitrogen). Each week, one-fifth of the culture medium volume was renewed.

Neuronal transfections with 5-HT_{2B}-HA, 5-HT_{2B}-ΔPDZ-HA, CIPP-flag, gephyrin–GFP (Hanus et al., 2006) (gift from A. Triller, Ecole Normale Supérieure, INSERM, Paris, France), and homer1c–GFP (Bats et al., 2007) (gift from D. Choquet, Centre National de la Recherche Scientifique, Bordeaux, France) were done at 13–14 d *in vitro* (DIV) using Transfectin (Bio-Rad), according to the instructions of the manufacturers (DNA/lipofectant ratio of 1:3), with 1 µg of plasmid DNA per 20 mm well. The following ratios of plasmid DNA were used in cotransfection experiments: 0.5:0.3:0.2 µg for 5-HT_{2B}-HA/ CIPP-flag/ homer1c–GFP or gephyrin–GFP or mCherry or eGFP. Experiments were performed 7–10 d after transfection.

Immunocytochemistry

The total (membrane plus intracellular) pools of 5-HT_{2B}-HA were revealed with immunocytochemistry in fixed and permeabilized cells, whereas the membrane pool of 5-HT_{2B}-HA was assessed by live cell staining. Cells were fixed for 15 min at room temperature (RT) in paraformaldehyde (PFA; 4% w/v; Sigma) and sucrose (20% w/v; Sigma) solution in 1X PBS. Cells were then washed in PBS and incubated for 30 min at RT in bovine serum albumin (BSA; 3% w/v; Sigma) and goat serum (GS; 20% v/v; Invitrogen) in PBS to block nonspecific staining. Neurons were then incubated for 1 h with rabbit antibody against HA (1:400; CST HA-Tag C29F4 Rabbit mAb #3724); mouse primary antibody against Flag (1:400; Sigma) or rabbit primary antibody against Flag (1:400; Sigma); mouse primary antibody against NR1 subunit of NMDA receptor (1:400 ,clone 54.1, Millipore, MAB363) in PBS supplemented with GS(3% v/v). After washes, cells were incubated for 45 min at RT with Cy3- or Cy5-conjugated goat anti-mouse antibody (1.9 µg/ml; JacksonImmunoResearch) or Cy3-conjugated goat anti-rabbit antibody (1.9 µg/ml; Jackson ImmunoResearch) in PBS–BSA–GS blocking solution, washed, and mounted on slides with mowiol 4-88 (48 mg/ml; Sigma). For live cell staining, neurons were washed in imaging medium and incubated for 20 min at 4°C with mouse primary antibody against HA (1:400; CST HA-Tag C29F4 Rabbit mAb #3724) in imaging medium. After washes with imaging medium, cells were fixed for 15 min with PFA and processed for immunodetection of Flag or NMDA receptor as above. The imaging medium consisted of phenol red-free MEM supplemented with glucose (33 mM; Sigma) and HEPES (20 mM), glutamine (2 mM), Na-pyruvate (1 mM), and B27 (1x) from Invitrogen. Sets of neurons compared for quantification were labeled and imaged simultaneously. In stimulation experiment, 5-HT_{2B}-receptor agonist (BW723C86 1µM Tocris) were diluted in imaging medium.

Fluorescence image acquisition and analyses

Images were obtained on a Leica SP5 confocal microscope using the LAS-AF program (Leica). Images were acquired using either a 63 X objective (stacks of 16–35 images acquired with an interval of 0.2 µm, and optical zoom of 2). Image exposure time was determined on bright cells to avoid pixel saturation. All images from a given culture were then acquired with the same exposure time.

Quantifications were performed on images acquired with standard light microscopy using MetaMorph software (Roper Scientific). For each image, a region of interest was chosen. A user-defined intensity threshold was applied to the sum intensity projections of confocal optical sections to select clusters and avoid their coalescence. Thresholded images were binarized, and binarized regions were outlined and transferred onto raw data to determine the mean cluster number, area, fluorescence intensity, and the mean fluorescence intensity per pixel within clusters. For quantifications of 5-HT_{2B}-HA clusters at excitatory or inhibitory synapses, only 5-HT_{2B}-HA clusters comprising at least three pixels and apposed on at least one pixel with Homer-GFP or Gephyrin-finger-GFP clusters were considered.

To study dendritic spines morphology, confocal stacks of 16–35 images acquired with an interval of 0.2 µm, and optical zoom of 2 from eGFP transfected neurons were analyzed with NeuronStudio (Dumitriu et al., 2011) (http://www. mssm.edu/cnic), blind to experimental conditions, to quantify changes in spine head diameter over time. Only spines that could be accurately followed over the entire experiments were measured. A total of 15–30 dendritic segments were analyzed per condition from three independent cultures. Dendritic spines were classify in different categories considering the neck ratio = 1.1 (spines with head to neck diameter ratio greater than this value are considered Thin or Mushroom); **thin Ratio = 2.5** (Spines that do not meet the Neck Ratio value and have a length to spine to head diameter above this value are classified as thin, otherwise as stubby); m**ushroom size** = 0.350 µm (spines that meet the Neck Ratio value and have a head diameter equal or greater than this value are labeled as mushroom, otherwise as stubby).

Calcium imaging acquisition and analyses

Neurons expressing 5-HT_{2B}-HA, mCherry and/or not CIPP-Flag were maintained at 37°C in a thermostated chamber and superfused with imaging medium preheated at 37°C. Time-lapse confocal images of neurons were acquired every 500ms using an inverted spinning-disc microscope (Leica DMI4000, Yokogawa CS20 spinning Nipkow disk, 63 objective). At every time point, neurons were illuminated by 491 nm light from an Ar/Kr laser in order to follow calcium activity using Fluo-4AM (Thermofisher). At first and last time point, neurons were illuminated by 561nm light to follow eventual morphological changes or displacement artifact. Importantly, laser intensity, time of illumination, and acquisition parameters of the camera remained identical to allow comparison between experiments and bleach correction. In order to analyze calcium variability after stimulation with BW723C86 (1µM) a 5-HT_{2B} agonist, region of interest are randomly selected in the dendrites of mCherry positives cells. In addition region of interest of precisely selected out of the mCherry neurons or other cells in order to identify the background fluorescence. The background intensity was substracted to the mean intensity values of Fluo-4AM calcium fluorescent probe. Basal intensity of each ROI was determined during the time before injection in order to determine F0 values. Then intensity after stimulation F was normalized by F0 in order to detect and compare each ROI by their specific F/F0. Finally each ROI were plot and analyzed using Graphpad Prism 6 software.

Acknowledgment.

We thank Mythili Savariradjane and the Imaging facility of the IFM.

This work has been supported by funds from the *Centre National de la Recherche Scientifique*, the *Institut National de la Santé et de la Recherche Médicale*, the *Université Pierre et Marie Curie*, and by grants from the *Fondation pour la Recherche Médicale* "Equipe FRM DEQ2014039529", the French Ministry of Research (Agence Nationale pour la Recherche ANR-12-BSV1-0015-01 and the Investissements d'Avenir programme ANR-11-IDEX-0004-02). LM's team is part of the École des Neurosciences de Paris Ile-de-France network and of the Bio-Psy Labex and as such this work was supported by French state funds managed by the ANR within the Investissements d'Avenir programme under reference ANR-11-IDEX-0004-02. E. Quentin by a PhD fellowship from the Region Ile de France DIM Cerveau et Pensée.

Financial Disclosures

The authors declare no conflict of interest.

References

Abbas, A.I., Yadav, P.N., Yao, W.-D., Arbuckle, M.I., Grant, S.G.N., Caron, M.G., and Roth, B.L. (2009). PSD-95 is essential for hallucinogen and atypical antipsychotic drug actions at serotonin receptors. The Journal of neuroscience : the official journal of the Society for Neuroscience *29*, 7124-7136.

Alpi, E., Landi, E., Barilari, M., Serresi, M., Salvadori, P., Bachi, A., and Dente, L. (2009). Channel-interacting PDZ protein, 'CIPP', interacts with proteins involved in cytoskeletal dynamics. Biochem J *419*, 289-300.

Anzai, N., Deval, E., Schaefer, L., Friend, V., Lazdunski, M., and Lingueglia, E. (2002). The multivalent PDZ domain-containing protein CIPP is a partner of acid-sensing ion channel 3 in sensory neurons. J Biol Chem *277*, 16655-16661.

Assémat, E., Crost, E., Ponserre, M., Wijnholds, J., Le Bivic, A., and Massey-Harroche, D. (2013). The multi-PDZ domain protein-1 (MUPP-1) expression regulates cellular levels of the PALS-1/PATJ polarity complex. Exp Cell Res *319*, 2514-2525.

Barilari, M., and Dente, L. (2010). The neuronal proteins CIPP, Cypin and IRSp53 form a tripartite complex mediated by PDZ and SH3 domains. Biological Chemistry *391*, 1169-1174.

Bats, C., Groc, L., and Choquet, D. (2007). The interaction between Stargazin and PSD-95 regulates AMPA receptor surface trafficking. Neuron *53*, 719-734.

Becamel, C., Gavarini, S., Chanrion, B., Alonso, G., Galeotti, N., Dumuis, A., Bockaert, J., and Marin, P. (2004). The serotonin 5-HT2A and 5-HT2C receptors interact with specific sets of PDZ proteins. J Biol Chem *279*, 20257-20266.

Bevilacqua, L., Doly, S., Kaprio, J., Yuan, Q., Tikkanen, R., Paunio, T., Zhou, Z., Wedenoja, J., Maroteaux, L., Diaz, S.*, et al.* (2010). A population-specific HTR2B stop codon predisposes to severe impulsivity. Nature *468*, 1061-1066.

Bigford, G.E., Chaudhry, N.S., Keane, R.W., and Holohean, A.M. (2012). 5-Hydroxytryptamine 5HT2C receptors form a protein complex with N-methyl-D-aspartate GluN2A subunits and activate phosphorylation of Src protein to modulate motoneuronal depolarization. J Biol Chem *287*, 11049-11059.

Black, J.W., and Leff, P. (1983). Operational models of pharmacological agonism. Proc R Soc Lond B Biol Sci *220*, 141-162.

Chamma, I., Heubl, M., Chevy, Q., Renner, M., Moutkine, I., Eugène, E., Poncer, J.C., and Lévi, S. (2013). Activity-dependent regulation of the K/Cl transporter KCC2 membrane diffusion, clustering, and function in hippocampal neurons. The Journal of neuroscience : the official journal of the Society for Neuroscience *33*, 15488-15503.

de Kock, C.P.J., Cornelisse, L.N., Burnashev, N., Lodder, J.C., Timmerman, A.J., Couey, J.J., Mansvelder, H.D., and Brussaard, A.B. (2006). NMDA receptors trigger neurosecretion of 5-HT within dorsal raphe nucleus of the rat in the absence of action potential firing. J Physiol *577*, 891-905.

Diaz, S.L., Doly, S., Narboux-Nême, N., Fernandez, S., Mazot, P., Banas, S., Boutourlinsky, K., Moutkine, I., Belmer, A., Roumier, A.*, et al.* (2012). 5-HT2B receptors are required for serotonin-selective antidepressant actions. Mol Psychiatry *17*, 154-163.

Dumitriu, D., Rodriguez, A., and Morrison, J.H. (2011). High-throughput, detailed, cell-specific neuroanatomy of dendritic spines using microinjection and confocal microscopy. Nat Protoc *6*, 1391-1411.

Dunn, H.A., and Ferguson, S.S.G. (2015). PDZ Protein Regulation of G Protein-Coupled Receptor Trafficking and Signaling Pathways. Mol Pharm *88*, 624-639.

Feng, W., and Zhang, M. (2009). Organization and dynamics of PDZ-domain-related supramodules in the postsynaptic density. Nature reviews Neuroscience *10*, 87-99.

Gauvain, G., Chamma, I., Chevy, Q., Cabezas, C., Irinopoulou, T., Bodrug, N., Carnaud, M., Levi, S., and Poncer, J.C. (2011). The neuronal K-Cl cotransporter KCC2 influences postsynaptic AMPA receptor content and lateral diffusion in dendritic spines. Proc Natl Acad Sci U S A *108*, 15474-15479.

Gavarini, S., Bécamel, C., Altier, C., Lory, P., Poncet, J., Wijnholds, J., Bockaert, J., and Marin, P. (2006). Opposite effects of PSD-95 and MPP3 PDZ proteins on serotonin 5-hydroxytryptamine2C receptor desensitization and membrane stability. Molecular biology of the cell *17*, 4619-4631.

Good, M.C., Zalatan, J.G., and Lim, W.A. (2011). Scaffold proteins: hubs for controlling the flow of cellular information. Science (New York, NY) *332*, 680-686.

Green, S., Issemann, I., and Sheer, E. (1988). A versatile in vivo and in vitro eukaryotic expression vector for protein engineering. Nucl Ac Res *16*, 396.

Hanus, C., Ehrensperger, M.V., and Triller, A. (2006). Activity-dependent movements of postsynaptic scaffolds at inhibitory synapses. J Neurosci *26*, 4586-4595.

Hering, H., and Sheng, M. (2001). Dendritic spines: structure, dynamics and regulation. Nature reviews Neuroscience *2*, 880-888.

Holohean, A.M., and Hackman, J.C. (2004). Mechanisms intrinsic to 5-HT2B receptor-induced potentiation of NMDA receptor responses in frog motoneurones. Br J Pharmacol *143*, 351-360.

Jones, K.A., Srivastava, D.P., Allen, J.A., Strachan, R.T., Roth, B.L., and Penzes, P. (2009). Rapid modulation of spine morphology by the 5-HT2A serotonin receptor through kalirin-7 signaling. Proc Natl Acad Sci USA *106*, 19575-19580.

Kenakin, T., and Christopoulos, A. (2013). Signalling bias in new drug discovery: detection, quantification and therapeutic impact. Nat Rev Drug Discov *12*, 205-216.

Kenakin, T., Watson, C., Muniz-Medina, V., Christopoulos, A., and Novick, S. (2012). A simple method for quantifying functional selectivity and agonist bias. ACS Chem Neurosci *3*, 193-203.

Kurschner, C., Mermelstein, P.G., Holden, W.T., and Surmeier, D.J. (1998). CIPP, a novel multivalent PDZ domain protein, selectively interacts with Kir4.0 family members, NMDA receptor subunits, neurexins, and neuroligins. Mol Cell Neurosci *11*, 161-172.

Lemmers, C., Médina, E., Delgrossi, M.-H., Michel, D., Arsanto, J.-P., and Le Bivic, A. (2002). hINADl/PATJ, a homolog of discs lost, interacts with crumbs and localizes to tight junctions in human epithelial cells. J Biol Chem *277*, 25408-25415.

Maletic-Savatic, M., Malinow, R., and Svoboda, K. (1999). Rapid dendritic morphogenesis in CA1 hippocampal dendrites induced by synaptic activity. Science (New York, NY) *283*, 1923-1927.

Maroteaux, L., Ayme-Dietrich, E., Aubertin-Kirch, G., Banas, S., Quentin, E., Lawson, R., and Monassier, L. (2017). New therapeutic opportunities for 5-HT2 receptor ligands. Pharmacol Ther *170*, 14-36.

Niwa, H., Yamamura, K., and Miyazaki, J. (1991). Efficient selection for high-expression transfectants with a novel eukaryotic vector. Gene *108*, 193-199.

Philipp, S., and Flockerzi, V. (1997). Molecular characterization of a novel human PDZ domain protein with homology to INAD from Drosophila melanogaster. FEBS Letters *413*, 243-248.

Pitychoutis, P., Belmer, A., Moutkine, I., Adrien, J., and Maroteaux, L. (2015). Mice lacking the serotonin Htr2B receptor gene present an antipsychotic-sensitive schizophrenic-like phenotype. Neuropsychopharmacology *40*, 2764-2773.

Ullmer, C., Schmuck, K., Figge, A., and Lubbert, H. (1998). Cloning and characterization of MUPP1, a novel PDZ domain protein. FEBS Lett *424*, 63-68.

Xia, Z., Gray, J.A., Compton-Toth, B.A., and Roth, B.L. (2003a). A direct interaction of PSD-95 with 5-HT2A serotonin receptors regulates signal transduction and receptor trafficking. J Biol Chem *278*, 21901-21908.

Xia, Z., Hufeisen, S.J., Gray, J.A., and Roth, B.L. (2003b). The PDZ-binding domain is essential for the dendritic targeting of 5-HT2A serotonin receptors in cortical pyramidal neurons in vitro. Neuroscience *122*, 907-920.

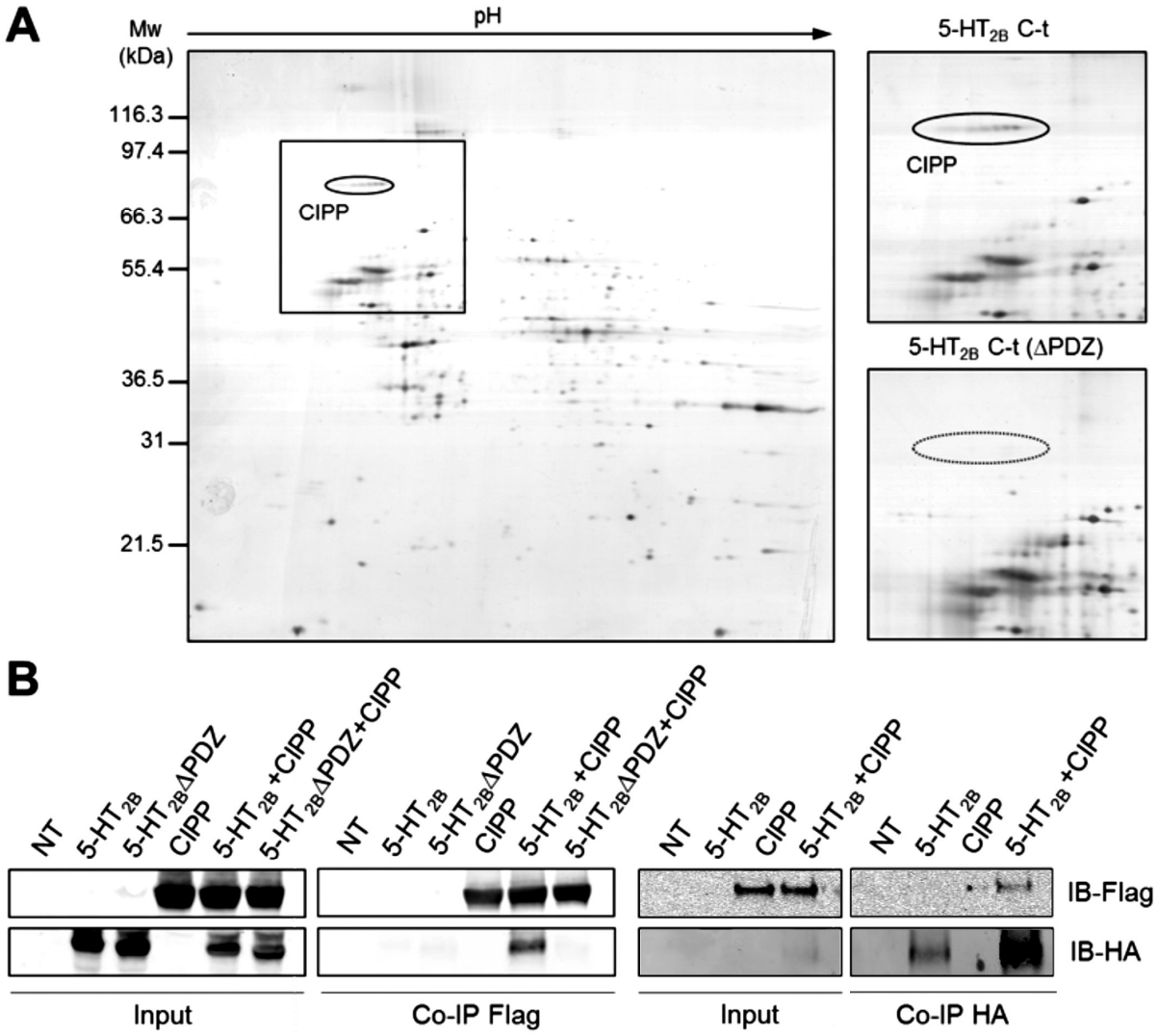

Figure 1 - CIPP protein and 5-HT$_{2B}$-receptor PDZ binding physically interact. (A) Recruitment of CIPP by the 5-HT$_{2B}$-receptor PDZ binding motif. The left panel shows a 2-D gel representative of three independent experiments performed with the 5-HT$_{2B}$ receptor C-terminal peptide as bait. The right panels show a magnification of the gel region comprising a train of protein spots otherwise absent in the corresponding region of 2-D gels obtained with the 5-HT$_{2B}$ receptor C-terminal peptide deleted of the receptor PDZ binding motif. This train of spot was identified as CIPP by MALDI-TOF mass spectrometry (16 out 26 detected peptides matching the CIPP sequence, corresponding to a protein sequence coverage of 25%, Mascot Score 153). **(B) Association of CIPP with full-length 5-HT$_{2B}$ receptor through a PDZ-dependent mechanism in COS-7 cells.** Immunoprecipitation of 5-HT$_{2B}$ receptor with CIPP protein. COS-7 cells co-transfected with plasmids coding for 5-HT$_{2B}$-HA, 5-HT$_{2B}$-ΔPDZ-HA and for CIPP-Flag proteins. Blot of input of proteins are revealed by Flag or HA antibody (IB-Flag, IB-HA) in order to show the presence of the proteins in each conditions. The immunoprecipitated proteins by anti-Flag beads (Co-IP Flag) or by anti-HA beads (Co-IP HA) revealed by Flag or HA antibody (IB-Flag, IB-HA), represent proteins that physically interact with CIPP and include 5-HT$_{2B}$ receptors (5-HT$_{2B}$) (NT non-transfected; n > 3 independent experiments).

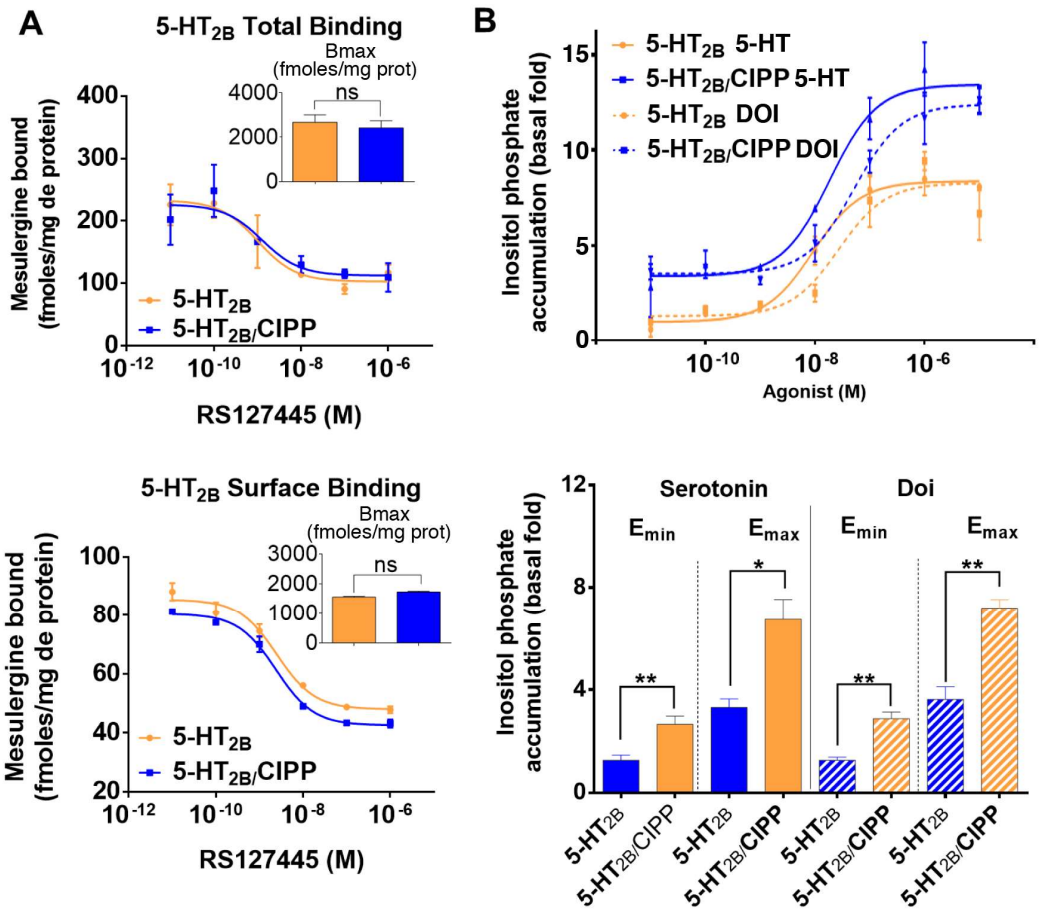

Figure 2 - CIPP increases 5-HT$_{2B}$ receptor signaling activity. (**A**) Pharmacological evaluation of 5-HT$_{2B}$ receptor expression in the presence (or not) of CIPP scaffold protein. Radioligand binding competition performed using transfected COS-7 cells expressing 5-HT$_{2B}$ receptor with or without CIPP showed similar total expression of the receptors, which is represented by the Bmax ($p = 0.7$). Similar result was obtained in experiment performed on living cell in order to identify 5-HT$_{2B}$ receptor expressed only at the plasma membrane ($p = 0.1$). Data were statistically analyzed by Welch corrected t-test; n = 3-5 independent experiments performed in duplicate. (**B**) Evaluation of the 5-HT$_{2B}$-receptor transduction when co-expressed with CIPP. Quantification of inositol phosphate signaling pathway activity was performed in Cos-7 cells transfected with 5-HT$_{2B}$ receptor with or without CIPP and stimulated by increasing concentrations of a full agonist of the receptor (5-HT) and a partial agonist (DOI). Co-expression of 5-HT$_{2B}$ receptors and CIPP increased the basal and stimulated inositol phosphate levels. The basal (E_{min}) and stimulated activity (E_{max}) of each condition were normalize by the basal activity of cells expressing 5-HT$_{2B}$ receptor alone. Bmax, Emin, Emax were statistically analyzed by Welch corrected t-test; n=3-5 independent experiments performed in duplicate.

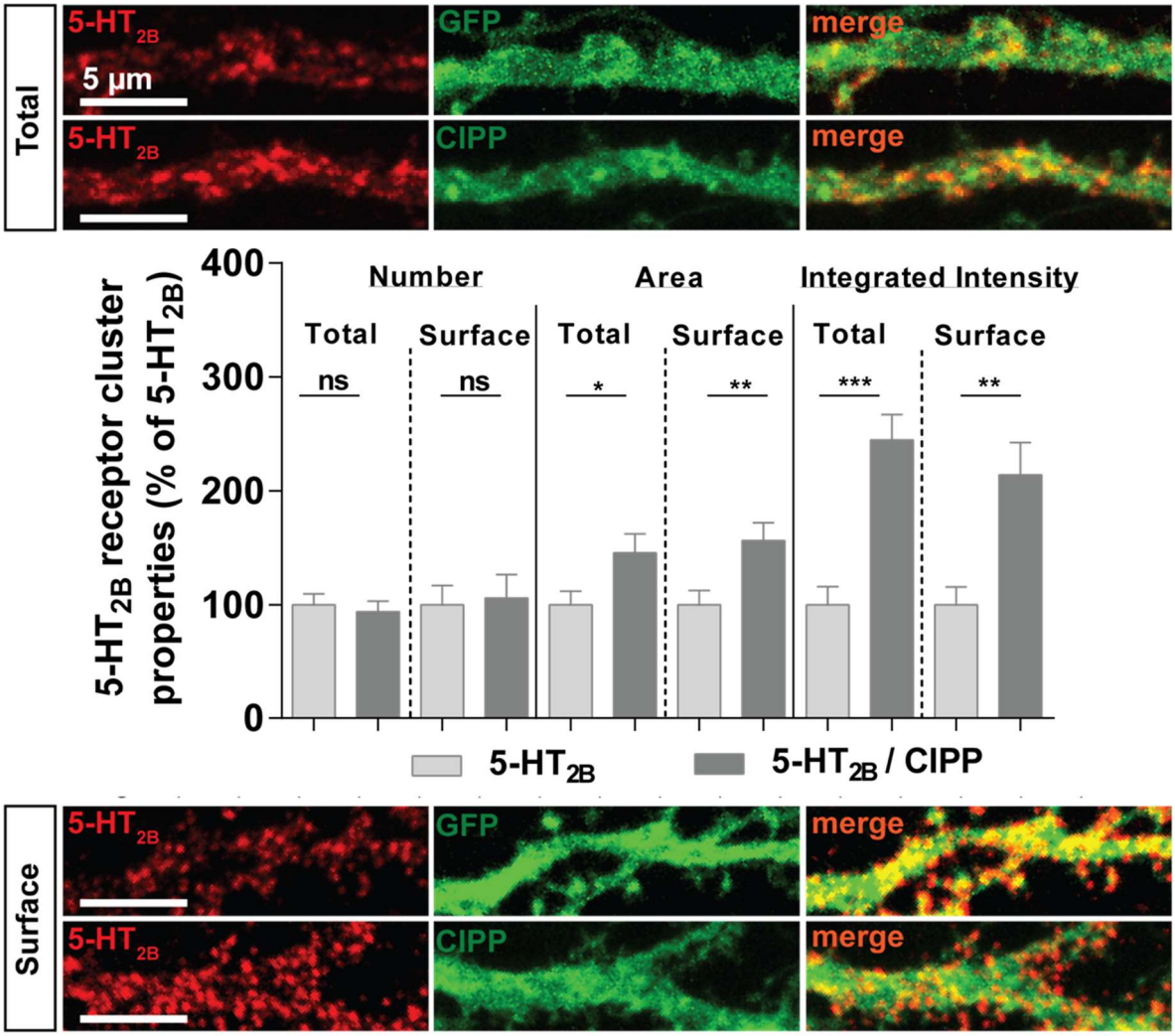

Figure 3 - CIPP shapes 5-HT$_{2B}$ receptors clusters at the surface of hippocampal neurons. Morphological analyses of 5-HT$_{2B}$ receptor clusters in the presence or not of CIPP in both total and surface area of secondary dendrites. The total 5-HT$_{2B}$ receptor and CIPP distribution was determined on fixed and permeabilized cells and revealed with anti-HA and/or anti-Flag antisera. Surface expression was determined by live labeling (performed at 4°C) of neurons. CIPP increased surface and total 5-HT$_{2B}$ receptor cluster area (total 5-HT$_{2B}$ receptors, *p = 0.04 and surface receptor, **p = 0.007) but not the cluster number. CIPP increased significantly the 5-HT$_{2B}$-receptor density per cluster (integrated intensity total 5-HT$_{2B}$ receptor, ***p = 0.0007 and surface receptor, **p = 0.004). Morphological parameters were analyzed by Mann-Withney t-test, n = 18-28 from 3-4 neuronal cultures. Scale bars 5µm.

Figure 4

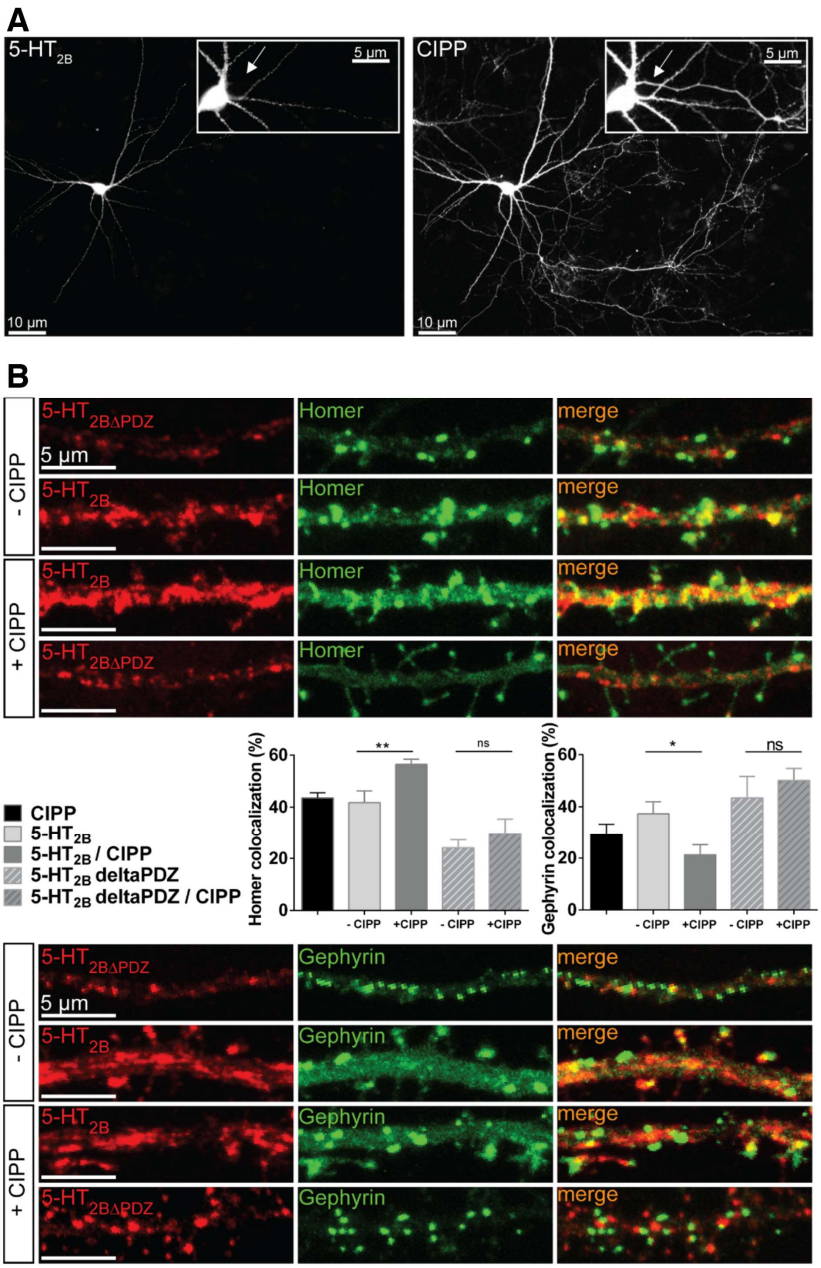

Figure 4 - CIPP targets 5-HT$_{2B}$ receptors at glutamatergic synapses by PDZ binding interaction. **A)** Hippocampal cultured neurons were transfected with 5-HT$_{2B}$-HA-tagged receptor and Flag-CIPP, and stained for their respective tag. 5-HT$_{2B}$-HA receptors (left) are distributed exclusively in the somatodendritic membrane while CIPP-flag protein (right) is also present in axons (white arrow). **B)** Co-expression of 5-HT$_{2B}$ receptor and CIPP scaffold protein increased the 5-HT$_{2B}$ receptor colocalization with Homer-GFP and thus receptor targeting at excitatory synapses (**p = 0.0097). Co-expression of 5-HT$_{2B}$ receptor and CIPP scaffold protein decreased the receptor colocalization with Gephyrin-finger-GFP and thus its distribution at inhibitory synapses (p = *0.026). Deletion of the PDZ binding domain of 5-HT$_{2B}$ receptor C-terminus suppressed the effect of CIPP and reduced receptor localization at excitatory synapses compared to non-truncated 5-HT$_{2B}$ receptor (#p = 0.0342 5-HT$_{2B}$ vs. 5-HT$_{2B}$ΔPDZ, ##p = 0.0023 5-HT$_{2B}$ vs. 5-HT$_{2B}$ΔPDZ). Data were statistically analyzed by Mann-Withney t-test; n = 9-11 from 3 neuronal cultures. Scale bar 5µm.

Figure 5

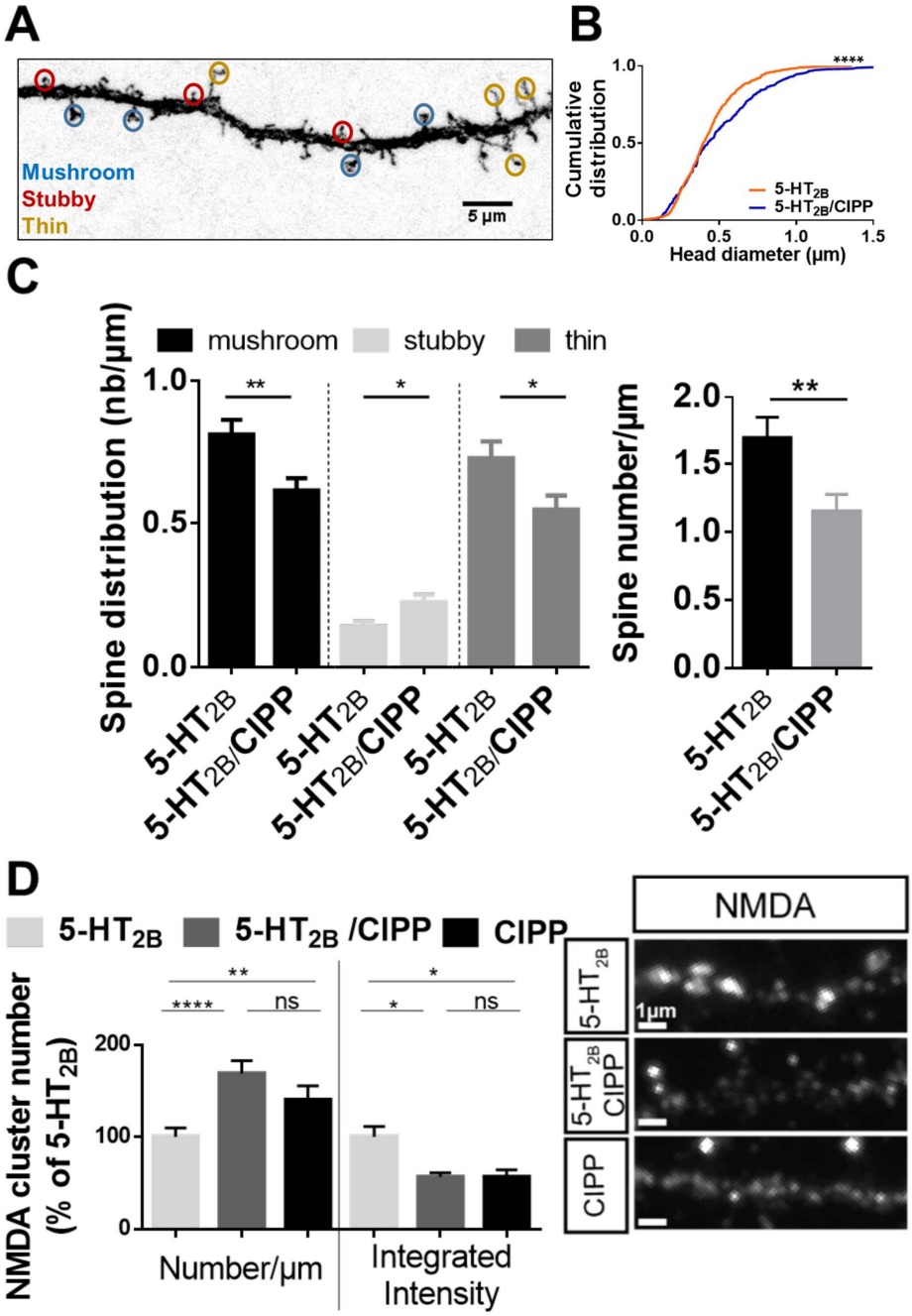

Figure 5 - CIPP modify 5-HT$_{2B}$ receptor spine number and morphology, and increases NMDA cluster number in hippocampal neurons A) Morphological classification of dendritic spines in eGFP transfected neurons **B**) CIPP co-expression with 5-HT$_{2B}$ receptors increased the density of spines with large diameter (Kolmogorov-Smirnov test ****p<0.0001) (n = 40-50 from 4-5 cultures). **C**) CIPP expression reduced the spine distribution and decreased the spine number per µm in eGFP transfected neurons (1.82 ± 0.13 spines/µm vs. 1.12 ± 0.17 spines/µm in the presence of CIPP, Mann-Whitney t-test **p = 0.01). **D**) CIPP significantly increased the NMDA receptor cluster number (**p = 0.016), but decreased the NMDA receptor density per cluster compared to 5-HT$_{2B}$ receptors (*p = 0.013). Data were statistically analyzed by Mann-Withney t-test; n = 30-40 from 3 independent neuronal cultures.

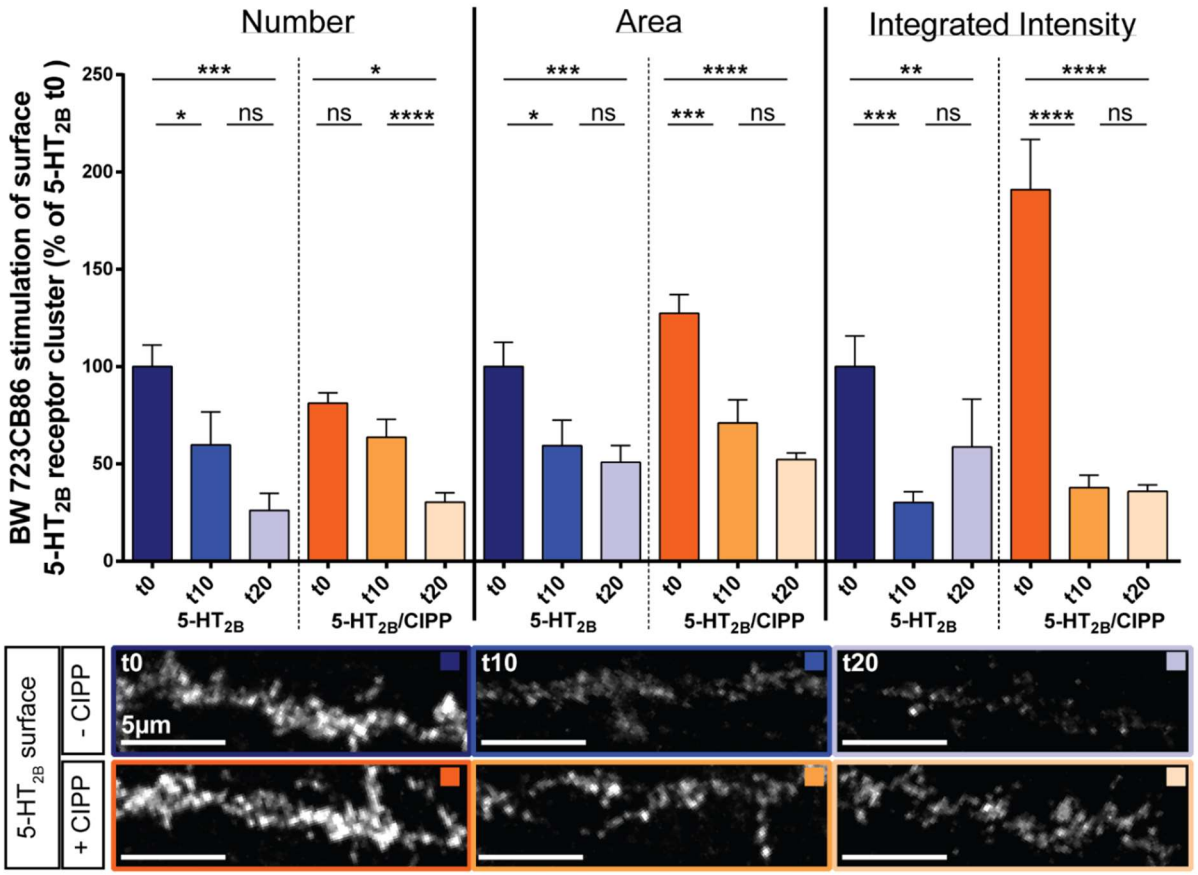

Figure 6 - CIPP does not prevent the BW723C86-dependent reduction in 5-HT$_{2B}$ receptor internalization. The number of 5-HT$_{2B}$ receptor clusters at the surface decreased faster in the absence of CIPP (*p = 0.04 t0 vs. t10) than in the presence of CIPP (ns t10 vs. t0). The area of 5-HT$_{2B}$ receptor clusters at the surface decreased after BW723C86 stimulation in the absence of CIPP (t20 vs. t0 ***p = 0.0006) or the presence of CIPP (t20 vs. t0 ****p<0.0001). Agonist stimulation decreased quickly the density of surface 5-HT$_{2B}$ receptor per clusters in the absence (integrated intensity t10 = 30.16%) or in the presence of CIPP (t10 = 37.83% ***p = 0.0003). Data, expressed as percentage of t0 of 5-HT$_{2B}$ receptor alone, were analyzed by Mann-Withney t-test; n=18-28 from 3-4 neuronal cultures. Scale bar 5 µm.

Figure 7

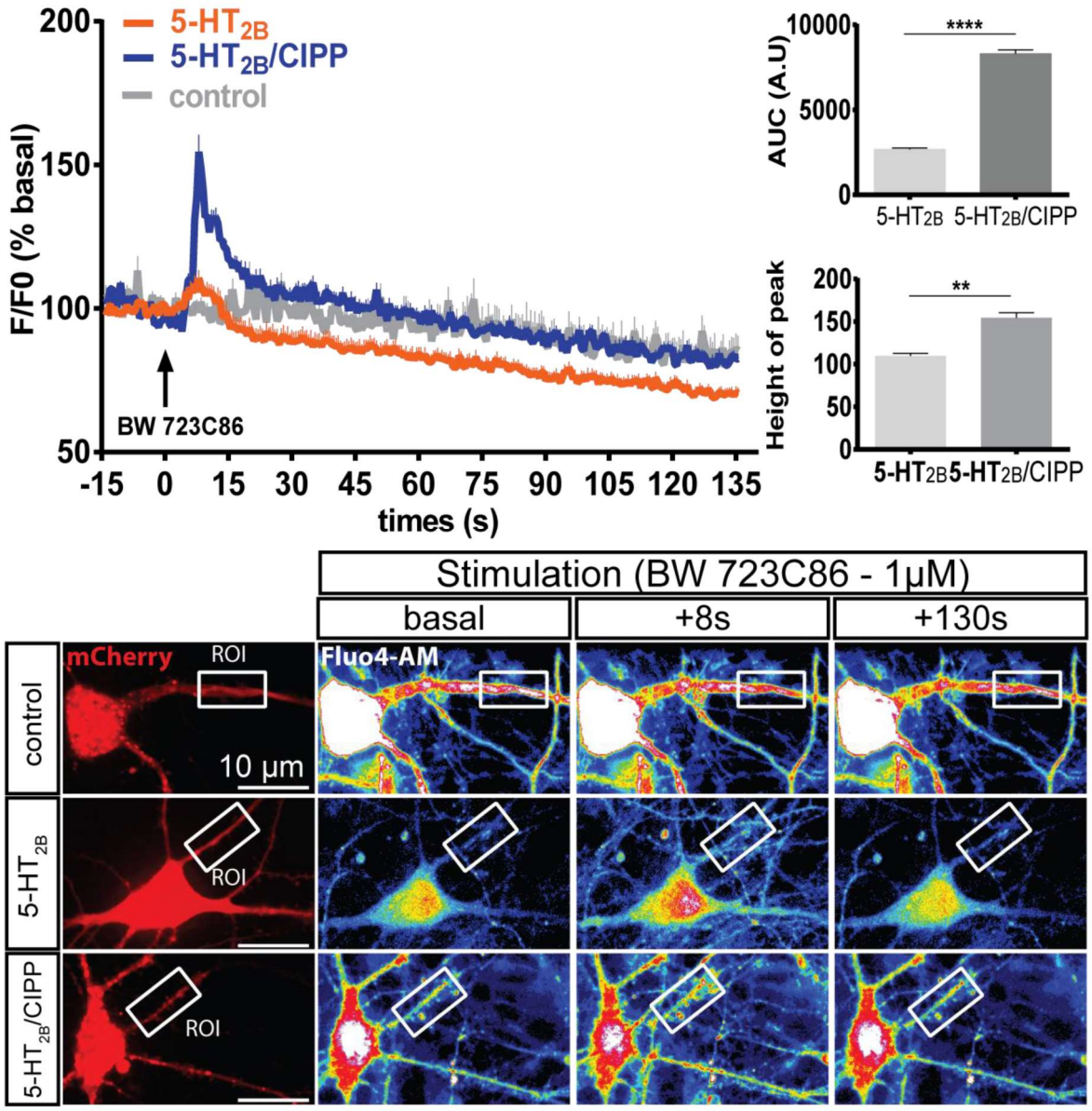

Figure 7 - CIPP increases calcium coupling of 5-HT$_{2B}$ receptors in hippocampal neurons Summed calcium transients recorded in primary hippocampal cells transfected with either 5-HT$_{2B}$ receptor (orange line), 5-HT$_{2B}$ and CIPP (blue line) and control (grey line) are shown. The curves were obtained from the means of 3–5 independent experiments, averaging at least 50 individual ROI measurements. The arrow indicates the time of BW723C86 stimulation. (right) The bar diagrams show statistical analysis of the height of the peak (F/F$_0$) in percent of 5-HT$_{2B}$ receptor alone, and the area under the curve (AUC) for the 5-HT$_{2B}$ receptor alone (light grey), or with CIPP at a stoichiometric ratio of 1:1 (dark grey). (****p<0.001; ** p = 0.016; Mann-Whitney t-test). Lower panels show example of selected image recordings and ROI definition at t0, t8, and t130s of BW723C86 stimulation.

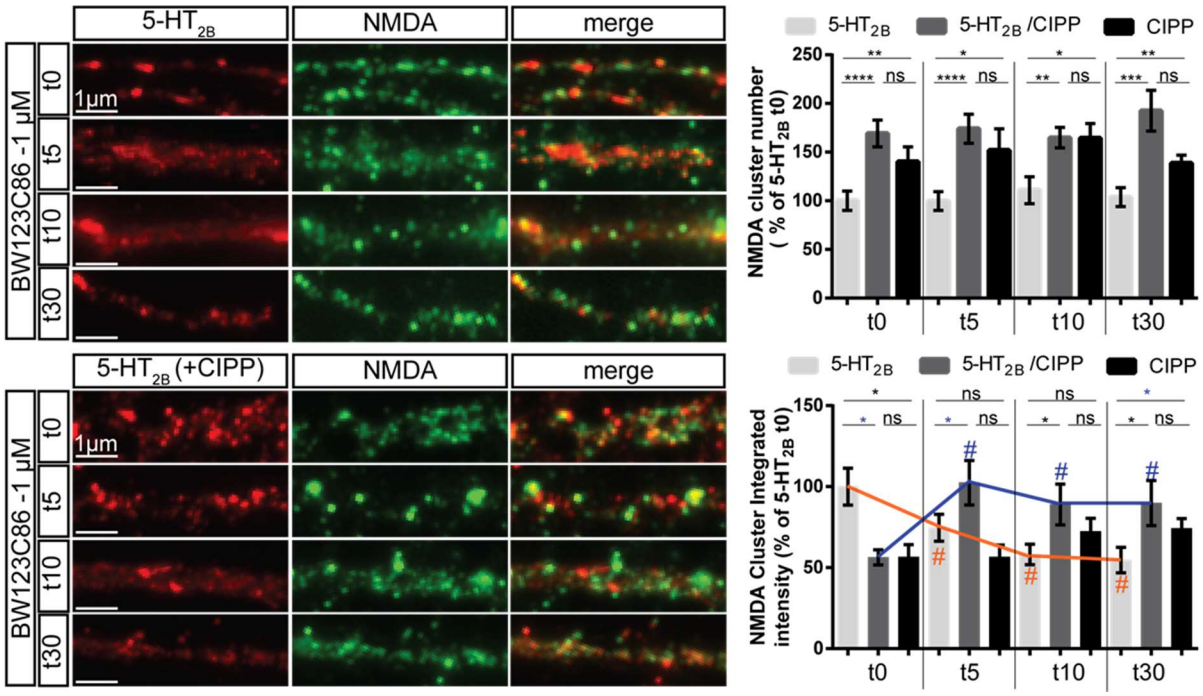

Figure 8 - The 5-HT$_{2B}$-receptor stimulation in the presence of CIPP promotes clustering of NMDA receptor. The BW723C86 stimulation of 5-HT$_{2B}$ receptor did not modify NMDA receptor cluster number in presence or not of CIPP from t0 to t30. By contrast, the NMDA receptor density per cluster gradually decreased with 5-HT$_{2B}$-receptor stimulation in the absence of CIPP but quickly increased in the presence of CIPP ($p = 0.0024$). Therefore, the presence of CIPP allows the 5-HT$_{2B}$ receptor stimulation to increase the clustering of NMDA receptor. Data were statistically analyzed by Mann-Withney t-test; # effect of treatment; * effect of transfection; n = 30-40 from 3 independent neuronal cultures.

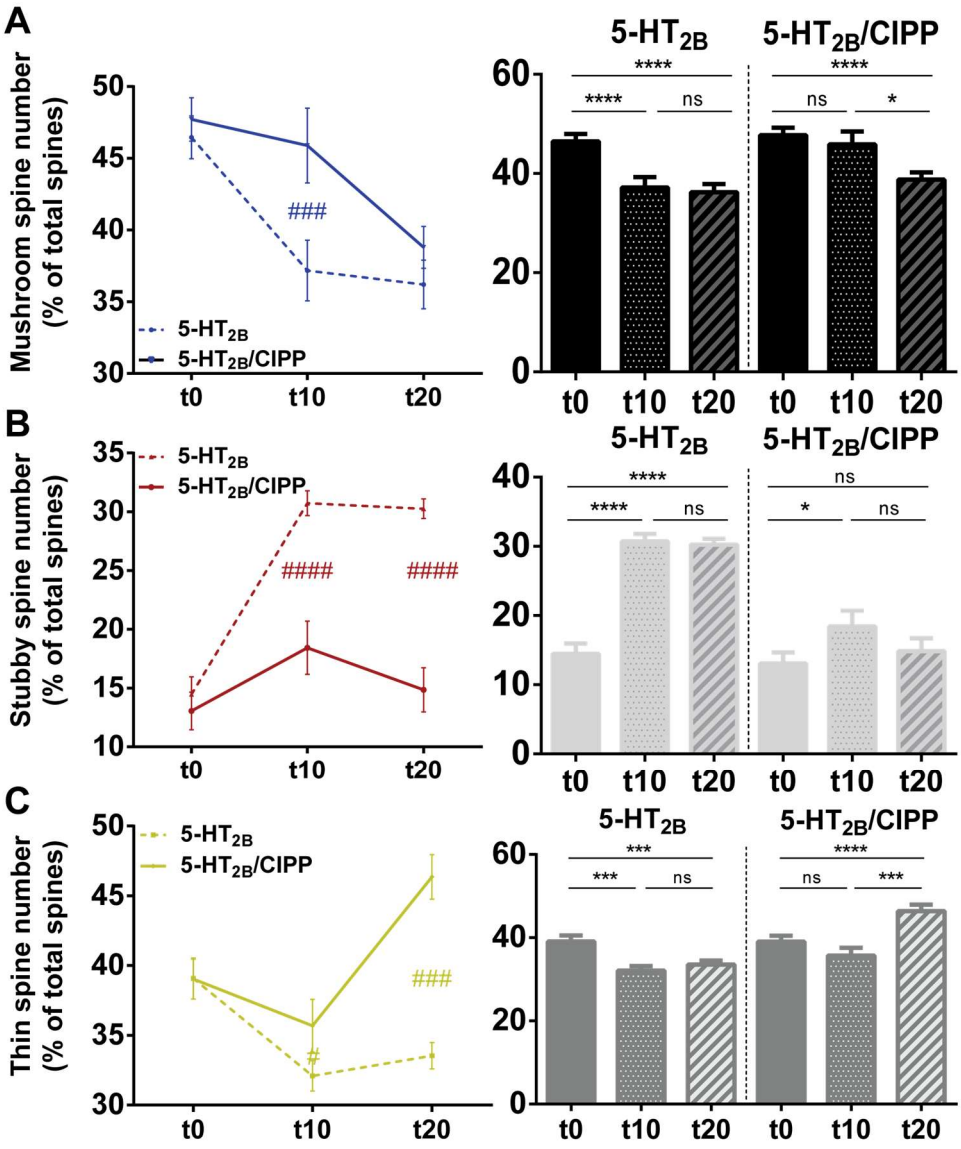

Figure 9 - Stabilization of spine morphology by CIPP upon 5-HT$_{2B}$-receptor stimulation. A) BW723C86 stimulation of 5-HT$_{2B}$ receptor induced a faster decrease in mushroom spine proportion (****p<0.0001) in the absence than in the presence of CIPP (****p<0.0001). B) BW723C86 stimulation increased the stubby spine density (****p<0.0001) in 5-HT$_{2B}$ receptor expressing cells but not in neurons expressing also CIPP. C) The 5-HT$_{2B}$ receptor stimulation induced a decrease in thin spine density (***p = 0.0001) in absence of CIPP while it increased the proportion of thin spines in presence of CIPP (****p<0.0001). Data were statistically analyzed by Mann-Withney t-test; n = 40-50 from 4-5 cultures.

DISCUSSION

L'absence d'outils permettant d'étudier la distribution, l'expression et ainsi la fonction du R-5-HT_{2B} a toujours été un frein dans les études *in vivo*. Cependant, le développement du modèle de souris n'exprimant pas ce récepteur (*Htr2b*$^{-/-}$) a permis de mettre évidence son rôle dans différents processus physiologiques au cours du développement et à l'âge adulte. Ce modèle a aussi permis de montrer que ce récepteur, bien que faiblement exprimé, est responsable de phénotypes provoquant une perturbation de la transmission sérotoninergique dans son ensemble. En effet, chez l'homme, un polymorphisme perte de fonction de ce récepteur est associé à des comportements impulsifs, agressifs et suicidaires (Bevilacqua et al., 2010). Des études complémentaires chez la souris ont montré que les animaux *Htr2b*$^{-/-}$ semblent insensibles aux molécules induisant une accumulation extracellulaire de 5-HT (MDMA, SSRI) (Diaz et al., 2012, 2016) et présentent des comportements psychotiques symptomatiques de la schizophrénie (Pitychoutis et al., 2015). Ces effets étant probablement le résultat d'une perturbation de la transmission sérotoninergique, il était important de comprendre les mécanismes moléculaires sous-jacents associés à ces récepteurs.

Les activités de recherche auxquelles j'ai participé au cours de mon doctorat ont permis de mettre en évidence le rôle du R-5-HT_{2B} dans la transmission sérotoninergique. L'invalidation génétique et/ou l'inhibition pharmacologique de ce récepteur dans les neurones sérotoninergiques ont permis de mettre en évidence sa contribution dans l'excitabilité des neurones. D'une part, nous avons démontré pour la première fois, que ce récepteur agit tel un modulateur positif capable de contrer le rétrocontrôle inhibiteur des R-5-HT_{1A} dans les neurones sérotoninergiques. D'autre part, le R-5-HT_{2B} exprimé par les neurones du raphé contribue aux effets moléculaires et comportementaux des molécules induisant une accumulation extracellulaire de 5-HT. Enfin, l'étude de l'interaction du R-5-HT_{2B} avec la protéine CIPP dans les cultures de neurones d'hippocampe a permis, pour la première fois, d'évaluer la distribution et l'adressage de ce récepteur dans des neurones. Par l'utilisation d'un agoniste spécifique du R-5-HT_{2B}, nous avons évalué la cinétique d'internalisation du récepteur, son impact sur la signalisation calcique et sur la distribution des R-NMDA.

Cette discussion sera répartie en deux sections dans lesquelles seront exposés le contexte ayant conduit à étudier nos projets de recherche puis les résultats principaux obtenus seront discutés. Cette discussion sera suivie d'une présentation des principales perspectives ouvertes par mon travail de thèse.

1. Participation des R-5-HT$_{2B}$ dans l'activité des neurones sérotoninergiques

A. Contexte

Les résultats antérieurs du laboratoire ont montré, par PCR sur cellule unique (*single cell PCR*), que certains neurones sérotoninergiques du DRN expriment le R-5-HT$_{2B}$ (10 neurones sur 12 testés) (Diaz et al., 2012). L'injection intrapéritonéale d'un agoniste du R-5-HT$_{2B}$ induit une augmentation significative des concentrations extracellulaires de 5-HT dans le raphé. Cette augmentation n'est plus observée suite à l'administration d'un antagoniste du R-5-HT$_{2B}$ (Doly et al., 2008). Ces données suggèrent que le R-5-HT$_{2B}$ participe à la libération de 5-HT.

Les phénotypes comportementaux induits par l'injection aigüe de MDMA ou un traitement chronique d'ISRSs ne sont pas observés chez les animaux *Htr2b*$^{-/-}$ et chez les animaux sauvages ayant reçu une injection d'antagonistes du R-5-HT$_{2B}$ (Doly et al., 2008; Diaz et al., 2012). En effet, des injections répétées de MDMA (10mg/kg) induisent une sensibilisation locomotrice chez les animaux sauvages, qui n'est pas observée en absence de R-5-HT$_{2B}$ (Doly et al., 2009). Cependant, la sensibilisation locomotrice induite par de fortes doses de MDMA (30mg/kg) est maintenue chez les animaux *Htr2b*$^{-/-}$ (Doly et al., 2009) **(Figure 31)**. A l'inverse, une injection chronique d'agonistes du R-5-HT$_{2B}$ reproduit les effets antidépresseurs chroniques des ISRSs chez les animaux sauvages (Diaz et al., 2012) **(Figure 31)**.

Les ISRS provoque une accumulation de 5-HT par blocage du SERT et le MDMA ainsi que les composés amphétaminergique un relargage par sortie des stocks vésiculaires de 5-HT. Le relargage de 5-HT induit par les ISRSs dans l'hippocampe n'est pas observé chez les animaux *Htr2b*$^{-/-}$ ou sauvages traités avec un antagoniste des R-5-HT$_{2B}$ (Diaz et al., 2012). Le MDMA provoque un relargage de 5-HT dans le Nac et l'ATV ainsi qu'une augmentation de dopamine dans le Nac. Ces effets ne sont pas non plus observés chez les animaux *Htr2b*$^{-/-}$ ou chez les animaux sauvages traités avec un antagoniste des R-5-HT$_{2B}$ suite à l'administration de faibles doses de MDMA (10 mg/kg). En revanche, de plus faibles augmentations de 5-HT et de dopamine sont toujours observées suite à l'administration de doses élevées de MDMA (30 mg/kg) (Doly et al., 2008, 2009) **(Figure 31)**.

		Témoins	Htr2b$^{-/-}$	Antagoniste 5-HT$_{2B}$
MDMA	10 mg/kg	↗Locomotion	×	×
		Sensibilisation	×	×
		↗ 5-HT (Nac, VTA)	×	×
		↗ Dopamine (Nac)	×	×
	30 mg/kg	↗Locomotion	×	×
		Sensibilisation	Sensibilisation	Sensibilisation
		↗ 5-HT (Nac, VTA)	Faible ↗ 5-HT (Nac)	Faible ↗ 5-HT (Nac)
		↗ Dopamine (Nac)	Faible ↗ Dopamine (Nac)	Faible ↗ Dopamine (Nac)
	Activité du SERT	↗ 5-HT extracellulaire	×	?
Agoniste 5-HT$_{2B}$	Aigu	Effet antidépresseur (nage forcée)	×	?
		↗ 5-HT extracellulaire (raphé)	?	×
ISRSs	Aigu	↗5-HT (hippocampe)	×	?
	chronique	Effet antidépresseur (neurogenèse)	×	×

Figure 31 Caractérisation phénotypique des animaux Htr2b$^{-/-}$ en réponse au MDMA, au ISRS et à l'agoniste du R-5-HT$_{2B}$. *× correspondent à une perte de l'effet observé chez les témoins ; ? les paramètres n'ont pas été testés.*

Les niveaux de base de 5-HT et de dopamine sont similaires chez les animaux sauvages et les animaux *Htr2b*$^{-/-}$, suggérant que l'expression et/ou de l'activité de SERT puissent être modifiées chez ce modèle animal. Néanmoins, les résultats ont montré que ni l'expression, ni l'activité de SERT ne sont modifiés chez les animaux *Htr2b*$^{-/-}$ indiquant que le transporteur est fonctionnel (Doly et al., 2008). De façon surprenante, les synaptosomes issus d'animaux *Htr2b*$^{-/-}$ ne libèrent pas de 5-HT en réponse au MDMA contrairement à ceux issus d'animaux sauvages (Doly et al., 2008) **(Figure 31)**.

Enfin, l'hypothèse d'une contribution du R-5-HT$_{1A}$ a été proposée du fait de son action inhibitrice sur l'activité des neurones sérotoninergiques et donc de la libération de 5-HT. L'expression du R-5-HT$_{1A}$ dans le raphé et l'hippocampe n'est pas affectée par la délétion du R-5-HT$_{2B}$ (Diaz et al., 2012). De même, l'hypothermie induite par l'agoniste du R-5-HT$_{1A}$ semble similaire chez les animaux sauvages et les animaux *Htr2b*$^{-/-}$ (Diaz et al., 2012). Le R-5-HT$_{1A}$ ne semble donc pas être impliqué dans les phénotypes des animaux *Htr2b*$^{-/-}$.

Cet ensemble de données suggèrent que le R-5-HT$_{2B}$ pourrait participer à la libération de 5-HT et/ou l'excitabilité des neurones sérotoninergiques. C'est dans cette optique que nous avons étudié le rôle du R-5-HT$_{2B}$ dans les neurones sérotoninergiques. Pour cela, nous avons généré 1) des animaux n'exprimant pas le R-5-HT$_{2B}$ uniquement dans les neurones sérotoninergiques (*5-HT$_{2B}^{5\text{-}HTKO}$*), et 2) avons effectué une surexpression virale du R-5-HT$_{2B}$ seulement dans les neurones sérotoninergiques. Ces modèles d'études ont été utilisés pour tester les effets comportementaux induits par le MDMA, les ISRSs et l'antagoniste du R-5-HT$_{1A}$ ainsi que dans les propriétés électrophysiologiques des neurones sérotoninergiques.

B. Discussion

1. Le R-5-HT$_{2B}$: un autorécepteur positif des neurones sérotoninergiques ?

Les résultats de l'Article 1 indiquent que la stimulation du R-5-HT$_{2B}$ augmente le taux de décharge des neurones sérotoninergiques et que sa surexpression augmente l'excitabilité de ces neurones. Des mesures électrophysiologiques *in vivo* dans le raphé effectuées sur des animaux *5-HT$_{2B}^{5\text{-}HTKO}$* montrent que la proportion des neurones déchargeant à une faible fréquence (0-1 Hz) est plus grande chez grande que chez les animaux sauvages. De plus, la proportion de neurones déchargeant à une forte fréquence (4-5Hz) est plus faible chez les animaux *5-HT$_{2B}^{5\text{-}HTKO}$* que chez les animaux sauvages. De plus, la stimulation du R-5-HT$_{2B}$ est capable de déplacer l'effet inhibiteur du R-5-HT$_{1A}$ sur le taux de décharge des neurones sérotoninergiques. Au niveau comportemental, l'injection d'agoniste du R-5-HT$_{1A}$ induit une hypothermie. Une injection préalable d'agoniste du R-5-HT$_{2B}$ raccourcie la durée de cette hypothermie.

Ces résultats nous permettent de proposer le R-5-HT$_{2B}$ en tant qu'autorécepteur positif des neurones sérotoninergiques.

Il est bien connu que les neurones sont modulés par différents mécanismes dépendants des R-5-HT$_{1A}$ et potentiellement des R-5-HT$_2$. En effet, en tant qu'autorécepteur négatif, le R-5-HT$_{1A}$ diminue l'activité des neurones sérotoninergiques, par son couplage à la protéine Gi

qui active l'ouverture des canaux potassiques de rectification entrante GIRK (Colino and Halliwell, 1987; Penington et al., 1992; Bayliss et al., 1997; Montalbano et al., 2015) et la fermeture des canaux calciques de type T (Penington and Kelly, 1990; Penington et al., 1992) favorisant ainsi l'hyperpolarisation des neurones **(Figure 32)**.

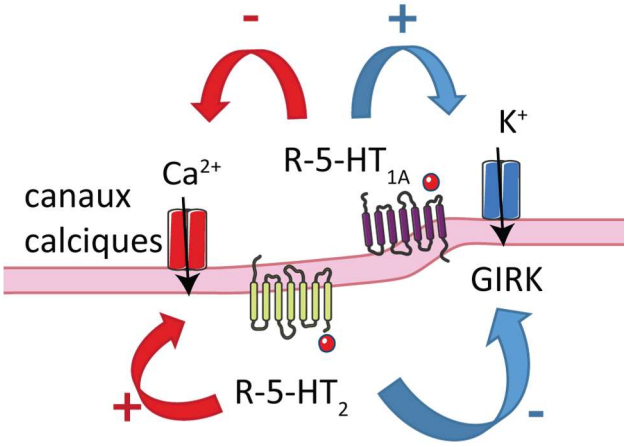

Figure 32 Action antagoniste des R-5-HT$_{1A}$ et des R-5-HT$_2$ sur les canaux calciques et les canaux GIRK. *Représentation schématique de l'action opposée des R-5-HT$_1$ et des R-5-HT$_2$ sur les canaux calciques et le canal GIRK.*

Il est probable que les R-5-HT$_2$, notamment les R-5-HT$_{2B}$, participent à l'activité des neurones sérotoninergiques par leur couplage à la protéine Gq. En effet, il a été montré que la stimulation des R-5-HT$_{2A}$ provoque l'ouverture des canaux calciques voltages dépendants, Cav1.2 (Day et al., 2002). De la même manière, la stimulation des R-5-HT$_{2B}$ peut induire l'ouverture des canaux calciques de type L (Baxter et al., 1994; Cox and Cohen, 1996; Sandén et al., 2000) et finalement la stimulation des R-5-HT$_{2C}$ induit la fermeture des canaux GIRK ou Kv (Day et al., 2002; Speake et al., 2004; Blomeley and Bracci, 2009) **(Figure 32)**. Cette hypothèse est renforcée par le fait que l'utilisation de différents antagonistes spécifiques des R-5-HT$_2$ (mésulergine, kétansérine) supprime la dépolarisation induite par la 5-HT (Craven et al., 2001), suggérant que les R-5-HT$_2$ seraient impliqués dans la dépolarisation des neurones induite par la 5-HT. De plus, dans certains neurones sérotoninergiques du DRN (47%), l'agoniste des récepteurs 5-HT$_2$ (DOI) induit des courants entrants dépolarisants et la totalité des neurones produisent des courants sortants hyperpolarisants dépendants des R-5-HT$_{1A}$ (Marinelli et al., 2004). Enfin, un tiers de neurones sérotoninergiques du DRN (37%) produisent des courants entrants et sortants en réponse aux agonistes 5-HT$_2$ et 5-HT$_{1A}$ indiquant qu'il existe

une population non négligeable de neurones capables d'être modulés par ces deux autorécepteurs (Marinelli et al., 2004).

Puisque le R-5-HT$_{1A}$ n'a pas de site de liaison au domaine PDZ, il ne semble pas avoir de protéines de pontage en commun avec le R-5-HT$_{2B}$ (Marin et al., 2012). Cependant, ils peuvent tous deux êtres internalisés dans des vésicules à clathrines (Della Rocca et al., 1999; Janoshazi et al., 2007) regroupées dans des radeaux lipidiques (pour revue Le Roy and Wrana, 2005). Ainsi, bien que cela reste à démontrer, les R-5-HT$_{1A}$ et les R-5-HT$_{2B}$ pourraient être distribués dans des microdomaines similaires.

Enfin, nos résultats indiquent que la délétion conditionnelle des R-5-HT$_{2B}$ diminue la proportion de neurones déchargeant à forte fréquence, renforçant l'hypothèse selon laquelle le R-5-HT$_{2B}$ participerait à l'excitabilité des neurones sérotoninergiques.

2. Les R-5-HT$_{2B}$ exprimés par les neurones sérotoninergiques sont nécessaires aux effets du MDMA et des ISRSs.

La délétion génétique du R-5-HT$_{2B}$ dans les neurones sérotoninergiques supprime les effets psychoactifs et antidépresseurs induits par le MDMA et les ISRSs. De plus, l'application aigüe d'antagoniste du R-5-HT$_{2B}$ reproduit les phénotypes observés chez les *Htr2b*$^{-/-}$. A l'inverse, l'administration aigüe ou chronique d'un agoniste du R-5-HT$_{2B}$ reproduit les effets induits par les ISRSs. Ces résultats suggèrent une action dynamique des R-5-HT$_{2B}$ sur les neurones sérotoninergiques (Diaz et al., 2012).

Les phénotypes comportementaux observés pourraient être expliqués par le fait qu'en absence des R-5-HT$_{2B}$, l'effet inhibiteur des autorécepteurs 5-HT$_{1A}$ n'est pas contrebalancé par l'effet activateur du R-5-HT$_{2B}$. Ainsi, cette « plus forte » inhibition diminuerait l'excitabilité des neurones sérotoninergiques et induit une hyposérotoninergie apparents.

3. Le R-5-HT$_{2B}$: un acteur de la transmission sérotoninergique ?

Cependant, chez les animaux *Htr2b*$^{-/-}$, les mécanismes expliquant que 1) les concentrations basales de 5-HT ne sont pas altérées, 2) SERT et les R-5-HT$_{1A}$ sont exprimés dans les même proportions, mais que 3) les synaptosomes ne libèrent pas de 5-HT en réponse au MDMA restent à déterminer. Une meilleure connaissance de la distribution et de la fonction du R-5-HT$_{2B}$ dans les neurones sérotoninergiques pourrait nous aider à répondre à cette problématique. Il est établi que, le R-5-HT$_{1A}$ est retrouvé au niveau somatodendritique dans les neurones sérotoninergiques où il exerce son action inhibitrice en réponse à la libération locale

de 5-HT. Des résultats préliminaires, par l'utilisation d'un modèle de surexpression virale des R-5-HT$_{2B}$-HA ou de *Tomato* dans les neurones sérotoninergiques ont mis en évidence que le R-5-HT$_{2B}$-HA est localisé au niveau somatodendritique dans les neurones sérotoninergiques **(Figure 33)**.

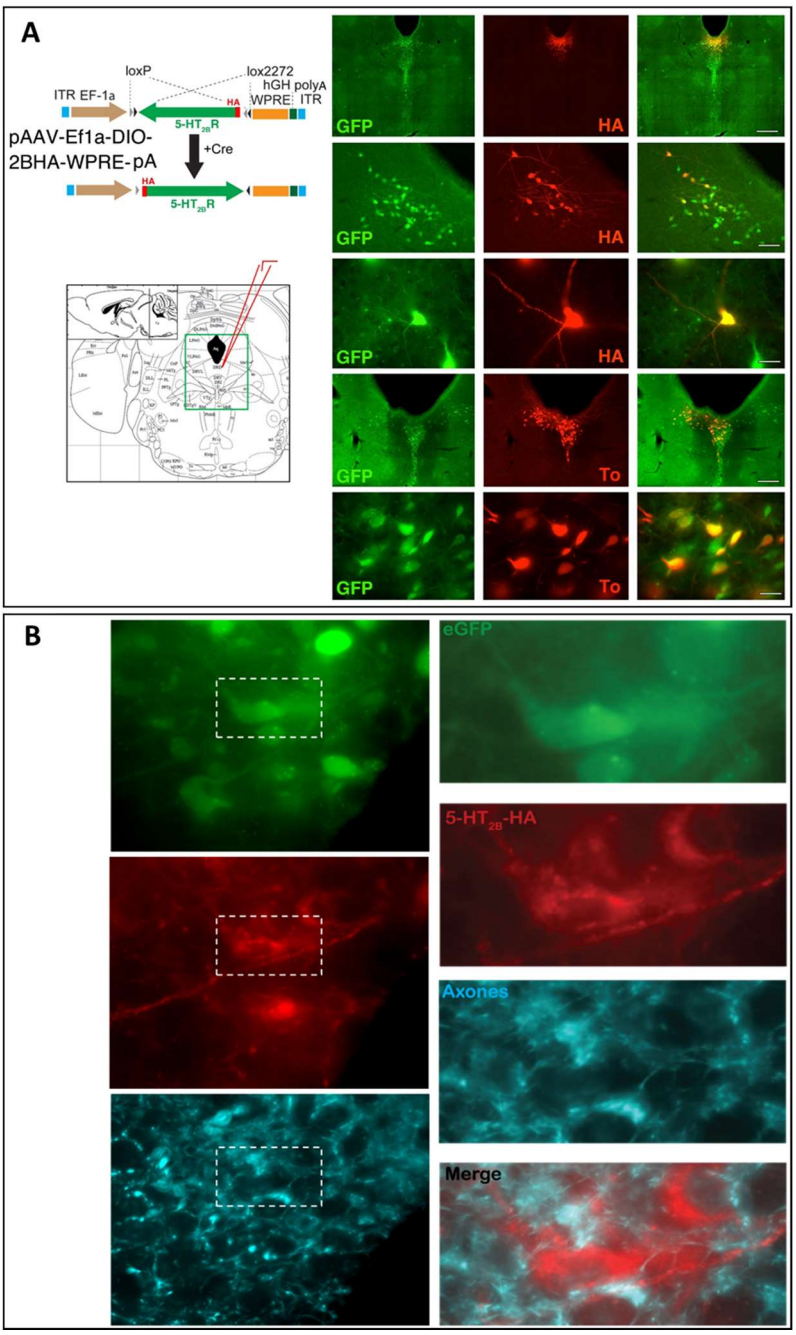

Figure 33 Expression virale de la protéine Tomato (To) et du R-5-HT$_{2B}$-HA dans les neurones sérotoninergiques. *(A) Construction virale DIO utilisée et site d'injection (noyau B7 du DRN). Vérification du site d'injection de la protéine Tomato et du R-5-HT$_{2B}$-HA en rouge. En vert, expression de la GFP dans les neurones sérotoninergiques. (B) Neurones sérotoninergiques GFP (vert), R-5-HT$_{2B}$-HA (rouge) et marquage axonal de la protéine neurofilament (bleu).*

Les R-5-HT_{1A} et 5-HT_{2B} semblent être exprimés dans les mêmes compartiments neuronaux. Les neurones sérotoninergiques libèrent de la 5-HT dans les boutons axonaux (transmission synaptique) et au niveau somatodendritique (transmission extrasynaptique). Il est envisageable que le R-5-HT_{2B} puisse participer à cette libération somatodendritique et ainsi participer à l'excitabilité des neurones. La libération de 5-HT n'est pas totalement dépendante du taux de décharge des neurones. La libération dendritique de 5-HT n'étant pas dépendante des potentiels d'actions (Colgan et al., 2012), il est possible de proposer que le R-5-HT_{2B} participe à la libération somatodendritique de 5-HT en jouant sur les processus de fusion des vésicules contenant les neuromédiateurs par sa signalisation calcique ou en potentialisant l'activité des R-NMDA par son couplage à la voie de la PLC. De plus, la libération dendritique de 5-HT induite par l'activation des R-NMDA est dépendante des canaux calciques de type L (Colgan et al., 2012). Les R-5-HT_{2B} sont capables de stimuler ces canaux calciques dans d'autres types cellulaires *via* la voie de la PLC (Baxter et al., 1994; Cox and Cohen, 1996; Sandén et al., 2000). Comme les canaux calciques de type L sont spécifiques de la libération extrasynaptique, le R-5-HT_{2B} pourrait participer à la libération somatodendritique de 5-HT. De plus, chez la sangsue dans les neurones sérotoninergiques Retzius, l'exocytose de 5-HT est aussi dépendante de l'ouverture des canaux calciques de type L, puis est renforcée par l'activation des R-5-HT_2 qui, par leur couplage à la voie de la PLC, va amplifier la libération de 5-HT (Trueta et al., 2003, 2004, 2012; Leon-Pinzon et al., 2014) renforçant l'hypothèse selon laquelle le R-5-HT_{2B} participerait à la libération extrasynaptique de 5-HT et ainsi à l'excitabilité des neurones sérotoninergiques **(Figure 35)**.

2. Interaction du R-5-HT$_{2B}$ avec la protéine CIPP

A. Contexte

La connaissance de la distribution subcellulaire du R-5-HT$_{2B}$ dans les neurones est importante pour faire le lien entre les phénotypes comportementaux observés chez les animaux *Htr2b*$^{-/-}$ et *5-HT*$_{2B}$$^{5\text{-}HTKO}$ et les mécanismes moléculaires physiologiques de la régulation des R-5-HT. Les interactions protéine-protéine sont des éléments clés dans la fonction des RCPGs, dont font partie les R-5-HT. En effet, les RCPGs sont associés à différents types de protéines comme 1) les protéines d'échafaudage qui sont souvent associées au cytosquelette, 2) les protéines de pontage qui régulent l'internalisation/maintien des RCPGs à la membrane ou encore 3) les protéines d'adressage qui régulent le trafic intracellulaire des RCPGs dans les différents compartiments cellulaires (pour revue : Dunn and Ferguson, 2015).

Ainsi, ces interactions protéiques sont cruciales dans l'activation des voies de signalisation associées aux RCPGs. Plusieurs protéines associées au R-5-HT$_{2B}$ ont été découvertes par des approches protéomiques mais leurs rôles n'ont pas encore été approfondis. C'est dans l'optique de clarifier ces mécanismes que je me suis intéressée à l'interaction du R-5-HT$_{2B}$ et de la protéine CIPP. Peu d'études ont porté sur la distribution subcellulaire du R-5-HT$_{2B}$ ou sur celle de CIPP. Cependant, quelques études ont été publiées quant au rôle de CIPP, une isoforme de la protéine INADL retrouvée dans le cerveau, composée de quatre domaines PDZ et capable d'interagir avec les R-NMDA, les R-5-HT$_{2A/2B/4}$ ainsi qu'avec SERT et les canaux potassique Kir (Kurschner et al., 1998; Bécamel et al., 2004; Chanrion et al., 2007). CIPP est aussi capable de former un complexe tripartite avec les protéines IRSp53 et Cypine dans la lignée neuronale HN9.10^{e} (Alpi et al., 2009). Dans cette lignée cellulaire, ce complexe protéique est retrouvé dans des structures semblables à des neurites. De façon surprenante, ces neurites sont absents lorsque les cellules ne sont pas transfectées avec CIPP (Barilari and Dente, 2010). Ces données suggèrent que CIPP peut participer à la modulation du cytosquelette, voir à la morphologie des épines dendritiques dans un modèle neuronal. Ceci est conforté par le fait que CIPP est aussi capable de s'associer aux protéines neuroligine et neurexine qui forment un complexe transynaptique permettant la différentiation et le maintien des éléments pré- et post-synaptiques (Dean et al., 2003; Chih et al., 2005).

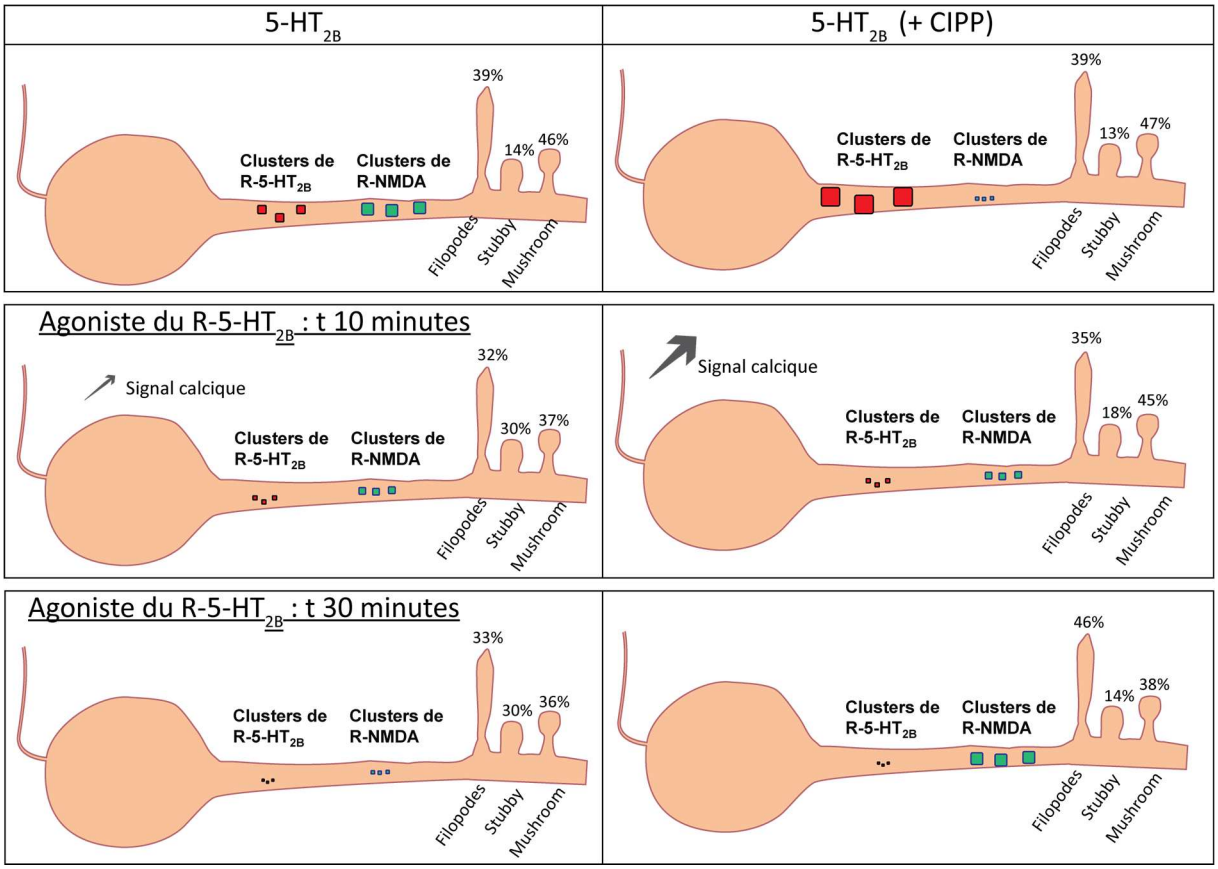

Figure 34 Représentation schématique des effets induits par la stimulation du R-5-HT$_{2B}$ dans des neurones exprimant ou non la protéine de pontage CIPP. *La distribution du R-5-HT$_{2B}$ est plus diffuse qu'en présence de CIPP tandis que les R-NMDA forment de plus gros clusters. La stimulation du R-5-HT$_{2B}$ provoque un pic de calcium, supérieur en présence de CIPP. La stimulation du R-5-HT$_{2B}$ induit son internalisation indépendamment de CIPP. La stimulation du R-5-HT$_{2B}$ induit une dispersion des R-NMDA (en absence de CIPP) ou le regroupement des R-NMDA (en présence de CIPP). La stimulation des R-5-HT$_{2B}$ induit des variations morphologiques de plus grandes ampleurs des épines dendritiques, en absence de CIPP.*

B. Discussion

1. Distribution subcellulaire du R-5-HT$_{2B}$

L'ensemble des résultats obtenus nous a permis, pour la première, fois de visualiser le R-5-HT$_{2B}$ au niveau somatodendritique. Nos résultats ont montré que le R-5-HT$_{2B}$ et CIPP sont fortement colocalisés et que cette interaction augmente la taille et l'intensité des clusters de R-5-HT$_{2B}$ dans les neurones. De plus, la présence de CIPP augmente significativement la distribution des R-5-HT$_{2B}$ dans les synapses excitatrices et la diminue dans les synapses

inhibitrices. Ces effets ne sont pas observés lorsque le site de liaison au domaine PDZ du R-5-HT_{2B} est tronqué. De plus, la forme tronquée du récepteur en présence de CIPP est moins ciblée dans les synapses excitatrices que la forme sauvage en absence de CIPP **(Figure 34)**. Cette observation indique que le domaine de liaison aux protéines PDZ est crucial pour l'adressage synaptique du récepteur. Ceci suggère aussi que d'autres protéines d'adressage pourraient intervenir dans la distribution subcellulaire du R-5-HT_{2B}.

Il aurait été préférable d'effectuer ces expériences sur des neurones sérotoninergiques qui contiennent la machinerie moléculaire nécessaire à la distribution et la fonction physiologique du R-5-$HT_{2B,}$ nous avons fait le choix d'utiliser des neurones primaire de l'hippocampe. En effet, les neurones sérotoninergiques sont difficiles à cultiver et à transfecter. Cependant, j'ai tout de même tenté de mettre au point une technique de dissociation des neurones sérotoninergiques issus de nos animaux exprimant la GFP dans les neurones sérotoninergiques dans le but de les trier par FACS (*« fluorescence activated cell sorting »*). Les résultats montrent que les purifications de neurones ont abouti, cependant le rendement était trop faible pour pouvoir envisager de le cultiver et de les infecter. Ainsi, l'utilisation de neurones primaires de l'hippocampe s'est avérée plus sûre. Néanmoins, il semble que CIPP ne soit pas exprimé dans l'hippocampe (Kurschner et al., 1998). Ainsi, en absence de CIPP endogène, les résultats obtenus par la surexpression pourraient ne pas refléter son rôle physiologique.

Lorsque j'ai effectué les injections virales *in vivo* de 5-HT_{2B}-HA dans les neurones sérotoninergiques, les marquages contre le motif HA montrent une distribution somatodendritique du R-5-HT_{2B}. Ceci permet de proposer que l'adressage du R-5-HT_{2B} serait similaire dans les neurones d'hippocampe et dans les neurones sérotoninergiques. La distribution somatodendritique du R-5-HT_{2B}, n'est pas totalement dépendante de CIPP car le R-5-HT_{2B} tronqué présente une distribution subcellulaire similaire à la construction sauvage du R-5-HT_{2B} dans les cultures de neurones d'hippocampe. Ainsi, d'autres mécanismes sont impliqués dans l'adressage du R-5-HT_{2B}. La protéine SAP-102 est un bon candidat car cette protéine est responsable de l'adressage des R-NMDA à partir de l'appareil de Golgi jusque dans les épines dendritiques (Pour revue Lau and Zukin, 2007). De plus, des expériences préliminaires, sur la lignée cellulaire COS-7, portant sur la co-expression du R-5-HT_{2B} et de SAP-102 ont montré un gain de fonction de la signalisation de base et après stimulation du R-5-HT_{2B} sur les lignées cellulaires COS-7.

2. Impact de la co-expression sur la fonction du R-5-HT$_{2B}$: CIPP protéine de pontage

Le R-5-HT$_{2B}$ a une activité de base potentialisée par la co-expression avec CIPP. La stimulation du R-5-HT$_{2B}$ par des concentrations croissantes d'agoniste total (5-HT) et partiel (DOI) induit une accumulation croissante de second messager. Ceci reflète l'activité de la voie de la PLC induite par la stimulation du récepteur. Nos résultats ont montré que la présence de CIPP induit un gain de fonction de l'activité de la PLC en réponse à la stimulation du récepteur **(Figure 34)**. En effet, dans les neurones, CIPP regroupe les R-5-HT$_{2B}$ qui forment des clusters plus grands et plus intenses, ce qui a pour conséquence de potentialiser l'activité du R-5-HT$_{2B}$ notamment dans la signalisation calcique. En accord avec nos résultats, un gain de fonction induit par CIPP a aussi été observé dans l'interaction de CIPP avec les canaux Kir dont les courants potassiques sont amplifiés (Kurschner et al., 1998). Ces données suggèrent que CIPP serait une protéine de pontage permettant de rassembler des protéines membranaires avec leurs effecteurs et non pas une protéine d'adressage.

3. Le complexe R-5-HT$_{2B}$/CIPP : implication dans la morphologie des épines dendritiques ?

De plus, il semble que CIPP renforce la stabilité des épines dendritiques en réponse à la stimulation du R-5-HT$_{2B}$ suggérant une action sur le cytosquelette d'actine **(Figure 34)**. Cette hypothèse est renforcée par le fait que CIPP forme des complexes tripartites avec les protéines IRSp53 et cypine induisant la formation de neurites faisant probablement intervenir des modulations du cytosquelette (Barilari and Dente, 2010). Cependant, les mécanismes impliqués restent à découvrir.

4. CIPP/ R-NMDA/ R-5-HT$_{2B}$: un complexe protéique fonctionnel ?

Dans les cultures de neurones d'hippocampe, CIPP module la distribution du R-NMDA qui est plus diffus (Article 1), cependant il est difficile de faire une interprétation fonctionnelle de cette observation. La stimulation du R-5-HT$_{2B}$ semble modifier la distribution des R-NMDA lorsque CIPP est présent **(Figure 34)**. Le R-5-HT$_{2B}$ pourrait, *via* sa signalisation calcique, moduler l'expression des R-NMDA. Ces derniers sont exportés le long des microtubules grâce un complexe protéique composé des protéines de pontage LIN2, LIN7 et SAP-102 dans des vésicules de transports dirigées *via* une kinésine (KIF17) (Setou et al., 2000; Guillaud et al., 2003). Il a été montré que la stimulation de la voie de la PKC facilite l'insertion des R-NMDA en quelques minutes (Lan et al., 2001). Ainsi, comme la signalisation des R-5-HT$_{2B}$ est augmentée en présence de CIPP, son couplage à la PKC pourrait faciliter l'insertion des R-NMDA.

En absence de CIPP, la stimulation du R-5-HT_{2B} induit une dispersion des clusters de R-NMDA **(Figure 34)**. Il a été montré que l'internalisation du R-5-HT_{2B} est dépendante des clathrines suite à une stimulation par la 5-HT ou par l'agoniste que j'ai utilisé dans mes expériences (BW723C86). L'internalisation des R-NMDA est aussi dépendante des clathrines (Lau and Zukin, 2007). Comme le R-5-HT_{2B} et les R-NMDA sont colocalisés à hauteur d'environ 40% indépendamment de la stimulation du R-5-HT_{2B} et de CIPP, l'internalisation du R-5-HT_{2B} suite à sa stimulation pourrait aussi entrainer l'internalisation des R-NMDA bien que cela reste à démontrer.

En accord avec cette hypothèse, Yuen et al, ont montré que les R-5-HT participent à la distribution des R-NMDA par l'action de la voie de la PLC dans des cultures de neurones de CPF (Yuen et al., 2005, 2008). La stimulation du R-5-HT_{1A} réduit les courants et l'expression membranaire des R-NMDA par un mécanisme dépendant des kinésines, participant au trafic des R-NMDA le long des microtubules (Yuen et al., 2005). L'activation des R-5-HT_{1A} favorise la dépolymérisation des microtubules et diminue leur stabilité, ce qui a pour conséquence fonctionnelle de diminuer l'export des vésicules contenant les récepteurs NMDA à la membrane plasmique (Yuen et al., 2005). La stimulation des R-5-$HT_{2A/2C}$ augmente les courants post-synaptiques excitateurs dépendants des R-NMDA, et que cet effet est associé à une diminution de la dépolymérisation des microtubules (Yuen et al., 2008). Ainsi, les R-5-HT_{1A} et 5-HT_2 participeraient à la transmission synaptique en modulant les processus de polymérisation / dépolymérisation des microtubules, et modulerait l'export des R-NMDA. Ces résultats sont cohérents avec ceux que nous avons obtenus *in vivo* dans le cadre de l'étude du R-5-HT_{2B} dont la stimulation est capable de contrer l'effet inhibiteur des R-5-HT_{1A} sur l'activité des neurones sérotoninergiques. Aussi, CIPP pourrait participer au maintien des R-5-HT_{2B} et des R-NMDA à la membrane. Ce qui signifierait que CIPP, en potentialisant la signalisation du R-5-HT_{2B}, permettrait le recrutement des récepteurs NMDA. Si l'on tient compte maintenant du fait que certains neurones sérotoninergiques sont capables de libérer du glutamate, la co-libération de ce neuromédiateur par la stimulation simultanée des R-5-HT_2 et NMDA induirait un signal plus fort et ainsi un renforcement rapide et solide de la transmission synaptique. Enfin, la libération extrasynaptique dendritique de 5-HT est dépendante des R-NMDA, de l'influx calcique dépendant des canaux de type L, et probablement des R-5-HT2 *via* la voie de la PKC (Colgan et al., 2012; Trueta et al., 2012; Leon-Pinzon et al., 2014). La libération dendritique de 5-HT pourrait être un bon modèle dans lequel le R-5-HT_{2B} pourrait participer à l'excitabilité des neurones sérotoninergiques **(Figure 35)**.

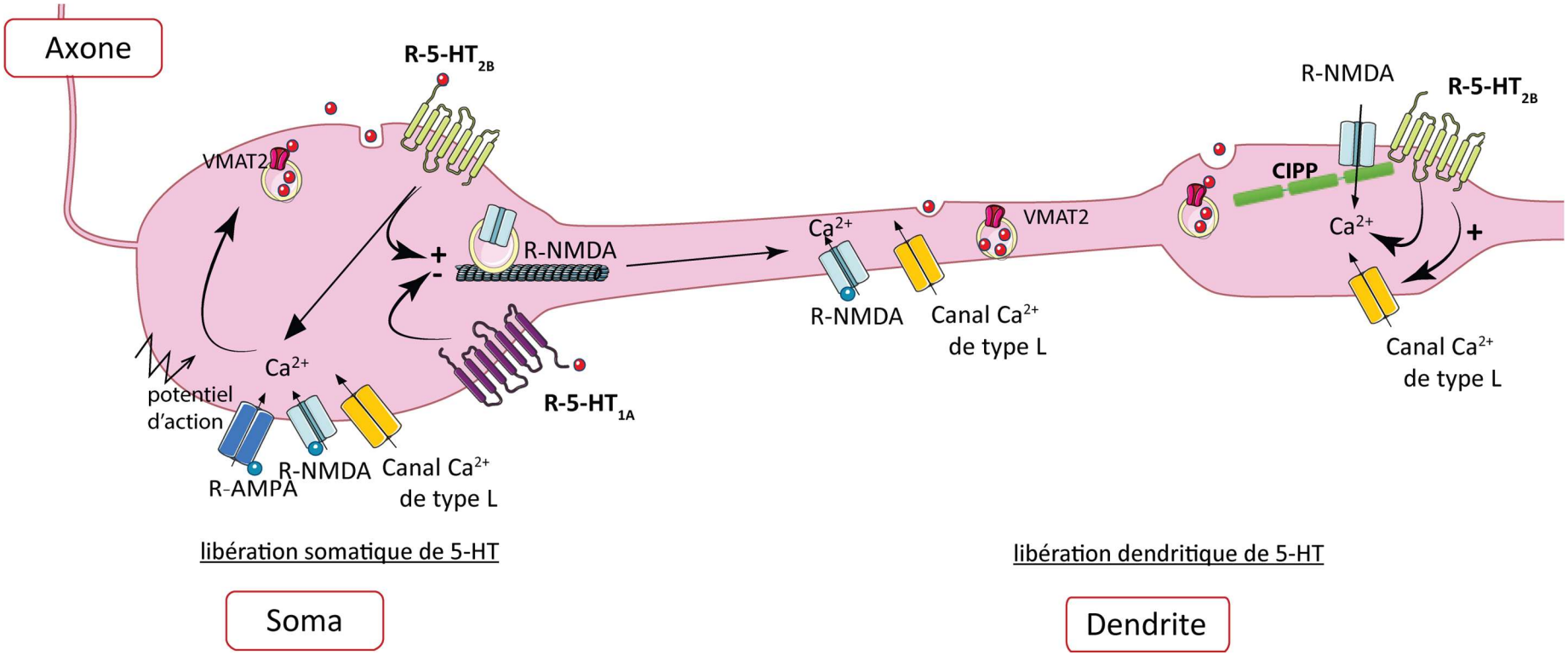

Figure 35 Représentation schématique du rôle potentiel du R-5-HT$_{2B}$ et de CIPP dans la libération extrasynaptique. *A gauche, dans le soma, la libération somatique de 5-HT dépendante des R-AMPA et NMDA, des canaux calcique de type L, et des potentiels d'action et potentiellement des R-5-HT$_2$ via leur couplage à la PKC (Trueta et al., 2003, 2004; De Kock et al., 2006; Colgan et al., 2012; Leon-Pinzon et al., 2014) L'activation des R-5-HT$_{1A}$ et des R-5-HT$_2$ augmente ou diminue l'expression membranaire des R-NMDA, respectivement, par leur action sur les microtubules (Yuen et al., 2005, 2008). A droite, la libération dendritique dépendante des R-NMDA et des canaux calcique de type L (Colgan et al., 2012) et hypothétiquement du R-5-HT$_{2B}$, en synergie avec CIPP au niveau de « puncta » dendritiques en forme de fuseau (Colgan et al., 2012).*

PERSPECTIVES

Ces deux études ont apporté de nouvelles données permettant de confirmer que le R-5-HT$_{2B}$ participe à la transmission sérotoninergique. Les résultats de l'Article 1 ont montré que le R-5-HT$_{2B}$ agit comme un autorécepteur positif de l'activité des neurones sérotoninergiques et participe à la libération de 5-HT. Les résultats de l'Article 2 ont montré que le R-5-HT$_{2B}$ est distribué au niveau somatodendritique dans les neurones d'hippocampe, majoritairement dans les synapses excitatrices. Cette étude a aussi permis d'approfondir le rôle de la protéine de pontage CIPP, notamment dans la distribution des R-5-HT$_{2B}$ et des R-NMDA. Cette protéine de pontage, en réorganisant la distribution du R-5-HT$_{2B}$, potentialise sa signalisation, ce qui a pour conséquence d'induire l'agrégation des R-NMDA suggérant un rôle dans la transmission synaptique. Cet ensemble de données nous a permis d'offrir de nouvelles perspectives dans l'étude de la fonction du R-5-HT$_{2B}$.

1. Trafic intracellulaire du R-5-HT$_{2B}$

Pour la première fois nous avons observé la distribution somatodendritique du R-5-HT$_{2B}$. Concernant son trafic intracellulaire, il serait important de définir les protéines impliquées dans sa distribution somatodendritique. Les premiers candidats à tester seraient les protéines PDZ associées avec le R-5-HT$_{2B}$: NHERF, SAP-102 et α-syntrophine).

Une autre piste serait d'évaluer l'impact des phosphorylations de l'extrémité C-terminale du R-5-HT$_{2B}$ dans la distribution cellulaire et/ou l'activité des voies de signalisation du R-5-HT$_{2B}$. J'ai effectué des clonages afin de transformer les sites putatifs de phosphorylation en résidus non phosphorylables de l'extrémité C-terminale du R-5-HT$_{2B}$. Pour l'instant, j'ai seulement observé que l'expression de ces constructions est similaire à celle de la construction non mutée du récepteur mais il serait intéressant d'approfondir cette étude.

2. Dualité R-5-HT$_{1A}$ et R-5-HT$_{2B}$

Sachant que le R-5-HT$_{1A}$ est distribué au niveau somatodendritique et que la stimulation du R-5-HT$_{2B}$ est capable de compenser l'action inhibitrice du R-5-HT$_{1A}$, il serait intéressant d'approfondir ces mécanismes.

Des expériences sont prévues pour évaluer la colocalisation des R-5-HT$_{1A}$ et les R-5-HT$_{2B}$, dans des cultures cellulaires et *in vivo* par infection virale. De plus, il serait intéressant d'évaluer l'impact de la stimulation de chacun de ces récepteurs sur leurs expressions et/ou leurs fonctions.

3. Contribution du R-5-HT$_{2B}$ dans la libération de 5-HT

Les deux articles présentés dans ce manuscrit ont apporté des évidences quant à la participation du R-5-HT$_{2B}$ dans la transmission synaptique. En effet, l'Article 1 montre que la surexpression du R-5-HT$_{2B}$ augmente l'excitabilité des neurones sérotoninergiques. Le fait que la délétion du R-5-HT$_{2B}$ dans les neurones sérotoninergiques supprime les effets induits par les molécules provoquant une accumulation de 5-HT (MDMA, ISRSs) suggère que le R-5-HT$_{2B}$ pourrait participer à la libération de 5-HT. L'Article 2 ayant montré que la stimulation du R-5-HT$_{2B}$ induit une agrégation rapide des R-NMDA dans les dendrites renforce cette hypothèse. Leur localisation dendritique renforce aussi l'hypothèse d'une action sur la libération extrasynaptique de 5-HT par les dendrites car cette libération est dépendante des R-NMDA, des canaux calciques de type L et de la PKC. Comme l'activation du R-5-HT$_{2B}$ potentialise ces trois paramètres il serait intéressant d'approfondir ces mécanismes en évaluant 1) la colocalisation des R-5-HT$_{2B}$ et des R-NMDA dans les neurones sérotoninergiques infectés avec le R-5-HT$_{2B}$-HA ainsi que, 2) la colocalisation des R-5-HT$_{2B}$ avec le transporteur VMAT2 qui est indispensable pour la libération dendritique de 5-HT. Pour étudier le rôle du R-5-HT$_{2B}$ *in vivo*, la mesure de la signalisation calcique en microscopie 2-photons en réponse à différents traitements pharmacologiques (ex: agoniste du R-5-HT$_{2B}$ ou des R-NMDA en présence d'un antagoniste du R-5-HT$_{2B}$) nous informerait sur la signalisation du récepteur dans les neurones sérotoninergiques. Enfin, à plus long terme ou en collaboration, il serait intéressant d'évaluer la libération somatodendritique de 5-HT, en microscopie 3-photons, en réponse à un agoniste ou un antagoniste des R-5-HT$_{2B}$ ou encore sur des tranches de cerveaux issus d'animaux *5-HT$_{2B}^{5\text{-}HTKO}$*.

ANNEXES

Annexe 1

Heterodimers of serotonin receptor subtypes 2 are driven by 5-HT2C protomers

Imane Moutkine, Emily Quentin, Bruno P. Guiard , Luc Maroteaux, and Stephane Doly

1. Impact fonctionnel de la dimérisation des récepteurs 5-HT$_2$

(Publié dans The Journal of Biological Chemistry en mars 2017)

Les récepteurs sérotoninergiques sont des RCPGs, qui participent à la transmission sérotoninergiques autant au niveau présynaptique que postsynaptique suite à la libération de 5-HT. Les RCPGs activent différentes voies de signalisation selon les protéines G auxquels ils sont couplés. Ces voies de signalisation peuvent varier notamment lorsque ces RCPGs forment des multimères. En effet, ces processus d'oligomérisation ont déjà été montrés pour certains récepteurs sérotoninergiques tels que les R-5-HT$_{1A/1B/1C/2A/2C/4/7}$ qui forment des homodimères (Xie et al., 1999; Salim et al., 2002; Herrick-Davis et al., 2004; Berthouze et al., 2005; Kobe et al., 2008; Mancia et al., 2008; Brea et al., 2009; Woehler et al., 2009; Teitler et al., 2010; Paila et al., 2011; Pellissier et al., 2011; Moutkine et al., 2017)..

Ils peuvent aussi former des hétérodimères, comme par exemple les R-5-HT$_{2A}$ avec les récepteurs mGlur2 (Moreno et al., 2012) ou les récepteurs dopaminergiques D1 (Łukasiewicz et al., 2010; Albizu et al., 2011), ainsi que les R-5-HT$_{2C}$ avec les récepteurs de la ghréline GHS-R1a (Schellekens et al., 2013). Les R-5-HT peuvent aussi s'hétérodimeriser entre eux, suggérant une complexité supplémentaire de la fonction sérotoninergique. En effet, des hétérodimérisations ont été décrites pour les R-5-HT$_{1B/1D}$ (Xie et al., 1999), et les R-5-HT$_{1A/7}$ (Renner et al., 2012). Ces hétérodimerisations peuvent induire des variations des propriétés pharmacologiques ou de l'expression des R-5-HT (pour revue Herrick-Davis, 2013).

Sachant que les sous-types de R-5-HT$_2$ sont exprimés en commun dans des certaines structures, il est apparu crucial, dans la compréhension de la transmission sérotoninergique, de savoir si ces récepteurs pouvaient s'oligomériser. En effet les R-5-HT$_{2A}$ et 5-HT$_{2C}$ sont exprimés par les interneurones GABAergiques et dans une population de neurones pyramidaux du CPF (Anastasio et al., 2015; Carr et al., 2002). De plus les R-5-HT$_{2C}$ et 5-HT$_{2B}$ sont co-exprimés dans les neurones dopaminergiques de l'ATV ainsi que dans les neurones POMC du noyau arqué de l'hypothalamus (Esposito, 2006; Yadav et al., 2009; Bubar et al., 2011).

A. Oligomérisation des R-5-HT$_2$

Dans un premier temps, nous avons mis en évidence que les R-5-HT$_{2A/B/C}$ peuvent former des homodimères (5-HT$_{2A/2A}$, 5-HT$_{2C/2C}$ mais pas 5-HT$_{2B/2B}$) ainsi que des hétérodimères (5-HT$_{2A/2B}$, 5-HT$_{2A/2C}$, 5-HT$_{2B/2C}$) par co-immunoprécipitation et BRET (*« Bioluminescence Resonance Energy Transfert »*).

B. Impact fonctionnel de la dimérisation des R-5-HT$_2$ *in vitro*

Ces récepteurs étant couplés à la voie de la PLC, nous avons étudié l'effet de ces dimérisations sur l'accumulation de second messager IP_3 en réponse à la stimulation de chacun des sous-types avec un agoniste partiel (DOI) ou total (5-HT), sur des cellules COS-7 simplement ou doublement transfectées avec ces récepteurs. Ensuite, nous avons analysé l'accumulation de second messager par un modèle pharmacologique (*« operationnal model »*) permettant de déterminer l'efficacité de couplage à la protéine G ainsi que l'affinité de l'agoniste pour le récepteur (Kenakin et al., 2012). Ces expériences ont montré que les R-5-HT$_2$ sont couplés de la même façon à la voie de PLC et que la dimérisation n'affecte pas l'activation de cette voie.

Des expériences de liaison montrent que les sites de liaison des R-5-HT$_{2A}$ et des R-5-HT$_{2B}$ sont masqués lorsqu'ils sont co-exprimés avec les R-5-HT$_{2C}$ bien que la production de second messager soit similaire. Ceci indique que l'activation de la voie de la PLC n'est dépendante que des R-5-HT$_{2C}$ lorsque les hétérodimères contiennent un protomère du R-5-HT$_{2C}$. Des études de cytométrie ont permis de montrer que les dimères comprenant les R-5-HT$_{2C}$, les R-5-HT$_{2A}$ ou les R-5-HT$_{2B}$ étaient bien des dimères « stimulables » car présent à la membrane plasmique. Ces observations indiquent donc que, lorsque les R-5-HT$_{2C}$ forment des dimères avec les R-5-HT$_{2A}$ ou les R-5-HT$_{2B}$, la présence des R-5-HT$_{2C}$ cache le site de liaison et empêche l'activation des voies de signalisation des R-5-HT$_{2A}$ et des R-5-HT$_{2B}$ et favorise celle du R-5-HT$_{2C}$.

C. Impact fonctionnel de la dimérisation des R-5-HT$_2$ *in vitro*

Enfin, pour vérifier que ce mécanisme existait aussi *in vivo*, nous avons injecté une construction virale de R-5-HT$_{2C\Delta Cter}$ dans le cortex et mesuré l'expression des R-5-HT$_{2A}$. Nous avons choisi d'injecter la construction de R-5-HT$_{2C}$ dont l'extrémité C-terminale est tronquée car son expression est similaire aux récepteurs intacts mais n'est pas en mesure d'activer la voie de la PLC et donc d'influer sur la signalisation intracellulaire. Cette expérience a montré une diminution apparente de l'expression des R-5-HT$_{2A}$ mais pas des R-5-HT$_{2C}$, comme cela a été observé en culture cellulaire.

Au niveau fonctionnel, l'agoniste des R-5-HT$_2$ (DOI) diminue la fréquence de décharge des neurones sérotoninergique du DRN. Cet effet est aboli chez les animaux 5-HT$_{2A}^{-/-}$ ou par la lésion des neurones noradrénergiques du LC qui projettent sur le DRN. En effet, le blocage des R-5-HT$_{2A}$ dans le LC diminue l'excitabilité des neurones noradrénergiques et donc l'inhibition

du DRN. Nous avons effectué une injection virale de R-5-$HT_{2C\Delta Cter}$ dans le LC afin de voir si la formation de dimères avec les R-5-HT_{2A} pouvait affecter l'action inhibitrice de ce dernier sur le taux de décharge des neurones sérotoninergiques du DRN. Le DOI induit une plus faible inhibition dans le LC lorsque les neurones du DRN sont infectés avec le R-5-$HT_{2C\Delta Cter}$. Suggérant que cet effet est la conséquence de la suppression de l'inhibition des neurones du LC dépendant des R-5-HT_{2A}, par la formation de dimères R-5-$HT_{2C\Delta Cter/2A}$ empêchant l'activité des R-5-HT_{2A}.

D. Conclusion

Cette étude est la première à mettre en évidence que les R-5-HT_2 forment des hétérodimères fonctionnels. Ainsi, que la présence de protomère du R-5-HT_{2C} masque le site de liaison des R-5-HT_{2A} ou des R-5-HT_{2B}. Au niveau fonctionnel, cette dimérisation favorise la signalisation des R-5-HT_{2C} au détriment de celles des R-5-HT_{2A} et R-5-HT_{2B} *in vitro* et *in vivo*. Ceci ouvre de nouvelles perspectives dans la compréhension du fonctionnement des R-5-HT_2 notamment dans les cellules exprimant un ou plusieurs sous-types de R-5-HT_2.

E. Contribution personnelle

Dans cette étude, j'ai effectué les expériences d'accumulation d'IP_3 en réponse à la 5-HT et au DOI. J'ai effectué les analyses en utilisant le modèle mathématique *«operationnal model»* afin de déterminer le couplage aux protéines G. J'ai aussi effectué les expériences de liaisons utilisant la mésulergine tritiée afin de confirmer que le protomère 5-HT_{2C} masque les sites du 5-HT_{2A} ou 5-HT_{2B}.

THE JOURNAL OF BIOLOGICAL CHEMISTRY VOL. 292, NO. 15, pp. 6352–6368, April 14, 2017

Heterodimers of serotonin receptor subtypes 2 are driven by 5-HT_{2C} protomers

Received for publication, January 30, 2017, and in revised form, March 2, 2017 Published, JBC Papers in Press, March 3, 2017, DOI 10.1074/jbc.M117.779041

Imane Moutkine[‡§¶1], Emily Quentin[‡§¶1], Bruno P. Guiard[‖], Luc Maroteaux[‡§¶2], and Stephane Doly[‡‡§§3]**

From the [‡]INSERM UMR-S839, Paris 75005, the [§]Université Pierre et Marie Curie, Paris 75005, the [¶]Institut du Fer à Moulin, Paris 75005, the [**]Institut Cochin, INSERM U1016, CNRS UMR8104, Paris 75014, the [‡‡]Université Paris Descartes, Sorbonne Paris Cité, Paris 75014, the [§§]Université Clermont Auvergne, INSERM, NEURO-DOL, F-63000 Clermont-Ferrand, and the [‖]Research Center on Animal Cognition, Center for Integrative Biology, Université Paul Sabatier, UMR5169 CNRS, 118, Route de Narbonne, 31062, Toulouse Cedex 9, France

Edited by Henrik G. Dohlman

The serotonin receptor subtypes 2 comprise 5-HT_{2A}, 5-HT_{2B}, and 5-HT_{2C}, which are Gα_q-coupled receptors and display distinct pharmacological properties. Although co-expressed in some brain regions and involved in various neurological disorders, their functional interactions have not yet been studied. We report that 5-HT_2 receptors can form homo- and heterodimers when expressed alone or co-expressed in transfected cells. Co-immunoprecipitation and bioluminescence resonance energy transfer studies confirmed that 5-HT_{2C} receptors interact with either 5-HT_{2A} or 5-HT_{2B} receptors. Although heterodimerization with 5-HT_{2C} receptors does not alter 5-HT_{2C} Gα_q-dependent inositol phosphate signaling, 5-HT_{2A} or 5-HT_{2B} receptor-mediated signaling was totally blunted. This feature can be explained by a dominance of 5-HT_{2C} on 5-HT_{2A} and 5-HT_{2B} receptor binding; in 5-HT_{2C}-containing heterodimers, ligands bind and activate the 5-HT_{2C} protomer exclusively. This dominant effect on the associated protomer was also observed in neurons, supporting the physiological relevance of 5-HT_2 receptor heterodimerization *in vivo*. Accordingly, exogenous expression of an inactive form of the 5-HT_{2C} receptor in the locus ceruleus is associated with decreased 5-HT_{2A}-dependent noradrenergic transmission. These data demonstrate that 5-HT_2 receptors can form functionally asymmetric heterodimers *in vitro* and *in vivo* that must be considered when analyzing the physiological or pathophysiological roles of serotonin in tissues where 5-HT_2 receptors are co-expressed.

Many members of the G-protein-coupled receptor (GPCR)[4] family have the capacity to form homo- or hetero-oligomers with biochemical and functional characteristics, including receptor pharmacology, signaling, and regulation, which are unique to these oligomeric conformations. These GPCR oligomers have been found not only to occur within a type of GPCR but also across different families and subtypes (1, 2).

Metabotropic serotonin (5-hydroxytryptamine, 5-HT) subtype 2 receptors (5-HT_2), which belong to the class A-1 GPCR family, display a widespread expression in the nervous system and are involved in an important array of physiological and pathological processes. The 5-HT_2 subfamily consists of three Gα_q/Gα_{11}-coupled receptors, 5-HT_{2A}, 5-HT_{2B}, and 5-HT_{2C}, which mediate excitatory neurotransmission (3). Interestingly, 5-HT_2 subtypes coexist in multiple areas of the brain (4, 5). For example, 5-HT_{2A} and 5-HT_{2C} receptors are co-expressed in GABAergic interneurons and in a subpopulation of pyramidal neurons of the PFC (6–8), in dopaminergic neurons of the ventral tegmental area (9, 10), and 5-HT_{2C} and 5-HT_{2B} receptors are expressed in pro-opiomelanocortin (POMC) neurons of the hypothalamic arcuate nucleus (11). Although 5-HT_2 receptors are similar in structure, there are differences in their pharmacology and signaling outputs (12). It has been reported that 5-HT_{2A} and 5-HT_{2C} receptors can function as stable homodimers (13–16), whereas the existence of 5-HT_{2B} homodimers has not yet been documented. Dimers have also been reported

This work was supported by funds from the Centre National de la Recherche Scientifique, Institut National de la Santé et de la Recherche Médicale, the Université Pierre et Marie Curie, the Université Paris Descartes, grants from the Fondation de France, Fondation pour la Recherche Médicale "Equipe FRM DEQ2014039529," and the French Ministry of Research (Agence Nationale pour la Recherche Grant ANR-12-BSV1-0015-01 and the Investissements d'Avenir Programme Grant ANR-11-IDEX-0004-02). The L. M. team is part of the École des Neurosciences de Paris Ile-de-France network and the Bio-Psy Labex, and as such this work was supported by French state funds managed by the ANR within the Investissements d'Avenir programme under Reference ANR-11-IDEX-0004-02. The authors declare that they have no conflicts of interest with the contents of this article.

[1] Both authors contributed equally to this work.
[2] To whom correspondence may be addressed. E-mail: Luc.maroteaux@upmc.fr.
[3] To whom correspondence may be addressed: Université Clermont Auvergne, INSERM, NEURO-DOL, F-63000 Clermont-Ferrand, France. E-mail: stephane.doly@inserm.fr.

[4] The abbreviations used are: GPCR, G-protein-coupled receptor; LC, locus coeruleus; 5-HT, serotonin, 5-hydroxytryptamine; DOI, (±)-2,5-dimethoxy-4-iodoamphetamine hydrochloride; NDF, nor-(+)-fenfluramine; IP, inositol phosphate; ΔCter, C-terminal deletion; Rluc, *Renilla* luciferase; DSP4, *N*-(2-chloroethyl)-*N*-ethyl-2-bromobenzylamine; RS127445, 2-amino-4-(4-fluoronaphth-1-yl)-6-isopropylpyrimidine hydrochloride; RS102221, 8-[5-(2,4-dimethoxy-5-(4-trifluoromethylphenylsulfonamido)phenyl-5-oxopentyl)]-1,3,8-triazaspiro[4.5]de cane-2,4-dione hydrochloride; SB242084, [6-chloro-5-methyl-1-(6-(2-methylpiridin-3-yloxy)pyridine-3-yl carbamoyl] inodoline dihydrochloride); MDL100907, *R*-(+)-α-(2,3-dimethoxyphenyl)-1-[2-(4-fluorophenylethyl)]-4-piperidine methanol; AAV, adeno-associated virus; IRES, internal ribosome entry site; DR, dorsal raphe; PLC, phospholipase C; BisTris, 2-[bis(2-hydroxyethyl)amino]-2-(hydroxymethyl)propane-1,3-diol; ANOVA, analysis of variance; PFC, prefrontal cortex; POMC, pro-opiomelanocortin; BRET, bioluminescence resonance energy transfer; IP_1, inositol 1-phosphate; IP_2, inositol 4,5-bisphosphate; IP_3, inositol 1,4,5-trisphosphate; LAD, lysergic acid diethylamide; HTRF, homogeneous time-resolved fluorescence; RA, activity ratio.

for other 5-HT receptors, including 5-HT$_{1A}$, 5-HT$_{1B}$, 5-HT$_{1D}$, 5-HT$_4$, and 5-HT$_7$ receptor subtypes in heterologous expression systems (13, 17–20). In addition, there are observations suggesting that the 5-HT$_2$ receptor subfamily can form heterodimeric complexes with other types of GPCRs. For example, the formation of heterodimers has been reported for the 5-HT$_{2A}$ with mGluR2, D$_2$-dopamine, and CB1 receptors (21–23), for 5-HT$_{2C}$ with ghrelin receptors (GHS-R1a) (24) and MT2 receptor (25), for 5-HT$_{1A}$ with μ-opioid (26) and adenosine A$_{2A}$ receptors (27), and for 5-HT$_{2B}$ with angiotensin AT1 receptors (28).

As mentioned above, oligomerization can occur between receptors of different GPCR families (*i.e.* 5-HT and dopamine for example) but also within the same family. A seminal study reported the identification of the first heterodimer between the 5-HT$_{1B}$ and 5-HT$_{1D}$ receptor subtypes (18). However, no significant pharmacological differences were reported between homo- and heterodimers for these closely related 5-HT receptor subtypes. Recently, a study identified other 5-HT receptor heterodimers with functional implication; heterodimers between 5-HT$_{1A}$ and 5-HT$_7$ receptors have been reported to regulate GIRK channel activity in heterologous systems and in hippocampal neurons (29). Heterodimerization was found to inhibit 5-HT$_{1A}$-mediated activation of Gα_i and GIRK channel activity, without affecting 5-HT$_7$ receptor-mediated signaling, indicating a unidirectional dominant effect of the 5-HT$_7$ protomer. Of note, cross-talks between 5-HT receptors have been reported without obligatory physical interaction. For instance, co-expression of the 5-HT$_{1B}$ and 5-HT$_{2B}$ receptors influences the internalization pathways and kinetics of both receptors without heterodimerization (*i.e.* lack of FRET signal) (30).

To date, neither the basic pharmacological profiles of putative 5-HT$_2$ heterodimers nor their signaling properties have been characterized. We specifically addressed this issue here by studying the interactions between the three members of the 5-HT$_2$ subfamily and their functional consequences *in vitro* and *in vivo*. Using co-immunoprecipitation and bioluminescence resonance energy transfer (BRET) approaches, we found that 5-HT$_{2A}$, 5-HT$_{2B}$, and 5-HT$_{2C}$ form heterodimers when co-expressed in heterologous expression systems. Although 5-HT$_{2C}$-containing heterodimers did not show alterations in coupling properties, the signaling of associated 5-HT$_{2A}$ or 5-HT$_{2B}$ protomers was blunted, whereas the 5-HT$_{2C}$ protomer maintained its signaling properties. Moreover, no blunting occurred in 5-HT$_{2A/2B}$ heterodimers. We next showed that this asymmetry in Gα_q protein activation was related to a dominant effect of the 5-HT$_{2C}$ protomer on ligand binding to the other partner. Using AAV-mediated exogenous expression of a 5-HT$_{2C}$ receptor-truncated C-tail mutant (5-HT$_{2C\Delta Cter}$) in brain regions expressing endogenous 5-HT$_{2A}$ receptor, we also observed a blunting effect of this inactive 5-HT$_{2C}$ receptor leading to a complete binding inhibition of the 5-HT$_{2A}$-selective ligand. Accordingly, this lack of ligand binding was associated with impaired 5-HT$_{2A}$-induced excitatory neurotransmission in neurons expressing the 5-HT$_{2C}$-inactive protomer.

Results

Interactions between 5-HT$_2$ receptors

The putative formation of heterodimers between 5-HT$_2$ receptor subtypes was investigated using BRET and co-immunoprecipitation experiments (Fig. 1). The coding region of *Renilla* luciferase (Rluc, BRET donor) or the yellow variant of the green fluorescent protein (YFP, BRET acceptor), were fused in-phase downstream of the coding region of 5-HT$_{2A}$, 5-HT$_{2B}$, and 5-HT$_{2C}$ receptors. Saturation BRET experiments were conducted in HEK293 cells co-transfected with constant amounts of BRET donor plasmids and increasing amounts of BRET acceptor plasmids. In case of a close proximity between the investigated partners, hyperbolic saturation of the BRET signal is expected (see under "Experimental procedures"). Hyperbolic curves were indeed obtained when 5-HT$_{2A}$ or 5-HT$_{2C}$ receptors were tested for self-association (5-HT$_{2A/2A}$ and 5-HT$_{2C/2C}$, respectively, Fig. 1*a*), confirming previous studies showing that these receptors are able to homodimerize in transfected cells (13, 14). Noteworthy, the same experiment with 5-HT$_{2B}$ BRET pairs led to a linear plot, consistent with a bystander (nonspecific) BRET and thus with the absence of self-association. Hyperbolic curves were also obtained with 5-HT$_{2A}$ and 5-HT$_{2C}$ BRET pairs (5-HT$_{2A/2C}$), 5-HT$_{2B}$ and 5-HT$_{2C}$ BRET pairs (5-HT$_{2B/2C}$), and 5-HT$_{2A}$ and 5-HT$_{2B}$ (5-HT$_{2A/2B}$) BRET pairs (Fig. 1*b*), suggesting that 5-HT$_2$ receptors can form heterodimers in intact cells. BRET$_{50}$ values (values of YFP/Rluc for half-maximal BRET) reflect the propensity of association between the investigated proteins. Interestingly, BRET$_{50}$ values for heterodimeric association are significantly lower than those measured for homodimeric association of 5-HT$_2$ subtypes, suggesting that in native cells expressing more than one 5-HT$_2$ receptor subtype heterodimerization is favored over homodimerization (Fig. 1*b*).

The physical interaction between these receptor subtypes was confirmed by co-immunoprecipitation studies in the same cells, using epitope (FLAG)- or GFP-tagged proteins (Fig. 1*c*). Consistent with BRET data, FLAG-5-HT$_{2C}$ receptor co-immunoprecipitated with 5-HT$_{2A}$-GFP and 5-HT$_{2C}$-GFP receptors. In complementary experiments FLAG-5-HT$_{2B}$ receptor co-immunoprecipitated with 5-HT$_{2A}$-GFP and 5-HT$_{2C}$-GFP receptors.

Impact of dimerization of 5-HT$_2$ receptors on signaling

We next examined the consequence of 5-HT$_2$-receptor heterodimerization on agonist-induced Gα_q activation. The 5-HT$_2$ receptors consistently activate the PLC-β pathway in native tissues and heterologous cells (3, 12). We first determined whether 5-HT$_2$ receptor signaling was altered when expressed in the presence of other 5-HT$_2$ receptors (Fig. 2). Dose-response curves of 5-HT$_2$-mediated production of IP in response to 5-HT or the partial agonist DOI in cells expressing 5-HT$_{2A}$, 5-HT$_{2B}$, or 5-HT$_{2C}$ receptors and in combination were analyzed using the operational model (31) to determine the Gα_q coupling efficiency of single receptors and heterodimers (Fig. 2). No significant difference in Gα_q coupling efficiency as determined by the transduction coefficient (τ/K_A) (32) was found among the groups, supporting a lack of major difference

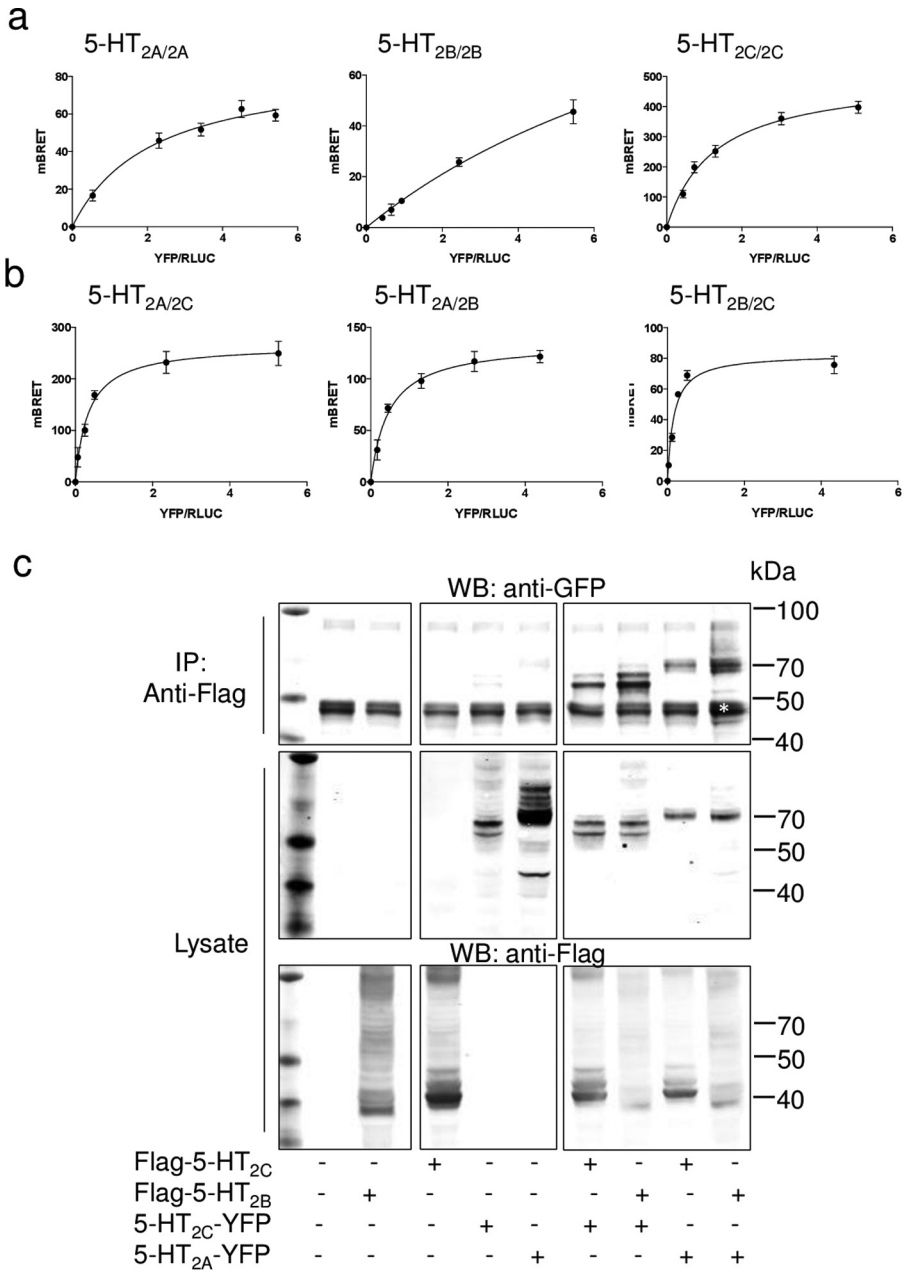

Figure 1. Constitutive heterodimerization of 5-HT$_2$ receptors and co-immunoprecipitation in living HEK293 cells. *a,* BRET proximity assays between homodimers of 5-HT$_{2A}$, 5-HT$_{2B}$, or 5-HT$_{2C}$ receptors. HEK293 cells were co-transfected with plasmids coding for a constant amount of RLuc-5-HT$_{2A}$, RLuc-5-HT$_{2B}$ or RLuc-5-HT$_{2C}$ (BRET donors) and increasing concentrations of the corresponding YFP tagged 5-HT$_2$ homodimer (the BRET acceptor). *b,* BRET proximity assays between heterodimers of 5-HT$_{2A}$, 5-HT$_{2B}$, or 5-HT$_{2C}$ receptors. HEK293 cells were co-transfected with plasmids coding for a constant amount of RLuc-5-HT$_{2A}$, RLuc-5-HT$_{2B}$, or RLuc-5-HT$_{2C}$ (BRET donors) and increasing concentrations of YFP-tagged 5-HT$_2$ heterodimer (the BRET acceptor). For each heterodimers, BRET donor and acceptor were swapped as a control experiment (data not shown). Energy transfer was measured after addition of membrane-permeable luciferase substrate coelenterazine-h. The BRET signal was determined by calculating the ratio of light emitted at 530 nm and that emitted at 485 nm, as described under "Experimental procedures." *Error bars* indicate S.E. of specific BRET-ratio values obtained from triplicate determinations. BRET values (B_{max}, BRET$_{50}$) were obtained from six independent experiments. Plots were established using GraphPad software. 5-HT$_{2A/2A}$: BRET$_{max}$ 76 ± 16, BRET$_{50}$ 2.4 ± 0.5; 5-HT$_{2B/2B}$ ambiguous: 5-HT$_{2C/2C}$: BRET$_{max}$ 434 ± 32, BRET$_{50}$ 1.2 ± 0.4; 5-HT$_{2A/2C}$: BRET$_{max}$ 266 ± 24, BRET$_{50}$ 0.33 ± 0.04; 5-HT$_{2A/2B}$: BRET$_{max}$ 90 ± 32, BRET$_{50}$ 0.19 ± 0.07; 5-HT$_{2B/2C}$: BRET$_{max}$ 85 ± 6, BRET$_{50}$ 0.16 ± 0.04. *c,* interactions of 5-HT$_2$ subtypes in co-immunoprecipitation experiments. COS-7 cells were transfected with various combinations of plasmids coding for 5-HT$_{2A}$-YFP, 5-HT$_{2C}$-YFP, and FLAG epitope-tagged 5-HT$_{2B}$ and 5-HT$_{2C}$, as indicated. Immunoprecipitation with a monoclonal anti-FLAG antibody-coated beads (EZview Red FLAG M2 affinity gel) was performed from 1 mg of protein of cell lysates. The presence of 5-HT$_2$-GFP and 5-HT$_2$-FLAG was revealed with anti-GFP and anti-FLAG antibodies, respectively. 100 μg of protein of cell lysates were analyzed to determine receptor-GFP receptor-FLAG expression (input). *White asterisk,* IgG heavy chain. *WB*, Western blotting; *IP*, immunoprecipitation.

in coupling efficiency between individual 5-HT$_2$ receptors to Gα_q activation and no modification of this coupling efficiency by heterodimers.

In the absence of highly selective, subtype-specific 5-HT$_2$ agonists, we next determined whether agonist-induced 5-HT$_2$ heterodimer signaling was altered in the presence of selective antagonist of the other protomer (Fig. 5). Affinity and selectivity of antagonists were first tested in transfected cells to define the optimal concentration that nearly fully inhibits each individual receptor and to avoid cross-reactivity (100 nM, Fig. 3).

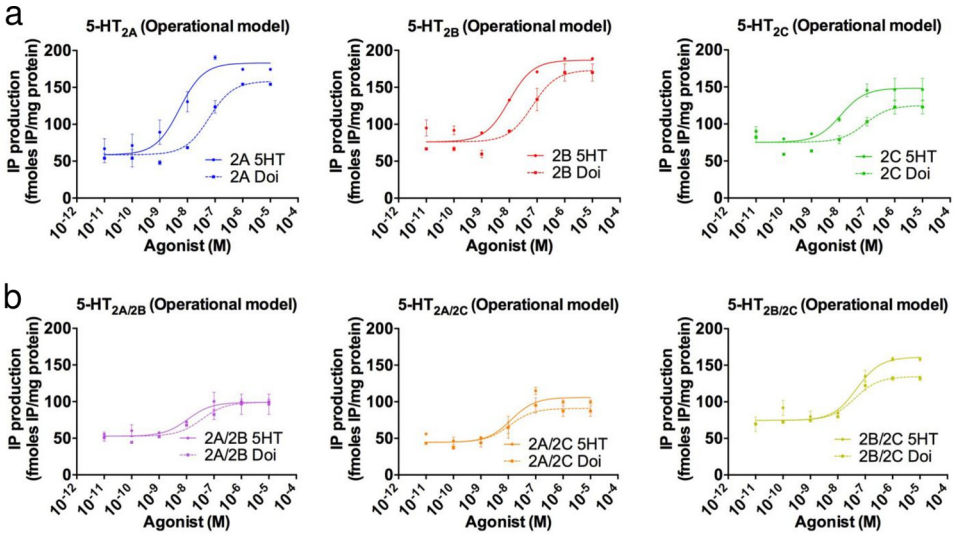

c

Log (τ/K_A)	5-HT$_{2A}$	5-HT$_{2B}$	5-HT$_{2C}$	5-HT$_{2A/2B}$	5-HT$_{2A/2C}$	5-HT$_{2B/2C}$
	-7.11±0.31	-7.58±0.19	-6.69±0.22	-7.30±0.20	-7.26±0.38	-7.22±0.19

Figure 2. IP production induced by stimulation by a full (5-HT) and a partial agonist (DOI). *a,* 5-HT and DOI dose-response curves in single receptor transfections. COS-7 cells transiently expressing 5-HT$_{2A}$, 5-HT$_{2B}$, 5-HT$_{2C}$, and receptor alone, were stimulated with serotonin (5-HT) or DOI, and IP levels were determined. For each condition, stimulation with 5-HT induces full dose-response curve and DOI a partial dose response that can be modelized using the operational model. *b,* 5-HT and DOI dose-response curves in two receptor transfections. COS-7 cells transiently co-expressing 5-HT$_{2A/2B}$, 5-HT$_{2A/2C}$, and 5-HT$_{2B/2C}$ receptors were stimulated with serotonin (5-HT), or DOI and IP levels were determined. These are representative curves of at least four independent experiments performed in duplicate. *c,* dose-response curves allow us to calculate the mean log(τ/K_A), which is not affected by dimerization (one-way ANOVA, $n = 4–5$). Values are given ± S.E.

Dose-response curves of 5-HT$_2$-mediated IP accumulation in response to 5-HT stimulation allowed the determination of the minimal agonist concentration inducing maximal IP response (1 μM, Fig. 4*a*). When expressed individually, 5-HT$_2$ receptors displayed significant 5-HT-stimulated IP production (Fig. 5*a*); in the presence of selective antagonists (MDL100970 for 5-HT$_{2A}$, RS127445 for 5-HT$_{2B}$, and RS102221 for 5-HT$_{2C}$ receptors), the agonist-stimulated IP response was reduced to basal level in cells expressing the cognate 5-HT$_2$ receptor (Fig. 5*a*).

In the 5-HT$_{2A/2B}$ heterodimers, the 5-HT$_{2A}$ receptor contributed to the activation of the Gα_q/PLC-β pathway in response to agonist, as demonstrated by the inhibitory effect of MDL100907 (Fig. 5*a*); reciprocally, the 5-HT$_{2B}$ receptor was also contributing to signaling when co-expressed with 5-HT$_{2A}$ receptors, as demonstrated by the inhibitory effect of RS127445 (Fig. 5*a*). By contrast in the 5-HT$_{2B/2C}$ heterodimers, only the 5-HT$_{2C}$ receptors continued mediating signaling, because blocking selectively the 5-HT$_{2B}$ receptors with RS127445 did not inhibit the 5-HT-mediated IP accumulation (Fig. 5*a*), although it can be blocked only by selective 5-HT$_{2C}$ receptor antagonists RS102221 or SB242084 (Figs. 5*a* and 4, *c* and *d*). The 5-HT$_{2A}$-mediated IP accumulation was similarly blunted by expression of the 5-HT$_{2C}$ receptor, as MDL100907 had no significant inhibitory effect on IP production but RS102221 did (Fig. 5*a*).

The same effect was reproduced for different agonists 5-HT or nor-(+)-fenfluramine (NDF) (Fig. 4, *e* and *f*) and in all tested cell lines, COS-7 (Fig. 2), HEK293 (Figs. 4–5), CHO (Fig. 6*c*), or LMTK (Fig. 6, *a* and *b*), and thus is likely independent of agonists or cell-specific effectors. Because it was shown above that under the same expression conditions these receptor isoforms constitute heterodimers, a plausible explanation for the observed effects is that heterodimerization with 5-HT$_{2C}$ prevents the ability of 5-HT$_{2A}$ or 5-HT$_{2B}$ receptors to signal, whereas in the case of heterodimerization of 5-HT$_{2A}$ with 5-HT$_{2B}$ receptors, both 5-HT$_{2A}$ and 5-HT$_{2B}$ protomers contribute to signal.

These results are consistent with a model where in the 5-HT$_{2A/2C}$ and 5-HT$_{2B/2C}$ heterodimers, only the 5-HT$_{2C}$ protomer couples to the G protein, while preventing coupling of the associated protomer. To investigate this issue, we co-expressed the 5-HT$_{2A}$ or 5-HT$_{2B}$ receptor with a 5-HT$_{2C}$ receptor deleted for the C-terminal tail (5-HT$_{2C\Delta Cter}$) (Fig. 5*b*), a mutant receptor incapable of activating Gα_q and stimulating IP production in response to 5-HT stimulation (Fig. 5*b*). Confirming the hypothesis, in cells expressing 5-HT$_{2A/2C\Delta Cter}$ and 5-HT$_{2B/2C\Delta Cter}$ heterodimers, IP accumulation was dramatically reduced (Fig. 5*b*). In addition, co-expressing 5-HT$_{2C}$ receptors with 5-HT$_{2B\Delta Cter}$, a 5-HT$_{2B}$ receptor similarly deleted for the C-terminal tail and impaired for IP accumulation, had no impact on 5-HT$_{2C}$ signaling (Fig. 5*b*) because it was still sensitive to RS102221, supporting that only the 5-HT$_{2C}$ protomer couples to the G$_q$ protein. We confirmed the proper plasma membrane expression of the 5-HT$_{2C\Delta Cter}$ and 5-HT$_{2B\Delta Cter}$ receptor constructs compared with the respective WT form, using a radioligand binding assay on non-permeabilized cells. Expression of 5-HT$_{2B}$, 5-HT$_{2B\Delta Cter}$, 5-HT$_{2C}$, or 5-HT$_{2C\Delta Cter}$ receptors in HEK cells leads to 37, 50, 20, and 53% of construct surface expression compared with total whole cell membrane expression (permeabilized cells), respectively, suggesting that ΔCter constructs are expressed properly at the cell membrane. Moreover, BRET assay confirms the ability of the two ΔCter

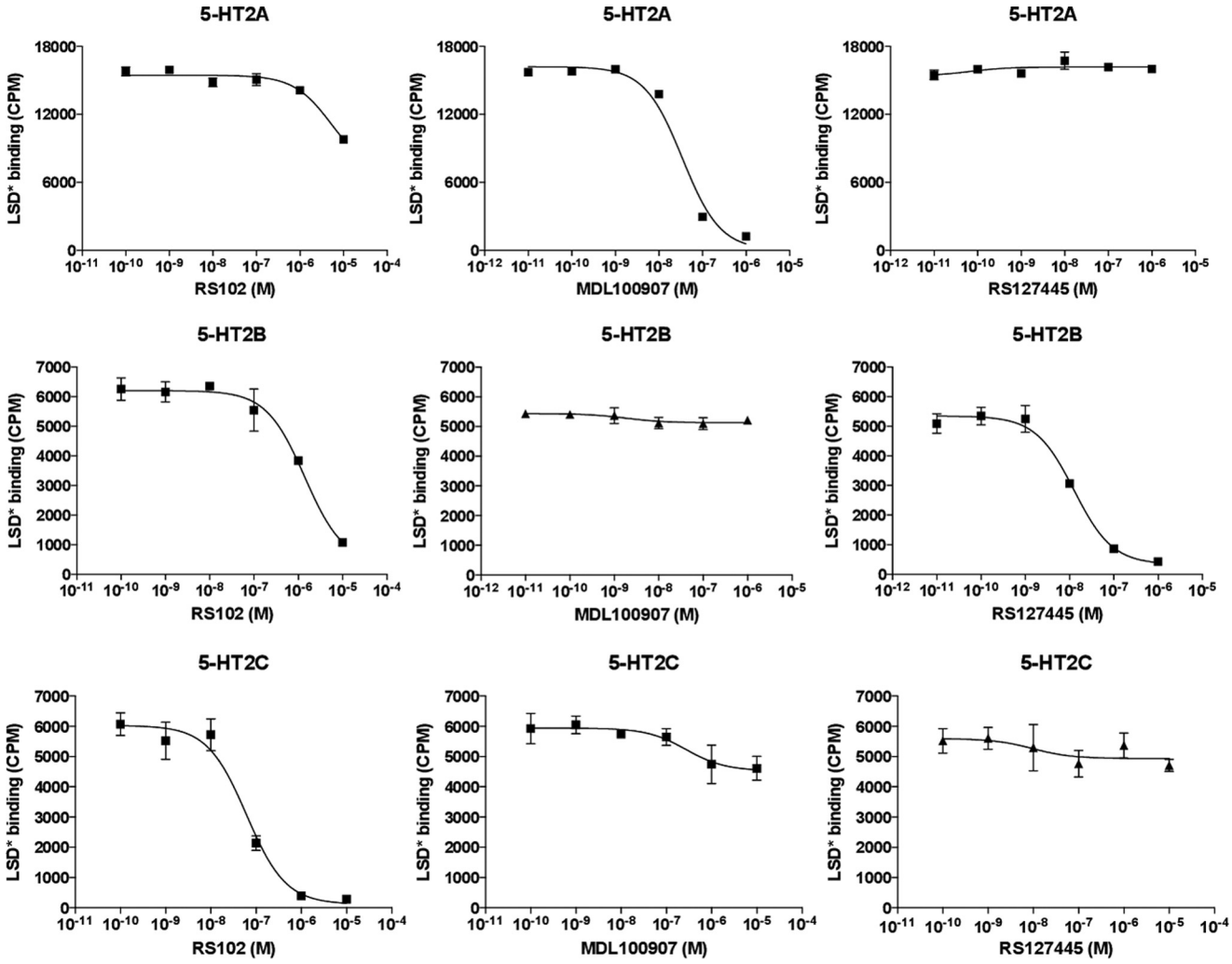

Figure 3. Affinity and selectivity of antagonists used in this study. Affinity and selectivity of antagonists were tested to define the optimal concentration and avoid cross-reactivity. Representative examples of [^{3}H]LSD radioligand binding heterologous competition experiments performed on membrane preparations are shown. HEK293 cells transiently expressing 5-HT$_{2A}$, 5-HT$_{2B}$, or 5-HT$_{2C}$ receptors were incubated with [^{3}H]LSD and increasing concentrations of the 5-HT$_{2A}$ (MDL100907), 5-HT$_{2B}$ (RS127445), and 5-HT$_{2C}$ (RS102221) antagonist. Thus, we used in this study 100 nM concentration for all the antagonists. *Graphs* are representative of one experiment performed in triplicate. *Bars* represent ± S.E. from triplicates. Binding curves were done using GraphPad software.

constructs to associate with 5-HT$_{2A}$, 5-HT$_{2B}$, or 5-HT$_{2C}$ protomers (Fig. 7, *a–d*). To confirm these findings, in cell expressing constant 5-HT$_{2B}$ and variable amounts of 5-HT$_{2C}$ receptors, the progressive decrease of 5-HT$_{2C}$ expression level allowed the recovery of 5-HT$_{2B}$ receptor-dependent signaling (the fraction of IP accumulation inhibited by the 5-HT$_{2B}$-selective RS127445), likely due to reduced formation of 5-HT$_{2B/2C}$ heterodimers (Fig. 7*e*).

Impact of dimerization on 5-HT$_2$ receptor-binding properties

The results above are thus consistent with a model where in the 5-HT$_{2A/2C}$ and 5-HT$_{2B/2C}$ heterodimers, only the 5-HT$_{2C}$ protomer couples to the G$_q$ protein, while preventing ligand binding of the associated protomer. To examine this hypothesis, agonist (5-[^{3}H]HT or [^{3}H]LSD) radioligand binding assays were conducted in the presence or absence of the 5-HT$_{2C}$ receptor and of increasing concentrations of selective antagonists (MDL100907 for 5-HT$_{2A}$, RS127445 for 5-HT$_{2B}$, and RS102221 for 5-HT$_{2C}$) in cells expressing similar quantities of receptors (Fig. 8). RS127445 could compete for 5-[^{3}H]HT (Fig. 8*a*) or [^{3}H]LSD (Fig. 8*c*) binding in cells only expressing 5-HT$_{2B}$ receptors, whereas no competition was observed in cells expressing 5-HT$_{2B/2C}$ receptors. In contrast, RS102221 could displace 5-[^{3}H]HT (Fig. 8*b*) or [^{3}H]LSD (Fig. 8*d*) binding in cells expressing either 5-HT$_{2C}$ receptors alone or 5-HT$_{2B}$/$_{2C}$ receptors. Similar findings were obtained for 5-HT$_{2A}$ receptors (Fig. 8, *e* and *f*). Noteworthy, 5-[^{3}H]HT or [^{3}H]LSD binding was comparable in cells expressing 5-HT$_{2C}$ alone or 5-HT$_{2C}$ receptor and another 5-HT$_2$ isoform, indicating that the presence of 5-HT$_{2C}$ receptors almost completely inhibits ligand binding to co-expressed 5-HT$_{2A}$ and 5-HT$_{2B}$ receptors. Strictly similar findings were observed with the 5-HT$_{2B\Delta Cter}$ receptor (Fig. 8, *g* and *h*) or with radiolabeled antagonist ([^{3}H]mesulergine) binding experiments (Fig. 8, *i–k*) supporting that 5-HT$_{2C}$ protomers somehow masked the ligand-binding site of the other protomer in 5-HT$_2$ heterodimers, independently of the coupling ability of the complex.

A possibility is that the presence of a 5-HT$_{2C}$ protomer is sufficient to compete with plasma membrane accessibility of either 5-HT$_{2A}$ or 5-HT$_{2B}$ protomers. Surface expression of

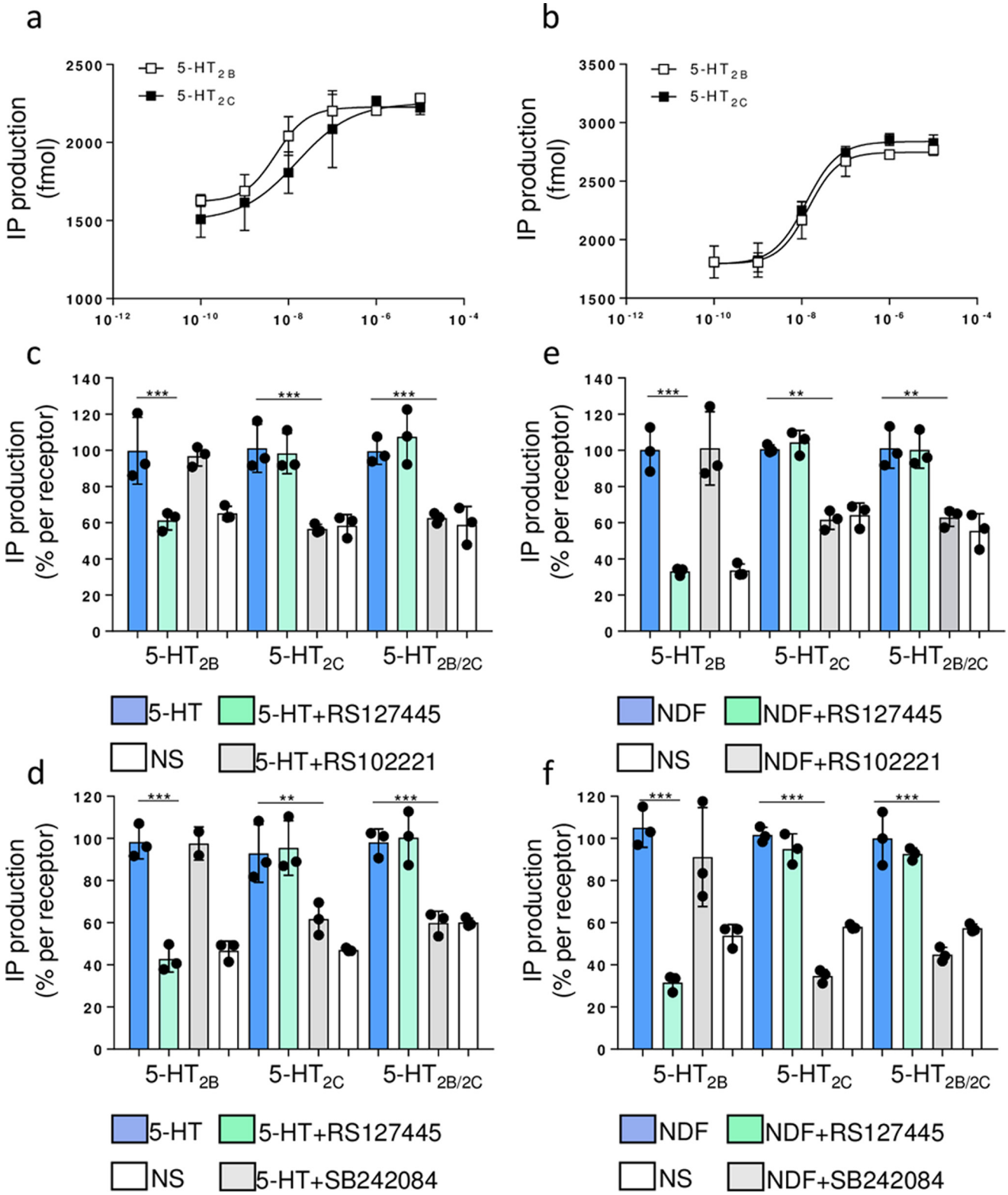

Figure 4. 5-HT$_{2C}$ receptor expression blocks 5-HT$_{2B}$ receptor signaling. *a, b,* agonist concentration-induced IP response. *a,* serotonin (5-HT) (*a*) and NDF (*b*) dose-response curves for stimulation of IP production in cells expressing the same amount of 5-HT$_{2B}$ (*white box*) or 5-HT$_{2C}$ (*dark box*) receptors were used to obtain the minimal agonist concentration-induced maximal IP response (1 μM for both agonists). *Bars* represent ± S.E. from triplicates. *c–f,* HEK293 cells transiently expressing 5-HT$_{2C}$ and 5-HT$_{2B}$ receptor alone or in combination (5-HT$_{2B/2C}$) were stimulated with 1 μM 5-HT$_2$ agonist serotonin (5-HT) or NDF, and IP accumulation was determined. The selective 5-HT$_{2B}$ (RS127445, *green*) or 5-HT$_{2C}$ antagonists RS102221 (*gray*) or SB242084 (*gray*) were co-incubated with agonists. Data are expressed as % of agonist response for each transfected condition. *Bars* represent ± S.D. of three independent experiments. *NS,* non-stimulated. Data were analyzed with one-way ANOVA within each independent transfection and a Bonferroni's multiple comparisons test. ***, $p < 0.005$; **, $p < 0.01$. Specific antagonist treatments were significantly different from 5-HT stimulation.

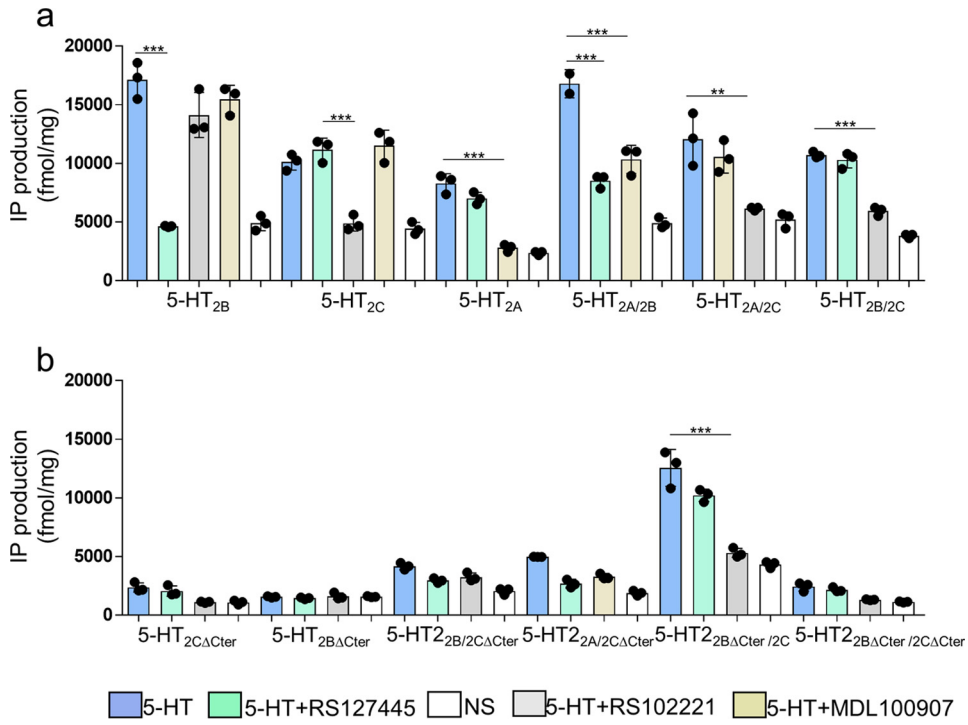

Figure 5. 5-HT$_{2C}$ receptor blunts 5-HT$_{2A}$ and 5-HT$_{2B}$ receptor signaling. HEK293 cells transiently expressing 5-HT$_{2A}$, 5-HT$_{2B}$, 5-HT$_{2C}$, 5-HT$_{2B\Delta Cter}$, and 5-HT$_{2C\Delta Cter}$ receptor, alone or in combination, were stimulated with 1 μM serotonin (5-HT), and IP levels were determined. The selective antagonists (100 nM), 5-HT$_{2B}$ (*green*, RS127445), 5-HT$_{2C}$ (*gray*, RS102221), or 5-HT$_{2A}$ (*brown*, MDL100907) were co-incubated with 5-HT as indicated. *a*, compared with receptors alone, which produce IP accumulation that can be blocked by the respective selective antagonists, IP accumulation can only be blocked by 5-HT$_{2C}$ receptor antagonist but not the 5-HT$_{2A}$ or 5-HT$_{2B}$ receptor antagonist in co-transfection of either 5-HT$_{2A}$ or 5-HT$_{2B}$ with 5-HT$_{2C}$ receptors. *b*, stimulation of 5-HT$_{2B\Delta Cter}$, 5-HT$_{2C\Delta Cter}$, or HT$_{2B\Delta Cter/2C\Delta Cter}$ receptors gives little IP accumulation. Stimulation of 5-HT$_{2A/2C\Delta Cter}$ or HT$_{2B/2C\Delta Cter}$ receptors gives also nearly no IP accumulation, whereas 5-HT$_{2C/2B\Delta Cter}$ leads to IP accumulation that can only be blocked by the 5-HT$_{2C}$ receptor antagonist. *Bars* represent $\pm$ S.D. of three independent experiments. *NS*, non-stimulated. Data were analyzed with one-way ANOVA within each independent transfection and a Bonferroni's multiple comparisons test. ***, $p < 0.005$; **, $p < 0.01$. Specific antagonist treatments are significantly different from 5-HT stimulation.

both receptors was measured by cytometry using a Pacific Blue-conjugated antibody directed against extracellular 3×FLAG-tagged 5-HT$_2$-YFP constructs, with YFP being intracellular and reflecting total expression of the receptor (Fig. 9). The ratio of cell-surface receptors over the total obtained (mean of Pacific Blue signal/mean of GFP) for each condition was normalized as the percentage of 5-HT$_{2A}$ (Fig. 9, *a* and *b*) or 5-HT$_{2B}$ receptor alone. 5-HT$_{2A}$ (Fig. 9*c*) or 5-HT$_{2B}$ (Fig. 9*d*) receptors in cells co-transfected with 5-HT$_{2C}$ receptors were not significantly different compared with control (single expression), although co-expression of 5-HT$_{2A}$ receptors slightly increased cell-surface expression of 5-HT$_{2B}$ receptors. Decreased ligand binding or Gα_q coupling of 5-HT$_{2A}$ or 5-HT$_{2B}$ receptors co-expressed with 5-HT$_{2C}$ receptor cannot be explained by reduced cell-surface expression.

Heterodimer properties in vivo

The inhibitory role of 5-HT$_{2C}$ on 5-HT$_{2A}$ and 5-HT$_{2B}$ receptor binding and coupling was next analyzed in neurons. Mouse prefrontal cortex (PFC) neurons, which have been shown to express 5-HT$_{2A}$ receptors (33, 34), were used as a model system. Accordingly, exogenous 5-HT$_{2C\Delta Cter}$ expression in PFC, upon infection with adeno-associated viruses carrying a 5-HT$_{2C\Delta Cter}$ construct (AAV-5-HT$_{2C\Delta Cter}$), was associated with an increase of [^{3}H]mesulergine able to bind to endogenous 5-HT$_{2A}$ and exogenous 5-HT$_{2C\Delta Cter}$ receptors (Fig. 10*a*). However, a dramatic inhibition of endogenous 5-HT$_{2A}$ receptor-dependent ligand binding compared with AAV-mediated GFP expression was also observed (absence of MDL100907-induced [^{3}H]mesulergine displacement) (Fig. 10*a*). We then investigated whether the 5-HT$_{2C}$ receptor was also able to suppress 5-HT$_{2A}$ receptor-dependent signaling *in vivo* via heterodimerization. We thus used the same adenoviral delivery system to express the inactive 5-HT$_{2C\Delta Cter}$ protomer in adrenergic locus ceruleus (LC) neurons. Previous studies reported that the 5-HT$_2$ receptor agonist DOI decreases the firing rate of 5-HT neurons in the dorsal raphe (DR) nucleus (35, 36). This inhibitory response was completely blunted in 5-*Htr*$_{2A}^{-/-}$ mice and was attenuated (30%) by inducing the loss of noradrenergic neurons with the DSP4 neurotoxin (37). Indeed, activation by DOI of 5-HT$_{2A}$ receptors expressed on GABAergic interneurons of the LC (38, 39) decreased noradrenergic tone thereby limiting its excitatory influence on DR 5-HT neurons. A corollary of these functional interactions between monoaminergic neurons is a significant decrease of DR 5-HT neuronal activity. We then used this paradigm as a functional read-out for norepinephrine transmission upon expression of the functionally inactive 5-HT$_{2C\Delta Cter}$ protomer (Fig. 10, *b–d*). Bilateral stereotaxic injections of AAV-5-HT$_{2C\Delta Cter}$ IRES GFP or AAV GFP in the LC were performed 1 month before *in vivo* electrophysiological recordings of DR 5-HT neurons (Fig. 10*b*). Mouse brains samples were examined to verify the distribution of adenovirus-encoded 5-HT$_{2C\Delta Cter}$ and GFP in the LC (Fig. 10*c*). In mice injected with

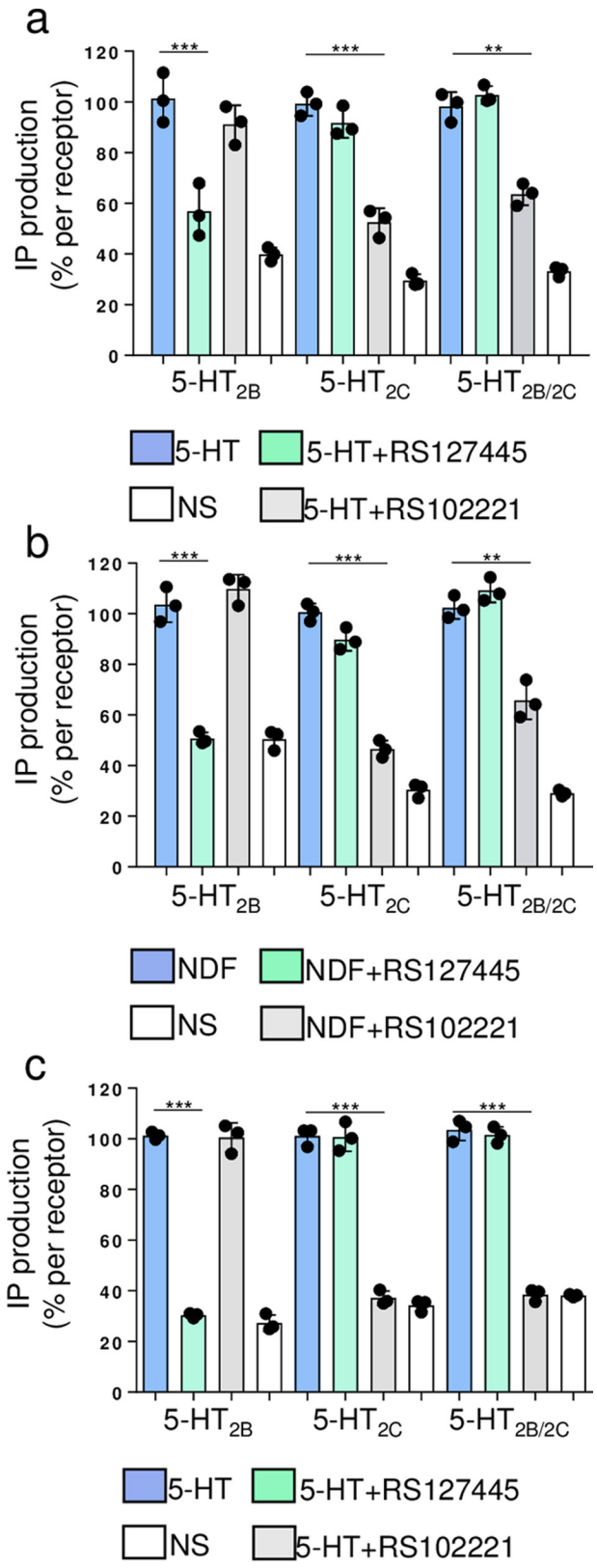

Figure 6. 5-HT$_{2C}$ receptor blunts 5-HT$_{2B}$ receptor signaling independently of the cell types. LMTK$^-$ (*a* and *b*) or CHO (*c*) cells transiently expressing 5-HT$_{2C}$ and 5-HT$_{2B}$ receptor alone or in combination (5-HT$_{2B/2C}$) were stimulated with 1 μM of the 5-HT$_2$ agonist serotonin (*5-HT*) or NDF, and IP accumulation was determined. The selective 5-HT$_{2B}$ (RS127445, *green*) or 5-HT$_{2C}$ antagonists (RS102221, *gray*) were co-incubated with agonist in some conditions, as indicated. Data are expressed as % of maximal agonist response for each transfected condition. *Bars* represent ± S.D. of three independent experiments. *NS*, non-stimulated. Data were analyzed with one-way ANOVA for each graph and a Bonferroni's multiple comparisons test. ***, $p < 0.005$; **, $p < 0.01$. Specific antagonist treatments are significantly different from 5-HT stimulation.

control AAV (AAV GFP), increasing DOI concentrations induced a progressive decrease of the firing rate of DR 5-HT neurons (Fig. 10*d*), as observed by previous reports (37). This inhibitory response was strongly reduced (50%) in AAV-5-HT$_{2C\Delta Cter}$-injected mice (Fig. 10*d*), consistent with an impaired signaling of 5-HT$_{2A}$ receptors. These data indicate that 5-HT$_{2C\Delta Cter}$ receptors inhibit 5-HT$_{2A}$ receptor-mediated signaling in neurons, likely via their heterodimerization with 5-HT$_{2A}$ receptors.

Discussion

Our data demonstrate that 5-HT$_{2A}$, 5-HT$_{2B}$, and 5-HT$_{2C}$ receptors heterodimers are favored and able to form *in vitro* and *in vivo*. Although heterodimerization with 5-HT$_{2C}$ receptors does not apparently modify the coupling ability to the Gα_q pathway, it appears to blunt binding properties of 5-HT$_{2A}$ and 5-HT$_{2B}$ protomers. These findings can be interpreted as uni-directional dominance of 5-HT$_{2C}$ over the two other protomers in 5-HT$_{2A/2C}$ and 5-HT$_{2B/2C}$ heterodimers. The masking effect exerted by the 5-HT$_{2C}$ protomer is specific, because no similar functional consequences could be observed in 5-HT$_{2A/2B}$ heterodimers. This dominance appears to be independent of ligands (agonists or antagonists), of the cell type or of the plasma membrane accessibility of the different protomers.

Uni-directional activating or inhibiting effects of protomers on ligand binding or coupling properties of the cognate partner were reported for few GPCR heterodimers (40). For example, G protein coupling of angiotensin AT1 receptor is inhibited in AT1/AT2 or AT1/APJ (the receptor for apelin) heterodimers (41, 42) but not in AT1/5-HT$_{2B}$ heterodimers (28). In this context, impaired coupling can be caused by different mechanisms. Ligand occupancy of one protomer of the heterodimer can induce conformational changes of the binding pocket of the second protomer resulting in ligand binding inhibition (43). The inhibitory effect of one protomer can also occur in the absence of its ligand. For example, the long C-terminal tail of the orphan receptor GPR50 indirectly prevents the binding of melatonin to the MT1 melatonin receptor in GPR50-MT1 heterodimers (44).

Here, we show that 5-HT$_{2C\Delta Cter}$, which lacks the capacity of activating Gα_q proteins, inhibits both Gα_q coupling and ligand binding of associated 5-HT$_2$ protomers. These data indicate that asymmetric "sequestration" of Gα_q by the C-terminal tail of the 5-HT$_{2C}$ receptor does not account for the observed effect. Consistent with previous observations, showing that a 5-HT$_2$ protomer can promote conformational changes across asymmetrical dimer interface (45, 46), 5-HT$_{2C}$-dependent inhibition of 5-HT$_{2A}$ and 5-HT$_{2B}$ protomer binding might occur via a similar mechanism.

Interestingly, when 5-HT$_{2C}$ receptors were co-expressed with 5-HT$_{2A}$ or 5-HT$_{2B}$ receptors, binding and functional studies indicated the absence of 5-HT$_{2A}$- or 5-HT$_{2B}$-dependent sig-

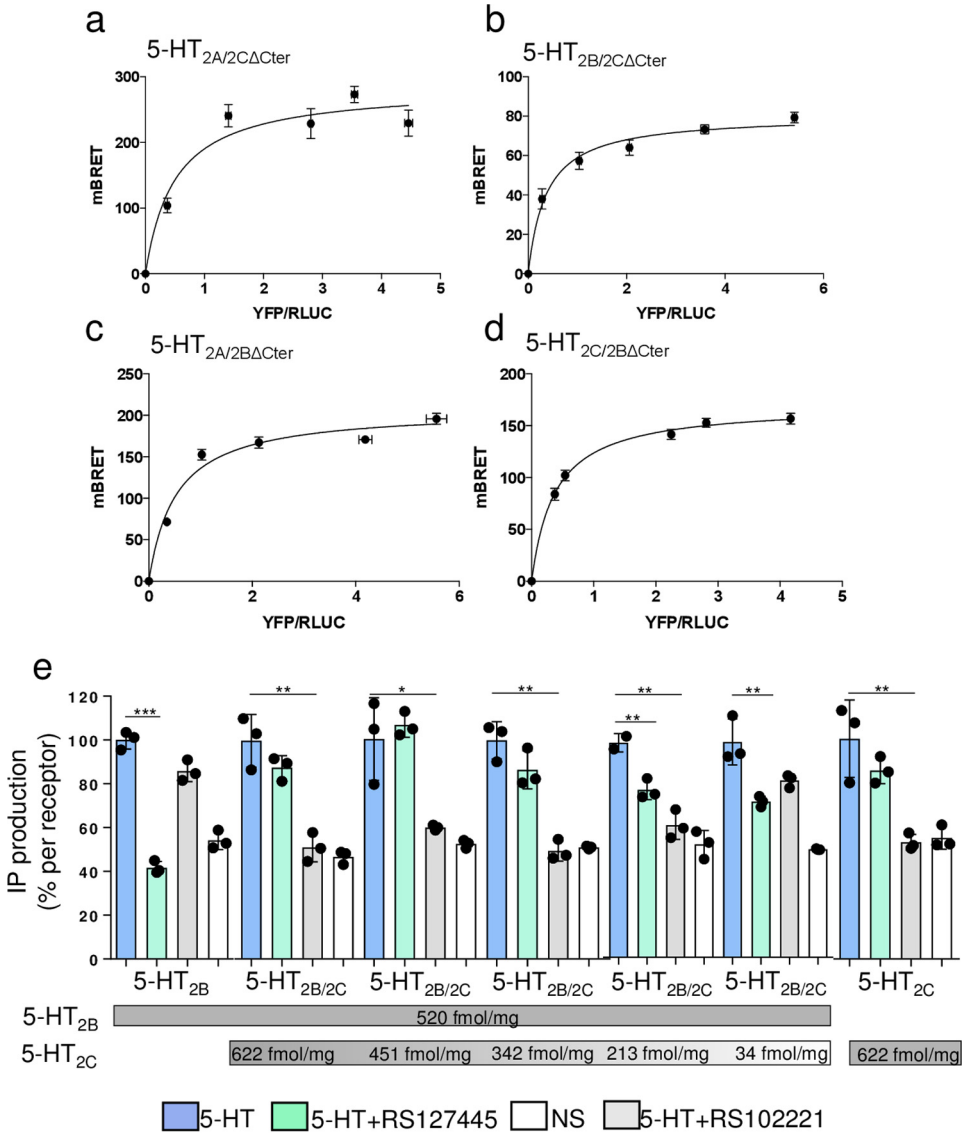

Figure 7. *a–d,* constitutive heterodimerization of 5-HT$_2$ receptors with 5-HT$_{2B\Delta Cter}$ and 5-HT$_{2C\Delta Cter}$ constructs in living HEK293 cells. HEK293 cells were co-transfected with plasmids coding for a constant amount of RLuc-5-HT$_{2A}$, RLuc-5-HT$_{2B}$, or RLuc-5-HT$_{2C}$ (BRET donors) and increasing concentrations of YFP tagged ΔCter constructs (the BRET acceptor). Energy transfer was measured after addition of membrane-permeable luciferase substrate coelenterazine-h. The BRET signal was determined by calculating the ratio of light emitted at 530 nm and that emitted at 485 nm, as described under "Experimental procedures." *Error bars* indicate S.E. of specific BRET-ratio values obtained from triplicate determinations. BRET values (B_{max}, BRET$_{50}$) were obtained from three independent experiments. Plots were established using GraphPad software. *a,* 5-HT$_{2A/2C\Delta Cter}$: BRET$_{max}$ 284 ± 27, BRET$_{50}$ 0.49 ± 0.22; *b,* 5-HT$_{2B/2C\Delta Cter}$: BRET$_{max}$ 80 ± 3, BRET$_{50}$ 0.36 ± 0.07; *c,* 5-HT$_{2A/2B\Delta Cter}$: BRET$_{max}$ 207 ± 12, BRET$_{50}$ 0.52 ± 0.13; *d,* 5-HT$_{2C/2B\Delta Cter}$: BRET$_{max}$ 170.0 ± 2.5, BRET$_{50}$ 0.37 ± 0.02. *e,* dose dependence of 5-HT$_{2C}$ blunting effect. Progressive reduction of the 5-HT$_{2C}$ receptor cDNA transfection (from 5 μg of DNA corresponding to 622 fmol/mg to 0.1 μg of DNA corresponding to 34 fmol/mg, as determined by radioligand binding assay) revealed the sensitivity of IP production to 5-HT$_{2B}$ receptor antagonism (starting from 213 fmol/mg). The 5-HT$_{2B}$ receptor expression was constant for each condition (5 μg of DNA corresponding to 520 fmol/mg). Data are expressed as % of maximal agonist response for each transfected condition. *Bars* represent ±S.D. of three independent experiments. *NS,* non-stimulated. Data were analyzed with one-way ANOVA within each independent transfection and a Bonferroni's multiple comparisons test. *, $p < 0.05$; **, $p < 0.01$; ***, $p < 0.001$: significantly different from 5-HT stimulation.

naling, consistent with the absence of 5-HT$_{2A}$ or 5-HT$_{2B}$ monomers or homodimers at the cell surface. The analysis of BRET$_{50}$ values in saturation BRET experiments, which reflect the propensity of association between protomers, suggests that in cells expressing simultaneously 5-HT$_{2C}$ and another 5-HT$_2$ receptor isoform the heterodimers are more likely to form than homodimers or monomers, and our cytometry analysis revealed that there was no impact of plasma membrane accessibility of 5-HT$_2$ receptor protomers.

Although many reports addressing the capacity of GPCRs to form heterodimeric complexes were based on investigations performed in transfected cells, only a few studies could document the existence and the functional significance of these complexes *in vivo* (21, 29, 47). Here, we show that the expression of exogenous 5-HT$_{2C\Delta Cter}$ receptors in PFC is associated with a dramatic inhibition of 5-HT$_{2A}$ receptor-dependent ligand binding, suggesting that both receptors are able to form heterodimers *in vivo*. Accordingly, we found that virus-mediated exogenous expression of the inactive protomer 5-HT$_{2C\Delta Cter}$ reduces 5-HT$_{2A}$ receptor-dependent neuronal inhibition of DR 5-HT neurons. Altogether, these results support that 5-HT$_{2C}$ receptors are able to form functional

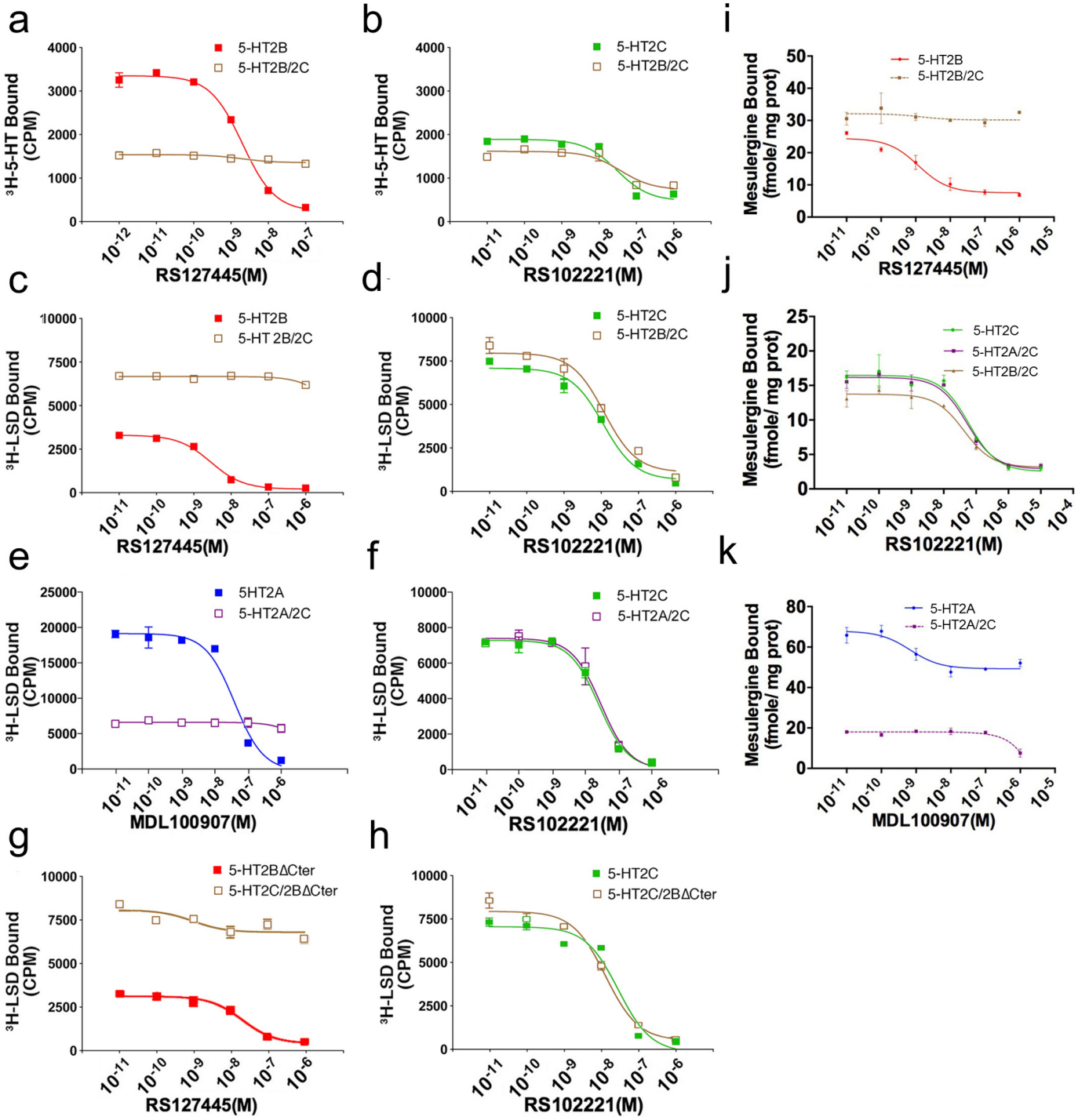

Figure 8. Co-expression of 5-HT$_{2C}$ receptors blunts 5-HT$_{2A}$ and 5-HT$_{2B}$ ligand binding. Transiently transfected cells were incubated with 5-[^{3}H]HT (*a* and *b*); [^{3}H]LSD (*c–h*); or [^{3}H]mesulergine and increasing concentrations of the 5-HT$_{2A}$ or 5-HT$_{2B}$ antagonist or 5-HT$_{2C}$ antagonist (*i–k*). *a* and *b*, 5-HT$_{2C}$ receptor transfection with 5-HT$_{2B}$ receptors abolishes the 5-[^{3}H]HT competition by 5-HT$_{2B}$ antagonist. *c–f*, 5-HT$_{2C}$ receptor transfection with 5-HT$_{2A}$ or 5-HT$_{2B}$ receptors abolishes the [^{3}H]LSD competition by 5-HT$_{2A}$ or 5-HT$_{2B}$ antagonists. *g* and *h*, 5-HT$_{2C}$ receptor transfection with 5-HT$_{2B\Delta Cter}$ receptors abolishes the [^{3}H]LSD competition by the 5-HT$_{2B}$ antagonist but not the 5-HT$_{2C}$ antagonist. *i–k*, 5-HT$_{2C}$ receptor transfection with 5-HT$_{2A}$ or 5-HT$_{2B}$ receptors abolishes the [^{3}H]mesulergine competition by 5-HT$_{2A}$ or 5-HT$_{2B}$ antagonists. These are representative curves of at least three independent experiments performed in duplicate, and *error bars* indicate S.E.

heterodimers with 5-HT$_{2A}$ or 5-HT$_{2B}$ receptors when co-expressed in neurons and pinpoint the physiological relevance of a putative switch in the pharmacological profile of these neurons, depending on 5-HT$_{2C}$ expression levels.

In line with this hypothesis, a recent study showed that high phenotypic motor impulsivity was associated with a diminished PFC 5-HT$_{2A}$·5-HT$_{2C}$ receptor complex (8). Independent findings about 5-HT$_{1A}$·5-HT$_7$ heterodimers (29) demonstrated that heterodimerization markedly decreases the ability of the 5-HT$_{1A}$ receptor to activate G-protein in hippocampal neurons. Interestingly, because 5-HT$_7$ receptor expression decreases during postnatal development, the concentration of

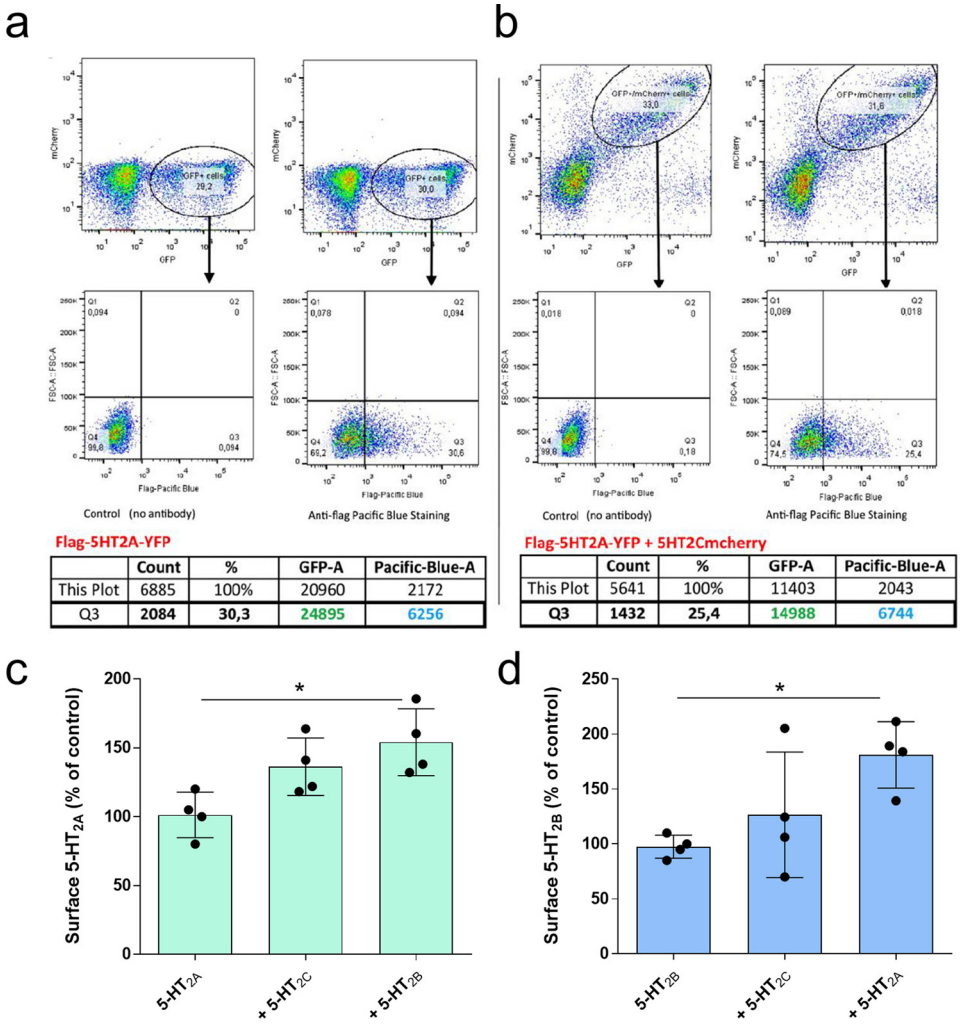

Flag-5HT2A-YFP	Count	%	GFP-A	Pacific-Blue-A
This Plot	6885	100%	20960	2172
Q3	2084	30,3	24895	6256

Flag-5HT2A-YFP + 5HT2Cmcherry	Count	%	GFP-A	Pacific-Blue-A
This Plot	5641	100%	11403	2043
Q3	1432	25,4	14988	6744

Figure 9. Receptor cell-surface export of 5-HT$_{2A}$ and 5-HT$_{2B}$ receptors is not affected by the co-expression with the 5-HT$_{2C}$ protomer. Surface 5-HT$_{2A}$ or 5-HT$_{2B}$ receptors in YFP-Cherry positive non-permeabilized cells were quantified by cytometry using anti-FLAG primary antibody conjugated to Pacific Blue dye. *a* and *b*, example of cell population analyzed for 5-HT$_{2A}$ receptor GFP and 5-HT$_{2C}$ receptor mCherry expression. Double-transfected cells (GFP$^+$/mCherry$^+$) were selected. FLAG-Pacific Blue staining (surface receptor expression) was analyzed on GFP$^+$/mCherry$^+$ cells. *Q3* shows % of Pacific Blue-positive cells. Ratio of cell-surface receptors over total were obtained (mean of Pacific Blue signal/mean of GFP) for each condition and normalized as percentage of 5-HT$_{2A}$ or 5-HT$_{2B}$ receptor alone (single transfection). *c*, FLAG-5-HT$_{2A}$-YFP alone or co-expressed with 5-HT$_{2B}$-Cherry or 5-HT$_{2C}$-Cherry. *d*, FLAG-5-HT$_{2B}$-YFP alone or co-expressed with 5-HT$_{2A}$-Cherry or 5-HT$_{2C}$-Cherry. Cell-surface 5-HT$_{2A}$ and 5-HT$_{2B}$ expression is shown by the histograms: *bars* indicate S.D. from three independent experiments. Data were analyzed with one-way ANOVA and a Bonferroni's multiple comparison test. *, $p < 0.05$ significantly different from control (receptor alone).

heterodimers and their functional significance should change over time. Similarly, it has been demonstrated that the expression of the 5-HT$_{2A}$ and 5-HT$_{2C}$ receptors varied during prenatal and early postnatal development (48), which represents a critical period for synaptogenesis and synaptic refinement (49). The 5-HT$_{2C}$ receptor is transiently expressed in the cortices from P10 to P28, whereas the 5-HT$_{2A}$ receptor expression increases progressively from P3 to P21, reaching the adult level. During the early postnatal period, pyramidal cells of layer V of the prefrontal cortex are profoundly depolarized by 5-HT, an effect that is mediated by the activation of the 5-HT$_{2A}$ receptor. However, 5-HT$_{2A}$ receptor-induced depolarization declines with increasing age (50, 51). In light of our results, 5-HT may progressively bind to the 5-HT$_{2C}$ protomer leading to a switch in signaling pathway activation and downstream membrane depolarization.

The operational model revealed no significant differences in the coupling ability to the Gα_q pathway between membranes expressing 5-HT$_2$ receptors alone and membranes expressing 5-HT$_2$ heterodimers. However, heterodimerization may affect the 5-HT$_2$ receptors signaling in many other ways; in addition to the activation of Gα_q, G$\alpha_{i/o}$, or G$\alpha_{12/13}$ proteins, activation of phospholipase A$_2$, and phospholipase D (ERK1/2 or β-arrestin-dependent pathways) (52, 53) can be mediated by 5-HT$_2$ receptors. All these pathways could be differentially affected by heterodimers. Interacting proteins like PSD-95, MUPP-1, and RSK2 (54) on 5-HT$_{2A}$ and 5-HT$_{2B}$ receptors might have also been affected by the dimerization with the 5-HT$_{2C}$ receptor. For example, the 5-HT$_{2C}$ and 5-HT$_{2B}$ receptors co-expressed in POMC neurons of the arcuate nucleus (11) are involved in feeding behavior but are not necessarily dependent on G$_q$ coupling. Additional studies on other signaling pathways should be performed to ascertain putative changes in 5-HT signaling associated with heterodimerization.

Another consequence of the dominant effect of the 5-HT$_{2C}$ receptor is a putative misleading link between pharmacological

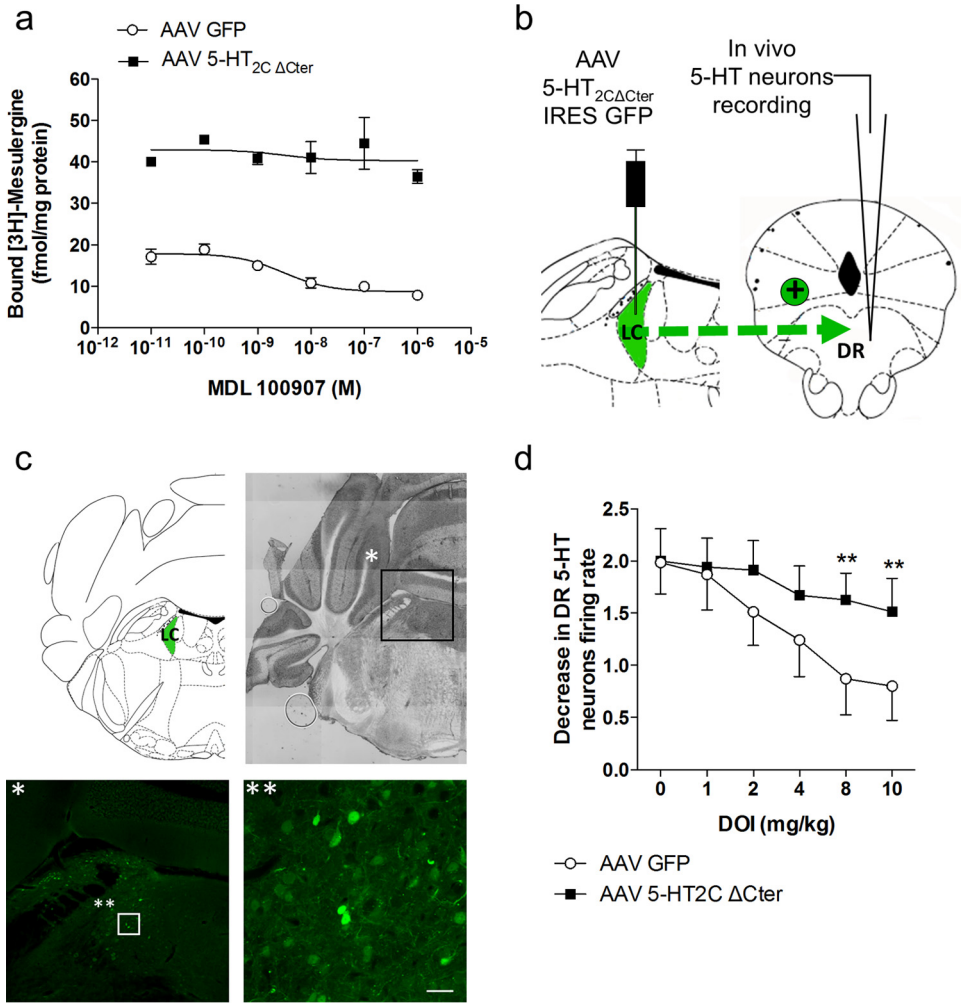

Figure 10. 5-HT$_{2C\Delta Cter}$-inactive protomer prevents 5-HT$_{2A}$ ligand binding in the PFC and reduces DOI-induced 5-HT$_{2A}$ receptor-dependent decrease of 5-HT neuron-firing rate. *a,* exogenous 5-HT$_{2C\Delta Cter}$ expression in PFC, upon bilateral infection with adeno-associated viruses carrying a 5-HT$_{2C\Delta Cter}$ construct (AAV-5-HT$_{2C\Delta Cter}$), was associated with a dramatic reduction of endogenous 5-HT$_{2A}$-dependent ligand binding compared with AAV-mediated GFP expression only. Representative example of [^{3}H]mesulergine binding (heterologous competition displacement with a selective 5-HT$_{2A}$ antagonist MDL100907) experiments performed on membrane preparation from one PFC. *Bars* represent ± S.E. from triplicates. Binding curve was done using GraphPad software. *b,* WT mice were bilaterally injected with AAV 5-HT$_{2C\Delta Cter}$ IRES GFP in the LC sending excitatory projections (*green arrow*) into the DR nucleus as shown in the diagram. After a 1-month recovery and transgene expression, *in vivo* recording of serotonin (5-HT) neurons in the DR was done. *c,* mouse brains were examined to verify the distribution of adenovirus-encoded 5-HT$_{2C\Delta Cter}$ and GFP in the LC. Fluorescence imaging of GFP in LC neurons is shown at increasing magnifications. The boxed * and ** correspond to magnified areas (*black* and *white square*). *d,* effect of the 5-HT$_{2A}$ receptor agonist DOI on the firing rate of DR 5-HT neurons in WT mice. DOI was administered using a cumulative dosing regimen, *i.e.* all mice received 1, 2, 4, 8, and 10 mg/kg (s.c.) with a 3-min interval between each injection. Data are presented as means ± S.E. of basal firing rate in mice injected with the control AAV (*open circle*) or AAV 5-HT$_{2C\Delta Cter}$ (*dark square*) ($n = 7$ mice per group). Data were analyzed with two-way ANOVA and a Bonferroni's multiple comparison test. **, $p < 0.01$: significantly different from sham AAV control-injected mice. *Scale bars,* 20 μm.

brain mapping expression and function of 5-HT$_2$ receptors. For example, in the *Globus pallidus*, the expression of 5-HT$_{2A}$ receptors, revealed by immunolabeling, had previously gone unnoticed due to absent or weak ligand binding. The 5-HT$_{2A}$ receptor immunostaining of the amygdala complex and in Purkinje cells of the cerebellum (55, 56) was also inconsistent with negative radioligand binding results previously reported (5, 57, 58). The reason for this expression discrepancy is unclear, but knowing that all these nuclei also express 5-HT$_{2C}$ receptors (4–6, 55, 59), a plausible explanation would be a pharmacological shielding of 5-HT$_{2A}$ by 5-HT$_{2C}$ receptors, without consequence for the immunocytochemistry detection. More importantly, pharmacological studies targeting 5-HT$_{2A}$ or 5-HT$_{2B}$ receptors in a physiological or a pathological context, like schizophrenia, food intake disorders, or depression, should take into account this dominant effect when brain areas of interest (*i.e.* frontal cortex, hypothalamus, or raphe nucleus, respectively) also express 5-HT$_{2C}$ receptors (8, 11, 47, 60, 61). This could lead to a misinterpretation of experimental results due to a mismatch between the consistent expression of 5-HT$_{2A}$ or 5-HT$_{2B}$ receptor in a particular nucleus, dedicated to a specific physiological function, and a lack of effect of selective pharmacological compounds. The putative formation of these heterodimers must now be taken into account when analyzing the physiological and/or pathophysiological role of 5-HT in tissues co-expressing 5-HT$_{2C}$/5-HT$_{2A}$ or 5-HT$_{2C}$/5-HT$_{2B}$ receptors.

Experimental procedures

Animals

Male mice (8–12 weeks old) used in these experiments are in a 129S2/SvPAS background (Charles River, France). Animals

were housed in groups of 3–5 per cage. The temperature was maintained at 21 ± 1 °C, under 12:12 h light/dark. Food for laboratory mice (SAFE A03, France; 3200 kcal/kg, moisture 12%, proteins 21%, lipids 5%, carbohydrates 52%, fibers 4%, and mineral ash 6%) and water were available *ad libitum*. Electrophysiological recording and animal care were conducted in accordance with the standard ethical guidelines ("Guide for the Care and Use of Laboratory Animals" from the National Institutes of Health and the European Communities Council European Communities Directive 86/609 EEC). All experiments involving mice were approved by the local ethical committee (number 1170.01).

Plasmid constructs

Human 5-HT$_{2A}$, 5-HT$_{2B}$, 5-HT$_{2CINI}$ receptor cDNAs were subcloned into the p513 vector, a derivative of the pSG5 mammalian expression vector (62), which replicates in SV40 T antigen-expressing cells and drives 5-HT receptor expression under the control of the SV40 early promoter. The C terminus truncated after amino acid 370 for the human 5-HT$_{2C}$ and amino acid 393 for the human 5-HT$_{2B}$ receptors (63) was generated by PCR deletion mutagenesis. 5-HT receptor-coding regions were amplified from their respective cDNAs using appropriate sense and antisense primers. The fragments were then subcloned in-frame in either a plasmid encoding C-terminal YFP (Clontech and BD Biosciences), N-terminal FLAG (Clontech and BD Biosciences), or Rluc. The coding regions of all constructs were entirely sequenced.

Cloning of mouse 5-HT$_{2C}$ receptor cDNA

From the full-length cDNA sequence of 5-HT$_{2CVNV}$ and 5-HT$_{VNI}$ receptors from mice that we previously reported (60), we selected the VNV-edited isoforms of 5-HT$_{2C}$ receptor for AAV injections, as VNV has been shown to be the most prevalent in C57BL/6J and 129S1/SvImJ mice (64). The C terminus of the mouse 5-HT$_{2CVNV}$ was truncated after amino acid 370.

Cell culture

COS-7, HEK293, LMTK$^-$, and CHO cells were cultured as monolayers in Dulbecco's modified Eagle's medium (DMEM) (Gibco, Invitrogen) supplemented with 10% fetal calf serum (Biowest) and 1% penicillin/streptomycin (Sigma), in 9-cm dishes (Falcon). Cells were incubated at 37 °C in a 5% CO_2 atmosphere. Cells were 80% confluent when transfected with 10 μg of DNA using nanofectin (PAA), according to the manufacturer's protocol, in an antibiotic-free medium. Four hours later, medium was replaced with fresh medium. Twenty four hours after transfection, cells were incubated in serum-free medium for membrane radioligand binding or trypsinized (trypsin 1× 0.05% EDTA, Invitrogen) and plated onto 24-well plates for IP accumulation.

AAV-mediated local LC or PFC 5-HT$_{2C\Delta Cter}$ expression

Adeno-associated virus (AAV9)-expressing GFP (7.5×10^{12} virus molecules/ml) and 5-HT$_{2C\Delta Cter}$ (IRES) GFP (8.8×10^{12} virus molecules/ml) under the control of the synapsin promoter (UNC Vector Core, Dr. R. Jude Samulski, Chapel Hill, NC) were stereotaxically injected into the LC (100 nl) or the PFC (600 nl). Mice were anesthetized with ketamine (50 mg/kg) and xylazine (2 mg/kg) and fixed in a stereotaxic apparatus. A burr hole was drilled above the LC (coordinates: 5.4 mm posterior to bregma, 1 lateral to midline) or the PFC (coordinates: 1.8 mm anterior to bregma, 2 lateral to midline). Stereotaxically guided injections were made through the hole in the dorsal surface of the cranium (3 mm deep for the LC and 1 mm for the PFC). Glass capillary tubes were pulled (HEKA pipette puller PIP5) and tips broken to 40-μm diameters. After 4 weeks of recovery and viral expression, the LC and PFC AAV-injected mice were used for electrophysiological or binding experiments, respectively. Proper viral infection was verified by GFP detection on brain-fixed sections.

In vivo electrophysiology of DR 5-HT neurons

Mice were anesthetized with chloral hydrate (400 m/kg; i.p.) and mounted in a stereotaxic frame. Additional anesthesia (50–100 mg/kg; i.p.) was given as necessary to maintain a full anesthetic state, characterized by the absence of response to a tail pinch. Body temperature was maintained at 37 °C throughout the experiments using a thermistor-controlled heating pad (Astro-Med, Elancourt, France). The extracellular recordings of the 5-HT neurons in the DR were performed using single-barreled glass micropipettes (Stoelting, Dublin, Ireland) pulled on a pipette puller (Narishige, Tokyo, Japan) preloaded with a 2 M NaCl solution. Their impedance typically ranged between 2.5 and 5 megohms. The single-barreled glass micropipettes were positioned 0.2–0.5 mm posterior to the interaural line on the midline and lowered using a hydraulic micropositioner (Kopf Instruments) into the DR, usually attained at a depth between 2.5 and 3.5 mm from the brain surface. To increase the signal-to-noise ratio, we used a current amplifier (BAK Electronics, Mount Airy, MD) connected to the active filter Humbug (Quest Scientific, DIPSI, Châtillon, France). The presumed DR 5-HT neurons were then identified according to the criteria of Aghajanian and Vandermaelen (65), *i.e.* a slow (0.5–2.5 Hz) and regular firing rate and long-duration (2–5 ms) bi- or triphasic extracellular waveform. Neuronal activity was recorded in real time using Spike2 software (Cambridge Electronic Design, Cambridge, UK), which was also used to analyze neurons off line. For all dose-response curves, only one neuron was recorded and tested from each animal.

^{3}H-radioligands and drugs

myo-[^{3}H]Inositol (51.0 Ci/mmol), [^{3}H]mesulergine (99 Ci/mmol), 5-[^{3}H]hydroxytryptamine (80.0 Ci/mmol), and [^{3}H]lysergic acid diethylamide (50.0 Ci/mmol) were purchased from PerkinElmer Life Sciences. (+)-Norfenfluramine hydrochloride (Sigma, France), RS127445 (Tocris), SB242084 (Sigma), 5-HT, DOI, mesulergine hydrochloride (Tocris), MDL100907 (Tocris), RS102221 (Tocris), and SB242084 (Tocris) were dissolved in DMSO as stock solution (1 mg/ml).

[^{3}H]IP accumulation assay

Twenty four hours before the experiment, cells were incubated in 24-well plates overnight with 20 nM *myo*-[^{3}H]inositol diluted in an inositol-free medium (BME, Lonza, Basel, Switzerland). Just before receptor stimulation, medium was

replaced by Krebs-Ringer/Hepes buffer (130 mM NaCl, 1.3 mM KCl, 2.2 mM $CaCl_2$, 1.2 mM NaH_2PO_4, 1.2 mM $MgSO_4$, 10 mM Hepes, 10 mM glucose, pH 7.4) supplemented with 20 mM LiCl to prevent IP_1 degradation. Cells were stimulated in duplicate in a final volume of 500 μl for 2 h. The experiment was stopped by replacing the stimulation medium with 10^{-3} M formic acid at room temperature for 20 min and at 4 °C overnight. Thus, IP_1 accumulated from IP_3 and IP_2 hydrolysis was released from lysed and fixed cells. The accumulated IP_1 was eluted on anion exchange columns (AG-1X8, Bio-Rad) with 0.2 M ammonium formate in 0.1 M formic acid. Scintillation mixture (Ultima Gold XR, PerkinElmer Life Sciences) was added to the eluted [^{3}H]IP sample, and radioactivity was counted in a Beckman Coulter scintillation counter. At least three independent experiments were performed in triplicate.

HTRF IP accumulation

COS-7 cells were transfected with 3 μg of DNA (1:1 ratio for co-transfection) in 6-well plates using Genjuice transfectant reagent in complete medium. Twenty four hours later the cells were trypsinized (trypsin 1× 0.05% EDTA; Invitrogen) and plated in 96-well plates (30,000 cells/well). The next day, complete medium was replaced by serum-free medium. The day of the experiment, media were replaced by stimulation buffer with LiCl to prevent IP_1 degradation (NaCl 146 mM, KCl 4.2 mM, $MgCl_2$ 0.5 mM, $CaCl_2$ 1 mM, Hepes 10 mM, glucose 5.5 mM, LiCl 50 mM, pH 7.4). Cells were stimulated during 2 h at 37 °C with a different concentration of full and partial agonists, 5-HT and DOI, respectively (10^{-11} to 10^{-6} M in stimulation buffer). Stimulation solution was replaced by lysis buffer (IP one HTRF Kit, Cisbio, France) during 1 h. Lysates were distributed to 384-well plates, and IP was labeled using HTRF reagents. The assay is based on a competitive format involving a specific antibody labeled with terbium cryptate (donor) and IP coupled to d_2 (acceptor). After a 1-h incubation with HTRF reagent, the plate was read using Mithras LB940 plate reader according to the manufacturer's instructions. At least five independent experiments were performed in duplicate.

Operational model

Data obtain in HTRF were transformed in femtomoles of IP per mg of protein per well using a standard dose-response curve. An operational model first described by Black and Leff in 1983 (31) was used to calculate coupling efficiency of each receptor in each condition for full (5-HT) and partial (DOI) agonists. This model allowed us to determine whether the dimerization could affect the coupling efficiency of the complex to the Gα_q/phospholipase C (PLC)/IP pathway. The power of a ligand to activate a specific cellular pathway is represented by the τ/K_A or RA (activity ratio). These values are extracted from the description of Model 1 and Equation 1,

$$\text{response A} = [A]^n\tau^n Em/[A]^n\tau^n + ([\text{A}] + K_A)^n$$

Model 1

where E_m is maximal response; n is slope; K_A is equilibrium constant dissociation of the agonist-receptor complex or affinity; τ is efficacy.

$$\text{RA} = \tau^n((2 + \tau^n)^{1/n} - 1)\,E_m/K_A(1 + t^n) \qquad \text{(Eq. 1)}$$

The operational model conditions show that for dose-response curves of unit slope ($n = 1$), it can be seen that RA reduces to the term E_m (τ/K_A). Ratios of these terms for particular agonists cancel the E_m term and are therefore system-independent. A theoretically complete term to describe the power of a ligand to active a cellular pathway is τ/K_A, which incorporates both elements of efficacy and affinity. Considering that the most common difference between systems is receptor density, ratios of τ/K_A account for these and are system-independent measures of the relative capacity of ligands to activate a specific pathway.

Radioligand binding assays on PFC

PFC freshly dissected from mouse brain was homogenized with 50 ml of ice-cold buffer per g of wet tissue containing 50 mM Tris and 5 mM $MgCl_2$, pH 7.4. The homogenate was centrifuged for 20 min at 15,000 × *g*. The pellet was resuspended and centrifuged under the same condition three times. Membrane preparations were resuspended in binding buffer to obtain a final concentration of 1 mg of protein/well. Radioligand binding assays were set up in a 96-well plate (1.2 ml/well capacity) using 5 nM [^{3}H]mesulergine (PerkinElmer Life Sciences) and increasing concentrations of MDL100907 for 60 min at room temperature. [^{3}H]Mesulergine ligand choice was based on the selective 5-HT$_2$ receptor-binding properties. This allows for the simultaneous measurement of 5-HT$_{2A}$ and 5-HT$_{2C}$ receptor expression, using the specific cold antagonists.

Membrane radioligand binding assay

Membrane binding assays were performed on transfected cells plated in 10-cm dishes. Cells were first washed with PBS, scraped into 10 ml of PBS on ice, and then centrifuged for 5 min at 1000 × *g*. Cell pellets were dissociated and lysed in 2 ml of binding buffer (50 mM Tris-HCl, 10 mM $MgCl_2$, 0.1 mM EDTA, pH 7.4) and centrifuged for 30 min at 10,000 × *g*. Membrane preparations were then resuspended in binding buffer to obtain a final concentration of 0.2–0.4 mg of protein/well. Aliquots of membrane suspension (200 μl/well) were incubated with 25 μl/well of ^{3}H-radioligand at a final concentration near the K_D value, diluted in binding buffer and 25 μl/well of increasing concentrations of homologous or heterologous compound (from 10^{-11} to 10^{-5} M, diluted in binding buffer) in 96-well plates for 60 min at room temperature. Membranes were harvested by rapid filtration onto Whatman GF/B glass fiber filters (Brandell) pre-soaked with cold saline solution and washed three times with cold saline solution to reduce nonspecific binding. Filters were placed in 6-ml scintillation vials and allowed to dry overnight. The next day, 4 ml of scintillation mixture were added to the samples, which were counted as before. Data in disintegrations/min were converted to femtomoles and normalized to protein content (ranging from 0.1 to 1 mg/well). At least three independent experiments were performed in duplicate.

Non-permeabilized whole cell radioligand binding assay

Cells expressing 5-HT$_{2B}$, 5-HT$_{2B\Delta Cter}$, 5-HT$_{2C}$, or 5-HT$_{2C\Delta Cter}$ receptors were plated in 24-well clusters. Twenty four hours

before the experiment, the cells were incubated in serum-free medium overnight. The next day, the medium was replaced by 400 μl/well of Krebs-Ringer/Hepes buffer (130 mM NaCl, 1.3 mM KCl, 2.2 mM $CaCl_2$, 1.2 mM NaH_2PO_4, 1.2 mM $MgSO_4$, 10 mM Hepes, 10 mM glucose, pH 7.4). Then, 50 μl of [^{3}H]mesulergine were diluted in Krebs-Ringer/Hepes buffer at a final concentration between half the K_d and the K_d for each 5-HT receptor. The radioligand was competed with 50 μl of increasing concentrations of non-radioactive ligand, also diluted in Krebs-Ringer/Hepes buffer. Cells were then incubated for 30 min at room temperature and then washed twice on ice with cold PBS. Washed cells were solubilized by the addition of 500 μl of SDS 1%. The next day, 4 ml of scintillation mixture were added to the samples, and the radioactivity was counted using a scintillation counter (Beckman Coulter). Data in disintegrations/min were converted to femtomoles and normalized to protein content (0.2–0.4 mg of protein/well). At least three independent experiments were performed in duplicate.

Co-immunoprecipitation

FLAG-tagged 5-HT$_{2B}$ and 5-HT$_{2C}$ receptor cDNA constructs were transfected in COS-7 cells with various combinations of YFP-tagged 5-HT$_2$ receptors. After 48 h, cells were washed in PBS, sonicated, and solubilized in lysis buffer (75 mM Tris, 2 mM EDTA, 12 mM $MgCl_2$, 10 mM CHAPS, protease inhibitor mixture EDTA free, pH 7.4) during 12 h at 4 °C. Lysates were centrifuged at 12,000 $\times$ *g* during 30 min at 4 °C. Immunoprecipitations were performed using EZview Red FLAG M2 affinity gel (Sigma) according to the manufacturer's recommendations. Immunoprecipitated proteins and 100 μg of total proteins were combined with Laemmli buffer, heated at 70 °C for 10 min, and run on 10% BisTris gel. Immunoblots were probed with rabbit anti-GFP (Abcam) or anti-FLAG rabbit (Sigma) antibodies diluted 1:2000, and immunoreactivity was revealed using secondary antibody coupled to 680-nm fluorophores using the Odyssey LI-COR infrared fluorescent scanner.

BRET assays

BRET assays were performed according to published methods (66). Briefly, HEK cells (5×10^5 per well of a 6-well plates) were transfected with 30–100 ng of plasmid DNA coding for the BRET donor (5-HT$_2$-Luc) and increasing amounts of BRET acceptor plasmids (5-HT$_2$-YFP; 100–4000 ng per well). Twenty four hours after transfection, cells were washed in PBS, detached using 10 mM EDTA in PBS, centrifuged (1400 $\times$ *g* for 5 min), resuspended in Hanks'-balanced salt solution, and distributed in 96-well plates (PerkinElmer Life Sciences plates; 10^5 cells per well). After addition of the luciferase substrate, coelenterazine-h (5 μM final concentration), luminescence, and fluorescence were measured simultaneously (at 485 and 530 nm, respectively) in a Mithras LB940 plate reader. The BRET ratio was calculated as ((emission at 530 nm/emission at 485 nm) − (background at 530 nm/background at 485 nm)), where background corresponds to signals in cells expressing the Rluc fusion protein alone under the same experimental conditions. For better readability, results were expressed in milli-BRET units (mBRET), with 1 mBRET corresponding to the BRET ratio multiplied by 1000. BRET ratios were plotted as a function of ((YFP − YFP0)/YFP0)/(Rluc/Rluc0), where YFP is the fluorescence signal at 530 nm after excitation at 485 nm, and Rluc is the signal at 485 nm after addition of coelenterazine-h. YFP0 and Rluc0 correspond to the same values in cells expressing the Rluc fusion protein alone.

Receptor cell-surface export analysis

To study the putative impact of 5-HT$_{2C}$ receptor co-expression on 5-HT$_{2A}$ or 5-HT$_{2B}$ receptor targeting at the cell surface, COS-7 cells were transiently co-transfected with 5-HT$_{2C}$-mCherry or 5-HT$_{2A}$-mCherry and a construct coding for 5-HT$_{2A}$ or 5-HT$_{2B}$ displaying the FLAG epitope at the N terminus and fused C-terminally to the YFP. Empty vector, p513, was used to maintain identically the total amount of transfected DNA. 48 h after transfection, cells were harvested, washed in PBS, and fixed in 4% paraformaldehyde. The expression of each receptor was assessed by measuring GFP and mCherry fluorescence using a Miltenyi MacsQuant VYB cytometer. These determinations allowed us to quantify the amount of single-transfected cells (less than 5%) of double-transfected cells (60%) and show that these values are identical whatever the combination of transfected receptors. To determine cell surface 5-HT$_{2A}$ or 5-HT$_{2B}$ expression, cell aliquots were stained with a primary antibody directed against the extracellular FLAG epitope conjugated to Pacific Blue dye (Cell Signaling) following the manufacturer's protocol. Pacific Blue and YFP signals correspond to surface and total FLAG-5-HT$_2$-YFP receptors. Cells expressing both GFP and mCherry were analyzed for Pacific Blue signal. Ratio of cell-surface receptors over total were obtained (mean of Pacific Blue signal/mean of GFP) for each condition and normalized as percentage of 5-HT$_{2A}$ or 5-HT$_{2B}$ receptor alone (single transfection), see Doly *et al.* (67).

Data analysis

Binding data were analyzed using the iterative non-linear regression model (GraphPad Prism 6.0). This allowed the calculation of inhibition constants (K_i) and the maximal number of sites (B_{max}). All values represent the average of independent experiments ± S.E. (n = number of experiments as indicated in the text).

Statistics

Comparisons between groups were performed using Student's unpaired *t* test, or one- or two-way ANOVA with Bonferroni's post hoc test were used depending on the experiment. Significance was set at $p < 0.05$ receptors.

Author contributions—S. D. and L. M. participated in research design. S. D., B. G., E. Q., and I. M. conducted the experiments. S. D., B. G., E. Q., and I. M. performed data analysis. S. D. and L. M. wrote or contributed to the writing of the manuscript.

Acknowledgment—We thank Dr. Stefano Marullo for helpful discussions and advice on BRET experiments.

References

1. Ferré, S., Baler, R., Bouvier, M., Caron, M. G., Devi, L. A., Durroux, T., Fuxe, K., George, S. R., Javitch, J. A., Lohse, M. J., Mackie, K., Milligan, G.,

Pfleger, K. D., Pin, J. P., Volkow, N. D., *et al.* (2009) Building a new conceptual framework for receptor heteromers. *Nat. Chem. Biol.* **5,** 131–134
2. Bulenger, S., Marullo, S., and Bouvier, M. (2005) Emerging role of homo- and heterodimerization in G-protein-coupled receptor biosynthesis and maturation. *Trends Pharmacol. Sci.* **26,** 131–137
3. Millan, M. J., Marin, P., Bockaert, J., and Mannoury la Cour, C. (2008) Signaling at G-protein-coupled serotonin receptors: recent advances and future research directions. *Trends Pharmacol. Sci.* **29,** 454–464
4. Bonhaus, D. W., Bach, C., DeSouza, A., Salazar, F. H., Matsuoka, B. D., Zuppan, P., Chan, H. W., and Eglen, R. M. (1995) The pharmacology and distribution of human 5-hydroxytryptamine 2B (5-HT2B) receptor gene products: comparison with 5-HT2A and 5-HT2C receptors. *Br. J. Pharmacol.* **115,** 622–628
5. Pompeiano, M., Palacios, J. M., and Mengod, G. (1994) Distribution of the serotonin 5-HT2 receptor family mRNAs: comparison between 5-HT2A and 5-HT2C receptors. *Brain Res. Mol. Brain Res.* **23,** 163–178
6. Carr, D. B., Cooper, D. C., Ulrich, S. L., Spruston, N., and Surmeier, D. J. (2002) Serotonin receptor activation inhibits sodium current and dendritic excitability in prefrontal cortex via a protein kinase C-dependent mechanism. *J. Neurosci.* **22,** 6846–6855
7. Nocjar, C., Alex, K. D., Sonneborn, A., Abbas, A. I., Roth, B. L., and Pehek, E. A. (2015) Serotonin-2C and -2a receptor co-expression on cells in the rat medial prefrontal cortex. *Neuroscience* **297,** 22–37
8. Anastasio, N. C., Stutz, S. J., Fink, L. H., Swinford-Jackson, S. E., Sears, R. M., DiLeone, R. J., Rice, K. C., Moeller, F. G., and Cunningham, K. A. (2015) Serotonin (5-HT) 5-HT2A receptor (5-HT2AR):5-HT2CR imbalance in medial prefrontal cortex associates with motor impulsivity. *ACS Chem. Neurosci.* **6,** 1248–1258
9. Bubar, M. J., Stutz, S. J., and Cunningham, K. A. (2011) 5-HT(2C) receptors localize to dopamine and GABA neurons in the rat mesoaccumbens pathway. *PLoS ONE* **6,** e20508
10. Esposito, E. (2006) Serotonin-dopamine interaction as a focus of novel antidepressant drugs. *Curr. Drug Targets* **7,** 177–185
11. Yadav, V. K., Oury, F., Suda, N., Liu, Z. W., Gao, X. B., Confavreux, C., Klemenhagen, K. C., Tanaka, K. F., Gingrich, J. A., Guo, X. E., Tecott, L. H., Mann, J. J., Hen, R., Horvath, T. L., and Karsenty, G. (2009) A serotonin-dependent mechanism explains the leptin regulation of bone mass, appetite, and energy expenditure. *Cell* **138,** 976–989
12. Raymond, J. R., Mukhin, Y. V., Gelasco, A., Turner, J., Collinsworth, G., Gettys, T. W., Grewal, J. S., and Garnovskaya, M. N. (2001) Multiplicity of mechanisms of serotonin receptor signal transduction. *Pharmacol. Ther.* **92,** 179–212
13. Brea, J., Castro, M., Giraldo, J., López-Giménez, J. F., Padín, J. F., Quintián, F., Cadavid, M. I., Vilaró, M. T., Mengod, G., Berg, K. A., Clarke, W. P., Vilardaga, J. P., Milligan, G., and Loza, M. I. (2009) Evidence for distinct antagonist-revealed functional states of 5-hydroxytryptamine(2A) receptor homodimers. *Mol. Pharmacol.* **75,** 1380–1391
14. Herrick-Davis, K., Grinde, E., Harrigan, T. J., and Mazurkiewicz, J. E. (2005) Inhibition of serotonin 5-hydroxytryptamine2c receptor function through heterodimerization: receptor dimers bind two molecules of ligand and one G-protein. *J. Biol. Chem.* **280,** 40144–40151
15. Herrick-Davis, K., Grinde, E., Lindsley, T., Teitler, M., Mancia, F., Cowan, A., and Mazurkiewicz, J. E. (2015) Native serotonin 5-HT2C receptors are expressed as homodimers on the apical surface of choroid plexus epithelial cells. *Mol. Pharmacol.* **87,** 660–673
16. Herrick-Davis, K., Grinde, E., Lindsley, T., Cowan, A., and Mazurkiewicz, J. E. (2012) Oligomer size of the serotonin 5-hydroxytryptamine 2C (5-HT2C) receptor revealed by fluorescence correlation spectroscopy with photon counting histogram analysis: evidence for homodimers without monomers or tetramers. *J. Biol. Chem.* **287,** 23604–23614
17. Berthouze, M., Ayoub, M., Russo, O., Rivail, L., Sicsic, S., Fischmeister, R., Berque-Bestel, I., Jockers, R., and Lezoualc'h, F. (2005) Constitutive dimerization of human serotonin 5-HT4 receptors in living cells. *FEBS Lett.* **579,** 2973–2980
18. Xie, Z., Lee, S. P., O'Dowd, B. F., and George, S. R. (1999) Serotonin 5-HT1B and 5-HT1D receptors form homodimers when expressed alone and heterodimers when co-expressed. *FEBS Lett.* **456,** 63–67
19. Smith, C., Toohey, N., Knight, J. A., Klein, M. T., and Teitler, M. (2011) Risperidone-induced inactivation and clozapine-induced reactivation of rat cortical astrocyte 5-hydroxytryptamine(7) receptors: evidence for *in situ* G protein-coupled receptor homodimer protomer cross-talk. *Mol. Pharmacol.* **79,** 318–325
20. Pellissier, L. P., Barthet, G., Gaven, F., Cassier, E., Trinquet, E., Pin, J. P., Marin, P., Dumuis, A., Bockaert, J., Banères, J. L., and Claeysen, S. (2011) G protein activation by serotonin type 4 receptor dimers: evidence that turning on two protomers is more efficient. *J. Biol. Chem.* **286,** 9985–9997
21. Albizu, L., Holloway, T., González-Maeso, J., and Sealfon, S. C. (2011) Functional crosstalk and heteromerization of serotonin 5-HT2A and dopamine D2 receptors. *Neuropharmacology* **61,** 770–777
22. Moreno, J. L., Muguruza, C., Umali, A., Mortillo, S., Holloway, T., Pilar-Cuéllar, F., Mocci, G., Seto, J., Callado, L. F., Neve, R. L., Milligan, G., Sealfon, S. C., López-Giménez, J. F., Meana, J. J., Benson, D. L., and González-Maeso, J. (2012) Identification of three residues essential for 5-hydroxytryptamine 2A-metabotropic glutamate 2 (5-HT2A.mGlu2) receptor heteromerization and its psychoactive behavioral function. *J. Biol. Chem.* **287,** 44301–44319
23. Viñals, X., Moreno, E., Lanfumey, L., Cordomí, A., Pastor, A., de La Torre, R., Gasperini, P., Navarro, G., Howell, L. A., Pardo, L., Lluís, C., Canela, E. I., McCormick, P. J., Maldonado, R., and Robledo, P. (2015) Cognitive impairment induced by Δ9-tetrahydrocannabinol occurs through heteromers between cannabinoid CB1 and serotonin 5-HT2A receptors. *PLoS Biol.* **13,** e1002194
24. Schellekens, H., van Oeffelen, W. E., Dinan, T. G., and Cryan, J. F. (2013) Promiscuous dimerization of the growth hormone secretagogue receptor (GHS-R1a) attenuates ghrelin-mediated signaling. *J. Biol. Chem.* **288,** 181–191
25. Kamal, M., Gbahou, F., Guillaume, J. L., Daulat, A. M., Benleulmi-Chaachoua, A., Luka, M., Chen, P., Kalbasi Anaraki, D., Baroncini, M., Mannoury la Cour, C., Millan, M. J., Prevot, V., Delagrange, P., and Jockers, R. (2015) Convergence of melatonin and serotonin (5-HT) signaling at MT2/5-HT2C receptor heteromers. *J. Biol. Chem.* **290,** 11537–11546
26. Cussac, D., Rauly-Lestienne, I., Heusler, P., Finana, F., Cathala, C., Bernois, S., and De Vries, L. (2012) μ-Opioid and 5-HT1A receptors heterodimerize and show signalling crosstalk via G protein and MAP-kinase pathways. *Cell. Signal.* **24,** 1648–1657
27. Łukasiewicz, S., Błasiak, E., Faron-Górecka, A., Polit, A., Tworzydło, M., Górecki, A., Wasylewski, Z., and Dziedzicka-Wasylewska, M. (2007) Fluorescence studies of homooligomerization of adenosine A2A and serotonin 5-HT1A receptors reveal the specificity of receptor interactions in the plasma membrane. *Pharmacol. Rep.* **59,** 379–392
28. Jaffré, F., Bonnin, P., Callebert, J., Debbabi, H., Setola, V., Doly, S., Monassier, L., Mettauer, B., Blaxall, B. C., Launay, J. M., and Maroteaux, L. (2009) Serotonin and angiotensin receptors in cardiac fibroblasts coregulate adrenergic-dependent cardiac hypertrophy. *Circ. Res.* **104,** 113–123
29. Renner, U., Zeug, A., Woehler, A., Niebert, M., Dityatev, A., Dityateva, G., Gorinski, N., Guseva, D., Abdel-Galil, D., Fröhlich, M., Döring, F., Wischmeyer, E., Richter, D. W., Neher, E., and Ponimaskin, E. G. (2012) Heterodimerization of serotonin receptors 5-HT1A and 5-HT7 differentially regulates receptor signalling and trafficking. *J. Cell Sci.* **125,** 2486–2499
30. Janoshazi, A., Deraet, M., Callebert, J., Setola, V., Guenther, S., Saubamea, B., Manivet, P., Launay, J. M., and Maroteaux, L. (2007) Modified receptor internalization upon coexpression of 5-HT1B receptor and 5-HT2B receptors. *Mol. Pharmacol.* **71,** 1463–1474
31. Black, J. W., and Leff, P. (1983) Operational models of pharmacological agonism. *Proc. R. Soc. Lond. B Biol. Sci.* **220,** 141–162
32. Kenakin, T., Watson, C., Muniz-Medina, V., Christopoulos, A., and Novick, S. (2012) A simple method for quantifying functional selectivity and agonist bias. *ACS Chem. Neurosci.* **3,** 193–203
33. Doly, S., Madeira, A., Fischer, J., Brisorgueil, M. J., Daval, G., Bernard, R., Vergé, D., and Conrath, M. (2004) The 5-HT2A receptor is widely distributed in the rat spinal cord and mainly localized at the plasma membrane of postsynaptic neurons. *J. Comp. Neurol.* **472,** 496–511
34. Cornea-Hébert, V., Riad, M., Wu, C., Singh, S. K., and Descarries, L. (1999) Cellular and subcellular distribution of the serotonin 5-HT2A receptor in the central nervous system of adult rat. *J. Comp. Neurol.* **409,** 187–209

35. Boothman, L. J., and Sharp, T. (2005) A role for midbrain raphe γ-aminobutyric acid neurons in 5-hydroxytryptamine feedback control. *Neuroreport* **16,** 891–896
36. Bortolozzi, A., and Artigas, F. (2003) Control of 5-hydroxytryptamine release in the dorsal raphe nucleus by the noradrenergic system in rat brain. Role of α-adrenoceptors. *Neuropsychopharmacology* **28,** 421–434
37. Quesseveur, G., Reperant, C., David, D. J., Gardier, A. M., Sanchez, C., and Guiard, B. P. (2013) 5-HT(2)A receptor inactivation potentiates the acute antidepressant-like activity of escitalopram: involvement of the noradrenergic system. *Exp. Br. Res.* **226,** 285–295
38. Szabo, S. T., and Blier, P. (2001) Functional and pharmacological characterization of the modulatory role of serotonin on the firing activity of locus coeruleus norepinephrine neurons. *Brain Res.* **922,** 9–20
39. Szabo, S. T., and Blier, P. (2002) Effects of serotonin (5-hydroxytryptamine, 5-HT) reuptake inhibition plus 5-HT(2A) receptor antagonism on the firing activity of norepinephrine neurons. *J. Pharmacol. Exp. Ther.* **302,** 983–991
40. Maurice, P., Kamal, M., and Jockers, R. (2011) Asymmetry of GPCR oligomers supports their functional relevance. *Trends Pharmacol. Sci.* **32,** 514–520
41. Siddiquee, K., Hampton, J., McAnally, D., May, L., and Smith, L. (2013) The apelin receptor inhibits the angiotensin II type 1 receptor via allosteric trans-inhibition. *Br. J. Pharmacol.* **168,** 1104–1117
42. AbdAlla, S., Lother, H., Abdel-tawab, A. M., and Quitterer, U. (2001) The angiotensin II AT2 receptor is an AT1 receptor antagonist. *J. Biol. Chem.* **276,** 39721–39726
43. Jastrzebska, B. (2013) GPCR: G protein complexes–the fundamental signaling assembly. *Amino Acids* **45,** 1303–1314
44. Levoye, A., Dam, J., Ayoub, M. A., Guillaume, J. L., Couturier, C., Delagrange, P., and Jockers, R. (2006) The orphan GPR50 receptor specifically inhibits MT1 melatonin receptor function through heterodimerization. *EMBO J.* **25,** 3012–3023
45. Herrick-Davis, K. (2013) Functional significance of serotonin receptor dimerization. *Exp. Br. Res.* **230,** 375–386
46. Mancia, F., Assur, Z., Herman, A. G., Siegel, R., and Hendrickson, W. A. (2008) Ligand sensitivity in dimeric associations of the serotonin 5HT2c receptor. *EMBO Rep.* **9,** 363–369
47. Fribourg, M., Moreno, J. L., Holloway, T., Provasi, D., Baki, L., Mahajan, R., Park, G., Adney, S. K., Hatcher, C., Eltit, J. M., Ruta, J. D., Albizu, L., Li, Z., Umali, A., Shim, J., *et al.* (2011) Decoding the signaling of a GPCR heteromeric complex reveals a unifying mechanism of action of antipsychotic drugs. *Cell* **147,** 1011–1023
48. Li, Q. H., Nakadate, K., Tanaka-Nakadate, S., Nakatsuka, D., Cui, Y., and Watanabe, Y. (2004) Unique expression patterns of 5-HT2A and 5-HT2C receptors in the rat brain during postnatal development: Western blot and immunohistochemical analyses. *J. Comp. Neurol.* **469,** 128–140
49. Gaspar, P., Cases, O., and Maroteaux, L. (2003) The developmental role of serotonin: news from mouse molecular genetics. *Nat. Rev. Neurosci.* **4,** 1002–1012
50. Béïque, J. C., Campbell, B., Perring, P., Hamblin, M. W., Walker, P., Mladenovic, L., and Andrade, R. (2004) Serotonergic regulation of membrane potential in developing rat prefrontal cortex: coordinated expression of 5-hydroxytryptamine (5-HT)1A, 5-HT2A, and 5-HT7 receptors. *J. Neurosci.* **24,** 4807–4817
51. Béïque, J. C., Chapin-Penick, E. M., Mladenovic, L., and Andrade, R. (2004) Serotonergic facilitation of synaptic activity in the developing rat prefrontal cortex. *J. Physiol.* **556,** 739–754
52. Wacker, D., Wang, C., Katritch, V., Han, G. W., Huang, X. P., Vardy, E., McCorvy, J. D., Jiang, Y., Chu, M., Siu, F. Y., Liu, W., Xu, H. E., Cherezov, V., Roth, B. L., and Stevens, R. C. (2013) Structural features for functional selectivity at serotonin receptors. *Science* **340,** 615–619
53. Bohn, L. M., and Schmid, C. L. (2010) Serotonin receptor signaling and regulation via β-arrestins. *Crit. Rev. Biochem. Mol. Biol.* **45,** 555–566
54. Roth, B. L. (2011) Irving Page Lecture: 5-HT(2A) serotonin receptor biology: interacting proteins, kinases and paradoxical regulation. *Neuropharmacology* **61,** 348–354
55. Bombardi, C. (2014) Neuronal localization of the 5-HT2 receptor family in the amygdaloid complex. *Front. Pharmacol.* **5,** 68
56. Maeshima, T., Shutoh, F., Hamada, S., Senzaki, K., Hamaguchi-Hamada, K., Ito, R., and Okado, N. (1998) Serotonin2A receptor-like immunoreactivity in rat cerebellar Purkinje cells. *Neurosci. Lett.* **252,** 72–74
57. Pazos, A., Cortés, R., and Palacios, J. M. (1985) Quantitative autoradiographic mapping of serotonin receptors in the rat brain. II. Serotonin-2 receptors. *Brain Res.* **346,** 231–249
58. Wright, D. E., Seroogy, K. B., Lundgren, K. H., Davis, B. M., and Jennes, L. (1995) Comparative localization of serotonin1A, 1C, and 2 receptor subtype mRNAs in rat brain. *J. Comp. Neurol.* **351,** 357–373
59. Ward, R. P., and Dorsa, D. M. (1996) Colocalization of serotonin receptor subtypes 5-HT2A, 5-HT2C, and 5-HT6 with neuropeptides in rat striatum. *J. Comp. Neurol.* **370,** 405–414
60. Banas, S. M., Doly, S., Boutourlinsky, K., Diaz, S. L., Belmer, A., Callebert, J., Collet, C., Launay, J. M., and Maroteaux, L. (2011) Deconstructing antiobesity compound action: requirement of serotonin 5-HT2B receptors for dexfenfluramine anorectic effects. *Neuropsychopharmacology* **36,** 423–433
61. Diaz, S. L., Doly, S., Narboux-Nême, N., Fernández, S., Mazot, P., Banas, S. M., Boutourlinsky, K., Moutkine, I., Belmer, A., Roumier, A., and Maroteaux, L. (2012) 5-HT(2B) receptors are required for serotonin-selective antidepressant actions. *Mol. Psychiatry* **17,** 154–163
62. Green, S., Issemann, I., and Sheer, E. (1988) A versatile *in vivo* and *in vitro* eukaryotic expression vector for protein engineering. *Nucleic Acids Res.* **16,** 396
63. Deraet, M., Manivet, P., Janoshazi, A., Callebert, J., Guenther, S., Drouet, L., Launay, J. M., and Maroteaux, L. (2005) The natural mutation encoding a C-terminal truncated 5-hydroxytryptamine 2B receptor is a gain of proliferative functions. *Mol. Pharmacol.* **67,** 983–991
64. Du, Y., Davisson, M. T., Kafadar, K., and Gardiner, K. (2006) A-to-I pre-mRNA editing of the serotonin 2C receptor: comparisons among inbred mouse strains. *Gene* **382,** 39–46
65. Aghajanian, G. K., and Vandermaelen, C. P. (1982) Intracellular recording *in vivo* from serotonergic neurons in the rat dorsal raphe nucleus: methodological considerations. *J. Histochem. Cytochem.* **30,** 813–814
66. Achour, L., Kamal, M., Jockers, R., and Marullo, S. (2011) Using quantitative BRET to assess G protein-coupled receptor homo- and heterodimerization. *Methods Mol. Biol.* **756,** 183–200
67. Doly, S., Shirvani, H., Gäta, G., Meye, F. J., Emerit, M. B., Enslen, H., Achour, L., Pardo-Lopez, L., Yang, S. K., Armand, V., Gardette, R., Giros, B., Gassmann, M., Bettler, B., Mameli, M., Darmon, M., and Marullo, S. (2016) GABA receptor cell-surface export is controlled by an endoplasmic reticulum gatekeeper. *Mol. Psychiatry* **21,** 480–490

Heterodimers of serotonin receptor subtypes 2 are driven by 5-HT_{2C} protomers

Imane Moutkine, Emily Quentin, Bruno P. Guiard, Luc Maroteaux and Stephane Doly

J. Biol. Chem. 2017, 292:6352-6368.
doi: 10.1074/jbc.M117.779041 originally published online March 3, 2017

Annexe 2

Serotonin 2B receptors in mesoaccumbens dopamine pathway regulate cocaine responses

Stéphane Doly, Emily Quentin, Raphaël Eddine, Stefania Tolu, Sebastian P. Fernandez, Jesus Bertran-Gonzalez, Emmanuel Valjent, Arnauld Belmer, Xavier Viñals, Jacques Callebert, Philippe Faure, Frank J. Meye, Denis Hervé, Patricia Robledo, Manuel Mameli, Jean-Marie Launay, Rafael Maldonado, and Luc Maroteaux

2. Le récepteur 5-HT$_{2B}$ dans les effets psychoactifs de la cocaïne

(Soumis dans Journal of neuroscience en avril 2017)

Le système sérotoninergique, du fait de ses nombreuses projections, joue un rôle majeur dans de nombreux processus physiologiques. C'est pourquoi de nombreuses pathologies psychiatriques sont associées à des perturbations de ce système. Le système de la récompense illustre parfaitement ces effets. Ce système est la source de la motivation poussant l'individu à se nourrir ou se défendre, il est donc indispensable à sa survie. La base structurale de ce circuit comprend les neurones dopaminergiques de l'ATV qui projettent sur le Nac et le CPF. Ces structures sont aussi innervées par d'autres systèmes de transmission comme celui de la sérotonine, du GABA ou du glutamate (pour revue Luscher, 2016). Un stimulus récompensant induit un renforcement des connexions synaptiques entre les structures du circuit de la récompense. Cependant, lorsque ces connexions sont renforcées par une stimulation non récompensant ou artificielle, cette stimulation va se substituer à un stimulus physiologique qui va mettre en péril la survie de l'individu. C'est le cas lors de la prise de drogues addictives telle que la cocaïne qui agit sur le système dopaminergique, sérotoninergique et noradrénergique.

Il est maintenant assez bien acquis que la composante sérotoninergique est très importante dans l'addiction à la cocaïne du fait de l'expression de R-5-HT par les neurones dopaminergiques de l'ATV et du NAcc (pour revue Howell and Cunningham, 2015). Il a aussi été montré que des comportements impulsifs sont corrélés avec une addiction à la cocaïne dans lesquels la dualité sérotonine/ dopamine est perturbée (pour revue Cunningham and Anastasio, 2014). Le laboratoire a montré qu'une délétion des R-5-HT$_{2B}$ est associée, chez l'homme et la souris, à des comportements impulsifs (Bevilacqua et al., 2010) et une perte de libération de 5-HT et de dopamine en réponse au MDMA (Doly et al., 2008, 2009).

Au vu de ces résultats, il est apparu d'étudier le rôle des R-5-HT$_{2B}$ dans les effets psychoactifs de la cocaïne. Dans cette optique, nous avons testé les effets psychoactifs et renforçant de la cocaïne dans une lignée de souris *Htr2b*$^{-/-}$ ou dépourvue de R-5-HT$_{2B}$ seulement dans les neurones dopaminergiques (*Htr2b*^{DAKO}). Enfin, nous avons testé l'activité des neurones dopaminergiques des animaux *Htr2b*$^{-/-}$ de façon basale ou en réponse à la cocaïne.

A. Expression du R-5-HT$_{2B}$ par les neurones dopaminergiques

Dans un premier temps il a fallu vérifier que les R-5-HT$_{2B}$ sont exprimés par les structures dopaminergiques du circuit de la récompense. Pour cela, nous avons injecté un traceur rétrograde dans le NAc de souris exprimant la protéine GFP seulement dans les neurones

dopaminergiques, afin d'identifier les neurones provenant de l'ATV. Ainsi, nous avons pu isoler le contenu cytoplasmique des neurones de l'ATV projetant dans le NAcc. Sur ces extraits de cytoplasme nous avons observé la présence ou non d'ARN messager du R-5-HT_{2B} et de marqueurs dopaminergiques tels que l'enzyme de synthèse de la dopamine TH et les récepteurs dopaminergiques D2 par PCR sur cellule unique. Ainsi, nous avons observé que 40% des neurones de l'ATV expriment le R-5-HT_{2B}, la TH et le récepteur dopaminergique D2. De plus, 100% des neurones provenant du Nac et projetant dans l'ATV expriment aussi ces marqueurs. Ces résultats prouvent donc la présence du R-5-HT_{2B} dans une sous-population de neurones dopaminergiques du circuit de la récompense.

B. Impact de la délétion du R-5-HT_{2B} sur les effets psychoactifs de la cocaïne

Nous avons testé les effets de la cocaïne sur différents modèles de délétion génétique ou de blocage pharmacologique du R-5-HT_{2B}. Chez les animaux sauvages, une injection de cocaïne induit une augmentation rapide de l'activité locomotrice. De façon surprenante, les souris *Htr2b*$^{-/-}$ présentent une locomotion plus forte que les souris sauvages. De plus, une seconde injection de cocaïne une semaine plus tard induit aussi une augmentation de l'activité locomotrice supérieure à la première injection. Ce phénomène est dû aux effets renforçants induits par la première injection de cocaïne, il s'agit de la sensibilisation locomotrice (Valjent, 2009). Les souris *Htr2b*$^{-/-}$ présentent une activité locomotrice supérieure aux souris sauvages, cependant elles ne présentent pas une sensibilisation plus forte. Cette observation a été reproduite chez les animaux *Htr2b*^{DAKO} indiquant que ce phénotype est dépendant du R-5-HT_{2B} exprimé par les neurones dopaminergiques.

Cet effet n'est pas reproduit par une simple injection d'antagonistes des R-5-HT_{2B}. Afin de savoir si ces phénotypes résultent d'une réorganisation des circuits neuronaux, nous avons effectué des traitements chroniques d'antagonistes du R-5-HT_{2B} de différentes durées sur des souris sauvages avant de tester les effets locomoteurs de la cocaïne. Un traitement de quatre semaines avec l'antagoniste reproduit les phénotypes des animaux *Htr2b*$^{-/-}$ et *Htr2b*^{DAKO}. Ces observations montrent que ces phénotypes résultent d'une inactivation des R-5-HT_{2B} à long terme probablement dû à des réorganisations synaptiques.

C. Contribution du R-5-HT_{2B} dans la transmission dopaminergique

L'injection de cocaïne provoque une forte accumulation de dopamine au niveau du NAc. Des expériences de microdialyse ont montré que cette accumulation est supprimée chez les animaux *Htr2b*$^{-/-}$, suggérant une perturbation de la transmission dopaminergique en absence de

R-5-HT_{2B}. Au niveau moléculaire, la cocaïne provoque une augmentation de l'activité des neurones dopaminergiques du NAc, de l'ATV et du striatum dorsal induisant une phosphorylation des protéines ERK1/2. Les souris *Htr2b*$^{-/-}$ présentent une plus faible proportion de neurones exprimant les protéines ERK1/2 phosphorylées dans le NAc shell. En effet, la libération de dopamine étant supprimée, l'activité des neurones est plus faible et donc les protéines ERK1/2 moins phosphorylées.

Enfin, nous avons voulu observer si l'absence de R-5-HT_{2B} pouvait affecter l'activité des neurones dopaminergiques. De façon surprenante, les souris *Htr2b*$^{-/-}$ présentent une plus forte activité basale que les souris sauvages. L'injection de cocaïne induit une diminution du taux de décharges des neurones dopaminergiques de l'ATV. Cette diminution est significativement plus forte chez les animaux *Htr2b*$^{-/-}$.

Dans l'optique d'évaluer la plasticité du système en présence ou non du R-5-HT_{2B}, nous avons mesuré les courants AMPA et NMDA dans l'ATV. Le calcul du ratio AMPA/NMDA est supérieur en absence de R-5-HT_{2B} indiquant qu'il y a renforcement des afférences glutamatergiques sur les neurones dopaminergiques, ce qui est couramment observé chez les animaux ayant déjà été exposés à la cocaïne.

D. Conclusion

Cette étude a permis de montrer que les R-5-HT_{2B} sont exprimés par les neurones dopaminergiques. Et qu'ils exercent un contrôle facilitateur de leur activité et de la libération de dopamine dans le NAC, notamment dans les effets psychostimulants et renforçant de la cocaïne.

E. Contribution personnelle

Dans cette étude j'ai pris en charge les lignées de souris *Htr2b*$^{-/-}$ et procédé aux croisements permettant d'obtenir les quatre lignées de transgéniques 5-HT_{2B} KO conditionnels dans les neurones dopaminergiques *Htr2b*^{DAKO} ou sérotoninergiques *Htr2b*$^{5\text{-}HTKO}$ exprimant la protéine GFP dans les neurones recombinés (DAT$^{cre/0}$; Htr2b$^{fl/fl}$; RCE/RCE et DAT$^{cre/0}$; RCE/RCE et Pet1$^{cre/0}$; Htr2b$^{fl/fl}$; RCE/RCE et Pet1$^{cre/0}$; RCE/RCE). J'ai effectué les tests de locomotion et de sensibilisation induit par la cocaïne dans ces lignées de KO conditionnelles. Sur les animaux *Htr2b*^{DAKO}, j'ai effectué les marquages contre la TH afin de montrer la colocalisation avec la GFP et vérifier que les neurones recombinés sont bien dopaminergiques. J'ai ensuite effectué les PCR sur des extraits cérébraux d'ATV afin de vérifier la présence de la forme floxée du récepteur 5-HT_{2B}.

Title: Serotonin 2B receptors in mesoaccumbens dopamine pathway regulate cocaine responses

***Abbreviated title: Htr2b* in mesolimbic dopamine neurons**

Authors: Stéphane Doly[1,7], Emily Quentin[1], Raphaël Eddine[2], Stefania Tolu[2], Sebastian P. Fernandez[1,8], Jesus Bertran-Gonzalez[1,9], Emmanuel Valjent[1,10], Arnauld Belmer[1,11], Xavier Viñals[5], Jacques Callebert[4], Philippe Faure[2], Frank J. Meye[1], Denis Hervé[1], Patricia Robledo[5,6], Manuel Mameli[1,12], Jean-Marie Launay[4], Rafael Maldonado[5,6], and Luc Maroteaux*[1]

Author affiliations: [1]INSERM, UMR-S839, F-75005, Paris, France; Sorbonne Universités, UPMC Univ Paris 06, UMR-S 839, F-75005, Paris, France; Institut du Fer à Moulin, F-75005, Paris, France.
[2]Neuroscience Paris Seine NPS, CNRS UMR 8246 INSERM U1130, Paris, France; Sorbonne Universités, UPMC Univ Paris 06, UMR 7102, F-75005, Paris, France.
[4]AP-HP, Hôpital Lariboisière, Service de Biochimie, Paris, 75010, France; INSERM U942, Paris, 75010, France.
[5]Laboratory of Neuropharmacology, Department of Experimental and Health Sciences, University Pompeu Fabra. Barcelona, Spain.
[6]Integrative Pharmacology and Systems Neuroscience, IMIM-Hospital del Mar Research Institute, Barcelona, Spain.

***Corresponding author:** Luc Maroteaux INSERM, U839, Institut du Fer à Moulin, 17 rue du du Fer à Moulin 75005 Paris, France. TEL: (33) 01 45 87 61 23; FAX: (33) 01 45 87 61 32; Email: luc.maroteaux@upmc.fr.

Current addresses: [7] Université Clermont Auvergne, INSERM, NEURO-DOL, F-63000 Clermont-Ferrand, France.
[8] IPMC – CNRS UMR7275 660 Route des Lucioles Sophia-Antipolis 06560 Valbonne France

[9] Clem Jones Centre for Ageing Dementia Research, Queensland Brain Institute, The University of Queensland, Brisbane, Queensland, Australia
[10] Institut de Génomique Fonctionnelle, INSERM U661; CNRS UMR 5203; University Montpellier I and II, Montpellier, France.
[11] Translational Research Institute, Queensland University of Technology, Brisbane Qld 4059, Australia

[12] Dept. Fundamental Neurosciences (DNF) The University of Lausanne, Rue du Bugnon 9 1005 Lausanne Switzerland

Number of words in abstract 203; **Number of words in introduction 644**; **Number of words in discussion 1390**; **Number of figures 8**; **Number of pages 45.**

Conflict of interest

The authors declare no competing financial interests.

Acknowledgments

We thank the Mouse Clinical Institute (Strasbourg) for *Htr2b* floxed mice production, François Tronche and Mark Ungless for providing *Dat-Cre*$^{+/0}$ mice, Evan Deneris for providing *Pet1-Cre*$^{+/0}$ mice, Mythili Savariradjane and the Imaging facility of the IFM, Natacha Roblot from the IFM animal facility, and Imane Moutkine for excellent technical assistance.
This work was supported by Ministerio de Economía y Competitividad (#SAF2014-59648-P to R.M., MINECO/FEDER, UE); Instituto de Salud Carlos III (RD06/0001/0001 to R.M.) and (PI14/00210 to P.R.), FEDER funds; the Generalitat de Catalunya ICREA (Institució Catalana de Recerca i Estudis Avançats) Academia (2015) to R.M, and the studies on *Htr2b*$^{-/-}$ mice were supported by funds from the *Centre National de la Recherche Scientifique*, the *Institut National de la Santé et de la Recherche Médicale*, the *Université Pierre et Marie Curie*, and by grants from the *Fondation pour la Recherche sur le Cerveau*, the *Fondation de France*, the *Fondation pour la Recherche Médicale* "Equipe FRM DEQ2014039529", the French Ministry of Research (Agence Nationale pour la Recherche ANR-12-BSV1-0015-01 and the Investissements d'Avenir programme ANR-11-IDEX-0004-02). S. Doly was supported by a Lefoulon-Lalande fellowship and E. Quentin by a PhD fellowship from the Region Ile de France DIM Cerveau et Pensée. LM's team is part of the École des Neurosciences de Paris Ile-de-France network and of the Bio-Psy Labex. None of these funding agencies had influence on the data presented in this paper.

Abstract:
Addiction is a maladaptive pattern of behavior following repeated use of reinforcing drugs in predisposed individuals, and leading to lifelong changes. A common substrate of these changes lies in alterations of neurons releasing dopamine in the ventral and dorsal territories of the striatum. The serotonin 5-HT$_{2B}$ receptor has been involved in various behaviors including impulsivity, response to antidepressants and to psychostimulants pointing toward putative interactions with the dopamine system. Despite these findings, it remains unknown whether the 5-HT$_{2B}$ receptor modulates dopaminergic activity and the possible mechanisms involved. To answer these questions, we investigated the contribution of the serotonin 5-HT$_{2B}$ receptor to cocaine-dependent behavioral responses. Mice permanently lacking 5-HT$_{2B}$ receptors, even restricted to dopamine neurons, developed heightened cocaine-induced locomotor responses. Retrograde tracing, combined with single cell mRNA amplification, *in-vivo* and *ex-vivo* electrophysiological recordings, and 5-HT$_{2B}$ receptor inactivation in dopamine neurons indicated that this receptor is expressed by mesolimbic dopamine neurons, and its lack affects their neuronal activity, and changes in AMPA- over NMDA-mediated excitatory synaptic currents. These changes are associated with lower ventral striatum dopamine activity and blunted cocaine self-administration. These data identify the 5-HT$_{2B}$ receptor as a pharmacological target and provide mechanistic insight into attenuated dopamine tone following exposure to drugs of abuse.

Significance Statement

Here we report that mice lacking 5-HT_{2B} receptors totally or exclusively in dopamine neurons exhibit heightened cocaine-induced locomotor responses. In spite of the sensitized state of these mice, we found that associated changes include lower ventral striatum dopamine activity, and lower cocaine operant self-administration. We described the selective expression of 5-HT_{2B} receptors in subpopulation of dopamine neurons sending axons to ventral striatum. An increased bursting *in-vivo* properties of these dopamine neurons and a concomitant increase in AMPA synaptic transmission to *ex-vivo* dopamine neurons was found in mice lacking 5-HT_{2B} receptors. These data support that the chronic 5-HT_{2B}-receptor inhibition makes mice behaving as animals already exposed to cocaine with higher cocaine-induced locomotion associated with changes in DA neuron reactivity.

Introduction

Vulnerability to drug addiction is moderately to highly heritable, but the genes involved are largely unknown (Goldman et al., 2005). The mesocorticolimbic dopamine (DA) system comprises midbrain projections from the ventral tegmental area (VTA) and substantia nigra to cortical territories and subcortical limbic areas including the striatum. A common substrate of addictive behaviors lies in neurons releasing DA in the striatum, as demonstrated via elegant and diverse investigations in both animals and humans (Hyman et al., 2006). Anatomical studies have shown in the ventral striatum that the nucleus accumbens (NAcc) is heterogeneous and includes a medio-ventral part, the shell, and a dorso-lateral part, the core. Whereas Pavlovian food conditioned stimuli release core but not shell DA, drug conditioned stimuli do the opposite, releasing shell but not core DA that initiates the drug addiction process. Neuroadaptative processes related to the chronic influence of drugs on DA secondarily impair the function of feed-back circuit loops, resulting in impairments in impulse control and decision making that form the basis for the compulsive features of drug seeking (Di Chiara and Bassareo, 2007). Evidence on how drug-evoked synaptic plasticity affects circuit adaptations is just emerging (Lüscher, 2016).

It has been established that serotonin (5-hydroxytryptamine, 5-HT) can enhance reinforcement induced by psychostimulants (Müller and Homberg, 2015) via regulation of DA neurons through 5-HT receptors expressed in the VTA and the NAcc (Hayes and Greenshaw, 2011). Both of these regions receive 5-HT projections from the dorsal raphe nucleus, which thereby can regulate DA neurotransmission (Di Giovanni et al., 2010). 5-HT has also been shown to modulate cocaine action both in clinical and preclinical studies (Filip et al., 2010). Human genetic association studies are largely consistent with a role of 5-HT in the effects of psychostimulants (Hnasko et al., 2007; Kirby et al., 2011). However, a detailed understanding of the roles of different 5-HT receptors in cocaine addiction remains to be clarified (Filip et al., 2010).

A single nucleotide substitution in the *HTR2B* gene was exclusively found in Finnish population and introduced a stop codon (Gln20Ter, rs79874540) at the beginning of the coding sequence of the 5-HT_{2B} receptor. This loss-of-function polymorphism is associated with impulsive, behaviors (Bevilacqua et al., 2010). Coherently, mice knockout for 5-HT_{2B} receptor gene (*Htr2b*$^{-/-}$) exhibit higher novelty-induced locomotion, and impulsive choice in delayed discounting task paradigm (Bevilacqua et al., 2010). We also found that pharmacological inhibition (5-HT_{2B} receptor antagonist) or genetic ablation of the 5-HT_{2B} receptor in mice (*Htr2b*$^{-/-}$) completely abolished hyperlocomotion and 5-HT and DA release in NAcc and VTA in response to MDMA (10 mg/kg) (Doly et al., 2008). However, these mice still respond to high dose of MDMA (30 mg/kg) distinguishing 5-HT-dependent from DA-dependent effects and illustrating the complex 5-HT/DA interactions (Doly et al., 2009). We also found that *Htr2b*$^{-/-}$

mice display an higher amphetamine-induced locomotion (Pitychoutis et al., 2015) and other reported that 5-HT_{2B} receptor selective antagonists can reduced significantly the increase in DA outflow induced by amphetamine in the NAcc shell, but not in the dorsal striatum (Auclair et al., 2010). However, the same authors reported that a single antagonist injection had no effect on cocaine-induced DA outflow in the striatum (Devroye et al., 2015), and decreased the firing rate of DA neurons in the VTA (Devroye et al., 2016). Despite these findings, it remains unclear whether the 5-HT_{2B} receptor modulates DA/reward and the mechanisms involved.

Here, we report that mice with permanent genetic ablation, even restricted to DA neurons or long-term pharmacologic blockade (chronic antagonist treatment) of 5-HT_{2B} receptors exhibit heightened cocaine-induced locomotor responses. Associated changes include lower ventral striatum DA activity, and lower cocaine operant self-administration. Furthermore, a lack of this receptor increases the cocaine reactivity of VTA DA neurons projecting to the NAcc shell and the ratio of AMPA- over NMDA-mediated excitatory postsynaptic currents in these neurons. These data support that the 5-HT_{2B} receptor is an intermediate in drug-evoked plasticity.

Materials and methods

Reagents.

Cocaine, SKF 81297 [(±)-6-chloro-7,8-dihydroxy-1-phenyl- 2,3,4,5-tetrahydro-1H-3-benzazepine hydrobromide] (Sigma-Aldrich, Saint-Quentin Fallavier, France) and 2-amino-4- (4-fluoronaphth-1-yl)-6-isopropylpyrimidine (RS127445) and quinpirole hydrochloride (Tocris Bioscience, USA) were slowly dissolved in 0.9% (wt/vol) NaCl solution (saline). All drugs were administered intraperitoneally (ip) (0.1 ml/10 g body weight). RS127445 was found to have sub-nanomolar affinity for the 5-HT_{2B} receptor (pK_i = 9.5±0.1) and at least 1,000 fold selectivity for this receptor as compared to numerous other receptors and monoamine uptake sites (Diaz et al., 2012). *Htr2b*$^{+/+}$ mice chronically treated with RS127445 continuously received the 5-HT_{2B} antagonist at 1mg/kg/day or vehicle (10 mM DMSO) control via subcutaneous (sc) osmotic pumps (Alzet® model 2004) for 4 weeks.

Animal studies

Animals. *Htr2b*$^{-/-}$ mice (MGI:1888735) used in these experiments were maintained in a 129S2/SvPas (129S2) background. Wild type 129S2 mice (8-10 week old) used as a control group were derived from heterozygote crosses and were bred at our animal facility. Swiss-Webster mice carrying *drd2*-EGFP bacterial artificial chromosome transgenes were generated by the Gene Expression Nervous System Atlas program at Rockefeller University (MGI:3843608) (Gong et al., 2003). Groups were composed of 50% male and 50% female for each experiment. All mice were maintained on a 12h light: 12h dark schedule (lights on at 8:00), and housed in groups of 3-5 of the same genetic background and sex after weaning. Mice were moved to experimental room in their home cage at least 5 days prior to testing to allow for habituation to the environment and stayed there until the end of the experiments. Behavioral studies were carried out in the afternoon (14:00–20:00). The observer was blind to experimental conditions being measured. Behavioral tests and animal care were conducted in accordance with standard ethical guidelines (National Institutes of Health's 'Guide for the Care and Use of Laboratory animals', and European Directive 2010/63/ UE) and were approved by the local Ethic Committee for Animal Experiments (No. 01170.02).

Experimental design and statistical analysis

The total number of animals per group was defined according to the standard deviation and the difference score observed for each small group in a pilot experiment. Mice were randomly assigned to different experimental groups of 4 to 6 animals and independent experiments were performed at least 3 times. Normal distributions and homoscedasticity were verified by Shapiro-Wilk's test and Levene's test, respectively. Putative outliers were determined by the ROUT method. The statistical analysis was developed with the software Infostat and GrapPad Prism 6. Microdialysis and locomotor activity data were analyzed by two-way ANOVA repeated measures (RM) with gene or drug treatment and time as factors. Food self-administration was analyzed by three-way ANOVA with hole, day and genotype as factors. Behavioral and biochemical assays were analyzed by two-way analysis of variance (ANOVA) with treatment and genotype as main factors. One-way ANOVA and t-test or Bonferroni test were used for post-hoc comparisons depending on the experiment. $P < 0.05$ was predetermined as the threshold for statistical significance.

Generation of *Htr2b* floxed mice. Genomic contigs of *Htr2b* encompassing exon 1 and 2 and flanking sequence were obtained by screening of a 129S2 mouse genomic library. For the gene targeting construct, a 10 kb BamHI-XhoI fragment containing the two first exons was selected, while a 4 kb SacI-SacI fragment containing exon 2, which includes the ATG start codon and 5' UTR was used to induce the targeted deletion. A LoxP site was inserted in the 5'-UTR and a neomycine-resistance (NEO) cassette flanked by two LoxP sites in the ClaI site of the second intron. Then, the SacI-SacI fragment comprising the floxed construct was excised and electroporated into 129S2 embryonic stem (ES) cells which were subjected to G418 selection. Targeted homologous recombination was confirmed by PCR and Southern blot analysis. A positive ES clone was injected into C57Bl/6NCrl blastocysts and implanted into pseudopregnant mice. A chimeric male displaying germ-line transmission was then used to propagate the floxed *Htr2b* (*Htr2b*$^{fl/fl}$) allele on a C57Bl/6NCrl background for the two first generations. More than ten backcrosses of *Htr2b*$^{fl/fl}$ mice with 129S2 (*Htr2b*$^{+/+}$) mice were performed. *Htr2b*$^{fl/fl}$ alleles were detected by PCR using the oligonucleotide F1: CTAACATTTTTCATCCACATCTA as forward primer located in the 5' UTR (position of the primers are indicated in Figure). Paired to this primer, the reverse primer R1: TCCCTCGAAGCTTATCGGCGCG, located in the 5' end of the second intron led to the amplification of a 1 kbp product in the presence of the *Htr2b*$^{fl/fl}$ allele, while the reverse primer R2: ACTTTAATTGGGACTCGCTGAT, located in the 3' side of the ClaI site permits amplification of a 309 bp amplicon indicative of the *Htr2b* null allele.

DA neurons selective ablation of *Htr2b*. Adults *Htr2b*$^{fl/fl}$ mice were exclusively inactivated in DA neurons for *Htr2b* by crossing with DAT-Cre$^{+/0}$ (BAC–Slc6-icre) mice (Turiault et al., 2007). *Htr2b*$^{fl/fl}$;DAT-Cre$^{+/0}$ (*Htr2b*^{DAKO}) were generated on a mixed 129S2.B6 background used as F3 on 129S2 strain with littermate *Htr2b*$^{fl/fl}$;DAT-Cre$^{0/0}$ (*Htr2b*$^{fl/fl}$) as control mice. Identification of DA neurons was performed in *DAT-Cre*$^{+/0}$;*Gt(ROSA)26Sor*$^{tm1.1(CAG-EGFP)Fsh}$ (*DAT-Cre*$^{+/0}$*;RCE*) mice, who expressed EGFP only after recombination (Jackson Lab, also named RCE:loxP mice harbor the R26R CAG-boosted EGFP (RCE) reporter allele with a *loxP*-flanked STOP cassette upstream of the enhanced green fluorescent protein (EGFP) gene-MGI:4412373).

Locomotor activity. Locomotor activity was measured in an actimeter (circular corridor with four infrared beams placed at every 90° Imetronic, France) as described (Doly et al., 2009). Counts were incremented by consecutive interruption of two adjacent beams (i.e., mice moving through one-quarter of the corridor). Mice were individually placed in the activity box for 30 min followed by an ip injection of a saline solution and recorded for another 60 min during 3 days consecutively for habituation before all locomotor experiments. The day of experiment, mice were individually placed in the activity box for

30 min before being ip injected with a saline or cocaine (7.5 to 20 mg/kg) solution and the locomotor activity was recorded for more than one hour.

Locomotor sensitization. For locomotor sensitization in this study, we used a two-injection protocol shown to be as efficient as repeated injections protocol but involving much less mice handling, thus minimizing stress and contextual habituation that can be confounding factors (Valjent et al., 2010). After 30 min in the actimeter, mice received a first injection of cocaine (7.5 to 20 mg/kg) and the locomotor activity was recorded for more than one hour. Mice were then challenged seven days later with a second injection of cocaine at the same concentration as the first injection, same injection protocol, and the locomotor activity was recorded for more than one hour.

Microdialysis in freely moving mice. The microdialysis experiment was performed using awake mice as described (Doly et al., 2009). Initially, anesthetized animals were placed in a stereotaxic frame (D. Kopf, Tujunga, CA, USA) and a stainless-steel guide cannula (CMA/12, CMA Microdialysis, North Chelmsford, MA, USA; outer diameter 0.7 mm) was implanted in the NAcc. The cannula was then secured to the skull with dental cement, and the skin was sutured. Animals were kept in individual cages for a seven-day recovery. Dialysis probes were equipped with a Cuprophan membrane (membrane length 1 mm and diameter 0.24 mm, cutoff: 5,000 Da, Microdialysis AB, Sweden). According to Praxinos and Franklin (Paxinos and Franklin, 2001), stereotaxic coordinates in mm were for NAcc AP +1.2, ML +0.6, DV -4.2 both to bregma and dura surface, respectively. After insertion, probes were perfused at a constant rate of 1µl/min with artificial CSF containing 154.1 mM Cl-, 147 mM Na+, 2.7 mM K+, 1 mM Mg2+, and 1.2 mM Ca2+, adjusted to pH 7.4 with 2 mM sodium phosphate buffer. The microdialysis experiment was performed using awake mice. Dialysates were collected every 20 min. All measurements were carried out 150 min after the beginning of perfusion, by which time a steady state was achieved. Mice were injected with cocaine (20 mg/kg; ip) 20 minutes after the beginning of measurements. At the end of the experiment, all brains were fixed in a 4% formaldehyde solution and serial coronal slices were made on a microtome. Histological examination of cannula tip placement was subsequently made on 100 µm safranine-stained coronal sections. Dialysate samples were injected without any purification into an HPLC system that consists of a pump linked to an automatic injector (Agilent 1100, Palo Alto, CA, USA), a reverse-phase column (Zorbax SB C18, 3.5 lm, 150·4.6 mm; Agilent Technologies, Palo Alto, CA, USA) and a coulometric detector (Coulochem III; ESA Inc., Chelmsford, USA) with a 5011 analytical cell to quantify DA or 5-HT. The first electrode was fixed at -100 mV and the second electrode at +300 mV. The gain of the detector was set at 50 nA. The signal of the second electrode was connected to an HP Chemstation for HPLC. The composition of the mobile phase was 50 mM NaH_2PO_4, 0.1 mM Na_2EDTA, 0.65 mM octyl sodium sulphate and 14% (v/v) methanol, pH 3.5. The flow rate was set at 1 ml/min. The quantity of neurotransmitters calculated based on standard injected in each HPLC run in the same range of concentrations as experimental samples.

Tissue preparation and immunofluorescence. Ten minutes after cocaine or saline injection, and locomotor recording, mice were rapidly anesthetized with pentobarbital (100 mg/kg, ip; Sanofi-Aventis) and perfused transcardially with 4% (w/v) paraformaldehyde in 0.1 M sodium phosphate buffer, pH 7.5 (Bertran-Gonzalez et al., 2008). Brains were postfixed overnight in the same solution and stored at 4°C. Thirty-µm-thick sections were cut with a Vibratome (Leica) and stored at –20°C in a solution containing 30% (v/v) ethylene glycol, 30% (v/v) glycerol, and 0.1 M sodium phosphate buffer, until they were processed for immunofluorescence. Free-floating sections were rinsed in Tris-buffered saline (TBS) (0.10 M Tris, 0.14 M NaCl), pH 7.4, incubated for 5 min in TBS containing 3% H_2O_2 (v/v) and 10% methanol (v/v), and rinsed three times 10 min in TBS. After 20 min incubation in 0.2% Triton X-100 in

TBS (v/v), sections were rinsed three times in TBS, blocked with 30 g/L BSA in TBS, and incubated overnight (or longer as indicated) at 4°C with the primary antibodies. Antibody for TH is a mouse monoclonal (1:750 with an incubation ≥ 2 d; Sigma-Aldrich) and for pERK using rabbit polyclonal antibodies against diphospho-Thr-202/ Tyr-204-ERK1/2 (1:400; Cell Signaling Technology). After incubation with primary antibody, sections were rinsed three times for 10 min in TBS and incubated for 45 min with chicken Cy3-coupled (1:400; The Jackson Laboratory) or goat Alexa Fluor 488-coupled (1:400; Invitrogen) secondary antibodies. Finally, sections were rinsed for 10 min twice in TBS and twice in Tris buffer (0.25 M Tris, pH 7.4) before mounting in Vectashield (Vector Laboratories). Brain regions were identified using a mouse brain atlas and sections equivalent to 1.54 mm from Bregma were taken. Sections were processed as previously described (Doly et al., 2008). Confocal microscopy and image analysis were performed at the Institut du Fer à Moulin Imaging Facility. Labeled images from each region of interest were obtained bilaterally using sequential laser-scanning confocal microscopy (SP2; SP5 Leica). Neuronal quantification was performed in 375 x 375 µm images by counting nuclear/cytoplasm Cy3 immunofluorescence (for pERK1/2). Cell counts were performed by an observer unaware of the treatment received by the mice.

Food and cocaine self-administration. Prior to cocaine self-administration testing, mice were individually housed and food deprived to 85-90% of their free-feeding body weight, and then trained to respond for food pellets in mouse operant chambers (Med Associates Inc. Georgia, VT, USA) equipped with two nose-pokes, one randomly selected as the active and the other as the inactive nose-poke. A cue light located above the active nose-poke was paired contingently with the delivery of the reinforcer. Animals were first trained to respond for food pellets (Testdiet, Richmond, IN, USA) in one-hour daily self-administration sessions on a fixed ratio 1 (FR1) schedule of reinforcement until responding for food criteria was acquired (a minimum of 20 reinforcers, more than 75% of correct responding, and stabilization for 2 to 3 days). After this initial training, mice were kept in ad libitum conditions in order to recover their body weight before proceeding with the catheter implantation as previously described (Soria et al., 2005). Mice were anesthetized with a mixture of ketamine/xylazine (5:1; 0.10 ml/10 g, ip) and implanted with indwelling intravenous silastic catheters on their right jugular vein as previously described (Soria et al., 2005). After surgery, animals were allowed to recover for 3 days before initiation of self-administration sessions. Saline solution self-administration sessions were performed until obtaining a low and stable responding pattern in order to prevent any food-seeking or food-extinction disturbance in succeeding cocaine self-administration. The mice included in the statistical analysis (18 WT and 13 KO mice) showed patent catheters up to the end of the experiment. Animals were then trained to self-administer cocaine at the dose of 0.250 mg/kg/infusion during 8 days on a FR1 schedule of reinforcement. Following stable responding, all mice underwent dose-response experiments, where cocaine was presented at the doses of 0.125, 0.250 and 0.500 mg/kg/infusion during 4 consecutive days respectively. Subsequently, a progressive ratio procedure was performed in order to test the motivation of the mice to work for cocaine at the dose of 0.125 mg/kg/infusion, where the response requirements to earn an infusion escalated according to the following series: 1-2-3-5-12-18-27-40-60-90-135-200-300-450-675-1000. The patency of intravenous catheters was evaluated at the end of the experiments by an infusion of 0.05 ml of thiopental sodium (5 mg/ml) (Braun Medical) through the catheter. If prominent signs of anesthesia were not apparent within 3 seconds of the infusion the mouse was removed from the experiment.

Sucrose preference. In the first phase two bottles of water were available to individually caged mice and liquid consumption was monitored during two consecutive days. Then, the liquid from one of the bottles was replaced with a 2% sucrose solution and liquid intake measurements were performed daily during 3 days. Total liquid intake, as well as, sucrose preference was evaluated in *Htr2b*$^{-/-}$ mice and *Htr2b*$^{+/+}$ controls.

Single-cell RT-PCR. Swiss-Webster mice carrying *Drd2-EGFP* bacterial artificial chromosome transgenes were generated by the Gene Expression Nervous System Atlas program at Rockefeller University (New York). For single-cell RT-PCR experiments, 1-2 week-old *Drd2-EGFP* mice were used to direct EGFP protein expression to D2 receptor expressing neurons. Mice were anesthetized and decapitated, and the brain was rapidly dissected out. Horizontal slices (250-µm thick) were prepared using a vibratome, in artificial cerebral spinal fluid aCSF supplemented with sucrose. After a 1-h recovery period, individual slices were placed in an electrophysiology chamber continuously perfused with aCSF bubbled with Carbogen and maintain at 22 °C. Neurons were visualized using an Olympus BX51WI upright microscope holding x5 and x40 objectives, a fluorescent lamp, and infrared, red, and green fluorescence filters. The methodology involving harvesting of cytoplasmic content and subsequent single cell PCR amplification has been described elsewhere (Cauli et al., 1997). Briefly, borosilicate glass pipettes (3-5 MΩ) were made in a HEKA PIP5 puller and filled with 8 µl of autoclaved RT-PCR internal solution (in mM): 144 K-gluconate; 3 $MgCl_2$; 0.5 EGTA; 10 HEPES, pH 7.2 (285/295 mOsm). Single DA neurons in the VTA and SNc were approached with a pipette and after a whole-cell connection was established, cytoplasmic content of the cell was harvested by applying gentle negative pressure to the pipette. Cell content was expelled into a tube where a reverse transcription (RT) reaction was performed in a final volume of 10 µl. Target cDNA sequences were thereafter amplified by conducting a multiplex nested PCR, designed to simultaneously detect the enzyme tryrosine hydroxylase (TH), D2 receptor and 5-HT_{2B} receptors. The following primers used were: TH, external sense CTGGCCTTCCGTGTGTTTCAGTG, external anti-sense CCGGCTGGTAGGTTTGATCTTGG, internal sense AGTGCACACAGTACATCCGTCAT and internal anti-sense GCTGGTAGGTTTGATCTTGGTA; D2 receptor external sense GCAGCCGAGCTTTCAGAGCC, external anti-sense CCTGCGGCTCATCGTCTTAAG, internal sense AGAGCCAACCTGAAGACACCAC and internal anti-sense CTTAAGGGAGGTCCGGGTTTTG; 5-HT_{2B} external sense CACTGGAGAAAAGGCTGCAGTA, external anti-sense TTGCACTGATTGGCCTGAATTG, internal sense GGCTATATGGCCCCTCCCAC and internal anti-sense GGTCCAGGGAAATGGCACAG.

Initially, all three genes were simultaneously amplified in a single tube using 10 µl of cDNA, 200 nM of each primer and 2.5 U of Taq polymerase in a final volume of 100 µl. The PCR reaction was carried out using a 6-min hot start at 94°C, followed by a 21-cycle program (94°C for 30 s, 60°C for 30 s and 72°C for 30 sec). Subsequently, 2 µl of the amplified cDNA was used as the template for the second amplification step. Here, each gene was individually amplified in a separate tube, and a 35-cycles program using the same cycling conditions as mentioned above, in a final volume of 100 µl. The products of the second PCR were analyzed by electrophoresis in 2.5% agarose gels using ethidium bromide. The sizes of the PCR-generated fragments were as predicted by the mRNA sequences and were further verified by direct sequencing of the final products.

***In-vivo* electrophysiology: extracellular single-cell recordings.** Mice were anesthetized with chloral hydrate, 400 mg/kg ip, supplemented as required to maintain optimal anesthesia throughout the experiment, and were positioned in a stereotaxic frame (David Kopf). Body temperature was kept at 37 °C by means of a thermostatically controlled heating blanket. Procedures for DA cell electrophysiological recording were described previously (Mameli-Engvall et al., 2006). An incision was made in the midline to expose the skull. A burr hole was drilled above the VTA (coordinates: between 3.5 ± 0.3 mm posterior to bregma and 0.5 ± 0.3 mm lateral to midline (Paxinos and Franklin, 2001). Recording electrodes were pulled with a Narishige electrode puller from borosilicate glass capillaries with outer and inner diameters of 1.50 and 1.17 mm, respectively (Harvard Apparatus Ltd.). The tips were broken under microscope control and filled with 1.5% Neurobiotine in 0.5% Na-acetate. These electrodes had tip diameters of 1–2 mm and impedances of 4–8 MΩ. They were lowered through

the burr hole with a micro drive, and a reference electrode was placed in the subcutaneous tissue. Electrical signals were amplified by a high-impedance amplifier (Axon Instruments) and monitored visually with an oscilloscope (Tektronix TDS 2002) and audibly through an audio monitor (A.M. Systems Inc.). When a single unit was well isolated, the oscilloscope sweep was triggered from the rising phase of the action potential and set sufficiently fast to display the action potential over the entire screen (usually 0.5 ms per unit). Such continuous observation of the expanded action potential provided assurance that the same single unit was being monitored throughout the experiment. The unit activity digitized at 25 KHz was stored in Spike2 program (Cambridge Electronic Design, CED, United Kingdom).

Firing Pattern Quantification. DA cell firing *in-vivo* was analyzed with respect to the average firing rate and the percentage of spikes within a burst (the number of spikes within burst divided by total number of spikes in a given window of 1-min duration; %SWB). Spontaneous firing rate and %SWB analysis. DA cell firing *in-vivo* was analyzed with respect to the average firing rate and the %SWB. Neuron basal activity was defined on the basis of at least 5 min or 500 spikes. The electrophysiological characteristics of ventral tegmental area (VTA) neurons were analyzed in the active cells encountered by systematically passing the microelectrode in a stereotaxically defined block of brain tissue including the VTA. Its margins ranged from 2.92–3.88 mm posterior to bregma, 0.24–0.96 mm mediolateral with respect to the bregma point, and 3.7–4.7 mm ventral to the cortical surface, according to the coordinates of Paxinos and Franklin (2001). Sampling was initiated on the right side and then on the left side. Each electrode descent was spaced at least 10 µm from the others.

DA cell identification. Extracellular identification of DA neurons was based on their location as well as on the set of unique electrophysiological properties that characterize these cells *in-vivo*: (i) a typical triphasic action potential with a marked negative deflection; (ii) a characteristic long-duration (>2.0 ms) action potential; (iii) an action potential width from start to negative of >1.1 ms; (iv) a slow firing rate (< 10 Hz) with an irregular single spiking pattern and occasional short, slow bursting activity. These electrophysiological properties distinguish DA from non-DA neurons. When possible, upon completion of the experiment, positive current pulses were applied to the electrode to electroporate the recorded neuron. The mouse was killed with an overdose of anesthetic. The brain was removed and placed in a 4% paraformaldehyde solution. VTA sections of 60 µm were cut and stained with Neurobiotin and Tyrosine Hydroxylase antibody (a mouse monoclonal antibody for TH, 1:500 with an incubation 2>d; Sigma-Aldrich), and the recorded neurons were identified by fluorescence microscopy. We also added two criteria: (i) that the recording be stable (i.e., the absence of cell perturbation following our saline solution injection); and (ii) that the recorded cells be more than 4 mm from the surface of the brain. These parameters have been used classically to identify DA cells (Mameli-Engvall et al., 2006).

Electrophysiological response to cocaine and quinpirole. The firing rate and % of spike within burst (SWB) were evaluated using a 60-s moving window and a 15-s time step. Each cell's activity was rescaled by its baseline value averaged during the 3-min period before 10 µl cocaine (20 mg/kg) or quinpirole (0.25-0.50 mg/kg) in 0.9% NaCl was injected ip For firing frequency, rescaling was defined using x*100/xb with xb being the baseline firing frequency. The results are presented as mean ± SEM. The effect of cocaine or quinpirole was tested by comparing the maximum observed during baseline and after cocaine injection. For each neuron we determined xav, the maximum of the fluctuations before cocaine injections (during the 2.5-min period used as baseline); xav = max (x)av − mean (x) av, and xap is the maximum after cocaine (or quinpirole) injection (during the 3-min period after drug injection).

We used a paired nonparametric Wilcoxon test (Wilcoxon signed rank test) to compare xav and xap for firing frequency in two populations.

Electrophysiological recordings from brain slices. AMPA/NMDA ratio of evoked excitatory postsynaptic currents (EPSCs) from putative DA neurons of the VTA were obtained with whole–cell voltage–clamp recordings using a CsCl-based internal medium, as described (Glangetas et al., 2015). Six to seven weeks old *Htr2b*$^{+/+}$ control and *Htr2b*$^{-/-}$ mice were anesthetized (Ketamine/Xylazine) for slice preparation. Horizontal 250-µm slices were prepared in bubbled ice-cold 95% O2/5% CO2-equilibrated solution containing (in mM): cholineCl 110; glucose 25; NaHCO3 25; ascorbic acid 11.6; Na+-pyruvate 3.1; KCl 2.5; NaH2PO4 1.25; MgCl2 7; CaCl2 0.5, were then heated for 10 minutes in the same medium at 32ºC. Subsequently, slices were stored at room temperature in 95% O2/5% CO2-equilibrated artificial cerebrospinal fluid (ACSF) containing (in mM): NaCl 124; NaHCO3 26.2; glucose 11; KCl 2.5; NaH2PO4 1; CaCl2 2.5; MgCl2 1.3. Slices were kept at 32–34°C in a recording chamber and were continuously superfused with 2.5 ml/min ACSF. Whole-cell voltage-clamp recording techniques were used to measure excitatory synaptic responses of the ventral tegmental area (VTA). Synaptic currents were evoked by pulses (60 µs) delivered at 0.1Hz through a glass pipette placed 200 µm rostral to the patched neurons. Recordings were made in the presence of picrotoxin (100 µM) to block $GABA_A$ receptor-mediated currents. Putative DA neurons were identified as large cells (>30 pF capacitance) in the lateral part of the VTA, which are prone to project to the nucleus accumbens (Lammel et al., 2008). Currents were amplified, filtered at 5 kHz and digitized at 20 kHz and recorded at a holding potential of +40 mV (IGOR PRO, Wavemetrics, USA). Access resistance was monitored by a step of -4 mV (0.1 Hz) and experiments were discarded if the access resistance increased more than 20%. The internal solution contained (in mM): CsCl 130; NaCl 4; $MgCl_2$ 2; EGTA 1.1; HEPES 5; Na_2ATP 2; Na^+-creatine-phosphate 5; Na_3GTP 0.6, and spermine 0.1, with a liquid junction potential of –3 mV. AMPA receptor (AMPAR)-EPSCs were pharmacologically isolated using NMDA receptor (NMDAR) antagonist APV (50 µM), while NMDAR-EPSCs were then calculated by subsequent digital subtraction. The ratio of AMPAR/NMDAR responses was calculated by taking the peak values of these averaged (20 sweeps) currents. All drugs were obtained from Abcam (Cambridge, UK), Tocris (Bristol, UK), and HelloBio (Bristol, UK). APV was dissolved in water, whereas picrotoxin was dissolved in DMSO (diluted 1000x in the final volume). Online/offline analysis was performed using IGOR-6 (Wavemetrics, USA) and Prism (Graphpad, USA). Compiled data are expressed as mean ± SEM

Immunoblot analysis. Wildtype and mutant mice (2-month-old, age-matched) were killed by decapitation and their brains were immediately dissected out from the skull and frozen on dry ice. Microdiscs of tissue were punched out from frozen slices (500-µm thick) within the striatum using a stainless steel cylinder (1.4 mm diameter). Samples were homogenized in 1% SDS, equalized for their protein content and analyzed by western blot. The antibody dilutions were 1/1000 and 1/500 for antibodies against Golf and D1 receptor, respectively. Antibody for Golf was from our laboratory (Corvol et al., 2001) and for D1 receptor was from Luedtke et al. (1999). Antibodies were revealed by Fluoprobes 682 goat anti-rabbit or mouse IgG (Interchim, Montluçon, France) at a 1:5000 dilution. The fluorescent immunocomplexes were detected with Odyssey (LI-COR Biosciences, Lincoln, Nebraska). Quantification was carried out by measuring the average intensity in regions of interest using the Odyssey software and data were analyzed with the Prism 6 software (GraphPad Software, San Diego, CA).

Retrograde tracing of VTA or SNc neurons. *Drd2-EGFP* mice were anesthetized with ketamine (50 mg/kg) and xylazine (2 mg/kg) and fixed in a stereotaxic apparatus. Stereotaxically guided injections

were made through holes in the dorsal surface of the cranium. Glass capillary tubes were pulled (HEKA pipette puller PIP5) and tips broken to 40 µm diameter. Capillaries were filled with Dextran Alexa Fluor 568 (Invitrogen). Pressure injections of tracer (0.1 µl for 10min) were targeted to the NAcc (80 nl) or dorsal striatum (200 nl) for VTA or SNc neurons labeling, respectively. Micropipettes were left in place 10 min before removal to minimize leakage. The stereotaxic coordinates used for these injections were obtained from the atlas (Paxinos and Franklin, 2001) adapted and checked in pilot experiments for P15 mice (NAcc AP +1, ML +0.6, DV -3.5; Dst AP +1, ML +1.5, DV -2 both to bregma and dura surface, respectively. Correct placement site was verified by red-dextran injection. After a 10 days survival, the animals were proceed for the single cell PCR experiment.

Binding assays. Mice were decapitated and brain regions, including the prefrontal cortex and striatum, were dissected on ice and homogenized with 25 ml of ice cold buffer containing 50mM Tris, 5mM MgCl2, pH 7.4. Homogenates were centrifuged for 20 min at 15,000x g. The pellet was resuspended and centrifuged under the same condition three times. To the final suspension (0.2-0.6 mg/ml) was added for one hour, [^{3}H]raclopride (81.3Ci/mmol; Perkin Elmer; USA) or [^{3}H]SCH23390 (85.6Ci/mmol; Perkin Elmer; USA) (2 nM) for D2 and D1 receptors binding, respectively. The process was terminated by immersing the tubes in ice-cold buffer followed by rapid filtration through Whatman GF/B filters. Radioactivity was measured using liquid scintillation counting. Binding data were analyzed using the iterative non-linear fitting software GraphPad Prism 6 to estimate dissociation constants (K_D) and maximum number of sites (B_{max}).

Results

Permanent genetic 5-HT$_{2B}$-receptor inactivation increases locomotor effects of cocaine. The dose-dependent locomotor activity recorded every 5 min was evaluated after an intraperitoneal (ip) injection of cocaine (7.5 and 15 mg/kg) 30 min after the start of the session and recorded for the following 60 min. A first injection of cocaine (7.5 mg/kg, **Fig. 1a** or 15 mg/kg, **Fig. 1b**) induced a stronger increase in locomotor activity in *Htr2b*$^{-/-}$ than *Htr2b*$^{+/+}$ mice. Behavioral sensitization can be measured by enhancement of drug-evoked locomotor responses following repeated drug exposure or injections performed a week apart (Stewart and Badiani, 1993; Valjent et al., 2010). A second cocaine injection, at the same dose, seven days after the first, increased locomotion of both *Htr2b*$^{-/-}$ and *Htr2b*$^{+/+}$ mice compared to the first injection, and the *Htr2b*$^{-/-}$ mice exhibited higher cocaine-induced locomotor response than *Htr2b*$^{+/+}$ mice. The fold increase in cocaine induced-locomotor activity at the second injection with respect to the first was similar in both genotypes (**Fig. 1a,b**) at either 7.5 or 15 mg/kg dose. Of note the locomotor activity at the first injection in *Htr2b*$^{-/-}$ was similar to that at the second in sensitized *Htr2b*$^{+/+}$ mice.

Permanent pharmacological 5-HT$_{2B}$-receptor blockade increases locomotor effects of cocaine. We used injection of 5-HT$_{2B}$ receptor antagonists in wildtype mice to confirm the effect of receptor ablation on cocaine-induced locomotion. Interestingly, we did not observe difference in cocaine-(15 mg/kg) induced locomotion in *Htr2b*$^{+/+}$ mice after a single ip injection of the highly selective and potent 5-HT$_{2B}$ receptor antagonist, RS127445 (0.5 mg/kg) (Bonhaus et al., 1999), compared to vehicle treated mice (**Fig. 2a**). Similar absence of differential effects was obtained with the 5-HT$_{2B/2C}$ receptor antagonist SB206553 (3 mg/kg) (**Fig. 2a**). We then evaluated whether the enhanced locomotor response to cocaine in *Htr2b*$^{-/-}$ mice was developmentally mediated or due to long-term neuroadaptations following permanent

inhibition of the receptor activity in adult *Htr2b*$^{+/+}$ mice. A four weeks treatment with RS127445 (1 mg/kg/d) by subcutaneous (sc) release with mini-osmotic pumps (Launay et al., 2002) of adult mice, significantly enhanced cocaine-(15 mg/kg) induced locomotor response after a first injection (**Fig. 2b**) compared to vehicle-treated mice. A second cocaine injection, at the same dose seven days after the first, increased more the locomotion of RS127445-chronically treated *Htr2b*$^{+/+}$ mice compared to vehicle-treated *Htr2b*$^{+/+}$ and to the first injection. The fold increase in cocaine induced-locomotor activity at the second injection with respect to the first was similar (**Fig. 2b)**. Together these results suggest that permanent inactivation of the 5-HT$_{2B}$ receptor leads to increased sensitivity to cocaine as measured by locomotor responses, independently of putative consequences of the receptor knockout during embryonic development.

The lack of 5-HT$_{2B}$ receptor reduces ventral striatal cocaine-induced DA accumulation and ERK1/2 phosphorylation. To further investigate the consequences of the loss of 5-HT$_{2B}$ receptor expression, we compared monoamine extracellular concentrations after cocaine injection in *Htr2b*$^{+/+}$ and *Htr2b*$^{-/-}$ mice first measured by microdialysis. In awake *Htr2b*$^{-/-}$ mice, cocaine (20 mg/kg) elicited a significantly lower increase (2.5-fold) in DA extracellular levels in the NAcc compared to *Htr2b*$^{+/+}$ mice, in which extracellular DA concentration increased 10-fold (**Fig. 3a).** Of note, no difference in extracellular 5-HT accumulation was observed (**Fig. 3a**). Striatal extracellular signal-regulated kinase (ERK)1/2 phosphorylation is a marker of DA-dependent D1 receptor stimulation and an essential component of signaling pathways initiating synaptic plasticity and long-term behavioral effects of drugs of abuse (Girault et al., 2007). After cocaine injection and locomotor recordings (**Fig. 3b**), we quantified phosphorylated-ERK1/2 (p-ERK1/2) immunoreactive neurons in various areas of the striatum of *Htr2b*$^{+/+}$ and *Htr2b*$^{-/-}$ mice (**Fig. 3c-e**). Activated neurons in vehicle and cocaine conditions displayed globally an equivalent amount of p-ERK1/2 staining, and immunoreactive areas of p-ERK1/2 (not illustrated). Cocaine induced a significantly lower number in p-ERK1/2 immuno-positive neurons in the NAcc shell of *Htr2b*$^{-/-}$ than *Htr2b*$^{+/+}$ mice (4-fold vs. 10-fold) (**Fig. 3e**). By contrast, the increase in the number of p-ERK1/2 immuno-positive neurons in NAcc core and dorsal striatum did not differ between genotypes (**Fig. 3e**). These results are in agreement with the microdialysis data for the whole NAcc. Altogether these results suggest that reduced extracellular accumulation of DA blunts cocaine-dependent activation of the ERK1/2 pathway in medium spiny neurons of the NAcc shell from *Htr2b*$^{-/-}$ mice without modification of activity in the dorsal striatum.

The lack of 5-HT$_{2B}$ receptor increases locomotor effects of D1 agonist. Since cocaine-dependent ERK1/2 activation relies on D1 receptor-expressing neurons, we assessed the locomotor response to D1 receptor agonist. An acute injection of the D1 receptor agonist, SKF81297 (2 mg/kg) increased locomotor activity significantly more in *Htr2b*$^{-/-}$ than in *Htr2b*$^{+/+}$ mice (**Fig. 4a**). A second SKF81297 injection, seven days after the first, increased locomotion of both *Htr2b*$^{-/-}$ and *Htr2b*$^{+/+}$ mice compared to the first injection (**Fig. 4a**), and *Htr2b*$^{-/-}$ mice exhibited higher SKF81297-induced locomotor response than *Htr2b*$^{+/+}$ mice (**Fig. 4a**). The fold increase in cocaine induced-locomotor activity at the second SKF81297 injection with respect to the first was similar in both genotypes. Nevertheless, basal expression of D1 and D2 receptors in *Htr2b*$^{-/-}$ mice did not differ from *Htr2b*$^{+/+}$ mice (**Fig. 4b,c**), and neither did D1 receptor coupling to Gαolf (**Fig. 4b,d**). Moreover, there was no difference in striatal DAT, SERT, NET expression between *Htr2b*$^{+/+}$ and *Htr2b*$^{-/-}$ mice (Doly et al., 2008; Banas et al., 2011; Diaz et al., 2012). These results suggest that D1 receptors are sensitized in *Htr2b*$^{-/-}$ mice without modification of receptor, Gαolf, or transporter expression.

Meso-accumbens DA neurons express 5-HT$_{2B}$ receptors. To understand how the 5-HT$_{2B}$ receptor could affect cocaine-induced activation of the NAcc, we evaluated its expression in VTA DA neurons. In the absence of reliable antibody against 5-HT$_{2B}$ receptors in mice, we performed single-cell RT-PCR by extracting cytoplasmic RNA of single identified DA neurons expressing GFP from brain slices of *Drd2-EGFP* mice. We found that among D2- and tyrosine hydroxylase (TH)-positive neurons of the VTA, 40% expressed *Htr2b* mRNA (**Fig. 5a**). The two primary efferent fiber projections of the DA neurons from VTA are the mesocortical and mesolimbic pathways, innervating the prefrontal cortex and the NAcc, respectively (Lammel et al., 2014). We anticipated that among the VTA neurons expressing *Htr2b*, some would send projections to the NAcc and dorsal striatum. To visualize these cells, we stereotactically injected red-dextran into the NAcc shell (**Fig. 5b-d)** or dorsal striatum **(Fig. 5e,f**) of *Drd2-EGFP* mice and traced retrograde transport. We found that DA neurons projecting to the NAcc shell originated from the parabrachial pigmented area of the VTA (**Fig. 5c,d)**, as previously reported (Ikemoto, 2007). Strikingly, by performing single cell RT-PCR on double-labeled neuron (**Fig. 5b)**, we found that all double-labeled (*Drd2-EGFP* and NAcc shell-injected red-dextran) neurons expressed the 5-HT$_{2B}$ receptor (n = 13 out of 13). These data support a selective expression of 5-HT$_{2B}$ receptors in mesolimbic DA neurons sending axons to NAcc shell.

Conditional knockout of 5-HT$_{2B}$ receptor genes in DA neurons increases locomotor effects of cocaine. To functionally validate the 5-HT$_{2B}$-receptor expression in DA neurons, we generated conditional knockout mice by inserting recombination sites (loxP) flanking the *Htr2b* first coding exon (*Htr2b$^{fl/fl}$*) (**Fig. 6a-c**). We crossed mice expressing the Cre recombinase under a DA transporter promoter (*Dat-Slc6a3*) (*Dat-Cre$^{+/0}$*) with these *Htr2b$^{fl/fl}$* mice, generating *Htr2b^{DAKO}*. We verified the proper recombination in TH-positive DA neurons (**Fig. 6b,c**). A first injection of cocaine (20 mg/kg) induced a stronger increase in locomotor activity in *Htr2b^{DAKO}* mice than in control littermates *Htr2b$^{fl/fl}$* mice (**Fig. 6d**). The locomotor effect of a challenge dose of cocaine seven days later (second injection) was also significantly enhanced in comparison to the first, and the *Htr2b^{DAKO}* mice exhibited higher cocaine-induced locomotor response than *Htr2b$^{fl/fl}$* control mice (**Fig. 6d**). The fold increase in cocaine induced-locomotor activity at the second injection with respect to the first was similar in both genotypes (**Fig. 6d**). Thus, mice that underwent selective *Htr2b* inactivation in DA neurons displayed increased locomotor responses to cocaine. These data confirmed that inactivation of the receptor in DA neurons is, at least in part, responsible for locomotor effects and potentially for modulation of DA neuron activity.

The lack of 5-HT$_{2B}$ receptors modulates VTA DA cell excitability. We next tested the hypothesis that 5-HT$_{2B}$ receptors expressed by VTA DA neurons directly modulate activity of these neurons, first, by recording electrophysiological activity *in-vivo* in *Htr2b$^{+/+}$* and *Htr2b$^{-/-}$* mice. Mice were anesthetized and electrophysiologically active cells encountered in a stereotactically defined block of brain tissue including the VTA were recorded; only cells that met all criteria for VTA DA neurons were recorded: (i) a typical triphasic action potential with a marked negative deflection; (ii) a characteristic long-duration (>2.0 ms) action potential; (iii) an action potential width from start to negative of >1.1 ms; (iv) a slow firing rate (<10 Hz) with an irregular single spiking pattern (tonic) and occasional short, slow bursting (phasic) activity (Grace and Bunney, 1984a, b; Gonon, 1988; Mameli-Engvall et al., 2006). Juxtacellular single unit recordings were obtained in anesthetized *Htr2b$^{+/+}$* and *Htr2b$^{-/-}$* mice, respectively (**Fig. 7a**). Activity of DA cells was then characterized using the firing rate and the percentage of spikes within a burst (% SWB). DA cells fired at an average rate of 1.6 ± 0.2 Hz in *Htr2b$^{+/+}$* and 1.8 ± 0.1 Hz in *Htr2b$^{-/-}$* mice (n = 57-58). The mean percentage of burst firing in individual cells

ranged from 0% to 16% in *Htr2b*$^{+/+}$ and 0% to 60% in *Htr2b*$^{-/-}$ mice, and was significantly higher in *Htr2b*$^{-/-}$ (5.2 ± 1.5%) than *Htr2b*$^{+/+}$ (1.4 ± 0.5%) mice (**Fig. 7a**).

After baseline recordings, the same mice were ip injected with cocaine and the evoked modification of firing rate was analyzed. Cocaine (20 mg/kg) decreased the firing rate by 62.3% in *Htr2b*$^{+/+}$ mice, while this decrease was significantly greater (90.9%) in *Htr2b*$^{-/-}$ mice (**Fig. 7b**). The decrease in firing rate lasted for more than 30 min after drug delivery and was not always followed by a return to pre-injection levels in *Htr2b*$^{-/-}$ mice. However, systemic ip injection of the D2 agonist quinpirole (0.25-0.5 mg/kg) produced a similar decrease of firing rate in *Htr2b*$^{+/+}$ and *Htr2b*$^{-/-}$ mice (**Fig. 7c**). Our results indicate that long term blockade of 5-HT$_{2B}$ receptor lead to a stronger cocaine-dependent inhibition of DA neurons firing rate and supports the hypothesis that 5-HT modulates VTA DA cell excitability via 5-HT$_{2B}$ receptors without modification of D2 autoreceptor function.

To test whether the lack of 5-HT$_{2B}$ receptors would produce long-lasting synaptic modifications in DA neurons, we used whole-cell patch recordings in acute brain slices. We measured AMPA- and NMDAR-mediated excitatory postsynaptic currents (EPSCs) in voltage clamp mode at +40 mV on horizontal brain slices, which included VTA from *Htr2b*$^{+/+}$ and *Htr2b*$^{-/-}$ mice, in DA neurons (large cells (>30 pF capacitance) from the lateral part of the VTA that are prone to project to the NAcc shell. In *Htr2b*$^{-/-}$, the AMPA/NMDA ratio was significantly increased compared to control mice (*Htr2b*$^{+/+}$: 0.63 ± 0.06, n=7 cells; *Htr2b*$^{-/-}$: 1.01 ± 0.15, n=7 cells) (**Fig. 7d**). Altogether, these results indicated that the lack of 5-HT$_{2B}$ receptors promotes an increase in DA neuron bursting *in-vivo* properties, a stronger reactivity to cocaine, and a concomitant potentiation of AMPA synaptic transmission of VTA DA neurons measured *ex-vivo*.

***Htr2b* inactivation modifies the reinforcing properties of cocaine.** To know if the locomotor activating effects of cocaine are associated with disruptions in the primary reinforcing effects of the drug, we tested whether 5-HT$_{2B}$ receptor deletion altered operant cocaine self-administration. *Htr2b*$^{+/+}$ and *Htr2b*$^{-/-}$ animals were first trained to respond for food pellets under an fixed ratio (FR)1 schedule of reinforcement (18 *Htr2b*$^{+/+}$ and 13 *Htr2b*$^{-/-}$ mice). The discrimination between active and inactive nose-poke responding was rapidly acquired by both *Htr2b*$^{+/+}$ and *Htr2b*$^{-/-}$ mice (**Fig. 8a**), and no statistically significant differences between genotypes were observed during acquisition of food responding (**Fig. 8b**). Following catheter implantation, animals were trained to intravenous saline self-administration until responding rates decreased in order to avoid interference from food responding. Animals were then trained to self-administer cocaine at the dose of 0.25 mg/kg/infusion during 8 days on a FR1 schedule of reinforcement. After acquisition of cocaine responding, *Htr2b*$^{-/-}$ mice earned a significantly lower number of cocaine infusions mainly at the dose of 0.125 and 0.5 mg/kg/infusion (**Fig. 8c**). In addition, *Htr2b*$^{-/-}$ animals showed a lower break point in the progressive ratio schedule of reinforcement test (**Fig. 8d**), although this difference was not statistically significant. We finally characterized the effects of 5-HT$_{2B}$ receptor deletion on post-cocaine reductions in reward system function by analyzing putative effect on sucrose preference. Both cohorts of *Htr2b*$^{+/+}$ and *Htr2b*$^{-/-}$ mice drank similar amounts of water during a 24 h period (**Fig. 8e**), and both showed comparable preference for sucrose-enriched water (**Fig. 8f**). Although learning ability is similar in *Htr2b*$^{-/-}$ mice to *Htr2b*$^{+/+}$, they self-administrate less cocaine, show a trend toward lower breaking point, and display no difference in post-cocaine reward system.

Discussion

Here, we report that mice lacking 5-HT$_{2B}$ receptors totally or exclusively in DA neurons exhibit heightened cocaine-induced locomotor responses independently of putative consequences of the

receptor knockout during embryonic development. The lack of 5-HT_{2B} receptors induces a reduced cocaine-induced DA-accumulation and activation of the NAcc shell medium spiny neurons, without modification of DA signaling in the dorsal striatum and is associated with an over-reactivity to D1 receptor agonist. We describe the selective expression of 5-HT_{2B} receptors in VTA DA neurons sending axons to NAcc shell. An increase in basal DA neuron bursting *in-vivo* properties and a concomitant increase in AMPA synaptic transmission to VTA DA neurons measured *ex-vivo* were found in mice lacking 5-HT_{2B} receptors. The lack of 5-HT_{2B} receptors leads to a stronger inhibition of DA neurons firing rate in response to cocaine without modification of D2 autoreceptor function. Finally, the absence of 5-HT_{2B} receptors is associated with a decreased cocaine operant self-administration with a trend toward a lower break point in the progressive ratio schedule of reinforcement test.

DA and 5-HT interactions are known to be important in mesolimbic and nigrostriatal DA pathways. 5-HT immunoreactive fibers are dense in both VTA and SNc (Hervé et al., 1987). 5-HT_{2A} and 5-HT_{2C} receptors have previously been shown to modulate the effects of cocaine (Cunningham and Anastasio, 2014). We show, here, that the genetic ablation of 5-HT_{2B} receptors increases cocaine-induced locomotor activity, even restricted to DA neurons. However, an acute pharmacologic inhibition does not reproduce this effect. These data are in agreement with previous neuropharmacological data indicating the inability of 5-HT_{2B} receptor antagonists to affect cocaine responses while acute blockade of 5-HT_{2A} and 5-HT_{2C} receptors generated opposing modulatory actions on cocaine-induced activity (Filip et al., 2010; Cunningham and Anastasio, 2014; Devroye et al., 2015). Nevertheless, we show here that a chronic (4 weeks) exposure to a 5-HT_{2B}-receptor antagonist is sufficient to increase the locomotor response to cocaine to the same extent as the increase observed in *Htr2b*$^{-/-}$ mice. Aside of the opposing actions of 5-HT_{2A} and 5-HT_{2C} receptors, 5-HT_{2B} receptors likely modulate directly and indirectly cocaine-induced locomotion via DA-dependent circuitry, since we found that 5-HT_{2B} receptors are expressed in VTA DA neurons projecting to the NAcc shell and that their selective elimination in DA neurons by conditional knockout is sufficient to reproduce the increased cocaine locomotor response. It is clear that 5-HT_{2B} receptor mode of action differs from that of 5-HT_{2A} and 5-HT_{2C} receptors and must affect different DA neuron subpopulation and/or different effectors.

One of our most striking finding is the dissociation between decreased cocaine-induced DA accumulation with subsequent blunted activation of the ERK1/2 pathway selectively in medium spiny neurons of the NAcc shell, and increased locomotor activity. Cocaine, like other drugs of abuse, is known to preferentially increase extracellular DA in the NAcc shell as compared to the core (Di Chiara and Bassareo, 2007). This preferential action has also been demonstrated in rats during acquisition of cocaine self-administration (Lecca et al., 2007). We identified that 100% of the retrogradely labeled DA neurons in the NAcc shell originating from VTA, express 5-HT_{2B} receptors. Interestingly, the reduced activation of the NAcc shell following cocaine injection in *Htr2b*$^{-/-}$ mice does not seem to take place in other striatal areas such as the core and the dorsal striatum as indicated by the lack of effect on cocaine-induced increase of phosphorylated ERK1/2. A similar difference between dorsal striatum and NAcc shell in DA activation was independently reported in rats following amphetamine injection in the presence of a selective 5-HT_{2B} receptor antagonist (Auclair et al., 2010): LY 266097 significantly diminished the increase in DA outflow induced by amphetamine in the NAcc shell, but not in the dorsal striatum. The reduction of DA transmission in the NAcc shell upon cocaine injection may result from a heightened sensitivity to the inhibitory effect of cocaine on the firing of DA neurons projecting to the NAcc shell since we observed that cocaine produced a stronger decrease in firing rate of VTA DA neurons in *Htr2b*$^{-/-}$ mice.

Another explanation to the dissociation between cocaine-induced decrease in DA accumulation, increase in locomotion, and reduction in cocaine self-administration is the increased post-synaptic responsiveness in other striatal areas. An important finding is the observation that a delay is necessary to allow adaptations that are responsible for these apparent paradoxical responses, the increased cocaine response being only an indirect consequence of the 5-HT_{2B} receptor-dependent reduction in DA tone

observed in NAcc and downstream adaptation. Our observation of the sensitized locomotor response to D1 agonists in *Htr2b*$^{-/-}$ mice may be the reason for the apparent discrepancy between the reduction of DA transmission in the NAcc shell associated with increased locomotion. The trend in reduction of the reinforcing properties of cocaine as indicated by reduction in breaking point for cocaine responding in a PR schedule is consistent with the reduction of the DA stimulant effects of cocaine in *Htr2b*$^{-/-}$ mice. These observations suggest that NAcc shell DA acting on D1 receptors (p–ERK findings) is critical for cocaine reinforcement. This conclusion is consistent with recent results obtained in rats, in which D1 receptors have been silenced by siRNA in the NAcc shell while sparing the core, and which were prevented from the acquisition of cocaine self administration (Pisanu et al., 2015). Interestingly, excitatory afferents of VTA DA neurons that project to the NAcc have been shown to be potentiated upon exposure of animals to addictive drugs (Lammel et al., 2012). This induction depends on NMDA and D1 receptors (Ungless et al., 2001), which are activated when DA neurons become active and release DA from their dendrites. The NMDARs that drive this induction are located on DA neurons themselves, supporting that this form of plasticity is a VTA-autonomous process. The ratio of the amplitude of AMPA/NMDA-mediated postsynaptic currents, a parameter often used to quantify synaptic strength in the acute brain slice preparation, becomes higher than normal upon exposure to addictive drugs (Ungless et al., 2001). Here, we found that permanent ablation of the 5-HT_{2B} receptor is associated with higher reactivity to cocaine of VTA DA neurons and higher AMPA/NMDA ratio. These data support that the 5-HT_{2B} receptor acts as an important mediator of drug-evoked synaptic plasticity.

Previous evidence indicated that 5-HT_{2B} receptors could directly modulate 5-HT neurons and indirectly DA neurons. Indeed, genetic (knockout) or pharmacologic manipulation (antagonist) of 5-HT_{2B} receptors interferes with the effects of molecules that directly target the 5-HT system including serotonin selective reuptake inhibitors (SSRI) antidepressant, or amphetamine-derivatives 5-HT releasers MDMA and dexfenfluramine (Doly et al., 2008; Doly et al., 2009; Banas et al., 2011; Diaz et al., 2012). For example, the enhanced locomotor response to the psychostimulant MDMA was abolished in *Htr2b*$^{-/-}$ mice (Doly et al., 2008). These mutant mice did not exhibit behavioral sensitization or conditioned place preference following MDMA (10 mg/kg) injections as following injection of a 5-HT_{2B}-receptor antagonist (RS127445) in wild type mice. Nevertheless, high doses (30 mg/kg) of MDMA induce DA-dependent but 5-HT-independent behavioral effects (Doly et al., 2009). It was also reported that 5-HT_{2B} receptor selective antagonists can reduced significantly the increase in DA outflow induced by amphetamine in the NAcc shell, but not in the dorsal striatum (Auclair et al., 2010). We independently found that *Htr2b*$^{-/-}$ mice display a higher amphetamine-induced locomotion (Pitychoutis et al., 2015). Together with our present findings, these observations clearly distinguish between a direct action of 5-HT_{2B} receptors on 5-HT neurons that is mimicked by antagonists, from an action at DA neurons that requires long term inhibition of 5-HT_{2B} receptors and neuroadaptations i.e., that is not reproduced by direct antagonist injections. This finding is of importance for genetic polymorphisms that permanently affect gene expression such as the *HTR2B* (Gln20Ter) (Bevilacqua et al., 2010).

Several parameters remain to be determined to fully explain our findings, e.g. the exact neural circuits that are modified, or the time during which the blockade of 5-HT_{2B} receptor activity is necessary to produced the observed changes in reactivity to cocaine. Nevertheless, this work established for the first time that permanently inactive 5-HT_{2B} receptor is associated with a local hypodopaminergy that paradoxically and ultimately results in increased cocaine psychostimulant responses and a trend toward blunted motivation to the drug. To sum up, the chronic 5-HT_{2B}-receptor inhibition makes mice behaving as animals already exposed to cocaine with higher cocaine-induced locomotion associated with changes in DA neuron reactivity.

References

Auclair AL, Cathala A, Sarrazin F, Depoortère R, Piazza PV, Newman-Tancredi A, Spampinato U (2010) The central serotonin 2B receptor: a new pharmacological target to modulate the mesoaccumbens dopaminergic pathway activity. J Neurochem 114:1323-1332.

Banas S, Doly S, Boutourlinsky K, Diaz S, Belmer A, Callebert J, Collet C, Launay J-M, Maroteaux L (2011) Deconstructing antiobesity compound action: requirement of serotonin 5-HT2B receptors for dexfenfluramine anorectic effects. Neuropsychopharmacology 36:423–433.

Bertran-Gonzalez J, Bosch C, Maroteaux M, Matamales M, Herve D, Valjent E, Girault JA (2008) Opposing patterns of signaling activation in dopamine D1 and D2 receptor-expressing striatal neurons in response to cocaine and haloperidol. J Neurosci 28:5671-5685.

Bevilacqua L, Doly S, Kaprio J, Yuan Q, Tikkanen R, Paunio T, Zhou Z, Wedenoja J, Maroteaux L, Diaz S, Belmer A, Hodgkinson C, Dell'Osso L, Suvisaari J, Coccaro E, Rose R, Peltonen L, Virkkunen M, Goldman D (2010) A population-specific HTR2B stop codon predisposes to severe impulsivity. Nature 468:1061-1066.

Bonhaus DW, Flippin LA, Greenhouse RJ, Jaime S, Rocha C, Dawson M, Van Natta K, Chang LK, Pulido-Rios T, Webber A, Leung E, Eglen RM, Martin GR (1999) RS-127445: a selective, high affinity, orally bioavailable 5-HT2B receptor antagonist. Br J Pharmacol 127:1075-1082.

Cauli B, Audinat E, Lambolez B, Angulo MC, Ropert N, Tsuzuki K, Hestrin S, Rossier J (1997) Molecular and physiological diversity of cortical nonpyramidal cells. J Neurosci 17:3894-3906.

Corvol JC, Studler JM, Schonn JS, Girault JA, Hervé D (2001) Galpha(olf) is necessary for coupling D1 and A2a receptors to adenylyl cyclase in the striatum. J Neurochem 76:1585-1588.

Cunningham KA, Anastasio NC (2014) Serotonin at the nexus of impulsivity and cue reactivity in cocaine addiction. Neuropharmacology 76 Pt B:460-478.

Devroye C, Cathala A, Di Marco B, Caraci F, Drago F, Piazza PV, Spampinato U (2015) Central serotonin2B receptor blockade inhibits cocaine-induced hyperlocomotion independently of changes of subcortical dopamine outflow. Neuropharmacology 97:329-337.

Devroye C, Cathala A, Haddjeri N, Rovera R, Vallee M, Drago F, Piazza PV, Spampinato U (2016) Differential control of dopamine ascending pathways by serotonin2B receptor antagonists: New opportunities for the treatment of schizophrenia. Neuropharmacology 109:59-68.

Di Chiara G, Bassareo V (2007) Reward system and addiction: what dopamine does and doesn't do. Current Opinion in Pharmacology 7:69-76.

Di Giovanni G, Esposito E, Di Matteo V (2010) Role of serotonin in central dopamine dysfunction. CNS Neuroscience & Therapeutics 16:179-194.

Diaz SL, Doly S, Narboux-Nême N, Fernandez S, Mazot P, Banas S, Boutourlinsky K, Moutkine I, Belmer A, Roumier A, Maroteaux L (2012) 5-HT2B receptors are required for serotonin-selective antidepressant actions. Mol Psychiatry 17:154-163.

Doly S, Valjent E, Setola V, Callebert J, Herve D, Launay JM, Maroteaux L (2008) Serotonin 5-HT2B receptors are required for 3,4-methylenedioxymethamphetamine-induced hyperlocomotion and 5-HT release in vivo and in vitro. J Neurosci 28:2933-2940.

Doly S, Bertran-Gonzalez J, Callebert J, Bruneau A, Banas SM, Belmer A, Boutourlinsky K, Herve D, Launay JM, Maroteaux L (2009) Role of serotonin via 5-HT2B receptors in the reinforcing effects of MDMA in mice PLoS ONE 4:e7952.

Filip M, Alenina N, Bader M, Przegaliński E (2010) Behavioral evidence for the significance of serotoninergic (5-HT) receptors in cocaine addiction. Addiction Biology 15:227-249.

Girault JA, Valjent E, Caboche J, Herve D (2007) ERK2: a logical AND gate critical for drug-induced plasticity? Curr Opin Pharmacol 7:77-85.

Glangetas C, Fois GR, Jalabert M, Lecca S, Valentinova K, Meye FJ, Diana M, Faure P, Mameli M, Caille S, Georges F (2015) Ventral Subiculum Stimulation Promotes Persistent Hyperactivity of Dopamine Neurons and Facilitates Behavioral Effects of Cocaine. Cell reports 13:2287-2296.

Goldman D, Oroszi G, Ducci F (2005) The genetics of addictions: uncovering the genes. Nat Rev Genet 6:521-532.

Gong S, Zheng C, Doughty ML, Losos K, Didkovsky N, Schambra UB, Nowak NJ, Joyner A, Leblanc G, Hatten ME, Heintz N (2003) A gene expression atlas of the central nervous system based on bacterial artificial chromosomes. Nature 425:917-925.

Gonon FG (1988) Nonlinear relationship between impulse flow and dopamine released by rat midbrain dopaminergic neurons as studied by in vivo electrochemistry. Neuroscience 24:19-28.

Grace AA, Bunney BS (1984a) The control of firing pattern in nigral dopamine neurons: single spike firing. J Neurosci 4:2866-2876.

Grace AA, Bunney BS (1984b) The control of firing pattern in nigral dopamine neurons: burst firing. J Neurosci 4:2877-2890.

Hayes DJ, Greenshaw AJ (2011) 5-HT receptors and reward-related behaviour: a review. Neurosci Biobehav Rev 35:1419-1449.

Hervé D, Pickel VM, Joh TH, Beaudet A (1987) Serotonin axon terminals in the ventral tegmental area of the rat: fine structure and synaptic input to dopaminergic neurons. Brain Research 435:71-83.

Hnasko TS, Sotak BN, Palmiter RD (2007) Cocaine-conditioned place preference by dopamine-deficient mice is mediated by serotonin. J Neurosci 27:12484-12488.

Hyman SE, Malenka RC, Nestler EJ (2006) Neural Mechanisms of Addiction: The Role of Reward-Related Learning and Memory. Annu Rev Neurosci 29:565-598.

Ikemoto S (2007) Dopamine reward circuitry: two projection systems from the ventral midbrain to the nucleus accumbens-olfactory tubercle complex. Brain Res Rev 56:27-78.

Kirby LG, Zeeb FD, Winstanley CA (2011) Contributions of serotonin in addiction vulnerability. Neuropharmacology 61:421-432.

Lammel S, Lim BK, Malenka RC (2014) Reward and aversion in a heterogeneous midbrain dopamine system. Neuropharmacology 76 Pt B:351-359.

Lammel S, Hetzel A, Häckel O, Jones I, Liss B, Roeper J (2008) Unique properties of mesoprefrontal neurons within a dual mesocorticolimbic dopamine system. Neuron 57:760-773.

Lammel S, Lim BK, Ran C, Huang KW, Betley MJ, Tye KM, Deisseroth K, Malenka RC (2012) Input-specific control of reward and aversion in the ventral tegmental area. Nature 491:212-217.

Launay JM, Hervé P, Peoc'h K, Tournois C, Callebert J, Nebigil C, Etienne N, Drouet L, Humbert M, Simonneau G, Maroteaux L (2002) Function of the serotonin 5-hydroxytryptamine 2B receptor in pulmonary hypertension. Nat Med 8:1129-1135.

Lecca D, Cacciapaglia F, Valentini V, Acquas E, Di Chiara G (2007) Differential neurochemical and behavioral adaptation to cocaine after response contingent and noncontingent exposure in the rat. Psychopharmacology (Berl) 191:653-667.

Luedtke RR, Griffin SA, Conroy SS, Jin X, Pinto A, Sesack SR (1999) Immunoblot and immunohistochemical comparison of murine monoclonal antibodies specific for the rat D1a and D1b dopamine receptor subtypes. J Neuroimmunol 101:170-187.

Lüscher C (2016) The Emergence of a Circuit Model for Addiction. Annual review of neuroscience 39:257-276.

Mameli-Engvall M, Evrard A, Pons S, Maskos U, Svensson TH, Changeux J-P, Faure P (2006) Hierarchical control of dopamine neuron-firing patterns by nicotinic receptors. Neuron 50:911-921.

Müller CP, Homberg JR (2015) The role of serotonin in drug use and addiction. Behav Brain Res 277:146-192.

Paxinos G, Franklin KBJ (2001) The mouse brain in stereotaxic coordinates. San Diego: Academic Press.

Pisanu A, Lecca D, Valentini V, Bahi A, Dreyer J-L, Cacciapaglia F, Scifo A, Piras G, Cadoni C, Di Chiara G (2015) Impairment of acquisition of intravenous cocaine self-

administration by RNA-interference of dopamine D1-receptors in the nucleus accumbens shell. Neuropharmacology 89:398-411.

Pitychoutis P, Belmer A, Moutkine I, Adrien J, Maroteaux L (2015) Mice lacking the serotonin Htr2B receptor gene present an antipsychotic-sensitive schizophrenic-like phenotype. Neuropsychopharmacology 40:2764-2773.

Soria G, Mendizabal V, Tourino C, Robledo P, Ledent C, Parmentier M, Maldonado R, Valverde O (2005) Lack of CB1 cannabinoid receptor impairs cocaine self-administration. Neuropsychopharmacology 30:1670-1680.

Stewart J, Badiani A (1993) Tolerance and sensitization to the behavioral effects of drugs. Behav Pharmacol 4:289-312.

Turiault M, Parnaudeau S, Milet A, Parlato R, Rouzeau J-D, Lazar M, Tronche F (2007) Analysis of dopamine transporter gene expression pattern -- generation of DAT-iCre transgenic mice. FEBS J 274:3568-3577.

Ungless MA, Whistler JL, Malenka RC, Bonci A (2001) Single cocaine exposure in vivo induces long-term potentiation in dopamine neurons. Nature 411:583-587.

Valjent E, Bertran-Gonzalez J, Aubier B, Greengard P, Hervé D, Girault J-A (2010) Mechanisms of locomotor sensitization to drugs of abuse in a two-injection protocol. Neuropsychopharmacology 35:401-415.

Figure 1

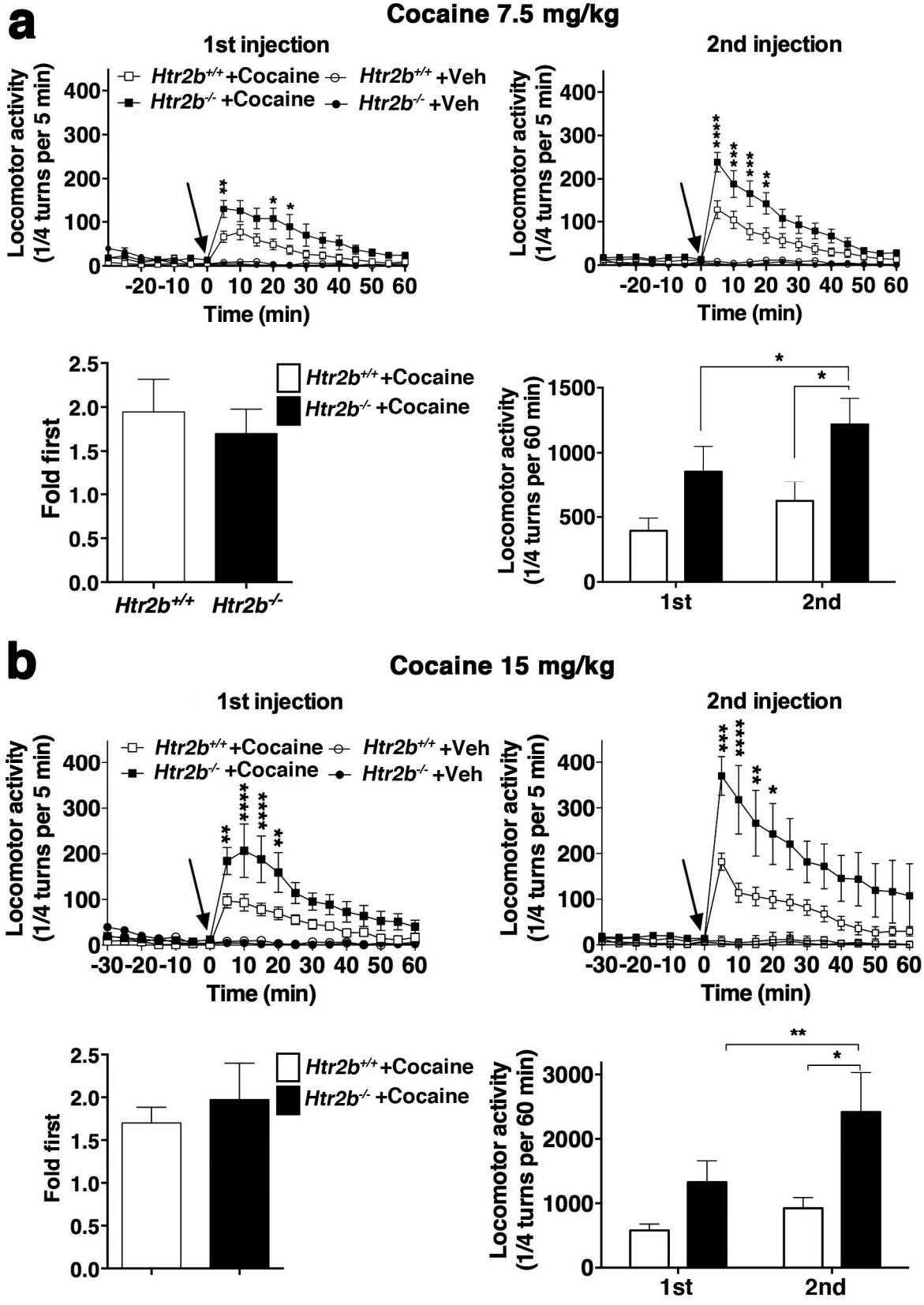
a
Cocaine 7.5 mg/kg
1st injection
2nd injection
Locomotor activity (1/4 turns per 5 min)
Htr2b+/+ +Cocaine
Htr2b-/- +Cocaine
Htr2b+/+ +Veh
Htr2b-/- +Veh
Time (min)
Fold first
Htr2b+/+
Htr2b-/-
Locomotor activity (1/4 turns per 60 min)
1st
2nd
b
Cocaine 15 mg/kg
1st injection
2nd injection
Locomotor activity (1/4 turns per 5 min)
Time (min)
Fold first
Locomotor activity (1/4 turns per 60 min)
1st
2nd

Fig. 1. Dose-dependent effects of 5-HT_{2B} receptor knockout on cocaine responses. a : Higher locomotor response to cocaine injection (7.5 mg/kg) of *Htr2b*$^{-/-}$ mice. The locomotor activity was recorded every 5 min. Cocaine was injected after 30 min of habituation and locomotion recorded for the following 60 min. An injection of cocaine (7.5 mg/kg) increased more the locomotor activity in *Htr2b*$^{-/-}$ (cocaine, black square; vehicle, black circle, n = 12-8) than in *Htr2b*$^{+/+}$ mice (cocaine, white square; vehicle, open circle, n = 12-8; 1st injection, left, arrow cocaine injection t = 0). Data analyzed by two-way ANOVA repeated measures (RM) showed a main effect of genotype ($F_{(1, 22)}$ = 6.04, *p=0.022*). The stimulant locomotor effect of a challenge dose of cocaine seven days later (2nd injection, right, arrow cocaine injection t = 0) was significantly higher in *Htr2b*$^{-/-}$ than in *Htr2b*$^{+/+}$ mice (effect of genotype $F_{(1, 22)}$ = 6.44, *p=0.022*). The increase in cocaine induced-locomotor activity at the second injection was similar in respect to the first (Fold first) (left, n=12-12; unpaired t-test t_{22} = 0.528, P = 0.60). Total locomotor activity recorded over 60 min after a 2nd injection (right) was significantly higher in *Htr2b*$^{-/-}$ (black bars) compared to *Htr2b*$^{+/+}$ mice (white bars) and to the 1st injection (Factor genotype $F_{(1, 22)}$ = 6.44, *p=0.019*; factor injection $F_{(1, 22)}$ = 776, *p=0.010*), as analyzed using two-way ANOVA RM for cocaine (means ± SEM, n = 12-12); Bonferroni post-hoc tests were applied to each graph, *P < 0.05; **P < 0.01; ***P < 0.001; ****P<0.0001. **b : Higher locomotor response to cocaine injection (15 mg/kg) of *Htr2b*$^{-/-}$ mice.** An injection of cocaine (15mg/kg) increased more the locomotor activity in *Htr2b*$^{-/-}$ (cocaine, black square; vehicle, black circle, n = 12-8) than in *Htr2b*$^{+/+}$ mice (cocaine, white square; vehicle, open circle, n = 12-8) (1st injection, left, arrow cocaine injection t = 0). Data analyzed by two-way ANOVA RM showed a main effect of genotype ($F_{(1, 22)}$ = 5.22, *p=0.032*). The stimulant locomotor effect of a challenge dose of cocaine seven days later (2nd injection, right, arrow cocaine injection t = 0) was also significantly higher in *Htr2b*$^{-/-}$ compared to *Htr2b*$^{+/+}$ mice (genotype $F_{(1, 22)}$ = 5.62, *p=0.027*). The increase in cocaine induced-locomotor activity at the second injection was similar in respect to the first (Fold first) (left, n=12-12; unpaired t-test t_{22} = 0.592, P = 0.56). Total locomotor activity recorded over 60 min after a 2nd injection (right) was significantly higher in *Htr2b*$^{-/-}$ (black bars) compared to *Htr2b*$^{+/+}$ mice (white bars) and to the 1st injection (Factor genotype $F_{(1, 22)}$ = 6.02, *p=0.022*; factor injection $F_{(1, 22)}$ = 9.76, *p=0.005*), as analyzed using two-way ANOVA RM (n = 12-12) (means ± SEM). Bonferroni post-hoc tests were applied to each graph, *P < 0.05; **P < 0.01; ***P < 0.001; ****P<0.0001.

Figure 2

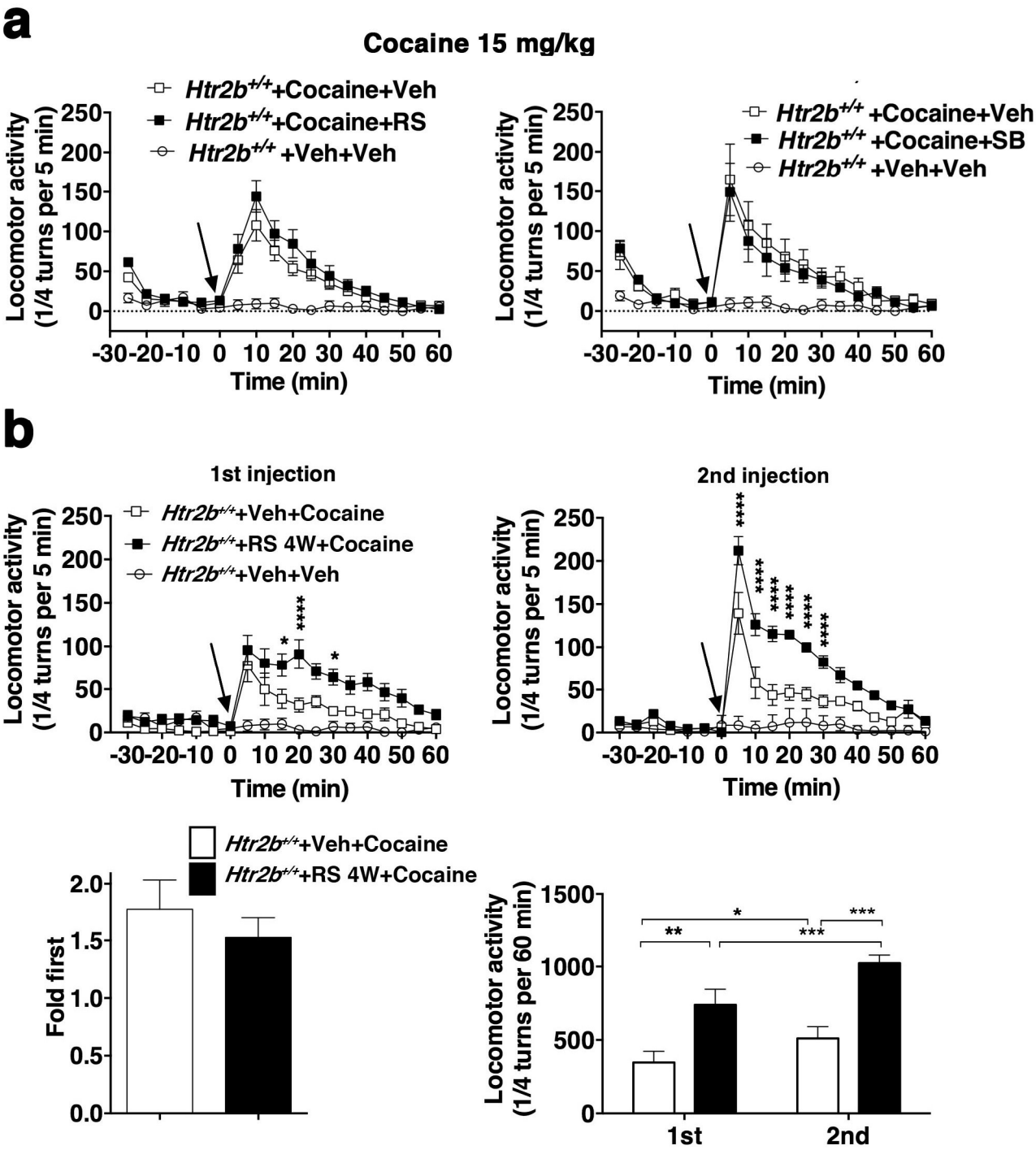
a
Cocaine 15 mg/kg
Htr2b+/+ +Cocaine+Veh
Htr2b+/+ +Cocaine+RS
Htr2b+/+ +Veh+Veh
Locomotor activity (1/4 turns per 5 min)
Time (min)
Htr2b+/+ +Cocaine+Veh
Htr2b+/+ +Cocaine+SB
Htr2b+/+ +Veh+Veh
b
1st injection
Htr2b+/+ +Veh+Cocaine
Htr2b+/+ +RS 4W+Cocaine
Htr2b+/+ +Veh+Veh
2nd injection
Fold first
Locomotor activity (1/4 turns per 60 min)
1st
2nd

Fig. 2. Effects of 5-HT_{2B} receptor pharmacological blockade on cocaine response. a : Lack of effect of a single injection of 5-HT_{2B} receptor antagonists on cocaine-induced locomotion. Locomotor activity was not different in response to 15 mg/kg of cocaine ip co-injected with saline vehicle (Veh-white square) or with a selective 5-HT_{2B} receptor antagonist (RS127445 0.5 mg/kg-RS, black square) (left) or a 5-$HT_{2B/2C}$ receptor antagonist (SB206553 3 mg/kg-SB) (right) (black square) in *Htr2b*$^{+/+}$ mice. Data were analyzed using two-way ANOVA RM for cocaine (means ± SEM, n = 7-12). **b : Mice exposed 4 weeks to RS127445 show increased locomotor responses to cocaine.** An injection of cocaine (15 mg/kg) increased locomotor activity more in 4 weeks RS127445-treated (cocaine, black square; vehicle, black circle, n =8-8) than in vehicle-treated *Htr2b*$^{+/+}$ mice (cocaine, white square; vehicle, open circle, n = 8-8) (1st injection, left, arrow cocaine injection t = 0). Two-way ANOVA RM showed a main effect of RS127445 ($F_{(1, 14)}$ = 6.02, *p=0.042*). The stimulant locomotor effect of a challenge dose of cocaine seven days later (2nd injection, right, arrow cocaine injection t = 0) was also significantly higher in 4 weeks RS127445-treated compared to vehicle-treated *Htr2b*$^{+/+}$ mice (cocaine, white square; vehicle, open circle) (effect of RS127445 $F_{(1, 14)}$ = 25.19, *p=0.0002*). The increase in cocaine induced-locomotor activity at the second injection was similar in respect to the first (Fold first) (n = 8-8, left; unpaired t-test t_{14} = 0.808, P = 0.43). Total locomotor activity recorded over 60 min after a 1st injection of cocaine and a 2nd injection (right) was significantly higher in 4 weeks RS127445-treated compared to vehicle-treated *Htr2b*$^{+/+}$ mice and to the first injection (effect of RS127445 $F_{(1, 14)}$ = 17.43, *p=0.0009*; factor injection $F_{(1, 14)}$ = 31.59, *p<0.0001*), as analyzed using two-way ANOVA RM (n = 8-8) (means ± SEM). Bonferroni post-hoc tests were applied to each graph, *P < 0.05; **P < 0.01; ***P < 0.001; ****P < 0.0001.

Figure 3

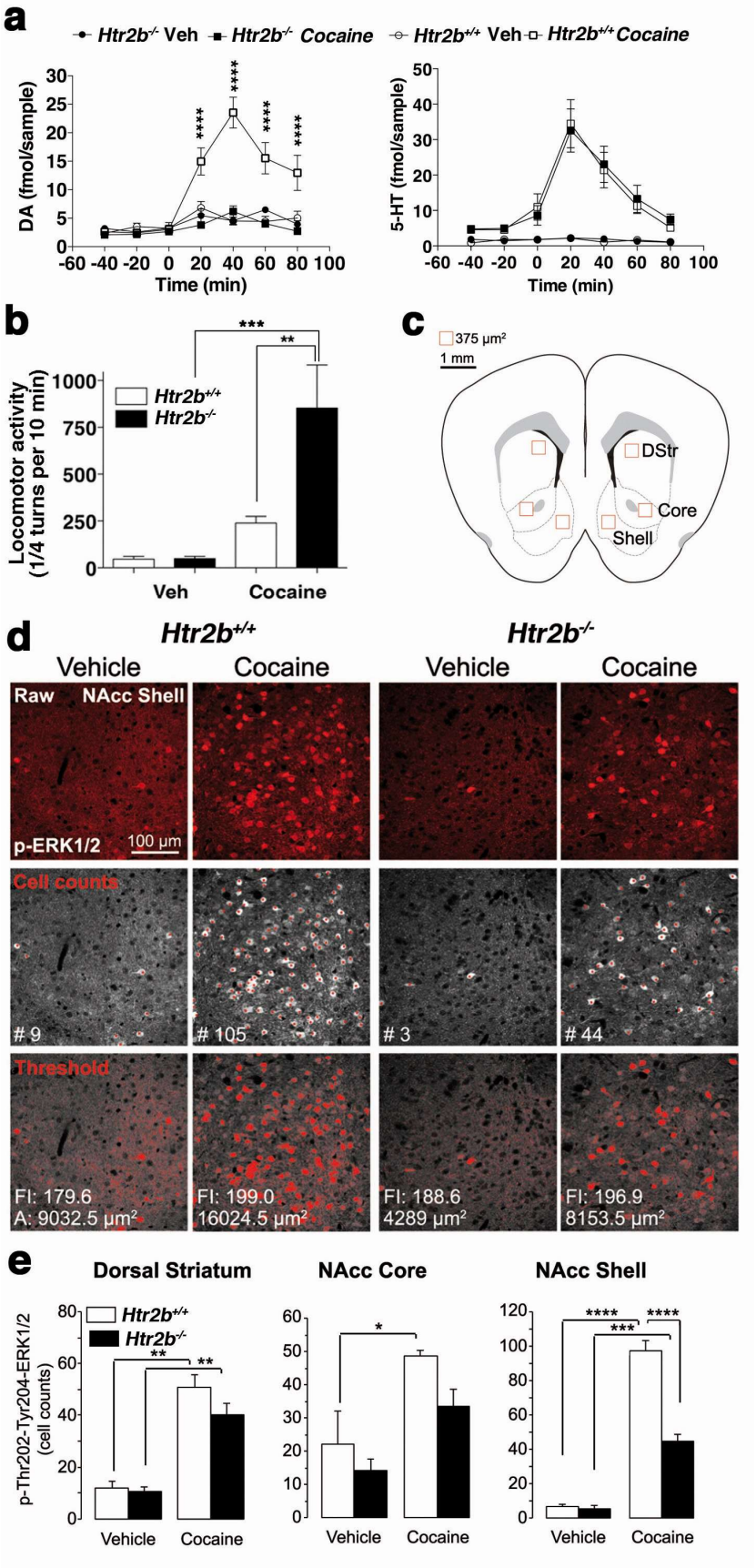
a
Htr2b-/- Veh
Htr2b-/- Cocaine
Htr2b+/+ Veh
Htr2b+/+ Cocaine
DA (fmol/sample)
Time (min)
5-HT (fmol/sample)
Time (min)
b
Locomotor activity (1/4 turns per 10 min)
Htr2b+/+
Htr2b-/-
Veh
Cocaine
c
375 µm²
1 mm
DStr
Core
Shell
d
Htr2b+/+
Htr2b-/-
Vehicle
Cocaine
Vehicle
Cocaine
Raw
NAcc Shell
p-ERK1/2
100 µm
Cell counts
9
105
3
44
Threshold
FI: 179.6
A: 9032.5 µm²
FI: 199.0
16024.5 µm²
FI: 188.6
4289 µm²
FI: 196.9
8153.5 µm²
e
Dorsal Striatum
NAcc Core
NAcc Shell
p-Thr202-Tyr204-ERK1/2 (cell counts)
Htr2b+/+
Htr2b-/-
Vehicle
Cocaine
Vehicle
Cocaine
Vehicle
Cocaine

Fig. 3. Effect of 5-HT$_{2B}$ receptor knockout on cocaine-dependent striatal activation. a : Lower extracellular DA but identical 5-HT accumulation in NAcc of cocaine-treated *Htr2b*$^{-/-}$ mice. 5-HT and DA extracellular concentrations were assessed by microdialysis in the NAcc of awake mice. After cocaine (20 mg/kg) injection (t = 0), extracellular DA was significantly elevated in *Htr2b*$^{+/+}$ (white square) compared to *Htr2b*$^{-/-}$ (black square) or saline control (black and white circle) mice. Two-way ANOVA RM showed a main effect of genotype ($F_{(1, 13)} = 43.29$, $p<0.0001$). No difference in NAcc 5-HT extracellular concentrations in *Htr2b*$^{+/+}$ (white square) and *Htr2b*$^{-/-}$ (black square) mice, as analyzed using two-way ANOVA RM for cocaine (means ± SEM, n = 7-8). Bonferroni post-hoc tests were applied to each graph, ****P < 0.0001 vs. *Htr2b*$^{+/+}$ cocaine. **b-g** : **Reduced ERK1/2 phosphorylation in ventral, but not in dorsal striatum of cocaine-treated *Htr2b*$^{-/-}$ mice**. **b** : The locomotion was first recorded during the first 10 minutes after saline (vehicle) or cocaine (20 mg/kg) injection. Locomotor activity was significantly higher in *Htr2b*$^{-/-}$ (black square) than in *Htr2b*$^{+/+}$ mice (white square). Data analyzed using two-way ANOVA (n = 3-5) (means ± SEM) showed a main effect of genotype ($F_{(1, 10)} = 9.23$, $p<0.0125$). Bonferroni post-hoc tests were applied to each graph, **P < 0.01; ***P < 0.001. Immediately after the 10 min of locomotor recording, the brains were fixed and sectioned. p-ERK1/2 immuno-positive neurons were counted. **c** : location of the images within the striatal tissue (red squares). **d** : raw images obtained in the confocal microscope (top panels), cell counts performed on each image (middle panels, red dots) and segmentation on each image through signal thresholding (bottom panels). **e** : quantification revealed significantly lower number of cells positive for p-ERK1/2 in the NAcc shell of cocaine--treated *Htr2b*$^{-/-}$ (black) compared to *Htr2b*$^{+/+}$ (white) mice (n = 3-4). Data analyzed using two-way ANOVA showed a main effect of genotype ($F_{(1, 10)} = 40.23$, $p<0.0001$). No difference between genotype was found in NAcc core or dorsal striatum. Bar scales: 100 µm. Bonferroni post-hoc tests were applied to each graph, *P < 0.05; **P < 0.01; ***P < 0.001; ****P < 0.0001.

Figure 4

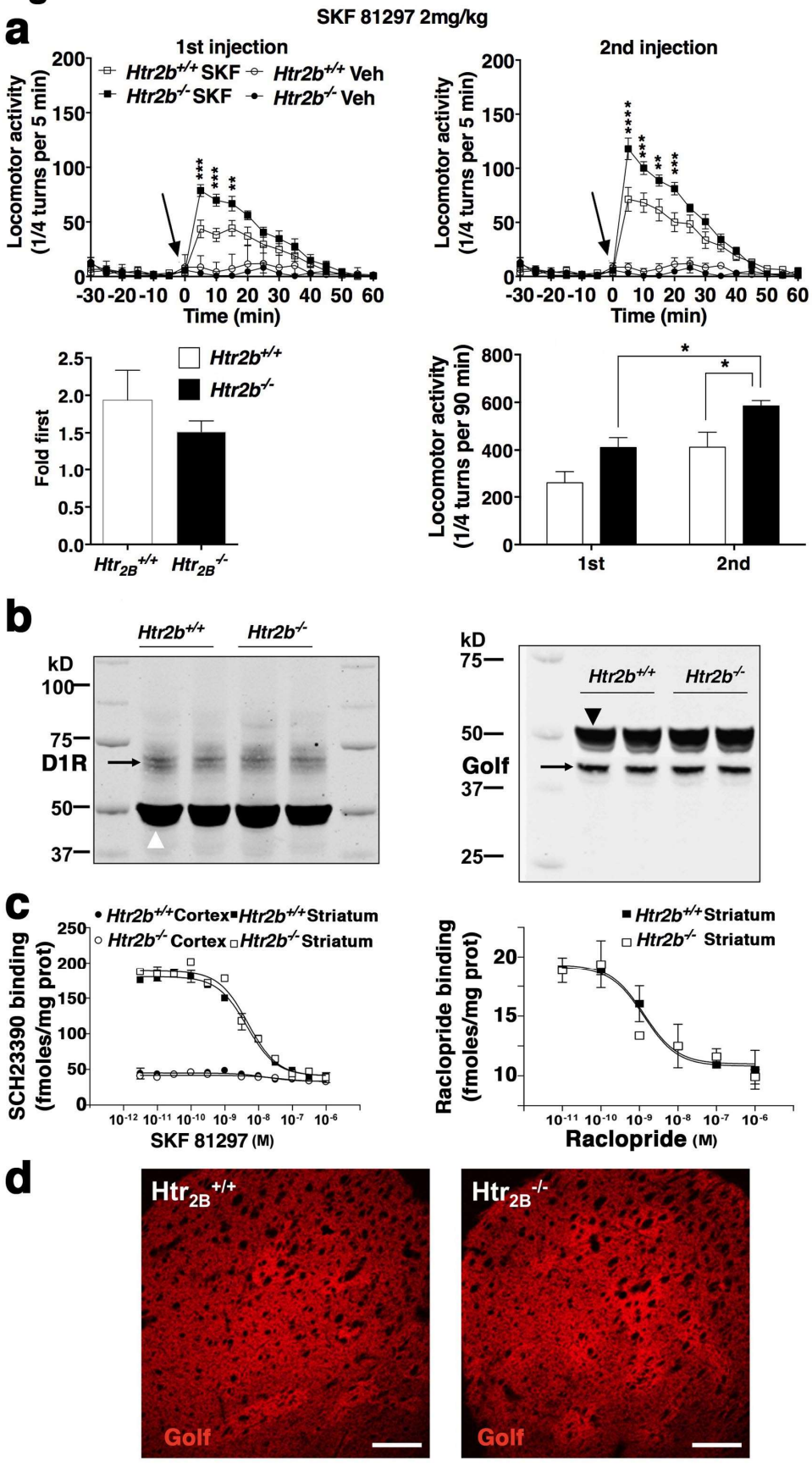
a
SKF 81297 2mg/kg
1st injection
2nd injection
Htr2b+/+ SKF
Htr2b-/- SKF
Htr2b+/+ Veh
Htr2b-/- Veh
Locomotor activity (1/4 turns per 5 min)
Time (min)
Fold first
Htr2B+/+
Htr2B-/-
Locomotor activity (1/4 turns per 90 min)
1st
2nd
b
kD
D1R
Golf
c
Htr2b+/+Cortex
Htr2b+/+Striatum
Htr2b-/- Cortex
Htr2b-/- Striatum
SCH23390 binding (fmoles/mg prot)
SKF 81297 (M)
Raclopride binding (fmoles/mg prot)
Raclopride (M)
d
Golf

Fig. 4. Assessment of DA system in *Htr2b*$^{-/-}$ mice. a : Increased locomotor activity in response to DA receptor D1 agonist in *Htr2b*$^{-/-}$ mice. An ip injection of D1 agonist SKF81297 (SKF, 2mg/kg) increased locomotor activity more in *Htr2b*$^{-/-}$ (cocaine, black square; vehicle, black circle, n = 8-8) than in *Htr2b*$^{+/+}$ mice (cocaine, white square; vehicle, open circle, n = 8-8; 1st injection, left, arrow cocaine injection t = 0). Data analyzed using two-way ANOVA RM showed a genotype effect ($F_{(1, 14)} = 5.30$ *p=0.037*). The stimulant effect of a challenge dose of SKF81297 seven days later (2nd injection, right, arrow cocaine injection t = 0) was also significantly higher in *Htr2b*$^{-/-}$ compared to *Htr2b*$^{+/+}$ mice (genotype effect, $F_{(1,14)} = 5.95$ *p=0.029*). The increase in SKF81297 induced-locomotor activity at the second injection was similar in respect to the first (Fold first) (left, n=8-8; unpaired t-test $t_{14} = 1.00$, P = 0.33). Total locomotor activity recorded over 60 min after a 2nd injection (right) was significantly higher in *Htr2b*$^{-/-}$ (black bars) compared to *Htr2b*$^{+/+}$ mice (white bars) and to the 1st injection (genotype effect $F_{(1, 14)} = 12.30$, *p=0.0035*; factor injection $F_{(1, 14)} = 13.19$, *p=0.0027*), as analyzed using two-way ANOVA RM for cocaine (means ± SEM, *n* = 8-8). Bonferroni post-hoc tests were applied to each graph, *P < 0.05; **P < 0.01; ***P < 0.001; ****P<0.0001. **b-d Similar D1 and D2 receptor expression level in *Htr2b*$^{+/+}$ and *Htr2b*$^{-/-}$ mice. b**, Western blots from *Htr2b*$^{+/+}$ and *Htr2b*$^{-/-}$ mouse striatum proteins (2 example for each genotype) were revealed using antibody against D1 receptor (left, black arrow) or using Gαolf antibody (right, black arrow). Normalization (using tubulin antibody; arrow head) revealed no significant difference between genotypes (n = 4 mice per genotype; Student's t-test). **c**, Radioligand binding assays with the selective D1 receptor ligand [^{3}H]SCH23390 on membranes prepared from cortex and striatum showed no differences between *Htr2b*$^{+/+}$ and *Htr2b*$^{-/-}$ mice (Bmax = *Htr2b*$^{+/+}$ cortex 18±2.7; *Htr2b*$^{-/-}$ cortex 14±2.5; *Htr2b*$^{+/+}$ striatum 211 ± 6; *Htr2b*$^{-/-}$ striatum 223 ± 7.4 fmoles/mg of proteins) (left). Radioligand binding assays with the selective D2 receptor ligand [^{3}H]raclopride on membranes prepared from striatum showed no differences between *Htr2b*$^{+/+}$ and *Htr2b*$^{-/-}$ mice (Bmax = *Htr2b*$^{+/+}$ striatum 11.4 ± 5.6; *Htr2b*$^{-/-}$ striatum 11.4 ± 5.7 fmoles/mg of proteins, 3 independent experiments in duplicate) (right). **d,** Immunohistochemistry with a selective antibody directed against Gαolf protein on striatum slices showed no pattern differences between *Htr2b*$^{+/+}$ and *Htr2b*$^{-/-}$ mice, respectively, (scale bars: 200 µm).

Figure 5

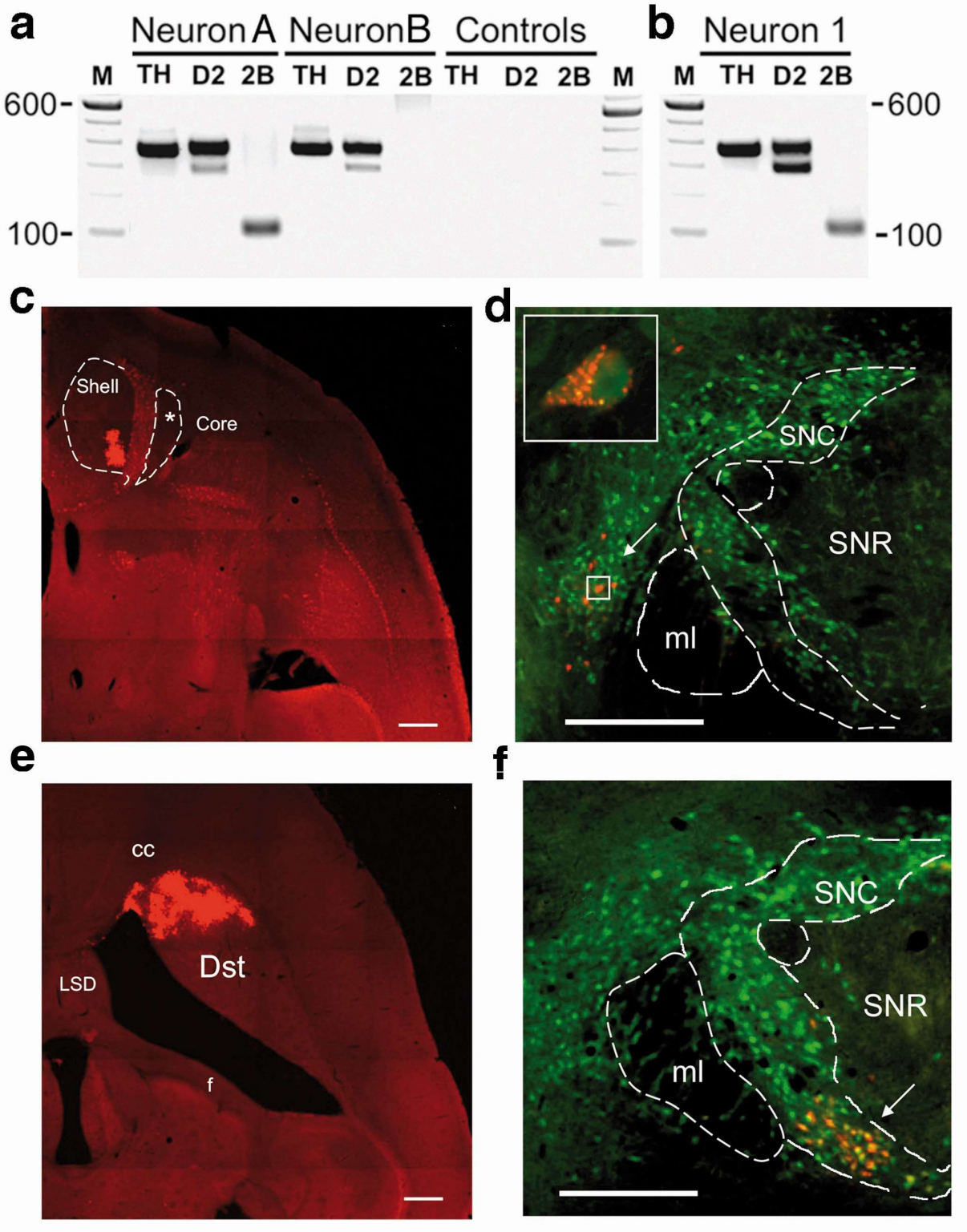
a
Neuron A
NeuronB
Controls
M
TH
D2
2B
600-
100-
b
Neuron 1
-600
-100
c
Shell
Core
d
SNC
SNR
ml
e
cc
Dst
LSD
f
SNC
SNR
ml

Fig. 5. 5-HT$_{2B}$ receptors are expressed by mesolimbic DA neurons. a : Coexpression of D2 receptors and tyrosine hydroxylase with 5-HT$_{2B}$-receptor mRNA in a subset of individual VTA neurons. RT-PCR was performed on cytoplasmic RNA extracted from individually identified *Drd2-EGFP*-positive VTA neurons. The displayed pattern illustrates a negative (Neuron B) and a positive neuron (Neuron A) expressing 5-HT$_{2B}$ receptor, which is representative of 4 out of 10 neurons in VTA. All neurons classes express tyrosine hydroxylase (TH) and D2 receptors (D2). Negative RT-PCR controls (GFP negative neuron) are also presented. M = molecular weight marker in base pairs. **b-d : VTA neurons expressing 5-HT$_{2B}$ receptor project to the NAcc. b,** Stereotactic red-dextran injection in NAcc of *Drd2-EGFP* mice allowed identifying, after retrograde tracing, VTA DA neurons projecting to NAcc (double-labeled). Cytoplasmic RNA from double labeled neuron in the VTA was analyzed by single cells RT-PCR (Neuron 1), which is representative of 13 out of 13 VTA neurons expressing 5-HT$_{2B}$ receptor and that project to NAcc. **c,** Representative horizontal section, showing NAcc shell stereotactic red-dextran injection site for retrograde tracing experiments using fluorescently red-labeled latex beads. Scale bars: 600 µm **d**, Representative horizontal section, showing red-dextran retrograde tracing in VTA of *Drd2-EGFP* mice that identified double-labeled DA neurons projecting to NAcc used for single cells RT-PCR (Arrow and inset). Scale bars: 200 µm. Star indicates the NAcc core nucleus. **e-f Controls of red dextran injection into dorsal striatum. e,** Representative horizontal section, showing dorsal striatum stereotactic red-dextran injection site for retrograde tracing experiments using fluorescently red-labeled latex beads. Scale bars: 600 µm **f**, Representative horizontal section, showing red-dextran retrograde tracing in the *substantia nigra reticulata* (SNR) of *Drd2-EGFP* mice that identify DA neurons projecting to dorsal striatum (Arrow). Scale bars: 200 µm. SNR: *substantia nigra reticulata*; SNC *substantia nigra compacta*; ml: medial lemniscus; Dst: dorsal striatum; f: fornix; cc: *corpus callosum*; LSD: lateral septal nucleus dorsal.

Figure 6

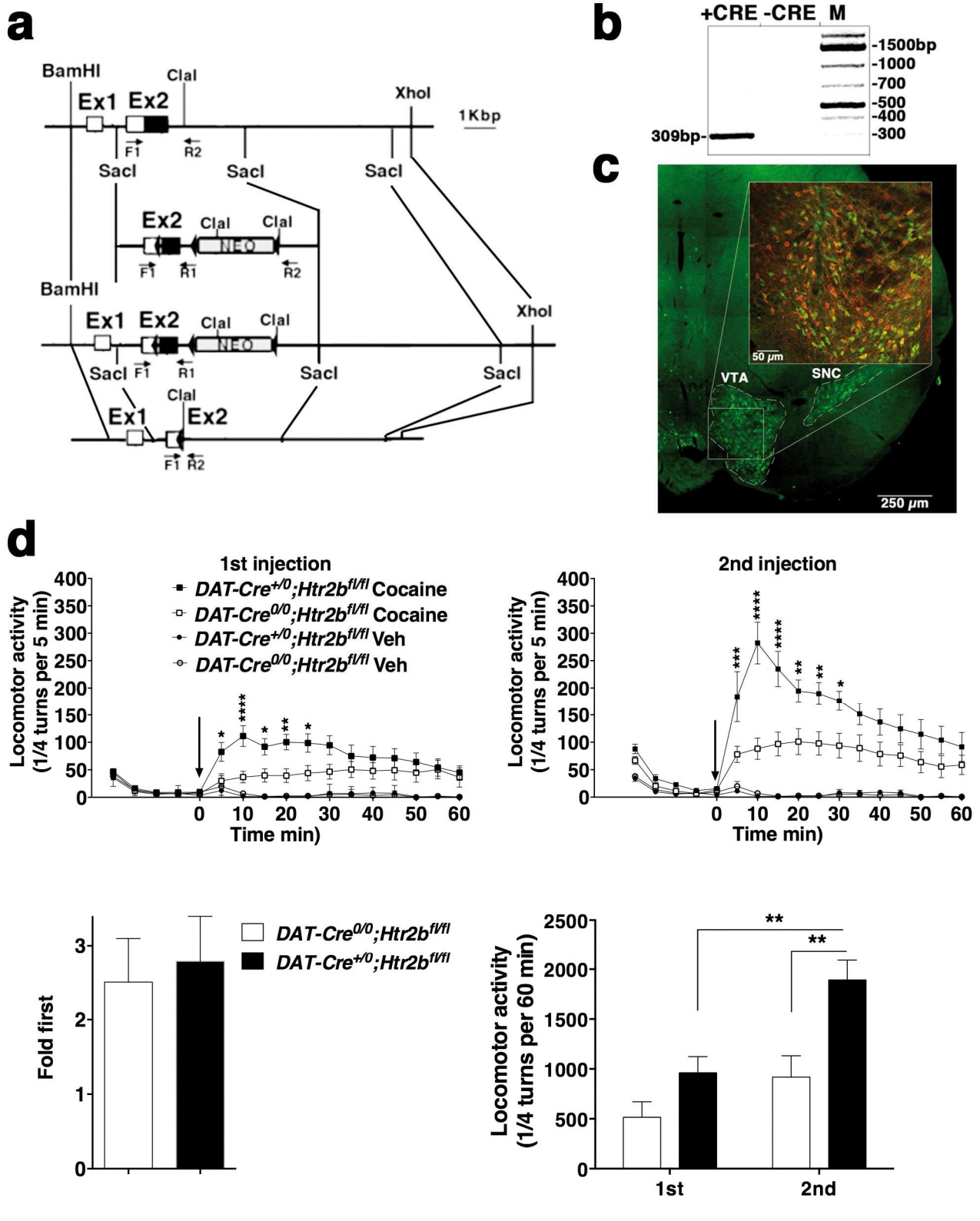
a
BamHI
ClaI
Ex1 Ex2
XhoI
1Kbp
F1
R2
SacI
SacI
SacI
Ex2
ClaI
ClaI
NEO
F1
R1
R2
BamHI
Ex1 Ex2
ClaI
ClaI
NEO
XhoI
SacI F1
R1
SacI
SacI
ClaI
Ex1
Ex2
F1 R2
b
+CRE -CRE M
-1500bp
-1000
-700
-500
-400
-300
309bp-
c
50 µm
VTA
SNC
250 µm
d
1st injection
DAT-Cre+/0;Htr2bfl/fl Cocaine
DAT-Cre0/0;Htr2bfl/fl Cocaine
DAT-Cre+/0;Htr2bfl/fl Veh
DAT-Cre0/0;Htr2bfl/fl Veh
Locomotor activity (1/4 turns per 5 min)
Time min)
2nd injection
Locomotor activity (1/4 turns per 5 min)
Time min)
DAT-Cre0/0;Htr2bfl/fl
DAT-Cre+/0;Htr2bfl/fl
Fold first
Locomotor activity (1/4 turns per 60 min)
1st
2nd

Fig. 6. Conditional deletion of 5-HT$_{2B}$ receptor in DA neurons, *Htr2b^{DAKO}* mutant mice. a-c : Mapping and genotyping of *Htr2b^{DAKO}* mutant mice. Top: 5-HT$_{2B}$ receptor locus indicating the positions of exons, (Exon 1, Ex1; Exon 2, Ex2) and restriction sites used for the targeting construct. Middle: targeting vector designed to floxed exon 2 by homologous recombination in genomic DNA generating the targeted locus (below). Exons 1– 2 are depicted by white (untranslated) and black boxes (coding) and Neomycin resistance by grey box (NEO). Bottom: sequenced-verified structure of the *Htr2b* null allele (KO) after excision by Cre recombinase of the sequence flanked by LoxP sites (triangles). Horizontal arrows illustrate the position of primers used for genotyping (F1, R1, R2). **b :** Genomic DNA of VTA from *Htr2b^{DAKO}* mice was extracted and analyzed by PCR, revealing the effective proper recombination (F1, R2 amplimers, 309 bp). **c:** Efficient Cre recombination in TH positive neurons. Immunofluorescence revealed the recombinase-dependent GFP expression in VTA, which colocalized with the TH antibody staining as seen by confocal microscopy in coronal section of VTA of *DAT-Cre$^{+/0}$;RCE* mice (inset); scale bars: 250 µm, inset 50 µm. **d : Restricted 5-HT$_{2B}$ receptor inactivation to DA neurons leads to increased locomotor response to cocaine.** An injection of cocaine (20 mg/kg) increased locomotor activity more in *Htr2b^{DAKO}* (*Dat-Cre$^{+/0}$*;*Htr2b$^{fl/fl}$* cocaine, black square; vehicle, black circle, n = 10-10) than in Cre negative littermate mice (*Htr2b$^{fl/fl}$* cocaine, white square; vehicle, open circle, n = 10-10; 1st injection, left, arrow cocaine injection t = 0). Data analyzed using two-way ANOVA RM showed a main effect of genotype ($F_{(1, 18)} = 4.03$, *p=0.05*). The stimulant locomotor effect of a challenge dose of cocaine seven days later (2nd injection, right, arrow cocaine injection t = 0) was also significantly higher in *Htr2b^{DAKO}* compared to *Htr2b$^{fl/fl}$* mice (genotype $F_{(1, 18)} = 10.63$, *p=0.0043*). The increase in cocaine induced-locomotor activity at the second injection was similar in respect to the first (Fold first) (n=10-10; unpaired t-test $t_{18} = 0.324$, P = 0.75). Total locomotor activity recorded over 60 min after a 2nd injection was significantly higher in *Htr2b^{DAKO}* compared to *Htr2b$^{fl/fl}$* littermate mice and compared to the 1st injection (factor genotype $F_{(1, 18)} = 10.31$, *p=0.0048*; factor injection $F_{(1, 18)} = 23.82$, *p=0.0001*), as analyzed using two-way ANOVA RM for cocaine (n = 10-10) (means ± SEM). Bonferroni post-hoc tests were applied to each graph, *P < 0.05; **P < 0.01; ***P < 0.001; ****P<0.0001.

Figure 7

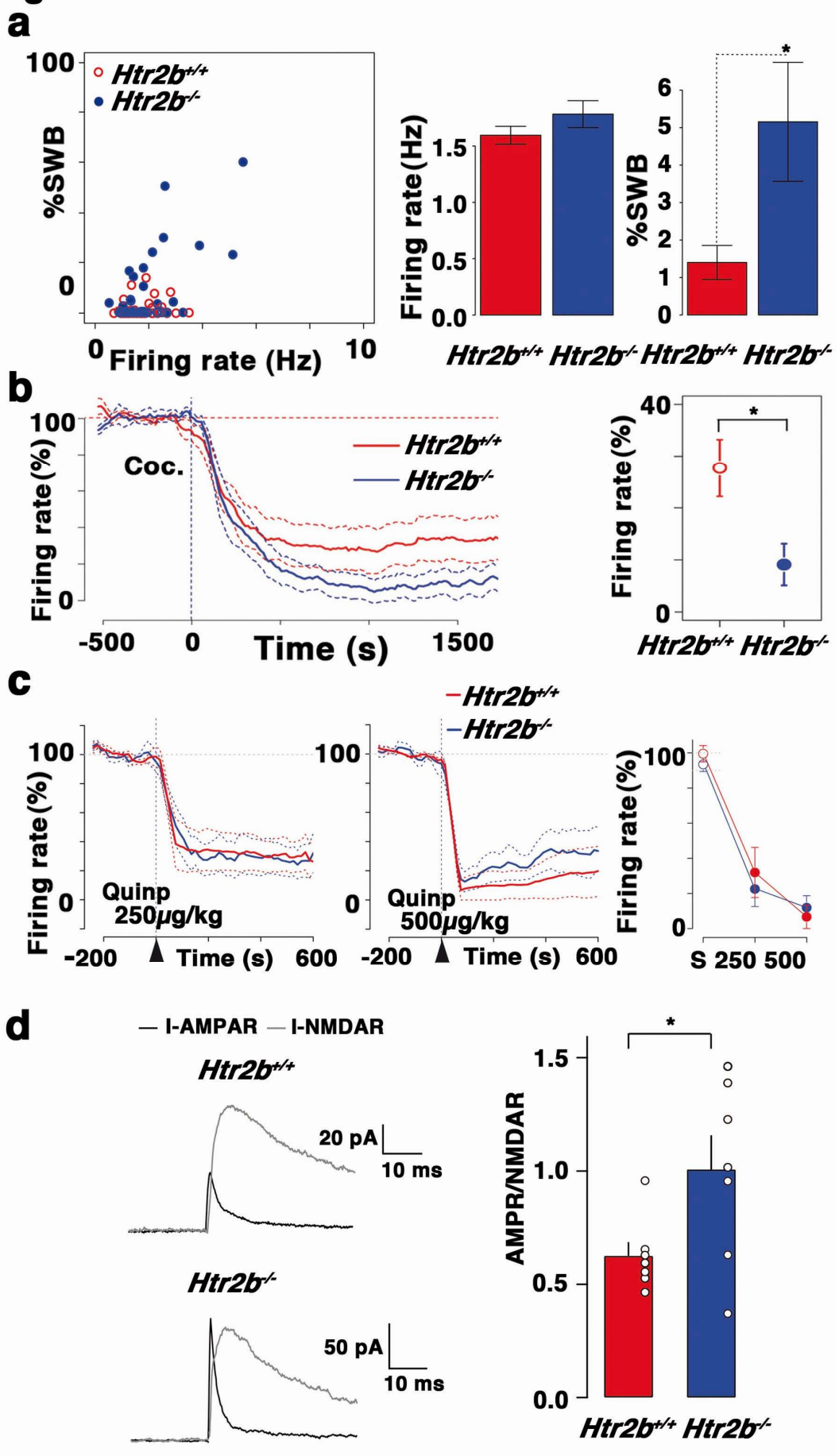
a
100
Htr2b+/+
Htr2b-/-
%SWB
0
0
Firing rate (Hz)
10
Firing rate(Hz)
1.5
1.0
0.5
0.0
%SWB
6
5
4
3
2
1
0
*
Htr2b+/+ Htr2b-/- Htr2b+/+ Htr2b-/-
b
100
Firing rate(%)
0
Coc.
Htr2b+/+
Htr2b-/-
-500
0
Time (s)
1500
40
Firing rate(%)
0
*
Htr2b+/+ Htr2b-/-
c
100
Firing rate(%)
0
Quinp
250μg/kg
-200
Time (s)
600
Htr2b+/+
Htr2b-/-
100
0
Quinp
500μg/kg
-200
Time (s)
600
100
Firing rate(%)
0
S 250 500
d
— I-AMPAR — I-NMDAR
Htr2b+/+
20 pA
10 ms
Htr2b-/-
50 pA
10 ms
AMPR/NMDAR
1.5
1.0
0.5
0.0
*
Htr2b+/+ Htr2b-/-

Fig. 7. Electrophysiological effect of 5-HT$_{2B}$ receptor knockout on VTA DA neurons. a : Changes in basal *in-vivo* firing of *Htr2b*$^{-/-}$ VTA DA neurons. After *in-vivo* recordings, the mean frequency (Hz) was plotted against the percentage of spikes within a burst (%SWB) of DA neurons in *Htr2b*$^{+/+}$ (red, n=57) and *Htr2b*$^{-/-}$ mice (blue, n=58). Barplot shows no change in the mean frequency (left) and a significant increase in percentage of SWB (right) for the same groups (t_{66} = 2.27, *P=0.026, unpaired t-test-Welch corrected). **b** : **Cocaine induced a stronger decrease in firing rate of VTA DA neurons in *Htr2b*$^{-/-}$ mice.** Systemic ip injection of cocaine (20 mg/kg) in *Htr2b*$^{+/+}$ (10 mice; red line) and *Htr2b*$^{-/-}$ (9 mice; blue line) mice produced a decrease of firing rate. On average, cocaine-induced decrease in firing rate was significantly stronger in *Htr2b*$^{-/-}$ than in *Htr2b*$^{+/+}$ mice. (t_{16} = 2.73, *P=0.015, unpaired t-test-Welch corrected). The percentage of variation in firing rate (right) is illustrated. **c : No change in quinpirole-dependent decrease in firing rate of VTA DA neurons in *Htr2b*$^{-/-}$ mice.** Systemic ip injection of the D2 agonist quinpirole (Quinp 250-500 µg/kg) in *Htr2b*$^{+/+}$ (6-5 mice; red line) and *Htr2b*$^{-/-}$ (7-6 mice; blue line) mice produced similar decrease of firing rate. The percentage of variation in firing rate (right) is illustrated for the two concentrations. **d : Strengthening of AMPA transmission in the VTA neurons of *Htr2b*$^{-/-}$ mice.** Representative sample traces for AMPAR- (black) and NMDAR-EPSCs (gray) recorded at +40 mV in DA neurons from the lateral part of the VTA that are prone to project to the NAcc shell of *Htr2b*$^{-/-}$ and *Htr2b*$^{+/+}$ mice. (right): Bar graph and scatter plot illustrate the significant increase in AMPA/NMDA ratio in the *Htr2b*$^{-/-}$ vs. *Htr2b*$^{+/+}$ mice (t_{12} = 2.35, *P=0.037, unpaired t-test).

Figure 8

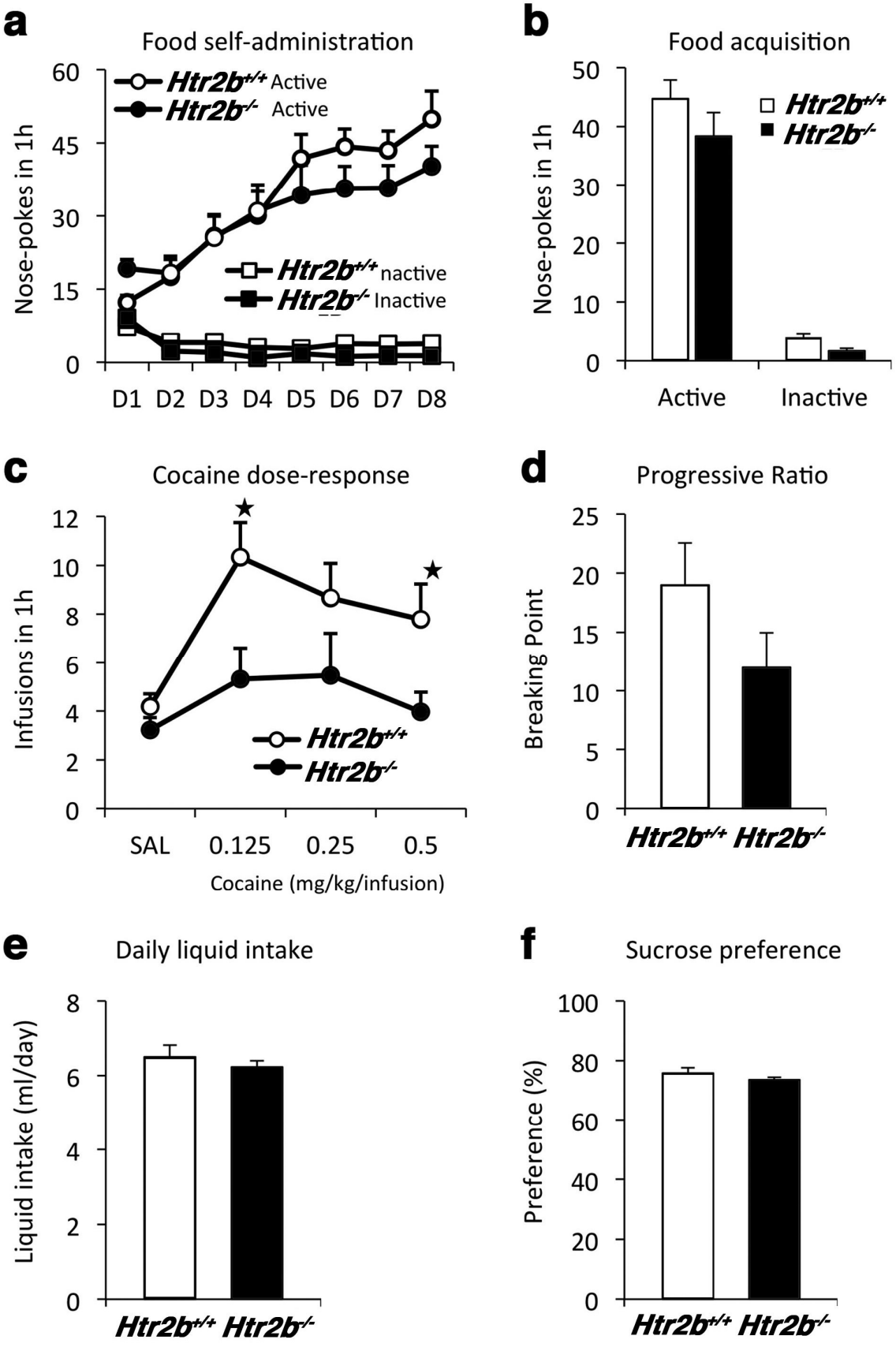
a
Food self-administration
Nose-pokes in 1h
Htr2b+/+ Active
Htr2b-/- Active
Htr2b+/+ nactive
Htr2b-/- Inactive
D1 D2 D3 D4 D5 D6 D7 D8
b
Food acquisition
Nose-pokes in 1h
Htr2b+/+
Htr2b-/-
Active
Inactive
c
Cocaine dose-response
Infusions in 1h
Htr2b+/+
Htr2b-/-
SAL
0.125
0.25
0.5
Cocaine (mg/kg/infusion)
d
Progressive Ratio
Breaking Point
Htr2b+/+ Htr2b-/-
e
Daily liquid intake
Liquid intake (ml/day)
Htr2b+/+ Htr2b-/-
f
Sucrose preference
Preference (%)
Htr2b+/+ Htr2b-/-

Fig 8. Cocaine self-administration in *Htr2b*$^{-/-}$ mice. a-b : Similar training of mice to food pellets in *Htr2b*$^{+/+}$ and *Htr2b*$^{-/-}$ animals. Mice were first trained to respond for food pellets under FR1 schedule of reinforcement in one-hour daily self-administration sessions until responding for food criteria was acquired. A significant increase in nose-poke responding was observed during the first sessions leading to a learning-curve pattern in both group of animals. Data analyzed by three-way ANOV showed an effect the day ($F_{(7, 203)} = 17.9$, $p<0.001$). The discrimination between active and inactive nose-poke responding was rapidly acquired in both, *Htr2b*$^{+/+}$ and *Htr2b*$^{-/-}$ mice (hole, $F_{(1, 29)} = 144.4$, $p<0.001$) (**a**). No statistical differences between genotypes were obtained when data from the acquisition days was analyzed (**b**). **c-d : Lower cocaine self-administration in *Htr2b*$^{-/-}$ mice.** A saline solution was presented first until a low and stable responding pattern was obtained. Animals were then trained to self-administer cocaine at the dose of 0.25 mg/kg/infusion during 8 days on a FR1 schedule of reinforcement, followed by cocaine at the doses of 0.125 or 0.5 mg/kg/infusion during 4 consecutive days. *Htr2b*$^{-/-}$ mice earned a significantly lower number of cocaine infusions by one-way ANOVA (genotype, $F_{(1, 29)} = 5.4$, $p=0.027$), mainly at the dose of 0.125 (genotype, $F_{(1, 29)} = 6.3$, $p=0.018$) and 0.5 mg/kg (genotype, $F_{(1, 29)} = 4.2$, $p=0.049$) (**c**). Subsequently, a progressive ratio procedure was performed in order to test the motivation of the mice to work for cocaine at the dose of 0.125 mg/kg/infusion. The trend toward a lower break point in the progressive ratio schedule of reinforcement test did not reach significance ($t_{29} = 2.10$, P = 0.162, unpaired t-test) (**d**). **e-f : No difference in post-cocaine reward system between genotypes.** To evaluate the effects of 5-HT_{2B} receptor deletion on post-cocaine reward system, two bottles of water were first available to individually caged mice and liquid consumption was monitored during two consecutive days (**e**). Then, the liquid from one of the bottles was replaced with a 2% sucrose solution and liquid intake measurements was performed daily during 3 days (**f**). Total liquid intake, as well as, sucrose preference was evaluated in *Htr2b*$^{+/+}$ and *Htr2b*$^{-/-}$ animals. No statistical differences between genotypes were obtained. (n = 18-13, unpaired t-test $t_{29} = 0.50$, P = 0.50 for liquid and $t_{29} = 1.00$, P = 0.325 for sucrose).

BIBLIOGRAPHIE

Adell, A., Castro, E., Celada, P., Bortolozzi, A., Pazos, A., and Artigas, F. (2005). Strategies for producing faster acting antidepressants. Drug Discov. Today *10*, 578–585.

Aghajanian, G.K., and Marek, G.J. (1997). Serotonin induces excitatory postsynaptic potentials in apical dendrites of neocortical pyramidal cells. Neuropharmacology *36*, 589–599.

Agnati, L.F., Zoli, M., Strömberg, I., and Fuxe, K. (1995). Intercellular communication in the brain: wiring versus volume transmission. Neuroscience *69*, 711–726.

Aira, Z., Buesa, I., García del Caño, G., Bilbao, J., Doñate, F., Zimmermann, M., and Azkue, J.J. (2013). Transient, 5-HT2B receptor–mediated facilitation in neuropathic pain: Up-regulation of PKCγ and engagement of the NMDA receptor in dorsal horn neurons. PAIN® *154*, 1865–1877.

Aira, Z., Buesa, I., Rada, D., Gómez-Esteban, J.C., and Azkue, J.J. (2014). Coupling of serotonergic input to NMDA receptor-phosphorylation following peripheral nerve injury via rapid, synaptic up-regulation of ND2. Exp. Neurol. *255*, 86–95.

Akum, B.F., Chen, M., Gunderson, S.I., Riefler, G.M., Scerri-Hansen, M.M., and Firestein, B.L. (2004). Cypin regulates dendrite patterning in hippocampal neurons by promoting microtubule assembly. Nat. Neurosci. *7*, 145–152.

Albizu, L., Holloway, T., González-Maeso, J., and Sealfon, S.C. (2011). Functional crosstalk and heteromerization of serotonin 5-HT2A and dopamine D2 receptors. Neuropharmacology *61*, 770.

de Almeida, J., and Mengod, G. (2008). Serotonin 1A receptors in human and monkey prefrontal cortex are mainly expressed in pyramidal neurons and in a GABAergic interneuron subpopulation: implications for schizophrenia and its treatment. J. Neurochem. *107*, 488–496.

Alpi, E., Landi, E., Barilari, M., Serresi, M., Salvadori, P., Bachi, A., and Dente, L. (2009). Channel-interacting PDZ protein, “CIPP”, interacts with proteins involved in cytoskeletal dynamics. Biochem. J. *419*, 289.

Alterio, J., Masson, J., Diaz, J., Chachlaki, K., Salman, H., Areias, J., Al Awabdh, S., Emerit, M.B., and Darmon, M. (2015). Yif1B Is Involved in the Anterograde Traffic Pathway and the Golgi Architecture. Traffic n/a-n/a.

Alvarez, F.J., Pearson, J.C., Harrington, D., Dewey, D., Torbeck, L., and Fyffe, R.E. (1998). Distribution of 5-hydroxytryptamine-immunoreactive boutons on alpha-motoneurons in the lumbar spinal cord of adult cats. J. Comp. Neurol. *393*, 69–83.

Amilhon, B., Lepicard, È., Renoir, T., Mongeau, R., Popa, D., Poirel, O., Miot, S., Gras, C., Gardier, A.M., Gallego, J., et al. (2010). VGLUT3 (Vesicular Glutamate Transporter Type 3) Contribution to the Regulation of Serotonergic Transmission and Anxiety. J. Neurosci. *30*, 2198–2210.

Anastasio, N.C., Stutz, S.J., Fink, L.H.L., Swinford-Jackson, S.E., Sears, R.M., DiLeone, R.J., Rice, K.C., Moeller, F.G., and Cunningham, K.A. (2015). Serotonin (5-HT) 5-HT2A Receptor (5-HT2AR):5-HT2CR Imbalance in Medial Prefrontal Cortex Associates with Motor Impulsivity. ACS Chem. Neurosci. *6*, 1248–1258.

Aoki, C., Joh, T.H., and Pickel, V.M. (1987). Ultrastructural localization of beta-adrenergic receptor-like immunoreactivity in the cortex and neostriatum of rat brain. Brain Res. *437*, 264–282.

Aoki, C., Venkatesan, C., Go, C.G., Mong, J.A., and Dawson, T.M. (1994). Cellular and subcellular localization of NMDA-R1 subunit immunoreactivity in the visual cortex of adult and neonatal rats. J. Neurosci. Off. J. Soc. Neurosci. *14*, 5202–5222.

Ashworth-Preece, M.A., Jarrott, B., and Lawrence, A.J. (1995). 5-Hydroxytryptamine3 receptor modulation of excitatory amino acid release in the rat nucleus tractus solitarius. Neurosci. Lett. *191*, 75–78.

Awabdh, S.A., Miserey-Lenkei, S., Bouceba, T., Masson, J., Kano, F., Marinach-Patrice, C., Hamon, M., Emerit, M.B., and Darmon, M. (2012). A New Vesicular Scaffolding Complex Mediates the G-Protein-Coupled 5-HT1A Receptor Targeting to Neuronal Dendrites. J. Neurosci. *32*, 14227–14241.

Awtry, T.L., Frank, J.G., and Werling, L.L. (2006). In vitro regulation of serotonin transporter activity by protein kinase A and nicotinic acetylcholine receptors in the prefrontal cortex of rats. Synap. N. Y. N *59*, 342–349.

Baki, L., Fribourg, M., Younkin, J., Eltit, J.M., Moreno, J.L., Park, G., Vysotskaya, Z., Narahari, A., Sealfon, S.C., Gonzalez-Maeso, J., et al. (2016). Cross-signaling in metabotropic glutamate 2 and serotonin 2A receptor heteromers in mammalian cells. Pflüg. Arch. - Eur. J. Physiol. 1–19.

Banas, S.M., Doly, S., Boutourlinsky, K., Diaz, S.L., Belmer, A., Callebert, J., Collet, C., Launay, J.-M., and Maroteaux, L. (2011). Deconstructing Antiobesity Compound Action: Requirement of Serotonin 5-HT2B Receptors for Dexfenfluramine Anorectic Effects. Neuropsychopharmacology *36*, 423–433.

Barilari, M., and Dente, L. (2010). The neuronal proteins CIPP, Cypin and IRSp53 form a tripartite complex mediated by PDZ and SH3 domains. Biol. Chem. *391*, 1169–1174.

Barnes, N.M., and Sharp, T. (1999). A review of central 5-HT receptors and their function. Neuropharmacology *38*, 1083–1152.

Baumann, P.A., and Waldmeier, P.C. (1984). Negative feedback control of serotonin release in vivo: comparison of 5-hydroxyindolacetic acid levels measured by voltammetry in conscious rats and by biochemical techniques. Neuroscience *11*, 195–204.

Baxter, G.S., Murphy, O.E., and Blackburn, T.P. (1994). Further characterization of 5-hydroxytryptamine receptors (putative 5-HT2B) in rat stomach fundus longitudinal muscle. Br. J. Pharmacol. *112*, 323–331.

Bayliss, D.A., Li, Y.W., and Talley, E.M. (1997). Effects of serotonin on caudal raphe neurons: activation of an inwardly rectifying potassium conductance. J. Neurophysiol. *77*, 1349–1361.

Bécamel, C., Figge, A., Poliak, S., Dumuis, A., Peles, E., Bockaert, J., Lübbert, H., and Ullmer, C. (2001). Interaction of Serotonin 5-Hydroxytryptamine Type 2C Receptors with PDZ10 of the Multi-PDZ Domain Protein MUPP1. J. Biol. Chem. *276*, 12974–12982.

Bécamel, C., Alonso, G., Galéotti, N., Demey, E., Jouin, P., Ullmer, C., Dumuis, A., Bockaert, J., and Marin, P. (2002). Synaptic multiprotein complexes associated with 5-HT(2C) receptors: a proteomic approach. EMBO J. *21*, 2332–2342.

Bécamel, C., Gavarini, S., Chanrion, B., Alonso, G., Galéotti, N., Dumuis, A., Bockaert, J., and Marin, P. (2004). The Serotonin 5-HT2A and 5-HT2C Receptors Interact with Specific Sets of PDZ Proteins. J. Biol. Chem. *279*, 20257–20266.

Beck, A., Lohr, C., Nett, W., and Deitmer, J.W. (2001). Bursting activity in leech Retzius neurons induced by low external chloride. Pflugers Arch. *442*, 263–272.

Beck, S.G., Pan, Y.-Z., Akanwa, A.C., and Kirby, L.G. (2004). Median and dorsal raphe neurons are not electrophysiologically identical. J. Neurophysiol. *91*, 994–1005.

Becquet, D., Faudon, M., and Hery, F. (1990). The role of serotonin release and autoreceptors in the dorsalis raphe nucleus in the control of serotonin release in the cat caudate nucleus. Neuroscience *39*, 639–647.

Becquet, D., Hery, M., Francois-Bellan, A.M., Giraud, P., Deprez, P., Faudon, M., Fache, M.P., and Hery, F. (1993a). Glutamate, GABA, glycine and taurine modulate serotonin synthesis and release in rostral and caudal rhombencephalic raphe cells in primary cultures. Neurochem. Int. *23*, 269–283.

Becquet, D., Héry, M., Deprez, P., Faudon, M., Fache, M.P., Giraud, P., and Héry, F. (1993b). N-methyl-D-aspartic acid/glycine interactions on the control of 5-hydroxytryptamine release in raphe primary cultures. J. Neurochem. *61*, 1692–1697.

Belmer, A., Doly, S., Setola, V., Banas, S.M., Moutkine, I., Boutourlinsky, K., Kenakin, T., and Maroteaux, L. (2014). Role of the N-Terminal Region in G Protein–Coupled Receptor Functions: Negative Modulation Revealed by 5-HT2B Receptor Polymorphisms. Mol. Pharmacol. *85*, 127–138.

Bengel, D., Jöhren, O., Andrews, A.M., Heils, A., Mössner, R., Sanvitto, G.L., Saavedra, J.M., Lesch, K.P., and Murphy, D.L. (1997). Cellular localization and expression of the serotonin transporter in mouse brain. Brain Res. *778*, 338–345.

Bermingham, D.P., and Blakely, R.D. (2016). Kinase-dependent Regulation of Monoamine Neurotransmitter Transporters. Pharmacol. Rev. *68*, 888–953.

Berthouze, M., Ayoub, M., Russo, O., Rivail, L., Sicsic, S., Fischmeister, R., Berque-Bestel, I., Jockers, R., and Lezoualc'h, F. (2005). Constitutive dimerization of human serotonin 5-HT4 receptors in living cells. FEBS Lett. *579*, 2973–2980.

Bevilacqua, L., Doly, S., Kaprio, J., Yuan, Q., Tikkanen, R., Paunio, T., Zhou, Z., Wedenoja, J., Maroteaux, L., Diaz, S., et al. (2010). A population-specific HTR2B stop codon predisposes to severe impulsivity. Nature *468*, 1061–1066.

Bhatnagar, A., Sheffler, D.J., Kroeze, W.K., Compton-Toth, B., and Roth, B.L. (2004). Caveolin-1 Interacts with 5-HT2A Serotonin Receptors and Profoundly Modulates the Signaling of Selected Gαq-coupled Protein Receptors. J. Biol. Chem. *279*, 34614–34623.

Black, J.W., and Leff, P. (1983). Operational models of pharmacological agonism. Proc. R. Soc. Lond. B Biol. Sci. *220*, 141–162.

Blakely, R.D., Berson, H.E., Fremeau, R.T., Caron, M.G., Peek, M.M., Prince, H.K., and Bradley, C.C. (1991). Cloning and expression of a functional serotonin transporter from rat brain. Nature *354*, 66–70.

Blakely, R.D., Ramamoorthy, S., Schroeter, S., Qian, Y., Apparsundaram, S., Galli, A., and DeFelice, L.J. (1998). Regulated phosphorylation and trafficking of antidepressant-sensitive serotonin transporter proteins. Biol. Psychiatry *44*, 169–178.

Blier, P., Steinberg, S., Chaput, Y., and de Montigny, C. (1989). Electrophysiological assessment of putative antagonists of 5-hydroxytryptamine receptors: a single-cell study in the rat dorsal raphe nucleus. Can. J. Physiol. Pharmacol. *67*, 98–105.

Blomeley, C.P., and Bracci, E. (2009). Serotonin excites fast-spiking interneurons in the striatum. Eur. J. Neurosci. *29*, 1604–1614.

Bockaert, J., and Dumuis, A. (1998). Localization of 5-HT4 Receptors in Vertebrate Brain and Their Potential Behavioral Roles. In 5-HT4 Receptors in the Brain and Periphery, R.M. Eglen, ed. (Springer Berlin Heidelberg), pp. 63–86.

Bockaert, J., Claeysen, S., Compan, V., and Dumuis, A. (2004). 5-HT4 receptors. Curr. Drug Targets CNS Neurol. Disord. *3*, 39–51.

Bockaert, J., Claeysen, S., Bécamel, C., Dumuis, A., and Marin, P. (2006). Neuronal 5-HT metabotropic receptors: fine-tuning of their structure, signaling, and roles in synaptic modulation. Cell Tissue Res. *326*, 553–572.

Boeijinga, P.H., and Boddeke, H.W. (1993). Serotonergic modulation of neurotransmission in the rat subicular cortex in vitro: a role for 5-HT1B receptors. Naunyn. Schmiedebergs Arch. Pharmacol. *348*, 553–557.

Bonaventure, P., Guo, H., Tian, B., Liu, X., Bittner, A., Roland, B., Salunga, R., Ma, X.-J., Kamme, F., Meurers, B., et al. (2002). Nuclei and subnuclei gene expression profiling in mammalian brain. Brain Res. *943*, 38–47.

Borroto-Escuela, D.O., Carlsson, J., Ambrogini, P., Narváez, M., Wydra, K., Tarakanov, A.O., Li, X., Millón, C., Ferraro, L., Cuppini, R., et al. (2017). Understanding the Role of GPCR Heteroreceptor Complexes in Modulating the Brain Networks in Health and Disease. Front. Cell. Neurosci. *11*.

Bortolozzi, A., Castañé, A., Semakova, J., Santana, N., Alvarado, G., Cortés, R., Ferrés-Coy, A., Fernández, G., Carmona, M.C., Toth, M., et al. (2012). Selective siRNA-mediated suppression of 5-HT1A autoreceptors evokes strong anti-depressant-like effects. Mol. Psychiatry *17*, 612–623.

Brea, J., Castro, M., Giraldo, J., López-Giménez, J.F., Padín, J.F., Quintián, F., Cadavid, M.I., Vilaró, M.T., Mengod, G., Berg, K.A., et al. (2009). Evidence for distinct antagonist-revealed functional states of 5-hydroxytryptamine(2A) receptor homodimers. Mol. Pharmacol. *75*, 1380–1391.

Brunner, H.G., Nelen, M., Breakefield, X.O., Ropers, H.H., and van Oost, B.A. (1993). Abnormal behavior associated with a point mutation in the structural gene for monoamine oxidase A. Science *262*, 578–580.

Bruns, D., and Jahn, R. (1995). Real-time measurement of transmitter release from single synaptic vesicles. Nature *377*, 62–65.

Bruns, D., Engert, F., and Lux, H.D. (1993). A fast activating presynaptic reuptake current during serotonergic transmission in identified neurons of Hirudo. Neuron *10*, 559–572.

Bruns, D., Riedel, D., Klingauf, J., and Jahn, R. (2000). Quantal release of serotonin. Neuron *28*, 205–220.

Bubar, M.J., Stutz, S.J., and Cunningham, K.A. (2011). 5-HT(2C) receptors localize to dopamine and GABA neurons in the rat mesoaccumbens pathway. PloS One *6*, e20508.

Bunin, M.A., and Wightman, R.M. (1999). Paracrine neurotransmission in the CNS: involvement of 5-HT. Trends Neurosci. *22*, 377–382.

Burnet, P.W., Eastwood, S.L., Lacey, K., and Harrison, P.J. (1995). The distribution of 5-HT1A and 5-HT2A receptor mRNA in human brain. Brain Res. *676*, 157–168.

Cabral, J.H.M., Petosa, C., Sutcliffe, M.J., Raza, S., Byron, O., Poy, F., Marfatia, S.M., Chishti, A.H., and Liddington, R.C. (1996). Crystal structure of a PDZ domain. Nature *382*, 649–652.

Carmignoto, G. (2000). Reciprocal communication systems between astrocytes and neurones. Prog. Neurobiol. *62*, 561–581.

Carr, G.V., and Lucki, I. (2011). The role of serotonin receptor subtypes in treating depression: a review of animal studies. Psychopharmacology (Berl.) *213*, 265–287.

Carr, D.B., Cooper, D.C., Ulrich, S.L., Spruston, N., and Surmeier, D.J. (2002). Serotonin Receptor Activation Inhibits Sodium Current and Dendritic Excitability in Prefrontal Cortex via a Protein Kinase C-Dependent Mechanism. J. Neurosci. *22*, 6846–6855.

Carrel, D., Masson, J., Awabdh, S.A., Capra, C.B., Lenkei, Z., Hamon, M., Emerit, M.B., and Darmon, M. (2008). Targeting of the 5-HT1A Serotonin Receptor to Neuronal Dendrites Is Mediated by Yif1B. J. Neurosci. *28*, 8063–8073.

Catterall, W.A. (2011). Voltage-Gated Calcium Channels. Cold Spring Harb. Perspect. Biol. *3*.

Cercós, M.G., De-Miguel, F.F., and Trueta, C. (2009). Real-time measurements of synaptic autoinhibition produced by serotonin release in cultured leech neurons. J. Neurophysiol. *102*, 1075–1085.

Chang, J.C., Tomlinson, I.D., Warnement, M.R., Ustione, A., Carneiro, A.M.D., Piston, D.W., Blakely, R.D., and Rosenthal, S.J. (2012). Single Molecule Analysis of Serotonin Transporter Regulation Using Antagonist-Conjugated Quantum Dots Reveals Restricted, p38 MAPK-Dependent Mobilization Underlying Uptake Activation. J. Neurosci. *32*, 8919–8929.

Chanrion, B., Cour, C.M. la, Bertaso, F., Lerner-Natoli, M., Freissmuth, M., Millan, M.J., Bockaert, J., and Marin, P. (2007). Physical interaction between the serotonin transporter and neuronal nitric oxide synthase underlies reciprocal modulation of their activity. Proc. Natl. Acad. Sci. *104*, 8119–8124.

Chazal, G., and Ralston, H.J. (1987). Serotonin-containing structures in the nucleus raphe dorsalis of the cat: an ultrastructural analysis of dendrites, presynaptic dendrites, and axon terminals. J. Comp. Neurol. *259*, 317–329.

Chen, J., Shen, C., and Meller, E. (2002). 5-HT1A receptor-mediated regulation of mitogen-activated protein kinase phosphorylation in rat brain. Eur. J. Pharmacol. *452*, 155–162.

Chih, B., Engelman, H., and Scheiffele, P. (2005). Control of Excitatory and Inhibitory Synapse Formation by Neuroligins. Science *307*, 1324–1328.

Choi, D.-S., and Maroteaux, L. (1996). Immunohistochemical localisation of the serotonin 5-HT2B receptor in mouse gut, cardiovascular system, and brain. FEBS Lett. *391*, 45–51.

Choi, D.-S., Birraux, G., Launay, J.-M., and Maroteaux, L. (1994). The human serotonin 5-HT2B receptor: Pharmacological link between 5-HT2 and 5-HT1D receptors. FEBS Lett. *352*, 393–399.

Choi, D.S., Loric, S., Colas, J.F., Callebert, J., Rosay, P., Kellermann, O., Launay, J.M., and Maroteaux, L. (1996). The mouse 5-HT2B receptor: homologous subtype or species variant? Behav. Brain Res. *73*, 253–257.

Choi, J., Ko, J., Racz, B., Burette, A., Lee, J.-R., Kim, S., Na, M., Lee, H.W., Kim, K., Weinberg, R.J., et al. (2005). Regulation of dendritic spine morphogenesis by insulin receptor substrate 53, a downstream effector of Rac1 and Cdc42 small GTPases. J. Neurosci. Off. J. Soc. Neurosci. *25*, 869–879.

Ciranna, L. (2006). Serotonin as a Modulator of Glutamate- and GABA-Mediated Neurotransmission: Implications in Physiological Functions and in Pathology. Curr. Neuropharmacol. *4*, 101.

Coggeshall, R.E. (1972). Autoradiographic and chemical localization of 5-hydroxytryptamine in identified neurons in the leech. Anat. Rec. *172*, 489–498.

Cohen, N.A., Brenman, J.E., Snyder, S.H., and Bredt, D.S. (1996). Binding of the inward rectifier K+ channel Kir 2.3 to PSD-95 is regulated by protein kinase A phosphorylation. Neuron *17*, 759–767.

Colas, J.-F., Choi, D.-S., Launay, J.-M., and Maroteaux, L. (1997). Evolutionary Conservation of the 5-HT2B Receptors. Ann. N. Y. Acad. Sci. *812*, 149–153.

Colgan, L.A., Putzier, I., and Levitan, E.S. (2009). Activity-dependent vesicular monoamine transporter-mediated depletion of the nucleus supports somatic release by serotonin neurons. J. Neurosci. Off. J. Soc. Neurosci. *29*, 15878–15887.

Colgan, L.A., Cavolo, S.L., Commons, K.G., and Levitan, E.S. (2012). Action potential-independent and pharmacologically unique vesicular serotonin release from dendrites. J. Neurosci. Off. J. Soc. Neurosci. *32*, 15737–15746.

Colino, A., and Halliwell, J.V. (1987). Differential modulation of three separate K-conductances in hippocampal CA1 neurons by serotonin. Nature *328*, 73–77.

Collet, C., Schiltz, C., Geoffroy, V., Maroteaux, L., Launay, J.-M., and Vernejoul, M.-C. de (2008). The serotonin 5-HT2B receptor controls bone mass via osteoblast recruitment and proliferation. FASEB J. *22*, 418–427.

Conn, P.J., and Sanders-Bush, E. (1984). Selective 5HT-2 antagonists inhibit serotonin stimulated phosphatidylinositol metabolism in cerebral cortex. Neuropharmacology *23*, 993–996.

Cour, C.M. la, Mestikawy, S.E., Hanoun, N., Hamon, M., and Lanfumey, L. (2006). Regional Differences in the Coupling of 5-Hydroxytryptamine-1A Receptors to G Proteins in the Rat Brain. Mol. Pharmacol. *70*, 1013–1021.

Cox, D.A., and Cohen, M.L. (1996). 5-HT2B receptor signaling in the rat stomach fundus: dependence on calcium influx, calcium release and protein kinase C. Behav. Brain Res. *73*, 289–292.

Craven, R.M., Grahame-Smith, D.G., and Newberry, N.R. (2001). 5-HT1A and 5-HT2 receptors differentially regulate the excitability of 5-HT-containing neurones of the guinea pig dorsal raphe nucleus in vitro. Brain Res. *899*, 159–168.

Cunningham, K.A., and Anastasio, N.C. (2014). Serotonin at the nexus of impulsivity and cue reactivity in cocaine addiction. Neuropharmacology *76 Pt B*, 460–478.

Cunningham, K. A., K.A., Anastasio, N.C., Fox, R.G., Stutz, S.J., Bubar, M.J., Swinford, S.E., Watson, C.S., Gilbertson, S.R., Rice, K.C., Rosenzweig-Lipson, S., et al. (2013). Synergism Between a Serotonin 5-HT2A Receptor (5-HT2AR) Antagonist and 5-HT2CR Agonist Suggests New Pharmacotherapeutics for Cocaine Addiction. ACS Chem. Neurosci. *4*, 110–121.

Cussac, D., Rauly-Lestienne, I., Heusler, P., Finana, F., Cathala, C., Bernois, S., and De Vries, L. (2012). μ-Opioid and 5-HT1A receptors heterodimerize and show signalling crosstalk via G protein and MAP-kinase pathways. Cell. Signal. *24*, 1648–1657.

D'Adamo, M.C., Servettini, I., Guglielmi, L., Matteo, V.D., Maio, R.D., Giovanni, G.D., and Pessia, M. (2013). 5-HT2 receptors-mediated modulation of voltage-gated K+ channels and neurophysiopathological correlates. Exp. Brain Res. *230*, 453–462.

Darmon, M., Al Awabdh, S., Emerit, M.-B., and Masson, J. (2015). Chapter Five - Insights into Serotonin Receptor Trafficking: Cell Membrane Targeting and Internalization. In Progress in Molecular Biology and Translational Science, G. Wu, ed. (Academic Press), pp. 97–126.

Day, M., Olson, P.A., Platzer, J., Striessnig, J., and Surmeier, D.J. (2002). Stimulation of 5-HT(2) receptors in prefrontal pyramidal neurons inhibits Ca(v)1.2 L type Ca(2+) currents via a PLCbeta/IP3/calcineurin signaling cascade. J. Neurophysiol. *87*, 2490–2504.

De Almeida, J., and Mengod, G. (2007). Quantitative analysis of glutamatergic and GABAergic neurons expressing 5-HT2A receptors in human and monkey prefrontal cortex. J. Neurochem. *103*, 475–486.

De Kock, C.P.J., Cornelisse, L.N., Burnashev, N., Lodder, J.C., Timmerman, A.J., Couey, J.J., Mansvelder, H.D., and Brussaard, A.B. (2006). NMDA receptors trigger neurosecretion of 5-HT within dorsal raphé nucleus of the rat in the absence of action potential firing. J. Physiol. *577*, 891–905.

Dean, C., Scholl, F.G., Choih, J., DeMaria, S., Berger, J., Isacoff, E., and Scheiffele, P. (2003). Neurexin mediates the assembly of presynaptic terminals. Nat. Neurosci. *6*, 708–716.

Della Rocca, G.J., Mukhin, Y.V., Garnovskaya, M.N., Daaka, Y., Clark, G.J., Luttrell, L.M., Lefkowitz, R.J., and Raymond, J.R. (1999). Serotonin 5-HT1A receptor-mediated Erk activation requires calcium/calmodulin-dependent receptor endocytosis. J. Biol. Chem. *274*, 4749–4753.

Deraet, M., Manivet, P., Janoshazi, A., Callebert, J., Guenther, S., Drouet, L., Launay, J.-M., and Maroteaux, L. (2005). The Natural Mutation Encoding a C Terminus-Truncated 5-Hydroxytryptamine2B Receptor Is a Gain of Proliferative Functions. Mol. Pharmacol. *67*, 983–991.

Descarries, L., and Mechawar, N. (2000). Ultrastructural evidence for diffuse transmission by monoamine and acetylcholine neurons of the central nervous system. Prog. Brain Res. *125*, 27–47.

Descarries, L., Watkins, K.C., Garcia, S., and Beaudet, A. (1982). The serotonin neurons in nucleus raphe dorsalis of adult rat: a light and electron microscope radioautographic study. J. Comp. Neurol. *207*, 239–254.

Descarries, L., Audet, M.A., Doucet, G., Garcia, S., Oleskevich, S., Séguéla, P., Soghomonian, J.J., and Watkins, K.C. (1990). Morphology of central serotonin neurons. Brief review of quantified aspects of their distribution and ultrastructural relationships. Ann. N. Y. Acad. Sci. *600*, 81–92.

Devroye, C., Cathala, A., Di Marco, B., Caraci, F., Drago, F., Piazza, P.V., and Spampinato, U. (2015). Central serotonin2B receptor blockade inhibits cocaine-induced hyperlocomotion independently of changes of subcortical dopamine outflow. Neuropharmacology *97*, 329–337.

Diaz, S.L., Doly, S., Narboux-Nême, N., Fernández, S., Mazot, P., Banas, S.M., Boutourlinsky, K., Moutkine, I., Belmer, A., Roumier, A., et al. (2012). 5-HT2B receptors are required for serotonin-selective antidepressant actions. Mol. Psychiatry *17*, 154–163.

Diaz, S.L., Narboux-Nême, N., Boutourlinsky, K., Doly, S., and Maroteaux, L. (2016). Mice lacking the serotonin 5-HT2B receptor as an animal model of resistance to selective serotonin reuptake inhibitors antidepressants. Eur. Neuropsychopharmacol. J. Eur. Coll. Neuropsychopharmacol. *26*, 265–279.

Dietzel, I.D., Drapeau, P., and Nicholls, J.G. (1986). Voltage dependence of 5-hydroxytryptamine release at a synapse between identified leech neurones in culture. J. Physiol. *372*, 191–205.

Doly, S., Valjent, E., Setola, V., Callebert, J., Hervé, D., Launay, J.-M., and Maroteaux, L. (2008). Serotonin 5-HT2B Receptors Are Required for 3,4-Methylenedioxymethamphetamine-Induced Hyperlocomotion and 5-HT Release In Vivo and In Vitro. J. Neurosci. *28*, 2933–2940.

Doly, S., Bertran-Gonzalez, J., Callebert, J., Bruneau, A., Banas, S.M., Belmer, A., Boutourlinsky, K., Hervé, D., Launay, J.-M., and Maroteaux, L. (2009). Role of Serotonin via 5-HT2B Receptors in the Reinforcing Effects of MDMA in Mice. PLoS ONE *4*, e7952.

Doyle, D.A., Lee, A., Lewis, J., Kim, E., Sheng, M., and MacKinnon, R. (1996). Crystal Structures of a Complexed and Peptide-Free Membrane Protein–Binding Domain: Molecular Basis of Peptide Recognition by PDZ. Cell *85*, 1067–1076.

Drake, M.T., Shenoy, S.K., and Lefkowitz, R.J. (2006). Trafficking of G Protein–Coupled Receptors. Circ. Res. *99*, 570–582.

Dunn, H.A., and Ferguson, S.S. (2015). PDZ Protein Regulation of GPCR Trafficking and Signaling Pathways. Mol. Pharmacol. mol.115.098509.

Emerit, M.B., Baranowski, C., Diaz, J., Martinez, A., Areias, J., Alterio, J., Masson, J., Boué-Grabot, E., and Darmon, M. (2016). A New Mechanism of Receptor Targeting by Interaction between Two Classes of Ligand-Gated Ion Channels. J. Neurosci. *36*, 1456–1470.

Erickson, J.D., Eiden, L.E., and Hoffman, B.J. (1992). Expression cloning of a reserpine-sensitive vesicular monoamine transporter. Proc. Natl. Acad. Sci. U. S. A. *89*, 10993–10997.

Esposito, E. (2006). Serotonin-dopamine interaction as a focus of novel antidepressant drugs. Curr. Drug Targets *7*, 177–185.

Fabre, V., Boutrel, B., Hanoun, N., Lanfumey, L., Fattaccini, C.M., Demeneix, B., Adrien, J., Hamon, M., and Martres, M.P. (2000). Homeostatic regulation of serotonergic function by the serotonin transporter as revealed by nonviral gene transfer. J. Neurosci. Off. J. Soc. Neurosci. *20*, 5065–5075.

Fei, H., Grygoruk, A., Brooks, E.S., Chen, A., and Krantz, D.E. (2008). Trafficking of Vesicular Neurotransmitter Transporters. Traffic *9*, 1425–1436.

Fernandez, S.P., Cauli, B., Cabezas, C., Muzerelle, A., Poncer, J.-C., and Gaspar, P. (2015). Multiscale single-cell analysis reveals unique phenotypes of raphe 5-HT neurons projecting to the forebrain. Brain Struct. Funct. *221*, 4007–4025.

Fitzgerald, L.W., Iyer, G., Conklin, D.S., Krause, C.M., Marshall, A., Patterson, J.P., Tran, D.P., Jonak, G.J., and Hartig, P.R. (1999). Messenger RNA Editing of the Human Serotonin 5-HT2C Receptor. Neuropsychopharmacology *21*, 82S–90S.

Fletcher, P.J., Korth, K.M., Robinson, S.R., and Baker, G.B. (2002). Multiple 5-HT receptors are involved in the effects of acute MDMA treatment: studies on locomotor activity and responding for conditioned reinforcement. Psychopharmacology (Berl.) *162*, 282–291.

Freund, T.F., and Buzsáki, G. (1996). Interneurons of the hippocampus. Hippocampus *6*, 347–470.

Fujita, M., Shimada, S., Maeno, H., Nishimura, T., and Tohyama, M. (1993). Cellular localization of serotonin transporter mRNA in the rat brain. Neurosci. Lett. *162*, 59–62.

Fuxe, K., Borroto-Escuela, D.O., Romero-Fernandez, W., Tarakanov, A.O., Calvo, F., Garriga, P., Tena, M., Narvaez, M., Millón, C., Parrado, C., et al. (2012a). On the existence and function of galanin receptor heteromers in the central nervous system. Front. Endocrinol. *3*.

Fuxe, K., Borroto-Escuela, D.O., Romero-Fernandez, W., Diaz-Cabiale, Z., Rivera, A., Ferraro, L., Tanganelli, S., Tarakanov, A.O., Garriga, P., Narváez, J.A., et al. (2012b). Extrasynaptic neurotransmission in the modulation of brain function. Focus on the striatal neuronal-glial networks. Front. Physiol. *3*, 136.

Gagnon, D., and Parent, M. (2014). Distribution of VGLUT3 in Highly Collateralized Axons from the Rat Dorsal Raphe Nucleus as Revealed by Single-Neuron Reconstructions. PLOS ONE *9*, e87709.

Gartside, S.E., Cole, A.J., Williams, A.P., McQuade, R., and Judge, S.J. (2007). AMPA and NMDA receptor regulation of firing activity in 5-HT neurons of the dorsal and median raphe nuclei. Eur. J. Neurosci. *25*, 3001–3008.

Gavarini, S., Bécamel, C., Chanrion, B., Bockaert, J., and Marin, P. (2004). Molecular and Functional Characterization of Proteins Interacting with the C-Terminal Domains of 5-HT2 Receptors: Emergence of 5-HT2 “Receptosomes.” Biol. Cell *96*, 373–381.

Gavarini, S., Bécamel, C., Altier, C., Lory, P., Poncet, J., Wijnholds, J., Bockaert, J., and Marin, P. (2006). Opposite Effects of PSD-95 and MPP3 PDZ Proteins on Serotonin 5-Hydroxytryptamine2C Receptor Desensitization and Membrane Stability. Mol. Biol. Cell *17*, 4619–4631.

Gérard, C., el Mestikawy, S., Lebrand, C., Adrien, J., Ruat, M., Traiffort, E., Hamon, M., and Martres, M.P. (1996). Quantitative RT-PCR distribution of serotonin 5-HT6 receptor mRNA in the central nervous system of control or 5,7-dihydroxytryptamine-treated rats. Synap. N. Y. N *23*, 164–173.

Ghavami, A., Baruscotti, M., Robinson, R.B., and Hen, R. (1997). Adenovirus-mediated expression of 5-HT1B receptors in cardiac ventricle myocytes; coupling to inwardly rectifying K+ channels. Eur. J. Pharmacol. *340*, 259–266.

González-Maeso, J., Ang, R.L., Yuen, T., Chan, P., Weisstaub, N.V., López-Giménez, J.F., Zhou, M., Okawa, Y., Callado, L.F., Milligan, G., et al. (2008). Identification of a serotonin/glutamate receptor complex implicated in psychosis. Nature *452*, 93–97.

Good, M.C., Zalatan, J.G., and Lim, W.A. (2011). Scaffold Proteins: Hubs for Controlling the Flow of Cellular Information. Science *332*, 680–686.

Goridis, C., and Rohrer, H. (2002). Specification of catecholaminergic and serotonergic neurons. Nat. Rev. Neurosci. *3*, 531–541.

Graeff, F.G., Guimarães, F.S., De Andrade, T.G., and Deakin, J.F. (1996). Role of 5-HT in stress, anxiety, and depression. Pharmacol. Biochem. Behav. *54*, 129–141.

Gras, C., Herzog, E., Bellenchi, G.C., Bernard, V., Ravassard, P., Pohl, M., Gasnier, B., Giros, B., and Mestikawy, S.E. (2002). A Third Vesicular Glutamate Transporter Expressed by Cholinergic and Serotoninergic Neurons. J. Neurosci. *22*, 5442–5451.

Guillaud, L., Setou, M., and Hirokawa, N. (2003). KIF17 dynamics and regulation of NR2B trafficking in hippocampal neurons. J. Neurosci. Off. J. Soc. Neurosci. *23*, 131–140.

Günther, S., Maroteaux, L., and Schwarzacher, S.W. (2006). Endogenous 5-HT2B receptor activation regulates neonatal respiratory activity in vitro. J. Neurobiol. *66*, 949–961.

Gurevich, I., Englander, M.T., Adlersberg, M., Siegal, N.B., and Schmauss, C. (2002). Modulation of Serotonin 2C Receptor Editing by Sustained Changes in Serotonergic Neurotransmission. J. Neurosci. *22*, 10529–10532.

Hagan, C.E., McDevitt, R.A., Liu, Y., Furay, A.R., and Neumaier, J.F. (2012). 5-HT(1B) autoreceptor regulation of serotonin transporter activity in synaptosomes. Synap. N. Y. N *66*, 1024–1034.

Hajjo, R., Grulke, C.M., Golbraikh, A., Setola, V., Huang, X.-P., Roth, B.L., and Tropsha, A. (2010). Development, Validation, and Use of Quantitative Structure−Activity Relationship Models of 5-Hydroxytryptamine (2B) Receptor Ligands to Identify Novel Receptor Binders and Putative Valvulopathic Compounds among Common Drugs. J. Med. Chem. *53*, 7573–7586.

Halazy, S., Perez, M., Fourrier, C., Pallard, I., Pauwels, P.J., Palmier, C., John, G.W., Valentin, J.-P., Bonnafous, R., and Martinez, J. (1996). Serotonin Dimers: Application of the Bivalent Ligand Approach to the Design of New Potent and Selective 5-HT1B/1D Agonists. J. Med. Chem. *39*, 4920–4927.

Hamon, M., Gozlan, H., el Mestikawy, S., Emerit, M.B., Bolaños, F., and Schechter, L. (1990). The central 5-HT1A receptors: pharmacological, biochemical, functional, and regulatory properties. Ann. N. Y. Acad. Sci. *600*, 114-129; discussion 129-131.

Hasuo, H., Matsuoka, T., and Akasu, T. (2002). Activation of Presynaptic 5-Hydroxytryptamine 2A Receptors Facilitates Excitatory Synaptic Transmission via Protein Kinase C in the Dorsolateral Septal Nucleus. J. Neurosci. *22*, 7509–7517.

Hata, Y., Butz, S., and Südhof, T.C. (1996). CASK: a novel dlg/PSD95 homolog with an N-terminal calmodulin-dependent protein kinase domain identified by interaction with neurexins. J. Neurosci. Off. J. Soc. Neurosci. *16*, 2488–2494.

Henderson, L.P. (1983). The role of 5-hydroxytryptamine as a transmitter between identified leech neurones in culture. J. Physiol. *339*, 309–324.

Hensler, J.G., Ferry, R.C., Labow, D.M., Kovachich, G.B., and Frazer, A. (1994). Quantitative autoradiography of the serotonin transporter to assess the distribution of serotonergic projections from the dorsal raphe nucleus. Synap. N. Y. N *17*, 1–15.

Herrick-Davis, K. (2013). Functional significance of serotonin receptor dimerization. Exp. Brain Res. *230*, 375–386.

Herrick-Davis, K., Grinde, E., and Mazurkiewicz, J.E. (2004). Biochemical and Biophysical Characterization of Serotonin 5-HT2C Receptor Homodimers on the Plasma Membrane of Living Cells†. Biochemistry (Mosc.) *43*, 13963–13971.

Herzog, E., Bellenchi, G.C., Gras, C., Bernard, V., Ravassard, P., Bedet, C., Gasnier, B., Giros, B., and Mestikawy, S.E. (2001). The Existence of a Second Vesicular Glutamate Transporter Specifies Subpopulations of Glutamatergic Neurons. J. Neurosci. *21*, RC181-RC181.

Herzog, E., Gilchrist, J., Gras, C., Muzerelle, A., Ravassard, P., Giros, B., Gaspar, P., and El Mestikawy, S. (2004). Localization of VGLUT3, the vesicular glutamate transporter type 3, in the rat brain. Neuroscience *123*, 983–1002.

Hioki, H., Nakamura, H., Ma, Y.-F., Konno, M., Hayakawa, T., Nakamura, K.C., Fujiyama, F., and Kaneko, T. (2010). Vesicular glutamate transporter 3-expressing nonserotonergic projection neurons constitute a subregion in the rat midbrain raphe nuclei. J. Comp. Neurol. *518*, 668–686.

Horton, Y.M., Lubbert, H., and Houslay, M.D. (1996). Localization of the gene for the human serotonin 5-HT(2B) receptor to chromosome 2. Mol. Membr. Biol. *13*, 29–31.

Howell, L.L., and Cunningham, K.A. (2015). Serotonin 5-HT2 Receptor Interactions with Dopamine Function: Implications for Therapeutics in Cocaine Use Disorder. Pharmacol. Rev. *67*, 176–197.

Imai, H., Steindler, D.A., and Kitai, S.T. (1986). The organization of divergent axonal projections from the midbrain raphe nuclei in the rat. J. Comp. Neurol. *243*, 363–380.

Innis, R.B., and Aghajanian, G.K. (1987). Pertussis toxin blocks 5-HT1A and GABAB receptor-mediated inhibition of serotonergic neurons. Eur. J. Pharmacol. *143*, 195–204.

Irie, M., Hata, Y., Takeuchi, M., Ichtchenko, K., Toyoda, A., Hirao, K., Takai, Y., Rosahl, T.W., and Südhof, T.C. (1997). Binding of neuroligins to PSD-95. Science *277*, 1511–1515.

Ishimura, K., Takeuchi, Y., Fujiwara, K., Tominaga, M., Yoshioka, H., and Sawada, T. (1988). Quantitative analysis of the distribution of serotonin-immunoreactive cell bodies in the mouse brain. Neurosci. Lett. *91*, 265–270.

Jacobs, B.L., and Fornal, C.A. (1993). 5-HT and motor control: a hypothesis. Trends Neurosci. *16*, 346–352.

Janoshazi, A., Deraet, M., Callebert, J., Setola, V., Guenther, S., Saubamea, B., Manivet, P., Launay, J.-M., and Maroteaux, L. (2007). Modified Receptor Internalization upon Coexpression of 5-HT1B Receptor and 5-HT2B Receptors. Mol. Pharmacol. *71*, 1463–1474.

Jayanthi, L.D., Samuvel, D.J., Blakely, R.D., and Ramamoorthy, S. (2005). Evidence for biphasic effects of protein kinase C on serotonin transporter function, endocytosis, and phosphorylation. Mol. Pharmacol. *67*, 2077–2087.

Jensen, P., Farago, A.F., Awatramani, R.B., Scott, M.M., Deneris, E.S., and Dymecki, S.M. (2008). Redefining the serotonergic system by genetic lineage. Nat. Neurosci. *11*, 417–419.

Johnson, M.D. (1994). Synaptic glutamate release by postnatal rat serotonergic neurons in microculture. Neuron *12*, 433–442.

Johnston, J.P. (1968). Some observations upon a new inhibitor of monoamine oxidase in brain tissue. Biochem. Pharmacol. *17*, 1285–1297.

Jones, K.A., Srivastava, D.P., Allen, J.A., Strachan, R.T., Roth, B.L., and Penzes, P. (2009). Rapid modulation of spine morphology by the 5-HT2A serotonin receptor through kalirin-7 signaling. Proc. Natl. Acad. Sci. *106*, 19575–19580.

Joo, S.H., and Pei, D. (2008). Synthesis and Screening of Support-Bound Combinatorial Peptide Libraries with Free C-Termini: Determination of the Sequence Specificity of PDZ Domains†. Biochemistry (Mosc.) *47*, 3061–3072.

Jørgensen, T.N., Christensen, P.M., and Gether, U. (2014). Serotonin-induced down-regulation of cell surface serotonin transporter. Neurochem. Int. *73*, 107–112.

Joubert, L., Hanson, B., Barthet, G., Sebben, M., Claeysen, S., Hong, W., Marin, P., Dumuis, A., and Bockaert, J. (2004). New sorting nexin (SNX27) and NHERF specifically interact with the 5-HT4(a) receptor splice variant: roles in receptor targeting. J. Cell Sci. *117*, 5367–5379.

Kanner, B.I., and Schuldiner, S. (1987). Mechanism of transport and storage of neurotransmitters. CRC Crit. Rev. Biochem. *22*, 1–38.

Kapadia, S.E., de Lanerolle, N.C., and LaMotte, C.C. (1985). Immunocytochemical and electron microscopic study of serotonin neuronal organization in the dorsal raphe nucleus of the monkey. Neuroscience *15*, 729–746.

Karila, D., Freret, T., Bouet, V., Boulouard, M., Dallemagne, P., and Rochais, C. (2015). Therapeutic Potential of 5-HT6 Receptor Agonists. J. Med. Chem. *58*, 7901–7912.

Katsurabayashi, S., Kubota, H., Tokutomi, N., and Akaike, N. (2003). A distinct distribution of functional presynaptic 5-HT receptor subtypes on GABAergic nerve terminals projecting to single hippocampal CA1 pyramidal neurons. Neuropharmacology *44*, 1022–1030.

Katz, B., and Miledi, R. (1970). Further study of the role of calcium in synaptic transmission. J. Physiol. *207*, 789–801.

Kaushalya, S.K., Nag, S., Ghosh, H., Arumugam, S., and Maiti, S. (2008a). A high-resolution large area serotonin map of a live rat brain section. Neuroreport *19*, 717–721.

Kaushalya, S.K., Desai, R., Arumugam, S., Ghosh, H., Balaji, J., and Maiti, S. (2008b). Three-photon microscopy shows that somatic release can be a quantitatively significant component of serotonergic neurotransmission in the mammalian brain. J. Neurosci. Res. *86*, 3469–3480.

Kawahara, Y., Grimberg, A., Teegarden, S., Mombereau, C., Liu, S., Bale, T.L., Blendy, J.A., and Nishikura, K. (2008). Dysregulated Editing of Serotonin 2C Receptor mRNAs Results in Energy Dissipation and Loss of Fat Mass. J. Neurosci. *28*, 12834–12844.

Kawashima, N., Karasawa, J., Shimazaki, T., Chaki, S., Okuyama, S., Yasuhara, A., and Nakazato, A. (2005). Neuropharmacological profiles of antagonists of group II metabotropic glutamate receptors. Neurosci. Lett. *378*, 131–134.

Kellermann, O., Loric, S., Maroteaux, L., and Launay, J.M. (1996). Sequential onset of three 5-HT receptors during the 5-hydroxytryptaminergic differentiation of the murine 1C11 cell line. Br. J. Pharmacol. *118*, 1161–1170.

Kenakin, T., Watson, C., Muniz-Medina, V., Christopoulos, A., and Novick, S. (2012). A Simple Method for Quantifying Functional Selectivity and Agonist Bias. ACS Chem. Neurosci. *3*, 193–203.

Kennett, G. a., Bright, F., Trail, B., Baxter, G. s., and Blackburn, T. p. (1996). Effects of the 5-HT2B receptor agonist, BW 723C86, on three rat models of anxiety. Br. J. Pharmacol. *117*, 1443–1448.

Kia, H.K., Miquel, M.C., Brisorgueil, M.J., Daval, G., Riad, M., El Mestikawy, S., Hamon, M., and Vergé, D. (1996). Immunocytochemical localization of serotonin1A receptors in the rat central nervous system. J. Comp. Neurol. *365*, 289–305.

Kiehn, O., Rostrup, E., and Møller, M. (1992). Monoaminergic systems in the brainstem and spinal cord of the turtle Pseudemys scripta elegans as revealed by antibodies against serotonin and tyrosine hydroxylase. J. Comp. Neurol. *325*, 527–547.

Kish, S.J., Furukawa, Y., Chang, L.-J., Tong, J., Ginovart, N., Wilson, A., Houle, S., and Meyer, J.H. (2005). Regional distribution of serotonin transporter protein in postmortem human brain: is the cerebellum a SERT-free brain region? Nucl. Med. Biol. *32*, 123–128.

Kishimoto, K., Koyama, S., and Akaike, N. (2001). Synergistic mu-opioid and 5-HT1A presynaptic inhibition of GABA release in rat periaqueductal gray neurons. Neuropharmacology *41*, 529–538.

Knoll, J., and Magyar, K. (1972). Some puzzling pharmacological effects of monoamine oxidase inhibitors. Adv. Biochem. Psychopharmacol. *5*, 393–408.

Kobe, F., Renner, U., Woehler, A., Wlodarczyk, J., Papusheva, E., Bao, G., Zeug, A., Richter, D.W., Neher, E., and Ponimaskin, E. (2008). Stimulation- and palmitoylation-dependent changes in oligomeric conformation of serotonin 5-HT1A receptors. Biochim. Biophys. Acta *1783*, 1503–1516.

Köhler, C., Chan-Palay, V., and Steinbusch, H. (1982). The distribution and origin of serotonin-containing fibers in the septal area: a combined immunohistochemical and fluorescent retrograde tracing study in the rat. J. Comp. Neurol. *209*, 91–111.

Kolodziejczak, M., Béchade, C., Gervasi, N., Irinopoulou, T., Banas, S.M., Cordier, C., Rebsam, A., Roumier, A., and Maroteaux, L. (2015). Serotonin Modulates Developmental Microglia via 5-HT2B Receptors: Potential Implication during Synaptic Refinement of Retinogeniculate Projections. ACS Chem. Neurosci. *6*, 1219–1230.

van der Kooy, D., and Hattori, T. (1980). Dorsal raphe cells with collateral projections to the caudate-putamen and substantia nigra: a fluorescent retrograde double labeling study in the rat. Brain Res. *186*, 1–7.

Kosofsky, B.E., and Molliver, M.E. (1987). The serotoninergic innervation of cerebral cortex: different classes of axon terminals arise from dorsal and median raphe nuclei. Synap. N. Y. N *1*, 153–168.

Koyama, S., Matsumoto, N., Murakami, N., Kubo, C., Nabekura, J., and Akaike, N. (2002). Role of presynaptic 5-HT1A and 5-HT3 receptors in modulation of synaptic GABA transmission in dissociated rat basolateral amygdala neurons. Life Sci. *72*, 375–387.

Kuffler, D.P., Nicholls, J., and Drapeau, P. (1987). Transmitter localization and vesicle turnover at a serotoninergic synapse between identified leech neurons in culture. J. Comp. Neurol. *256*, 516–526.

Kurrasch-Orbaugh, D.M., Parrish, J.C., Watts, V.J., and Nichols, D.E. (2003). A complex signaling cascade links the serotonin2A receptor to phospholipase A2 activation: the involvement of MAP kinases. J. Neurochem. *86*, 980–991.

Kursar, J.D., Nelson, D.L., Wainscott, D.B., and Baez, M. (1994). Molecular cloning, functional expression, and mRNA tissue distribution of the human 5-hydroxytryptamine2B receptor. Mol. Pharmacol. *46*, 227–234.

Kurschner, C., and Morgan, J.I. (1995). The maf proto-oncogene stimulates transcription from multiple sites in a promoter that directs Purkinje neuron-specific gene expression. Mol. Cell. Biol. *15*, 246–254.

Kurschner, C., Mermelstein, P.G., Holden, W.T., and Surmeier, D.J. (1998). CIPP, a Novel Multivalent PDZ Domain Protein, Selectively Interacts with Kir4.0 Family Members, NMDA Receptor Subunits, Neurexins, and Neuroligins. Mol. Cell. Neurosci. *11*, 161–172.

Kvachnina, E., Liu, G., Dityatev, A., Renner, U., Dumuis, A., Richter, D.W., Dityateva, G., Schachner, M., Voyno-Yasenetskaya, T.A., and Ponimaskin, E.G. (2005). 5-HT7 receptor is coupled to G alpha subunits of heterotrimeric G12-protein to regulate gene transcription and neuronal morphology. J. Neurosci. Off. J. Soc. Neurosci. *25*, 7821–7830.

Labasque, M., Reiter, E., Becamel, C., Bockaert, J., and Marin, P. (2008). Physical interaction of calmodulin with the 5-hydroxytryptamine2C receptor C-terminus is essential for G protein-independent, arrestin-dependent receptor signaling. Mol. Biol. Cell *19*, 4640–4650.

Lan, J.Y., Skeberdis, V.A., Jover, T., Grooms, S.Y., Lin, Y., Araneda, R.C., Zheng, X., Bennett, M.V., and Zukin, R.S. (2001). Protein kinase C modulates NMDA receptor trafficking and gating. Nat. Neurosci. *4*, 382–390.

Lanfumey, L., and Hamon, M. (2000). Central 5-HT(1A) receptors: regional distribution and functional characteristics. Nucl. Med. Biol. *27*, 429–435.

Lau, C.G., and Zukin, R.S. (2007). NMDA receptor trafficking in synaptic plasticity and neuropsychiatric disorders. Nat. Rev. Neurosci. *8*, 413–426.

Lau, T., Horschitz, S., Bartsch, D., and Schloss, P. (2009). Monitoring mouse serotonin transporter internalization in stem cell-derived serotonergic neurons by confocal laser scanning microscopy. Neurochem. Int. *54*, 271–276.

Launay, J.-M., Birraux, G., Bondoux, D., Callebert, J., Choi, D.-S., Loric, S., and Maroteaux, L. (1996). Ras Involvement in Signal Transduction by the Serotonin 5-HT2B Receptor. J. Biol. Chem. *271*, 3141–3147.

Launay, J.-M., Hervé, P., Peoc'h, K., Tournois, C., Callebert, J., Nebigil, C.G., Etienne, N., Drouet, L., Humbert, M., Simonneau, G., et al. (2002). Function of the serotonin 5-hydroxytryptamine 2B receptor in pulmonary hypertension. Nat. Med. *8*, 1129–1135.

Launay, J.-M., Schneider, B., Loric, S., Prada, M.D., and Kellermann, O. (2006). Serotonin transport and serotonin transporter-mediated antidepressant recognition are controlled by 5-HT2B receptor signaling in serotonergic neuronal cells. FASEB J. *20*, 1843–1854.

Le Coniat, M., Choi, D.-S., Maroteaux, L., Launay, J.-M., and Berger, R. (1996). The 5-HT2B Receptor Gene Maps to 2q36.3–2q37.1. Genomics *32*, 172–173.

Le Grand, B., Panissié, A., Pauwels, P.J., and John, G.W. (1998). Activation of recombinant h 5-HT1B and h 5-HT1D receptors stably expressed in C6 glioma cells produces increases in Ca2+-dependent K+ current. Naunyn. Schmiedebergs Arch. Pharmacol. *358*, 608–615.

Le Roy, C., and Wrana, J.L. (2005). Clathrin- and non-clathrin-mediated endocytic regulation of cell signalling. Nat. Rev. Mol. Cell Biol. *6*, 112–126.

Leon-Pinzon, C., Cercós, M.G., Noguez, P., Trueta, C., and De-Miguel, F.F. (2014). Exocytosis of serotonin from the neuronal soma is sustained by a serotonin and calcium-dependent feedback loop. Front. Cell. Neurosci. *8*, 169.

Levine, E.S., and Jacobs, B.L. (1992). Neurochemical afferents controlling the activity of serotonergic neurons in the dorsal raphe nucleus: microiontophoretic studies in the awake cat. J. Neurosci. Off. J. Soc. Neurosci. *12*, 4037–4044.

Leysen, J.E. (2004). 5-HT2 receptors. Curr. Drug Targets CNS Neurol. Disord. *3*, 11–26.

Lin, S.L., Setya, S., Johnson-Farley, N.N., and Cowen, D.S. (2002). Differential coupling of 5-HT(1) receptors to G proteins of the G(i) family. Br. J. Pharmacol. *136*, 1072–1078.

Lin, S.-Y., Chang, W.-J., Lin, C.-S., Huang, C.-Y., Wang, H.-F., and Sun, W.-H. (2011). Serotonin Receptor 5-HT2B Mediates Serotonin-Induced Mechanical Hyperalgesia. J. Neurosci. *31*, 1410–1418.

Lin, Z., Walther, D., Yu, X.-Y., Drgon, T., and Uhl, G. (2004). The human serotonin receptor 2B: coding region polymorphisms and association with vulnerability to illegal drug abuse. Pharmacogenetics Dec. 2004 *14*, 805–811.

Liposits, Z., Görcs, T., and Trombitás, K. (1985). Ultrastructural analysis of central serotoninergic neurons immunolabeled by silver-gold-intensified diaminobenzidine chromogen. Completion of immunocytochemistry with X-ray microanalysis. J. Histochem. Cytochem. Off. J. Histochem. Soc. *33*, 604–610.

Liu, C., Maejima, T., Wyler, S.C., Casadesus, G., Herlitze, S., and Deneris, E.S. (2010). Pet-1 is required across different stages of life to regulate serotonergic function. Nat. Neurosci. *13*, 1190–1198.

Liu, R., Jolas, T., and Aghajanian, G. (2000). Serotonin 5-HT2 receptors activate local GABA inhibitory inputs to serotonergic neurons of the dorsal raphe nucleus. Brain Res. *873*, 34–45.

Liu, Y., Peter, D., Roghani, A., Schuldiner, S., Privé, G.G., Eisenberg, D., Brecha, N., and Edwards, R.H. (1992). A cDNA that suppresses MPP+ toxicity encodes a vesicular amine transporter. Cell *70*, 539–551.

Liu, Z., Zhou, J., Li, Y., Hu, F., Lu, Y., Ma, M., Feng, Q., Zhang, J., Wang, D., Zeng, J., et al. (2014). Dorsal Raphe Neurons Signal Reward through 5-HT and Glutamate. Neuron *81*, 1360–1374.

Llinás, R., Steinberg, I.Z., and Walton, K. (1981). Relationship between presynaptic calcium current and postsynaptic potential in squid giant synapse. Biophys. J. *33*, 323–351.

Lohr, C., Beck, A., and Deitmer, J.W. (2001). Activity-dependent accumulation of Ca2+ in axon and dendrites of the leech Leydig neuron. Neuroreport *12*, 3649–3653.

López-Giménez, J.F., Mengod, G., Palacios, J.M., and Vilaró, M.T. (1997). Selective visualization of rat brain 5-HT2A receptors by autoradiography with [3H]MDL 100,907. Naunyn. Schmiedebergs Arch. Pharmacol. *356*, 446–454.

Loric, S., Launay, J.M., Colas, J.F., and Maroteaux, L. (1992). New mouse 5-HT2-like receptor. Expression in brain, heart and intestine. FEBS Lett. *312*, 203–207.

Lucas, G., and Debonnel, G. (2002). 5-HT4 receptors exert a frequency-related facilitatory control on dorsal raphé nucleus 5-HT neuronal activity. Eur. J. Neurosci. *16*, 817–822.

Łukasiewicz, S., Błasiak, E., Faron-Górecka, A., Polit, A., Tworzydło, M., Górecki, A., Wasylewski, Z., and Dziedzicka-Wasylewska, M. (2007). Fluorescence studies of homooligomerization of adenosine A2A and serotonin 5-HT1A receptors reveal the specificity of receptor interactions in the plasma membrane. Pharmacol. Rep. PR *59*, 379–392.

Łukasiewicz, S., Polit, A., Kędracka-Krok, S., Wędzony, K., Maćkowiak, M., and Dziedzicka-Wasylewska, M. (2010). Hetero-dimerization of serotonin 5-HT2A and dopamine D2 receptors. Biochim. Biophys. Acta BBA - Mol. Cell Res. *1803*, 1347–1358.

Łukasiewicz, S., Faron-Górecka, A., Kędracka-Krok, S., and Dziedzicka-Wasylewska, M. (2011). Effect of clozapine on the dimerization of serotonin 5-HT(2A) receptor and its genetic variant 5-HT(2A)H425Y with dopamine D(2) receptor. Eur. J. Pharmacol. *659*, 114–123.

Lummis, S.C.R. (2012). 5-HT3 Receptors. J. Biol. Chem. *287*, 40239–40245.

Luscher, C. (2016). The Emergence of a Circuit Model for Addiction. Annu. Rev. Neurosci. *39*, 257–276.

Maejima, T., Masseck, O.A., Mark, M.D., and Herlitze, S. (2013). Modulation of firing and synaptic transmission of serotonergic neurons by intrinsic G protein-coupled receptors and ion channels. Front. Integr. Neurosci. *7*.

Mancia, F., Assur, Z., Herman, A.G., Siegel, R., and Hendrickson, W.A. (2008). Ligand sensitivity in dimeric associations of the serotonin 5HT2c receptor. EMBO Rep. *9*, 363–369.

Manivet, P., Mouillet-Richard, S., Callebert, J., Nebigil, C.G., Maroteaux, L., Hosoda, S., Kellermann, O., and Launay, J.-M. (2000). PDZ-dependent Activation of Nitric-oxide Synthases by the Serotonin 2B Receptor. J. Biol. Chem. *275*, 9324–9331.

Manivet, P., Schneider, B., Smith, J.C., Choi, D.-S., Maroteaux, L., Kellermann, O., and Launay, J.-M. (2002). The Serotonin Binding Site of Human and Murine 5-HT2BReceptors MOLECULAR MODELING AND SITE-DIRECTED MUTAGENESIS. J. Biol. Chem. *277*, 17170–17178.

Mao, X., Fujiwara, Y., Chapdelaine, A., Yang, H., and Orkin, S.H. (2001). Activation of EGFP expression by Cre-mediated excision in a new ROSA26 reporter mouse strain. Blood *97*, 324–326.

Marcos, B., Cabero, M., Solas, M., Aisa, B., and Ramirez, M.J. (2010). Signalling pathways associated with 5-HT6 receptors: relevance for cognitive effects. Int. J. Neuropsychopharmacol. *13*, 775–784.

Marin, P., Becamel, C., Dumuis, A., and Bockaert, J. (2012). 5-HT Receptor-Associated Protein Networks: New Targets for Drug Discovery in Psychiatric Disorders? Curr. Drug Targets *13*, 28–52.

Marinelli, S., Schnell, S.A., Hack, S.P., Christie, M.J., Wessendorf, M.W., and Vaughan, C.W. (2004). Serotonergic and Nonserotonergic Dorsal Raphe Neurons Are Pharmacologically and Electrophysiologically Heterogeneous. J. Neurophysiol. *92*, 3532–3537.

Marion, S., Weiner, D.M., and Caron, M.G. (2004). RNA Editing Induces Variation in Desensitization and Trafficking of 5-Hydroxytryptamine 2c Receptor Isoforms. J. Biol. Chem. *279*, 2945–2954.

Maroteaux, L., Ayme-Dietrich, E., Aubertin-Kirch, G., Banas, S., Quentin, E., Lawson, R., and Monassier, L. (2017). New therapeutic opportunities for 5-HT2 receptor ligands. Pharmacol. Ther. *170*, 14–36.

Masson, J., Emerit, M.B., Hamon, M., and Darmon, M. (2012). Serotonergic signaling: multiple effectors and pleiotropic effects. Wiley Interdiscip. Rev. Membr. Transp. Signal. *1*, 685–713.

Matthes, H., Boschert, U., Amlaiky, N., Grailhe, R., Plassat, J.L., Muscatelli, F., Mattei, M.G., and Hen, R. (1993). Mouse 5-hydroxytryptamine5A and 5-hydroxytryptamine5B receptors define a new family of serotonin receptors: cloning, functional expression, and chromosomal localization. Mol. Pharmacol. *43*, 313–319.

Miller, K.J., and Hoffman, B.J. (1994). Adenosine A3 receptors regulate serotonin transport via nitric oxide and cGMP. J. Biol. Chem. *269*, 27351–27356.

Misener, V.L., Luca, P., Azeke, O., Crosbie, J., Waldman, I., Tannock, R., Roberts, W., Malone, M., Schachar, R., Ickowicz, A., et al. (2004). Linkage of the dopamine receptor D1 gene to attention-deficit/hyperactivity disorder. Mol. Psychiatry *9*, 500–509.

Mlinar, B., Montalbano, A., Baccini, G., Tatini, F., Palmini, R.B., and Corradetti, R. (2015). Nonexocytotic serotonin release tonically suppresses serotonergic neuron activity. J. Gen. Physiol. *145*, 225–251.

Mlinar, B., Montalbano, A., Piszczek, L., Gross, C., and Corradetti, R. (2016). Firing Properties of Genetically Identified Dorsal Raphe Serotonergic Neurons in Brain Slices. Front. Cell. Neurosci. *10*.

Monassier, L., Laplante, M.A., Ayadi, T., Doly, S., and Maroteaux, L. (2010). Contribution of gene-modified mice and rats to our understanding of the cardiovascular pharmacology of serotonin. Pharmacol. Ther. *128*, 559–567.

Montalbano, A., Corradetti, R., and Mlinar, B. (2015). Pharmacological Characterization of 5-HT1A Autoreceptor-Coupled GIRK Channels in Rat Dorsal Raphe 5-HT Neurons. PLOS ONE *10*, e0140369.

Moreno, J.L., Holloway, T., Albizu, L., Sealfon, S.C., and González-Maeso, J. (2011). Metabotropic glutamate mGlu2 receptor is necessary for the pharmacological and behavioral effects induced by hallucinogenic 5-HT2A receptor agonists. Neurosci. Lett. *493*, 76–79.

Moreno, J.L., Muguruza, C., Umali, A., Mortillo, S., Holloway, T., Pilar-Cuéllar, F., Mocci, G., Seto, J., Callado, L.F., Neve, R.L., et al. (2012). Identification of Three Residues Essential for 5-Hydroxytryptamine 2A-Metabotropic Glutamate 2 (5-HT2A·mGlu2) Receptor Heteromerization and Its Psychoactive Behavioral Function. J. Biol. Chem. *287*, 44301–44319.

Morikawa, H., Manzoni, O.J., Crabbe, J.C., and Williams, J.T. (2000). Regulation of central synaptic transmission by 5-HT(1B) auto- and heteroreceptors. Mol. Pharmacol. *58*, 1271–1278.

Mosienko, V., Beis, D., Pasqualetti, M., Waider, J., Matthes, S., Qadri, F., Bader, M., and Alenina, N. (2015). Life without brain serotonin: Reevaluation of serotonin function with mice deficient in brain serotonin synthesis. Behav. Brain Res. *277*, 78–88.

Moukhles, H., Bosler, O., Bolam, J.P., Vallée, A., Umbriaco, D., Geffard, M., and Doucet, G. (1997). Quantitative and morphometric data indicate precise cellular interactions between serotonin terminals and postsynaptic targets in rat substantia nigra. Neuroscience *76*, 1159–1171.

Moutkine, I., Quentin, E., Guiard, B.P., Maroteaux, L., and Doly, S. (2017). Heterodimers of serotonin receptor subtypes 2 are driven by 5-HT2C protomers. J. Biol. Chem. jbc.M117.779041.

Murphy, D.L., and Lesch, K.-P. (2008). Targeting the murine serotonin transporter: insights into human neurobiology. Nat. Rev. Neurosci. *9*, 85–96.

Muzerelle, A., Scotto-Lomassese, S., Bernard, J.F., Soiza-Reilly, M., and Gaspar, P. (2014). Conditional anterograde tracing reveals distinct targeting of individual serotonin cell groups (B5–B9) to the forebrain and brainstem. Brain Struct. Funct. 1–27.

Nebigil, C.G., and Maroteaux, L. (2001). A Novel Role for Serotonin in Heart. Trends Cardiovasc. Med. *11*, 329–335.

Nebigil, C.G., Choi, D.-S., Dierich, A., Hickel, P., Meur, M.L., Messaddeq, N., Launay, J.-M., and Maroteaux, L. (2000). Serotonin 2B receptor is required for heart development. Proc. Natl. Acad. Sci. *97*, 9508–9513.

Nebigil, C.G., Etienne, N., Messaddeq, N., and Maroteaux, L. (2003a). Serotonin is a novel survival factor of cardiomyocytes: mitochondria as a target of 5-HT2B receptor signaling. FASEB J. Off. Publ. Fed. Am. Soc. Exp. Biol. *17*, 1373–1375.

Nebigil, C.G., Jaffré, F., Messaddeq, N., Hickel, P., Monassier, L., Launay, J.-M., and Maroteaux, L. (2003b). Overexpression of the Serotonin 5-HT2B Receptor in Heart Leads to Abnormal Mitochondrial Function and Cardiac Hypertrophy. Circulation *107*, 3223–3229.

Nelson, D.L. (2004). 5-HT5 receptors. Curr. Drug Targets CNS Neurol. Disord. *3*, 53–58.

Niebert, M., Vogelgesang, S., Koch, U.R., Bischoff, A.-M., Kron, M., Bock, N., and Manzke, T. (2011). Expression and Function of Serotonin 2A and 2B Receptors in the Mammalian Respiratory Network. PLOS ONE *6*, e21395.

Norum, J.H., Hart, K., and Levy, F.O. (2003). Ras-dependent ERK activation by the human G(s)-coupled serotonin receptors 5-HT4(b) and 5-HT7(a). J. Biol. Chem. *278*, 3098–3104.

Norum, J.H., Méthi, T., Mattingly, R.R., and Levy, F.O. (2005). Endogenous expression and protein kinase A-dependent phosphorylation of the guanine nucleotide exchange factor Ras-GRF1 in human embryonic kidney 293 cells. FEBS J. *272*, 2304–2316.

Nusser, Z., Mulvihill, E., Streit, P., and Somogyi, P. (1994). Subsynaptic segregation of metabotropic and ionotropic glutamate receptors as revealed by immunogold localization. Neuroscience *61*, 421–427.

Okaty, B.W., Freret, M.E., Rood, B.D., Brust, R.D., Hennessy, M.L., deBairos, D., Kim, J.C., Cook, M.N., and Dymecki, S.M. (2015). Multi-Scale Molecular Deconstruction of the Serotonin Neuron System. Neuron *88*, 774–791.

Oleskevich, S., Descarries, L., Watkins, K.C., Séguéla, P., and Daszuta, A. (1991). Ultrastructural features of the serotonin innervation in adult rat hippocampus: an immunocytochemical description in single and serial thin sections. Neuroscience *42*, 777–791.

Page, I.H., Rapport, M.M., and Green, A.A. (1948). The crystallization of serotonin. J. Lab. Clin. Med. *33*, 1606.

Paila, Y.D., Kombrabail, M., Krishnamoorthy, G., and Chattopadhyay, A. (2011). Oligomerization of the serotonin(1A) receptor in live cells: a time-resolved fluorescence anisotropy approach. J. Phys. Chem. B *115*, 11439–11447.

Pan, Z.Z., and Williams, J.T. (1989). GABA- and glutamate-mediated synaptic potentials in rat dorsal raphe neurons in vitro. J. Neurophysiol. *61*, 719–726.

Pazos, A., and Palacios, J.M. (1985). Quantitative autoradiographic mapping of serotonin receptors in the rat brain. I. Serotonin-1 receptors. Brain Res. *346*, 205–230.

Pazos, A., Cortés, R., and Palacios, J.M. (1985). Quantitative autoradiographic mapping of serotonin receptors in the rat brain. II. Serotonin-2 receptors. Brain Res. *346*, 231–249.

Pellissier, L.P., Barthet, G., Gaven, F., Cassier, E., Trinquet, E., Pin, J.-P., Marin, P., Dumuis, A., Bockaert, J., Banères, J.-L., et al. (2011). G protein activation by serotonin type 4 receptor dimers: evidence that turning on two protomers is more efficient. J. Biol. Chem. *286*, 9985–9997.

Penington, N.J., and Kelly, J.S. (1990). Serotonin receptor activation reduces calcium current in an acutely dissociated adult central neuron. Neuron *4*, 751–758.

Penington, N.J., Kelly, J.S., and Fox, A.P. (1992). Action potential waveforms reveal simultaneous changes in ICa and IK produced by 5-HT in rat dorsal raphe neurons. Proc. Biol. Sci. *248*, 171–179.

Perrier, J.-F., and Cotel, F. (2008). Serotonin differentially modulates the intrinsic properties of spinal motoneurons from the adult turtle. J. Physiol. *586*, 1233–1238.

Pieczynski, J., and Margolis, B. (2011). Protein complexes that control renal epithelial polarity. Am. J. Physiol. - Ren. Physiol. *300*, F589–F601.

Pitychoutis, P.M., Belmer, A., Moutkine, I., Adrien, J., and Maroteaux, L. (2015). Mice Lacking the Serotonin Htr2B Receptor Gene Present an Antipsychotic-Sensitive Schizophrenic-Like Phenotype. Neuropsychopharmacology *40*, 2764–2773.

Pompeiano, M., Palacios, J.M., and Mengod, G. (1992). Distribution and cellular localization of mRNA coding for 5-HT1A receptor in the rat brain: correlation with receptor binding. J. Neurosci. Off. J. Soc. Neurosci. *12*, 440–453.

Pompeiano, M., Palacios, J.M., and Mengod, G. (1994). Distribution of the serotonin 5-HT2 receptor family mRNAs: comparison between 5-HT2A and 5-HT2C receptors. Brain Res. Mol. Brain Res. *23*, 163–178.

Portas, C.M., Bjorvatn, B., and Ursin, R. (2000). Serotonin and the sleep/wake cycle: special emphasis on microdialysis studies. Prog. Neurobiol. *60*, 13–35.

Porter, R.H.P., Malcolm, C.S., Allen, N.H., Lamb, H., Revell, D.F., and Sheardown, M.J. (2001). Agonist-induced functional desensitization of recombinant human 5-HT2 receptors expressed in CHO-K1 cells2. Biochem. Pharmacol. *62*, 431–438.

Prasad, H.C., Zhu, C.-B., McCauley, J.L., Samuvel, D.J., Ramamoorthy, S., Shelton, R.C., Hewlett, W.A., Sutcliffe, J.S., and Blakely, R.D. (2005). Human serotonin transporter variants display altered sensitivity to protein kinase G and p38 mitogen-activated protein kinase. Proc. Natl. Acad. Sci. U. S. A. *102*, 11545–11550.

Prosser, R.A., Miller, J.D., and Heller, H.C. (1990). A serotonin agonist phase-shifts the circadian clock in the suprachiasmatic nuclei in vitro. Brain Res. *534*, 336–339.

Rainer, Q., Nguyen, H.T., Quesseveur, G., Gardier, A.M., David, D.J., and Guiard, B.P. (2012). Functional Status of Somatodendritic Serotonin 1A Autoreceptor after Long-Term Treatment

with Fluoxetine in a Mouse Model of Anxiety/Depression Based on Repeated Corticosterone Administration. Mol. Pharmacol. *81*, 106–112.

Ramamoorthy, S., Giovanetti, E., Qian, Y., and Blakely, R.D. (1998). Phosphorylation and regulation of antidepressant-sensitive serotonin transporters. J. Biol. Chem. *273*, 2458–2466.

Ramamoorthy, S., Samuvel, D.J., Buck, E.R., Rudnick, G., and Jayanthi, L.D. (2007). Phosphorylation of threonine residue 276 is required for acute regulation of serotonin transporter by cyclic GMP. J. Biol. Chem. *282*, 11639–11647.

Rapport, M.M. (1949). Serum vasoconstrictor (serotonin) the presence of creatinine in the complex; a proposed structure of the vasoconstrictor principle. J. Biol. Chem. *180*, 961–969.

Rapport, M.M., Green, A.A., and Page, I.H. (1948). Serum vasoconstrictor, serotonin; chemical inactivation. J. Biol. Chem. *176*, 1237–1241.

Raymond, J.R., Mukhin, Y.V., Gelasco, A., Turner, J., Collinsworth, G., Gettys, T.W., Grewal, J.S., and Garnovskaya, M.N. (2001). Multiplicity of mechanisms of serotonin receptor signal transduction. Pharmacol. Ther. *92*, 179–212.

Renner, U., Zeug, A., Woehler, A., Niebert, M., Dityatev, A., Dityateva, G., Gorinski, N., Guseva, D., Abdel-Galil, D., Fröhlich, M., et al. (2012). Heterodimerization of serotonin receptors 5-HT1A and 5-HT7 differentially regulates receptor signalling and trafficking. J Cell Sci *125*, 2486–2499.

Reynolds, K.A., McLaughlin, R.N., and Ranganathan, R. (2011). Hot spots for allosteric regulation on protein surfaces. Cell *147*, 1564–1575.

Riad, M., Garcia, S., Watkins, K.C., Jodoin, N., Doucet, É., Langlois, X., El Mestikawy, S., Hamon, M., and Descarries, L. (2000). Somatodendritic localization of 5-HT1A and preterminal axonal localization of 5-HT1B serotonin receptors in adult rat brain. J. Comp. Neurol. *417*, 181–194.

Richardson-Jones, J.W., Craige, C.P., Guiard, B.P., Stephen, A., Metzger, K.L., Kung, H.F., Gardier, A.M., Dranovsky, A., David, D.J., Beck, S.G., et al. (2010). 5-HT1A Autoreceptor Levels Determine Vulnerability to Stress and Response to Antidepressants. Neuron *65*, 40–52.

Ridet, J.L., Rajaofetra, N., Teilhac, J.R., Geffard, M., and Privat, A. (1993). Evidence for nonsynaptic serotonergic and noradrenergic innervation of the rat dorsal horn and possible involvement of neuron-glia interactions. Neuroscience *52*, 143–157.

Ridet, J.L., Tamir, H., and Privat, A. (1994). Direct immunocytochemical localization of 5-hydroxytryptamine receptors in the adult rat spinal cord: a light and electron microscopic study using an anti-idiotypic antiserum. J. Neurosci. Res. *38*, 109–121.

Rosenbaum, D.M., Rasmussen, S.G.F., and Kobilka, B.K. (2009). The structure and function of G-protein-coupled receptors. Nature *459*, 356–363.

Ruat, M., Traiffort, E., Arrang, J.M., Tardivel-Lacombe, J., Diaz, J., Leurs, R., and Schwartz, J.C. (1993). A novel rat serotonin (5-HT6) receptor: molecular cloning, localization and stimulation of cAMP accumulation. Biochem. Biophys. Res. Commun. *193*, 268–276.

Rude, S., Coggeshall, E., and Van Orden, L.S. (1969). Chemical and ultrastructural identification of 5-hydroxytryptamine in an identified neuron. J. Cell Biol. *41*, 832–854.

Ryan, T.A., Reuter, H., Wendland, B., Schweizer, F.E., Tsien, R.W., and Smith, S.J. (1993). The kinetics of synaptic vesicle recycling measured at single presynaptic boutons. Neuron *11*, 713–724.

Sabol, S.Z., Hu, S., and Hamer, D. (1998). A functional polymorphism in the monoamine oxidase A gene promoter. Hum. Genet. *103*, 273–279.

Sakurai, A., and Katz, P.S. (2003). Spike timing-dependent serotonergic neuromodulation of synaptic strength intrinsic to a central pattern generator circuit. J. Neurosci. Off. J. Soc. Neurosci. *23*, 10745–10755.

Salim, K., Fenton, T., Bacha, J., Urien-Rodriguez, H., Bonnert, T., Skynner, H.A., Watts, E., Kerby, J., Heald, A., Beer, M., et al. (2002). Oligomerization of G-protein-coupled Receptors Shown by Selective Co-immunoprecipitation. J. Biol. Chem. *277*, 15482–15485.

Samuvel, D.J., Jayanthi, L.D., Bhat, N.R., and Ramamoorthy, S. (2005). A role for p38 mitogen-activated protein kinase in the regulation of the serotonin transporter: evidence for distinct cellular mechanisms involved in transporter surface expression. J. Neurosci. Off. J. Soc. Neurosci. *25*, 29–41.

Sanchez-Armass, S., Merz, D.C., and Drapeau, P. (1991). Distinct receptors, second messengers and conductances underlying the dual responses to serotonin in an identified leech neurone. J. Exp. Biol. *155*, 531–547.

Sandén, N., Thorlin, T., Blomstrand, F., Persson, P.A., and Hansson, E. (2000). 5-Hydroxytryptamine2B receptors stimulate Ca2+ increases in cultured astrocytes from three different brain regions. Neurochem. Int. *36*, 427–434.

Sanders-Bush, E., and Breeding, M. (1988). Putative selective 5-HT-2 antagonists block serotonin 5-HT-1c receptors in the choroid plexus. J. Pharmacol. Exp. Ther. *247*, 169–173.

Santarelli, L., Saxe, M., Gross, C., Surget, A., Battaglia, F., Dulawa, S., Weisstaub, N., Lee, J., Duman, R., Arancio, O., et al. (2003). Requirement of Hippocampal Neurogenesis for the Behavioral Effects of Antidepressants. Science *301*, 805–809.

Sarkar, B., Das, A.K., Arumugam, S., Kaushalya, S.K., Bandyopadhyay, A., Balaji, J., and Maiti, S. (2012). The dynamics of somatic exocytosis in monoaminergic neurons. Front. Physiol. *3*, 414.

Schappi, J.M., Krbanjevic, A., and Rasenick, M.M. (2014). Tubulin, actin and heterotrimeric G proteins: Coordination of signaling and structure. Biochim. Biophys. Acta BBA - Biomembr. *1838*, 674–681.

Schellekens, H., van Oeffelen, W.E.P.A., Dinan, T.G., and Cryan, J.F. (2013). Promiscuous dimerization of the growth hormone secretagogue receptor (GHS-R1a) attenuates ghrelin-mediated signaling. J. Biol. Chem. *288*, 181–191.

Schmuck, K., Ullmer, C., Engels, P., and Lübbert, H. (1994). Cloning and functional characterization of the human 5-HT2B serotonin receptor. FEBS Lett. *342*, 85–90.

Schneider, B., Pietri, M., Mouillet-Richard, S., Ermonval, M., MuŢEL, V., Launay, J.-M., and Kellermann, O. (2006). Control of Bioamine Metabolism by 5-HT2B and α1D Autoreceptors through Reactive Oxygen Species and Tumor Necrosis Factor-α Signaling in Neuronal Cells. Ann. N. Y. Acad. Sci. *1091*, 123–141.

Séguéla, P., Watkins, K.C., and Descarries, L. (1988). Ultrastructural features of dopamine axon terminals in the anteromedial and the suprarhinal cortex of adult rat. Brain Res. *442*, 11–22.

Séguéla, P., Watkins, K.C., and Descarries, L. (1989). Ultrastructural relationships of serotonin axon terminals in the cerebral cortex of the adult rat. J. Comp. Neurol. *289*, 129–142.

Séguéla, P., Watkins, K.C., Geffard, M., and Descarries, L. (1990). Noradrenaline axon terminals in adult rat neocortex: an immunocytochemical analysis in serial thin sections. Neuroscience *35*, 249–264.

Sesack, S.R., Aoki, C., and Pickel, V.M. (1994). Ultrastructural localization of D2 receptor-like immunoreactivity in midbrain dopamine neurons and their striatal targets. J. Neurosci. Off. J. Soc. Neurosci. *14*, 88–106.

Setou, M., Nakagawa, T., Seog, D.H., and Hirokawa, N. (2000). Kinesin superfamily motor protein KIF17 and mLin-10 in NMDA receptor-containing vesicle transport. Science *288*, 1796–1802.

Sharp, T., Bramwell, S.R., Clark, D., and Grahame-Smith, D.G. (1989). In vivo measurement of extracellular 5-hydroxytryptamine in hippocampus of the anaesthetized rat using microdialysis: changes in relation to 5-hydroxytryptaminergic neuronal activity. J. Neurochem. *53*, 234–240.

Sheng, M., and Sala, C. (2001). Pdz Domains and the Organization of Supramolecular Complexes. Annu. Rev. Neurosci. *24*, 1–29.

Sierralta, J., and Mendoza, C. (2004). PDZ-containing proteins: alternative splicing as a source of functional diversity. Brain Res. Brain Res. Rev. *47*, 105–115.

Soiza-Reilly, M., and Commons, K.G. (2011). Quantitative analysis of glutamatergic innervation of the mouse dorsal raphe nucleus using array tomography. J. Comp. Neurol. *519*, 3802–3814.

Soiza-Reilly, M., Anderson, W.B., Vaughan, C.W., and Commons, K.G. (2013). Presynaptic gating of excitation in the dorsal raphe nucleus by GABA. Proc. Natl. Acad. Sci. *110*, 15800–15805.

Soiza-Reilly, M., Saggau, P., and Arenkiel, B.R. (2015). Neural circuits revealed. Front. Neural Circuits 35.

Sørensen, L., Strømgaard, K., and Kristensen, A.S. (2014). Characterization of Intracellular Regions in the Human Serotonin Transporter for Phosphorylation Sites.

Sotelo, C., Cholley, B., El Mestikawy, S., Gozlan, H., and Hamon, M. (1990). Direct Immunohistochemical Evidence of the Existence of 5-HT1A Autoreceptors on Serotoninergic Neurons in the Midbrain Raphe Nuclei. Eur. J. Neurosci. *2*, 1144–1154.

Speake, T., Kibble, J.D., and Brown, P.D. (2004). Kv1.1 and Kv1.3 channels contribute to the delayed-rectifying K+ conductance in rat choroid plexus epithelial cells. Am. J. Physiol. - Cell Physiol. *286*, C611–C620.

Sprouse, J.S., and Aghajanian, G.K. (1987). Electrophysiological responses of serotoninergic dorsal raphe neurons to 5-HT1A and 5-HT1B agonists. Synap. N. Y. N *1*, 3–9.

Steiner, J.A., Carneiro, A.M.D., and Blakely, R.D. (2008). Going with the Flow: Trafficking-Dependent and -Independent Regulation of Serotonin Transport. Traffic *9*, 1393–1402.

Stockmeier, C.A., Shapiro, L.A., Haycock, J.W., Thompson, P.A., and Lowy, M.T. (1996). Quantitative subregional distribution of serotonin1A receptors and serotonin transporters in the human dorsal raphe. Brain Res. *727*, 1–12.

Sullivan, N.R., Crane, J.W., Damjanoska, K.J., Carrasco, G.A., D'Souza, D.N., Garcia, F., and Van de Kar, L.D. (2005). Tandospirone activates neuroendocrine and ERK (MAP kinase) signaling pathways specifically through 5-HT1A receptor mechanisms in vivo. Naunyn. Schmiedebergs Arch. Pharmacol. *371*, 18–26.

Sur, C., Betz, H., and Schloss, P. (1996). Immunocytochemical detection of the serotonin transporter in rat brain. Neuroscience *73*, 217–231.

Suzuki, R., Rygh, L.J., and Dickenson, A.H. (2004). Bad news from the brain: descending 5-HT pathways that control spinal pain processing. Trends Pharmacol. Sci. *25*, 613–617.

Svenningsson, P., and Greengard, P. (2007). p11 (S100A10)--an inducible adaptor protein that modulates neuronal functions. Curr. Opin. Pharmacol. *7*, 27–32.

Svenningsson, P., Chergui, K., Rachleff, I., Flajolet, M., Zhang, X., El Yacoubi, M., Vaugeois, J.-M., Nomikos, G.G., and Greengard, P. (2006). Alterations in 5-HT1B receptor function by p11 in depression-like states. Science *311*, 77–80.

Szule, J.A., Harlow, M.L., Jung, J.H., De-Miguel, F.F., Marshall, R.M., and McMahan, U.J. (2012). Regulation of synaptic vesicle docking by different classes of macromolecules in active zone material. PloS One *7*, e33333.

Tao, R., and Auerbach, S.B. (2000). Regulation of serotonin release by GABA and excitatory amino acids. J. Psychopharmacol. Oxf. Engl. *14*, 100–113.

Tao, R., and Auerbach, S.B. (2003). Influence of inhibitory and excitatory inputs on serotonin efflux differs in the dorsal and median raphe nuclei. Brain Res. *961*, 109–120.

Tao, R., Ma, Z., and Auerbach, S.B. (1996). Differential regulation of 5-hydroxytryptamine release by GABAA and GABAB receptors in midbrain raphe nuclei and forebrain of rats. Br. J. Pharmacol. *119*, 1375–1384.

Teitler, M., Toohey, N., Knight, J.A., Klein, M.T., and Smith, C. (2010). Clozapine and other competitive antagonists reactivate risperidone-inactivated h5-HT7 receptors: radioligand binding and functional evidence for GPCR homodimer protomer interactions. Psychopharmacology (Berl.) *212*, 687–697.

Thomas, D.R. (2006). 5-ht5A receptors as a therapeutic target. Pharmacol. Ther. *111*, 707–714.

Torres, G.E., and Amara, S.G. (2007). Glutamate and monoamine transporters: new visions of form and function. Curr. Opin. Neurobiol. *17*, 304–312.

Torres-Escalante, J.L., Barral, J.A., Ibarra-Villa, M.D., Pérez-Burgos, A., Góngora-Alfaro, J.L., and Pineda, J.C. (2004). 5-HT1A, 5-HT2, and GABAB receptors interact to modulate neurotransmitter release probability in layer 2/3 somatosensory rat cortex as evaluated by the paired pulse protocol. J. Neurosci. Res. *78*, 268–278.

Tournois, C., Mutel, V., Manivet, P., Launay, J.M., and Kellermann, O. (1998). Cross-talk between 5-hydroxytryptamine receptors in a serotonergic cell line. Involvement of arachidonic acid metabolism. J. Biol. Chem. *273*, 17498–17503.

Trueta, C., and De-Miguel, F.F. (2012). Extrasynaptic exocytosis and its mechanisms: a source of molecules mediating volume transmission in the nervous system. Front. Physiol. *3*, 319.

Trueta, C., Méndez, B., and De-Miguel, F.F. (2003). Somatic exocytosis of serotonin mediated by L-type calcium channels in cultured leech neurones. J. Physiol. *547*, 405–416.

Trueta, C., Sánchez-Armass, S., Morales, M.A., and De-Miguel, F.F. (2004). Calcium-induced calcium release contributes to somatic secretion of serotonin in leech Retzius neurons. J. Neurobiol. *61*, 309–316.

Trueta, C., Kuffler, D.P., and De-Miguel, F.F. (2012). Cycling of dense core vesicles involved in somatic exocytosis of serotonin by leech neurons. Front. Physiol. *3*, 175.

Turner, J.H., and Raymond, J.R. (2005). Interaction of Calmodulin with the Serotonin 5-Hydroxytryptamine2A Receptor A PUTATIVE REGULATOR OF G PROTEIN COUPLING AND RECEPTOR PHOSPHORYLATION BY PROTEIN KINASE C. J. Biol. Chem. *280*, 30741–30750.

Turner, J.H., Gelasco, A.K., and Raymond, J.R. (2004a). Calmodulin interacts with the third intracellular loop of the serotonin 5-hydroxytryptamine1A receptor at two distinct sites: putative role in receptor phosphorylation by protein kinase C. J. Biol. Chem. *279*, 17027–17037.

Turner, T.J., Mokler, D.J., and Luebke, J.I. (2004b). Calcium influx through presynaptic 5-HT3 receptors facilitates GABA release in the hippocampus: in vitro slice and synaptosome studies. Neuroscience *129*, 703–718.

Ullmer, C., Schmuck, K., Figge, A., and Lübbert, H. (1998). Cloning and characterization of MUPP1, a novel PDZ domain protein. FEBS Lett. *424*, 63–68.

Ursin, R. (2002). Serotonin and sleep. Sleep Med. Rev. *6*, 55–69.

Urtikova, N., Berson, N., Van Steenwinckel, J., Doly, S., Truchetto, J., Maroteaux, L., Pohl, M., and Conrath, M. (2012). Antinociceptive effect of peripheral serotonin 5-HT2B receptor activation on neuropathic pain. PAIN *153*, 1320–1331.

Valjent, E. (2009). Neuropsychopharmacology - Mechanisms of Locomotor Sensitization to Drugs of Abuse in a Two-Injection Protocol. Neuropsychopharmacology *35*, 401–415.

Van Bockstaele, E.J., and Pickel, V.M. (1993). Ultrastructure of serotonin-immunoreactive terminals in the core and shell of the rat nucleus accumbens: cellular substrates for interactions with catecholamine afferents. J. Comp. Neurol. *334*, 603–617.

Van Bockstaele, E.J., Cestari, D.M., and Pickel, V.M. (1994). Synaptic structure and connectivity of serotonin terminals in the ventral tegmental area: potential sites for modulation of mesolimbic dopamine neurons. Brain Res. *647*, 307–322.

Varga, V., Sik, A., Freund, T.F., and Kocsis, B. (2002). GABAB receptors in the median raphe nucleus: distribution and role in the serotonergic control of hippocampal activity. Neuroscience *109*, 119–132.

Varga, V., Kocsis, B., and Sharp, T. (2003). Electrophysiological evidence for convergence of inputs from the medial prefrontal cortex and lateral habenula on single neurons in the dorsal raphe nucleus. Eur. J. Neurosci. *17*, 280–286.

Varga, V., Losonczy, A., Zemelman, B.V., Borhegyi, Z., Nyiri, G., Domonkos, A., Hangya, B., Holderith, N., Magee, J.C., and Freund, T.F. (2009). Fast Synaptic Subcortical Control of Hippocampal Circuits. Science *326*, 449–453.

Vizi, E.S., Kiss, J.P., and Lendvai, B. (2004). Nonsynaptic communication in the central nervous system. Neurochem. Int. *45*, 443–451.

Voigt, M.M., Laurie, D.J., Seeburg, P.H., and Bach, A. (1991). Molecular cloning and characterization of a rat brain cDNA encoding a 5-hydroxytryptamine1B receptor. EMBO J. *10*, 4017–4023.

Voisin, A.N., Mnie-Filali, O., Giguère, N., Fortin, G.M., Vigneault, E., El Mestikawy, S., Descarries, L., and Trudeau, L.-É. (2016). Axonal Segregation and Role of the Vesicular Glutamate Transporter VGLUT3 in Serotonin Neurons. Front. Neuroanat. 39.

Wacker, D., Wang, C., Katritch, V., Han, G.W., Huang, X.-P., Vardy, E., McCorvy, J.D., Jiang, Y., Chu, M., Siu, F.Y., et al. (2013). Structural Features for Functional Selectivity at Serotonin Receptors. Science *340*, 615–619.

Wacker, D., Wang, S., McCorvy, J.D., Betz, R.M., Venkatakrishnan, A.J., Levit, A., Lansu, K., Schools, Z.L., Che, T., Nichols, D.E., et al. (2017). Crystal Structure of an LSD-Bound Human Serotonin Receptor. Cell *168*, 377–389.e12.

Wainscott, D.B., Cohen, M.L., Schenck, K.W., Audia, J.E., Nissen, J.S., Baez, M., Kursar, J.D., Lucaites, V.L., and Nelson, D.L. (1993). Pharmacological characteristics of the newly cloned rat 5-hydroxytryptamine2F receptor. Mol. Pharmacol. *43*, 419–426.

Wainscott, D.B., Lucaites, V.L., Kursar, J.D., Baez, M., and Nelson, D.L. (1996). Pharmacologic characterization of the human 5-hydroxytryptamine2B receptor: evidence for species differences. J. Pharmacol. Exp. Ther. *276*, 720–727.

Wang, C., Zhang, N., Zhang, Y.L., Zhang, J., Yang, H., Timothy, T.C., Wang, C., Zhang, N., Zhang, Y.L., Zhang, J., et al. (2013). Comparison of the neurobiological effects of attribution retraining group therapy with those of selective serotonin reuptake inhibitors. Braz. J. Med. Biol. Res. *46*, 318–326.

Warner-Schmidt, J.L., Flajolet, M., Maller, A., Chen, E.Y., Qi, H., Svenningsson, P., and Greengard, P. (2009). Role of p11 in cellular and behavioral effects of 5-HT4 receptor stimulation. J. Neurosci. Off. J. Soc. Neurosci. *29*, 1937–1946.

Weber, E.T., and Andrade, R. (2010). Htr2a Gene and 5-HT2A Receptor Expression in the Cerebral Cortex Studied Using Genetically Modified Mice. Front. Neurosci. *4*.

Weiger, W.A. (1997). Serotonergic modulation of behaviour: a phylogenetic overview. Biol. Rev. Camb. Philos. Soc. *72*, 61–95.

Whitaker-Azmitia, P.M. (1999). The discovery of serotonin and its role in neuroscience. Neuropsychopharmacol. Off. Publ. Am. Coll. Neuropsychopharmacol. *21*, 2S–8S.

White, S.R., Fung, S.J., Jackson, D.A., and Imel, K.M. (1996). Serotonin, norepinephrine and associated neuropeptides: effects on somatic motoneuron excitability. Prog. Brain Res. *107*, 183–199.

Williams, J.T., Colmers, W.F., and Pan, Z.Z. (1988). Voltage- and ligand-activated inwardly rectifying currents in dorsal raphe neurons in vitro. J. Neurosci. Off. J. Soc. Neurosci. *8*, 3499–3506.

Wimalasena, K. (2011). Vesicular monoamine transporters: Structure-function, pharmacology, and medicinal chemistry. Med. Res. Rev. *31*, 483–519.

Winstanley, C.A., Eagle, D.M., and Robbins, T.W. (2006). Behavioral models of impulsivity in relation to ADHD: translation between clinical and preclinical studies. Clin. Psychol. Rev. *26*, 379–395.

Wirth, A., Holst, K., and Ponimaskin, E. (2016). How serotonin receptors regulate morphogenic signalling in neurons. Prog. Neurobiol.

Woehler, A., Wlodarczyk, J., and Ponimaskin, E.G. (2009). Specific oligomerization of the 5-HT1A receptor in the plasma membrane. Glycoconj. J. *26*, 749–756.

Wölfel, M., and Schneggenburger, R. (2003). Presynaptic capacitance measurements and Ca2+ uncaging reveal submillisecond exocytosis kinetics and characterize the Ca2+ sensitivity of vesicle pool depletion at a fast CNS synapse. J. Neurosci. Off. J. Soc. Neurosci. *23*, 7059–7068.

Wong, A., Zhang, Y.-W., Jeschke, G.R., Turk, B.E., and Rudnick, G. (2012). Cyclic GMP-dependent Stimulation of Serotonin Transport Does Not Involve Direct Transporter Phosphorylation by cGMP-dependent Protein Kinase. J. Biol. Chem. *287*, 36051–36058.

Wyler, S.C., Spencer, W.C., Green, N.H., Rood, B.D., Crawford, L., Craige, C., Gresch, P., McMahon, D.G., Beck, S.G., and Deneris, E. (2016). Pet-1 Switches Transcriptional Targets Postnatally to Regulate Maturation of Serotonin Neuron Excitability. J. Neurosci. Off. J. Soc. Neurosci. *36*, 1758–1774.

Xia, Z., Gray, J.A., Compton-Toth, B.A., and Roth, B.L. (2003a). A Direct Interaction of PSD-95 with 5-HT2A Serotonin Receptors Regulates Receptor Trafficking and Signal Transduction. J. Biol. Chem. *278*, 21901–21908.

Xia, Z., Hufeisen, S.J., Gray, J.A., and Roth, B.L. (2003b). The PDZ-binding domain is essential for the dendritic targeting of 5-HT2A serotonin receptors in cortical pyramidal neurons in vitro. Neuroscience *122*, 907–920.

Xie, Z., Lee, S.P., O'Dowd, B.F., and George, S.R. (1999). Serotonin 5-HT1B and 5-HT1D receptors form homodimers when expressed alone and heterodimers when co-expressed. FEBS Lett. *456*, 63–67.

Xu, T.L., Pang, Z.P., Li, J.S., and Akaike, N. (1998). 5-HT potentiation of the GABA(A) response in the rat sacral dorsal commissural neurones. Br. J. Pharmacol. *124*, 779–787.

Yadav, V.K., Oury, F., Suda, N., Liu, Z.-W., Gao, X.-B., Confavreux, C., Klemenhagen, K.C., Tanaka, K.F., Gingrich, J.A., Guo, X.E., et al. (2009). A serotonin-dependent mechanism explains the leptin regulation of bone mass, appetite, and energy expenditure. Cell *138*, 976–989.

Yakel, J.L., and Jackson, M.B. (1988). 5-HT3 receptors mediate rapid responses in cultured hippocampus and a clonal cell line. Neuron *1*, 615–621.

Yuen, E.Y., Jiang, Q., Chen, P., Gu, Z., Feng, J., and Yan, Z. (2005). Serotonin 5-HT1A Receptors Regulate NMDA Receptor Channels through a Microtubule-Dependent Mechanism. J. Neurosci. *25*, 5488–5501.

Yuen, E.Y., Jiang, Q., Chen, P., Feng, J., and Yan, Z. (2008). Activation of 5-HT2A/C Receptors Counteracts 5-HT1A Regulation of N-Methyl-D-aspartate Receptor Channels in Pyramidal Neurons of Prefrontal Cortex. J. Biol. Chem. *283*, 17194–17204.

Zhang, Y., Chen, K., Sloan, S.A., Bennett, M.L., Scholze, A.R., O'Keeffe, S., Phatnani, H.P., Guarnieri, P., Caneda, C., Ruderisch, N., et al. (2014). An RNA-Sequencing Transcriptome and Splicing Database of Glia, Neurons, and Vascular Cells of the Cerebral Cortex. J. Neurosci. *34*, 11929–11947.

Zhang, Y.-W., Gesmonde, J., Ramamoorthy, S., and Rudnick, G. (2007). Serotonin transporter phosphorylation by cGMP-dependent protein kinase is altered by a mutation associated with obsessive compulsive disorder. J. Neurosci. Off. J. Soc. Neurosci. *27*, 10878–10886.

Zhou, F.C., Tao-Cheng, J.H., Segu, L., Patel, T., and Wang, Y. (1998). Serotonin transporters are located on the axons beyond the synaptic junctions: anatomical and functional evidence. Brain Res. *805*, 241–254.

Zhu, C.-B., Hewlett, W.A., Feoktistov, I., Biaggioni, I., and Blakely, R.D. (2004a). Adenosine receptor, protein kinase G, and p38 mitogen-activated protein kinase-dependent up-regulation of serotonin transporters involves both transporter trafficking and activation. Mol. Pharmacol. *65*, 1462–1474.

Zhu, C.-B., Hewlett, W.A., Francis, S.H., Corbin, J.D., and Blakely, R.D. (2004b). Stimulation of serotonin transport by the cyclic GMP phosphodiesterase-5 inhibitor sildenafil. Eur. J. Pharmacol. *504*, 1–6.

Zhu, C.-B., Steiner, J.A., Munn, J.L., Daws, L.C., Hewlett, W.A., and Blakely, R.D. (2007). Rapid stimulation of presynaptic serotonin transport by A(3) adenosine receptors. J. Pharmacol. Exp. Ther. *322*, 332–340.

Zoli, M., and Agnati, L.F. (1996). Wiring and volume transmission in the central nervous system: the concept of closed and open synapses. Prog. Neurobiol. *49*, 363–380.